Whole System Approaches to Railway Asset Management

By
Jack Litherland



University of Nottingham
UK | CHINA | MALAYSIA

Thesis submitted to the University of Nottingham for the degree of Doctor of Philosophy

October 2019

‘Essentially, all models are wrong, but some are useful’

George Box



The evolution of British railways [1]

Abstract

As the world population continues to grow, the demand for rail transport increases. The requirements on railway networks already at capacity continues to expand. In 2017-2018 there were 1.7 billion passenger journeys made on the UK railway network, compared to just over 700 million in 1994. Yet the number of track kilometres in the UK has remained near constant over that same time period. These changes are making maintenance scheduling more challenging; increased usage is leading to faster degradation yet, with more trains per hour and services starting earlier and finishing later, the time available to perform maintenance is shrinking. In many areas, it is extremely difficult to build new railways as land is both limited and expensive, additionally there are a range of legal challenges. Therefore innovative approaches to railway asset management are needed to maximise the performance of the existing network.

This research will investigate how whole system approaches to railway asset management, which consider whole system condition and whole life cost, can be used to make maintenance as streamlined and efficient as possible and tackle these challenges. A range of models have been created to aid railway asset management including Markov models and Petri net models. Nonetheless, previous models have generally only considered a single asset class and only considered a small section of the railway. The aim of this thesis is to investigate the feasibility of a framework, which allows a range of different railway assets to be modelled simultaneously, over a large section of railway.

In order to create a whole system model this thesis begins by developing Petri net models for a range of assets within the railway network namely: track (rails and ballast), sleepers, switches and crossings (S&C), tunnels and the signalling system. The asset models were developed based on Network Rail data, literature and expert judgement.

The Petri net models for the various assets were then converted into modules and combined using the hierarchical Petri net (HPN) framework, to form a system model. The hierarchy proposed contained three levels, allowing different phenomena to impact the system in different ways. The system model enabled the effects of dependencies between assets to be explored as well as allowing opportunistic maintenance to be considered. The framework was constructed in such a way as to allow additional asset classes to be included, in the framework, in the future.

The system model was applied to the Bletchley Delivery Unit, a busy railway corridor, as a test case. The test case contained; a master/control module, 849 track modules, 849 sleeper modules (705 concrete, 53 timber, 91 steel), 61 S&C modules, 21 tunnel modules and a signalling module.

Due to the size of the whole system model, the simulation time and memory required needs careful consideration. The final part of this research explores a range of means to speed up

the simulation of Petri nets, and reduce the memory required to solve them. A range of techniques for streamlining the Petri net algorithm were explored. The research also investigated the benefits of using parallel processing to solve Petri net models. Heterogeneous programming, which combines the central processing unit (CPU) and the graphics processing unit (GPU) was also explored. It was concluded that the memory requirement is likely to limit performance before computation time, and also limits the benefit that can be achieved from heterogeneous programming.

Acknowledgments

First of all I would like to express my gratitude to my supervisors: Professor John Andrews, Dr Rasa Remenyte-Prescott and Dr Darren Prescott. I would like to thank them for the opportunities they have given me throughout my PhD studies and for their continuous guidance and input to my PhD project. Without this the project would not have been possible.

I would also like to give a massive thanks to Andy Kirwan and the Advanced Analytics team at Network Rail; both for their sponsorship and huge input to the project. I would also like to specifically thank Matthew Hamer and Julian Williams for providing both extensive time and resources to my PhD project, without which I would not have completed this PhD.

I would also like to thank all the members of the Resilience Engineering Research Group and Nottingham Engineering Transport Centre (NTEC), for creating such a friendly and helpful working environment over the number of years I have spent in Nottingham.

A special thanks must also go to my amazing girlfriend, Anqi Chen, for the support given to me at the end of the PhD journey. A huge thanks must also go to my friends in Nottingham and back home in Plymouth who have kept me smiling throughout the PhD project, a particular thanks to Arthur Argles for the hours he spent reading my thesis.

Lastly, I think the biggest thanks of all must go to my parents; Margaret and Julian and the other members of my family, including the members that are sadly no longer with us, for their continuous support and encouragement throughout my PhD project.

Thank you!

Publications

Conference Papers

J. Litherland, G. Calvert, J. Andrews and A. Kirwan “Developing an extended RAMS framework for railway networks” *in Proceedings of the 29th European Safety and Reliability Conference (ESREL 2019)*, 2019, pp. 3489–3496

J. Litherland and J. Andrews “A Petri net methodology for modelling the maintenance of railway route sections” *in Proceedings of the 29th European Safety and Reliability Conference (ESREL 2019)*, 2019, pp. 452–459

Contents

Abstract ..... **IV**
Acknowledgments ..... **VI**
Publications ..... **VII**
Glossary ..... **XII**
List of Figures ..... **XIV**
List of Tables ..... **XIX**
1 Introduction **1**
1.1 Background 1
1.2 Outline of the Problem 3
1.3 Aims and Objectives 3
1.4 Research Novelty 4
1.5 Outline of the Thesis 4
2 Background 6
2.1 Introduction 6
2.2 Terminology 6
2.3 Railway Assets 8
2.3.1 Ballast 9
2.3.2 Rails 16
2.3.3 Slab Track 23
2.3.4 Sleepers 23
2.3.5 Sleeper Pads 27
2.3.6 Fastening System 27
2.3.7 Switches and Crossings (S&C) 28
2.3.8 Tunnels 30
2.3.9 Signalling Systems 31
2.4 Other Assets: Not Considered in this Research 32
2.5 Summary 32
3 Asset Management Modelling Techniques 34
3.1 Introduction 34
3.2 Asset Management 34
3.2.1 Reliability 35
3.2.2 Maintainability 35
3.2.3 Availability 36
3.2.4 Safety 37
3.2.5 Whole Lifecycle Cost (LCC) 37
3.3 Asset Management Modelling Techniques 37
3.3.1 Markovian Methods 38
3.3.2 Petri Net Models 42
3.3.3 Petri Net Extensions 47
3.3.4 Monte Carlo Simulations 49
3.3.5 Combination of Methods 50
3.4 Summary 50

4 Railway Asset Management Models 52
4.1 Introduction 52
4.2 Track Geometry Models 52
4.3 Review of Sleeper Models 58
4.4 Review of Tunnel Literature 59
4.5 Review of Switches and Crossings Literature and Models 61
4.6 Whole System Asset Management Applications 62
4.7 Conclusions and Evaluation of Modelling Techniques 63
5 System Analysis 66
5.1 Introduction 66
5.2 Data Available and Data Limitations 67
5.3 Distribution Fitting 68
5.4 Track Analysis 69
5.4.1 Track Deterioration Analysis 69
5.4.2 Track Maintenance Analysis 73
5.4.3 Analysis of Location Factors 95
5.4.4 Maintenance History 101
5.5 Sleeper Analysis 102
5.5.1 Deterioration Rates 102
5.5.2 Maintenance Analysis 104
5.6 Switch and Crossing Analysis 108
5.7 Analysis of the Signalling System 116
5.8 Inspections 120
5.9 Summary and Conclusions 121
6 Individual Models for Railway Assets 123
6.1 Introduction 123
6.2 Petri Net Transitions and Notation 123
6.2.1 Places 123
6.2.2 Standard Transitions 123
6.2.3 Conditional Transitions 125
6.2.4 Reset Transitions 126
6.2.5 Probabilistic Transitions 127
6.2.6 Conditional Probabilistic Transitions 127
6.2.7 Conflicting Transitions 128
6.2.8 Labelling System 128
6.3 Petri Net Asset Models 129
6.3.1 Track Section Petri Net Model 129
6.3.2 Sleepers, Fastenings and Pads Petri Net Model 154
6.3.3 Tunnel Petri Net Model 187
6.3.4 Switches and Crossings Petri Net Model 188
6.3.5 Signalling System Petri Net Model 196
6.4 Summary and Conclusions 201
7 System Framework 203
7.1 Introduction 203

7.2 System Hierarchy 203
7.2.1 System Dependencies 204
7.3 Whole System Petri Net Modules 207
7.3.1 Master Module 207
7.3.2 Additions to the Track Section Model for use in the Whole System Framework 213
7.3.3 Additions to the Sleeper Models for use in the Whole System Framework 221
7.3.4 Additions to the S&C Model for use in the Whole System Framework 222
7.3.5 Additions to the Tunnel Model for use in the Whole System Framework 224
7.3.6 Additions to the Signalling System Model for use in the Whole System Framework 224
7.4 A Test Case: Bletchley Delivery Unit 225
7.4.1 Results of Bletchley Delivery Unit Case Study 227
7.5 Model Validation 234
7.5.1 Cost Outputs 234
7.5.2 Ballast Condition Profile Condition 235
7.6 Discussion and Conclusions 237
8 Simulating Large Petri Nets and Code Validation 238
8.1 Introduction 238
8.2 Code Validation 238
8.2.1 Calculating Solution in Special Cases 238
8.2.2 Comparison to Other Codes and Software 239
8.2.3 CPU V GPGPU Results 240
8.3 Reducing Computer Resources Required 240
8.3.1 The Petri Net Solution Routine 240
8.3.2 Petri Net Solution Routine Improvements Implemented 245
8.3.3 Parallel Programming 246
8.3.4 GPGPU Programming 247
8.3.5 Parallel Processing in this Research 254
8.4 Convergence Rates 257
8.5 Simulation Times 258
8.6 Summary and Conclusions 260
9 Conclusions 261
9.1 Introduction 261
9.2 Summary of Work Completed 261
9.3 Conclusions 262
9.3.1 Conclusions Drawn from the Asset Models 262
9.3.2 Conclusions Drawn from the System Framework 263
9.3.3 Conclusions Drawn on the Computational Requirements 264
9.4 Overall Conclusions 264
9.5 Completion of Aims and Contributions to Research 265
9.6 Limitations 267
9.7 Future Work 267
9.7.1 Future Developments of Tamping and Stoneblowing Scheduling 269

References 274
Appendix A: Ballast Parameters 283
Appendix B: Rail Parameters 284
Appendix C: Sleeper Parameters 288
Appendix D: Switches and Crossings Summary 299
Appendix E: Inspection Costs 301
Appendix F: Budget Parameters 302
Appendix G: System Level Asset Module Petri Nets 303
Appendix H: Special Case Solutions to the System Model 309
Appendix I: System Model Initial Marking Distributions 311
Appendix J: Location Parameters 313

Glossary

ART	Active Repair Time
AWS	Automatic Warning System
CDF	Cumulative Density Function
CP	Control Period *Normally followed by a number e.g. CP5*
CPN	Coloured Petri Net
CPU	Central Processing Unit
CTRI	Combined Track Record Index
CUDA	Compute Unified Device Architecture
CWR	Continuous Welded Rail
DC	Direct Current
DP	Double Precision
ELR	Engineer's Line Reference
BBM	Bletchley →Bedford
RBS1	Rugby →Birmingham
HNR	Northampton Loop
LEC1	Euston →Rugby
LEC2	Rugby →Stafford
ERTMS	European Rail Traffic Management System
EMGTPA	Equivalent Million Gross Tonnes per Annum
E&P	Electrification and Power
FD	Fixed Diamond (Crossing)
FLOPS	Floating Point Operations per Second
FMS	Fault Management System (Database)
ft	Feet
GB	Gigabytes
GB/s	Gigabytes per Second
GIPS	Giga Instructions per Cycle
GPGPU	General-purpose Computing on Graphics Processing Unit
GPU	Graphics Processing Unit
HOM	High Output Machine *Used for track renewal*
HPN	Hierarchical Petri Net
HS2	High Speed 2 *Proposed high speed rail link between London, Birmingham and the North*
IAM	Institute of Asset Management
IMDM	Infrastructure Maintenance Delivery Manager
IDD	Independently and Identically Distributed
IDE	Intergraded Development Environment
kg	Kilograms
km	Kilometres
kph	Kilometres per Hour
LCC	Lifecycle Cost
LI	Location Index
LNW	London North Western *Network Rail strategic route*
MGT	Million Grose Tonnes
MLE	Maximum Likelihood Estimator
mm	Millimetres
mph	Mile per Hour
MTBSAF	Mean Time Between Service Affecting Failures
MTTF	Mean Time To Failure
MTTR	Mean Time To Repair

MSC	Multi Spin Code
NMT	New Measurement Train
NHPP	Non Homogenous Poisson Process
ODE	Ordinary Differential Equation
OLE	Overhead Line Equipment
ORR	Office of Road and Rail *Formally Office of Rail Regulation*
PCI	Peripheral Component Interconnect *Local computer bus for connecting hardware devices*
PDF	Probability Density Function
POE	Point Operating Equipment
RAIB	Rail Accident Investigation Branch
RCF	Rolling Contact Fatigue
RAM	Random-access Memory
S&C	Switches and Crossings
SD	Standard Deviation
SM	Streaming Microprocessor
SNCF	Société Nationale des Chemins de fer Français *French railway operator*
SPAD	Signal Passed At Danger
SSC	Single Spin Code
TD	Transverse Defects
TEX	Read Only Texture Memory
TFLOPS	Trillion Floating Point Operations per Second
TGI	Track Geometry Index
TSI	Track Structure Index
TSR	Temporary Speed Restriction
TQI	Track Quality Index
UIC	Union Internationale des Chemins de fer *International Union of Railways*
UK	United Kingdom
USP	Under Sleeper Pad
WCML	West Coast Mainline
X	Random number on the open interval $0 \rightarrow 1$

List of Figures

Figure 1.1: Passenger Usage 1950→2016 [4] 1
Figure 1.2: UK Route Kilometres 1900 →2016 [7] 2
Figure 1.3: Rail Technical Strategy; Capability Delivery Plan [9] 2
Figure 2.1: Network Rail Track Categories Based on Tonnage and Line Speed 7
Figure 2.2: Electrified Ballasted Railway (Taken From Tallington Level Crossing on the East Coast Mainline, UK) 8
Figure 2.3: Wet Bed [22] 10
Figure 2.4: New Measurement Train (NMT) at Derby Station 11
Figure 2.5: The Tamping Process 12
Figure 2.6: The Stoneblowing Process 13
Figure 2.7: Track Profile 14
Figure 2.8: The Ballast Re-profiling Process [26] 14
Figure 2.9: Ballast Cleaner [13] 15
Figure 2.10: Evolution of Ballast Vertical Alignment (SD) with Time 15
Figure 2.11: Jointed Rail with a Fishplate. The Rail is in Tension so there is a Gap Between the Rails 16
Figure 2.12: Extreme Rail Shelling [29] 19
Figure 2.13: Squat Development 20
Figure 2.14: Short and Long Pitch Corrugations 21
Figure 2.15: Extreme Wheel Burn 21
Figure 2.16: Slab Track [33] 23
Figure 2.17: Common Causes of Timber Sleeper Failure [36] 24
Figure 2.18: Twin Block Concrete Sleeper 26
Figure 2.19: Mono Block Concrete Sleeper 26
Figure 2.20: Serious Rail Seat Abrasion [45] 26
Figure 2.21: Steel Sleepers [47] 27
Figure 2.22: (Left) Pandrol ‘e’ Clip, (Right) Pandrol ‘Fastclip’ Clip [51] 28
Figure 2.23: UK Switch Size Breakdown, Further Information in Appendix D-1.1 30
Figure 2.24: Key Components of the Signalling System 31
Figure 3.1: IAM Conceptual Asset Management Model [64] 34
Figure 3.2: Types of Maintenance; Adapted from [63], [68], [69] 36
Figure 3.3: Modelling Techniques 38
Figure 3.4: Three State Markov Chain Model 39
Figure 3.5: Two State Markov Process 40
Figure 3.6: Solution to the Markov Model Shown in Figure 3.5, with Failure Rate =0.01 and Repair Rate =0.1 41
Figure 3.7: Hidden Markov Model 42
Figure 3.8: Firing of an Untimed Transition 44
Figure 3.9: Evolution of a Petri Net 45
Figure 3.10: Reachability Graph of Petri Net Shown in Figure 3.9 45
Figure 3.11: A Simple Petri Net 48

Figure 3.12: A Simple Hierarchical Petri Net 48
Figure 4.1: Evolution of Track Profile [95] 53
Figure 4.2: Degradation Petri Net Model Andrews [21] 57
Figure 4.3: Finite Element Model for Prestressed Concrete Sleeper You et al. [43] 58
Figure 4.4: Average Vertical Settlement Comparison [114] 59
Figure 4.5: Tunnel Age [115] 59
Figure 4.6: Tunnel Construction Type [115] 60
Figure 4.7: Laser Scanning of Railway Tunnels in Finland [118] 61
Figure 5.1: Key Parameter Require to Develop Railway Asset Models 66
Figure 5.2 Probability of Failure for Different Defect Types (List in Table 5.3) (25 MGT per Year Traffic Flow) [135] 72
Figure 5.3: Mean LCC Versus Renewal Tonnage [134] 72
Figure 5.4 Yearly Average Tamping Volumes 75
Figure 5.5 Tamping Volumes by Track Category 2009 →2014 75
Figure 5.6: Time to Schedule Tamping by Track Category CP4 '*Normal'* 78
Figure 5.7: Time to Schedule Tamping by Track Category CP4 '*Emergency*' 78
Figure 5.8: ART for Tamping by Track Category CP4 79
Figure 5.9: Comparison of Data and Distribution Fit for ART For Categories 1A →5 80
Figure 5.10: Probability Plot[136] for the Active Repair Time for Tamping 81
Figure 5.11: Proportion of the Number of Sections Tamped 83
Figure 5.12: Average Stoneblowing Volume per Year CP4 84
Figure 5.13: Distribution for the Time to Scheduling Stoneblowing by Track Category for CP4 '*Normal*' 85
Figure 5.14: Distribution for the Time to Scheduling Stoneblowing by Track Category for CP4 '*Emergency'* 86
Figure 5.15: ART Distributions for Stoneblowing by Track Category for CP4 86
Figure 5.16: Length Stoneblown During CP4 Interventions 87
Figure 5.17: Average Grinding Volume Per Year By Track Category for CP4 88
Figure 5.18: Grinding Scheduling Time Distribution by Track Category 90
Figure 5.19: Grinding Repair Time Distribution by Track Category 90
Figure 5.20: Average Length Ground Per Intervention For CP4 by Track Category 91
Figure 5.21: CP4 Welding Volumes 92
Figure 5.22: Distribution for the Time to Scheduling Weld Repairs by Track Category for CP4 93
Figure 5.23: ART Distributions for the Time to Perform Weld Repairs by Track Category CP4 94
Figure 5.24: Proportion of the Number of Sections Welded per Intervention by Track Category CP4 94
Figure 5.25: LI Used to Access Location Factors 97
Figure 5.26 Geology of the Bletchley Delivery Unit [141] 99
Figure 5.27 Concrete Sleeper Construction by Tonnage (Cumulative) 103
Figure 5.28 Sleeper Replacement Percentage By Year By Tonnage Band For Concrete Sleepers 103
Figure 5.29 Sleeper Maintenance Volumes by Construction Type and Track Category 105

Figure 5.30 Spread of the Number of Sleepers Replaced During CP4 Interventions By Sleeper Type 105
Figure 5.31: PDFs of the Distributions Found for the Time to Schedule Concrete, Timber and Steel Sleeper Repair Based on the Number of Defective Sleepers 107
Figure 5.32: PDFs of the Distributions Found for the ART for Concrete, Timber and Steel Sleepers Based on the Number of Defective Sleepers 107
Figure 5.33: Turnout S&C 109
Figure 5.34: NHPP CDF for First Eight Failures ($F_1(y) \rightarrow F_8(y)$), ($a>1$) 111
Figure 5.35: Number of Failures per Quarter by Switch Size (A→H) [147] 115
Figure 5.36 UK Signalling Repair/Maintenance 2014-2015 116
Figure 5.37 Bletchley Delivery Unit Signalling Repair/Maintenance 2014-2015 117
Figure 5.38: Bletchley Delivery Unit Signalling Component Degradation Distributions 118
Figure 5.39 Number of Failures in 2014-2015 118
Figure 6.1: Marking of the System Before and After a Conditional Transition Fires 126
Figure 6.2: Marking of the System Before and After a Reset Transition Fires 126
Figure 6.3: Marking of the System Before and After a Probabilistic Transition Fires 127
Figure 6.4: Marking of the System Before and After a Conditional Probabilistic Transition Fires 128
Figure 6.5: Conflicting Transitions 128
Figure 6.6: Ballast Condition Petri Net Model 130
Figure 6.7: Inspection Petri Net 132
Figure 6.8: Maintenance Scheduling Petri Net 132
Figure 6.9: Performing Maintenance 133
Figure 6.10: Update Condition 133
Figure 6.11: Petri Net for Speed Restrictions and Line Closures 134
Figure 6.12: Renewal and Cleaning Scheduler Petri Net 135
Figure 6.13: Rail Condition Model 137
Figure 6.14: Rail Renewal Schedule Petri Net 139
Figure 6.15: Rail Lubrication Model 139
Figure 6.16: Ballast Deterioration Profiles (Maintenance Not Considered) 146
Figure 6.17: Rail Deterioration Profiles (Maintenance Not Considered) 147
Figure 6.18: Probability of an Interventions Per 10.5 Week Period (Categories 1A, 1, 2 and 3) or 13 Week Period (Categories 4 and 5) 148
Figure 6.19: Convergence of Total Cost (Log Scale) 149
Figure 6.20: Cost Breakdown 150
Figure 6.21: Cost By Track Category 151
Figure 6.22: Sensitivity Analysis on the Total Cost 153
Figure 6.23 Concrete Sleeper Petri Net Model 156
Figure 6.24: Combining Exponential Distributions 157
Figure 6.25: Concrete Sleeper Total Cost Convergence 165
Figure 6.26: Concrete Sleeper Cost Breakdown 166
Figure 6.27: Concrete Sleeper Maintenance Frequency Per 16 weeks 167
Figure 6.28: Timber Sleeper Petri Net Model 174
Figure 6.29: Timber Sleeper Cost Convergence 175

Figure 6.30: Timber Sleeper Cost Breakdown....176
Figure 6.31: Timber Sleeper Maintenance Frequency Per 16 weeks....177
Figure 6.32: Steel Sleeper Petri Net....182
Figure 6.33: Steel Sleeper Total Cost Convergence....183
Figure 6.34: Steel Sleeper Cost Breakdown....184
Figure 6.35: Steel Sleeper Maintenance Per 16 Weeks....185
Figure 6.36: Comparison of the LCC Cost for the Three Different Sleeper Types (50 Years)....186
Figure 6.37: Tunnel Petri Net Model....188
Figure 6.38: S&C Petri Net Model (Size D)....192
Figure 6.39: S&C Convergence (Log Scale)....193
Figure 6.40: S&C Cost Breakdown (50 Years, Size D)....194
Figure 6.41: S&C Maintenance Per 16 Week Period (for 50 Years) by S&C Size....195
Figure 6.42: Petri Net Model for the Signalling System....198
Figure 6.43: Convergence of the Overall Cost of the Signalling Model....199
Figure 6.44: Signalling System Cost Breakdown....200
Figure 7.1: System Hierarchy....206
Figure 7.2: Master Module Petri Net....212
Figure 7.3: Tamping Scheduling Petri Net with Additional Port and Socket Places....214
Figure 7.4: Tamping Scheduling Petri Net for Opportunistic Maintenance of a Different Component in the Same Section with Additional Port and Socket Places....218
Figure 7.5: Tamping Scheduling Petri Net for Opportunistic Maintenance of a Similar Component in a Neighbouring Section with Additional Port and Socket Places....218
Figure 7.6: Implementation of Speed Restrictions and Line Closures....220
Figure 7.7: Bletchley Delivery Unit....225
Figure 7.8: Bletchley Delivery Unit Map, Including Stations and Key Assets....226
Figure 7.9: Bletchley Delivery Unit Heat Map of Cost, Normalised....230
Figure 7.10: Bletchley Delivery Unit Cost Breakdown Sections 1-400....231
Figure 7.11: Bletchley Delivery Unit Cost Breakdown by Year....232
Figure 7.12: Bletchley Delivery Unit Total Cost Breakdown....232
Figure 7.13: Delivery Unit Condition....233
Figure 7.14: Bletchley Delivery Unit Convergence Plot....233
Figure 7.15: Comparison Between Model Outputs for CP6→CP12 (35 Years) and Network Rail's CP5 Expenditure on Renewals and Track Maintenance....235
Figure 7.16: Comparison Between the Ballast Geometry Recorded by the NMT and a Ballast Profile Generated in One Simulation of the Petri Net....236
Figure 8.1: Sample Petri Net Model....239
Figure 8.2: Parallel and Series Petri Net Structure....242
Figure 8.3: Effect of the Number of Transitions (Constant Number of Time Steps) on the Simulation Time....242
Figure 8.4: Effect of the Number of Transitions that Fire (Number of Time Steps) on the Simulations Time (Constant Number of Transitions)....242
Figure 8.5: The Effect of a Parallel Vs Series Net Structure (see Figure 8.2) on Simulation Time (Constant Number of Transitions and Constant Number of Steps)....242

Figure 8.6: The Effect of Increasing the Number of Transitions and the Number of Transitions that Fire (Time Steps) on the Simulation Time....242
Figure 8.7: Flowchart of The Petri Net Solution Algorithm....244
Figure 8.8: Increase in Processor Speed 1980→2000 [161]....246
Figure 8.9: Tasks in Series (Left) and Tasks in Parallel (Right)....247
Figure 8.10: GPU v CPU GFLOPS from 2008 to 2016 (Left) and GPU v CPU Memory Bandwidth 2008 to 2016 (Right) [164]....248
Figure 8.11: Block, Grid, Thread and Warp Configuration....249
Figure 8.12: Kepler Streaming Multiprocessor....250
Figure 8.13: Tesla K40 Schematic, Comprising 15 MSs....252
Figure 8.14: CPU v GPU Simulation Time for Randomly Generate Biological Models with Varying Numbers of Processes [169]....254
Figure 8.15: Simulation Time For Various CPU and GPU Setups....255
Figure 9.1: Causes of Delay Minutes by Asset Class (TransPennine Route 2014-2019)....268
Figure 9.2: Tamping Scheduling Method A....272
Figure 9.3: Tamping and Stoneblowing Scheduling Method B....273

List of Tables

Table 2.1: Track Category Summary 8
Table 2.2: Rail Types in the UK 17
Table 2.3: Rail Maintenance Options 22
Table 2.4: Total Number of Sleeper and Demand for Various Countries [36] 23
Table 2.5: UK Sleeper Types 24
Table 2.6: Fastening System Breakdown 28
Table 2.7: Asset Summary 33
Table 3.1: Petri Net Symbols 46
Table 3.2: A→C Port and Socket Places 48
Table 3.3: Summary of Modelling Methods 51
Table 4.1: Suitability Evaluation of Techniques 65
Table 5.1: Network Rail Databases used in this Research 67
Table 5.2: Distribution of the Time Taken to Progress Between Ballast Condition States and the Transitions used to Model them for the Seven Track Categories 70
Table 5.3: UIC Rail Defect Codes 73
Table 5.4: Category 1A Estimated Rail Deterioration Distributions 73
Table 5.5: Schedule Time for ‘Normal’ and ‘Emergency’ Tamping Maintenance 77
Table 5.6: ART Distributions and Transitions for Tamping Maintenance 77
Table 5.7: Correlation Coefficient, ρ, for the ART Distributions Shown in Table 5.6 77
Table 5.8: Number of Section Tamped by Track Category 82
Table 5.9: Distributions and Transitions for Time to Scheduled ‘Normal’ and ‘Emergency’ Stoneblowing Maintenance 84
Table 5.10: ART Distributions and Transitions for Stoneblowing 85
Table 5.11: Number of Section Stoneblown per Intervention 87
Table 5.12: Schedule time Distributions for Grinding 89
Table 5.13: ART for Grinding Maintenance 89
Table 5.14: Schedule Time Distributions for Welding 92
Table 5.15: ART for Weld Repairs 93
Table 5.16: LI Proposed in this Research 97
Table 5.17: Statistics on the LI Scores for Bletchley Delivery Unit 97
Table 5.18: Typical C_v Values for Various Soil Types 98
Table 5.19: Rock Types in the Bletchley Area, their Assumed C_v Values and LI Scores 100
Table 5.20: Sleeper LI Values 101
Table 5.21: S&C Components 108
Table 5.22: Distributions used to Model S&C Deterioration and Failure, and Justification 112
Table 5.23: Degrade, Failure, Schedule and Repair Time Information For a Single Size D S&C Unit 114
Table 5.24: Degradation, Failure, Schedule and Repair Distributions and Transitions for Signalling System for Bletchley Delivery Unit 119

Table 5.25: Basic Visual Inspection Frequency, Sourced from NR/L2/TRK/001/mod11 [24] 121
Table 5.26: NMT Inspection Frequency, Sourced from NR/L2/TRK/001/mod02 [23] 121
Table 5.27: Ultrasonic Inspection Frequency, Sourced from NR/L2/TRK/001/mod06 [32] 121
Table 5.28: Key Conclusions From The System Analysis 122
Table 6.1: Node Types 123
Table 6.2: Reset Places and Marking 127
Table 6.3: Asset Petri Net Model Labels 129
Table 6.4: Condition That Lead to Speed Restrictions and Line Closures 133
Table 6.5: Summary of Rail Maintenance in the Rail Subnet 140
Table 6.6: Summary of Maintenance Interventions by Track Category 144
Table 6.7: Track Section Costs 145
Table 6.8: Number of Missing or Ineffective Fastenings Permitted per 60 Feet of Track 159
Table 6.9: Maximum Number of Defective Sleepers Permitted Per 60 Feet of Track for Various Line Speeds. 160
Table 6.10: Cost Breakdown for Concrete Sleepers by Track Category 162
Table 6.11: Mean, SD Minimum and Maximum Number of Each Cause of Concrete Sleeper Failure 163
Table 6.12: Mean, SD, Minimum and Maximum Number For Concrete Sleeper Maintenance Interventions 164
Table 6.13: Timber Sleeper Costs 171
Table 6.14: Mean, SD, Minimum and Maximum Number of Defective Sleepers Based on the Four Deterioration Modes 172
Table 6.15: Mean, SD, Minimum and Maximum Number of All Sleeper Replacements Considered 173
Table 6.16: Steel Sleeper Cost Breakdown 179
Table 6.17: Mean, SD, Minimum and Maximum Number of Sleepers Repaired 180
Table 6.18: Mean, SD, Minimum and Maximum For Steel Sleeper Failure Modes by Track Category 181
Table 6.19: S&C Failures 190
Table 6.20: S&C Repairs 190
Table 6.21: S&C Cost Breakdown for Various Switch Sizes 191
Table 6.22: Distribution used to Determine the Marking of Places $P2SG, P6SG, P10SG, P14SG$ and $P18SG$ (Total Number of Signalling Maintenance Interventions in Bletchley Delivery Unit in 50 Years) 197
Table 6.23: Signalling System Costs 197
Table 6.24: Signal Module Failure Results 197
Table 6.25: Signal Module Repair Results 197
Table 7.1: Condition Dependencies Between Assets Considered in the System Petri Net Model 205
Table 7.2: Transition used to Model the Planned Unavailability of Maintenance Machines 209

Table 7.3: Transition used to Model the Unplanned Unavailability of Maintenance Machines 209
Table 7.4: Number of Restrictions Permitted in Each of the Condition States 210
Table 7.5: Estimate of Bletchley Delivery Unit Maintenance and Renewal Expenditure (Millions). 211
Table 7.6: Possession Time Units Required for Track Maintenance Actions 217
Table 7.7: Conditions for Different Types of Renewal 219
Table 7.8: Repair Time Units for Various Sleeper Maintenance Tasks 222
Table 7.9: Time Units Required for S&C Maintenance Tasks 223
Table 7.10: Summary of Modules in the Bletchley Delivery Unit System Model 227
Table 8.1: Marking of the Expenditure Place After 100,000 Time Units Based on 20,000 Simulations 240
Table 8.2: Time to Perform Various Operations in C++ 243
Table 8.3: CPU and GPU used in this Research 248
Table 8.4: GPU v CPU [167] 253
Table 8.5: GPU v CPU for Solving Bridge Asset Management Petri Net [168] 253
Table 8.6: Summary of Models and Simulation Times 259
Table 9.1: Completion of Objectives Listed in Chapter 1 266
Table 9.2: Condition Scaling Factor, α 270
Table 9.3: Condition Scaling Factor, β 270
Table 9.4: Condition Scaling Factor, γ 271
Table 9.5: Threshold Values For Work Bank Placement, Method B 271

1 Introduction

1.1 Background

Railway networks worldwide are complex systems, containing a wide range of assets; the French railway network, managed by the Société Nationale des Chemins de fer Français (SNCF), consists of 30,000km of track, 1500 tunnels and 2,220 signal boxes [2]. The Chinese railway network comprises over 12,183km of high speed track [3], and the railway network in the United Kingdom (UK) contains 32,000 km of track and 31,000 bridges.

With global population rising and the demand for transport increasing, the strain on railway networks around the world continues to grow. Railway asset managers have to make strategic decisions on where and how the available budget will be spent, while also ensuring safety limits are maintained and performance targets are delivered. The aim of this research is to explore the feasibility of a whole system asset management framework, which can be used to assist railway asset managers in their decision making.

This research will focus on the UK as a case study, however, the methodology developed can easily be applied to other networks. One of the biggest challenges facing the UK railway network is the dramatic rise in passenger numbers. In 1994-95 there were 735.1 million passenger journeys made on the UK network, however 20 years later, in 2015-16, that number had risen to 1.65 billion [4], see Figure 1.1.

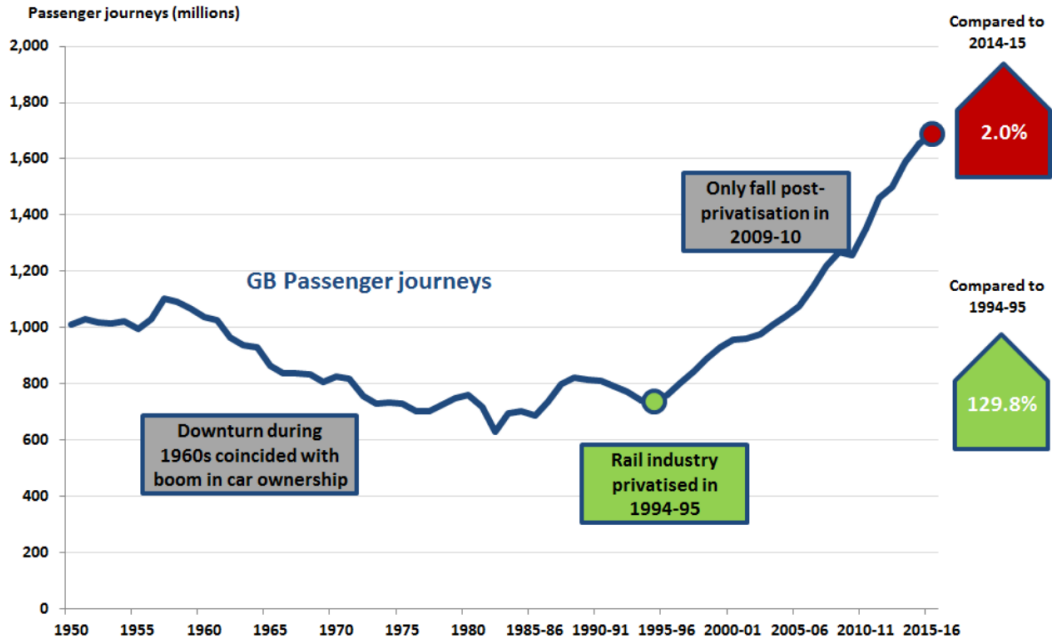


FIGURE 1.1: PASSENGER USAGE 1950→2016 [4]

However, due to the expense and legal difficultly in acquiring new land, in the UK, there has been little growth in the number of track km since the Beeching cuts [5] in the 1960s as shown in Figure 1.2. In 2016-17 just 12 km of new track were added to the UK railway network [6]. Furthermore with the exception of HS2 and Crossrail there are no large scale plans to expand the UK railway network in the coming decades.

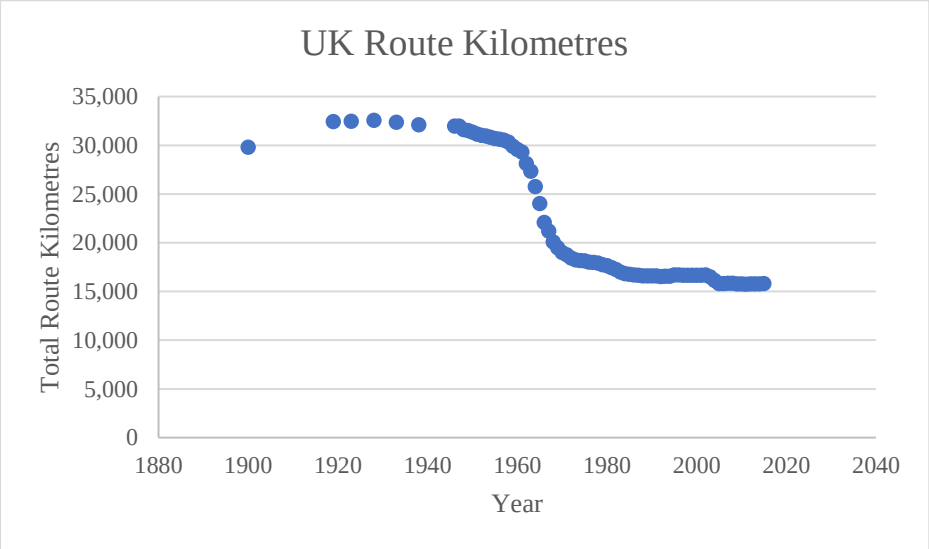


FIGURE 1.2: UK ROUTE KILOMETRES 1900 →2016 [7]

As a consequence, the UK railway needs to adapt and innovate if it is to continue to meet the growing demand on the network. The Rail Technical Strategy [8] published in 2012 identifies the 30 year vision for the UK railway, to meet the needs of the UK in the coming years and remain competitive compared to other modes of transport. The strategy states that by 2040 the railway should be '*available seven days a week and is reliable, resilient, safe and sustainable'*. The subsequent Rail Technical Strategy-Capability Delivery Plan [9] focuses on 12 ways these improvements can be achieved as shown in Figure 1.3.

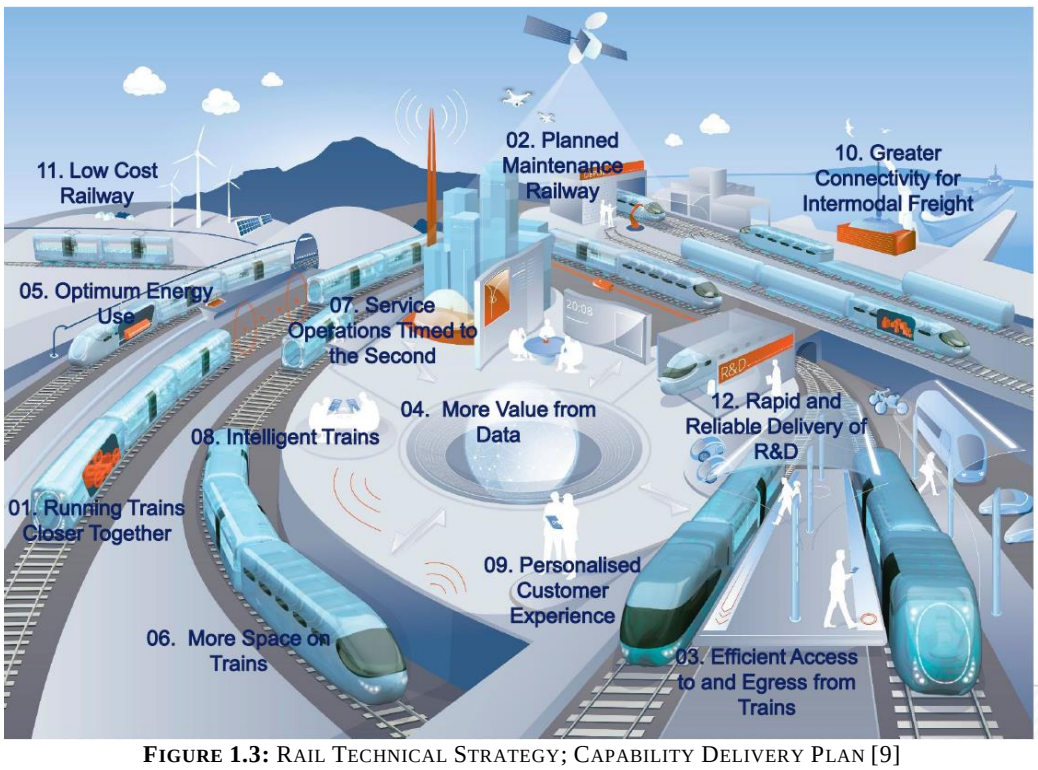


FIGURE 1.3: RAIL TECHNICAL STRATEGY; CAPABILITY DELIVERY PLAN [9]

This research will focus on point two in the delivery plan by creating a framework to aid asset managers in maintenance planning and scheduling. The delivery plan suggests that by 2040:

'The railway is 100% available during peak hours and there is no unplanned maintenance activity anywhere on the railway (infrastructure, rolling stock and associated assets). Plus, there are sufficient operational railway assets to meet predicted demand with a 99.996% confidence figure.'

Currently the UK railway network falls far short of achieving this; unplanned maintenance still forms a significant portion of the work performed. The lack of progress towards the goals of the Rail Technical Strategy are already affecting the railway, with passenger numbers dropping in 2018 by the largest amount since 1994 [10]. This highlights the urgent need for improvements on the UK railway.

1.2 Outline of the Problem

Implementing effective asset management on railway networks is difficult. Railway networks are complex systems with many interconnected assets, therefore building a model to simulate the entire railway network is difficult and the time needed to solve such a model can be prohibitive. As such, many of the models created to date have only been able to model a single asset class and often only focus on a small section of railway.

This research will attempt to build a whole system framework to model railway infrastructure, using the Petri net technique. By modelling a diverse range of assets over a large section of the railway it will allow asset managers to make more informed maintenance decisions based on the whole system condition and whole life cost, thus increasing the availability of the railway and reducing costs. The results of this research should help to streamline maintenance and address some of the issues discussed above. The model will allow various maintenance strategies and their effects on the whole system condition and whole life cost to be explored. From this suggestions about the best practise for maintenance can be attained.

1.3 Aims and Objectives

The fundamental aim of this research is to develop a whole system model for a railway network which is capable of modelling a range of railway assets for a large section of railway. The model can then be used to aid effective asset management, by predicting the future evolution of the railway. The findings will then be reported to the rail industry. These aims will be achieved through the following objectives:

(i) Gain an understanding of railway systems and current asset management strategies.
(ii) Review asset management models for assets which influence the whole system performance of a railway.
(iii) Identify the best modelling approach which will support maintenance decision making, taking a whole system, whole life prospective.
(iv) Analyse Network Rail data to determine deterioration and repair times.

(v) Develop asset state models for each asset group considered.
(vi) Establish dependencies and links between asset types relevant to the whole system model.
(vii) Link track section models together to create a whole system model for a railway corridor (100 mile section of railway).
(viii) Investigate the simulation times for such large-scale models.
(ix) Investigate the factors that might limit the size of system model that could be created such as computation time and memory use.

1.4 Research Novelty

There are two main novelties in this research:

(i) The size of the system being modelled and the diversity of assets being considered. Although various Petri net models have been proposed for asset management previously, none have been able to model a large section of the railway network (over 100 miles), and such a diverse range of assets (ballast, rails, sleepers, pads, fastenings, tunnels, switches and crossings (S&C) and the signalling system) simultaneously. By modelling many assets classes simultaneously, the model gives the most accurate prediction of whole system condition and long-term costs, allowing the maintenance regime to be streamlined in a way, which has until now, has not been possible.

(ii) The second novelty is ensuring that the Petri net model can be solved adequately with the time and computer resources available. As Petri net models increase in size the computer resources required to simulate them increases, methodologies such as heterogeneous computing, which maximise computer resources and performance, will be presented.

1.5 Outline of the Thesis

The remainder of this thesis is structured as follows:

Chapter 2: Provides a background on railways, and outline the key assets that will be modelled in this research, for each of the asset groups, deterioration modes are listed and the various maintenance options are discussed.

Chapter 3: Provides an overview of asset management and presents a number of current modelling techniques such as Markov models which are often used within asset management.

Chapter 4: Reviews literature on railway specific examples of asset management. The literature was used to determine the best framework for use in this study.

Chapter 5: Presents an analysis of Network Rail data which was used to investigate six key areas:

(i) Inspection regimes

(ii) Maintenance regimes
(iii) Maintenance scheduling times
(iv) Deterioration rates
(v) Repair rates
(vi) Effect of local environmental factors, a location index (LI) is introduced to consider this

Chapter 6: Presents Petri net models for the five asset types considered in this research:

(i) Track (ballast and rail)
(ii) Sleepers (wooden, concrete and steel)
(iii) Switches and crossings (S&C) of various sizes (A→G and fixed diamond)
(iv) Tunnels
(v) Signalling system

The models are populated based on the analysis in Chapter 5.

Chapter 7: Explains how the models in Chapter 6 were converted in to *modules* and combined together to create a hierarchical Petri net (HPN), to model a railway corridor. The system framework comprised of a three level hierarchy. The top level modelled phenomena that impact the whole railway corridor such as resources. The second level considered the track sections and the third level considered the assets within the track section. The system model was demonstrated on the Bletchley Delivery Unit, a 100 mile long railway corridor in England. The model for the Bletchley Delivery Unit contained 1783 sub modules; one master module, 849 track section modules, 705 concrete sleeper modules, 53 timber sleeper modules, 91 steel sleeper modules, 61 S&C modules, 21 tunnel modules and one module for the signalling system.

Chapter 8: Is split into two parts. Part one looks at how the code was validated and part two, explores techniques that can be used to solve large Petri nets, three main areas were explored:

(i) Developing Petri net solution algorithms to produce an acceptable simulation time.
(ii) Exploring the effectiveness of using parallel processing and heterogeneous computing (combined simulation on central processing unit (CPU) and graphics processing unit (GPU)) to deliver acceptable simulation times.
(iii) Ensuring that the memory required to solve large scale models is commonly available to engineers.

Chapter 9: Summarises the work, presents the key findings and conclusions and details how the research can progress in the future.

2 Background

2.1 Introduction

This chapter will provide a background on railway systems, it introduces the terminology that will be used and the assets that will be considered. The chapter begins by introducing key railway terminology. Section 2.3 introduces the assets that will be studied; for each asset the following information will be provided:

(i) Asset description
(ii) How the asset degrades and it's failure mechanisms
(iii) How the asset is inspected
(iv) How the asset can be maintained

The chapter concludes with a tabular summary of each of the assets for easy reference.

2.2 Terminology

Throughout this thesis a range of railway terminology will be used:

(i) Delivery Unit
The UK network is broken down into Delivery Units. Each Delivery Unit is managed by an Infrastructure Maintenance Delivery Manager (IMDM) and contains local works teams which are responsible for maintenance within the Delivery Unit. Delivery Units are typically about 100 miles in length. In this study Bletchley Delivery Unit, a railway corridor in England, will be used as a case study, a detailed description of Bletchley Delivery Unit is given in Chapter 7.

(ii) Eighth Mile (220 yard) Track Section
Network Rail measure the alignment of the track over eighth mile lengths called Poskeys. It is therefore consistent to measure track assets in eighth mile lengths.

(iii) Engineer's Line Reference (ELR)
Engineer's Line References or simply ELRs are used to describe routes within the UK. Each ELR has a given start and end yard. Therefore, given an ELR and yardage, it is possible to calculate the exact position of an asset on the network.

(iv) Plain Line Track
Plain line track refers to track that does not contain any S&C units.

(v) Railway Corridor
For the purpose of this study, a railway corridor is defined as a length of railway which links or forms part of the link between two key areas.

(vi) Temporary Speed Restrictions (TSRs) and Line Closures
Safety is critical on the railway network. Therefore if the condition of assets is found to be 'too' degraded, then a TSR may be put in place to ensure that it is still safe to run trains. The level of speed restriction will depend on the severity of the defect, a more serious defect will require a more major speed restriction. In some cases, for example if a rail fracture occurs, it will not be safe to run trains, and the line will be blocked/closed. TSRs and line closures cause delays

to trains and for this Network Rail have to pay compensation to the train operating companies (TOCs); these costs are known as schedule 4 and schedule 8 costs. Schedule 4 costs compensate train operators for the impact of planned service disruption [11], and schedule 8 costs compensates train operators for the impact of unplanned service disruption [11].

(vii) Office of Rail and Road (ORR)

The ORR are an independent regulator for the railways and roads in the UK, who operate within frameworks set by UK and EU legislation and are accountable through Parliament and the courts [12].

(viii) Control Period (CP)

Network Rail operates in five year funding timeframes called Control Periods (CP). Network Rail is currently in CP6 (April 2019 →April 2024).

(ix) Tier Models

For lifecycle costing (LCC) purposes, Network Rail currently model assets according to a three level system, called the Tier system. Tier 1 models, are portfolio level models and forecast the volume of work, outputs and expenditure required for a portfolio of assets. Tier 2 models are used to calculate the whole life cost for a particular asset type. Finally, Tier 3 are used to model the whole life cost of a particular asset type on a particular route.

(x) Track Category

Network Rail divides the UK network into seven track categories. The category is determined based on both speed and tonnage as shown in Figure 2.1. Category 1A classification is given to the highest speed, most heavily trafficked lines, such as the West Coast Mainline (WCML), whereas Category 6 classification generally describes sidings or goods yards with very low line speed and tonnage. Table 2.1 shows a breakdown of the UK network by track category.

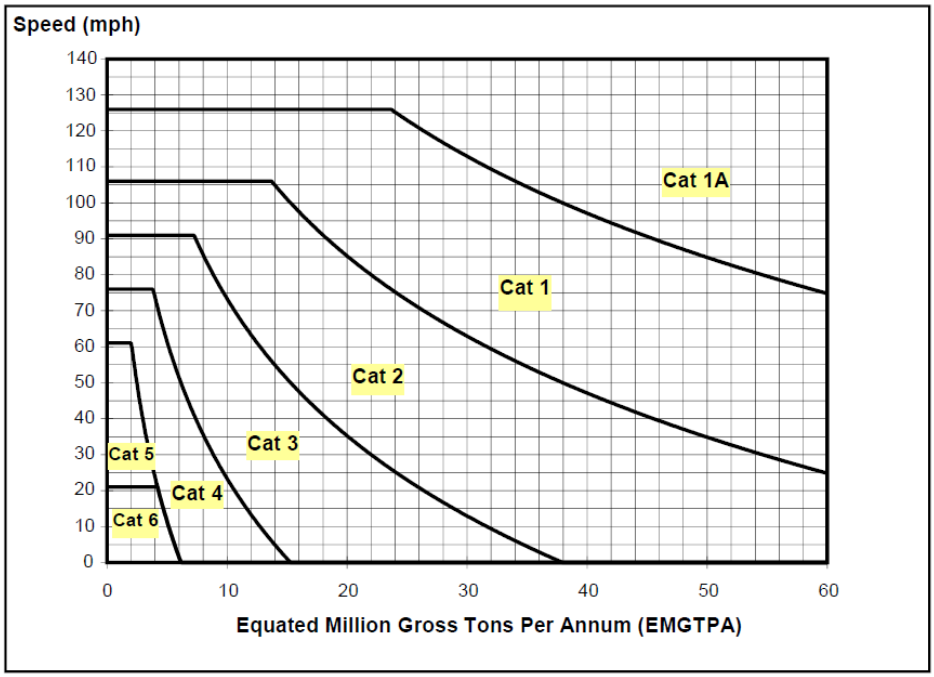


FIGURE 2.1: NETWORK RAIL TRACK CATEGORIES BASED ON TONNAGE AND LINE SPEED

Category	Length (Miles)	Percentage of the Network
1A	780	4%
1	2578	13%
2	3493	18%
3	4302	22%
4	3790	20%
5	3460	18%
6	989	5%

TABLE 2.1: TRACK CATEGORY SUMMARY

2.3 Railway Assets

There are two main types of track construction; ballasted track and slab track (See section 2.3.3). Ballasted track or *'classical track'* is the most common form of track in the UK forming over 99% of the network and is the focus of this study. It is made of three key components; rails, sleepers and ballast. The rails and sleepers make up a flat framework which is supported by the ballast [13].

Figure 2.2 shows a typical ballasted railway track in the UK. The following sections explain the assets in more detail.

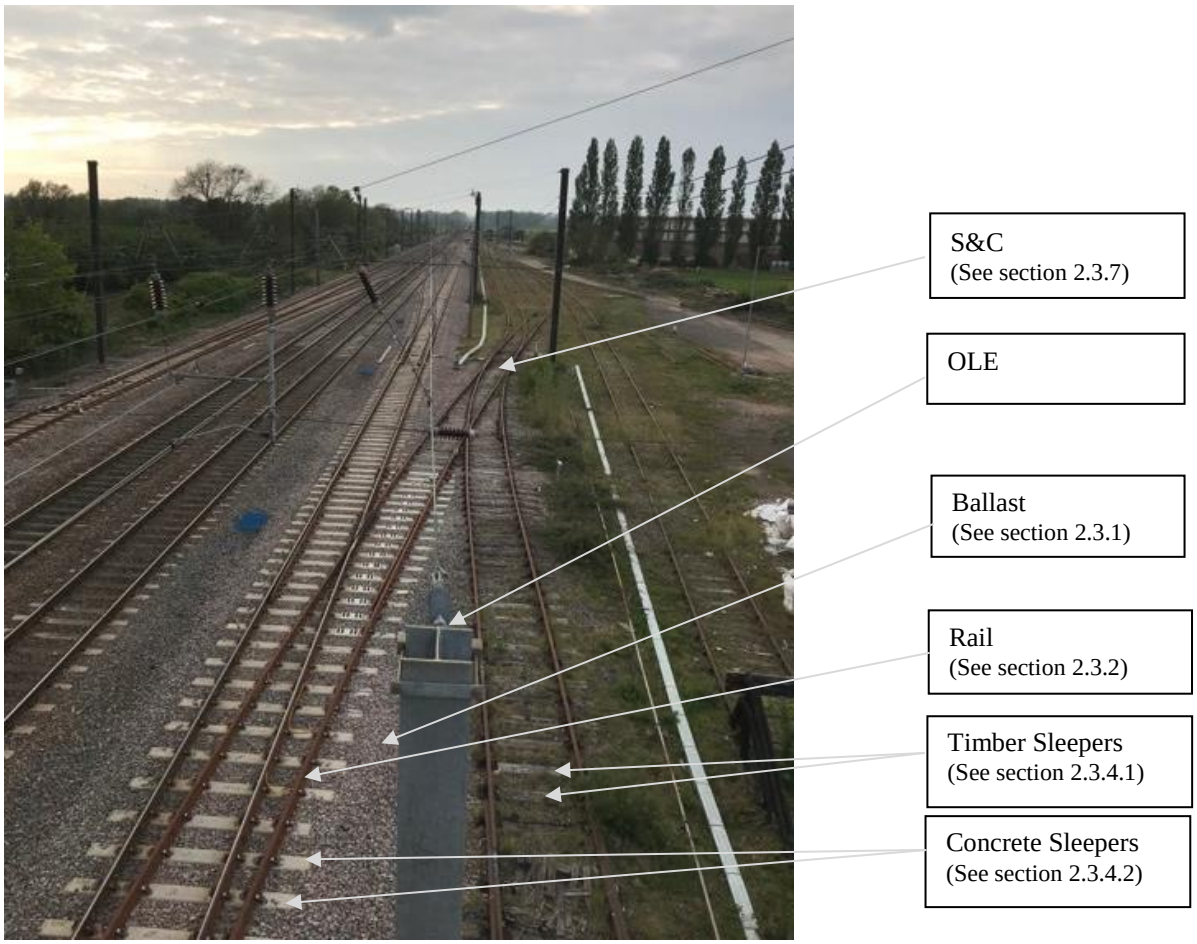


FIGURE 2.2: ELECTRIFIED BALLASTED RAILWAY (TAKEN FROM TALLINGTON LEVEL CROSSING ON THE EAST COAST MAINLINE, UK)

2.3.1 Ballast

Ballast is the crushed granular material placed as the top layer of the substructure in which the sleepers are embedded [14]. It is composed of medium to coarse gravel-sized aggregates (10–60 mm), with a small percentage of cobble-sized particles [15]. The optimum thickness is 250-300 mm [13]. Some of the main properties of the ballast as described in Selig and Waters [14] are:

(i) Resist vertical, lateral and longitudinal forces applied to the sleepers.
(ii) Provide some of the resiliency and energy absorption for the track.
(iii) Provide large voids for the storage of fouling material in the ballast and the movement of particles through the ballast.
(iv) Provide immediate drainage for water falling onto the track.
(v) Reduce pressure from the sleeper bearing area to acceptable stress levels for the underlying material.

2.3.1.1 Degradation and Failure Mechanisms

As the train passes along the rails forces are transmitted to the ballast from the sleepers. This causes the ballast to undergo elastic and plastic deformation. Gradually the plastic deformation causes the ballast to settle and the rails to move from their correct alignment.

During loading, parts of the ballast may break and produce fines or fouling material. Over time fines/fouling material can fill the voids in the ballast preventing water drainage [16]. This can lead to water-logged ballast causing wet beds (see Figure 2.3) and mud/silt pumping can occur. Over time the track overlying the wet bed settles disproportionately more, sleepers become progressively more voided, and train ride quality deteriorates [17]. Another way in which the ballast can degrade is shoulder slip and loss of profile.

The alignment of track and hence the ballast quality can be assessed according to five parameters:

(i) Vertical Geometry Standard Deviation (Top)

The New Measurement Train (NMT) passes over the track measuring the vertical alignment, the standard deviation (SD) of the values over 220 yard sections is then calculated, the higher the SD the greater the variation in vertical alignment and hence the worse the ride. It is recorded over 35m (short) and 70m (long) wavelength.

(ii) Lateral Geometry Standard Deviation (Alignment)

This is also recorded over 35m (short) and 70m (long) wavelength and records the variation in horizontal track geometry.

(iii) Gauge

The gauge is the distance between the left and right rails, if the gauge is not maintained then there is a high risk of derailment, such as that which occurred at Paddington Station [18].

(iv) Cyclic Top

Cyclic top is a series of dips or vertical irregularities in one or both rails. These dips cause wagons to experience a bouncing motion, which is particularly severe in certain types of freight wagons which have susceptible suspension [19]. Serious cases of cyclic top can cause derailments [20].

(v) Twist

Twist refers to the difference in rail height between the right and left rail.

It is generally the vertical geometry (short-wave) measurements which are the most significant when deciding the condition of the track and the requirement for maintenance, although they all have acceptable tolerances [21].

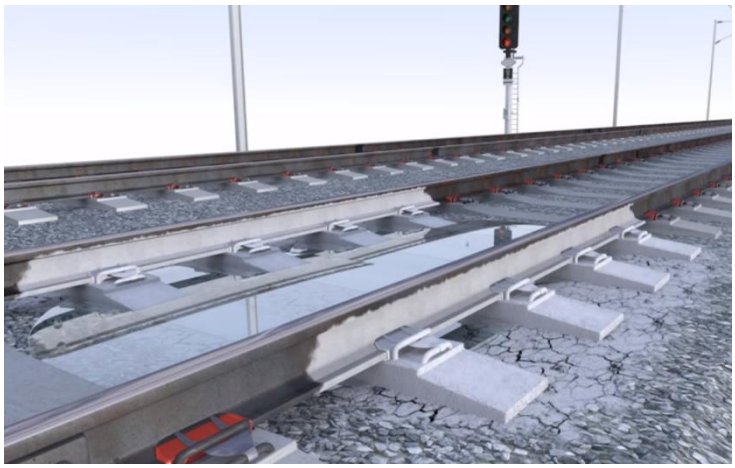


FIGURE 2.3: WET BED [22]

2.3.1.2 Inspection

A periodic inspection plan is put in place for all track assets [23]. The ballast can be inspected in two main ways, visually or using the NMT (Figure 2.4). Measurement of track geometry (top, alignment, gauge, cyclic top and twist) will be undertaken on all passenger running lines, goods running lines, carriage lines and loops, including all crossovers and turnouts [24]. Measurements are taken on a periodic basis with the minimum frequency between geometry inspections determined by the track category [24]. If serious defects are found during an inspection then a line closure or TSR can be put in place. Once a defect has been identified more regular inspections can take place.

Using the alignment data collected by the NMT, Network Rail place the track in one of five quality bands; '*Good'*, '*Satisfactory*', '*Poor*', '*Very poor'*, '*Super red*'. These quality bands are dependent on the line speed, and are used to determine the priority at which improvement work is completed.



FIGURE 2.4: NEW MEASUREMENT TRAIN (NMT) AT DERBY STATION

2.3.1.3 Maintenance Options

In the case of ballasted railway track, the cost of substructure maintenance can be significantly reduced if a better understanding is obtained of the physical and mechanical characteristics of the rail substructure and of the ballast layer in particular [15]. There are a number of different maintenance options available to improve the ballast condition and restore the track alignment. In general it is relatively easy to correct the alignment by adjusting the ballast. It is more difficult to remove fouled ballast and fines. There are four main methods to improve the alignment:

Tamping

A typical tamping machine is self-propelled and, by means of lifting and lining rollers that grip the head of the rail, is able to move the track to a pre-determined 'correct' position. The tamping process is as follows and is outlined in Figure 2.5:

- Identify that the track alignment needs correcting (This is usually done with the NMT).
- Position the tamping machine above the sleeper(s) that need to be tamped, (A).
- Raise the sleeper(s) to the correct position using the lifting rollers; this will create a void under the sleeper(s), (B).
- Insert tines into the ballast on either side of the sleeper(s), (C).
- Tines vibrate/squeeze the ballast into the void around the sleeper(s), (D).
- The tines and rollers are removed and the tamping machine moves on to the next sleeper(s), (E).

It is common practise to tamp a large section of track at a time rather than just a few individual sleepers, particularly for higher track categories. However there are several disadvantages of tamping. Firstly, the insertion of the tines and the squeezing of ballast leads to ballast breakdown and accelerates ballast fouling. For this reason there is only a limited number of tamps possible before some sort of ballast replacement will be needed, it also makes it critical not to over tamp, as tamping a section too often will lead to accelerated ballast degradation and shorten the ballast lifetime. Secondly, the tamping machine can damage the sleepers, this is particularly likely when inserting tines. Thirdly, tamping

machines are difficult to use at S&C, as the tines cannot be inserted. There are specialist tamping machines for S&C but these specialist S&C tampers are in short supply. Nonetheless tamping is the most common type of ballast maintenance performed on the UK railway network.

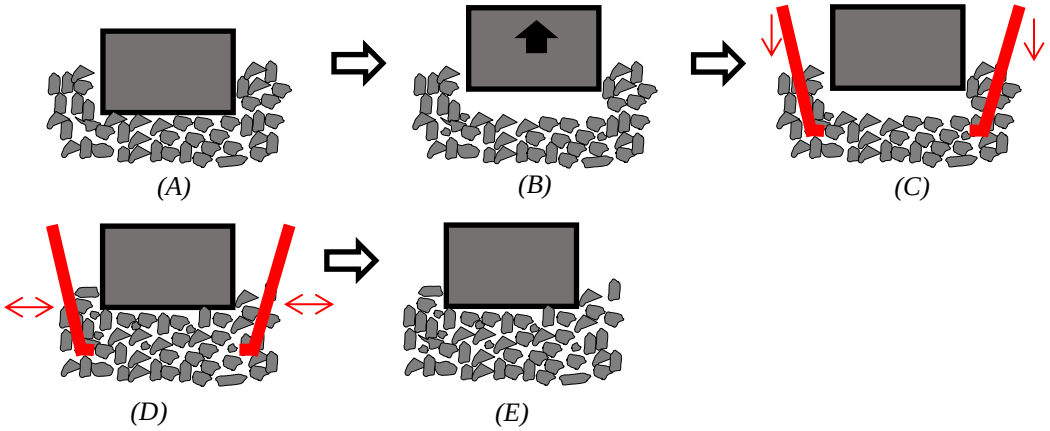


FIGURE 2.5: THE TAMPING PROCESS

Stoneblowing

Another option to improve the alignment is stoneblowing. The stoneblowing process is as follows and is shown in Figure 2.6.

- The geometry of the track is measured, (A).
  From this the exact track lift required at each sleeper (to unify the track level and reduce the SD) is calculated and the volume of stones needed to fill each void is subsequently determined.
- The sleeper is then lifted above the correct alignment leaving a void under the sleeper, (B).
- A tube is then inserted into the void and stone is blown into the gap until the correct amount of stone is blown in as calculated in step A, (C).
- The tube is then removed, (D).
- The sleeper is lowered onto the new ballast, (E).

Network Rail have 11 plain line stoneblowers. Stoneblowing tends to give a more durable result than using a tamper, and so can extend the life of the track by many years, saving the railway significant amounts of money [25]. However, stoneblowing cannot deliver the high quality alignment provided by tamping, therefore stoneblowing is not used as much on high category lines.

Network Rail also have three specialist multipurpose stoneblowers that can be used on S&C units as well as on plain line track. They are the only multipurpose stoneblowers in the world. They have been so successful at extending the life of older S&C units that Network Rail are looking at buying more to replace the old and life-expired plain line stoneblower machines [25].

A disadvantage of stoneblowing is that, the stones blown under the sleeper are fines (much smaller than regular ballast) and subsequently once a section has been stoneblown it should not be tamped.

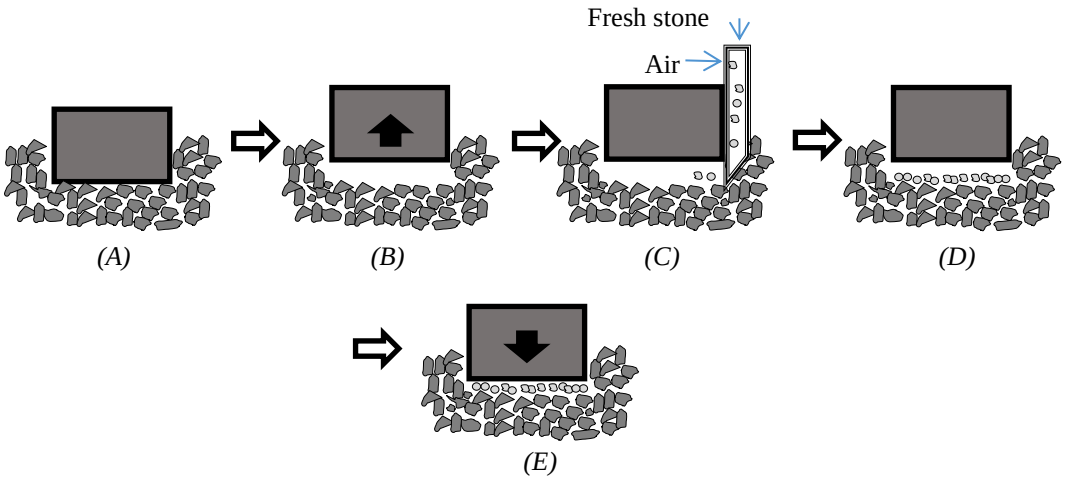


FIGURE 2.6: THE STONEBLOWING PROCESS

Ballast Re-Profiling

The ballast profile is vital to ensure that the sleepers are supported correctly and the track is drained adequately. There should be sufficient shoulder to support the sleepers and the profile should be inclined towards the drainage trench to ensure water is drained effectively (Figure 2.7). Over time plastic deformation of the ballast causes the profile to change, the shoulders in particular can be affected with ballast sliding away. Ballast re-profiling restores the ballast profile through ballast redistribution and by adding clean ballast. In the UK the ballast profile is usually assessed manually by a track inspector. A sweeper unit is then used to collect the surplus ballast and ballast is dropped in areas of deficit. However as this process is based on visual inspections it has several shortcomings such as no measurement is made of the exact position or precise quantity of ballast required to re-establish the correct ballast profile. To address this issue it is possible to measure the ballast profile more accurately using a laser profiling device. When the laser pulse hits the ballast profile, it is reflected and the distance is measured. The contour of the ballast profile is computed from a sequence of pulses received from the measuring device. The actual ballast profile is plotted and then the correct ballast profile is superimposed. From this the areas of deficit and surplus ballast can be precisely identified. An example output from a laser profiling device is shown in Figure 2.8. The red areas have surplus ballast and the green areas have a ballast deficit.

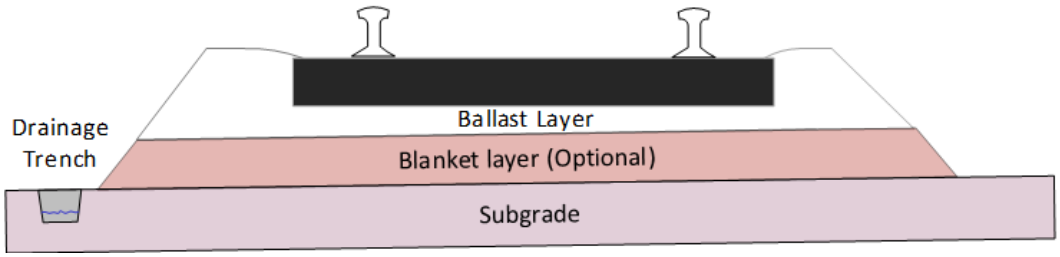


FIGURE 2.7: TRACK PROFILE

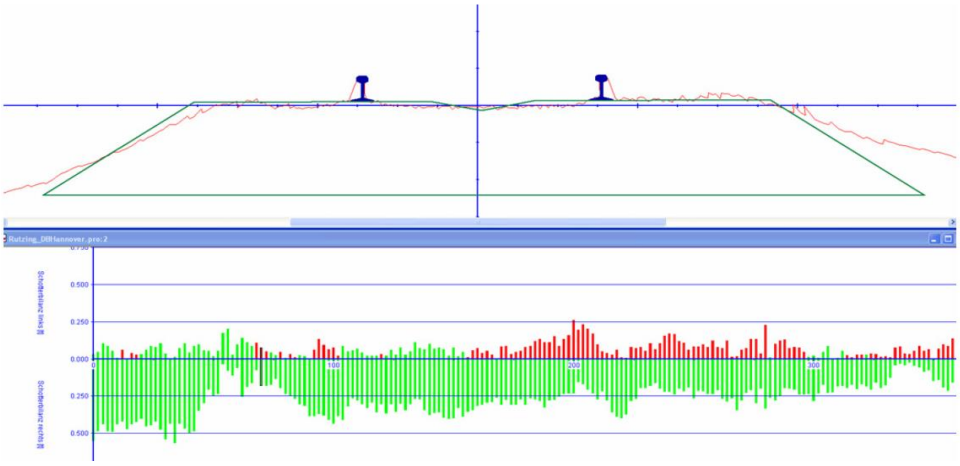


FIGURE 2.8: THE BALLAST RE-PROFILING PROCESS [26]

Manual Interventions

It is also possible to carry out interventions manually, with handheld tools. Manual interventions are normally carried out when urgent maintenance is needed and a tamper or stoneblower is not available. Manual interventions will usually be less effective than tamping or stoneblowing, as such, following a manual intervention the ballast condition is likely to degrade more rapidly.

Removing fines and fouled ballast is difficult. There are two main options to remove fines; clean the ballast or renew the ballast. However ballast cleaning and ballast renewal are costly and time consuming operations which can be disruptive to traffic [14]. The impact on traffic can be reduced by performing work at night, however this is more expensive and it is not always possible to complete larger work volumes in a single night possession. Therefore longer periods of closure are needed; major works are often scheduled during holiday periods such as Christmas or Easter.

Ballast Cleaning

Ballast cleaning is carried out using a specialist machine. The machine digs away ballast up to a minimum depth of 250 mm below the sleeper [13]. The removed ballast is sieved and material smaller than 35 mm is filtered out. The cleaned material is then replaced with new ballast to make up the deficiency. Figure 2.9 shows a drawing of a ballast cleaner, the dark grey ballast is the fouled ballast which is removed and the light grey ballast is the cleaned ballast that is replaced.



FIGURE 2.9: BALLAST CLEANER [13]

Ballast Renewal

Ballast renewal removes the entire ballast layer and replaces it with new ballast. Ballast renewal should return the ballast and track geometry to a very good condition. During a ballast renewal the rails and sleepers are often also renewed. Renewals are generally carried out by a High Output Machine (HOM), in the UK around 70% of renewals are performed by a HOM [27].

Figure 2.10 shows an example of how the vertical alignment changes over time as the track section is subject to loading cycles. At time zero the track has just been renewed and hence the vertical alignment, σ, is good $\sigma<\sigma_{crit}$. The SD of the vertical alignment increases with time. At time $t=\theta$ the inspection train passes, but since $\sigma<\sigma_{crit}$ no action is taken. At time $t=2\theta$ the inspection train passes again the value of σ is now such that $\sigma>\sigma_{crit}$ and maintenance is requested. At time $t= 2\theta+T_1$ the maintenance is complete and the SD is reduced to some improved value; where T_1 is the time to schedule and complete maintenance. Following maintenance the ballast starts to deteriorate once again. At time $t=3\theta$ the maintenance train passes again, this time the track has degraded faster and the SD has already reached σ_{speed} and a temporary speed limit has to be imposed until improvement work is completed. At time $t= 3\theta+T_2$ maintenance is complete and the SD is improved once again.

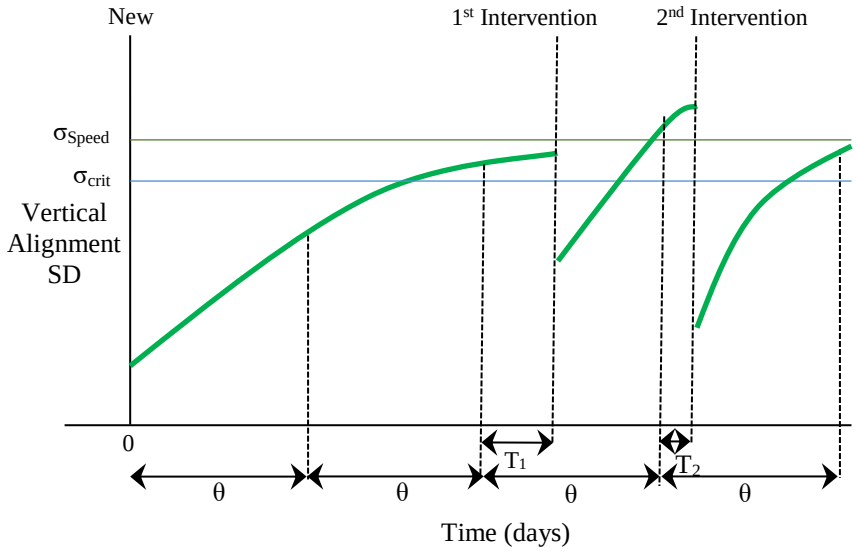


FIGURE 2.10: EVOLUTION OF BALLAST VERTICAL ALIGNMENT (SD) WITH TIME

2.3.2 Rails

Rails are the longitudinal steel members that directly guide the train wheels [14] and are the most important part of the track structure [13]. The rails are attached to the sleepers (or slab track) using fastening systems (section 2.3.6). The rails' primary function is to guide the train wheels, spread the loads onto the sleepers and maintain the gauge (the separation between the rails). They can also act as conductors for use within the signalling system (section 2.3.9). The rail can be split into three main sections; head, web and foot. The head is the top part of the rail on which the wheels run, the foot is the bottom part of the rail that sits on the sleepers/slab track and the web is the narrow section that connects the two. There are a wide range of rail profiles used on railway networks [28] but all have these three distinct parts. Most of the rail in the UK is flat-bottom rail, which as a very wide foot. Some older parts of the network use Bullhead Rail; Bullhead Rail has a much narrower but deeper foot. Table 2.2 gives a breakdown of the main rail types used on the UK network.

Rails can be either bolted together (with fishplates) (see Figure 2.11) or welded together to form continuous welded rail (CWR) [14]. As the rail is made of steel the rail must be able to expand and contract, in the UK temperatures can go below freezing in winter and the rail surface temperature can exceed 50 ^{o}C in summer. For jointed rail expansion gaps are left between sections. For CWR, when sections are joined the rail temperature is set at 27 ^{0}C before welding. Nonetheless the rail can still crack or buckle during extreme temperatures.



FIGURE 2.11: JOINTED RAIL WITH A FISHPLATE. THE RAIL IS IN TENSION SO THERE IS A GAP BETWEEN THE RAILS

Rail Type	Mass/unit Length (kg/m)	Percentage of the Network	Comment
Bullhead Rail	42 or 47	7%	This type of rail is the lightest type of rail and the foot is much narrower and deeper than flat-bottom rail. This type of rail is not widely used on the network, only around 7% of the UK network is Bullhead Rail. It is mainly used on tight curves and lightly trafficked lines such as branch lines.
Pre1976 Flat-bottom Rail	54.5 or 56	84%	Flat-bottom rail has a very wide and thin foot. This is designed to spread the load onto the sleepers more effectively and increase rail life. This sort of rail forms the majority of the network.
Post 1976 Flat-bottom Rail	56		
CEN-60 Flat-bottom Rail	60	8%	This is the highest quality rail that Network Rail currently uses. It has a wider foot, larger head and deeper web then other Flat-bottom rail types making it stiffer and stronger. It is used on heavily trafficked lines

TABLE 2.2: RAIL TYPES IN THE UK

2.3.2.1 Degradation and Failure Mechanisms

The rail is subject to transverse and longitudinal forces. These forces are influenced by a range of factors. Clearly the fundamental transverse force is the train weight; the heavier the train the faster the rail will degrade. The number of loadings also influences the degradation rate and service life. The other big factor that influences the transverse force on the rails is the curvature of the track. As the train travels around a curve with radius of curvature R a centrifugal force F_c acts on the train. F_c is influenced by the train's mass and velocity as described in equation (2.1).

$$F_C = M_t \frac{V^2}{R}. \tag{2.1}$$

When there is a centrifugal force acting on the train the resultant force no longer acts through the centre of the train, this means the force is no longer distributed evenly between the two rails. To reduce the effect of this the track can be canted. Cant is achieved by raising the height of one of the rails so the track is sloped, this helps bring the resultant force back through the centre of the track. Note however that the resultant force when cornering is greater than the weight alone hence, even if the track has the perfect cant the rails will wear faster than if the track was straight. The difference between the cant and equilibrium cant is called *cant deficiency*. In areas with high cant deficiency one of the rails will have a higher degradation rate than the other.

The rail is also subject to longitudinal forces including:

(i) Rail creep/plastic deformation: over time the rail naturally changes shape due to the forces applied to it.

(ii) Temperature forces: Steel naturally expands and contracts as its temperature changes. As the temperature drops tensile stress grows in the rail and in extreme cold weather the rail can crack. Conversely as the temperature rises the rail will enter compression and in extreme heat the rail can buckle. To minimise the risk of this, certain maintenance actions, which put extra stress on the rail, such as tamping, are not performed during extremely hot or cold weather.

(iii) Joint forces: In jointed track (Figure 2.11) there are additional forces as the train wheel passes over the gap in the rail, the wheel passing over the gap is what causes the traditional 'clickety clack' sound of a train.

As time passes, these transverse and longitudinal forces can cause defects to develop in the rail, which, if not treated, can eventually cause the rail to fail. These defects include (but are not limited to):

Rolling Contact Fatigue (RCF)

Rolling contact fatigue (RCF) is a generic term that is used to describe a range of cracks that are caused by high shear stresses at the wheel/rail contact interface. RCF defects commonly occur in the gauge corner region of the rails. The gauge corner region is the top of the rail head on the side closest to the centre of the track. There are three main types of RCF defect:

(i) Gauge corner cracking

For the reasons discussed previously these normally occur on the high rail of tight curves, they are cracks in the rail that normally occur at about 2-5 mm intervals along the rail. They can grow to 2-5 mm in depth at an angle of about 10^{o}-30^{o} to the rail surface, and look like 'fish scales' [29].

(ii) Shelling

These are cracks which develop within the rail and are initially seen as dark spots on the rail surface. They are most common in the upper rail of corners. As they develop they can lead to sections of the rail breaking away, see Figure 2.12.

(iii) Flaking

This can occur in the upper and lower rails at corners. They are initially small cracks but can grow to 10-15 mm and cause part of the rail to flake away.

RCF defects are caused by high stresses in the rail/wheel contact region. Poor track geometry and tight corners are key reasons for high stress. The wheel radius can also affect RCF defects as smaller wheels have a smaller contact area leading to higher contact forces. RCF defects can eventually lead to rail breaks/failures if they are not dealt with. They can also interfere with ultrasonic signals during inspections, which can lead to more serious internal rail faults not being detected. There are a number of ways that RCF defects can be reduced including:

(i) Higher strength rail steel
(ii) Better quality rail steel
(iii) Better lubrication of the wheels/rails

They can also be removed through rail maintenance such as grinding. However some actions that could initially seem like a solution can actually increase RCF defects. For example, the top 8-10 mm of the rail can undergo plastic deformation, when subject to heavy and repeated loadings, leading to a 'work hardened layer' on the top of the rail. This layer exhibits a high compression residual stress making it difficult for surface defects such as flaking or gauge corner cracking to develop. However stronger grades of rail such as CEN 60 are much less likely to develop a 'work hardened layer' so may be less resistant to flaking or gauge corner cracking. Similarly it may be considered that reducing wear on the rail would improve the situation. However wear can actually remove many RCF defects so it is desirable to find an optimum amount of wear such that the rail/wheel life is not overly shortened but RCF is reduced, this is known as the 'magic' wear rate.



FIGURE 2.12: EXTREME RAIL SHELLING [29]

Squats

Squats are subsurface lamination defects which initiate at small cracks [29]. The cracks initially propagate at a shallow angle to the rail surface, once the cracks have reached 3-5 mm below the surface they grow horizontally and if not treated will spread throughout the rail, as shown diagrammatically in Figure 2.13.

There are two main classifications of squats:

(i) Running surface squats

These are thought to develop from cracks caused by minor wheel slips.

(ii) Gauge corner squats

These develop from pre-existing cracks in the rail normally caused by RCF defects.

Squats cause dips in the running surface which can be observed as dark areas as they will not be polished as highly as other parts of the rail. Squats can increase the contact force on the rail as less of the rail will be in contact with the train wheel. Once squats have occurred they can be removed by:

(i) Head repair welding; using the wire feed process, however this process is expensive.

(ii) Grinding; but due to the depth of squats the rail will require extensive grinding, significantly reducing rail life.

(iii) Re-railing, this is very expensive and can be disruptive to traffic.

The list shows that each of the removal methods has difficulties so instead the focus is on prevention. There are a number of ways of doing this including; reducing RCF through the methods discussed above and by reducing wheel slips.

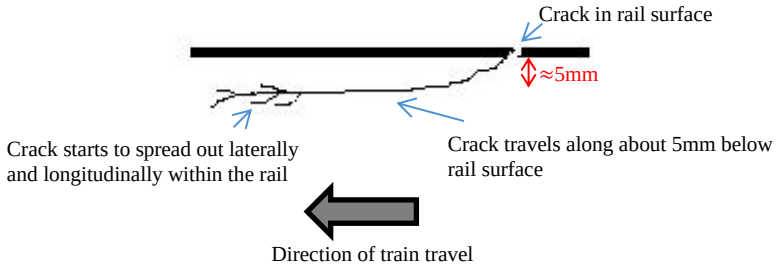


FIGURE 2.13: SQUAT DEVELOPMENT

Tache Ovales

Tache ovales are cracks around 10-15 mm below the rail surface in the rail head. They are mainly caused by hydrogen accumulations in the manufacturing process. However, improvements in the manufacturing process in 1976 made this sort of defect far less common. Tache ovales are the main reason why pre and post 1976 rail is considered separately. There are few rails left on the network that are more than 40 years old so the number of Tache ovales defects has significantly reduced.

Rail Corrugations

Rail corrugations are cyclic (wave like), generally vertical, irregularities on the running surface of the rails [29]. There are two main types of corrugation: short pitch corrugations and long pitch corrugations [30]. Short pitch corrugations have a wavelength of 30 mm to 90mm and the depth of these corrugations is normally less than 0.3 mm, see Figure 2.14. They tend to develop under light axle loads (less than 20 tonnes). Short pitch corrugations are thought to form from differential wear due to repetitious longitudinal wheel sliding [29]. Long pitch corrugations have a wavelength greater than 300 mm and the depth of these corrugations is normally between 0.1 mm and 2 mm, see Figure 2.14. They tend to develop under heavy axle loads (greater than 20 tonnes). Long pitch corrugations develop because of the plastic flow of the steel in the rail. This is usually caused by excessive contact stresses and the combined vertical resonance of the wheelset un-sprung mass and the track [29]. Any factors that increase the dynamic forces on the rail will increase the risk of long pitch corrugations. However, there is still some uncertainty as to why different rails suffer from different pitch corrugations. Although corrugations themselves do not pose a high risk of rail failure, they can increase noise, lead to the generation of squats and increase dynamic forces on track leading to accelerated deterioration of the rails as well as the sleepers and ballast. One of the most common ways to tackle rail corrugations is by reducing the causes; these include using higher strength steel (CEN 60) and improving wheel rail profiles. Corrugations can be removed by rail grinding.

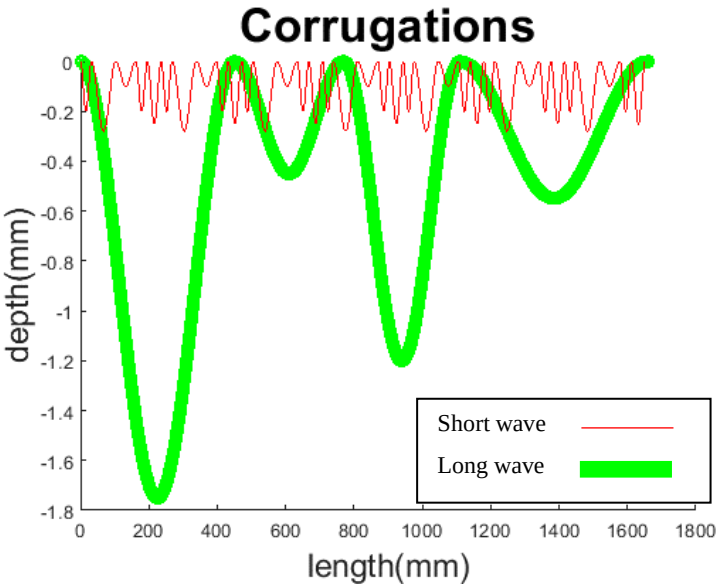


FIGURE 2.14: SHORT AND LONG PITCH CORRUGATIONS

Wheel Burns

Wheel burns are very similar in appearance to squats. However they form very differently and unlike squats, which form slowly, wheel burns form instantaneously. They are caused by the train wheel slipping on the rail for a large amount of time. The wheel slipping causes the rail to become very hot and the subsequent rapid cooling (due to the properties of steel) causes the top of the rail to become brittle. In serious cases a large portion of the rail head can become brittle and leads to rapid deterioration and a potential rail break. Wheel slipping and hence wheel burns can be caused by violent acceleration or braking and ineffective rail lubrication. They are particularly common on inclines and in autumn when there is a high concentration of leaves on the line. Figure 2.15 shows an extreme example of wheel burn, likely caused when a train lost traction when starting to move.



FIGURE 2.15: EXTREME WHEEL BURN

2.3.2.2 Inspection

Rails are inspected visually and using ultrasonic inspections. According to Network Rail standards [32]; 'All rails in running lines, through sidings and sidings separated from running lines by 10 ft (3050 mm) or less shall be ultrasonically tested as part of a cyclical programme of rail examinations'. The frequency of inspection depends on the inspection type and the track category. If serious rail defects are discovered during an inspection then a TSR or line closure is imposed. In areas where minor defects are known to be present the frequency of inspection is increased.

2.3.2.3 Maintenance Options

The previous section described the various defects and failure modes the rail could suffer from. For each failure mode listed in section 2.3.2.1, the maintenance options considered in the model development are given in Table 2.3. Note however in this research no distinction is made between the different types of weld repair, they are all grouped under the term 'weld repair'. Rail grinding can only be performed on the top 5 mm of the rail, therefore it can only remove defects that are in this region of the rail. Defects that are greater in depth than 5 mm (or are not located in the running surface) have to be removed using a weld repair. If a serious defect occurs then it is likely that a section of rail will be removed and replaced (partial re-rail).

Type of Maintenance		Description
1. Weld	Flux-cored arc welding	A section of rail is replaced using the arc weld process [31].
	Shielded metal arc welding	A section of rail is repaired using shielded metal arc welding [31].
	Thermit L80 weld	Head harden rail has a much higher hardness in the rail head then the web and foot. Hence when performing a weld on the complete rail the weld should also have a higher hardness in the rail head if the best result is to be achieved. In Thermit L80 weld molten steel flows in from the bottom (rail foot). In the rail head an alloy is introduced the molten steel mixes with the alloy in the rail head **only.** This gives the weld in the rail head a higher hardness than the rest of the weld.
	Aluminothermic rail head repair	This type of weld is used on the rail head, a section of the head is removed and repaired.
2. Grinding		Plain line grinding is performed by a grinding machine. The top of the rail is ground away to leave a smooth defect free running surface. Grinding will only remove defects in the top 5mm of the rail head.
3. Partial Re-rail		A section of rail is replaced.
4.Full Re-rail	Complete renewal	All of the rail is replaced.
	Complete track section renewal	The rail, sleepers and ballast are all removed and renewed.

TABLE 2.3: RAIL MAINTENANCE OPTIONS

2.3.3 Slab Track

An alternative railway construction method is slab track. Slab track removes the need for sleepers and ballast and instead the rail is fastened directly to a concrete base, see Figure 2.16. The main advantages of slab track are: elimination of ballast maintenance and fewer traffic interruptions, high track fixity increasing safety against track buckling and reduction of construction depth (allowing more clearance at structures). Some of the disadvantages are; it needs a strong and stable foundation to minimise the risk of settlement, construction time is considerably greater than ballasted track, and the initial construction cost is considerably higher than ballasted track. There are numerous different designs of slab track and extensive research into their properties [33], [34]. However none have proved popular in the UK, in 2015 just 0.2% of the UK railway network was slab track construction, and it was almost exclusively used to create greater clearance. As slab track forms such a small part of the network it is not considered in this research.

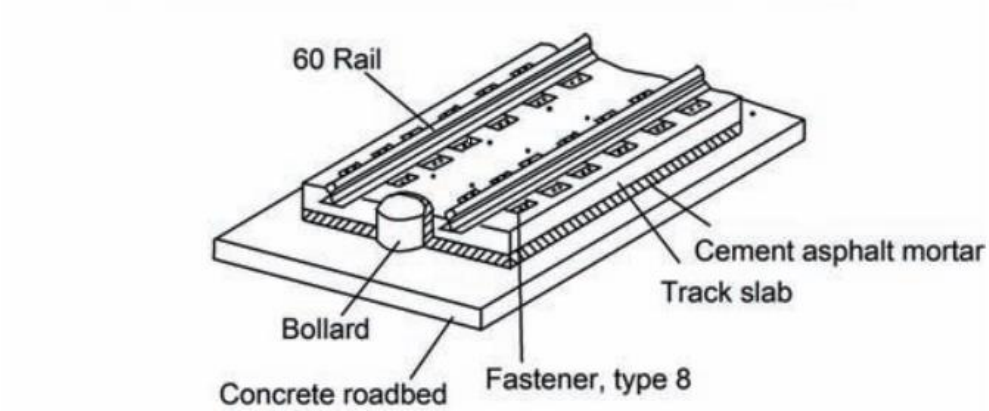


FIGURE 2.16: SLAB TRACK [33]

2.3.4 Sleepers

The sleepers (or bearers (S&C)) are positioned in the ballast. The main requirement of sleepers is the transmission of vertical, lateral and longitudinal loads from the rails to the ballast or other supports [35]. The sleepers also support the rails at the correct alignment and gauge. A bearer is a custom made sleeper used in S&C and is normally longer than a standard sleeper. There are three main types of sleepers used: concrete, wooden/timber and steel. Table 2.4 shows the total number of sleepers in several countries and the demand for new sleepers [36]. Table 2.4 shows that just over 2% of UK rail sleepers are replaced every year. Table 2.5 shows the sleeper breakdown in the UK currently; ¾ of sleepers used in the UK are concrete sleepers.

Country	Total Number of Sleepers (x1000)	Demands per Year (x1000)		
		Concrete	Steel	Wooden/Timber
UK	45,000	500	400	100
France	60,000	800	0	400
Germany	70,000	1400	100	100
Australia	600,000	-	150	200
USA	600,000	1,000	10	13,000

TABLE 2.4: TOTAL NUMBER OF SLEEPER AND DEMAND FOR VARIOUS COUNTRIES [36]

	Sleeper Type		
	Concrete	Steel	Wooden/Timber
Amount (x1000)	33,750	4,500	6750
Percentage	75%	10%	15%

TABLE 2.5: UK SLEEPER TYPES

2.3.4.1 Wooden Sleepers

Timber is the most widely used material for railway sleepers, however, as a sleeper material it deteriorates with time and needs appropriate replacement [37]. A timber sleeper is a cuboid with dimensions approximately 0.15*0.25*2.65 m, they have a typical weight of around 100 kg. There are two main types of wooden sleepers: softwood such as Pine and hardwood such as Oak. As the compression strength of softwoods such as Pine is low, softwood sleepers are usually fitted with a steel baseplate to spread the load to a larger area. The typical service life of a softwood (Pine) sleeper is 20-25 years [13]. Hardwood sleepers do not require a baseplate and are commonly used in S&C units as they are easy to attach fastenings to. The typical service life of an Oak sleeper is 40-60 years [13].

The main disadvantage of using timber sleepers is their susceptibility to biological degradation [38]. Australia is one of the biggest consumers of wooden sleepers, Figure 2.17 taken from [36] shows common causes of timber sleeper deterioration in Australia. It can be seen that over 50% of the failures were due to fungal decay, another 10% is due to termite infestations. However split ends, again accounting for about 10% of failures, are not due to age, they commonly occurs in timber sleepers as they support very large transverse shear loadings [39].

The primary driver of timber sleeper deterioration is time and environment. Regardless of loading, a softwood timber sleeper will fail after around 20 years due to biological attack. When modelling timber sleepers, it is of critical importance to consider the age of the sleeper as in many cases this will be the limiting factor for the service life.

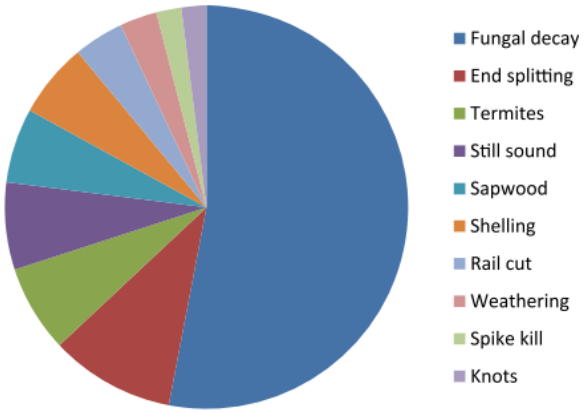


FIGURE 2.17: COMMON CAUSES OF TIMBER SLEEPER FAILURE [36]

The use of wooden/timber sleepers is in decline in the UK, however they are still used extensively in tunnels and for S&C. Traditionally wooden sleepers would be treated with creosote which would prevent biological attack. However in 2003 under EU legislation the use of creosote was banned due to the cancer risk it can pose, this has further decreased the use of wooden sleepers in the UK, as most alternative preservatives are more expensive and less effective.

2.3.4.2 Concrete Sleepers

Concrete sleepers grew in popularity in the 1950's in part due to improvements in concrete production technology and reductions in production cost. There are two main types of concrete sleeper: mono block and twin block. Mono block sleepers are made of a single block of concrete and twin block sleepers are made of two concrete blocks joined together with a steel rod. Concrete sleepers come in a range of sizes however the basic shapes are shown in Figure 2.18 and Figure 2.19 respectively. Concrete sleepers weigh approximately 300kg (three times that of a wooden sleeper); this makes them very stable and good at supporting the track; however the extreme weight makes them difficult to transport. Concrete sleepers are precast; they are constructed in an area that is not the final destination. Precast concrete is of the highest possible quality, both in terms of strength and durability; [40] therefore concrete sleepers have a very long service life. Nonetheless concrete sleepers are much less flexible than timber, meaning that more force is transferred to the ballast.

Concrete sleepers have three main failure modes according to Lutch et al. [41]:

(i) Seat abrasion [42] [43],

Rail seat abrasion is the gradual wearing away of concrete in the area around the rail pad and is the most common failure mode [41]. Accelerated rail seat abrasion occurs when water is present, tonnage is higher or curvature is tight. It can be reduced by placing pads between the sleepers and rails. Figure 2.20 shows an example of serious rail seat abrasion, if this level of rail seat abrasion occurs the sleeper needs replacing.

(ii) Flexural cracking

Damage occurs in the tie/fastening region. This commonly occurs when ballast conditions are beyond the scope of the tie design. It can also be caused by poor ballast alignment.

(iii) Rail fastening/clip failure

Damage occurs to the tie/fastening

All of the above failure modes are governed by loading cycles and are independent of the age of the sleeper, although Mohammadzadeh and Vahabi [44] found that corrosion due to the presents of chloride ions also influences concrete sleeper deterioration. It is widely believed the deterioration of concrete is primarily governed by the number of loading cycles and the environment it is in. If a concrete sleeper is not loaded and left in reasonable conditions (e.g. not immersed in water, not close to the sea) it can last for over one hundred years.



FIGURE 2.18: TWIN BLOCK CONCRETE SLEEPER

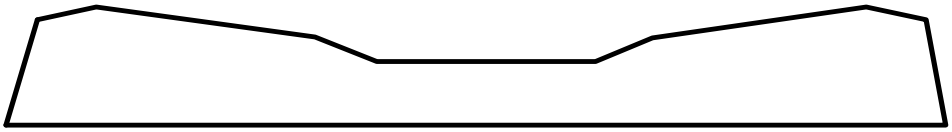


FIGURE 2.19: MONO BLOCK CONCRETE SLEEPER



FIGURE 2.20: SERIOUS RAIL SEAT ABRASION [45]

2.3.4.3 Steel Sleepers

Steel sleepers are the least commonly used worldwide. Just one in ten sleepers on the UK network is of steel construction (Table 2.5). However they have been growing in popularity and are now used extensively in Africa, India and the UK. Unlike concrete and wooden sleepers, steel sleepers are hollow and, consequently, are filled with ballast at installation time. Steel sleepers are not widely used as:

(i) New designs and long term effects are not fully understood.
(ii) High initial purchase price and large fluctuation in purchase price.
(iii) Insulation issues when using track circuits and overhead line equipment (OLE).
(iv) As the sleeper is filled with ballast it is not possible to use a tamping machine.

Nonetheless steel sleepers have a very long service life and whole life cost analysis [46], [47] suggests that in the long term steel sleepers could be cheaper than concrete. The main failure mode of steel sleepers is corrosion; this is accelerated by the fact the sleeper is in contact with the ballast and subgrade [36].

In the UK their use is generally restricted to lower priority lines. Steel sleepers are often used when ballast renewal can be postponed for at least 10 years, as, unlike concrete and timber sleepers, steel sleepers can be laid on the existing compacted ballast [48].



FIGURE 2.21: STEEL SLEEPERS [47]

2.3.4.4 Maintenance Options

There are very few ways in which sleepers can be maintained. In almost all cases if a sleeper becomes defective it is removed and replaced, this is done due to the insignificant cost of a single sleeper £30-£55 (depending on size and type) [49]. Wooden sleepers can be treated to reduce the effect of biological attacks and increase service life.

Sleepers have a long service life, compared to other track assets such as ballast and rails. Therefore renewal of track is normally governed by the condition of the rails or ballast as these generally have a shorter service life than sleepers, particularly on higher category routes. The sleepers are generally only renewed during complete track section renewal.

2.3.4.5 Inspection

The sleepers are inspected visually at regular intervals to ensure the number of defective sleepers adheres to standards [50].

2.3.5 Sleeper Pads

When using concrete sleepers (section 2.3.4.2) or steel sleepers (section 2.3.4.3), sleeper pads are placed between the rail and sleepers (see Figure 2.22). These dampen the transverse force applied to the sleepers. Originally Network Rail used 5 mm sleeper pads however sleeper pads were found to be so successful at increasing the sleeper service life that the standard has been increased from 5 mm to 10 mm. When sleeper pads become defective they are replaced.

2.3.6 Fastening System

Fastening systems or ‘clips’ are used to attach the rails to the sleepers or slab track. All over the world a great variety of fastening systems exist to which new types are regularly added, in order to keep up with changes in requirements and options or due to the availability of new materials [13]. Figure 2.22 shows a Pandrol ‘e’ clip, the clip (shown in blue) can be removed and re-inserted to the cast in shoulder (red). In the UK in recent years there has been a move to use ‘fast clips’ systems. These can easily be unfastened and refastened. A Pandrol ‘fastclip’ is shown in Figure 2.22. Table 2.6 summarises the different fastening systems used on the UK network. The ‘other’ section includes older fastening and fastening systems with a baseplate (used for wooden sleepers). The fastening system is critical in maintaining the gauge of the track.

Asset Description	Track (km)	Percentage of UK Network
Pandrol Fast Clips	5,100	17%
Pandrol ‘e’ Clips	18,000	62%
Other	6,100	21%

TABLE 2.6: FASTENING SYSTEM BREAKDOWN

2.3.6.1 Inspection and Maintenance

The clips are inspected visually to look for loose or broken clips. Any loose clips are secured and broken clips are replaced. The maximum number of defective clips must not exceed the values set in standards [50]. The maximum number of permitted defective sleepers is dependent on the rail type (see Table 6.8).

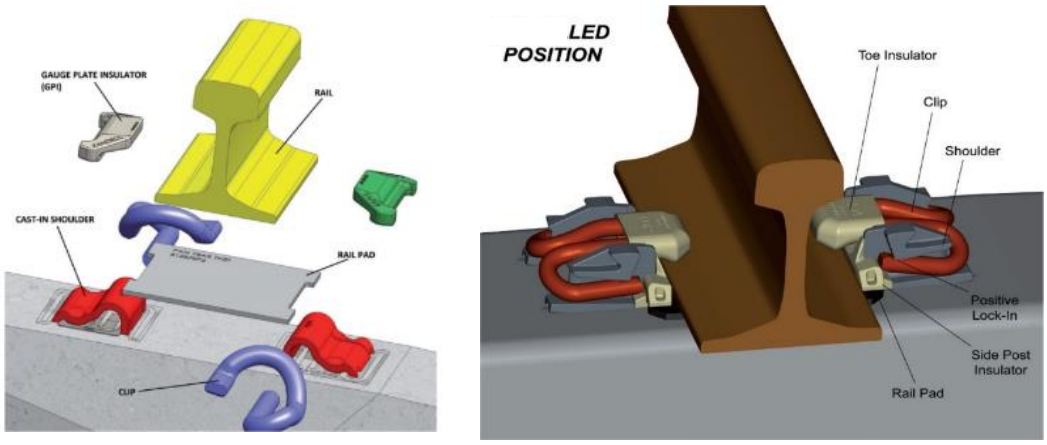


FIGURE 2.22: (LEFT) PANDROL ‘E’ CLIP, (RIGHT) PANDROL ‘FASTCLIP’ CLIP [51]

2.3.7 Switches and Crossings (S&C)

Switches and crossings (S&C), also called turnouts or points, are one of the most important assets on the UK railway network. An S&C unit is a trackside installation enabling railway vehicles to change tracks or crossover another track [52]. Any failure of an S&C unit usually leads to train delays and cancelations, having a negative impact on the quality of service delivered [53].

There are a range of switch types, the most common being turnout. Other types include:

(i) Fixed Diamond Crossings
These allow trains to cross another track but not change to that track.

(ii) Scissor Crossings
These can allow a train to crossover another track and join another track.

(iii) Catch Points
Catch points are typically used in sidings and goods yards; they are designed to deliberately derail trains rather than allowing the train to enter the mainline and potentially collide with a train travelling at high speed.

Network Rail classifies turnout S&C units based on their size (length). Type A are the smallest switches with the tightest radius curve and type H are the larger switches with the

shallowest radius curve. Figure 2.23 shows a breakdown of the different switch sizes, more information on switch types is given in Appendix D-1.1.

2.3.7.1 Description

An S&C unit is made up of electrical and mechanical components. There are eleven key components in an S&C unit:

(i) Ballast
(ii) Check Rail
(iii) Crossing
(iv) Fastening
(v) Point Operating Equipment (POE) (Including Point Heater)
(vi) Sleepers/Bearers
(vii) Slide Chair
(viii) Stretcher Bar
(ix) Stock Rail
(x) Switch Rail
(xi) Wing Rail

The type and number of each of the components within the switch will depend on the switch type. This information is listed in Appendix D-1.1. The ballast used for S&C units acts in the same way as plain line track and has similar failure modes, however it has to be maintained using a specialist S&C tamper or multipurpose stoneblower. The sleepers used in S&C are called bearers and are often longer than standard sleepers. Wooden bearers are still widely used in S&C design as they are much easier to customise than concrete or steel. There are two main rail types in an S&C unit, the stock rails which are fixed and the switch rails which move. In addition, there are check and wing rails used to guide the train wheels and ensure the train stays on the correct track as it passes over the switch. Sections where the two rails cross and there is a gap for the train wheel to pass through are called crossings. The rails are attached to the sleepers using a fastening system. The fixed rails (stock rails) are attached using the traditional fastening systems discussed in section 2.3.6. Slide chairs are used to guide the switch rails as they move. Stretcher bars are used to join the two switch rails and maintain them at the correct distance apart. Failure of stretcher bars can lead to derailment. Stretcher bar failure was found to be the cause of the fatal crash at Potters Bar in 2002 [54]. The switch rails are moved using POE. The POE can be electric, hydraulic or pneumatic [53].

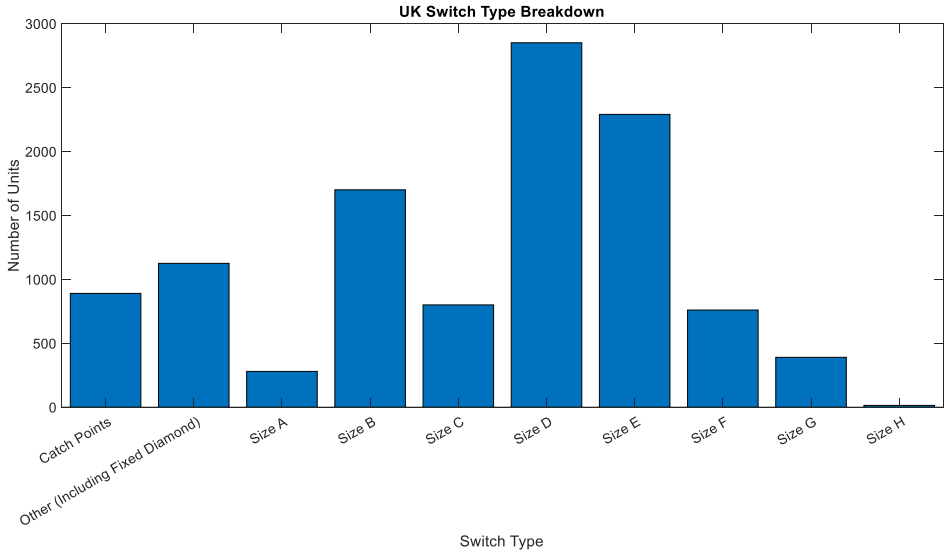


FIGURE 2.23: UK SWITCH SIZE BREAKDOWN, FURTHER INFORMATION IN APPENDIX D-1.1

2.3.7.2 Inspection and Maintenance

Many of the mechanical components within S&C units, such as the fastenings, sleepers, rails and ballast, are maintained and inspected in a similar way to the plain line track components discussed previously. Nonetheless the maintenance is made more difficult due to the shape of S&C. For this reason specific machines are often used to perform maintenance, such as a specialist S&C tamper or a multipurpose stoneblower. These machines are not as abundant as regular maintenance machines, there is often a considerable waiting time for one to become available. The condition of electrical components can be assessed using condition monitoring [55], [56]. Condition monitoring is used in a wide range of applications and measures a range of electrical parameters such as voltage, current and resistance in real time. By monitoring the components in real time any irregularities will immediately be identified and investigated in order for worn components to be identified and replaced before full failure occurs.

2.3.8 Tunnels

Trains are unable to climb steep gradients, for this reason tunnels are critical in allowing trains to pass through hilly areas. This research will not attempt to model tunnel deterioration in detail, however the effect being in a tunnel has on other components is of interest. For assets in a tunnel the following need to be considered:

(i) Accelerated deterioration rates, particularly for metallic and organic materials, due to damp conditions.

(ii) Increased repair times due to the dark, enclosed and cramped conditions. Maintenance in tunnels often takes longer as lighting needs to be installed and the air quality needs to be closely monitored [57].

As well as modelling the assets within the tunnel a basic model to predict the cost of maintaining the tunnel will also be included.

2.3.9 Signalling Systems

The signalling system ensures the safe control of railway traffic [58]. Almost all of the UK network is currently controlled using a fixed blocks signalling system which uses track circuits and axle counters to locate trains. A track circuit is a train detection system, the respective rails are attached to either side of a DC power source (battery) when the track section is empty there is an open circuit. However if there is a train in the section the circuit is complete and current flows through the axles. This energises a relay to indicate to the signaller that the section is occupied. Each block is protected by its own signal (Figure 2.24), which ensures that there can only ever be one train in a block at a time.

There have been several serious train accidents in the UK due to signals being passed at danger (SPAD), this includes the fatal train crash at Ladbroke Grove in 1999 [59]. As a result additional safety features have been added to the signalling system. The most common used in the UK is the automatic warning system (AWS), used to relay information to the driver if the signal is set at 'stop' or 'caution'. The AWS track equipment (Figure 2.24) consists of a permanent magnet and an electromagnet. When the train passes over the permanent magnet the AWS device is activated causing an alarm in the driver's cab. If the signal is 'clear' then the electromagnet is also energised which disarms the warning system. If the signal is at the 'caution' or 'stop' aspect the electromagnet is not energised, in this case the warning siren remains on and must be acknowledged by the driver. If the warning is not acknowledged then emergency brakes will be applied.

As the signalling system is safety critical, any failure of the system normally means at least part of the track will be non-operational until the issue is fixed, which can cause lengthy delays. Delays caused by signal failures are of considerable interest in this research as they will have a significant bearing on the whole life cost. The signalling system is also considered as, unlike the other assets, it effects the whole route and cannot be assigned to a specific track section, hence a different style of model will be required to consider this asset.

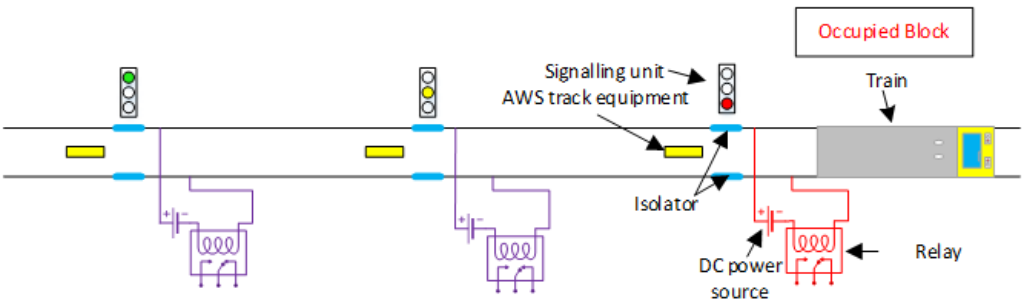


FIGURE 2.24: KEY COMPONENTS OF THE SIGNALLING SYSTEM

2.4 Other Assets: Not Considered in this Research

The previous sections have provided an overview of the key assets that will be considered in this research; track (rails, sleepers, fastenings, pads, and ballast), tunnels, S&C units and the signalling system. There are a number of other assets within a railway network, such as structures, buildings, stations, earthworks and overhead line equipment (OLE). The system model created will be flexible enough that these other asset classes can easily be linked to the framework in the future.

2.5 Summary

The purpose of this chapter was to outline the key railway assets that will be modelled in this research. All the assets discussed in this chapter are summarised in Table 2.7, this table will be referred to throughout the subsequent chapters.

Asset		Overview	Failure Modes	Inspection	Maintenance
1.Ballast		Crushed granular material; supports the sleepers and allows rapid drainage.	Ballast breakdown (fines) Geometry faults; vertical and lateral alignment, gauge, cyclic top and twist[1].	Visual inspection NMT (geometry measurements).	Tamping Stoneblowing Cleaning
2.Rail		Longitudinal steel members that directly guide the train wheel.	Can develop a range of defects due to longitudinal and transverse forces applied to the rail. Defects include; corrugations and squats.	Visual and ultrasonic inspection for defects.	Weld repair Rail grinding Rail replacement
3.Sleepers	Concrete	Transmit forces to the ballast, maintain the gauge.	Cracking and spalling	Visual inspection	Replacement
	Wooden/ Timber		Biological attack		Treatment against biological attacks Replacement
	Steel		Corrosion		Replacement
4.Fastening		Affix the rails to the sleepers.	Become lose Break	Visual inspection	Tighten bolts Replacement
5.Sleeper Pads		Placed between concrete and steel sleepers and the rails.	Wear out	Visual inspection	Replacement
6.Switches and Crossings (S&C)		S&C units allow trains to switch to another track or cross another track, comprising many electrical and mechanical components.	There are many components within a switch and crossing unit, each has its own failure modes.	Visual inspection NMT Ultrasonic Condition monitoring[2]	Wide range including welding, grinding and tamping[3].
7.Tunnel		Used to take trains through hills. Have a noticeable effect on degradation rates and maintenance completion times.	Wide range including bulging, however this will not be modelled in this research.	Visual inspection/ detailed inspection policy[4].	Range of repair techniques[5].
8.Signalling System		The signalling system is a global asset that affects the whole network. It is made up of a range of components including lineside signals and track circuits[6].	A wide range of failure modes. Safety critical system.	Each component is inspected in its own way.	Wide range of repair techniques.

TABLE 2.7: ASSET SUMMARY

[1] Vertical geometry (top) is the only geometry measurement considered in this research.
[2] Not considered at this stage.
[3] Specialist S&C tamper or multipurpose stoneblower required.
[4] Detailed modelling of tunnel inspections will not be considered in this research.
[5] Detailed modelling of tunnel maintenance will not be considered in this research.
[6] In the next 30 years it is likely there may be a significant overhaul of the signalling system in the UK.

3 Asset Management Modelling Techniques

3.1 Introduction

The aim of this research is to create a whole system model for railway networks capable of making detailed forecasts for the maintenance and expenditure on a wide range of railway assets. This can be used by asset managers to make more informed decisions on which maintenance tasks should be performed and how the budget available will affect the overall condition of the railway. This chapter will provide an introduction to asset management, explaining what asset management is and exploring some of the modelling techniques that are popular in asset management, with a particular focus on railways.

3.2 Asset Management

There are numerous definitions of asset management being used in different sectors and in different countries. The majority are slightly different expressions of the same basic concepts, based around optimising asset performance to deliver business objectives at the minimum whole life cost [60]. The International Standard ISO 55000 [61] defines asset management as the '*co-ordinated activity of an organisation to realise value from assets'*. Where an asset is described as '*an item, thing or entity that has potential or actual value to an organisation'*. Hence asset management entails finding strategies which effectively administrate all of the assets within the company's portfolio and deliver maximum benefit (usually profit).

The Institute of Asset Management (IAM) [62] have developed the '*Conceptual Asset Management Model'*, the model groups asset management into six areas; as shown in Figure 3.1. A number of tools and models have been developed to support asset management decisions especially in the areas of reliability, availability, maintainability and safety (RAMS) [63].

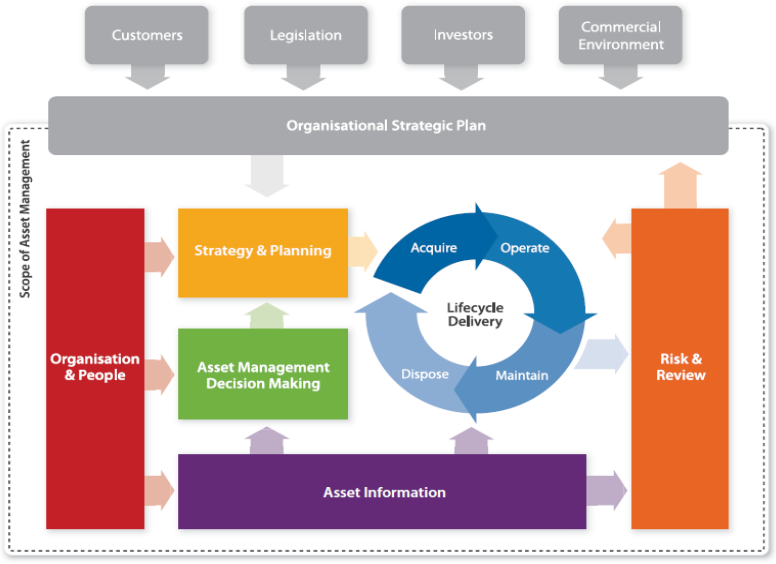


FIGURE 3.1: IAM CONCEPTUAL ASSET MANAGEMENT MODEL [64]

3.2.1 Reliability

The international definition of the reliability (of an item) is:
'Ability to perform as required, without failure, for a given time interval, under given conditions' (192-01-24) [65].

And can be expressed mathematically as:
'The probability that a component remains operational from time zero to some later time τ given that it was operational at time zero'. Closely linked to reliability is the failure rate, which is defined as '*the frequency at which a failure occurs at time t, given that no failure has occurred before t'* (3-7) [66]
The reliability is linked to the failure rate according to:

$$R(t) = e^{\int_0^t -\lambda(\tau)d\tau}. \quad (3.1)$$

In the case of a constant failure rate, λ:

$$R(t) = e^{-\lambda t}. \quad (3.2)$$

The component reliability can be used to determine the mean time to failure (MTTF) according to:

$$MTTF = \int_0^\infty tf(t)\,dt = \int_0^\infty R(u)\,du, \quad (3.3)$$

where $f(t)$ is the distribution of the failure times.

In railway systems it is common to only consider service affecting failures when calculating the reliability of a railway network. Therefore the reliability of railway networks is often expressed as the Mean Time Between Service Affecting Failures (MTBSAF).

3.2.2 Maintainability

Maintainability is a measure of how easily a system can be repaired. The maintainability (of an item) is formally defined as:
'Ability to be retained in, or restored to a state to perform as required, under given conditions of use and maintenance' (192-01-27) [65].

In an engineering sense it is common to consider the maintainability as:
'*the probability that the system will be restored to a fully operational condition within a specified period of time'* [67].

If the repair rate, μ, is constant then the maintainability, *M(t)*, is given by:

$$M(t) = 1 - e^{-\mu t}, \quad (3.4)$$

And the Mean Time To Repair (MTTR), is given as:

$$MTTR = \frac{1}{\mu}. \quad (3.5)$$

Figure 3.2 shows a diagram of the different types of maintenance. Maintenance can be split into two main types:

(i) Preventive maintenance; maintenance carried out to mitigate degradation and reduce the probability of failure [63].
(ii) Corrective maintenance; maintenance carried out after a fault occurs to restore the system to the working state [63].

Corrective or reactive maintenance tends to be the least cost effective, particularly if they have to be performed immediately, a premium will have to be paid to get the work performed at short notice. Preventative maintenance tends to be cheaper as downtime is avoided and maintenance can be planned in advance which generally reduces the cost. However replacing components before failure reduces the service life of components and increases the number of repairs/replacements required which can, in the long term, be more expensive. Asset managers can use predictive models to explore which strategy is better in the long term.

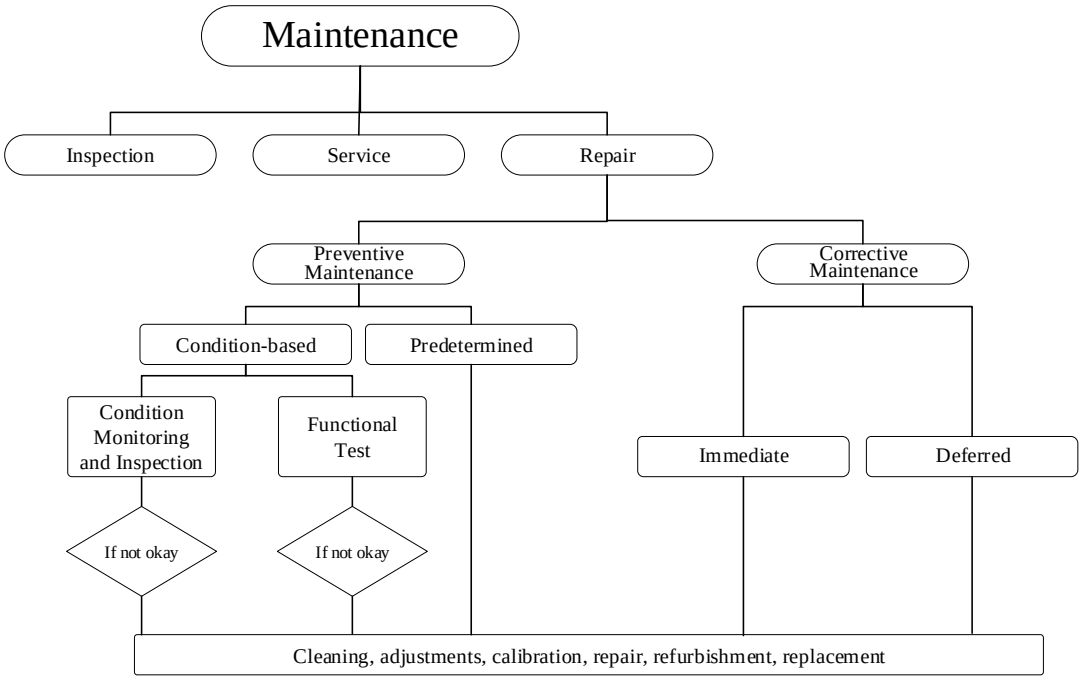


FIGURE 3.2: TYPES OF MAINTENANCE; ADAPTED FROM [63], [68], [69]

3.2.3 Availability

The international definition of availability is:
'Ability to be in a state to perform as required' (192-01-23) [65].

In an engineering sense availability can be defined as:
'*the fraction of the total time that a device or system is able to perform its required function*' [67].

The availability of a railway network is of critical importance to both asset managers and customers. Availability is formally calculated as:

$$A = \frac{MTTF}{MTTF + MTTR}. \quad (3.6)$$

For railway networks availability is generally assessed based on the number of days on which a TSR or line closure is in place. It is also important to consider the time the network may have to be closed to perform maintenance and renewals.

3.2.4 Safety

Safety is of paramount importance to railway asset managers. The UK railway network is one of the safest in Europe and fatalities are extremely rare. In 2016-17 there were 15 passenger fatalities on the UK railway network [70] that compares to 1,710 deaths on the UK road network [71].

Safety is closely linked to risk. In many asset management models it is common practice to assign cost to the safety risk, making higher risk strategies less favourable.

3.2.5 Whole Lifecycle Cost (LCC)

Another important consideration within asset management is LCC. Life cycle costing, or whole-life costing, is the process of estimating how much money you will spend on an asset or portfolio of assets over the course of its/their useful life. LCC considers the cost from the design stage/when the asset is purchase to the time the asset is sold or decommissioned. Considering the LCC is key to decision making, a wide range of techniques have been developed to assist with LCC decision making [72].

3.3 Asset Management Modelling Techniques

There are a large range of techniques that can be used by asset managers to evaluate the condition, remaining life and LCC of the assets in their portfolio, and help them to make decisions on which assets to maintain and how to maximise the value from their assets. Figure 3.3 shows the spectrum of techniques available from combinatorial methods, such as Fault Trees, through to complex simulation methods such as Petri nets. To combine the degradation of an asset with its asset management processes (inspection, maintenance and renewal), in order to predict its future condition, requires the use of state-based models. These are reviewed in the following sections.

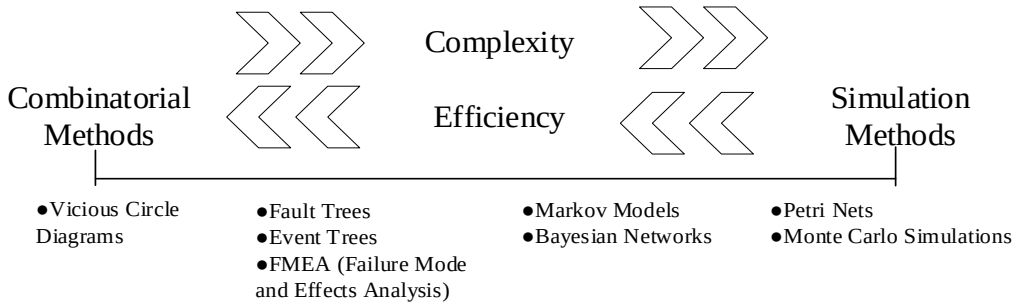


FIGURE 3.3: MODELLING TECHNIQUES

3.3.1 Markovian Methods

Markov models are a fundamental class of stochastic processes and have been applied to a wide range of disciplines including engineering, computer science, networking and physics [73]. They are frequently used in reliability analysis to assess different measurements of interest such as reliability, availability and maintainability [74]. They are state based models. The states of a Markov model typically represent states of a system, for example working or failed. A process is said to be Markovian if it is memoryless such that:

$$P(X_t=x_t|X_0=x_0,X_1=x_1,\ldots,X_{t-1}=x_{t-1})=P(X_t=x_t|X_{t-1}=x_{t-1}). \quad (3.7)$$

And homogenous such that:

$$P(X_t=z|X_{t-1}=y)=P(X_{t+k}=z|X_{t+k-1}=y) \quad \forall\, k\geq 0. \quad (3.8)$$

From equation (3.7) it can be seen that the probability of moving to state X_t given the system is currently in state X_{t-1} is constant regardless of the past states of the system $X_0, X_1,\ldots,X_{t-2}$. Hence information about the past is irrelevant in predicting future states of the system. Equation (3.8) makes the system homogenous as it implies the probabilities of changing state remains constant for all time. This implies that all transitions are governed by the Exponential distribution.

There are two main groups of Markov model: Markov chain models and Markov process models (continuous time Markov chain). A Markov chain is discrete in time and hence state changes happen in discrete steps, whereas a Markov process is continuous in time and state changes can happen at any point.

3.3.1.1 Markov Chain Models (Discrete Time)

A Markov chain contains a finite number of states. The sum of the probability of all the transitions leaving a state must equal one, these probabilities are typically expressed in a transition probability matrix, where the first row of the matrix represents the probability of transitioning to each state from the first row and the second from the second state and so on. A simple three state Markov model is shown in Figure 3.4 the transition matrix for the system is shown in equation (3.9). Given an initial state of the system, it is possible to work out the probability of being in each of the states in the next time step by multiplying the initial marking by the transition matrix as shown in equation (3.10).

$$\boldsymbol{T} = \begin{bmatrix} 0.7 & 0.3 & 0 \\ 0.8 & 0.1 & 0.1 \\ 0 & 0.9 & 0.1 \end{bmatrix}. \tag{3.9}$$

$$\boldsymbol{P1} = [1 \quad 0 \quad 0]. \begin{bmatrix} 0.7 & 0.3 & 0 \\ 0.8 & 0.1 & 0.1 \\ 0 & 0.9 & 0.1 \end{bmatrix} = [0.7 \quad 0.3 \quad 0]\,. \tag{3.10}$$

As the current state of the system is totally independent of all past states, it is possible to generalise equation (3.10) to calculate the probability of being in any state at any time step given any starting vector. This relationship is described by the Chapman-Kolmogorov equation shown in (3.11).

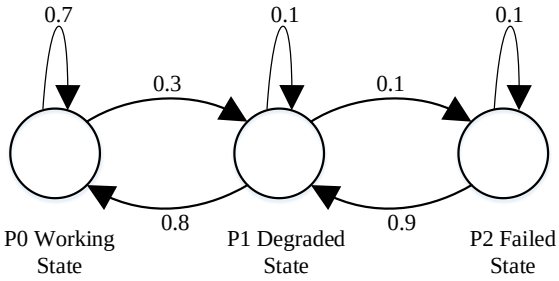


FIGURE 3.4: THREE STATE MARKOV CHAIN MODEL

$$\boldsymbol{p}(m+t) = \boldsymbol{p}(m).\boldsymbol{T^t} \qquad \forall\, t, \quad m \in N. \tag{3.11}$$

Another aspect of Markovian methods regularly used in asset management is Markov absorption theory. An absorbing state in a Markov chain is a state whereby once the state is entered it is not possible to transition to any other state. A Markov chain can be described as absorbing if there is at least one absorbing state and it is possible to go from every non-absorbing state to an absorbing state in a finite number of time steps.

Markov absorption theory can be used to calculate the expected number of steps required to reach an absorbing state from each of the non-absorbing states. To apply Markov absorption theory the transition matrix, ***T***, must be expressed in standard form (canonical form). The standard form for the transition matrix is:

$$\boldsymbol{P} = \begin{bmatrix} \boldsymbol{I} & \boldsymbol{0} \\ \boldsymbol{R} & \boldsymbol{Q} \end{bmatrix}, \tag{3.12}$$

where ***I*** is the *m***m* identity matrix, where *m* is equal to the number of absorbing states, **0** is a zero matrix, and ***R*** and ***Q*** are two nonzero matrices.

From the standard form matrix ***P,*** the fundamental matrix ***F*** can be calculated as:

$$\boldsymbol{F} = [\boldsymbol{I} - \boldsymbol{Q}]^{-1}, \tag{3.13}$$

where $\boldsymbol{I}$ is the k*k identity matrix where k is equal to the number of absorbing states subtracted from the total number of states, $\boldsymbol{Q}$ is the k*k square matrix in the bottom right portion of the matrix $\boldsymbol{P}$.

Finally the column vector $\boldsymbol{t}$ which lists the number of steps to absorption from each of the states can be calculated according to:

$$\boldsymbol{t} = \boldsymbol{F}.\mathbf{1}, \tag{3.14}$$

where **1** is a column vector of 1's.

3.3.1.2 Markov Process Models (Continuous Time)

In a Markov process (or continuous time Markov chain) the probability of being in each state is expressed as a continuous function of time, based on the transition rates between states. It is common practise to express the transition rates in a transition matrix. Figure 3.5 shows a simple two state Markov process, the component can either be working or failed, the component has a failure rate, λ and a repair rate, μ. The transition rate matrix for the system is shown in equation (3.15).

$$\begin{bmatrix} -\lambda & \lambda \\ \mu & -\mu \end{bmatrix}. \tag{3.15}$$

A system of ordinary differential equations (ODEs) can be developed for the system using the transition rate matrix according to equation (3.16). The solutions to the system of ODEs, assuming that the system starts in the working state, are shown in equations (3.17) and (3.18). A plot of the solutions assuming a failure rate of 0.01 and a repair rate of 0.1 is shown in Figure 3.6. For small systems it is possible to solve the equations analytically and get exact solutions. For larger systems numerical methods such as Runge–Kutta can be used to approximate the solutions to the ODEs.

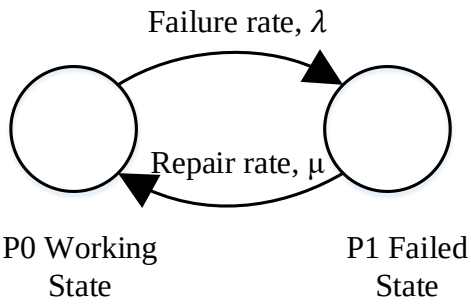


FIGURE 3.5: TWO STATE MARKOV PROCESS

$$\begin{bmatrix} \frac{dx_0}{dt} & \frac{dx_1}{dt} \end{bmatrix} = [x_0(t) \quad x_1(t)].\begin{bmatrix} -\lambda & \lambda \\ \mu & -\mu \end{bmatrix}. \tag{3.16}$$

$$x_0(t) = \frac{\mu}{\lambda+\mu} + \lambda\frac{e^{-(\lambda+\mu)t}}{\lambda+\mu}, \tag{3.17}$$

$$x_1(t) = \frac{\lambda}{\lambda+\mu} + \lambda\frac{e^{-(\lambda+\mu)t}}{\lambda+\mu}. \quad (3.18)$$

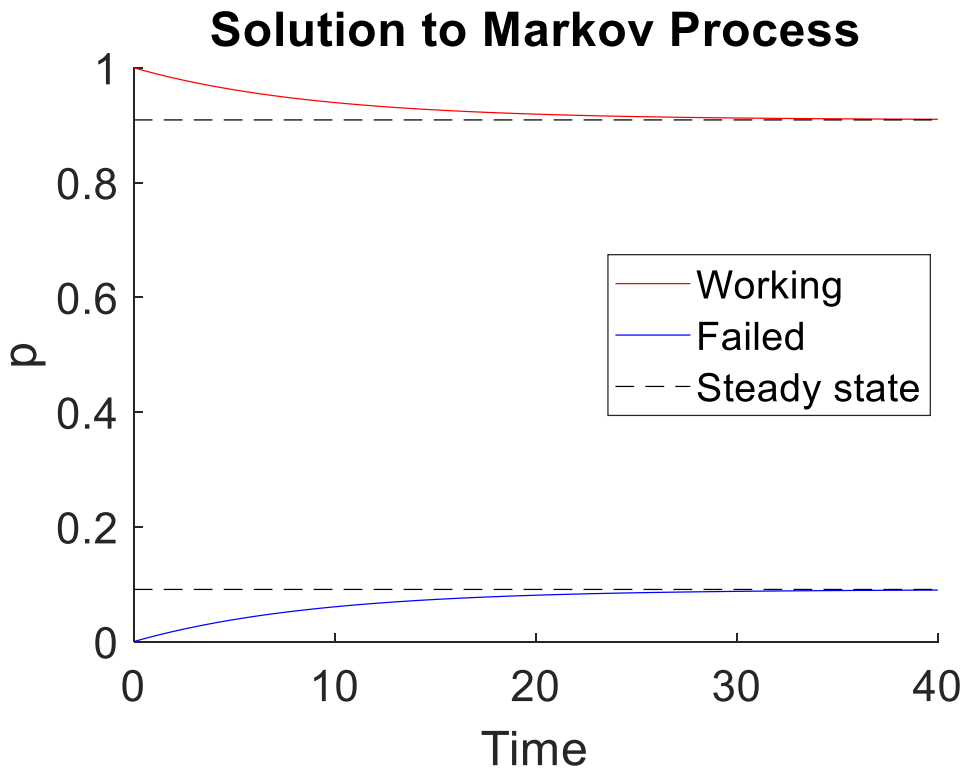


FIGURE 3.6: SOLUTION TO THE MARKOV MODEL SHOWN IN FIGURE 3.5, WITH FAILURE RATE =0.01 AND REPAIR RATE =0.1

After a large amount of time the Markov process will converge to a steady state value, this can be seen in Figure 3.6. The steady state value is determined by considering the limit as *t* tends to infinity in equations (3.17) and (3.18), it can be seen as *t* tends to infinity the exponential terms tend to zero leaving the steady state values shown in equations (3.19) and (3.20).

$$\frac{\mu}{\lambda+\mu}, \quad (3.19)$$

$$\frac{\lambda}{\lambda+\mu}. \quad (3.20)$$

3.3.1.3 Markov Variations

There are a number of variants that have been made to the Markov process to make it possible to model a wider range of real world systems. Variations of the Markov process include: hidden Markov models [75], semi-Markov models [76] and hidden semi-Markov models [77].

In a hidden Markov model the states of the system, Z_i, cannot be observed directly, however a set of observables, X_i, are known. The values Z_i, are linked to X_i by an Emission matrix E,

where the rows of E, are the probabilities of being in state, Z_i, given the system is observed to be in X_i.

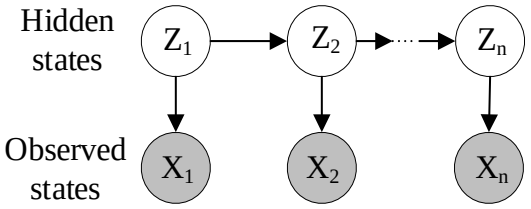


FIGURE 3.7: HIDDEN MARKOV MODEL

3.3.2 Petri Net Models

Petri nets were first proposed by Carl Petri in his 1962 thesis [78]. They have grown in popularity in recent years, they have been extensively analysed [79], and the original concepts have been added to [21], [80].

The theoretical features of the Petri net allow detailed modelling and investigation of system behaviour, while their graphical representation supports the visualisation of state changes of the modelled system [80]. Similar to Markov models they are state-based models, and the state of the model represents information about the system. However the transitions between states are not restricted to an Exponential distribution.

The formal mathematical definition given by Murata [79] is as follows:

A Petri net is a five tuple, $PN=(P, T, F, W, M_0)$ where

$P=\{p_1,p_2,...,p_4\}$	(finite set of places)
$T=\{t_1,t_2,...,t_n\}$	(finite set of transitions)
$F\subseteq(P \times T)\cup(T \times P)$	(set of arcs (flow relations))
$W:F\rightarrow\{1,2,3\ldots\}$	(weight function)
$M_o:P\rightarrow\{0,1,2,3\ldots\}$	(initial marking)
$P\cap T=\{\emptyset\}$ and $P\cup T\neq\{\emptyset\}$	

Petri nets are normally expressed diagrammatically, where possible the symbols in diagrams used match British Standards [81], however some of the Petri net extensions used are not listed in standards. The complete list of Petri net symbols used are shown in Table 3.1. The Petri net is created from four main parts:

Places

Places normally represent the state of the system such as working or failed, or contain information about the system such as the number of times a component has been maintained. The information expressed by the place is dependent on the number of tokens in the place. There is no limit on the number of tokens a place can hold. Places are represented in a Petri net diagram using circles.

Tokens
Tokens reside in places and provide information about the system, such as its condition. Increasing the number of tokens in a place will change the information/state of the system. Tokens are added, removed or transferred to places by the transitions. The number of tokens in a place is often called the marking of the system. Tokens are represented in a Petri net diagram as black dots. The system must be provided with an initial marking.

Arcs
Arcs are used to transfer tokens between places and update the marking of the system. The multiplicity or weight of the arc represents the number of tokens that the arc will move. There are two special types of arc: test arcs and inhibitor arcs. A test arc is used to test if a place is marked without altering the marking of that place, test arcs are represented with a double-ended arrow. An inhibitor arc is used to stop a transition firing based on the state of the system. Inhibitor arcs are represented as lines with a circle on the end in Petri net diagrams.

Transitions
Transitions are used to change the state of the system by moving tokens from input places to output places. There are various different transition types. The standard transition is introduced here and the Petri net extension transitions are introduced in Section 6.2. Transitions are represented as rectangles, the fill style is dependent on the transition firing type (Table 3.1) and the colour is dependent on the transition type.

An example Petri net is shown in Figure 3.8. The system is updated when a transition fires, transition firing occurs in the following way:

(i) The transition has to be '*enabled'*. A transition is enabled when all of the input places contain at least a number of tokens equal to their weight and it is not inhibited. The transition in Figure 3.8 is therefore enabled as the marking of both places *P0* and *P2* are greater than or equal to their arc weights, the test place, *P1*, is marked and there is no token in the inhibiting place, *P3*.

(ii) Once the transition is enabled it will *'fire'*, there can be a delay between the transition being enabled and the transition firing, this is discussed in the next section.

(iii) When a transition fires, a weight of tokens equal to the multiplicity of arcs is removed from each input place and a weight of tokens equal to the multiplicity of arcs is added to each of the output places. The total number of tokens does not need to be conserved in the firing process. In Figure 3.8 the marking of *P0* is reduced by one, the marking of *P2* is reduced by two and the marking of *P4* is increased by one. The marking of the test and inhibitor places remains unchanged. Following firing the state of the system will change.

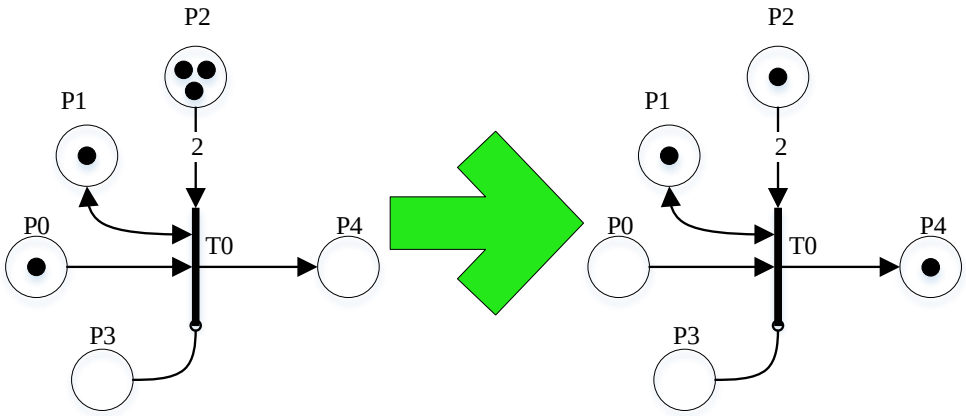


FIGURE 3.8: FIRING OF AN UNTIMED TRANSITION

3.3.2.1 Timed Petri Nets

In a timed Petri net there can be a delay between the transition being enabled and the transition firing. This duration can either be stochastic or deterministic. For the remainder of this thesis all Petri nets are assumed to be timed Petri nets.

A simple example of a timed Petri net is shown in Figure 3.9, the figure shows the evolution of a Petri net from $t=0$ to $t<2D$. The Petri net contains two transitions, a transition where the delay time is zero (instant transition) and a deterministic delay transition, with a delay of D. In the initial marking, Figure 3.9(a), transition *T0* is not enabled as it is inhibited by the tokens in place *P2*. Transition *T1* is enabled but has a delay time of D, so does not fire until time D has elapsed Figure 3.9(b). Once D time has elapsed transition *T1* fires removing one token from place *P2* an adding four to *P3*. Once the marking of *P2* is reduced to two, transition *T0* is no longer inhibited and becomes enabled. *T0* then fires instantaneously Figure 3.9(c).

Asset managers may wish to understand what will happen to the system after a large amount of time, reachability graphs can be used to show how the marking of a Petri net will evolve with time. A reachability graph allows dead transitions (transitions that cannot become enabled again) to be identified. Figure 3.10 shows the complete reachability graph for the system shown in Figure 3.9. It can be seen that *T0* initially becomes dead and then *T1* also becomes dead, meaning the net has become dead. Reachability graphs are useful for studying simple Petri nets however, their usefulness decreases significantly for larger nets.

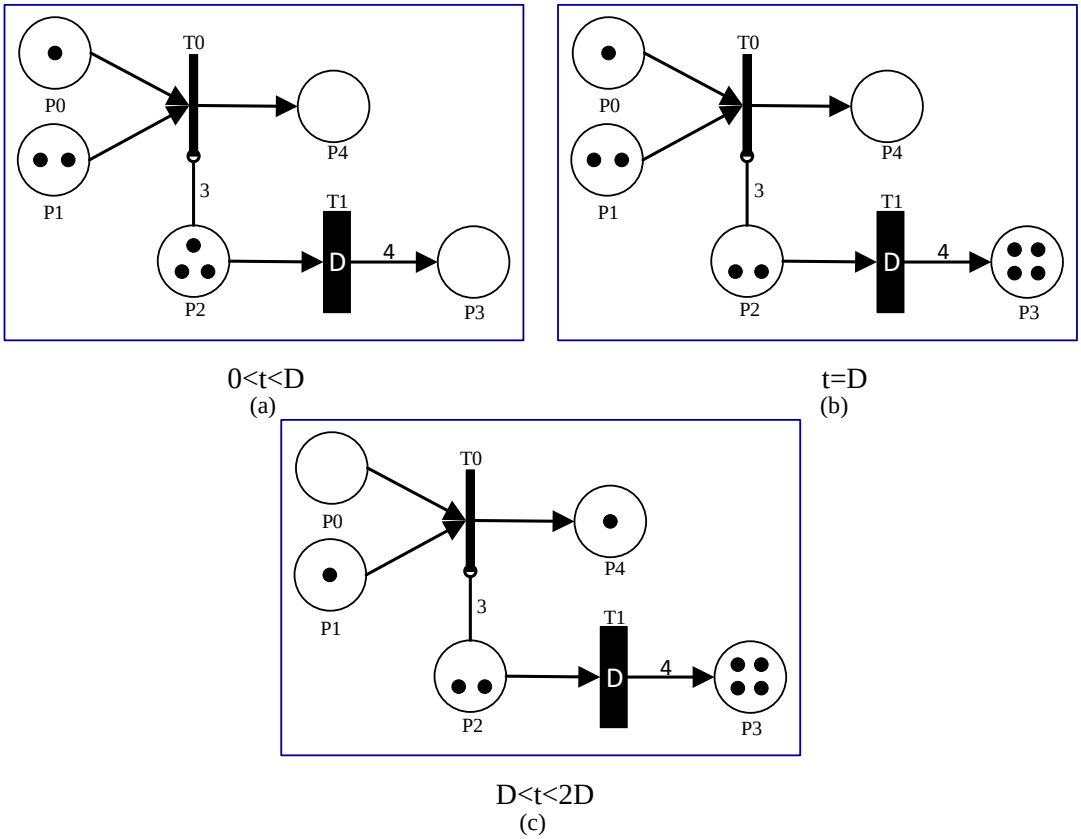


FIGURE 3.9: EVOLUTION OF A PETRI NET

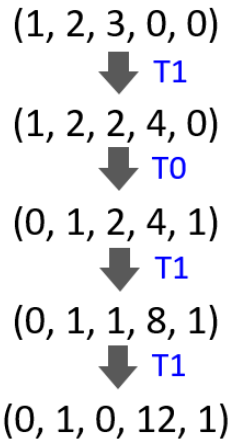


FIGURE 3.10: REACHABILITY GRAPH OF PETRI NET SHOWN IN FIGURE 3.9

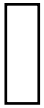
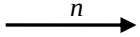
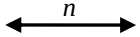
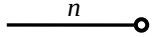
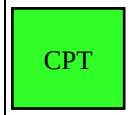
Place	Transition					Token	Arc	Test Arc	Inhibitor Arc
		Delay time of zero	Constant delay time	Delay time sampled from an Exponential distribution	Delay time sample from an arbitrarily distributed				
	Standard								
Used to represent the condition state of the system.	Conditional					Used to mark places, the number of tokens in a place will provide information on the state of the system.	Moves tokens (Tokens moved in direction of arrow)	Checks a test place, transition only fire if test place marking is great than or equal to n, however the marking of test place unchanged	Stops a transition firing if the number of tokens in the place it is connected to is greater than or equal to n. If the arc has no weight displayed then its value is unity
	Reset								
	Probabilistic		n/a	n/a	n/a				
	Conditional Probabilistic		n/a	n/a	n/a				
	Used to update the condition of the system by moving the tokens from place to place								

TABLE 3.1: PETRI NET SYMBOLS

3.3.3 Petri Net Extensions

The basic Petri net method has been expanded in a number of ways. This section will provide an overview of some of the main extensions.

3.3.3.1 Hierarchical Petri Nets (HPNs)

To accommodate the need to model larger and more complex systems, Jensen and Kristensen [82] proposed the hierarchical Petri net (HPN). A HPN divides a large Petri net model into a number of structured subnets or modules. The main benefit to using a HPN rather than a traditional Petri net is the simplification in expressing the Petri net diagrammatically. The HPN provides a clear way to identify a number of key aspects in a very large Petri net. Due to the size and number of assets that need to be modelled HPNs are thought to be a very useful tool in this research.

The fundamental aim of a HPN is to reduce the complexity of a Petri net diagram by replacing complex parts of the Petri net with '*substitution transitions'*. There are two types of modules within the HPN framework: '*master*' and '*slave*'. The master module is at the top of the hierarchy and the '*slave*' module feeds into it. If there are more than two layers to the hierarchy then certain modules will be '*slave'* to some modules but master to others. In the '*master*' module the '*slave*' net is replaced with a substitution transition to simplify the diagram. Substitution transitions are drawn as rectangles with a double line boarder to distinguish them from standard transitions.

The interface between modules and substitution transitions is achieved using '*port*' and '*socket*' places. '*Port'* and '*socket*' places are drawn with a double boarder to distinguish them from standard places. '*Socket*' places are located in the '*master*' module and have a corresponding *'port'* place in the '*slave*' module. The *'port'* places in the '*slave*' module plug into the '*socket*' places allowing modules to be linked together. When a '*port*' place is plugged into a '*socket*' place, all information is shared between the two. The number of tokens in a '*port*' place must always equal the number of tokens in its corresponding *'socket'* place. For clarity in this research the names will likewise always be the same; however this does not have to be the case.

Figure 3.11 shows a standard Petri net with eight places, Figure 3.12 shows how the Petri net in Figure 3.11 can be split into three modules and expressed as a HPN, which in its simplest form, has just two places and a substitution transition. The substitution transition *'Module2'* is used instead of places *P3, P4, P5,* three transitions and the substitution transition *'Module3'*. And the substitution transition *'Module3'* is used to represent two transitions and the places *P6, P7* and *P8*.

'Module 1' is at the top of the hierarchy, it is master to '*Module 2'* and hence only contains '*socket*' places. *'Module 2'* is '*slave*' to '*Module 1*' but '*master*' to *'Module 3'* therefore it has '*socket*' and *'port'* places. Finally *'Module 3'* is '*slave*' to *'Module 2'* and so only contains '*ports*'. As well as *'port'* and *'socket'* places the modules may contain any number of standard places such as *P3* which has no interface with other modules. The full list of

place types are shown in the tables next to the figures. It is possible, although not shown in Figure 3.12 for a single place to be a *'port'* and '*socket*' within the same module; if a '*master*' and '*slave*' module are linked to the same module via the same place.

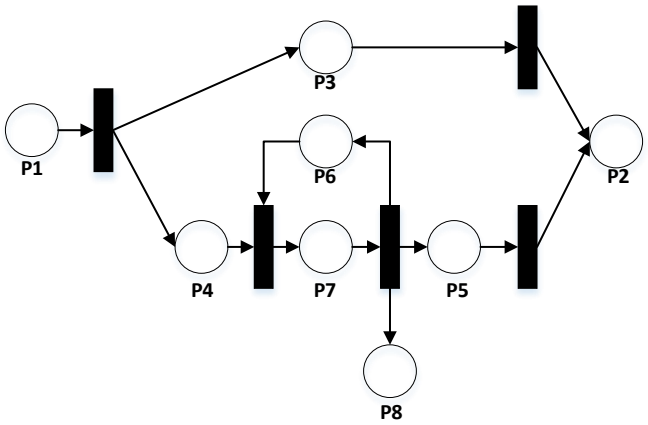
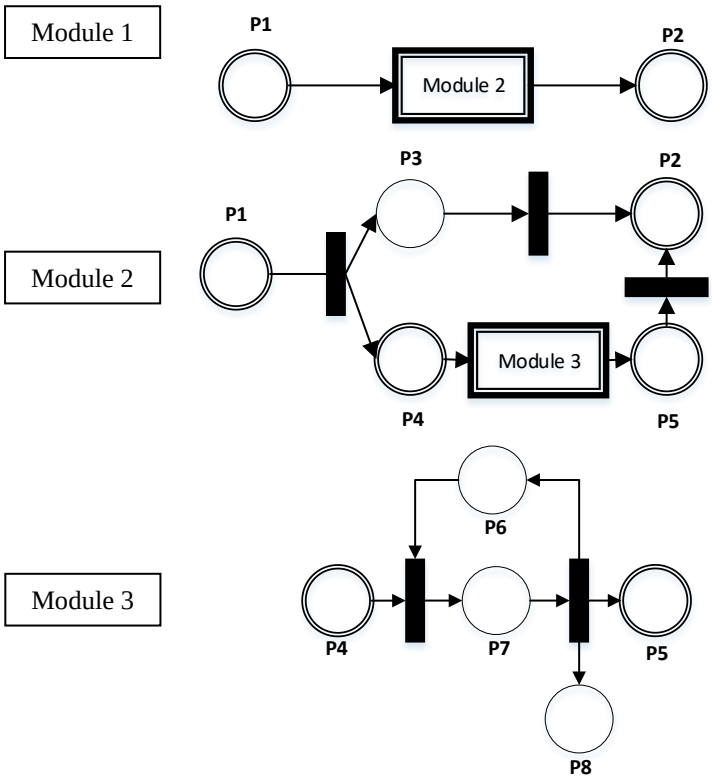


FIGURE 3.11: A SIMPLE PETRI NET



Place	Type
P1	Socket
P2	Socket

Place	Type
P1	Port
P2	Port
P3	Standard
P4	Socket
P5	Socket

Place	Type
P4	Port
P5	Port
P6	Standard
P7	Standard
P8	Standard

TABLE 3.2: A→C PORT AND SOCKET PLACES

FIGURE 3.12: A SIMPLE HIERARCHICAL PETRI NET

3.3.3.2 Coloured Petri Net (CPN)

Another Petri net extension is the coloured Petri net (CPN), again proposed by Jensen and Kristensen [82]. In a CPN the tokens contain information and this information can change during the evaluation of the model. CPNs allow the overall size of the net to be reduced by increasing the complexity of the transitions, arcs and tokens. Transitions in a CPN are able to distinguish between different 'colour' tokens and treat them differently. The colour of input tokens can determine the colour of the output tokens [83], this means that when a transition fires as well as moving the token it can change the 'colour' (information) of the token. The weighting of the arcs is also considerably more complex as only certain types of token will be able to travel along certain arcs. CPNs have been applied to a wide range of areas including production [84] and automotive industry [85] as well as the railway industry [86].

3.3.3.3 Continuous and Hybrid Petri Net

A limitation of traditional Petri nets, in some applications, is that the marking of the system is limited to a discrete number of tokens; this means traditional Petri nets are not elaborate enough to model continuous aspects of some systems. To address this the continuous Petri net has been developed. Continuous Petri nets mark places with a non-negative real number known as its value [87]. Hence the evolution rules for continuous Petri nets are different to a traditional Petri net and are not restricted to integer amounts. Consequently the markings are not forced to be integers [88]. Traditional (discrete) and continuous Petri nets have been combined to form the hybrid Petri net to provide further enhanced capabilities, an example of a hybrid Petri net model is given in [89].

3.3.4 Monte Carlo Simulations

Monte Carlo simulations are widely used to solve many mathematical problems, they can be used to solve Markov and Petri net models. At the heart of any Monte Carlo method is random number generation [90]. Random number generation creates an infinite series of values that are independently and identically distributed (IID). Most computer programs, such as Microsoft Visual Studio, have a built in pseudo random number generator, which simply requires a seed. The seed is the number used to initialise the random number generator, for a given seed the generator will produce the same sequence of pseudo random numbers. A sequence of pseudo random numbers generated by a computer will not be truly random, however their properties will be indistinguishable from IID random variables.

The Monte Carlo method is firmly based on two mathematical theorems: '*The law of large numbers'* and '*the central limit theorem*' [91]. One of the important features of Monte Carlo is that not only can one obtain an estimate of an expected value (by the law of large numbers) but also one can obtain an estimate of the uncertainty in the estimated value (using the central limit theorem).

The confidence limit for the expected value can be determined according to [91]:

$$\bar{x} \pm \frac{\lambda \bar{s}}{\sqrt{N}}, \tag{3.21}$$

where, $\bar{x}$ is the sample mean, $\bar{s}$ is the sample variance, N is the number of simulations, and λ is selected based on the confidence limit chosen, for example 0.95%.

3.3.5 Combination of Methods

When creating a large scale model it may be the case that using one modelling technique for the whole system may not be completely appropriate. A better result could be achieved by combining methods. For example Wootton [92] proposed combining Petri nets with Pseudo-Bond graphs to model the shutdown of nuclear power plants.

In the context of railway modelling it could be beneficial to include physical models within the Petri net to model certain assets, as it would allow continuous modelling of their physical properties. However combining modelling techniques can significantly increase the complexity of the model as an interface between the frameworks is required; transferring data across the interface can be inefficient and time intensive. Having multiple frameworks can also increase the complexity when expressing the model to users.

3.4 Summary

This chapter has provided an introduction to asset management, and explored some of the techniques that are commonly used within asset management. Table 3.3 summaries the simulation methods presented in this chapter, the following chapter will look at their applications in asset management and conclude which is the most appropriate for use in this study.

Method	Characteristic	Benefits	Disadvantages
Markov Model	●State based model ●Memoryless and homogenous	●Can be continuous in time ●Efficient to solve ●Analytical solution can be found (but only for simple models)	●Probability /rate of changing state are fixed ●Considers the probability of being in a state so decision processes based on the actual state cannot be modelled. ●State explosion
Petri Net	●State based model ●Transitions allow state changes based on any distribution	●Not restricted to constant rates, can model an extensive range of processes including Weibull and Gamma process. ●Petri nets simulate the actual state of the system so complex decision processes based on the state of the system can be modelled. ●Flexibility to model a wide range of complex processes.	●Have to be solved numerically, normally using Monte Carlo simulations which can take a large amount of time.
HPN	●Complex system drawn in single diagram	●Allow larger systems to be represented in a single diagram, making them easier to understand.	-
CPN	●Information is stored in tokens, the information can be changed by transitions	●Makes it easier to store asset information such as age and type within tokens.	●Software available to solve them is inflexible. ●The complexity of CPN diagrams can remove the benefit of the diagrammatic side of Petri nets.
Combination of Methods	●Two or more modelling frameworks combined.	●Allows tailored models for each asset, specifically capturing asset properties.	●The interface between the two models can be complex to implement and be computationally expensive. ●Can also increase the complexity when communicating the model to users.

TABLE 3.3: SUMMARY OF MODELLING METHODS

4 Railway Asset Management Models

4.1 Introduction

This chapter will review the application of asset management models to the railway asset classes that will be considered in this thesis (Table 2.7). The asset that has been studied the most is track, whereas literature on some of the other assets is limited.

After literature on the individual asset models has been considered, system models will be reviewed, to gain an understanding of current system models. However there is limited literature on this topic as it has not been studied extensively before, and it forms the novelty in this research. The chapter will conclude by evaluating which of the techniques considered is the most appropriate to create the whole system model.

4.2 Track Geometry Models

Ballasted track deforms due to loading. Most of this deformation will be elastic, however, some of the deformation will be plastic leading to ballast settlement. The settlement means that gradually the track alignment deteriorates, and after a given number of loadings the ballast will require maintenance such as tamping to restore the track to the correct alignment. One of the earliest models for ballast deterioration was proposed by Alva-Hurtado and Selig [93]. The authors developed a deterministic model to predict the settlement of railway ballast under repeated loading. The methodology involved laboratory testing of the ballast material under cyclic conditions, mimicking those in reality, to investigate the elastic and plastic deformation of the ballast. From their experiments they found that, permanent strain was a function of only the permanent strain after the first cycle and the number of cycles as shown in equation (4.1).

$$\varepsilon_N = \varepsilon_1(1 + 0.19\, ln(N)), \tag{4.1}$$

where N is the number of loading cycles, ε_N is the permanent strain after N loading cycles and ε_1 is the permanent strain after the first loading cycle estimated according to equation (4.2).

$$\varepsilon_1 = \varepsilon_v - \varepsilon_r, \tag{4.2}$$

where ε_v is the axial strain under the maximum deviator stress and ε_r is the resilient strain upon unloading.

The model suggests that the permanent strain is proportional to the logarithm of the number of cycles, hence the amount of settlement decreases with each loading, this reflects the fact that, after each loading the amount of plastic deformation in the ballast would be expected to decrease.

Not all experimental works agree with this model however Shenton [94] suggested that the relationship in equation (4.1) was not good at modelling a high number of loadings, instead an alternative model for the settlement, *y*, was proposed as shown in equation (4.3).

$$y = K_1 \sqrt[5]{N} + K_2 N, \tag{4.3}$$

where N is the number of cycles and the constants K_1 and K_2 depend on factors including axle load, rail section, sleeper spacing and foundation stiffness. The values of K_1 and K_2 are chosen such that for values of $N<10^6$ the equation is dominated by the $\sqrt[5]{N}$ term simulating rapid initial degradation, and for values of $N>10^6$ the equation is dominated by N simulating linear degradation.

More recently Lichtberger [95] proposed an exponential function to model longitudinal level decreases with exponential decreasing effectiveness of maintenance following a tamp, these assumptions led to a longitudinal level, *NL*, profile governed by equation (4.4) where *n* increases after each tamping intervention, Figure 4.1 shows a plot of the function.

$$NL(t) = NLinitail_n e^{b_n(t-t_n)}, \quad n = 0,1,2,3,\ldots \tag{4.4}$$

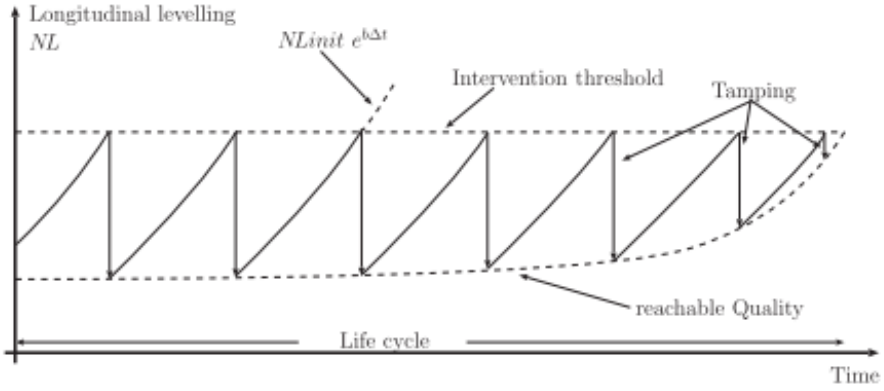


FIGURE 4.1: EVOLUTION OF TRACK PROFILE [95]

Quiroga and Schnieder [96] proposed replacing the constant parameters in equation (4.4), *NLinitail* and *b*, with log-normally distributed stochastic variables to address the stochastic nature of railway deterioration.

A wide range of deterministic models have been developed to consider a wider range of factors that influence track deterioration including speed, tonnage and curvature [97]–[100]. One of the most detailed deterministic models was proposed by Sadeghi and Askarinejad [101]. The authors worked on the Iranian railway network, and assessed the track condition based on track geometry index (TGI) and track structure index (TSI).

The TGI indicates only the geometry conditions of the track, such as profile, twist, gauge and alignment that have a direct influence on track riding comfort. The TGI can be obtained from statistical analysis of track geometry data recorded by track geometry recording cars and is calculated as:

$$TGI = \frac{2UI + TI + 6AI + GI}{10}, \quad (4.5)$$

where UI is the unevenness, TI is the twist, AI is the alignment and GI is the gauge.

On the other hand, the TSI represents the structural conditions of the track, which includes the condition of rail, sleeper, fastening system, subgrade and drainage system. The TSI is defined as:

$$TSI = 0.5CI(low) + 0.35CI(mid) + 0.5CI(high), \quad (4.6)$$

where CI (low), CI (mid) and CI (high) are the lowest, medium and highest amounts from rail condition index, sleeper condition index and ballast condition index, respectively.

Their models for the evolution of TGI and TSI (TGI_2, TSI_2) based on the current TGI and TSI values (TGI_1, TSI_1) are shown in equations (4.7) and (4.8) respectively.

$$\frac{TGI_2}{TGI_1} = \{\alpha_4 e^{\beta_1 V + \beta_2 EMGT + \beta_3 TGI_1}.[\lambda_1 T^4 + \lambda_2 T^3 + \lambda_3 T^2 + \lambda_4 T + 1]\} NL_1, \quad (4.7)$$

$$\frac{TSI_2}{TSI_1} = \{\alpha'_4 e^{\beta'_1 V + \beta'_2 EMGT + \beta'_3 TSI_1}.[\lambda'_1 T^4 + \lambda'_2 T^3 + \lambda'_3 T^2 + \lambda'_4 T + 1]\} NL_1, \quad (4.8)$$

where T is time, V is the line speed, $EMGT$ is the tonnage the line experienced and TGI_1 is the initial geometry value. Finally $\alpha_4, \beta_1, \ldots, \beta_3$ and $\lambda_1, \ldots, \lambda_4$ are constants selected based on the line type.

Selig and Waters [14] observed that two identical sections of track, which had been used and maintained in exactly the same way, may exhibit completely different behaviours. This observation was revolutionary in the way railway asset degradation was modelled. It suggests that there is an inherent degree of randomness involved in the degradation process and hence deterministic models are not appropriate for modelling this phenomenon. As such recent models for railway degradation are almost exclusively stochastic models. By using a stochastic model it is accepted that the future of the system cannot be predicted with certainty.

Track deterioration has been modelled with a wide range of stochastic modelling techniques including Bayesian Networks [102], [103], Markov models [104] and Petri nets [21]. This thesis will focus on state-based models, as Bayesian Networks require the relationship between failures to be well understood, and this information is currently lacking for some railway assets.

Shafahi & Hakhamaneshi [104] proposed a Markov Chain model for the deterioration of track quality, arguing that the probabilistic nature of Markov models made them good for including the randomness associated with the track degradation process. They measured the quality of the track using a track quality index (TQI). Shafahi & Hakhamaneshi used the combined track record index (CTRI) TQI to measure the quality of the track. The CTRI value was between zero and 100, with 100 representing the best possible track, however the index is not defined in their paper. Two assumptions are made about the CTRI scale; firstly

it is assumed that the scores can be grouped into five states, and secondly that these states will be chosen such that it is reasonable to assume that it is not possible for the track to deteriorate by more than one state per year. Therefore the track either remains in the same state or degrades by one. A further assumption of the model is that in year zero all track has a CTRI score close to 100.

The transition probability matrix was found by minimising the sum of the square differences between the values predicted by the model and the values suggested by the data. Their investigations suggested, as expected, that heavily loaded mountainous terrain deteriorated fastest, however the difference between the different conditions was relatively small, with the plain, light loaded track having a CTRI score of ≈30 after 21 years and the heavily-loaded mountainous track having a CTRI score of ≈20 after the same period.

Prescott & Andrews [105] developed on the ideas of Shafahi & Hakhamaneshi by creating a Markov model that includes maintenance and inspection as well as degradation. The states in their model were defined according to the vertical track geometry rather than a TQI. The track was considered to be in one of four conditions; *'good', 'maintenance requested', 'speed restriction imposed'* and '*line closed'*. One of the key differences between the two models was the inclusion of inspections. This meant that each state had an understood and actual condition, and the actual condition would only be known after an inspection. To model this a continuous Markov process with a discrete phase was used. The deterioration was modelled as a Markov process (continuous); however as inspections occur at fixed intervals this process was modelled using a discrete phase.

Prescott & Andrews also considered the effect of maintenance history on the deterioration rates. Instead of returning the system to the '*good*' condition following tamping, the state of the system becomes '*good with one previous tamp*'. The deterioration rates from this state are increased. This was repeated up until the seventh tamp and each time the deterioration rates were increased. After the seventh tamp no new state was considered, and after the seventh tamp there is assumed to be no effect on the deterioration rates. After 30 years it is assumed the track is replaced and hence the system returns to the '*good*' condition state.

Other examples of Markov models in literature include Lyngby [106], who proposed using a 50-state Markov model to investigate twist and Bai et al. [107], who proposed using a Markov model to investigate track irregularities.

As discussed in Chapter 3, two fundamental properties of the Markov process are:

(i) Memoryless property, meaning that all state changes are independent of the past states of the system.
(ii) Homogenous property, meaning all transition rates are constant throughout time.

The literature has shown how these properties can limit the usefulness of Markov models in railway asset management. To create a whole system framework for a railway network a vastly complex model is required, the number of states needed to model this using a Markov

models would be prohibitive. Additionally being restricted to exponentially distributed transitions limits the capability of Markov models in railway asset management.

A more advanced state-based stochastic modelling technique that can be used is Petri nets. Several papers have appeared in the literature using Petri nets to model railway degradation. Petri nets are very flexible and can easily be adapted. Andrews [21] exploited the flexibility of Petri nets by proposing additional aspects to the Petri net framework tailored specifically to modelling railway track degradation. Andrews proposed three new transitions: the reset transition, the conditional transition and the convolution transition, the reset and conditional transitions are used in this research and are explained in section (6.2.3) and section (6.2.4) respectively, when the Petri net models are introduced. These additional transitions are useful when modelling railway deterioration and have been used numerous times in subsequent research [108], [109], [110].

Andrews [21] used his new transitions to create a Petri net to model an eighth mile (220 yard) section of railway. His Petri net model was able to simulate the whole life of ballast in detail; the model included deterioration, inspection, maintenance and renewal. The model explored how ballast degrades over time and how maintenance is used to improve it. Data was analysed from sample track sections around the UK and two key assumptions were made. Firstly, in the time duration that was of interest the relationship between the alignment and time was approximately linear. Secondly, maintenance interventions became less effective with each intervention, after maintenance the track condition was improved but not returned to the '*good as new*' state.

The degradation part of the Petri net is shown in Figure 4.2. There are five track condition places corresponding to various alignment values. Place *P1* represents the track being in new condition. Upon entering place *P2* routine maintenance is requested, in place *P3* emergency maintenance is requested and a TSR is imposed, and finally in place *P4* emergency maintenance is requested and the line is closed. The track starts in the new condition (*P1*). Place *P10* is marked following maintenance (rather than *P1*) to model the fact that the condition is improved but not return to the '*good as new*' state. The main benefit of using a Petri net is that it allows the transitions between places to be modelled using a two parameter Weibull distribution, $W(\beta,\eta)$ rather than just an Exponential distribution. These distribution parameters can be changed based on the state of the system (for example number of previous interventions).

The final part of Andrews' model considers renewals. Various means to decide when a renewal should take place can be considered:

(i) When the ballast condition gets too poor
(ii) After a fixed number of maintenance interventions
(iii) When the time between maintenance intervals gets too short
(iv) After a fixed lifetime *L*

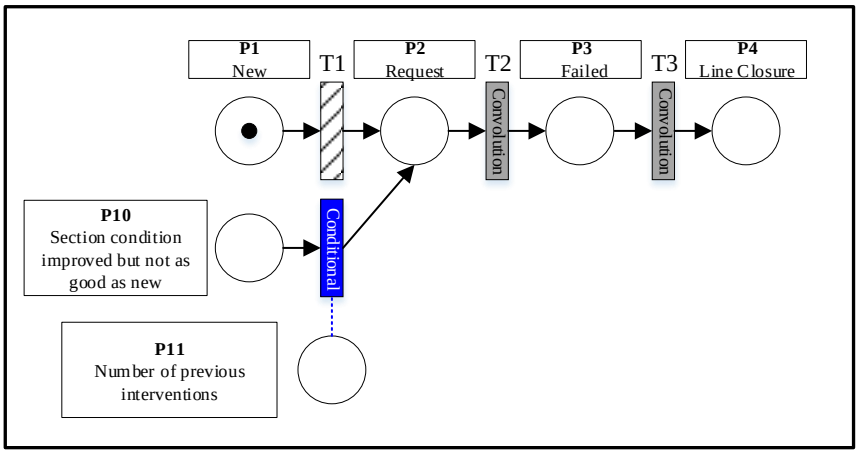


FIGURE 4.2: DEGRADATION PETRI NET MODEL ANDREWS [21]

The effect of altering various parameters is compared to a base case, where the base case is considered the most likely option. The parameters varied were:

(i) Inspection interval.
(ii) Lifetime of the ballast (time between renewals).
(iii) The average time to perform a routine repair.
(iv) Threshold for routine maintenance (Note the threshold of speed restriction and line closure cannot be varied as these are set by the regulator).

A detailed analysis of the model is presented in [111].

As part of his PhD thesis, Audley [109] proposed a Petri net model for ballast alignment. Similar to Andrews [21] his model considers degradation, inspection and maintenance of the track based on the vertical alignment. However, several additions were made by Audley. He considered five condition states in series, '*Very good*', '*Good*', '*Satisfactory*', '*Poor*' and '*Super red*', based on the vertical geometry. He also acknowledged that lower speed lines did not need to be maintained to such a high standard and consequently the criteria for '*Very good*', '*Good*', '*Satisfactory*', '*Poor*' and '*Super red*' was altered depending on the line speed, four line speeds were considered. However the big additions made by Audley were in the capability to model maintenance. He made several advances: firstly stoneblowing as well as tamping was included in his model as a form of maintenance. Secondly he accounted for the fact that maintenance can have varying degrees of success and after maintenance the condition could return to any of the five condition states. Audley went on to examine how the time between inspections and the maintenance performed affects track condition. Audley concluded that allowing stoneblowing straight away greatly reduced the amount of maintenance needed which would suggest a large cost saving. It was also concluded that having a shorter inspection interval (seven days) kept the overall track condition better however there is likely to be a large cost associated with such a high inspection frequency.

Another approach was proposed by Mercier et al. [112]. The authors proposed using the Gamma process to model the longitudinal and transverse levelling. They applied their methodology to a test case on the French railway. They used the longitudinal and transverse levelling to predict when interventions should be carried out. Using the bivariate Gamma process, the time to the next maintenance action was chosen as the maximum value which

ensures that the process stays below the thresholds with a given probability. The choice of the Gamma process was based on engineering judgement.

4.3 Review of Sleeper Models

Sleepers are a fundamental part of the railway network. As discussed in Chapter 2 there are three main types of sleeper construction; concrete, wooden/timber and steel. Concrete sleepers have perhaps been the most widely studied in literature. Most of the literature on concrete sleepers focuses on modelling the behaviour of the sleeper under various different loading scenarios.

You et al. [43] proposed a nonlinear finite element model for determining the structural capacity of a prestressed concrete sleeper with rail seat abrasion, their finite element model is shown in Figure 4.3. They validated their results using laboratory tests. A number of models have also been proposed for fatigue life assessment of concrete sleepers including the Dynamic Accumulation Methods and Damage Equivalent Stress Methods [113].

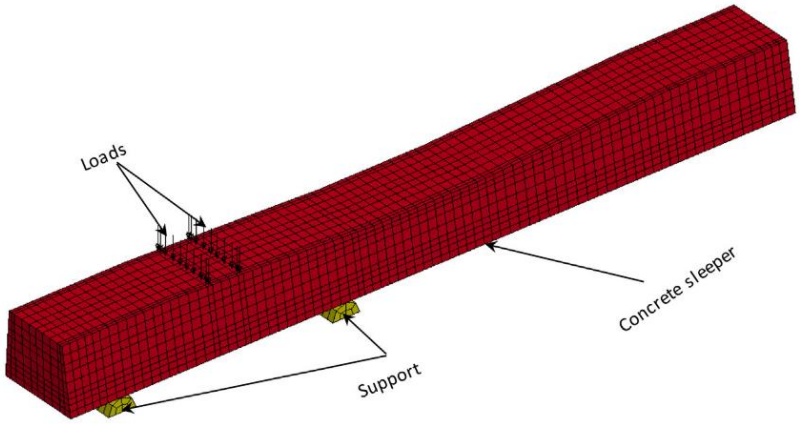


FIGURE 4.3: FINITE ELEMENT MODEL FOR PRESTRESSED CONCRETE SLEEPER YOU ET AL. [43]

Laryea et al. [114] performed a comparison between concrete and steel sleepers under repeated loading cycles, the results are shown in Figure 4.4. It can be seen that for up to about 100,000 loading cycles steel sleepers show less settlement. Beyond this the settlement of steel sleepers starts to exceed concrete sleepers. High levels of displacement are undesirable as lateral displacement of sleepers is a major issue in continuous welded rail (CWR) and is the leading cause of buckling due to the lack of resistance against lateral forces. This is further support of the argument that steel sleepers are best used on lower category lines, with a lower number of loading cycles.

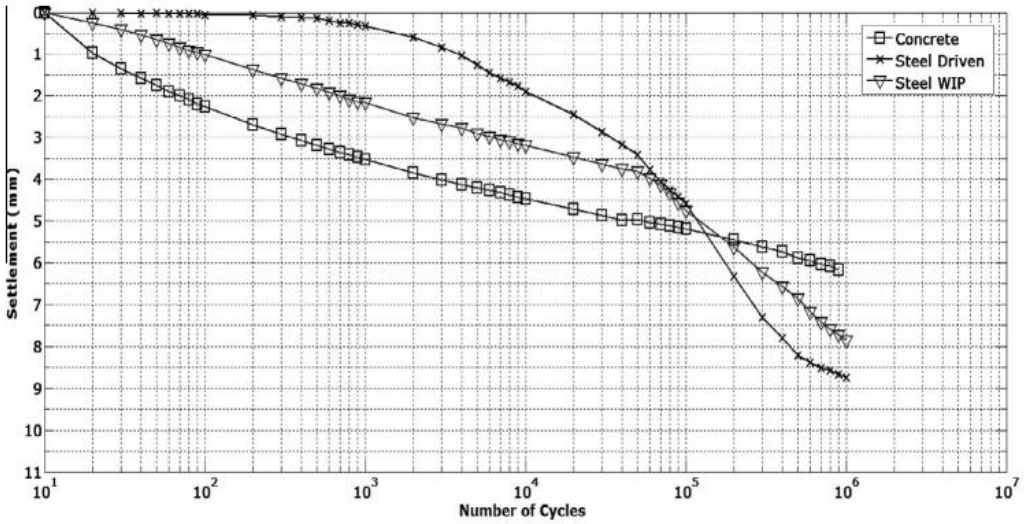


FIGURE 4.4: AVERAGE VERTICAL SETTLEMENT COMPARISON [114]

All of the literature found was used to model the failure modes of concrete sleepers. Literature on modelling the complete lifecycle of sleepers is very limited.

4.4 Review of Tunnel Literature

Tunnels have a very long service life. Figure 4.5 shows the average age of tunnels for a number of European railways, it can be seen that for a number of countries, including the UK, that the average tunnel age is over 100 years.

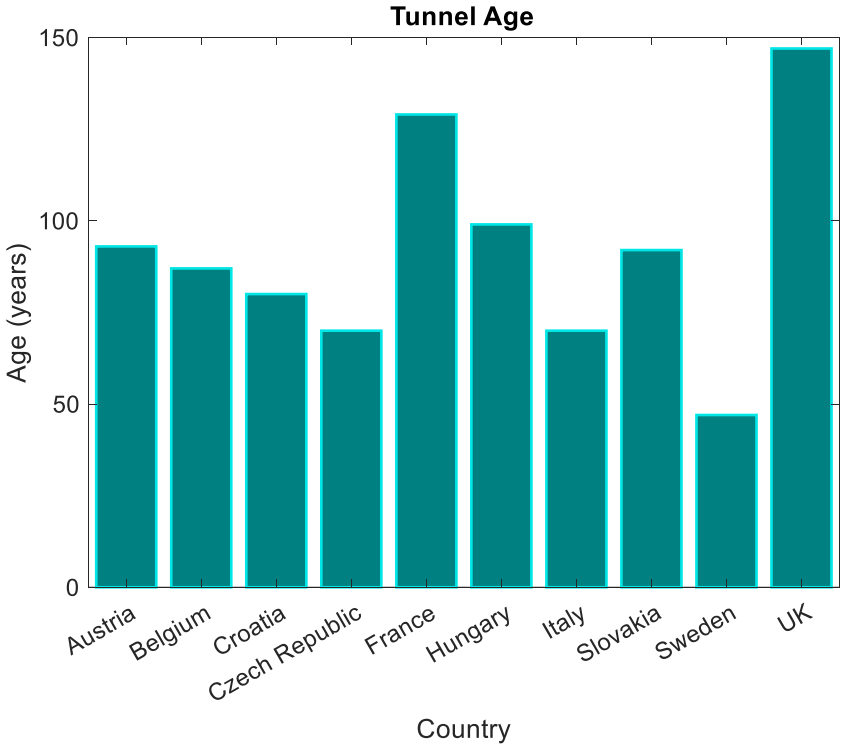


FIGURE 4.5: TUNNEL AGE [115]

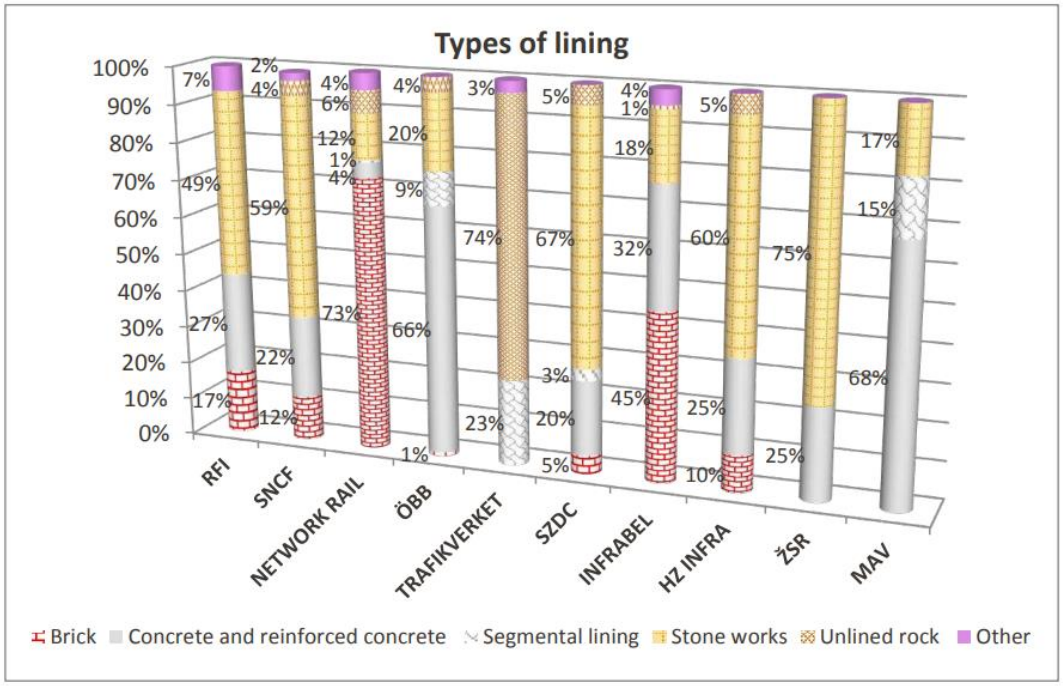


FIGURE 4.6: TUNNEL CONSTRUCTION TYPE [115]

There are many different types of tunnel construction [115], [116] see Figure 4.6. In this thesis the effect the tunnel has on the assets within the tunnel is of primary concern. Maintenance, inspection and degradation of track are all affected if they occur in a tunnel.

Inspection of tunnels is often carried out by specialist machine:
Eurotunnel is getting a new measurement train, 'Vectoor'. Information collected by Vectoor will be used to create big data models capable of evaluating the lifespan of equipment, anticipating breakdowns and developing a predictive approach to maintenance, to further increase the availability of the tunnel. The first carriage of Vectoor is capable of checking rail integrity via ultrasound at a standard speed of between 100km/h and 140km/h. The second contains all the equipment already used for inspecting, measuring and analysing track, catenary, GSM networks, track circuits, sleeper blocks, apron, tunnel lining, etc. [117]. Tunnel can also be inspected using laser profiling (Figure 4.7).

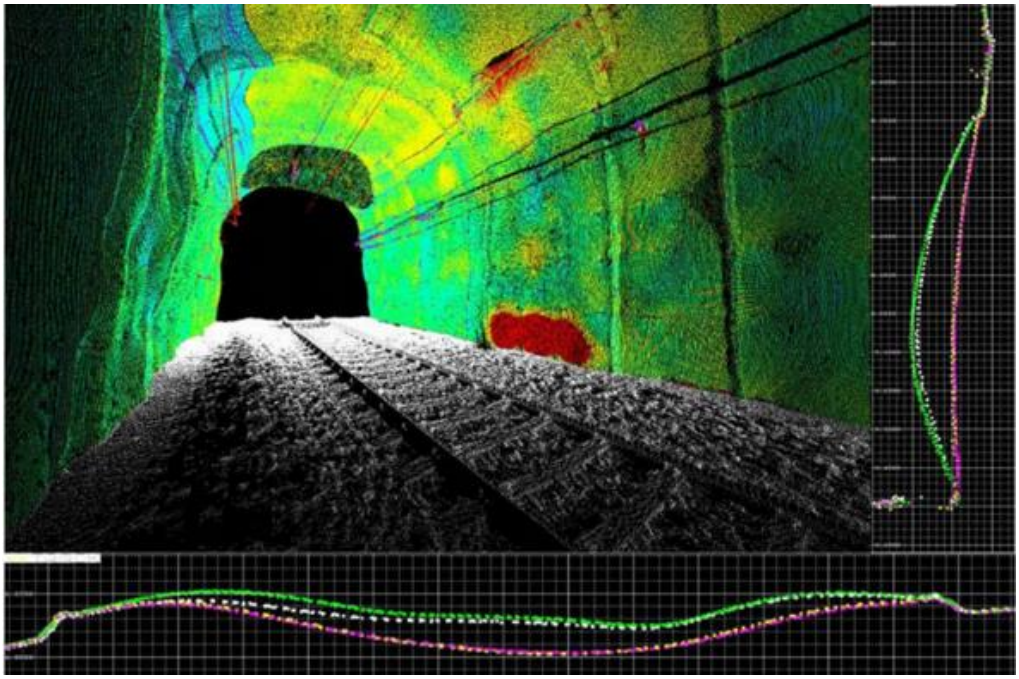


FIGURE 4.7: LASER SCANNING OF RAILWAY TUNNELS IN FINLAND [118]

There are a number of tunnel deterioration modes, these include:

(i) Water infiltration; moisture, leakage and outflow
(ii) Open joints
(iii) Deformed zones
(iv) Horizontal and vertical cracks
(v) Alteration of the surface due to ageing or mechanical strains
(vi) Coating delamination
(vii) Drainage malfunctions

Vibration levels in railway tunnels are also different to standard track [119] and the concrete in tunnels can suffer from sulphate attack [120].

Maintenance in tunnels can be hampered by the damp, dark and cramped conditions. The constraints of working in a confined environment often make it difficult to perform routine maintenance operations on a regular basis, therefore they are often combined with repair works [115].

Maintenance in tunnels can often take longer and require additional equipment (such as lighting and air control). These factors mean that it is often not possible to perform maintenance to such a high standard, for this reason tunnels such as the Kilsby and Stoke tunnel are subject to permanent speed restrictions.

4.5 Review of Switches and Crossings Literature and Models

S&C units allow trains to change tracks and crossover tracks. S&C units tend to have a higher failure rate than plain line track, there are two main reasons for this:

- S&C units contain moving parts

- The forces generated as a train passes over an S&C unit is greater than on the rest of the network

Due to the high number of failures on S&C units they have been studied extensively in literature. Rama and Andrews [53], analysed failures of S&C units to understand their reliability. They found that the Weibull distribution was the best for modelling the lifetime of S&C components, however they observed for many of the S&C components the shape factor was less than one, indicating a decreasing failure rate, which for mechanical components seems unrealistic. They attributed this to a high amount of poor maintenance producing short lifetimes, and concluded that data needs to be obtained for a longer period to completely understand the process.

Condition monitoring has been used extensively in POE analysis to enable the condition to be monitored in real time and to attempt to predict failures [55], [56], [121]. The aim is to replace components before catastrophic failure occurs.

To help reduce the forces at the crossing, the wheel rail interaction has also been studied extensively. Wheel designs have been investigated to find those that are best at reducing deterioration rates [122], [123].

4.6 Whole System Asset Management Applications

Literature on whole system approaches to railway asset management is in its infancy. Both Audley [109] and Prescott and Andrews [110] examined how Petri net models for the vertical geometry for short sections (⅛ mile) could be linked together to form regions and networks. To model this effectively a decision making transition [124] was introduced. The decision making transition was used to generate work orders where maintenance is scheduled based on the location of the maintenance machine (which region it is in) and the severity of the maintenance required.

Audley [109] went on to apply his work to a real section of the UK railway network near Manchester. He modelled 418 plain line 220 yard track sections (52.25 miles) with varying speed limits. As multiple track sections are being considered it allows for opportunistic maintenance to be considered. Opportunistic maintenance allows sections which are spatially close (in the same region) to be tamped early, if there is a section in the region already being tamped. Audley found that the inclusion of maintenance history (many of the sections he modelled had over ten tamps at the start of simulation) significantly influenced his results, and the case study had significantly more interventions than his single track section model. These models provide a good framework to start to build a whole system model, they do consider a larger scale of railway network and some of the benefits of a whole system model are already apparent, however these models only considered one factor, vertical geometry (top), no consideration is given to the rails or other assets within the system.

In other infrastructure disciplines work to develop multi phenomenon-models has been undertaken, this section will review a few of these, in the hope of gaining ideas of how to achieve similar for a railway network.

Shang [125] proposed using a Coloured Petri net to model the deterioration of railway track. By using coloured Petri nets it allowed the system to be modelled differently to Audley and Andrews. Shang was able to create nets for the various different processes such as deterioration and then use different coloured tokens to represent various track components. The work also explored a system model which contained six regions, each region contained two track components. This research shows the first stages of a whole system model however many more track sections need to be considered as well as a wider range of components if a whole system model, useful to asset managers, is to be created.

There has been research into the optimisation of worksites on highways [126], [127]. It is detrimental to close one section of the highway for work and then a short time later close it again to work on another section '*close by*'. Hajdin and Adey [127] attempted to find the optimum work program for a section of highway on the Canton of Vaud, Switzerland. They modelled a 15km section of motorway which consisted of 38 nodes and 37 sections. Traffic was assumed to enter the network at node one and could leave at four of the remaining nodes. They solved the problem using dynamic programing to maximise the objective function (benefit-cost) subject to five conditions. Clemens et al. [128] developed this idea by developing work programs for multiple infrastructure networks within a city including roads. Five infrastructure networks were considered in their research: electricity network, gas network, road network, sewer network and water distribution network. Each of these networks were found to have different properties and so were modelled differently.

4.7 Conclusions and Evaluation of Modelling Techniques

The literature review shows that a huge range of techniques have been explored to simulate railway deterioration. There are two broad classes of modelling technique that have been used to model railway networks; deterministic and stochastic. In terms of simulating railway deterioration many of the early attempts were deterministic; equations were developed to link factors such as tonnage to degradation, based on laboratory experiments. However more recently it has been agreed that there is inherent randomness involved in the deterioration of railway assets. For this reason, stochastic modelling techniques, which are solved through simulation, have grown in popularity among railway asset managers.

The chapter has outlined a number of key features that would be needed in a whole system model:

(i) Be stochastic in nature

Seemingly identical railway assets, under similar conditions, often degrade in very different ways. For this reason a stochastic technique is the most appropriate to create the whole system model.

(ii) Be flexible and modular

The aim of this research is to create a whole system model and investigate the advantages of whole system approaches compared to individual models. For this reason it is a fundamental requirement to have a technique that is flexible and modular to enable parts of the model to be removed and others added with ease.

(iii) Be able to map condition states in an effective way

Many railway operators such as Network Rail assess the condition of their assets according to condition states or indexes; for example ballast quality can be assessed according to the vertical geometry which is grouped into five conditions: '*Good*', 'S*atisfactory*', '*Poor*', '*Very poor*' and '*Super red*'. Any modelling technique chosen must easily be able to model these condition states and the progression between them.

(iv) Be able to simulate a large system in an effective amount of time

The model in this research will need to simulate a very large system so it must be capable of modelling a large and complex system in a reasonable amount of time.

Based on these assumptions it is clear that a simulation method will be needed. Table 4.1 shows a suitability assessment of the methods introduced in Chapter 3 and reviewed in this chapter. Green indicates that the methodology meets the requirement well, yellow or orange means that the methodology does not meet the requirement exactly but meets it to a workable standard. Red indicates the methodology meets the requirement very poorly or not at all.

Table 4.1 shows that Petri nets are the best suited to the needs of this research as they are stochastic in nature and can be easily mapped into a hierarchical structure, which allows modules to be added and removed with ease. Additionally the states of a Petri net are ideal for mapping condition states and, the rates between the condition states are totally flexible. Furthermore there are a range of techniques that can be used to reduce the computation time for solving Petri nets (see Chapter 8).

Technique	Stochastic	Flexible and Modular	Able to Represent Condition States Effectively	Capable of Simulating Large Systems
Deterministic Models	Not stochastic.	Extra terms can be included in equation to model extra parameters.	These techniques cannot represent condition states, only really useful for modelling single asset, single phenomena situations.	The scope that can be considered within a single deterministic model is limited. Possible to make a system model made of various deterministic models however it is then not possible to considered dependencies.
Markov Models	This modelling technique is stochastic in nature.	Extra states can be added to Markov models relatively straight forwardly (minor change to the transition matrix). However adding more states can lead to state space explosion.	The asset condition states can easily be translated into states of a Markov model. However the rates between the states are constant (Exponentially distributed). Additionally modelling maintenance decisions based on the state of the system, is not possible.	As Markov models increase in size the number of states increases exponentially and hence the computation time can become prohibitive.
Petri Net Models	This modelling technique is stochastic in nature.	If a HPN is used modules can be added to a core Petri net with ease.	The asset condition states can easily be translated into places in a Petri net, and the transitions between them can be governed by any distribution.	The simulation time for a Petri net is dependent on a number of factors (see Chapter 8). However effective coding should mean the computation time scales close to linearly as the model size is increased.
Combined Methods	Can be stochastic and deterministic.	Can be flexible to model a wide range of assets with different model types for each asset. However the interface between different model types can be difficult to define and time consuming to simulate. The interface can also be complex to communicate.	Can represent the condition states as well as a continuous condition profile if required.	Can simulate a large range of assets however the interface between different model types can often have significant simulation cost and often only happen at discrete points, leading to the different models becoming siloed.

TABLE 4.1: SUITABILITY EVALUATION OF TECHNIQUES

5 System Analysis

5.1 Introduction

The aim of this thesis is to develop and implement a framework for whole system railway asset management. This chapter will analyse condition records, maintenance records and industry standards, for the assets introduced in Chapter 2, to:

(i) Develop a better understanding of maintenance processes.
(ii) Develop an understanding of the amount of work currently performed by Network Rail, to use as a baseline in the asset models developed.
(iii) Develop an understanding of the six key areas of asset models shown in Figure 5.1, in order to populate the Petri net asset models developed.

The five asset classes considered in this research are: track (including rails, ballast), sleepers (concrete, timber and steel), S&C, signalling and tunnels. Track was chosen as it forms the heart of the railway network. S&C units were considered as they are a critical part of the infrastructure, S&C failure causes significant delays. Tunnels were considered as they can have a significant effect on the track within them. Lastly the signalling system was chosen as it is somewhat different to the other asset classes and forms a silo in its own right.

The main aim of this research is to investigate whole system approaches to railway asset management and not to establish new trends in the deterioration of railway assets through data analysis. Therefore this chapter will only provide a basic analysis to determine reasonable values that can be used as a proof of concept in the whole system model.

Figure 5.1 shows the key information that is required to build railway asset models. This chapter will attempt to quantify each of the six areas based on literature, condition and maintenance records provided by Network Rail, industry standards and engineering judgement.

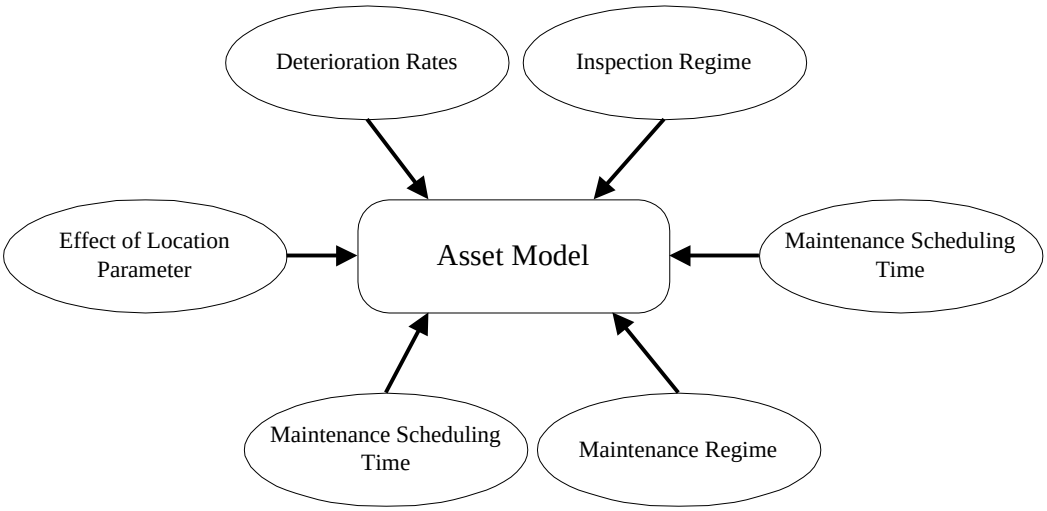


FIGURE 5.1: KEY PARAMETER REQUIRE TO DEVELOP RAILWAY ASSET MODELS

As described in Chapter 2 (see section 2.2), Network Rail classify the network as being in one of seven track categories 1A, 1, …, 6. The deterioration, maintenance and inspection

varies significantly depending on the track category; therefore, where possible, the analysis is divided by track category.

5.2 Data Available and Data Limitations

Network Rail provided various data sources for use in this project. Table 5.1 shows the seven databases that were used and lists the information contained in each. Database seven linked section IDs to Eastings and Northings coordinates which were used to generate maps of the route.

	Database	Records	Overview
1	Track Summary	646,628	A list of all track on the UK network, detail to the yard. Includes: (i) Tonnage (ii) Track category (iii) Rail type (iv) Sleeper type (v) Curvature (vi) Line speed (vii) Station and tunnel locations (viii) Where applicable switch name
2	FMS (2002-2017)	1,000,016	A list of all failures, locations and rectification actions. (All service affecting failures are recorded, but some failures which did not affect service may not be recorded).
3	Ellipse Control Period 4 (CP4) (2009-2014)	18,992,956	A list of maintenance records, including: (i) Job number and description (ii) Raised date (iii) Start date (iv) Yard start (v) Yard end (vi) Yards complete (vii) Hours complete (on site) (viii) Units complete
4	Ellipse Cut Control Period 5 (CP5) (2014-2015)	4,671,304	As above.
5	Geometry Records (2006-2016)	7,820,850	A record of 35 metre and 70 metre filtered vertical and horizontal alignment by Poskey (eighth mile section).
6	GEOGIS S&C Subset	15,028	A list of switches detailing: (i) Type (ii) Size (iii) Crossing angle (iv) Switch name
7	Bletchley Easting and Northings	8,518	Links track IDs to Eastings and Northings co-ordinates.

TABLE 5.1: NETWORK RAIL DATABASES USED IN THIS RESEARCH

5.3 Distribution Fitting

As determining distributions for deterioration is generally difficult, where possible these will be taken from previous literature. For the schedule and repair times, and where previous data on distributions for deterioration do not exist, distributions are determined based on the data sets listed in Table 5.1.

The aim of distribution fitting is to fit some probability distribution to a sample data set, where the distribution selected is the best possible reflection of the population the sample came from. There are multiple different methods of fitting distributions to data, these include:

(i) Method of Moments
(ii) Generalised Method of Moments
(iii) Maximum Likelihood Estimator (MLE)
(iv) Least Square Regression Method

Based on the literature four distributions are considered in this study: Weibull, Lognormal, Normal and Exponential distributions. All of the distributions presented in this chapter were fitted using the ReliaSoft-Weibull++ package [129]. There is no exact rule on which method is best for fitting a distribution to a data set. However as the sample sets in this research were large and some contained censored data, the MLE method was employed in Weibull++ to estimate the parameters.

Having used the MLE method to fit distributions to the data a means of determining which of the distributions is the best fit to the data is needed. There are a range of *goodness of fit tests* that can be used to assess the goodness of fit between a distribution and a data set. Weibull ++ considers three goodness of fit values:

- AVGOF from Kolmogorov-Smirnov
  The modified Kolmogorov-Smirnov is used as the distribution parameters are unknown. The modified Kolmogorov-Smirnov test uses D_{max}, the maximum of the absolute difference between $S_N(t)$ and the fitted cumulative distribution function, $Q(t)$ [130].
- AVPLOT a normalized correlation coefficient (rho)
- LKV likelihood value

For each of the methods, each of the distributions is ranked based on its goodness of fit to the data. From this an overall assessment is given on which distribution is most appropriate. The best distribution was the one chosen. The goodness of fit to the data for the final distribution can also be assessed visually using a probability plot.

The main aim of the data analysis was to make inferences about the population (true) characteristics, θ, based on an estimator, $\hat{\theta}$, determined from a sample of the population. Using the MLE method to fit known distributions such as Weibull to the data observed was simple to implement and for the purpose of this study, to demonstrate the capability of a system model, it was decided that the method provided adequate fitting. Nonetheless, it

should be noted that there are limitations to this method, which should be taken into account when refining the model in the future. Two issues identified were:

(i) Long distribution tails leading to extreme values being sampled.
The Weibull distribution in particular can have a very long right tail, this means there is the possibility when sampling to get an extreme result, values multiple standard deviations from the mean. An implication of this when using a Weibull distribution to model deterioration is that an unrealistically large time between changes of condition state can be obtained. A possible solution to this could be truncating the distribution or resampling values that are more than a given number of standard deviations from the mean.

(ii) Multimodal data sets.
A number of the data sets had multiple modes, this feature cannot be encapsulated with either the Lognormal, Normal, Exponential or Weibull distribution. A possible solution to this issue would be to use an empirical distribution function, to create a cumulative density function based directly on the data. This method would be able to account for the multiple modes and would ensure no values could be sampled outside the range of values observed in the real world data. A limitation of this method is that it is heavily based on the data, and the data may not be a completely accurate representation of reality particularly as the observation period is short compared to the lifetime of many of the assets modelled. An alternative approach could be a bootstrapping approach [131]. For a large sample, the central limit theorem can be used to analytically make inference about the population mean and variance. However, if the sample size is small or if the characteristic of interest is more obscure, for example the difference between the 5^{th} and 95^{th} percentile, then a bootstrapping approach could be considered. Bootstrapping is a computationally intensive, nonparametric technique; it differs from the traditional parametric approach in that it employs large numbers of repetitive computations rather than strong distributional assumptions and analytic formulas.

5.4 Track Analysis

The following sections will explore how the six areas outlined in Figure 5.1 can be quantified for track. As discussed in Chapter 4 there has been significant research in the field of railway track deterioration modelling. The work undertaken by Audley and Andrews [21], [109], [132] is of particular importance as it contains some of the most detailed analysis of Petri net applications to railway track deterioration. The research undertaken by Clarke and Prescott [133] into the factors that influence track deterioration is also of high importance when creating a system model.

5.4.1 Track Deterioration Analysis

Deterioration rates for railway track are affected by many factors, hence determining distributions for the time to degrade is a complex process. This section will explain how the distributions for the time to degrade for ballast and rails were determined.

Ballast Deterioration

The Weibull distributions for the time taken to transition between various ballast condition states (based on the vertical geometry), prior to first tamp, found by Audley and Andrews [132] are used as a baseline. The distribution parameters are adapted slightly as the geometry bands used in this research are slightly different to the ones adopted by Audley and Andrews, additionally the distributions will be divided by track category as opposed to line speed. The distributions used are detailed in Table 5.2 along with the threshold for each quality band and the transitions used to model them in the Petri net model (Chapter 6). The transition notation is explained in Section 6.2. The distribution listed in Table 5.2 were used as a baseline. In the system model they were adjusted based on a location index and the maintenance history, this is discussed in sections 5.4.3 and 5.4.4, respectively.

Category	State	Transition	SD (mm)	Time Unit	Distribution
1A	Good→Satisfactory	CT_7^{T-1A}	>1.7	Days	Weibull(0.80, 1500)
	Satisfactory→Poor	CT_8^{T-1A}	>2.4	Days	Weibull(1.00, 2800)
	Poor→Very poor	CT_9^{T-1A}	>3.0	Days	Weibull(1.10, 3000)
	Very poor→Super red	CT_{10}^{T-1A}	>4.7	Days	Weibull(1.30, 4000)
1	Good→Satisfactory	CT_7^{T-1}	>1.7	Days	Weibull(0.90, 1735)
	Satisfactory→Poor	CT_8^{T-1}	>2.4	Days	Weibull(1.08, 3168)
	Poor→Very poor	CT_9^{T-1}	>3.0	Days	Weibull(1.19,3750)
	Very poor→Super red	CT_{10}^{T-1}	>4.7	Days	Weibull(1.37, 4576)
2	Good→Satisfactory	CT_7^{T-2}	>1.9	Days	Weibull(0.96, 2724)
	Satisfactory→Poor	CT_8^{T-2}	>2.7	Days	Weibull(1.05, 3260)
	Poor→Very poor	CT_9^{T-2}	>3.4	Days	Weibull(1.19, 4008)
	Very poor→Super red	CT_{10}^{T-2}	>5.0	Days	Weibull(1.43, 4805)
3	Good→Satisfactory	CT_7^{T-3}	>2.7	Days	Weibull(0.96, 2503)
	Satisfactory→Poor	CT_8^{T-3}	>3.8	Days	Weibull(1.10, 3284)
	Poor→Very poor	CT_9^{T-3}	>4.8	Days	Weibull(1.2, 63,852)
	Very poor→Super red	CT_{10}^{T-3}	>5.7	Days	Weibull(1.32, 4224)
4	Good→Satisfactory	CT_7^{T-4}	>3.5	Days	Weibull(1.03, 2910)
	Satisfactory→Poor	CT_8^{T-4}	>5.0	Days	Weibull(1.26, 3582)
	Poor→Very poor	CT_9^{T-4}	>5.9	Days	Weibull(1.32, 4224)
	Very poor→Super red	CT_{10}^{T-4}	>6.3	Days	Weibull(1.39, 4528)
5	Good→Satisfactory	CT_7^{T-5}	>4.1	Days	Weibull(1.00, 2800)
	Satisfactory→Poor	CT_8^{T-5}	>5.8	Days	Weibull(1.07, 3079)
	Poor→Very poor	CT_9^{T-5}	>6.7	Days	Weibull(1.16, 3718)
	Very poor→Super red	CT_{10}^{T-5}	>7.2	Days	Weibull(1.20, 4027)
6	Good→Satisfactory	CT_7^{T-6}	>4.3	Days	Weibull(1.05, 3000)
	Satisfactory→Poor	CT_8^{T-6}	>6.1	Days	Weibull(1.11, 3367)
	Poor→Very poor	CT_9^{T-6}	>7.0	Days	Weibull(1.20, 4027)
	Very poor→Super red	CT_{10}^{T-6}	>7.7	Days	Weibull(1.24, 4189)

TABLE 5.2: DISTRIBUTION OF THE TIME TAKEN TO PROGRESS BETWEEN BALLAST CONDITION STATES AND THE TRANSITIONS USED TO MODEL THEM FOR THE SEVEN TRACK CATEGORIES

Rail Deterioration

The rail of the railway track is one of the most important components of the entire track structure and significantly influences maintenance costs [134]. Quantifying the deterioration of rails is more difficult than for ballast, there are a number of reasons for this:

(i) Unlike ballast there is no easy way of measuring the condition of rails.
(ii) Some rail defects can be difficult to detect.
(iii) It is common practice to assess the condition of rails based on the number of defects, however the assessment method is subjective.

Nonetheless there have been several attempts to quantify rail deterioration. Figure 5.2 taken from [135] shows the probability of various defects developing over time (the UIC code definitions are given in Table 5.3). It can be seen that the defects develop quickest between six and 12 years, up until six years there is a less than 15% chance of any of the defects occurring, however after 12 years all the defects (with the exception of code 411) are well established (Between 35% and 95% likelihood depending on defect type).

Several studies have been undertaken to estimate the service life of rails. Figure 5.3, taken from Kumar et al. [134], shows the optimum renewal tonnage in million gross tonnes (MGT) with respect to LCC. The figure shows the function is minimised around 350 MGT. Using the optimum value of about 350 MGT, the study suggests that for a route experiencing 25 million gross tonnes per annum it would be expected to need replacing after 14 years.

Network Rail service life estimations for rail are 20-35 years for a rail experiencing 25 MGPTA. This value is somewhat higher than the values suggested by Vandoorne and Gra [134] and Kumar et al. [135], this is likely to be due to their research being based on heavy haul routes, where there would be less frequent, but heavier trains.

Based on the service life estimations the distribution of the time taken for various defects to occur were estimated for use as a proof of concept in the system model. The distributions chosen for Category 1A track are shown in Table 5.4. The values for the remaining categories are shown in Appendix B-1.1→B-1.5. The rail Petri net model is introduced in section 6.3.1.2.

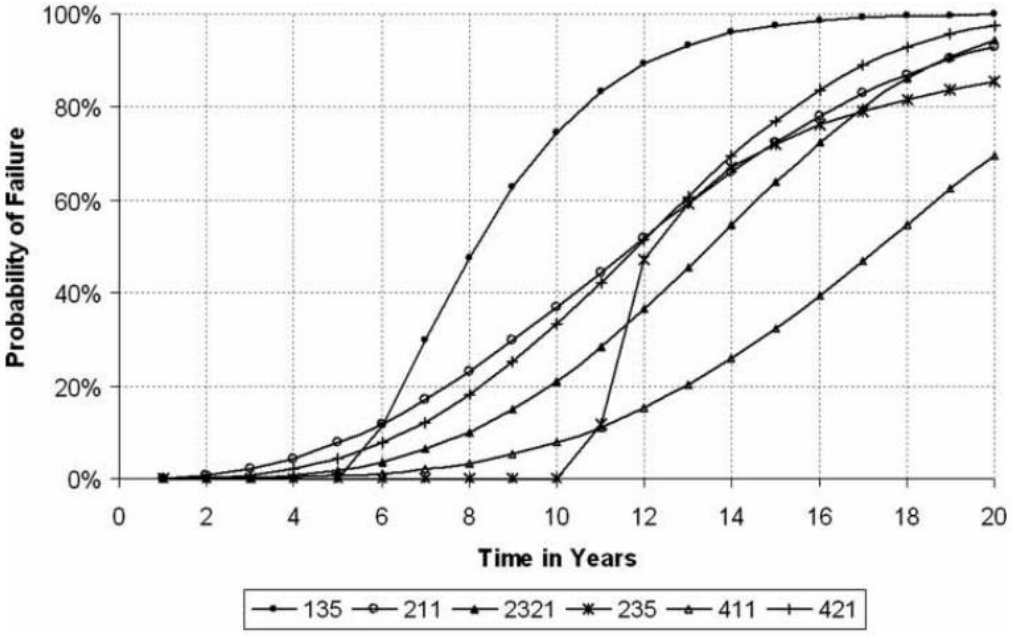


FIGURE 5.2 PROBABILITY OF FAILURE FOR DIFFERENT DEFECT TYPES (LIST IN TABLE 5.3) (25 MGT PER YEAR TRAFFIC FLOW) [135]

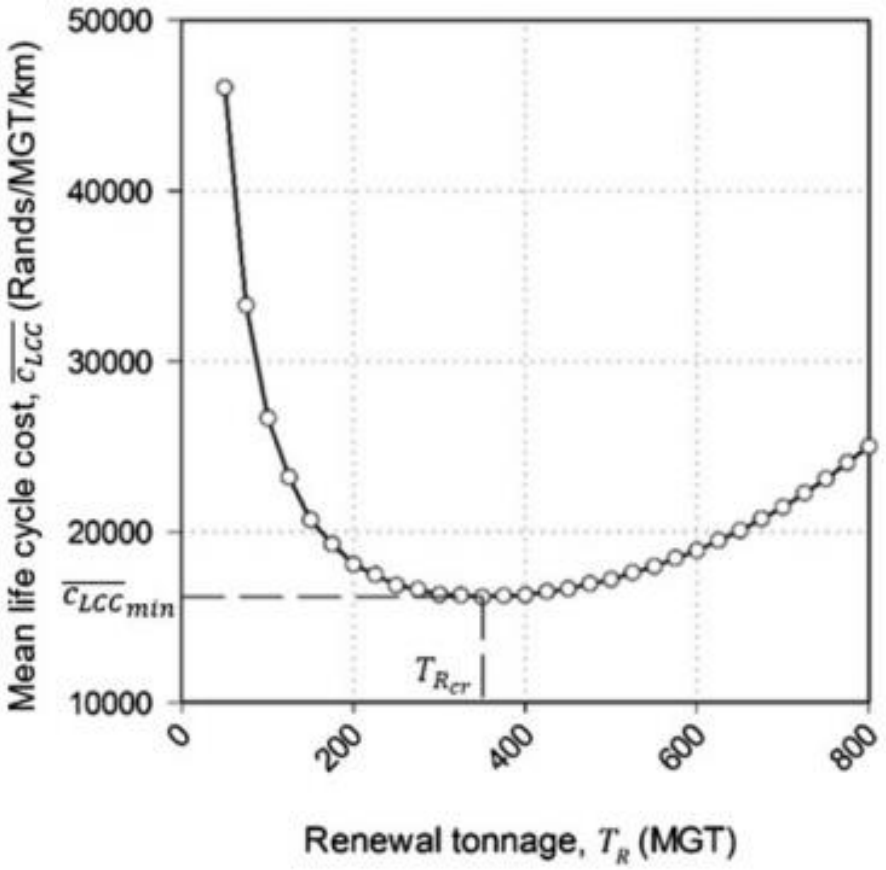


FIGURE 5.3: MEAN LCC VERSUS RENEWAL TONNAGE [134]

UIC Defect Code	Description
Defect code 135	Star cracking of fishbolt holes, this defect consists of progressive cracks that radiate from the fishbolt hole. They are mostly located near the rail ends.
Defect code 211	Progressive transverse cracking (kidney-shaped fatigue crack), this defect develops from a defect inside the rail head from an internal horizontal crack or deep shelling of the gauge corner.
Defect code 2321	Horizontal cracking at the web-head filler radius. Thus crack initially develops in the rail web, parallel to the web-head fillet radius and may curve either upwards or downwards as it progresses.
Defect code 235	Cracking around the holes other than fishbolt holes, this defect has the same appearance as that of defect code 135, but they occur away from the rail ends.
Defect code 421	Transverse cracking of the profile, this is a welding and resurfacing defect occurring in near the thermal welding.
Defect code 411	Transverse cracking of the profile it's a resurfacing defect occurring in electric flash-but welding. The crack develops in the weld cross-section either from an internal defect of the head in the weld or from a defect located in the foot of the rail.

TABLE 5.3: UIC RAIL DEFECT CODES

Category	State	Transition	Time Unit	Distribution
1A	New→ Minor Surface Defects	CT_{11}^{T-1A}	Days	Weibull(1.7, 455)
	Minor Surface Defects→ Major Surface Defects	CT_{12}^{T-1A}	Days	Weibull(1.7, 200)
	New→ Minor Transverse Defects	CT_{13}^{T-1A}	Days	Weibull(1.7, 435)
	Minor Transverse Defects → Major Transverse Defects	CT_{14}^{T-1A}	Days	Weibull(1.7, 195)
	Minor Surface Defects→ Surface Defects and Transverse Defects	CT_{15}^{T-1A}	Days	Weibull(1.7, 215)
	Major Surface Defects→ Major Surface Defects and Transverse Defects	CT_{16}^{T-1A}	Days	Weibull(1.7, 315)
	Minor Transverse Defects → Surface Defects and Transverse Defects	CT_{17}^{T-1A}	Days	Weibull(1.7, 215)
	Major Transverse Defects → Major Surface Defects and Transverse Defects	CT_{18}^{T-1A}	Days	Weibull(1.7, 315)
	Surface Defects and transverse → Major Surface Defects and Transverse Defects	CT_{19}^{T-1A}	Days	Weibull(1.7, 300)
	Major Surface Defects and Transverse Defects→ Serious Faults	CT_{20}^{T-1A}	Days	Weibull(1.7, 150)

TABLE 5.4: CATEGORY 1A ESTIMATED RAIL DETERIORATION DISTRIBUTIONS

5.4.2 Track Maintenance Analysis

This section will provide an analysis of the track maintenance regimes based on Network Rail maintenance records. There are three main objectives of the analysis in this section:

(i) Develop a better understanding of the maintenance process.

(ii) Determine distributions for the time to schedule and complete track maintenance which can be used to populate the asset models.

(iii) Establish the volume of track maintenance currently being performed by Network Rail, to help validate the models.

To fulfil these aims four areas were analysed:

- Work volumes: the average amount of work that is currently performed each year by Network Rail.
- Scheduling time: the number of days between a job being raised and maintenance being performed.
- Completion time/active repair time (ART): the number of hours spent on site performing the maintenance.
- Work lengths: the average number of yards currently maintained during an intervention.

5.4.2.1 Tamping Analysis

There were 22,978 tamping records, detailing the length of track tamped and the amount of time taken, recorded for Control Period 4 (CP4) (2009→2014). The tamping records were grouped by track category. This process required a number of steps as the *Ellipse* records were only recorded by start and end yards and did not contain Poskey or Track ID information.

A visual inspection of the tamping records highlighted some suspicious results regarding the yards recorded and the hours on site. In some cases to have repaired the number of yards recorded in the time listed was not realistic. There are two possible reasons for this:

(i) Several small sections were tamped within the length of track recorded in the database rather than the whole section.
(ii) Data recorded inaccurately.

Regardless of the cause these records should not be used in the analysis, as it is not possible to ascertain exactly how much track was tamped during these interventions. To address this a filter was added to the data whereby any record where the rate equated to more than five miles being tamped in an hour was removed. In the rest of this study this will be referred to as the '*speed filter'*. The *speed filter* caused about 900 tamping records (4%) to be removed.

Volume of Tamping Performed Each Year

The tamping records were analysed to determine the number of yards tamped in CP4. The records were subdivided by track category. However as the network is not split evenly between the track categories (see Table 2.1), to allow comparison between track categories, the amount tamped per year as a fraction of the total length of the category is expressed. For example; there are 780.33 miles of Category 1A track and, in CP4, 1015.94 miles of Category 1A track was tamped. Hence, approximately 203.19 miles of the Category 1A track was tamped each year, thus on average 26.04% of Category 1A track is tamped each year. From this it can be concluded that Category 1A track would be tamped on average once every 3.84 years. By contrast, only 4.99% of the Category 6 track was tamped per year meaning that the Category 6 track would be expected to last up to 20 years between tamps.

Figure 5.4 shows the percentage of track tamped by category per year (based on the CP4 average). The figure shows a strong correlation between track category and frequency of tamping; the higher the track category the more regularly it is tamped. This would be

expected as higher category tracks have higher loads, faster speeds and need to be maintained to a higher standard.

To investigate the volumes further, and to validate the assumption that tamping volumes per year are approximately constant, the volumes were subdivided by year; the results are shown in Figure 5.5. It can be seen that the values remain approximately constant from 2009 to 2014. The large spike in Category 1A is likely to have been caused by an enhancement project.

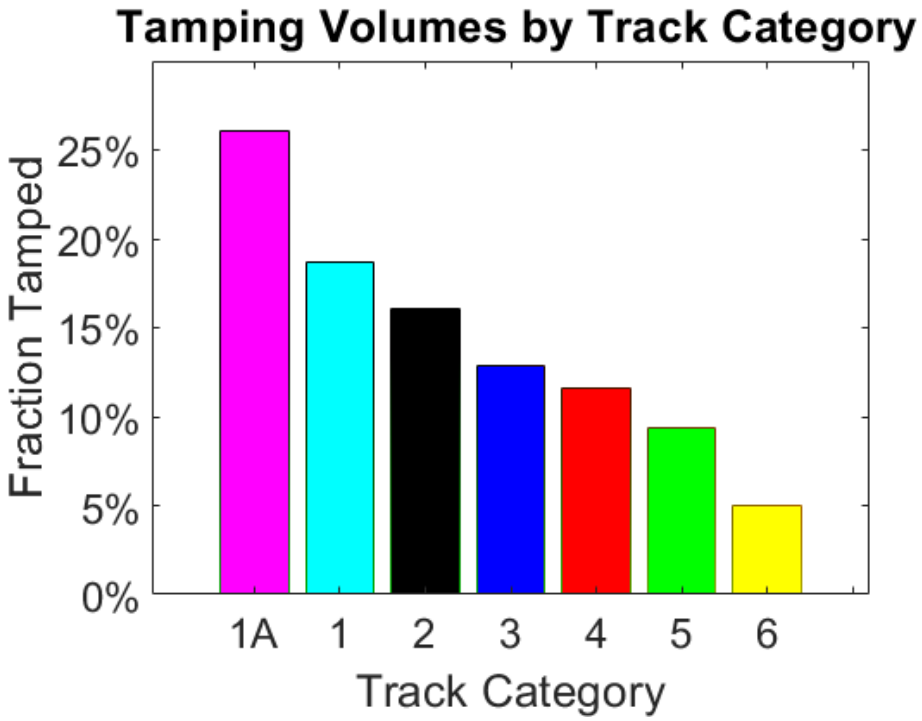


FIGURE 5.4 YEARLY AVERAGE TAMPING VOLUMES

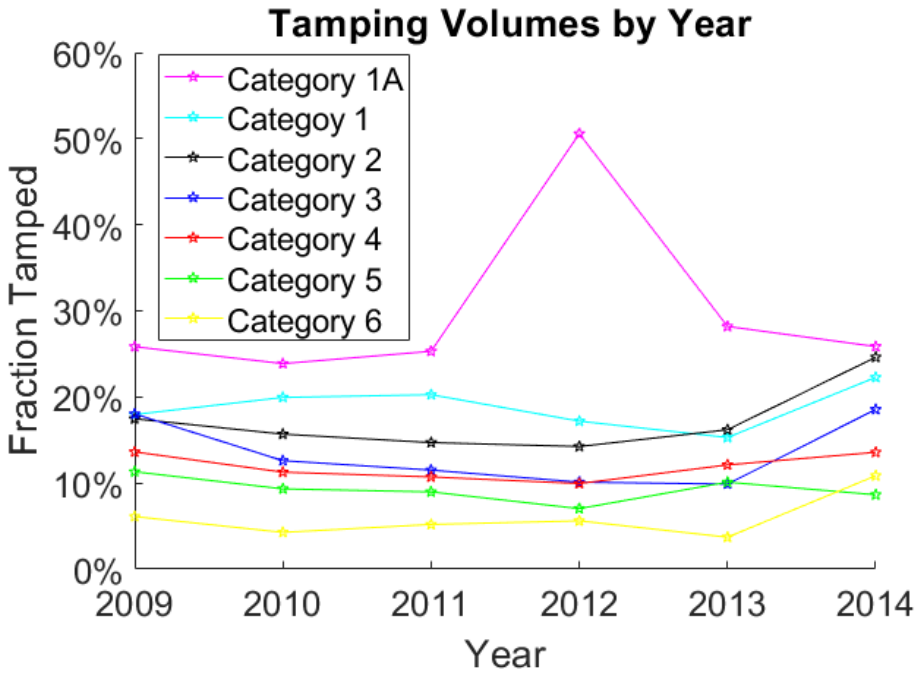


FIGURE 5.5 TAMPING VOLUMES BY TRACK CATEGORY 2009 →2014

Scheduling Time

The schedule time was evaluated as the number of days between the *raised date* and the *start date.* An additional filter was applied whereby records with a non-positive schedule time were removed from the analysis. This was done as these records were assumed to be incorrect or refer to opportunistic work which would need to be modelled differently.

To investigate the schedule time further, it was decided to look at the condition of the assets at the time work was requested. The alignment quality band ('*Good*', '*Satisfactory*'; '*Poor*', '*Very poor*', '*Super red'*) at the time the work was requested, was explored. Using this information the schedule times were split into two groups '*Normal'*, where the ballast was in '*Good*', '*Satisfactory*' or '*Poor*'; and '*Emergency*' when the ballast condition was '*Very poor'* or '*Super red'*. Figure 5.6 and Figure 5.7 show the probability density function (PDF) of the distributions for the schedule time of *'Normal'* and '*Emergency*' maintenance for the seven track categories considered. The distribution parameters are shown in Table 5.5 along with the transitions used to model them in the Petri net model.

There are clear differences between the '*Normal*' and '*Emergency*' categories, however, it is difficult to quantify any relationships as there are a range of factors that influence them including traffic density and traffic type.

Active Repair Time (ART)

The distributions for the ART were determined based on the '*hours completed*' listed in ellipse. Figure 5.8 shows, the PDF of the distribution for, the ART of each track category. The distribution parameters are listed in Table 5.6 along with the transitions used to model them.

To assess the goodness of fit, the data was plotted alongside the distribution fitted and the Weibull ++ package was used to generate quantile-quantile plots or probability plots [136]. Figure 5.9 shows a plot of the frequency density alongside the distribution PDF for the ART, for tamping, for each of categories 1A→6. It can be seen that the initial increase in the ART is captured well for all categories, however in all cases the distribution decreases faster than the data. Category 1A has the best fit between the distribution and the data. As mentioned there is some evidence of multiple modes particularly for categories 4 and 5, although the fit is good enough for the purpose of this research alternative methods such as an empirical distribution could be considered. Figure 5.10 shows the probability plot produced in Weibull++, which can be used to visually assess the goodness of fit. It can be observed again that Category 1A line has the best fit to the data, Category 1 also performs well in the probability plot. For lower categories there is a good fit in the centre but considerable deviation in the bottom tail.

The Weibull++ package was also used to determine the correlation coefficient, ρ, for the fitted distribution. The correlation coefficient is a measure of how well the linear regression model (the probability line) fits the data. In the case of life data analysis, it is a measure of the strength of the linear relation (correlation) between the median ranks and the data. A

value of one indicates perfect positive correlation and a value of minus one indicates perfect negative correlation. A value of zero indicates no correlation. The ρ value for the distributions found for the ART are shown in Table 5.7, it can be seen that all values are close to 1 suggesting a good fit to the data.

Category	Type	Transition	Sample Size	Time Unit	Distribution
1A	Normal	T_{19}^{T-1A}	1302	Days	Lognormal(3.505, 1.563)
	Emergency	T_{22}^{T-1A}	109	Days	Lognormal(2.671, 1.699)
1	Normal	T_{19}^{T-1}	3012	Days	Lognormal(3.215, 1.689)
	Emergency	T_{22}^{T-1}	207	Days	Lognormal(3.220, 1.801)
2	Normal	T_{19}^{T-2}	3626	Days	Lognormal(2.710, 1.562)
	Emergency	T_{22}^{T-2}	217	Days	Lognormal(2.662, 1.531)
3	Normal	T_{19}^{T-3}	3604	Days	Lognormal(3.029,1.729)
	Emergency	T_{22}^{T-3}	161	Days	Lognormal(2.838, 1.710)
4	Normal	T_{19}^{T-4}	2542	Days	Lognormal(3.288, 1.770)
	Emergency	T_{22}^{T-4}	94	Days	Lognormal(3.292, 1.816)
5	Normal	T_{19}^{T-5}	1780	Days	Lognormal(3.332, 1.808)
	Emergency	T_{22}^{T-5}	77	Days	Lognormal(3.085, 1.884)
6	Normal	T_{19}^{T-6}	146	Days	Lognormal(2.880, 1.756)
	Emergency	T_{22}^{T-6}	5	Days	–

TABLE 5.5: SCHEDULE TIME FOR 'NORMAL' AND 'EMERGENCY' TAMPING MAINTENANCE

Category	Transition	Sample Size	Time Unit	Distribution
1A	$RT_0^{T-1A}, RT_1^{T-1A}, RT_2^{T-1A}$	1604	Hours	Lognormal(1.029, 0.742)
1	$RT_0^{T-1}, RT_1^{T-1}, RT_2^{T-1}$	3701	Hours	Lognormal(0.949, 0.724)
2	$RT_0^{T-2}, RT_1^{T-2}, RT_2^{T-2}$	4736	Hours	Lognormal(0.868, 0.756)
3	$RT_0^{T-3}, RT_1^{T-3}, RT_2^{T-3}$	4705	Hours	Lognormal(0.820, 0.780)
4	$RT_0^{T-4}, RT_1^{T-4}, RT_2^{T-4}$	3437	Hours	Lognormal(0.923, 0.783)
5	$RT_0^{T-5}, RT_1^{T-5}, RT_2^{T-5}$	2612	Hours	Lognormal(0.910, 0.885)
6	$RT_0^{T-6}, RT_1^{T-6}, RT_2^{T-6}$	503	Hours	Weibull(2.911, 1.029)

TABLE 5.6: ART DISTRIBUTIONS AND TRANSITIONS FOR TAMPING MAINTENANCE

Category	Distribution	Correlation coefficient, ρ
1A	Lognormal	0.9898
1	Lognormal	0.9901
2	Lognormal	0.9816
3	Lognormal	0.9690
4	Lognormal	0.9741
5	Lognormal	0.9663
6	Weibull	0.9841

TABLE 5.7: CORRELATION COEFFICIENT, P, FOR THE ART DISTRIBUTIONS SHOWN IN TABLE 5.6

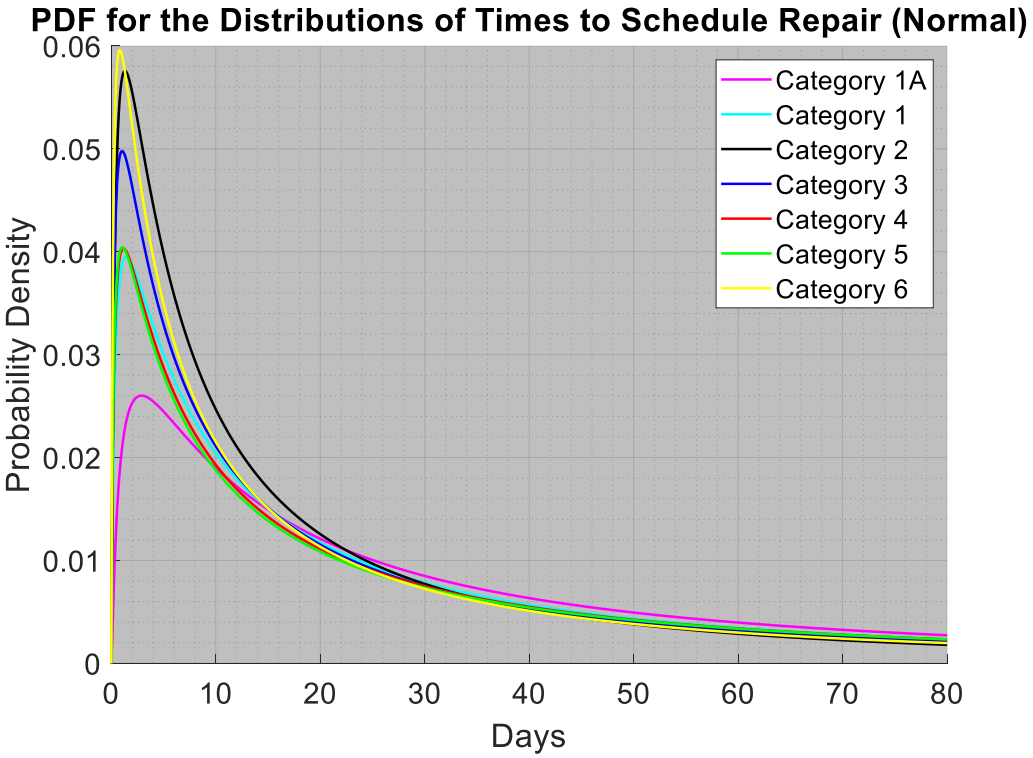


FIGURE 5.6: TIME TO SCHEDULE TAMPING BY TRACK CATEGORY CP4 '*NORMAL*'

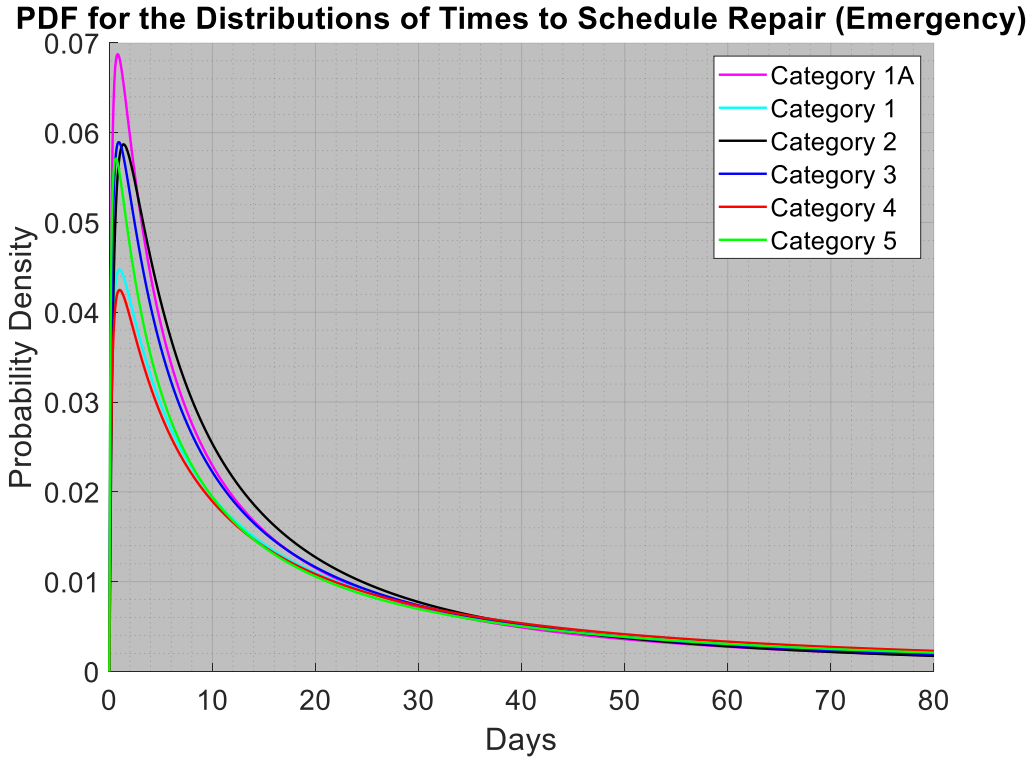


FIGURE 5.7: TIME TO SCHEDULE TAMPING BY TRACK CATEGORY CP4 '*EMERGENCY*'

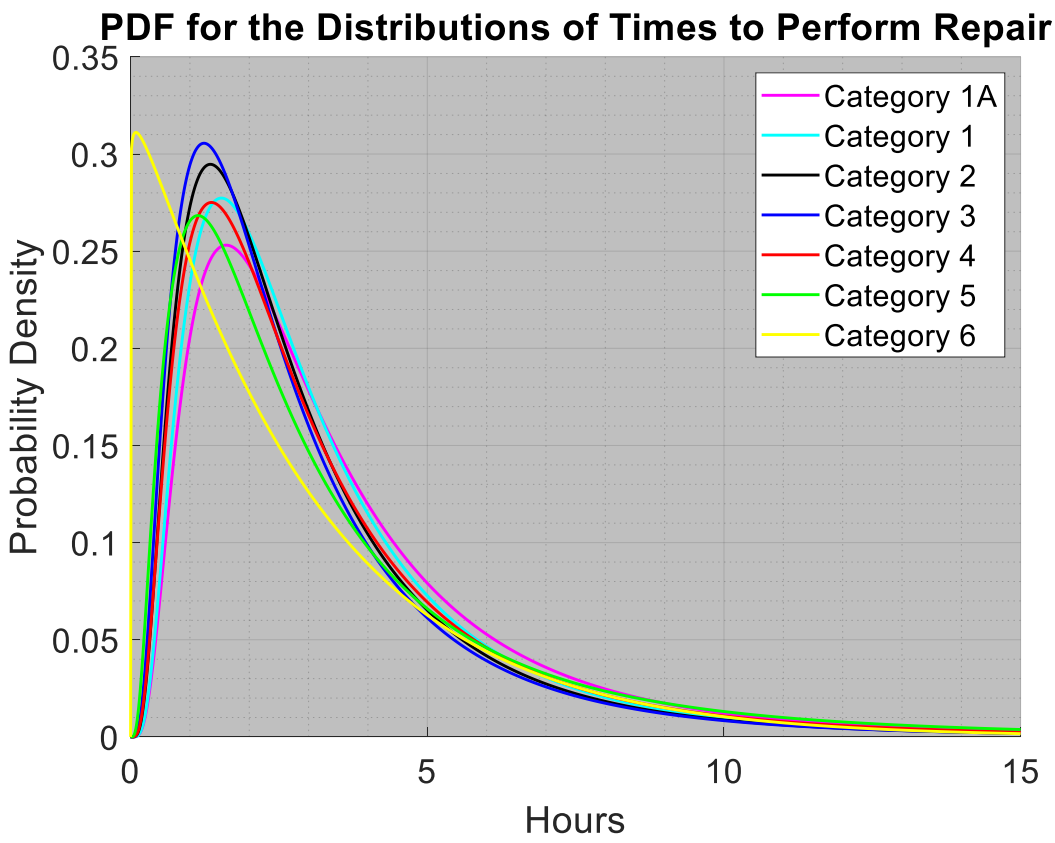


FIGURE 5.8: ART FOR TAMPING BY TRACK CATEGORY CP4

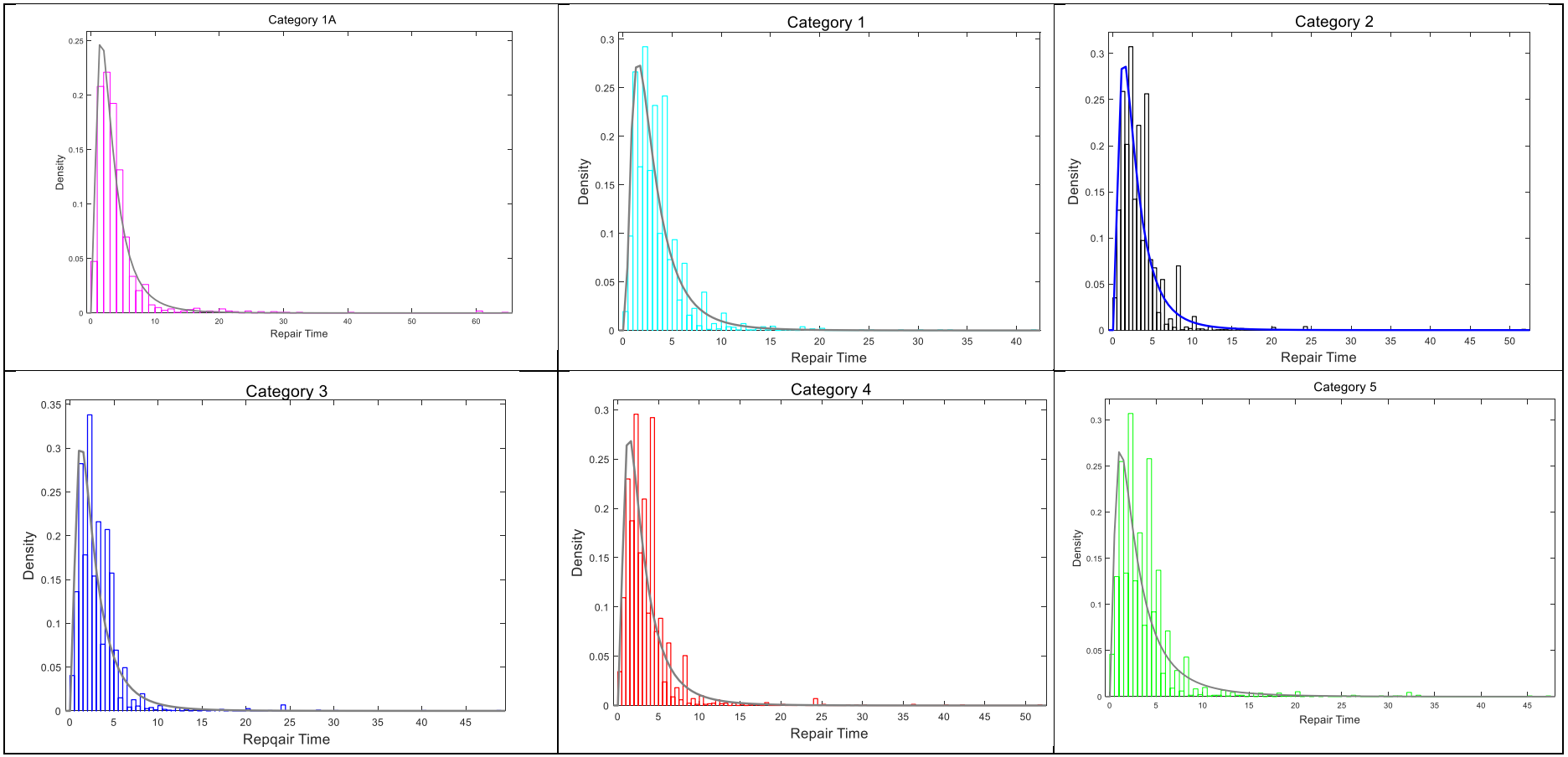


FIGURE 5.9: COMPARISON OF DATA AND DISTRIBUTION FIT FOR ART FOR CATEGORIES 1A →5

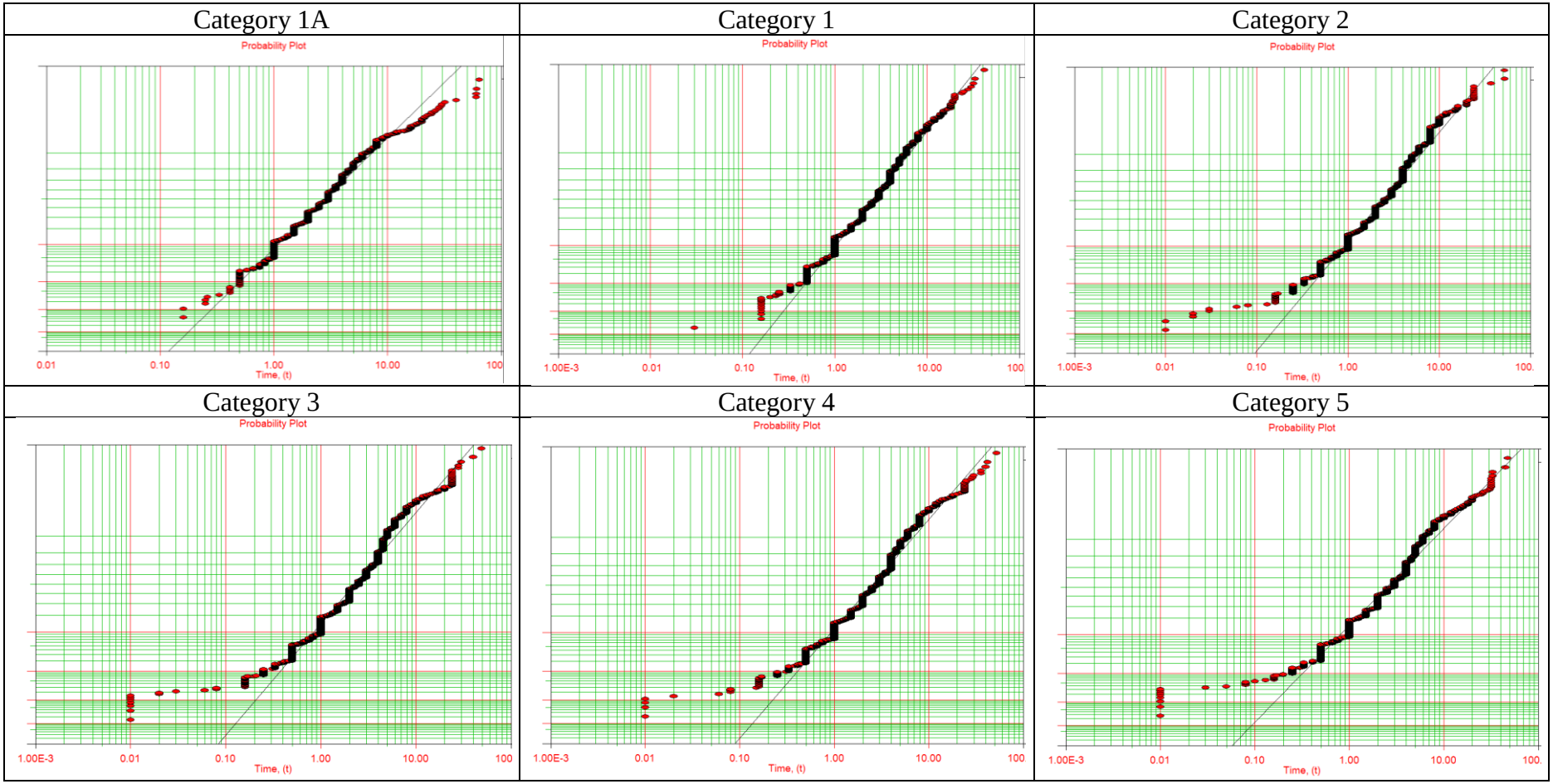


FIGURE 5.10: PROBABILITY PLOT[136] FOR THE ACTIVE REPAIR TIME FOR TAMPING

Length of Track Maintained During an Intervention

The amount of track tamped during an intervention varies significantly. Maintenance records were analysed to determine the length of track maintained; calculated by subtracting the *start yard* from the *end yard*. The mean, μ, and SD, σ, for the length of track tamped for each category is shown in Table 5.8. From this two key observations were made:

(i) There is significant variation in the length tamped.
(ii) In most cases more than one section (220 yards) is tamped during an intervention.

To allow modelling to be as accurate as possible, the length of tamping performed during an intervention was investigated further. The length tamped was converted from yards to eighth mile sections. The section lengths were then grouped into 11 bins: one section, two sections, three sections,..., nine sections, ten sections and more than ten sections.

Figure 5.11 shows the proportion in each of the bins, subdivided by track category. It can be seen that about 5 % of intervention (1200 records) reported more than ten sections tamped (more than 2200 yards). These are likely to have been completed during an extended possession, for example at Christmas or Easter or as part of an enhancement project. It can also be observed that there is a relationship between the length tamped and the track category; the length tamped for Category 6 is often short, in almost 60% of cases only one or two sections were tamped. However for Category 1A, in less than a quarter of cases, only one or two sections were tamped. Network Rail engineers explained a possible reason for this; when track is tamped the track is normally raised and realigned. The raising can cause a '*bump*' between the section that has been tamped and the section that has not, for Category 1A lines it is very important that this '*bump'* does not occur, and so extra work is undertaken to ensure there is a smooth transition between tamped and untamped track. For this reason it is preferential to tamp longer sections for Category 1A lines. Whereas for Category 6 lines the '*bump'* is much less of an issue.

Category	Sample Size	Mean	SD
1A	1644	5.204	7.147
1	3762	5.368	5.657
2	4780	4.963	4.560
3	4747	4.885	7.639
4	3469	5.344	9.640
5	2651	4.393	6.743
6	512	4.234	10.087

TABLE 5.8: NUMBER OF SECTION TAMPED BY TRACK CATEGORY

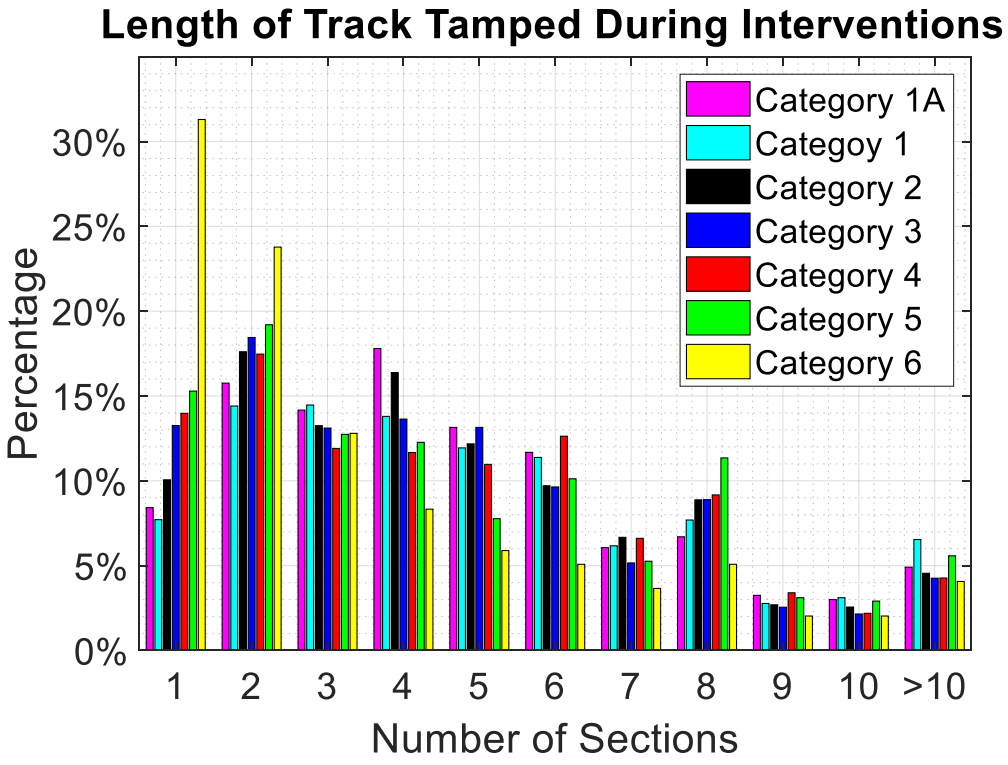


FIGURE 5.11: PROPORTION OF THE NUMBER OF SECTIONS TAMPED

5.4.2.2 Stoneblowing

There were 7565 stoneblowing records for CP4, 184 were removed by the *speed filter* (applied to records where over five miles of track was stoneblown in an hour or less). Stoneblowing is an alternative form of track maintenance; it is used much more widely in the UK than other countries, it is often used to extend the life of heavily fouled ballast [25].

Volumes of Stoneblowing Performed Each Year

As with tamping it was important to get a handle on the volume of stoneblowing currently performed by Network Rail, this would be used as a baseline in the proposed Petri net model. The volume of work was assessed in the same way as for tamping; using the percentage maintained each year for each track category, the results are shown in Figure 5.12. Unlike tamping there is not such a straightforward trend. The proportion of Category 1A line is lower than Category 1 and Category 2, this is due to stoneblowing not being able to deliver the high quality of alignment required for Category 1A lines. Stoneblowing is often used to extend the life of heavily fouled ballast, which explains why it may be used disproportionally more on Category 6 routes. Another important observation is that broadly speaking tamping is performed three times as often as stoneblowing.

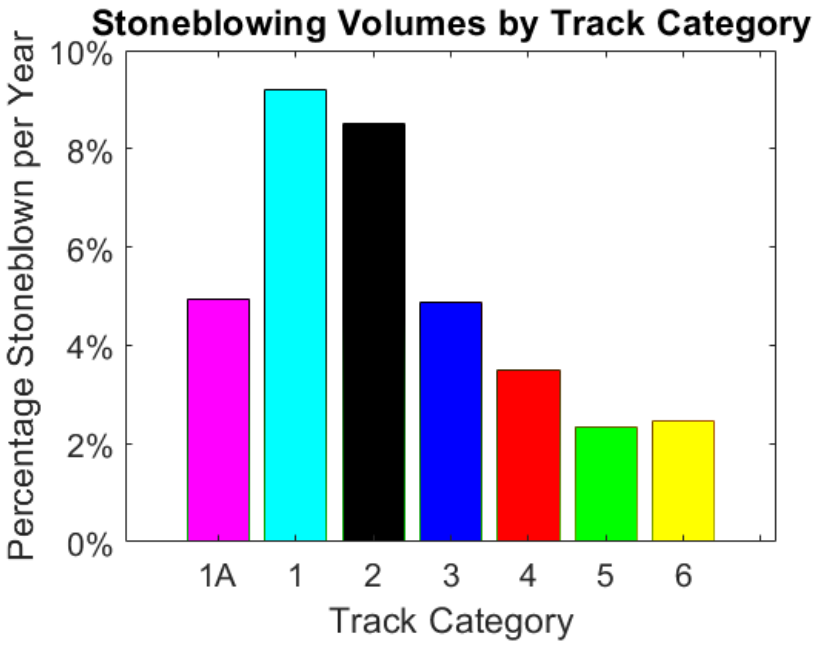


FIGURE 5.12: AVERAGE STONEBLOWING VOLUME PER YEAR CP4

Scheduling Time

Similar to tamping the time to schedule maintenance, was divided into '*Emergency*' and '*Normal*' priority, based on the condition of the ballast at the time maintenance was requested. The distribution of the time to schedule stoneblowing for the seven track categories for '*Normal*' and '*Emergency*' priority are shown in Figure 5.13 and Figure 5.14 respectively. The parameter values are shown in Table 5.9 along with the transitions used to model them in the Petri net.

Category	Type	Transition	Sample Size	Time Unit	Distribution
1A	Normal	T_{25}^{T-1A}	254	Days	Lognormal(2.766, 1.557)
	Emergency	T_{27}^{T-1A}	13	Days	Weibull(0.738, 58.980)
1	Normal	T_{25}^{T-1}	1479	Days	Weibull(0.795, 52.836)
	Emergency	T_{27}^{T-1}	56	Days	Lognormal(2.873, 1.398)
2	Normal	T_{25}^{T-2}	1772	Days	Lognormal(2.931, 1.526)
	Emergency	T_{27}^{T-2}	47	Days	Lognormal(2.963, 1.364)
3	Normal	T_{25}^{T-3}	1151	Days	Lognormal(2.867, 1.769)
	Emergency	T_{27}^{T-3}	34	Days	Lognormal(2.917, 1.785)
4	Normal	T_{25}^{T-4}	630	Days	Lognormal(3.227, 1.818)
	Emergency	T_{27}^{T-4}	14	Days	Lognormal(3.463, 1.997)
5	Normal	T_{25}^{T-5}	416	Days	Lognormal(2.855, 1.930)
	Emergency	T_{27}^{T-5}	27	Days	Lognormal(2.755, 1.632)
6	Normal	T_{25}^{T-6}	32	Days	Lognormal(2.083, 2.039)
	Emergency	T_{27}^{T-6}	0	Days	–

TABLE 5.9: DISTRIBUTIONS AND TRANSITIONS FOR TIME TO SCHEDULED 'NORMAL' AND 'EMERGENCY' STONEBLOWING MAINTENANCE

Active Repair Time (ART)

The distributions for the ART for stoneblowing, for each of the seven track categories, are shown in Figure 5.15 the distribution parameters and transitions used to model them in the Petri net model are shown in Table 5.10.

Category	Transition	Sample Size	Time Unit	Distribution
1A	RT_3^{T-1A}, RT_4^{T-1A}	287	Hours	Lognormal(1.305, 0.786)
1	RT_3^{T-1}, RT_4^{T-1}	1658	Hours	Lognormal(1.106, 0.631)
2	RT_3^{T-2}, RT_4^{T-2}	2246	Hours	Lognormal(1.073, 0.660)
3	RT_3^{T-3}, RT_4^{T-3}	1508	Hours	Lognormal(1.082, 0.671)
4	RT_3^{T-4}, RT_4^{T-4}	851	Hours	Weibull(1.597, 4.421)
5	RT_3^{T-5}, RT_4^{T-5}	584	Hours	Weibull(1.400, 4.198)
6	RT_3^{T-6}, RT_4^{T-6}	128	Hours	Weibull(1.368, 3.769)

TABLE 5.10: ART DISTRIBUTIONS AND TRANSITIONS FOR STONEBLOWING

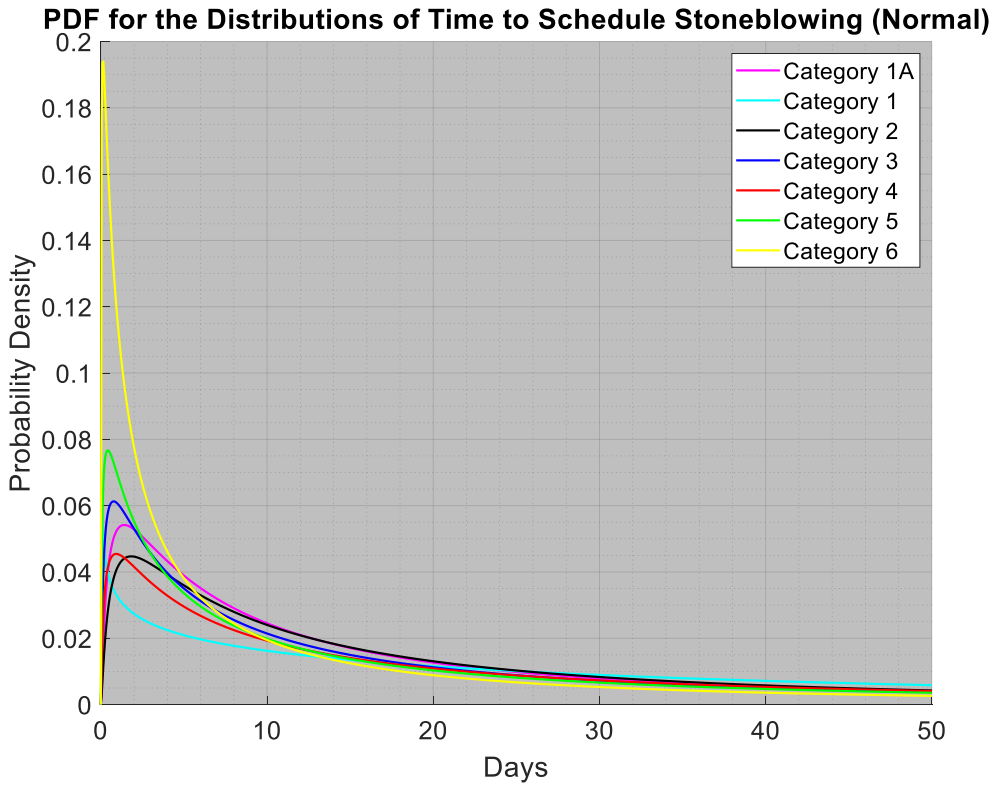


FIGURE 5.13: DISTRIBUTION FOR THE TIME TO SCHEDULING STONEBLOWING BY TRACK CATEGORY FOR CP4 '*NORMAL*'

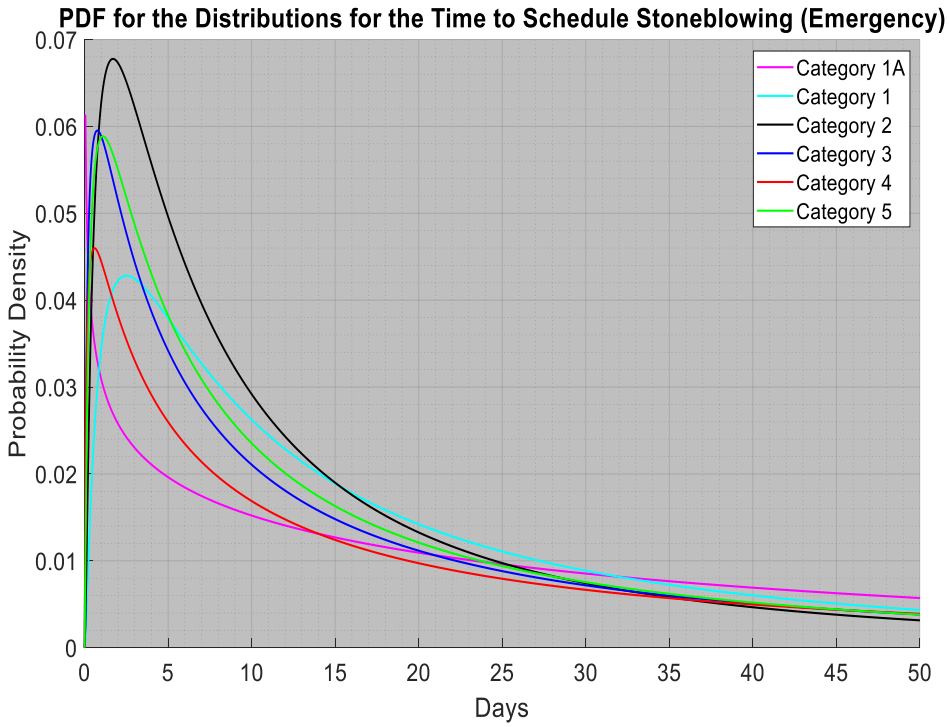


FIGURE 5.14: DISTRIBUTION FOR THE TIME TO SCHEDULING STONEBLOWING BY TRACK CATEGORY FOR CP4 '*EMERGENCY*'

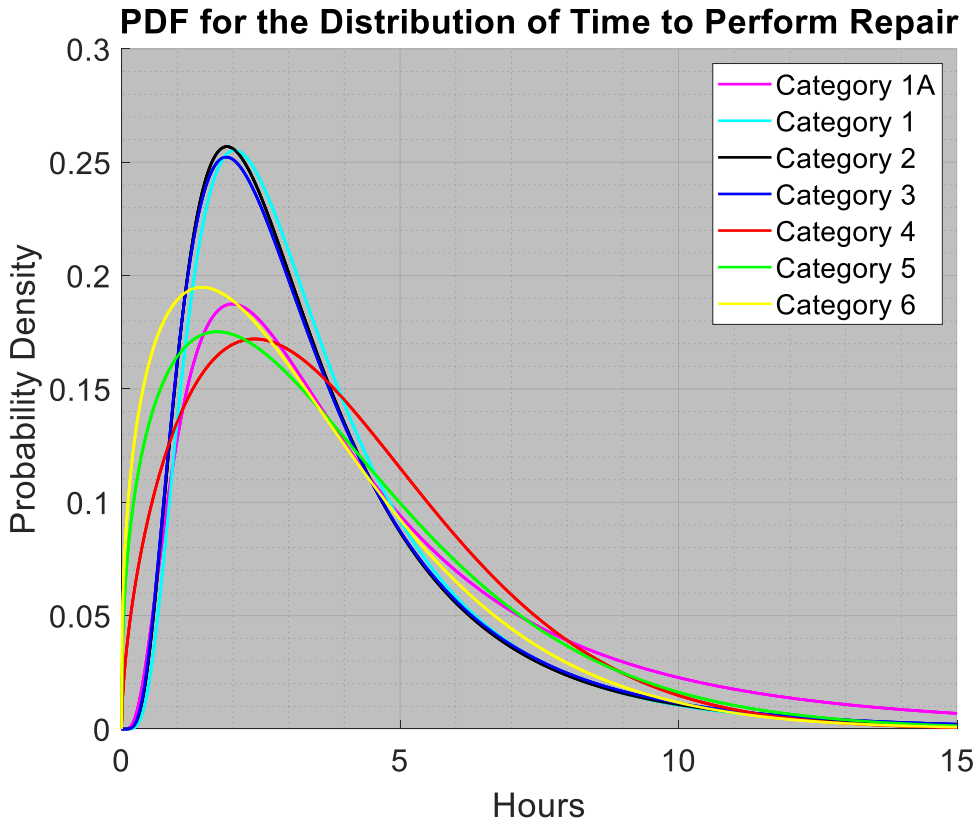


FIGURE 5.15: ART DISTRIBUTIONS FOR STONEBLOWING BY TRACK CATEGORY FOR CP4

Length of Track Maintained During an Intervention

Each of the stoneblowing records was analysed to determine the length of track maintained, this was calculated by subtracting the *start yard* from the *end yard*. The mean, μ, and SD, σ, for the length of track stoneblown for each category is shown in Table 5.11. Similar to tamping it can be observed that the mean is a little over five and there is a large variation in the length stoneblown, in most cases $\sigma > \mu$.

Again, to allow modelling to be as accurate as possible, the length stoneblown during an intervention was analysed further. The length stoneblown was converted from yards to eighth mile sections. These values were then grouped into the same 11 bins as the tamping analysis. Figure 5.16 shows the proportion in each of the bins, subdivided by track category.

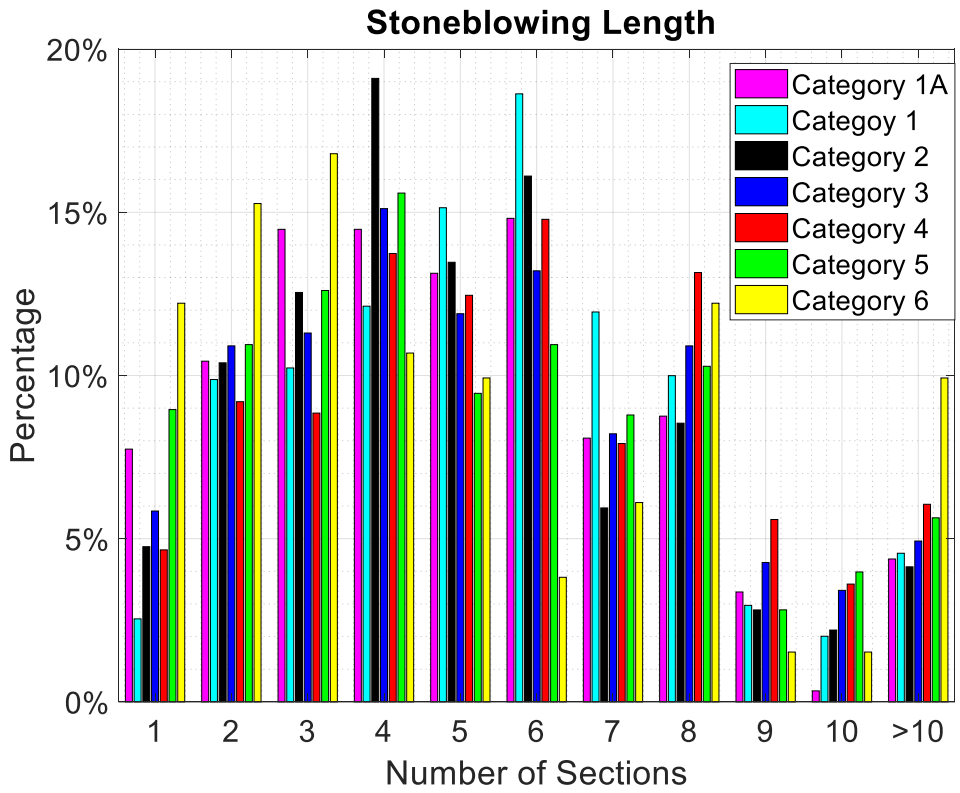


FIGURE 5.16: LENGTH STONEBLOWN DURING CP4 INTERVENTIONS

Category	Sample Size	Mean	SD
1A	297	5.43	5.72
1	1961	5.81	4.63
2	2272	5.48	5.34
3	1522	5.76	7.22
4	859	6.45	7.43
5	603	5.67	6.12
6	131	7.84	15.66

TABLE 5.11: NUMBER OF SECTION STONEBLOWN PER INTERVENTION

5.4.2.3 Grinding

Rail grinding is a form of maintenance which involves grinding away the top surface of the rail to remove shallow cracks and defects. Maintenance records (containing *raised date*, *start date*, *start yards*, *end yards* and *hours completed*) were analysed to determine:

(i) The volume of grinding maintenance currently completed by Network Rail each year which will be used as a baseline in the Petri net models.
(ii) The time to schedule grinding maintenance (time between work being requested and work being complete).
(iii) The ART (Number of hours on site required to complete grinding maintenance).
(iv) The length of rail repaired during a grinding intervention.

Volumes of Grinding Performed Each Year

Figure 5.17 shows the average percentage that each category was ground per year. It can be seen that the volume varies between 3.5% and 6%. There is no clear relationship between the track category and the grinding volume, however it could be argued that the lower track categories (Category 5 and 6) appear to be ground disproportionately more than Category 1A and Category 1. Category 5 and 6 have a similar percentage of grinding each year to Category 1A and 1, however the deterioration of rails on Category 5 and 6 would be expected to be significantly slower due to the much lower use. This phenomena could be explained by poorer rail grades being used on lower category lines.

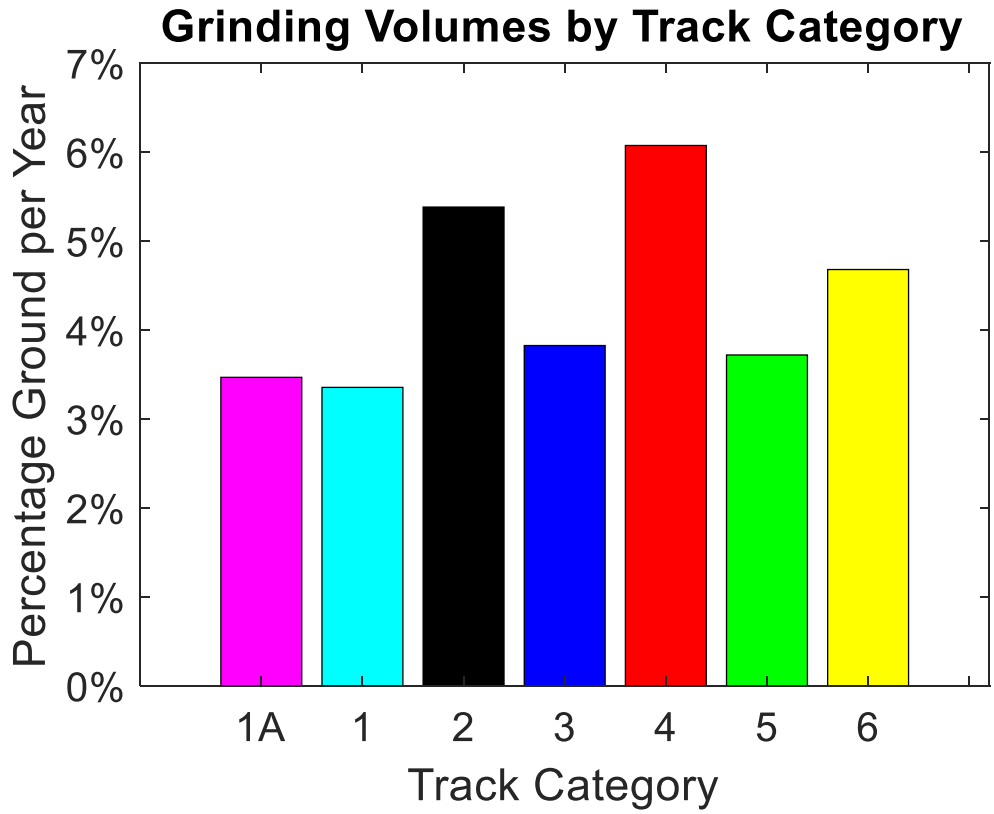


FIGURE 5.17: AVERAGE GRINDING VOLUME PER YEAR BY TRACK CATEGORY FOR CP4

Scheduling Time

The PDFs of the distributions for the time to schedule grinding maintenance for each of the track categories considered are shown in Figure 5.19. Unlike the ballast, data on the condition of the rail was not available so it was not possible to investigate a link between rail condition and the schedule time. The distribution parameters for scheduling time are shown in Table 5.12 alongside the transitions used to model them.

Category	Transition	Sample Size	Time Unit	Distribution
1A	T_{62}^{T-1A}	1025	Days	Lognormal(2.250, 1.544)
1	T_{62}^{T-1}	1855	Days	Lognormal(2.389, 1.592)
2	T_{62}^{T-2}	3170	Days	Lognormal(2.268, 1.528)
3	T_{62}^{T-3}	3638	Days	Lognormal(2.329, 1.667)
4	T_{62}^{T-4}	2536	Days	Lognormal (2.280, 1.641)
5	T_{62}^{T-5}	2574	Days	Lognormal (2.515, 1.654)
6	T_{62}^{T-6}	1183	Days	Lognormal (2.490, 1.689)

TABLE 5.12: SCHEDULE TIME DISTRIBUTIONS FOR GRINDING

Active Repair Time (ART)

The distributions for the ART for rail grinding are shown in Figure 5.20, the distribution parameters are shown in Table 5.13 alongside the transitions used to model them.

Category	Transition	Sample Size	Time Unit	Distribution
1A	$RT_9^{T-1A}, RT_{10}^{T-1A}, RT_{11}^{T-1A}$	1025	Hours	Lognormal(0.928, 1.084)
1	$RT_9^{T-1}, RT_{10}^{T-1}, RT_{11}^{T-1}$	1855	Hours	Lognormal(0.804, 1.119)
2	$RT_9^{T-2}, RT_{10}^{T-2}, RT_{11}^{T-2}$	3170	Hours	Lognormal(0.910, 1.154)
3	$RT_9^{T-3}, RT_{10}^{T-3}, RT_{11}^{T-3}$	3638	Hours	Lognormal(1.072, 1.221)
4	$RT_9^{T-4}, RT_{10}^{T-4}, RT_{11}^{T-4}$	2536	Hours	Lognormal (1.261, 1.133)
5	$RT_9^{T-5}, RT_{10}^{T-5}, RT_{11}^{T-5}$	2574	Hours	Lognormal (1.224, 1.145)
6	$RT_9^{T-6}, RT_{10}^{T-6}, RT_{11}^{T-6}$	1183	Hours	Weibull (0.949, 7.283)

TABLE 5.13: ART FOR GRINDING MAINTENANCE

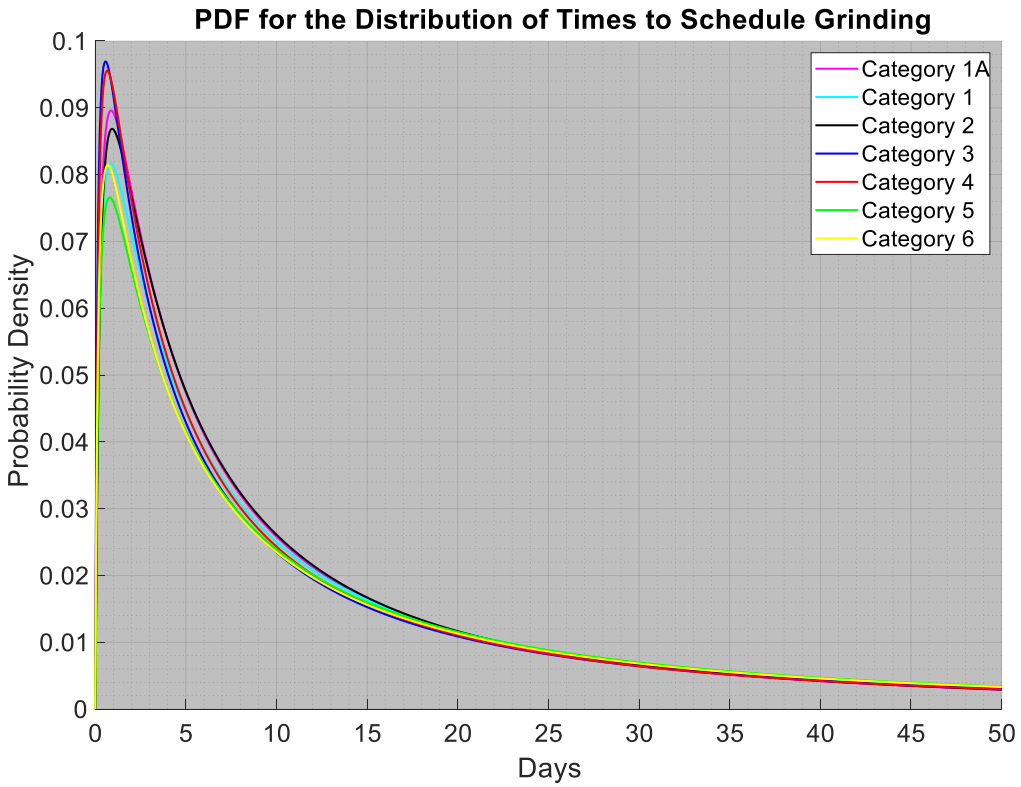


FIGURE 5.18: GRINDING SCHEDULING TIME DISTRIBUTION BY TRACK CATEGORY

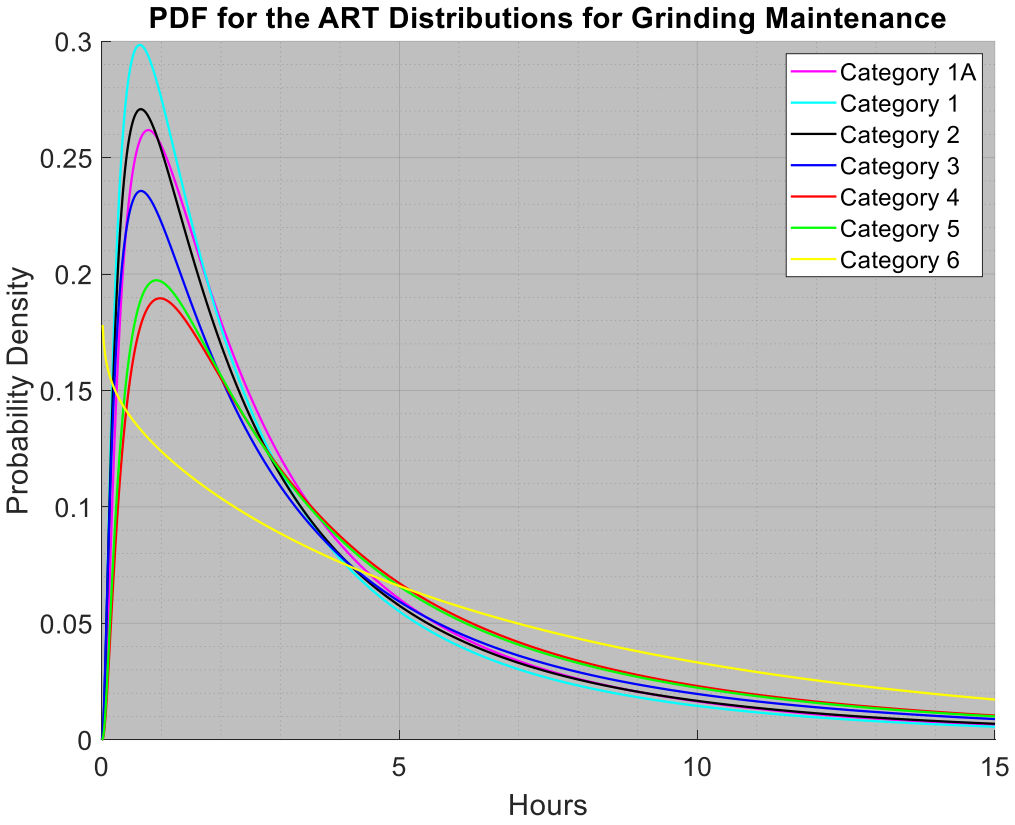


FIGURE 5.19: GRINDING REPAIR TIME DISTRIBUTION BY TRACK CATEGORY

Length of Track Maintained During an Intervention

The length of rail ground during an intervention was also investigated; the results are shown in Figure 5.20. It can be seen that unlike for stoneblowing and tamping, the majority of grinding work is carried out on a single section. This is important to consider in the Petri net model.

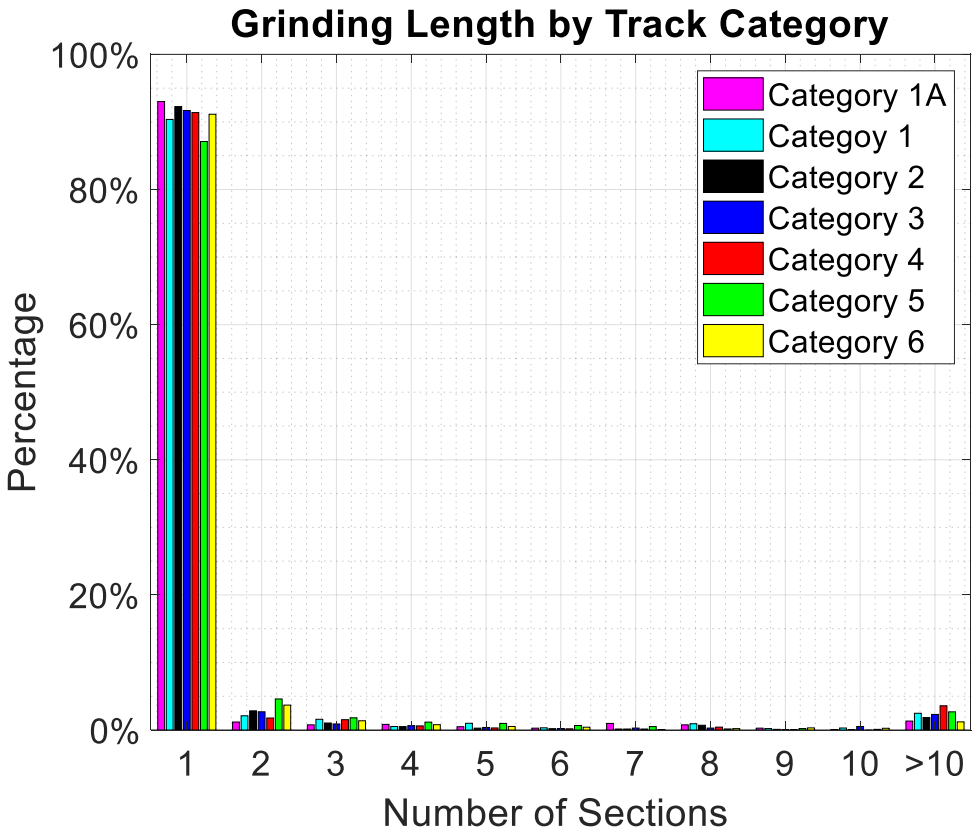


FIGURE 5.20: AVERAGE LENGTH GROUND PER INTERVENTION FOR CP4 BY TRACK CATEGORY

5.4.2.4 Welding

The final type of track maintenance considered is welding. Welding is used to treat rail defects that are not in the surface or have progressed deeper into the rail head. As discussed in section 2.3.2.3 there are various different types of weld repair, however in this research no distinction is made between the different types of weld repair. Maintenance records (containing *raised date*, *start date*, *start yard*, *end yard* and *hours completed*) were analysed to determine:

(i) The percentage of the track currently experiencing welding maintenance performed by Network Rail each year.
(ii) The time to schedule welding maintenance.
(iii) ART (Number of hours on site required to complete the maintenance).
(iv) The length of track repaired during an intervention.

Volumes of Welding Performed Each Year

Welding volumes by track category for CP4 are shown in Figure 5.22, there seems to be little correlation between track category and welding volumes.

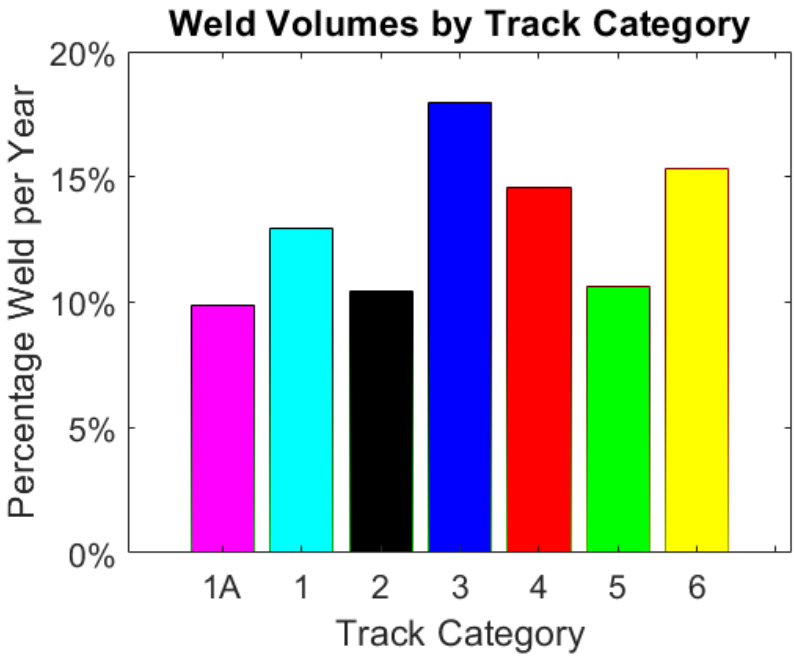


FIGURE 5.21: CP4 WELDING VOLUMES

Scheduling Time

The schedule times for weld repairs were determined using the maintenance records, the results are shown in Figure 5.22. As in the case of grinding there was no way of determining the rail condition so it was not possible to investigate a link between rail condition and the schedule time. The distribution parameters for the schedule times are shown in Table 5.14 , along with the transitions used to model them in the Petri net.

Category	Transition	Sample Size	Time Unit	Distribution
1A	T_{56}^{T-1A}	3002	Days	Lognormal(2.483, 1.228)
1	T_{56}^{T-1}	6839	Days	Lognormal(2.010, 1.300)
2	T_{56}^{T-2}	10527	Days	Lognormal(2.049, 1.399)
3	T_{56}^{T-3}	10301	Days	Lognormal(1.920, 1.394)
4	T_{56}^{T-4}	8148	Days	Lognormal (1.865, 1.335)
5	T_{56}^{T-5}	5326	Days	Lognormal (2.081, 1.452)
6	T_{56}^{T-6}	1202	Days	Lognormal (1.760, 1.294)

TABLE 5.14: SCHEDULE TIME DISTRIBUTIONS FOR WELDING

Active Repair Time (ART)

The ART for weld repairs were determined using the maintenance records, the results are shown in Figure 5.23, the ART distribution parameters are shown in Table 5.15 alongside the transitions used to model them.

Category	Transition	Sample Size	Time Unit	Distribution
1A	RT_7^{T-1A}, RT_8^{T-1A}	4199	Hours	Weibull(1.397, 8.119)
1	RT_7^{T-1}, RT_8^{T-1}	8749	Hours	Weibull (1.346, 8.825)
2	RT_7^{T-2}, RT_8^{T-2}	13107	Hours	Weibull (1.385, 8.598)
3	RT_7^{T-3}, RT_8^{T-3}	12858	Hours	Weibull (1.208, 8.860)
4	RT_7^{T-4}, RT_8^{T-4}	10190	Hours	Weibull (1.375, 9.080)
5	RT_7^{T-5}, RT_8^{T-5}	7018	Hours	Weibull (1.263, 9.115)
6	RT_7^{T-6}, RT_8^{T-6}	1652	Hours	Weibull (1.386, 8.477)

TABLE 5.15: ART FOR WELD REPAIRS

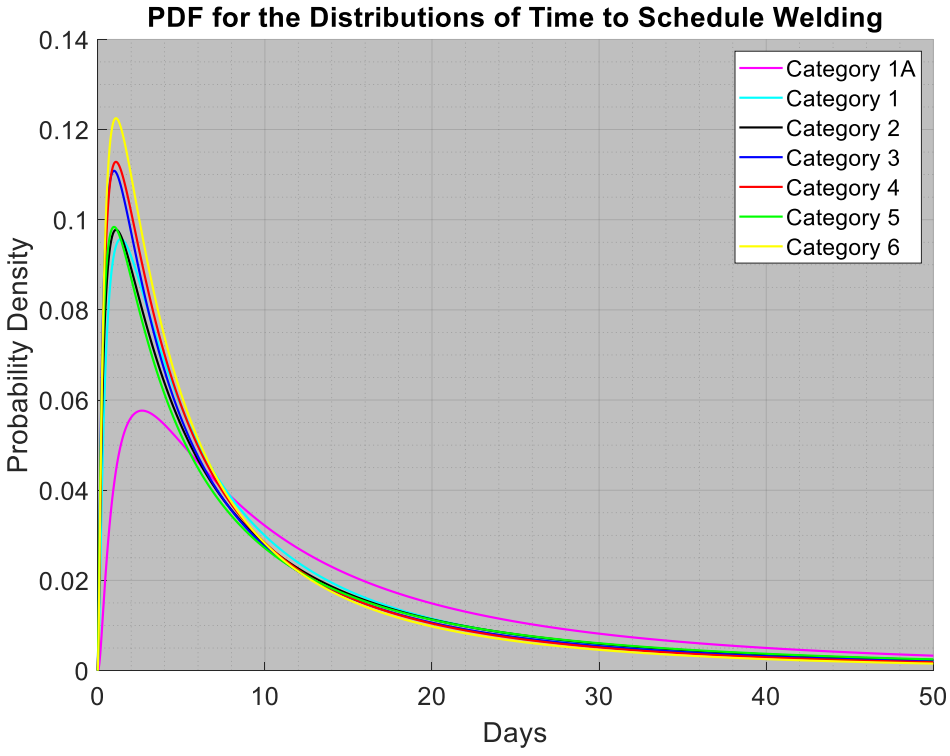


FIGURE 5.22: DISTRIBUTION FOR THE TIME TO SCHEDULING WELD REPAIRS BY TRACK CATEGORY FOR CP4

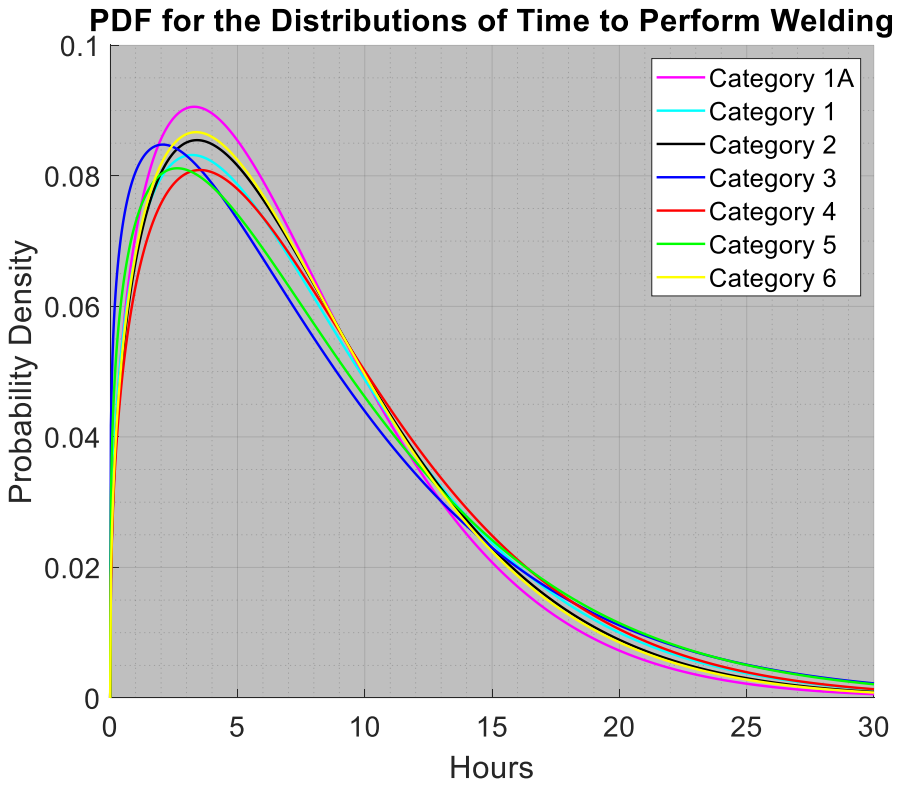


FIGURE 5.23: ART DISTRIBUTIONS FOR THE TIME TO PERFORM WELD REPAIRS BY TRACK CATEGORY CP4

Length of Track Maintained During an Intervention

Finally the length of rail repaired during a welding intervention was investigated. The results are shown in Figure 5.24. Weld repairs are normally performed on a short section of rail (a section of rail is removed and a new section welded in) the results reflected this as the majority of welding interventions only affect a single section.

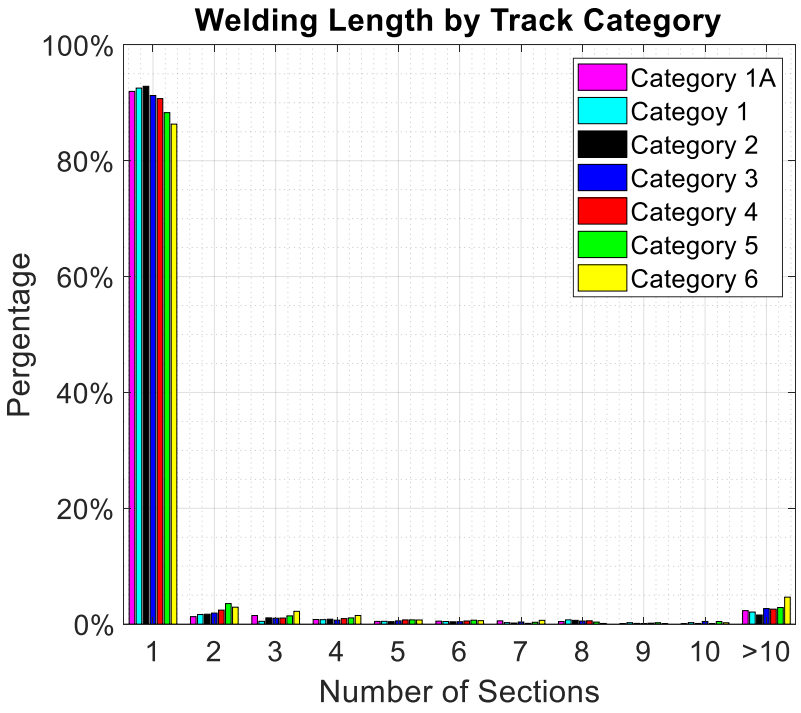


FIGURE 5.24: PROPORTION OF THE NUMBER OF SECTIONS WELDED PER INTERVENTION BY TRACK CATEGORY CP4

5.4.3 Analysis of Location Factors

The model in this research is designed to simulate a railway corridor, comprised of a number of eighth mile sections. By modelling the route at the level of granularity of eighth mile sections, factors local to each track section can be considered. Location parameters such as line speed have an impact on the behaviour of assets. To demonstrate the modelling capabilities of the whole system model it was decided to vary the parameters in the degradation distributions detailed in section 5.4.1 based on location parameters.

It is common practice to use a Cox Proportional Hazard Model [137] to relate a range of covariates to the occurrence of an event. The Cox model is used widely in survival analysis, reliability analysis and biomedical studies. The Cox model is used to relate lifetime distributions to a set of covariates by modelling hazard rates [138]. It allows an assessment of how a range of parameters affect a placebo or baseline case. To apply the Cox model event occurrence time under each of the different scenarios and the base case are required. Although information on location parameters, such as track speed, was available, information on the time of events (changes of ballast condition state) were difficult to obtain. For this reason in this study a Location Index (LI) is proposed to take account of location factors to demonstrate the capability of the model.

Analysis of the relationship between track deterioration rates and location factors was carried out by Clarke and Prescott [133]. The authors found that the following factors had a measurable impact on track deterioration rates:

(i) Usage/tonnage/number of loading cycles
(ii) Maximum line speed
(iii) Rail joint type
(iv) Geology
(v) Electrification
(vi) '*Dirty traffic'*, including coal freight trains which lead to a disproportionally large amount of fines in the ballast
(vii) Curvature
(viii) Sleeper design

Quantifying the effects of these parameters on deterioration is difficult for a number of reasons:

(i) It is hard to isolate the effects of a specific factor and assess its influence on deterioration.
(ii) The data available is often only for a short period of time, so long term effects can be hard to understand/predict.
(iii) There is an underlying element of randomness in the ballast deterioration process.

Therefore a simple LI is proposed to allow the location parameters to be included and vary the deterioration parameters for each of the track sections, to demonstrate the capability of the model. The LI created is based on the works of Clarke and Prescott [133], An et al. [139] and engineering judgement. One of the main disadvantages of using a LI is that extreme

values can be masked if all other parameters are good. However in this research the LI is only being used to demonstrate the model's capability to consider the variation in deterioration rates between neighbouring track sections. As a future study more detailed analysis of location factors can be undertaken to develop a better understanding of the relationships between deterioration and location parameters, and from this an alternative means to assess them can be developed.

The LI was applied only to the deterioration of ballast. Although in the future it could be applied to all of the asset classes. The LI score proposed is calculated based on the eight factors identified by Clarke and Prescott [133]. However '*Dirty traffic*' was not considered, since this data was difficult to obtain and was hard to quantitatively measure. An additional parameter was included to consider if the section was in a tunnel or not.

Table 5.16 details how the LI score was calculated, each of the eight factors was given a score and the LI value was calculated by adding each of the eight scores together. The values are such that the overall score is always between zero and 1000. A section with a LI score of 500 would be assigned the baseline degradation distribution shown in Table 5.2. For sections with a score different from 500, the scale parameter in the Weibull degradation distributions were adjusted to give a different time profile. The LI is shown in Figure 5.25, a section with a score of 1000 (max) would have a scale factor half the value of the baseline and a section with zero would receive a scale factor twice as big as the baseline scale factor. Hence a higher score implies faster deterioration.

The *importance factor* in Table 5.16, acts as a weighting and allows some parameters to influence the deterioration more than others. Parameter with a large *importance factor* influence deterioration the most whereas factors with small importance effect it the least. The *score range* refers to the range of values that a specific factor can be assigned.

The *units* column refers to how the parameter is measured for example the line speed is measured in mph. A *Y/N* entry refers to yes/no, this is used when the parameter assesses a phenomena which is either present or not, for example jointed rail. The *relationship column* describes how the score was calculated for that parameter, three relationships are considered:

(i) *Linear*: this is used when the parameter value can take a continuous value, for example line speed. The score for this parameter is determined based on a linear relationship between the best and worst value (indicated in the last two columns).

(ii) *Boolean*: the parameter can only take one of two values, yes or no. A *Yes* received the maximum score (fastest deterioration) and *No* received a score of zero (slowest deterioration).

(iii) *Categorical*: the parameter can take one of a number of discrete values. Each of the discrete values is assigned a score. The bedrock and sleeper design were determined using a categorical score; sections 5.4.3.1 and 5.4.3.2 explain the categorical values for bedrock and sleeper design respectively.

The last two columns show the best performing and worst performing values. At this stage of the research the LI scores for each section are assumed to remain constant throughout.

The parameter values for each of the 849 track sections considered in the whole system model and the associated LI scores are shown in Appendix J-1.1, the key statistics for the LI scores are shown in Table 5.17. It can be seen that the mean, median and mode of the scores are all less than 500, indicating a better than baseline performance in general.

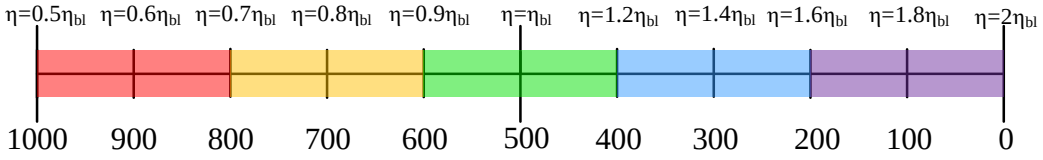


FIGURE 5.25: LI USED TO ACCESS LOCATION FACTORS

	Location Factor	Importance	Score Range	Unit	Relationship	Best Performing	Worst Performing
1	Tonnage	Large	0→280	EMGTPA	Linear	**< 1 (Least** heavily trafficked routes)	**>65 (Most** heavily trafficked routes)
2	Maximum Line Speed	Large	0→280	mph	Linear	5 (**Lowest** speed routes)	125 (**Highest** speed routes)
3	Jointed Rail	Large	0→120	Y/N	Boolean	CWR	Jointed Rail
4	Sleeper Design	Large	0→120	N/A	Categorical (see 5.4.3.2)	Large Concrete	Softwood
5	Bedrock	Medium	0→80	C_v	Categorical (see 5.4.3.1)	<10 >150	70
6	No electrification	Small	0→40	Y/N	Boolean	OLE	Non electrified lines
7	Curvature	Small	0→40	m^{-1}	Linear	0 (straight track)	>1/1000 (tight corner)
8	Tunnel	Small	0→40	Y/N	Boolean	Not in a tunnel	In a tunnel

TABLE 5.16: LI PROPOSED IN THIS RESEARCH

Statistic	Values
Mean	410.2
Mode	405.5
Median	429.0
SD	106.9
Range	498.5
Minimum	138.8
Maximum	637.3

TABLE 5.17: STATISTICS ON THE LI SCORES FOR BLETCHLEY DELIVERY UNIT

5.4.3.1 Geology and Bedrock

The geology of the soil the railway is constructed on has an effect on the settlement of the track. Soil is made up of three parts; air, water and the soil itself. When a load is applied to the soil the water and air are forced out and cause the soil to compress. If the soil is assumed to be saturated, then Terzaghi's One-Dimensional Consolidation Equation (Equation(5.1)) [140], can be used to relate excess pore pressures, *u*, (due to infrastructure dead and live loads) the depth *z* and time *t* according to a coefficient of consolidation C_v. C_v is dependent on the soil properties, and hence the soil can affect the rate of settlement.

$$C_v \frac{\partial^2 u}{\partial z^2} = \frac{\partial u}{\partial t}. \tag{5.1}$$

The C_v value for different soil types can be sourced from textbooks or calculated directly from laboratory testing of borehole samples. Some example C_v values are given in Table 5.18. For each eighth mile section it is possible to determine the coefficient of consolidation, C_v. In this research, the soil type will be estimated based on bedrock data from the British Geological Survey [141].

Soil	C_v (cm^2/sec) $x10^{-4}$
Mexico City Clay	0.9→1.5
Soft Blue Clay	1.6→26
Organic Silt	5→170
Chicago Silty Clay	8→11
Sandy Silty Clay	5→20
Organic Silts and Clays	1→10

TABLE 5.18: TYPICAL C_V VALUES FOR VARIOUS SOIL TYPES

Figure 5.26 shows the geology of the Bletchley Delivery Unit; this was used to determine the bedrock type for each eighth mile track section within Bletchley Delivery Unit. From the bedrock type the C_v value was estimated. The British Geological Survey did also provide borehole data, which contained the exact C_v value, however the values were not in a digital format and would have taken a significant amount of time to process, therefore at this stage this information was not used. From Figure 5.26 it was concluded that there were seven types of bedrock in the Bletchley Delivery Unit, these are listed in Table 5.19 along with the assumed C_v values.

The C_v values were used to estimate the impact on deterioration distributions. At this stage it is assumed that sections with a very high C_v value or very low C_v value perform best, as ground with a low C_v value (less porous) such as hard clay settle slowly and the settlement is insignificant during the life of the track. Sections with a high C_v value such as sand will settle very quickly and hence most of the consolidation will happen during construction. Soil with properties between the two extremes are thought to be the worst to build track on as they settle at a significant rate during the life of the ballast. As a future study more detailed analysis should be undertaken to establish the exact relationship between the coefficient of consolidation and track deterioration rates. The final column of Table 5.19 shows the LI values that were assigned to each bedrock type based on the assumptions above.

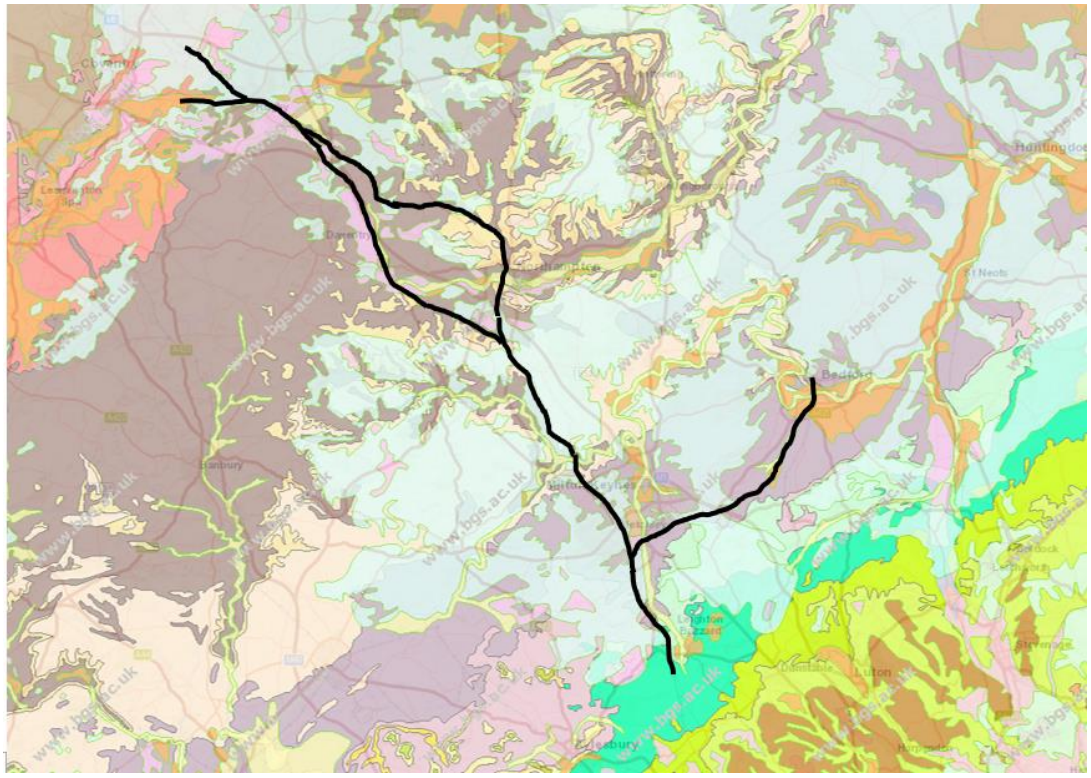


FIGURE 5.26 GEOLOGY OF THE BLETCHLEY DELIVERY UNIT [141]

	Rock Type	Description	Assumed C_v Value ($cm^2/sec\ x10^{-4}$)	LI Score
1	Lias Group	**Mudstone, Siltstone, Limestone And Sandstone.** Sedimentary Bedrock formed approximately 172 to 204 million years ago in the Jurassic and Triassic Periods. Local environment previously dominated by shallow seas.	20-30	40
2	Triassic Rocks	**Mudstone, Siltstone And Sandstone.** Sedimentary Bedrock formed approximately 200 to 251 million years ago in the Triassic Period. Local environment previously dominated by hot deserts.	1-10	0
3	Great Oolite Group	**Sandstone, Limestone And Argillaceous Rocks.** Sedimentary Bedrock formed approximately 165 to 168 million years ago in the Jurassic Period. Local environment previously dominated by shallow carbonate seas.	50-70	85
4	Inferior Oolite Group	**Limestone, Sandstone, Siltstone And Mudstone.** Sedimentary Bedrock formed approximately 165 to 176 million years ago in the Jurassic Period. Local environment previously dominated by shallow carbonate seas.	30-40	60
5	Kellaways Formation And Oxford Clay Formation	**Mudstone, Siltstone And Sandstone.** Sedimentary Bedrock formed approximately 156 to 165 million years ago in the Jurassic Period. Local environment previously dominated by shallow seas.	1-10	0
6	Gault Formation And Upper Greensand Formation	**Mudstone, Sandstone And Limestone.** Sedimentary Bedrock formed approximately 94 to 112 million years ago in the Cretaceous Period. Local environment previously dominated by shallow seas.	15-25	30
7	Lower Greensand Group	**Sandstone And Mudstone.** Sedimentary Bedrock formed approximately 100 to 125 million years ago in the Cretaceous Period. Local environment previously dominated by shallow seas.	5-15	15

TABLE 5.19: ROCK TYPES IN THE BLETCHLEY AREA, THEIR ASSUMED C_V VALUES AND LI SCORES

5.4.3.2 Sleeper Type

There are a range of different sleeper types used on the UK railway network, an LI score was assigned to each sleeper type, size of the sleeper and when the sleeper was first produced. Larger Concrete sleepers were thought to provide the best ballast support and so receive a score of zero. F40 was given a score of ten as it is an older type of concrete, more prone to defects. Softwood sleepers are thought to provide the worst support and so receive the largest score of 120. Steel, smaller concrete designs and hardwood sleepers are somewhere between the two. The LI score for a range of sleeper types are shown in Table 5.20.

ID	Sleeper Type	Description	LI Score
1	5F40 Concrete Sleeper	Large Concrete	0
2	EF29 Concrete Sleeper	Small Concrete	40
3	EF33 Concrete Sleeper	Small Concrete	40
4	EG47 Concrete Sleeper	Large Concrete	0
5	F19 Concrete Sleeper	Small Concrete	60
6	F23 Concrete Sleeper	Small Concrete	60
7	F27 Concrete Sleeper	Small Concrete	40
8	F27AS Concrete Sleeper	Small Concrete	40
9	F27P Concrete Sleeper	Small Concrete	40
10	F40 Concrete Sleeper	Large Concrete	10
11	F40AS Concrete Sleeper	Large Concrete	0
12	F40BS Concrete Sleeper	Large Concrete	0
13	G44 Concrete Sleeper	Large Concrete	0
14	Hardwood Sleeper / Bearer	Timber	60
15	Softwood Sleeper / Bearer	Timber	120
16	W560 Steel Sleeper	Large Metal	80
17	W560H Steel Sleeper	Large Metal	60
18	560D Steel Sleeper	Small Metal	60

TABLE 5.20: SLEEPER LI VALUES

5.4.4 Maintenance History

Maintenance history is also thought to have an effect on the ballast life cycle. Antoni [142] demonstrated that the effectiveness of maintenance on the track is related to the number of maintenance actions performed since its last renewal. This phenomena was modelled by Lichtberger [89], who proposed that the effectiveness of maintenance exponentially decreased with the number of interventions. One of the most comprehensive studies on the effectiveness of tamping on ballast deteriorating which appears in literature is arguably the work undertaken by Audley and Andrews [122]. The authors found that the probability of achieving the desired geometry following maintenance decreases as the number of tamps increases and that a Lognormal distribution was the most appropriate for modelling this. Additionally it was concluded the ballast deterioration rate was best modelled with a two

parameter Weibull distribution, the characteristic life parameter of which decreased with the number of tamping interventions. Providing further evidence to the theory, that tamping damages the ballast and causes the geometry to deteriorate faster. The above studies highlight two areas that need considering in the whole system model:

(i) The number of interventions influences their effectiveness.
(ii) The number of interventions influences the deterioration rate.

5.5 Sleeper Analysis

Sleepers are a fundamental component of ballasted track and three main materials are used to make sleepers: timber/wood, concrete and steel. Each of these sleeper types behaves in a different way and so was investigated separately. This section will look to develop an understanding of the six key areas shown in Figure 5.1, for the three sleeper types.

5.5.1 Deterioration Rates

There are approximately 14,500 miles of track of concrete sleeper construction in the UK. As discussed in Chapter 2 it is widely believed that tonnage is one of the biggest causes of concrete sleeper deterioration. To investigate this hypothesis the tonnage experienced by concrete sleepers was explored.

Figure 5.27 shows the UK tonnage breakdown for concrete sleepers. It can be seen that there are a considerable amount of lightly-trafficked routes constructed using concrete sleepers, around half the concrete sleepers experience less than 10 EMGTPA. Additionally it is important to note that less than 5% of concrete sleepers experience more than 40 EMGTPA.

Maintenance records for concrete spot re-sleepering were then analysed to determine the number of yards that were replaced in each of the tonnage bands. To allow comparison between different tonnage bands, rather than expressing the number of sleepers that were replaced, the number replaced as a percentage of the total is given. The results are shown in Figure 5.28.

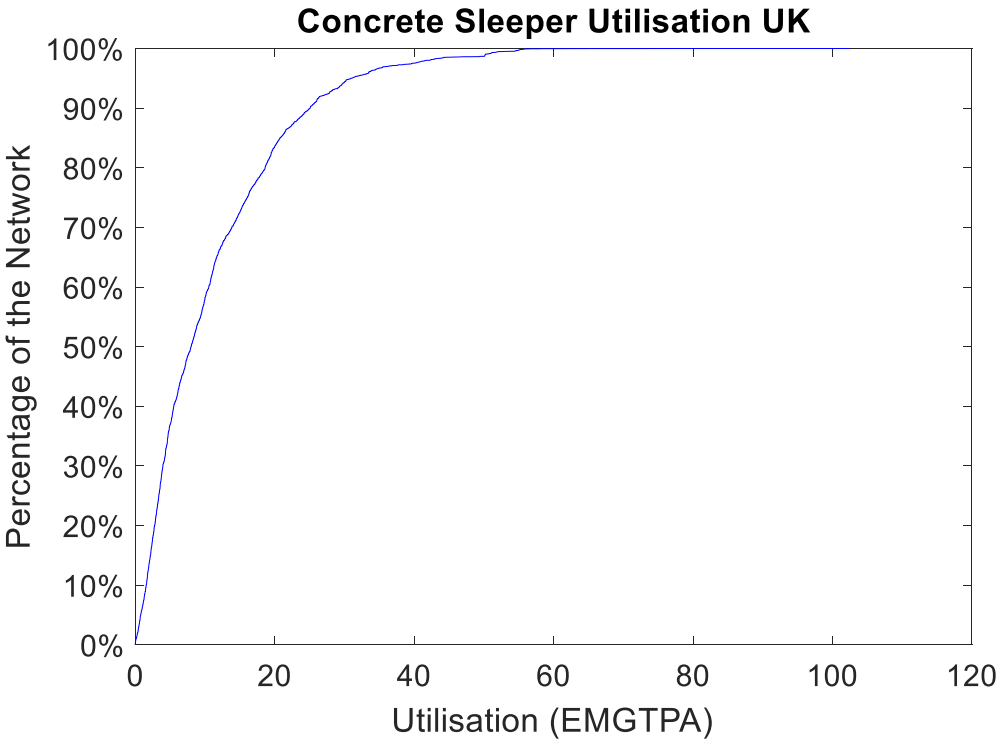


FIGURE 5.27 CONCRETE SLEEPER CONSTRUCTION BY TONNAGE (CUMULATIVE)

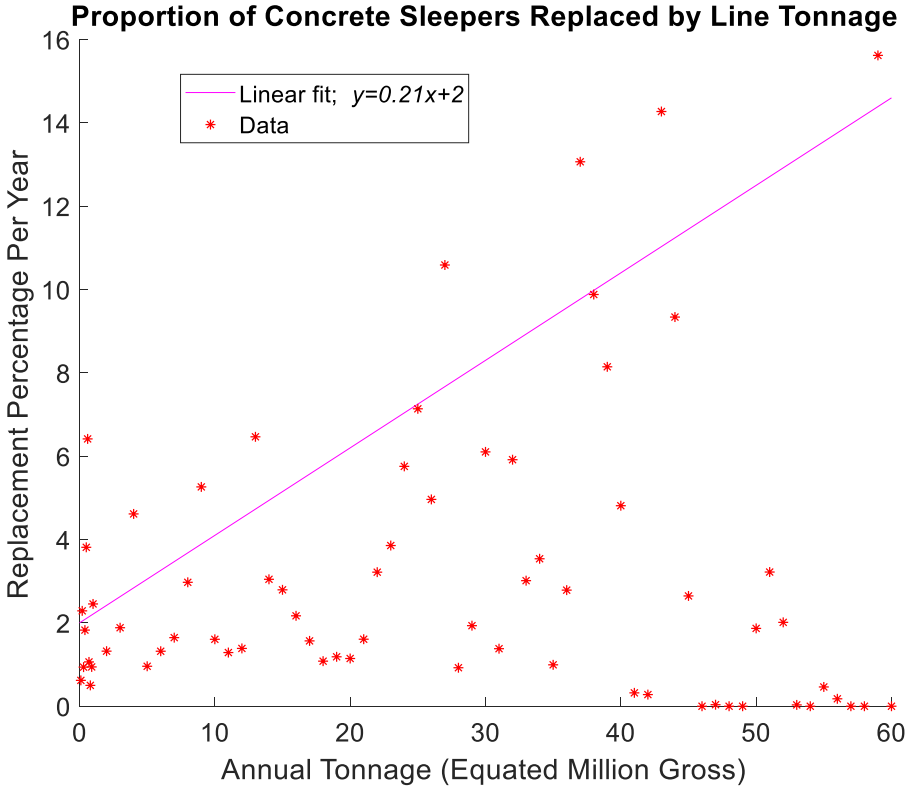


FIGURE 5.28 SLEEPER REPLACEMENT PERCENTAGE BY YEAR BY TONNAGE BAND FOR CONCRETE SLEEPERS

Despite the literature suggesting that there is a relationship between usage and service life, the correlation found between the tonnage experienced and the replacement rates was poor. There are thought to be a number of reasons for this:

(i) It was unclear in some records exactly how many sleepers were replaced during the intervention.
(ii) The sleeper design is not specified in the maintenance data, yet different designs would be expected to perform better, for example larger concrete sleepers would be expected to perform better than smaller designs.
(iii) Location parameters such as chloride ion concentration and weather patterns were not considered.
(iv) The ballast condition was not taken into account.
(v) The type and number of loads was not considered, only the overall tonnage.
(vi) Sleeper replacement may not have been like for like; wooden sleepers may have been replaced with concrete and some concrete sleepers may have been replaced with steel ones on lower category lines.
(vii) Only a very small fraction of the network experiences tonnage greater than 40 EMGTPA, therefore, many of the bins greater than 40 EMGTPA contained no records during the observation period.
(viii) The observation period was short in comparison to the service life of sleepers.
(ix) The time since renewal of the sleepers was not known.

It would have been advantageous to explore a relationship between the replacement rate and the age of the sleeper, however information on the age of sleepers was not available.

Data was analysed for wooden and steel sleepers, however the correlation was equally poor and did not reveal anything meaningful. For wooden sleepers this is likely to be because there is a drive to remove wooden sleepers from the network and so the assumption of like for like replacement is not valid. Steel sleepers are the least widely used and have only been adopted recently so there was limited data on these, and the data is in its infancy.

5.5.2 Maintenance Analysis

As with the other assets, to better understand the behaviour of the sleepers maintenance records (containing *raised date*, *start date*, *units complete* and *hours completed*) were analysed to determine:

(i) The volume of sleepers currently replaced each year by Network Rail.
(ii) The number of sleepers replaced during an intervention, as the number of defective sleepers may affect the maintenance performed.
(iii) The time to schedule sleeper replacement (time between work being requested and work being complete).
(iv) The ART (Number of hours on site required to complete the maintenance).

Volumes of Sleepers Replaced each Year

As in the case of the ballast and rail, the CP4 sleeper maintenance was used to determine the number of spot re-sleepers (replacement of individual sleepers). Figure 5.29 shows the average volumes for concrete, timber and steel per year in CP4. It can be seen timber sleeper replacements are some of the highest, particularly for low category tracks, this is likely to be as softwood sleepers (Beach or Pine) are used for lower category track and have a much

shorter service life than hardwoods, concrete or steel. This is offset by the cheaper cost of softwood sleepers.

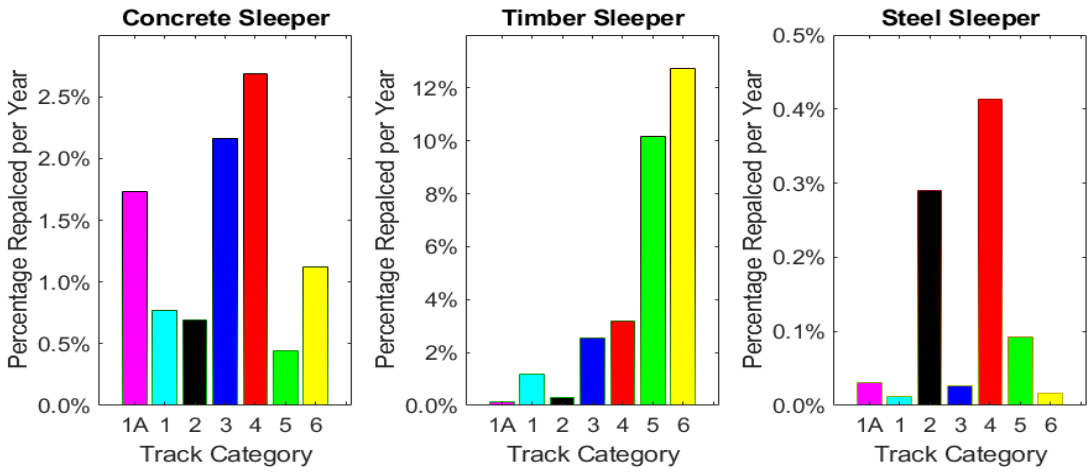


FIGURE 5.29 SLEEPER MAINTENANCE VOLUMES BY CONSTRUCTION TYPE AND TRACK CATEGORY

Number of Sleepers Replaced During an Intervention

As opposed to looking at the length of sleepers maintained in yards, the *number of units complete* (number of sleepers replaced) during an intervention was investigated, the results are shown in Figure 5.30. The number of sleepers replaced was grouped into 11 bins; one→ ten and then more than ten. The figure shows the proportion of the number of interventions in each bin as a fraction of the total number of interventions. For concrete sleepers (pink) it can be seen that over 60% of interventions involved replacing just one or two sleepers. This is likely to be due to concrete sleepers being significantly heavier than wooden/steel sleepers hence it takes considerably longer to install them, meaning less can be installed during a possession. By contrast only a little over 20% of wooden sleeper interventions only affected one or two sleepers. It can be seen that for wooden and steel sleepers a high proportion of interventions affected more than ten sleepers.

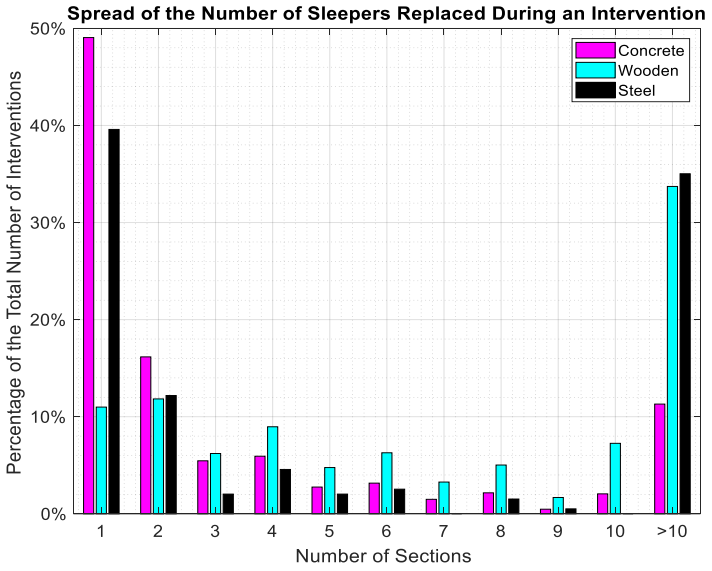


FIGURE 5.30 SPREAD OF THE NUMBER OF SLEEPERS REPLACED DURING CP4 INTERVENTIONS BY SLEEPER TYPE

Scheduling Time and ART

As the number of sleepers changed during an intervention is likely to affect the schedule time different distributions were determined for the schedule time based on the number of sleepers that were defective. The results are shown in Figure 5.31. For concrete and steel sleepers it was decided not to consider 7, …, 10 sleepers replaced due to the lack of data in these bins. The distribution parameter values, number of data points in each bin and the transitions used to model them in the Petri net model are detailed in Appendix C-2.

Active Repair Time (ART)

The number of sleepers changed is likely to have a significant impact on the ART. Therefore, it was also decided to determine a distribution for ART based on the number of sleepers replaced during the intervention. The results are shown in Figure 5.32. The distribution parameter values, number of data points in each bin and the transitions used to model them in the Petri net model are detailed in Appendix C-3.

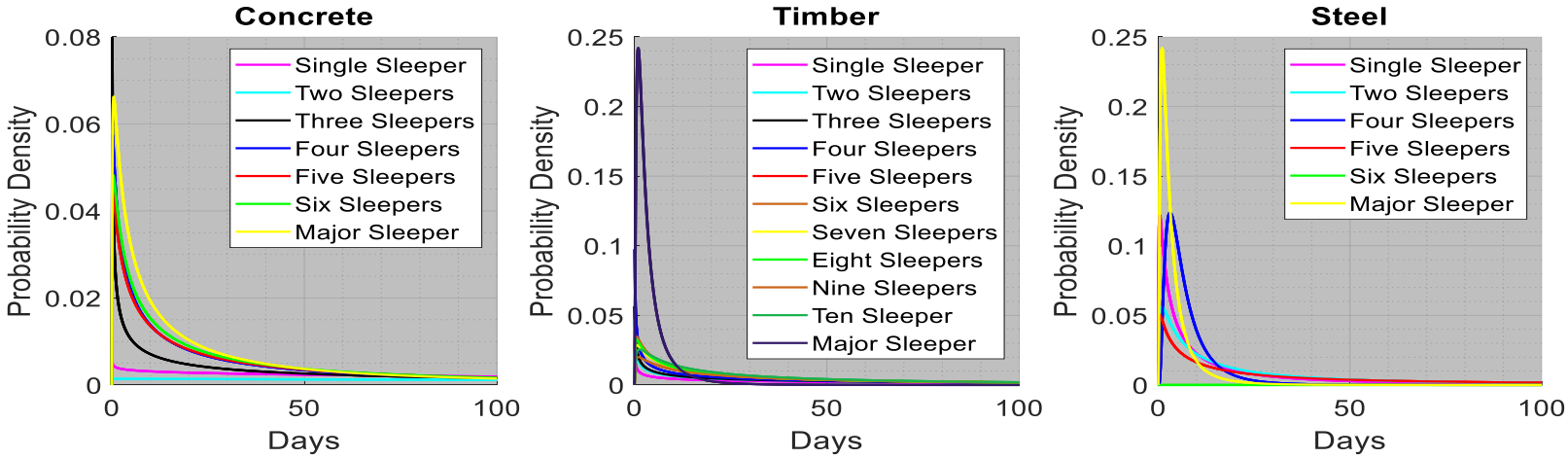


FIGURE 5.31: PDFS OF THE DISTRIBUTIONS FOUND FOR THE TIME TO SCHEDULE CONCRETE, TIMBER AND STEEL SLEEPER REPAIR BASED ON THE NUMBER OF DEFECTIVE SLEEPERS

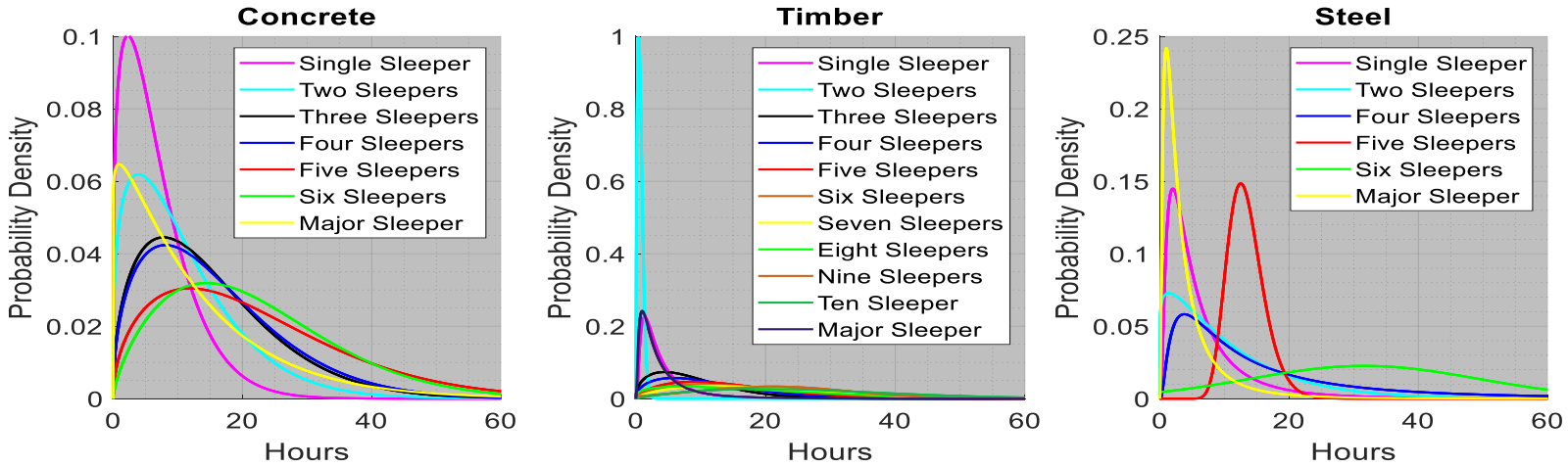


FIGURE 5.32: PDFS OF THE DISTRIBUTIONS FOUND FOR THE ART FOR CONCRETE, TIMBER AND STEEL SLEEPERS BASED ON THE NUMBER OF DEFECTIVE SLEEPERS

5.6 Switch and Crossing Analysis

S&C are a vital part of the railway infrastructure. An S&C unit is a trackside installation enabling railway vehicles to change tracks or crossover another track [52]. On the UK network there are over 18,000 S&C units which are managed and maintained by Network Rail.

S&C units are made up of a number of components as shown in Figure 5.33 and listed in Table 5.21, further information is given in Appendix D-1.1. Due to the range of components that make up an S&C unit, and their different degradation characteristics, it became apparent that one single methodology would not be suitable to model all the components.

Maintenance records for S&C units; which contain information on the *S&C name, raised date*, *complete date* and *number of units complete*, were analysed to determine how often specific S&C components were maintained, in addition to this failure data was also reviewed to determine the number of failures of S&C components. A number of key observations were made:

(i) Interventions of the same S&C often occurred in clusters with several repairs in quick succession and then long periods with no maintenance.

(ii) Many of the S&C units had no recorded repairs in the five year observation period.

(iii) For a number of components such as bearers and slide chairs it was not possible to determine which component had been repaired/replaced and hence it was not possible to determine if subsequent repairs were on the same or different components.

(iv) With the exception of stretcher bars, components were generally repaired, following a defect and not replaced.

Type of Components in an S&C Unit	
1	Ballast
2	Check
3	Crossing
4	Fastening
5	POE, including point heater
6	Sleepers/bearer
7	Slide chair
8	Stretcher bars
9	Stock rail
10	Switch rail
11	Wing rail

TABLE 5.21: S&C COMPONENTS

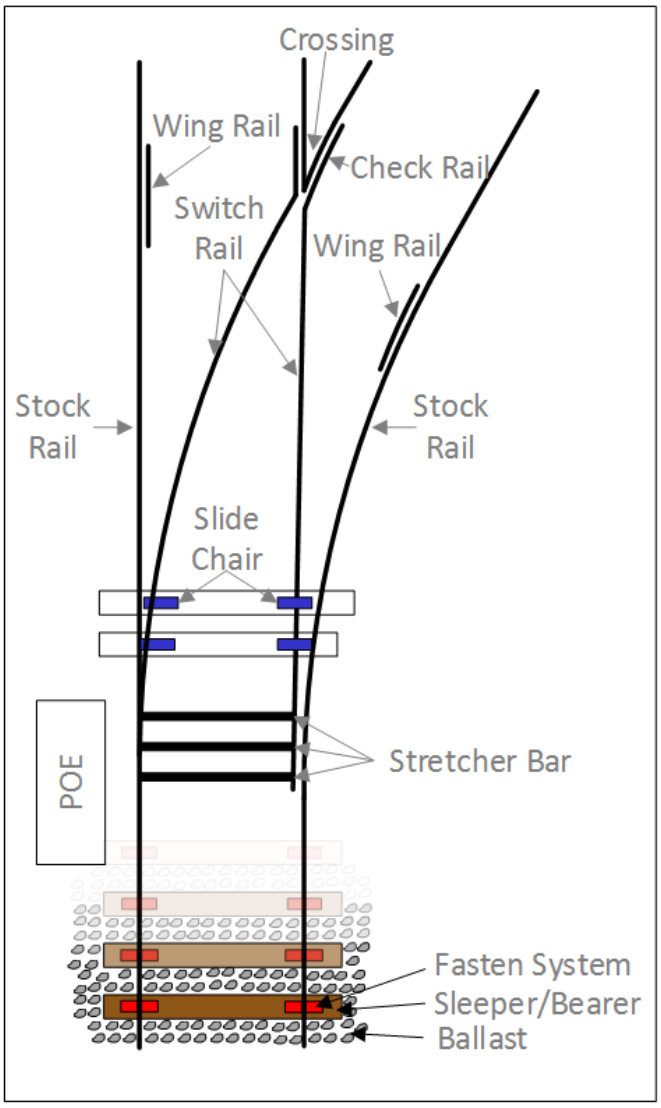


FIGURE 5.33: TURNOUT S&C

Based on these observations it was decided that three methodologies would be used to model the distribution of time between condition states. These were:

(i) Weibull Distribution

As discussed, the Weibull distribution is employed extensively in the analysis of equipment lifetime data [67]. To fit a Weibull distribution the data required is complete or censored lifetime information.

(ii) Poisson Process/ Exponential Distribution

The Poisson Process is one of the most widely used stochastic models [143]. The Poisson Process assumes that failures occur completely at random but at a constant rate. It is convenient to use the Poisson Process for systems where the only information known is the rate of occurrence of failure. This is typically the case for components such as

bearers/sleepers where there is a high density of components and yet information on specific assets is unavailable.

(iii) Non Homogenous Poisson Process (NHPP)

The NHPP [144], is a special case of the Poisson Process where the rate of occurrence is non-constant. It can be used to model a system where components fail more or less regularly with age and when repaired, the system does not return to the good as new state, for example stock/switch rail.

In the NHPP the rate of occurrence of failures, *u*, is a function of time. The number of failures is now dependent on the location and the length of the interval. This property makes it fundamentally different from the Weibull analysis, in the NHPP after a failure the component does not return to the as good as new state. One of the most common choices for *u* is:

$$u(t) = abt^{a-1} \tag{5.2}$$

This choice was proposed by Crow [145] and is known as the Power Law NHPP or Power Law Process.

Let failure events occur at successive failure times, $\tau_0 = 0$ and $\tau_1 < \tau_2 < \tau_3$. Then, if the system is modelled using a Power law NHPP, the cumulative distribution function $F_i(y)$ for the time to the next (i^{th}) failure is as shown below:

$$F_i(y) = \frac{F(\tau_{i-1}+y) - F(\tau_{i-1})}{1 - F(\tau_{i-1})}, i = 1,2,3, \dots, \tag{5.3}$$

where $y>0$, $F(x)=1-e^{-U(x)}$ with $U(x) = \int_0^x u(t)dt$

If $u(t)$ is as described in equation (5.2), then equation (5.3) can be used to estimate the cumulative distribution function $F_i(y)$ of the time to the next (i^{th}) failure:

$$F_i(y) = 1 - e^{b\{\tau_{i-1}{}^a - [\tau_{i-1}+y]^a\}}. \tag{5.4}$$

From equation (5.4) it can be seen that the cumulative distribution function for the time to first failure, F_1, is equal to that of a Weibull distribution, with shape parameter, a, and scale parameter, $\frac{1}{\sqrt[a]{b}}$, $W(a, \frac{1}{\sqrt[a]{b}})$. As the distribution of F_i changes after each failure, the failure rate depends both on the location and the length of the interval. Similarly to the Weibull distribution, the parameters are capable of representing an increasing failure rate, $a>1$, constant failure rate, $a=1$, and decreasing failure rate, $0<a<1$.

By rearranging equation (5.4), and substituting $F_i(y)$ with the random number X, equation (5.5) is obtained, from which firing times can be sampled for the various, $F_i(y)$.

$$y = \sqrt[a]{\tau_{i-1}{}^a - \frac{\ln(X)}{b}} - \tau_{i-1} \quad \text{i=1, 2, 3, …,} \tag{5.5}$$

where τ_{i-1} is the time the previous failure occurred.

To show the changing distributions, Figure 5.34 plots $F_1(y)$, …, $F_8(y)$ with parameters a = 1.581, b=0.056 as well as the Weibull distribution, $W(a, \frac{1}{a\sqrt{b}})$. It can be seen that:

(i) The time to first failure is equal to the Weibull distribution; $W(a, \frac{1}{a\sqrt{b}})$.

(ii) Subsequent failures happen more quickly (increasing failure rate).

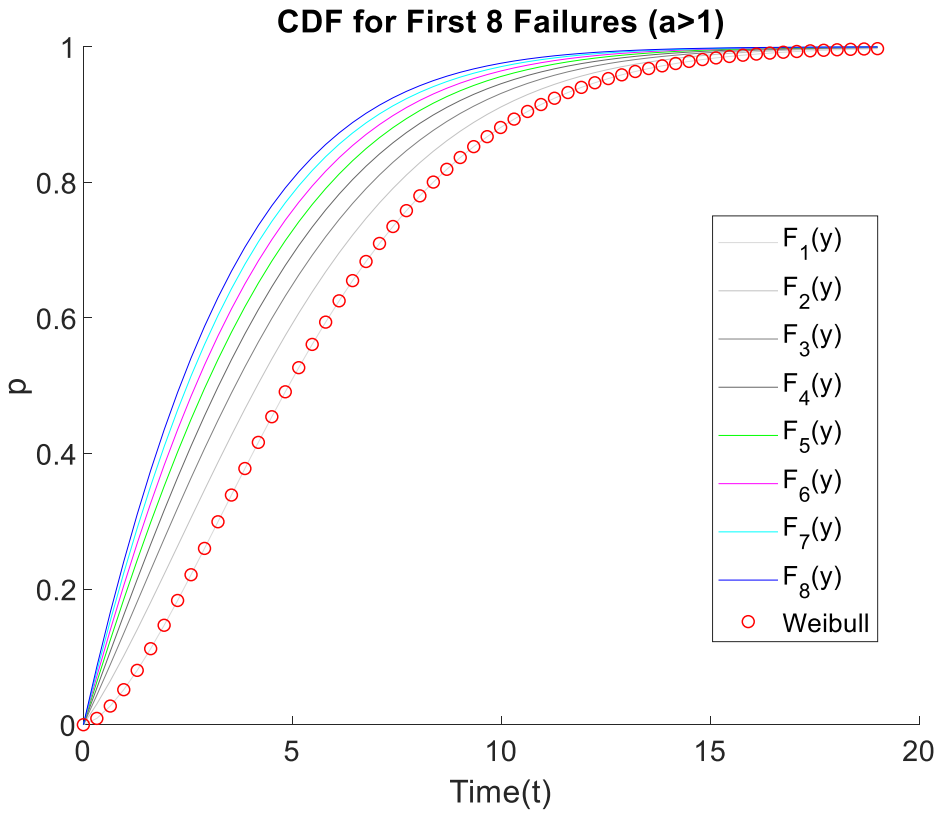


FIGURE 5.34: NHPP CDF FOR FIRST EIGHT FAILURES ($F_1(Y) \rightarrow F_8(Y)$), ($a$>1)

Table 5.22 lists the methodology that was used to model the distribution of times between state changes and explains why that method was chosen. The POE is used to move the switch rails and is an electrical component. The condition of the POE is often monitored in real time using condition monitoring [55], [56]. The Petri net framework is not well suited to processing a constant supply of condition data from condition monitoring, so the POE was not considered at this stage.

Compoent	Condition Change	Modelling Technique	Reasoning
1 Ballast	Good→ Minor Degradation	Conditional Weibull	Geometry data for S&C units is abundant so it was possible to obtain complete lifetime data information for ballast. It was decided to make the distribution conditional as the number of previous tamps is thought to influence the deterioration rate.
	Minor→ Major Degradation	Conditional Weibull	
2 Check and wing rail	Good → Degraded	Poisson Process	Rate determined based on the number of maintenance interventions recorded.
	Degraded → Failure	NHPP	The NHPP was chosen to model check and wing rail failures for two reasons. A lack of complete lifetime data (from the FMS database, it was not possible to establish any complete lifetimes) and following failure the check/wing rail is likely to be repaired and not replaced.
3 Crossing	Good → Degraded	Poisson Process	Rate determined based on the number of maintenance interventions recorded
	Degraded → Failure	NHPP	The NHPP is used to model failures due to a lack of lifetime data and because Ellipse records suggest repairs are performed far more regularly than renewals
4 POE	As POE is an electrical component it was decided that an alternative method capable of processing condition data was required.		
Sleepers/ bearers	Working → Failed	Poisson Process	The Poisson Process is used for two reasons. There are a high number of bearers within an S&C unit and from the data available it was not possible to determine exactly which bearer had failed, therefore it was not possible to determine complete lifetime data. Secondly following failure bearers are nearly always renewed and not repaired.
6 Slide chair	Working → Failed	Weibull Analysis	There are 2822 complete lifetimes and 5254 censored lifetimes recorded in the FMS database, so it is possible to fit a Weibull distribution.
7 Stretcher bars	Working → Failed	Poisson Process	The stretcher bars were modelled using a Poisson Process as complete life data was not available (as it was not possible to determine which stretcher bar had failed). Following a failure stretcher bars are normally renewed and not repaired.
8 Stock rail	Working → Degraded (through life)	Weibull Analysis (with varying stages of life)	There was considerable complete lifetime data for the stock rail, so the Weibull distribution was chosen, however in the data there were a high number of cases were multiple failures of the same component would be recorded followed by periods of no failures. The reason for this was thought to be poor maintenance or component burn in. To model this the stock rail life is divided into three parts with a separate Weibull distribution for each.
	Degraded→ Failed	Poisson Process	Failures are assumed to happen at a constant rate so a Poisson Process was used to model the occurrence of failures (from the degraded state).
9 Switch rail	Working → Degraded (through life)	Weibull Analysis (with varying stages of life)	Similar to the stock rail, there were found to regularly be clusters of failures of the same component followed by periods with no failures. So again three Weibull distributions are used.
	Degraded→ Failed	Poisson Process	Failures are assumed to happen at a constant rate so a Poisson Process was used to model the occurrence of failures (from the degraded state).

TABLE 5.22: DISTRIBUTIONS USED TO MODEL S&C DETERIORATION AND FAILURE, AND JUSTIFICATION

For the eight components considered the methodology shown in Table 5.22 was used to model the distribution of times between state changes. The distributions for the Weibull analysis and Poisson Process were determined using the MLE method in Weibull++ as described in section 5.3. The Weibull++ package does not provide a tool for fitting the NHPP so bespoke MATLAB code was written to do this. The NHPP parameters were estimated using a maximum likelihood estimator. The maximum likelihood estimators, $\hat{a}$ and $\hat{b}$ for the NHPP parameters *a* and *b* are shown in equations (5.6) and (5.7) respectively.

$$\hat{a} = \frac{n}{n\ln(T) - \sum_{i=1}^{N(T)} \ln(\tau_i)}, \tag{5.6}$$

$$\hat{b} = \frac{n}{T^{\hat{a}}}, \tag{5.7}$$

where *T* is the length of the observation period, *N(T)* is the number of failures in the observation period and τ_i is the time the ith failure occurred.

The aim was to determine distributions for the time for individual S&C components to change state, so a model for an individual S&C unit could be developed. In the case of the Weibull analysis the distribution fitted was based on component data and could be used directly. In the case of the Exponential distribution, it was assumed that events happen uniformly across the portfolio, consequently the value of λ was divided by 18,000 (total number of S&C units in the population) to determine the λ value for an individual S&C. In the case of the NHPP, the *a* parameter was kept constant and simulated annealing [146] was used to determine the *b* parameter which, for a population of 18,000 S&C units, led to the required number of events.

The distributions for the time to schedule and complete maintenance for the various tasks was calculated directly from maintenance records by considering the difference between '*Raised date'* and *'Complete date*' and '*Hours completed*' respectively.

The distributions for the time to degrade, time to fail, time to schedule maintenance and time to complete repairs, for each of the eight components are shown in Table 5.23, along with the transitions used to model them in the Petri net.

As discussed in Chapter 2, Network Rail classify turnout switches into ten groups A→H based on the switch size (information on the switch size is given in Appendix D-1.1). The values calculated in Table 5.23 did not consider switch size. Analysis was undertaken by Amey [147], to investigate the relationship between switch type and the number of failures, the results are shown in Figure 5.35.

The figure shows the normalised frequency of faults per switch per quarter for the ten switch types, as well as unclassified switches. It can be seen that small switch types (A, B) seem to have significantly fewer failures than the large switch types (G, H). Over 60% of type A switches had zero failures, whereas only around 20% of size H switches had zero failures.

To demonstrate the modelling capability the values in Table 5.23 were used for size D switches and for the remaining switch sizes the values were adjusted. This is discussed more in Chapter 6 when the Petri net model is introduced.

Component	Attribute	Observations	Transitions	Time Unit	Distributions
1 Ballast	Good → Poor	Estimated	CT_0^{SC}	Days	Conditional Weibull
	Poor → Very poor	Estimated	CT_1^{SC}	Days	Conditional Weibull
	Schedule tamping	2380	T_{59}^{SC}, T_{60}^{SC}	Days	Exponential(0.0064)
	Repair time	2993	$RT_1^{SC}, RT_2^{SC}, RT_3^{SC}$	Hours	Lognormal(0.859, 1.11)
2. Check and Wing	Time to degrade	849	T_{43}^{SC}	Days	Exponential(0.000026)
	Time to failure	54	CT_3^{SC}	Days	NHPP(1.035, 0.00014)
	Schedule	517	T_{46}^{SC}	Days	Exponential(0.0040)
	Repair time	727	$T_{47}^{SC}, T_{48}^{SC}, T_{49}^{SC}$	Hours	Exponential(0.0814)
3. Crossing	Time to degrade	21878	T_{36}^{SC}	Days	Exponential(0.000712)
	Time to failure	400	CT_2^{SC}	Days	NHPP(0.989, 0.0797)
	Schedule	18167	T_{39}^{SC}	Days	Exponential(0.0110)
	Repair time	21710	$T_{40}^{SC}, T_{41}^{SC}, T_{42}^{SC}$	Hours	Lognormal(1.579, 0.967)
4. Stock Rail	Early life duration	Estimated	T_{10}^{SC},	Days	Normal(500,4)
	Normal life duration	Estimated	T_{11}^{SC}	Days	Normal(5000,100)
	Early life failure	3202	T_7^{SC}	Days	Weibull(0.8931, 403.1)
	Normal life	3404	T_8^{SC}	Days	Weibull(1.856, 3531.2)
	Wear out phase	Estimated	T_9^{SC}	Days	Weibull(2.0, 2800.0)
	Schedule	2018	T_5^{SC}	Days	Exponential(0.0204)
	Repair time	2433	$T_0^{SC}, T_1^{SC}, T_6^{SC}$	Hours	Exponential (0.5063)
	Time to failure	Estimated	T_3^{SC}	Days	Exponential (0.0001)
5. Switch Rail	Early life duration	Estimated	T_{22}^{SC},	Days	Normal(750,5)
	Normal life duration	Estimated	T_{23}^{SC}	Days	Normal(5000, 100)
	Early life failure	4212	T_{19}^{SC}	Days	Weibull(0.965, 326.4)
	Normal life	814	T_{20}^{SC}	Days	Weibull(1.007, 30217)
	Wear out phase	Estimated	T_{21}^{SC}	Days	Weibull(3,5000.0)
	Schedule	2018	T_{17}^{SC}	Days	Exponential(0.0204)
	Repair time	2433	$T_{12}^{SC}, T_{13}^{SC}, T_{18}^{SC}$	Hours	Exponential (0.5063)
	Time to failure	Estimated	T_{15}^{SC}	Days	Exponential (0.0001)
6. Stretcher Bar	Time to degrade	9233[7]	T_{50}^{SC}	Days	Exponential(0.000304)
	Schedule	6918	T_{53}^{SC}	Days	Exponential(0.0096)
	Repair time	9046	T_{54}^{SC}, T_{55}^{SC}	Hours	Lognormal(1.276, 1.149)
7. Sleeper	Time to degrade	6422	T_{24}^{SC}	Days	Exponential(0.000195)
	Schedule	5579	T_{27}^{SC}	Days	Exponential(0.0032)
	Repair time	6363	T_{28}^{SC}, T_{29}^{SC}	Hours	Weibull(1.056, 24.183)
8. Slide Chair	Time to degrade	1270	T_{30}^{SC}	Days	Weibull(5.209, 4516.2)
	Schedule	932	T_{33}^{SC}	Days	Exponential(0.00411)
	Repair time	1255	T_{34}^{SC}, T_{35}^{SC}	Hours	Exponential(0.1678)

TABLE 5.23: DEGRADE, FAILURE, SCHEDULE AND REPAIR TIME INFORMATION FOR A SINGLE SIZE D S&C UNIT

[7]A breakdown of stretcher bar maintenance tasks is shown in Appendix D-2.1

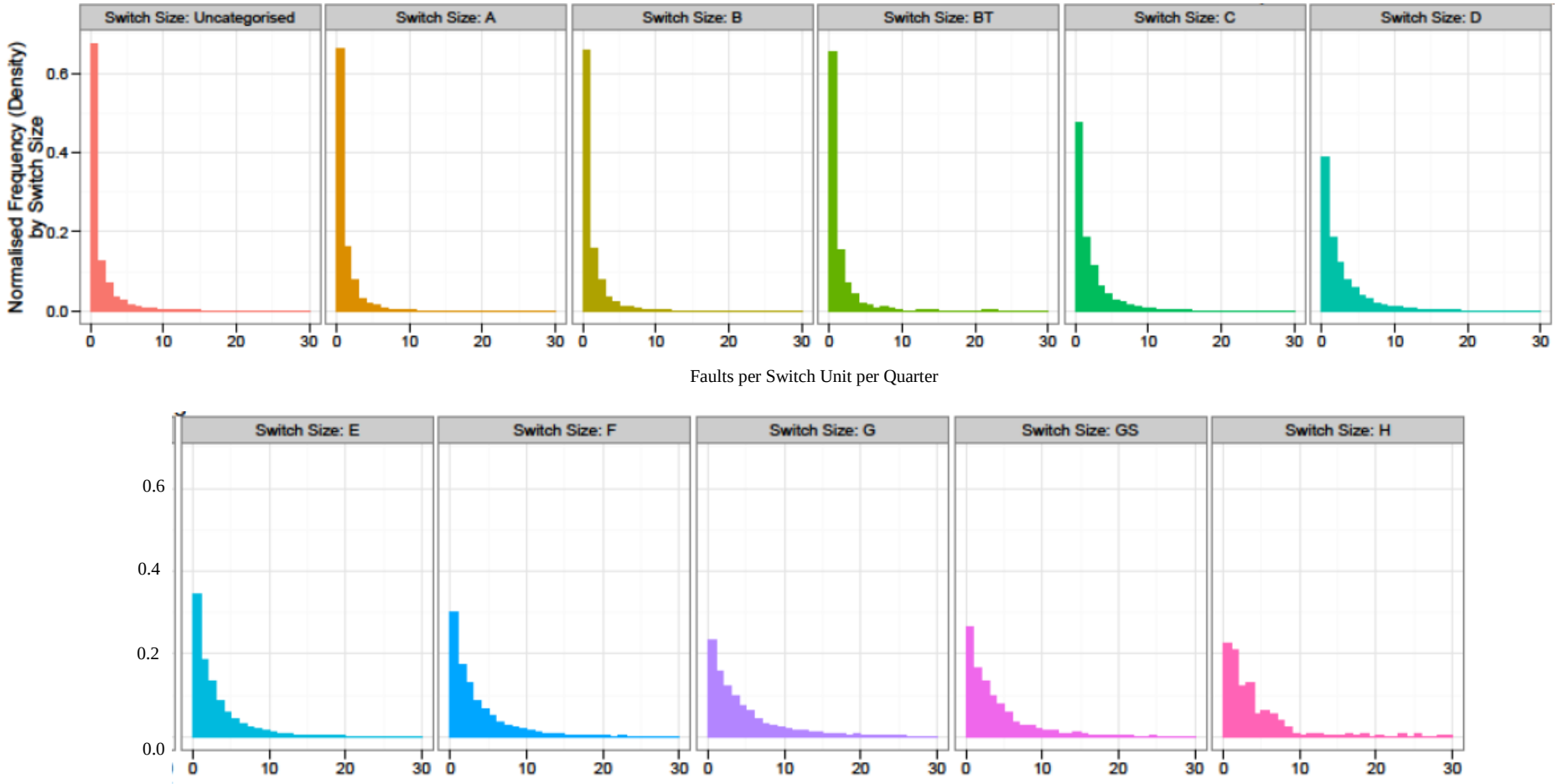


FIGURE 5.35: NUMBER OF FAILURES PER QUARTER BY SWITCH SIZE (A→H) [147]

5.7 Analysis of the Signalling System

The last asset considered is the signalling system. There are two main differences between the signalling system and the assets discussed so far in this study:

(i) The signalling system is largely independent of the other assets considered; the condition of the track and other assets has little effect on the signalling system, unless a catastrophic event such as a derailment occurs.

(ii) The signalling system tends to cover a large area, it cannot be broken down into small sections, and if any components in the signalling system fail the whole route is likely to be affected.

For this reason the signalling system will be modelled at route level, rather than eighth mile section level. Similarly to S&C the signalling system is made up of a high number of subsystems. Five subsystems will be considered:

(i) Axle Counters
(ii) Automatic Warning System (AWS)
(iii) Direct Current (DC) Track Circuits
(iv) Cables
(v) Signal Lamps

The number of interventions on the UK network (excluding Northern Ireland) for the financial year (March 2014 - April 2015) for each of the five subsystems is shown in Figure 5.36. It can be seen that track circuits have the highest number of interventions/repairs with axle counters and signal lamps having the least.

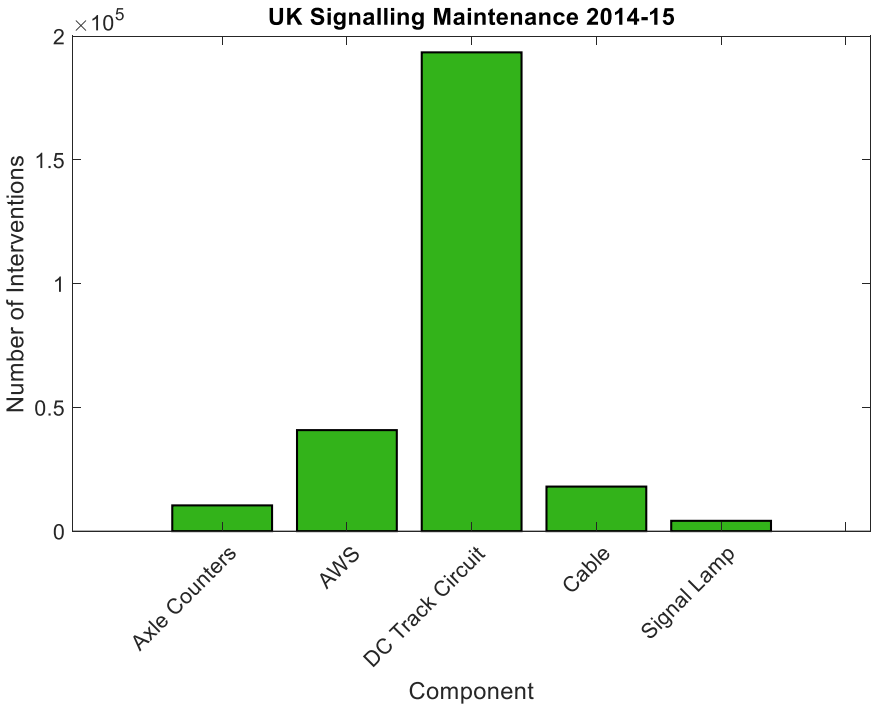


FIGURE 5.36 UK SIGNALLING REPAIR/MAINTENANCE 2014-2015

To model the signalling system in Bletchley Delivery Unit it was decided to only consider maintenance interventions that occurred in Bletchley Delivery Unit, the results are shown in

Figure 5.37. It can be seen for Bletchley Delivery Unit, DC track circuits again have the highest number of interventions.

As the Petri net model for the signalling system was created at route level it was not necessary to determine distributions for individual components. The deterioration was modelled using an Exponential distribution where the rates of occurrence were based on the number of occurrences for Bletchley Delivery Unit shown in Figure 5.37. An Exponential distribution was used as it was unclear how the deterioration rate would change over time, many of the electrical components would show no signs of deterioration prior to failure and, as it was unclear exactly which component had been repaired, it was not possible to determine lifetime data. Figure 5.38 shows the PDF of the Exponential distributions found for the time to degrade for the various signalling components.

In addition to the number of maintenance interventions the number of signalling faults was also considered. The number of faults in Bletchley Delivery Unit for the financial year (March 2014 - April 2015) for each of the five subsystems is shown in Figure 5.39. It can be seen that for Bletchley Delivery Unit the highest number of faults are attributed to axle counters. The failure distribution was also modelled using an Exponential distribution, the rates were based on the values shown in Figure 5.39. The Exponential distribution was thought to be the most appropriate distribution due to the low number of failures.

Using the *raised* and *complete* data in the maintenance records, distributions for the time to schedule maintenance for each of the five component types were calculated. The *actual hours* were used to determine distributions for the time to complete maintenance.

Table 5.24, summarises the distributions found for the deterioration, failure, schedule time and ART for the signalling system in Bletchley Delivery Unit. The transitions used to model them, which will be introduced in Chapter 6, are also listed.

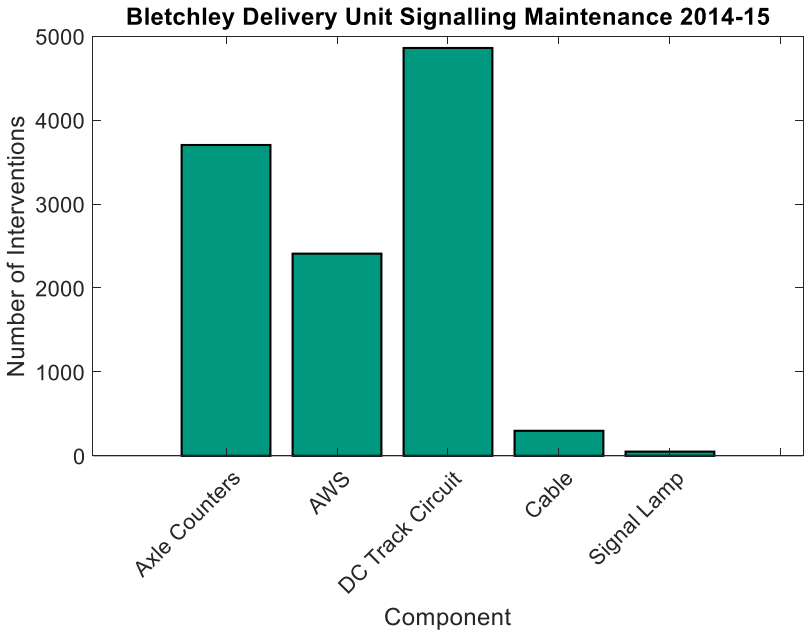


FIGURE 5.37 BLETCHLEY DELIVERY UNIT SIGNALLING REPAIR/MAINTENANCE 2014-2015

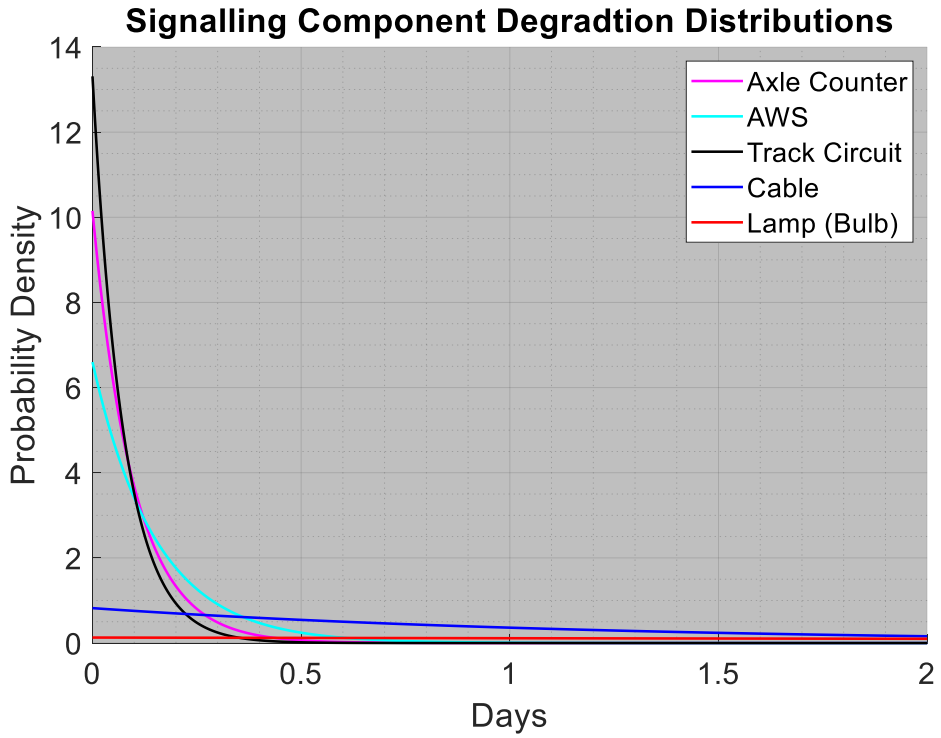


FIGURE 5.38: BLETCHLEY DELIVERY UNIT SIGNALLING COMPONENT DEGRADATION DISTRIBUTIONS

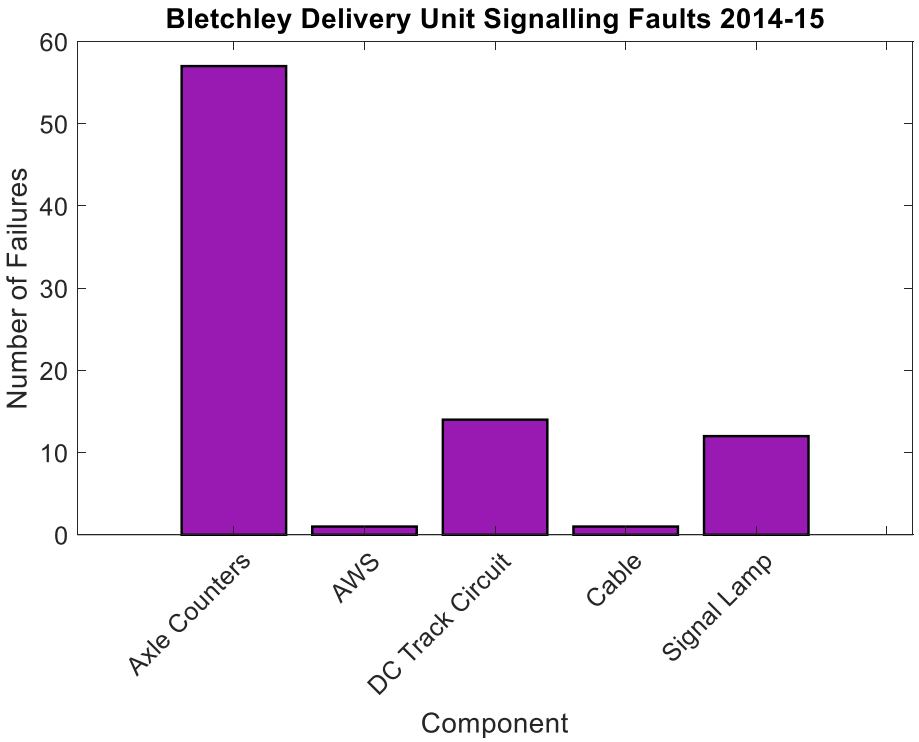


FIGURE 5.39 NUMBER OF FAILURES IN 2014-2015

	To Time Degrade			Time to Failure			Schedule Time			ART		
	Distribution	Time Unit	Transition	Distribution	Time Unit	Transition	Distribution	Time Unit	Transition	Distribution	Time Unit	Transition
Axle Counter	Exponential(10.15)	Days	T^{SG}_{13}	Exponential (0.156)	Days	T^{SG}_{14}	Lognormal(2.37, 0.64)	Days	T^{SG}_{11}	Weibull(1.33, 0.96)	Hours	T^{SG}_{10}, T^{SG}_{15}
AWS	Exponential(6.6)	Days	T^{SG}_{19}	Exponential (0.003)	Days	T^{SG}_{20}	Lognormal(2.45, 0.90)	Days	T^{SG}_{17}	Weibull(1.11, 0.89)	Hours	T^{SG}_{16}, T^{SG}_{21}
Track Circuit	Exponential(13.31)	Days	T^{SG}_{25}	Exponential (0.038)	Days	T^{SG}_{26}	Lognormal(2.35, 0.70)	Days	T^{SG}_{23}	Weibull(1.40, 0.91)	Hours	T^{SG}_{22}, T^{SG}_{27}
Cable	Exponential(0.82)	Days	T^{SG}_{31}	Exponential (0.003)	Days	T^{SG}_{32}	Lognormal(3.92, 1.52)	Days	T^{SG}_{29}	Weibull(0.96, 3.71)	Hours	T^{SG}_{28}, T^{SG}_{33}
Lamp (blub)	Exponential(0.129)	Days	T^{SG}_{6}	-		-	Lognormal(1.16, 0.93)	Days	T^{SG}_{4}	Lognormal(0.09, 0.63)	Hours	T^{SG}_{3}, T^{SG}_{8}, T^{SG}_{9}
Signal unit	Exponential(0.008)	Days	T^{SG}_{1}	Exponential (0.032)	Days	T^{SG}_{7}	-		-	-		-

TABLE 5.24: DEGRADATION, FAILURE, SCHEDULE AND REPAIR DISTRIBUTIONS AND TRANSITIONS FOR SIGNALLING SYSTEM FOR BLETCHLEY DELIVERY UNIT

5.8 Inspections

To be able to manage assets effectively and to ensure safety thresholds are maintained it is important to know the condition of assets. For this reason Network Rail regularly inspects all the assets in their portfolio. The inspection interval (time between inspections) is dependent on a number of things:

(i) The deterioration rate of the asset; assets such as bridges and tunnels which degrade very slowly can have lengthy periods between inspections. Whereas, the alignment of the track can be measured as frequently as fortnightly.

(ii) The condition of assets; assets which are known to be in a poorer condition are likely to be inspected more frequently.

(iii) The criticality of the asset/route; higher category lines will generally be inspected more frequently.

(iv) The type of inspection; visual inspections will be performed much more regularly than detailed inspections; the condition during a visual inspection can often trigger a full detailed inspection.

Four types of inspection are considered:

(i) Basic Visual Inspection

This type of inspection will reveal serious defects such as rail breaks and broken sleepers. The visual inspection frequencies specified in Network Rail standards are shown in Table 5.25. Transitions used to model visual inspections are shown with a blue outline in diagrams ● (see Figure 6.23).

(ii) Geometry Inspection

This type of inspection is performed by the NMT and measures the horizontal and vertical geometry. The geometry inspection frequencies specified in Network Rail standards are shown in Table 5.26. Transitions used to model visual inspections are shown with a yellow outline in diagrams ● (See Figure 6.7).

(iii) Ultrasonic Inspection

This type of inspection reveals rail defects that are not detected by the visual inspection. The ultrasonic inspection frequencies specified in Network Rail standards are shown in Table 5.27. Transitions used to model visual inspections are shown with a green outline in diagrams ● (See Figure 6.38).

(iv) Tunnel Inspections

Tunnels are visually inspected every 12 months. Detailed examinations of tunnels are also performed, however they are much less frequent than visual inspections. The interval between detailed examinations is determined by the risk of structural failure, technical specifications of the tunnel and the condition at previous detailed and visual inspections. The time between detailed examinations ranges between one and six years based on these factors.

Category	Frequency (Days)
1A	14
1	14
2	14
3	28
4	28
5	56
6	56

TABLE 5.25: BASIC VISUAL INSPECTION FREQUENCY, SOURCED FROM NR/L2/TRK/001/MOD11 [24]

Category	Frequency (Days)
1A	42
1	70
2	98
3	126
4	182
5	182
6	182

TABLE 5.26: NMT INSPECTION FREQUENCY, SOURCED FROM NR/L2/TRK/001/MOD02 [23]

Category	Frequency (Days)
1A	56
1	56
2	112
3	182
4	182
5	182
6	182

TABLE 5.27: ULTRASONIC INSPECTION FREQUENCY, SOURCED FROM NR/L2/TRK/001/MOD06 [32]

5.9 Summary and Conclusions

This chapter has provided an analysis of the five asset classes that will be modelled in this research. Six areas were identified as critical to changing the state of the system:

(i) Deterioration rates
(ii) Inspection regimes
(iii) Maintenance regimes
(iv) Time to schedule maintenance
(v) Time to complete maintenance, ART
(vi) Location parameters

This chapter attempted to quantify each of these aspects for the five asset groups. Maintenance records and condition records were used alongside engineering judgement and Network Rail standards to quantitatively quantify each of the six areas. Significant variation between track categories was observed it was therefore concluded the data should be segregated by track category where possible. The key conclusions from the analysis for each of the asset classes are shown in Table 5.28.

Asset Class	Conclusions
Track Section	**Ballast** • The higher the track category, the more tamping and stoneblowing maintenance performed. The exception to this was stoneblowing of Category 1A lines, stoneblowing is generally not used for Category 1A as it cannot deliver the required alignment. • Tamping is performed approximately three times as often as stoneblowing. • The average length of track maintained during an intervention is half a mile. However, there is significant variation in the length of track maintained. • Interventions on high track categories (1A, 1) tend to cover a longer length of track than lower categories. • The volume of tamping remained relatively constant during CP4. • In general tamping was scheduled more quickly if the track alignment was '*Very poor*' or '*Super red*'; however, a strong correlation between ballast condition and schedule time was not found. • There are a range of location parameters, such as sleeper design and bedrock which influence the deterioration of ballast and hence the frequency of tamping and stoneblowing. An LI was presented to model this. • The effectiveness of tamping decreases with each intervention. **Rail** • There was no clear link between track category and the volume of rail work performed. • Generally grinding and welding did not cover more than a single track section (less than eighth mile).
Sleepers	• It was not possible to establish a clear link between tonnage and the deterioration of sleepers. • Wooden sleeper replacement volumes were higher than steel and concrete. • During an intervention the number of sleepers replaced varies, in general during an intervention the number of timber sleepers replaced is greater than for concrete or steel.
S&C	• S&C units are made up of a number of components, it was therefore, not appropriate to use one method to model the deterioration of S&C, three methods were considered: Poisson Process (Exponential), NHPP and Weibull Analysis. • The switch size affects the number of failures, with larger switches (G and H) experiencing more failures than smaller sizes (A and B).
Tunnel	• Tunnels degrade slowly compared to other assets, the average tunnel age in the UK is 150 years. • Assets in tunnels exhibit different characteristics than those not.
Signalling System	• The signalling system is a single system, which covers the whole route; it cannot be broken down into different sections, and therefore is modelled at route level. • The deterioration of the signalling system is not dependent on factors such as line speed and tonnage.

TABLE 5.28: KEY CONCLUSIONS FROM THE SYSTEM ANALYSIS

6 Individual Models for Railway Assets

6.1 Introduction

This chapter describes the development of Petri net models for the degradation and maintenance of five asset classes which occur on railway networks: track, sleepers, S&C, tunnels and the signalling system. Initially the Petri net notation will be explained alongside the Petri net extensions used in this research. Petri net asset models for each of the five asset types will then be presented alongside the results of the individual models.

6.2 Petri Net Transitions and Notation

This section will outline the Petri net transitions that will be used and the labelling system that will be employed. Four non-standard transition types are used: conditional transitions [21], reset transitions [21], probabilistic transitions [80] and conditional probabilistic transitions [148] alongside the standard transition [81] introduced in section 3.3.2. Note in C++ counting starts from zero, hence all numbering of places and transitions within the Petri nets starts from zero. Table 6.1 shows the six different node types used, the following sections will discuss each of the node types in more detail.

	Node	Source	Symbol	Section
1	Place	[79]	P	6.2.1
2	Standard Transition	[79]	T	6.2.2
3	Conditional Transition	[21]	CT	6.2.3
4	Reset Transition	[21]	RT	6.2.4
5	Probabilistic Transition	[80]	PT	6.2.5
6	Conditional Probabilistic Transition	[148]	CPT	6.2.6

TABLE 6.1: NODE TYPES

6.2.1 Places

The marking of a place (number of tokens in the place) is used to represent the state of the system or information about the system. The marking of the system determines which transitions are enabled and consequently how the system will evolve.

6.2.2 Standard Transitions

A standard transition is enabled when all of the input places contain at least a number of tokens equal to their associated arc weight and it is not inhibited as explained in section 3.3.2. Once a transition is enabled it can fire. There can be a delay between the transition being enabled and it firing. This can be determined in one of six ways:

1. Exponential Distribution

The firing time is sampled from an Exponential distribution, to achieve this the distribution CDF is used. The CDF of the Exponential distribution is shown in equation (6.1):

$$CDF = 1 - e^{-\lambda t}, \tag{6.1}$$

A random number $X \in (0,1)$ is set equal to the CDF, equation (6.1) is then rearranged to make t the subject as shown in equation (6.2); t is the firing time assigned to the transition.

$$t = \frac{-\ln(1-X)}{\lambda}. \tag{6.2}$$

Note that as X is a randomly generated variable from a uniform distribution between one and zero; using X or $1 - X$ when sampling has no impact on the overall distribution obtained so $1 - X$ can be replaced with just X, this is done in all subsequent equations where appropriate.

2. Weibull Distribution

The firing time is sampled from a Weibull distribution. The CDF of the Weibull distribution is shown in equation (6.3):

$$CDF = 1 - e^{-(\frac{t}{\eta})^{\beta}}. \tag{6.3}$$

A random number $X \in (0,1)$ is set equal to the CDF, equation (6.3) is then rearranged to make t the subject as shown in equation (6.4). t is the firing time assigned to the transition.

$$t = \eta[(-\ln(X))^{\frac{1}{\beta}})], \tag{6.4}$$

where β is the shape factor of the Weibull distribution and η is the scale factor.

3. Normal Distribution

The CDF of the Normal distribution is shown in equation (6.5).

$$CDF = \frac{1}{2}[1 + ecf\left(\frac{t-\mu}{\sigma\sqrt{2}}\right)], \tag{6.5}$$

where $ecf(x)$ is the error function defined as:

$$ecf(x) = \frac{2}{\sqrt{\pi}}\int_0^x e^{-t^2}dt\,. \tag{6.6}$$

A random number $X \in (0,1)$ is set equal to the CDF, equation (6.5) is then rearranged to make t the subject as shown in equation (6.7). t is the firing time assigned to the transition:

$$t = \sigma\sqrt{2} * ecf^{-1}(2X - 1) + \mu, \tag{6.7}$$

where $ecf^{-1}(x)$ is the inverse error function and is defined such that:

$$ecf^{-1}\big(ecf(x)\big) = x. \tag{6.8}$$

The inverse error function, $ecf^{-1}(x)$, is approximated using the formula proposed in [149], shown in equation (6.9).

$$ecf^{-1}(x) = sgn(x)\sqrt{\sqrt{\left(\frac{2}{\pi a} + \frac{\ln(1-x^2)}{2}\right)^2 - \frac{\ln(1-x^2)}{a}} - \left(\frac{2}{\pi a} + \frac{\ln(1-x^2)}{2}\right)}, \tag{6.9}$$

where:

$$a = \frac{8(\pi - 3)}{3\pi(4 - \pi)} \approx 0.140012. \tag{6.10}$$

And *sgn*(*x*) is the sign function defined as:

$$sgn(x) = \begin{cases} -1 & \text{if } x < 0 \\ 0 & \text{if } x = 0 \\ 1 & \text{if } x > 0 \end{cases} \quad (6.11)$$

The maximum error in this approximation is 0.00035.

It should be noted that when sampling from a normal distribution theoretically it is possible to obtain a negative value as $X \rightarrow 0$ in equation (3.7). To account for this when sampling using computer software, the smallest nonzero value of *X* was calculated and substituted into equation (3.7), the value of *t* was then checked to ensure it was non negative. This was done for all normal distributions used.

4. Lognormal Distribution

The CDF of the Lognormal distribution is shown in equation (6.12).

$$CDF = \frac{1}{2}\left[1 + ecf\left(\frac{\ln(t)-\mu}{\sigma\sqrt{2}}\right)\right], \quad (6.12)$$

where $ecf(x)$ is the error function as defined in equation (6.6). A random number *X* is set equal to the CDF, equation (6.12) is then rearranged to make *t* the subject as shown in equation (6.13). *t* is the firing time assigned to the transition:

$$t = e^{\sigma\sqrt{2} * ecf^{-1}(2X-1)+\mu}, \quad (6.13)$$

where $ecf^{-1}(x)$ is the inverse error function as defined in equation (6.8).

5. Non Homogenous Poisson Process (NHPP)

As discussed in section 5.6, for some of the S&C components following maintenance the component was not as good as new. These components were modelled with the NHPP. Values can be sampled from an NHPP according to:

$$t = \sqrt[a]{\tau_{i-1}{}^{a} - \frac{\ln(X)}{b}} - \tau_{i-1} \quad \text{i=1, 2, 3, …,} \quad (6.14)$$

where τ_{i-1} is the time the last failure occurred, and *a* and *b* are the parameters of the NHPP.

6. Fixed Amount of Time

The firing time of the transition is fixed and the transition always fires after the same amount of time has elapsed. Note this time could be zero meaning it fires immediately.

6.2.3 Conditional Transitions

The enabling and firing rules for the conditional transition [21], are the same as for the standard transition. However the delay between the transition being enabled and it firing is dependent on the marking of a number of other places in the net. Conditional transitions were used to govern the degradation of rails, ballast and S&C components; the deterioration rates were altered based on the maintenance history. Figure 6.1 shows a conditional transition (shown in blue) firing. The input places are *P0* and *P1* and the output place is *P3*. The distribution used in the transition is dependent on the marking of places *P8* and *P32*.

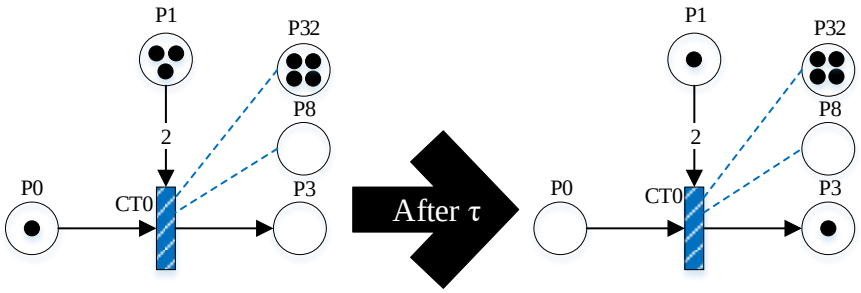


FIGURE 6.1: MARKING OF THE SYSTEM BEFORE AND AFTER A CONDITIONAL TRANSITION FIRES

6.2.4 Reset Transitions

The enabling and firing rules for the reset transition [21], are the same as the standard transition, however when a reset transition fires a number of places and transitions in the net are reset. The marking of places is returned to the initial marking and the firing time of the transitions is re-sampled when the reset transition fires. Figure 6.2 shows a reset transition firing and the effect it has on the subnet. In Figure 6.2 transition *T44* is enabled, when transition *RT0* fires however the marking of *P19* is set to zero (see Table 6.2). This means that transition *T44* is no longer enabled, the delay time of the transition must therefore be re-sampled. For clarity, in figures, the places and transitions reset when a reset transition fires are not shown, as in most cases the reset transition resets a high number of places and transitions; if all these arcs were shown in the figure it would become meaningless. Instead where appropriate the places and transitions reset will be listed in a table. In the case of the Petri net shown in Figure 6.2, Table 6.2 details the places that will be reset (the places whose marking will be changed after the reset transition fires).

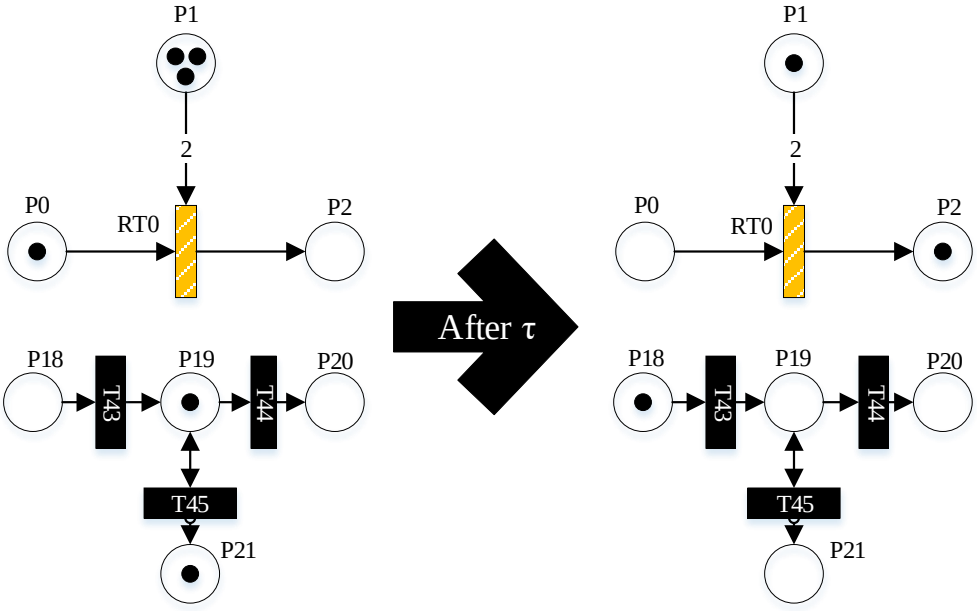


FIGURE 6.2: MARKING OF THE SYSTEM BEFORE AND AFTER A RESET TRANSITION FIRES

Place	Reset	Marking
P0	No	n/a
P1	No	n/a
P2	No	n/a
P18	Yes	1
P19	Yes	0
P20	Yes	0
P21	Yes	0

TABLE 6.2: RESET PLACES AND MARKING

6.2.5 Probabilistic Transitions

The probabilistic transition [80] is used to select one outcome from a choice of many. In Figure 6.3 there are three possible outputs; there is a 50% chance of *P2* being marked a 30% chance of *P3* being marked and a 20% chance of *P4* being marked. In addition to probability outputs, there may also be constant outputs, this place is marked every time the transition fires. In Figure 6.3 there is one constant output *P5*, this place is always marked when probabilistic transition *PT0* fires regardless of which output place is selected. All probabilistic transitions are assumed to have zero delay time and fire as soon as they are enabled.

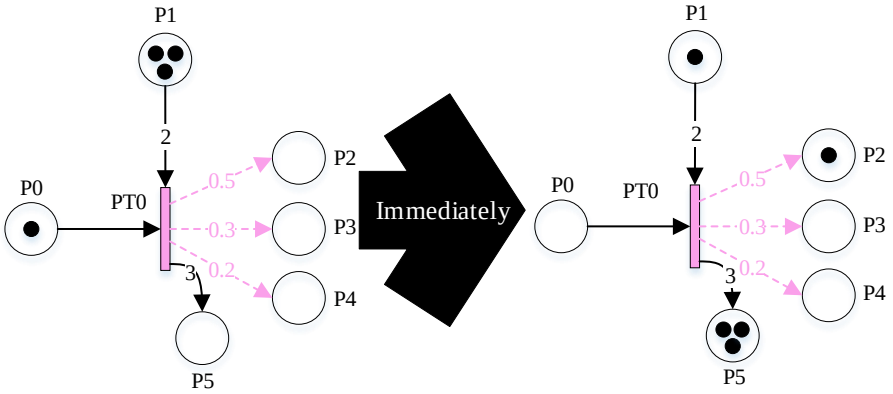


FIGURE 6.3: MARKING OF THE SYSTEM BEFORE AND AFTER A PROBABILISTIC TRANSITION FIRES

6.2.6 Conditional Probabilistic Transitions

The final transition type is the conditional probabilistic transition [148]. It is a hybrid of the conditional and probabilistic transitions. It is identical to the probabilistic transition (see section 6.2.5) except that the probabilities that govern which output place is marked are conditional on the marking of other places is the net. In Figure 6.4 the probabilities of moving to *P0* or *P1* changes based on the marking of place *P19* and *P69.* The marking of *P19* and *P69* does not change when the transition fires.

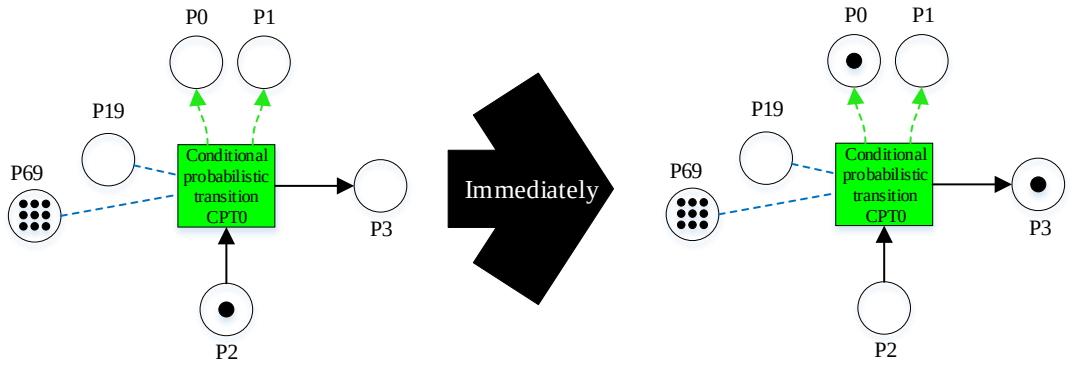


FIGURE 6.4: MARKING OF THE SYSTEM BEFORE AND AFTER A CONDITIONAL PROBABILISTIC TRANSITION FIRES

6.2.7 Conflicting Transitions

One additional feature that needs to be addressed is conflicting transitions. A conflicting transition occurs if a single place feeds multiple transitions. Figure 6.5 shows an example of the unique scenario that can cause a conflict to arise. A conflict has arisen as both *T0* and *T1* have the same firing time and hence after time τ will both attempt to fire, however there is only one token in place *P0*. To address this issue, it is assumed that in the event of a conflict the transition with the lowest number will fire. So in the case of Figure 6.5, transition *T0* would fire. The transition(s) prevented by the conflict are treated as if they were never enabled and their firing time is resampled the next time the transition becomes enabled.

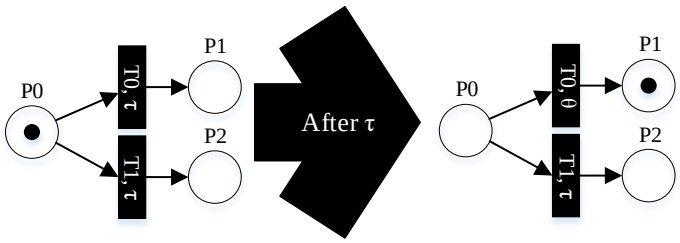


FIGURE 6.5: CONFLICTING TRANSITIONS

6.2.8 Labelling System

Before creating any Petri nets it was important to decide on a robust numbering system to ensure that the model is flexible enough to allow different asset modules to be added and removed from the structure with ease. A conventional numbering system, for places and transitions, from zero to *n* was not suitable. There are two problems with a conventional numbering system; firstly the numbers become extremely high and lose meaning. Secondly the system cannot handle adding additional modules easily. To address this issue an alternative numbering system is chosen. The numbering system adopted is shown in equation (6.15) .

$$YY_{nn}^{t-c} \quad (6.15)$$

The labelling system comprises of four aspects:

i. *YY* used to define the node type, for example place (listed in Table 6.1)
ii. *t* used to define the module type, for example track section (see in Table 6.3)
iii. *nn* used to define the node number
iv. *c* used to define the track category

For example CT_{23}^{T-1A} would describe conditional transition number *23* in a *Category 1A*, *track section* module.

	Model/Module	Label	Section
1	Master	M	Chapter 7
2	Track Section	T	6.3.1
3	Concrete Sleeper	CS	6.3.2.1
4	Wooden Sleeper	WS	6.3.2.2
5	Steel Sleeper	SS	6.3.2.3
6	Tunnel	TN	6.3.3
7	S&C	SC	6.3.4
8	Signalling	SG	6.3.5

TABLE 6.3: ASSET PETRI NET MODEL LABELS

6.3 Petri Net Asset Models

The remainder of this chapter will present Petri net models for the five asset classes considered in this research, using the numbering system introduced and the five transition types discussed.

6.3.1 Track Section Petri Net Model

The first step in creating the whole system model was to create a model for an individual track section to simulate the ballast and rails. Ideally their condition would be expressed as a continuous function along their length. However, modelling the system at that level of detail would be difficult and the computation time needed to solve the model would be prohibitive. Therefore the network is discretised into a finite number of segments *track sections,* over which the condition is considered to be uniform.

Choosing the length of the track section is a balance between computation time (the smaller the track section the more track sections required hence the longer the simulation time) and the level of accuracy required (if the track section is too large then the approximation of the true condition using a uniform representation is not valid). Network Rail records track geometry data over 220 yard sections called Poskeys [150]. Therefore the track section length used is 220 yards (eighth mile) to correspond with the condition data. The 220 yard track section Petri net model is described below; the model contains subnets to simulate the degradation, inspection and maintenance of the ballast and rails.

6.3.1.1 Ballast Petri Net Model

The first part of the track section model simulates the deterioration, inspection, maintenance and renewal of ballast. The track alignment is governed by the condition of the ballast and over time as the ballast condition worsens the track alignment deteriorates. Network Rail assess each Poskey (220 yards section) as being in one of five quality bands based on the geometry and line speed. These categories are '*Good*', '*Satisfactory*', '*Poor*', '*Very poor*' and '*Super red*'. Therefore the ballast condition was modelled using five places, one for each quality band; hence a series Petri net consisting of five places and four conditional transitions was developed to model the deterioration of the ballast as shown in Figure 6.6.

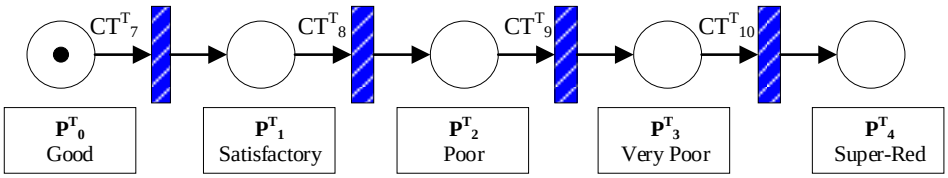


FIGURE 6.6: BALLAST CONDITION PETRI NET MODEL

The firing times of the conditional transitions $CT_7^T \rightarrow CT_{10}^T$ are sampled from Weibull distributions. The parameter values were those found in Chapter 5 and are shown in Table 5.2. The scale parameter of these Weibull distributions is then adjusted based on:

(i) The number of previous interventions

It has been shown that track deterioration is related to the number of maintenance actions performed since the last renewal [142]. Therefore, after each intervention the Weibull distribution scale parameter was decreased.

(ii) Location parameters

The LI introduced in section (5.4.3) was used to adjust the distributions for the time to degrade, based on the eight location factors. In the individual track section model the location parameters were not considered and the LI score is always assumed to be 500 (baseline value). However in the whole system model the LI was calculated based on the attributes of each eighth mile section, hence the parameters in the distributions used to model the deterioration rates for each section were different. The LI scores used in the system model are shown in Appendix J-1.1.

Once the model for the deterioration was developed the next step was to model the inspection. To model this, each of the four deteriorated ballast condition states (P_1^T, P_2^T, P_3^T and P_4^T) are connected (via transitions T_0^T, T_1^T, T_2^T and T_3^T) to degradation revealed (known) states (P_{14}^T, P_{15}^T, P_{17}^T and P_{19}^T). For clarity in diagrams, places that represent a revealed (known) condition state are drawn with a red outline.

As discussed in section 5.8 ballast alignment is assessed during a geometry inspection carried out by the NMT. The geometry inspection frequencies are shown in Table 5.26. Transitions used to model geometry inspections are shown with a yellow outline in diagrams (See Figure 6.7). The inspection frequency is dependent on the track category and it is assumed that all inspections are perfect.

Figure 6.7 shows the Petri net used to simulate the inspection of ballast in '*Poor*' condition. The marking of P_2^T indicates poor ballast condition. Transition T_1^T links the unrevealed state to the revealed state and is only enabled when P_{101}^T is marked; simulating an inspection is ongoing. Place P_{15}^T will remain marked until either the condition worsens (CT_9^T fires) and the known condition is updated (following an inspection) or the condition is reset following completion of maintenance. Due to the inhibitor arc between T_1^T and P_{15}^T, T_1^T will only fire when the deterioration is revealed for the first time.

Once degradation is revealed following an inspection, maintenance can be scheduled. The scheduling of maintenance is one of the most important decisions asset managers have to make and one of the most difficult features to model. In the single track section model maintenance is scheduled based solely on the condition of the track section. However in the whole system framework, a range of alternative strategies are proposed which will consider the condition of all track sections before scheduling maintenance.

In the track section model three types of ballast maintenance are considered: tamping, stoneblowing and manual interventions. A conditional probabilistic transition decides whether tamping or stoneblowing should be performed based on the number of previous interventions in the section, see Figure 6.8. Three rules are considered when scheduling tamping and stoneblowing:

(i) Tamping is performed approximately three times as often as stoneblowing (Categories 1→6).
(ii) For Category 1A track, stoneblowing is only considered after eight tamps (Tamping is the preferred method for Category 1A track as stoneblowing cannot deliver the required alignment accuracy).
(iii) Following a stoneblow it is bad practice to tamp the section.

Once the decision was made to tamp or stoneblow the section, a standard transition was used to implement the distributions for the scheduling times found in Chapter 5. The schedule time was split into two groups: '*Normal schedule time*' if the alignment was '*Good*', '*Satisfactory*' or '*Poor*' at the time of maintenance being requested and '*Emergency schedule time*' if the alignment was '*Very poor*' or '*Super red*' at the time of maintenance being requested. The distribution parameters used and the transitions used to model them are shown in Table 5.5.

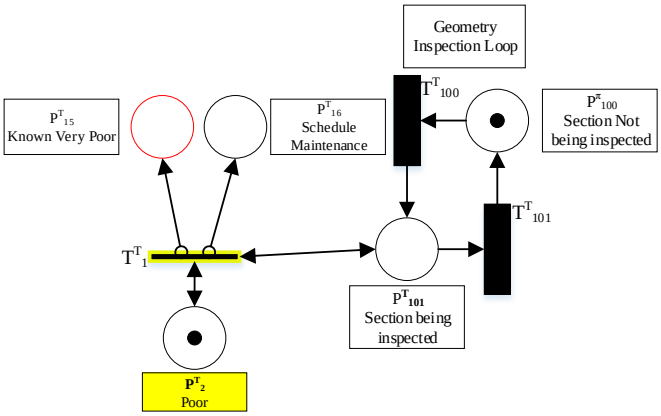


FIGURE 6.7: INSPECTION PETRI NET

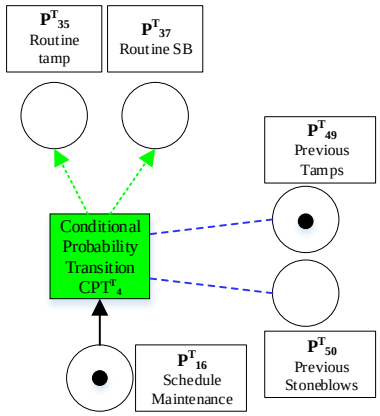


FIGURE 6.8: MAINTENANCE SCHEDULING PETRI NET

Figure 6.9 shows the Petri net used to simulate a tamp taking place. Once P^T_{35} is marked transition T^T_{19} is enabled, the firing time of T^T_{19} is sampled from the '*Normal schedule time*' Lognormal distribution found in Chapter 5 (see Table 5.5). Following the firing of T^T_{19}, RT^T_0 is enabled, the firing time of RT^T_0 is sampled from a Lognormal or Weibull distribution based on the distributions found in Chapter 5 (see Table 5.6). When RT^T_0 fires it adds one to the marking of place P^T_{49} and P^T_{99}; this in turn influences the degradation rates of the ballast and the effectiveness of the repair. The firing of RT^T_0 removes all unrevealed and revealed condition markings. The conditional probabilistic transition, CPT^T_1, then marks either P^T_1, P^T_2 or P^T_3 with respective probabilities q_1, q_2, q_3 based on the marking of P^T_{99}. Initially q_1 is approximately one and q_2 and q_3 are approximately zero; however, in time, the values evolve such that q_1 and q_2 are approximately zero and q_3 is approximately one. This was used to simulate the decreasing effectiveness of maintenance. At this stage these values are estimated, the values used are shown in Appendix A.

One final piece of housekeeping in the Petri net is needed to ensure that only one known condition place is marked at once, Figure 6.10 shows the Petri net that is used to achieve this.

Safety is critical on the railway. If an asset becomes heavily degraded then it may no longer be safe to run trains under normal conditions. When this occurs two types of action can be taken: impose a TSR, or in extreme cases close the line. Network Rail have detailed rules and regulations on when to impose speed restrictions and line closures set by the ORR.

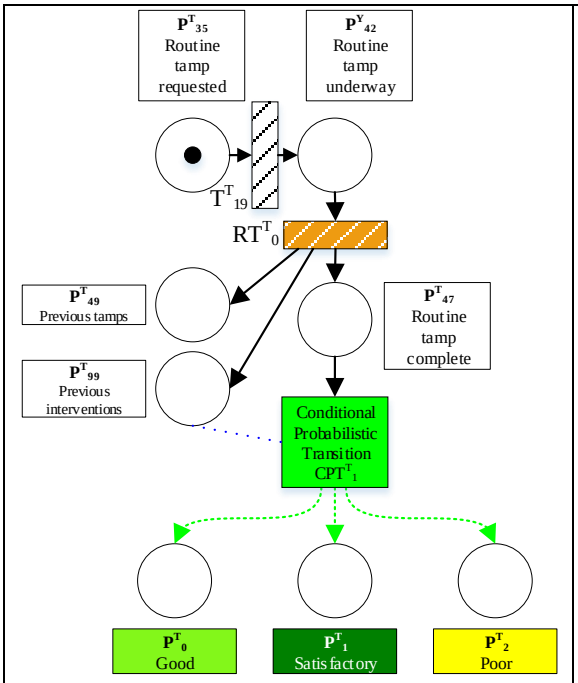


FIGURE 6.9: PERFORMING MAINTENANCE

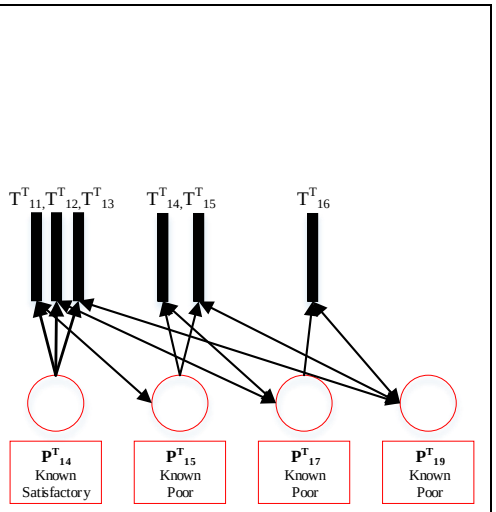


FIGURE 6.10: UPDATE CONDITION

Speed restrictions were modelled in the Petri net in the following way. The overall track section condition was modelled as being in one of four states: No speed restriction (P_{80}^T), Level 1 speed restriction (P_{82}^T), Level 2 speed restriction (P_{83}^T) and Line closure (P_{84}^T). There were five condition states in the track section Petri net model that would require a speed restriction or line closure, as shown in Table 6.4. It is important to note the restriction can only be put in place once the asset is known to be degraded. Therefore all the TSR and line closure triggers are linked to known condition places.

	Ballast		**Rail**	
	Condition	Place	Condition	Place
Level 1 Speed restriction	*'Very poor'*	P_{17}^T	*'Major surface defects and transverse defects'*	P_{30}^T
Level 2 Speed restriction	*'Super red'*	P_{19}^T	*'Critical number of defects'*	P_{32}^T
Line closure	n/a[8]		*'Rail break'*	P_{33}^T

TABLE 6.4: CONDITION THAT LEAD TO SPEED RESTRICTIONS AND LINE CLOSURES

The Petri net in Figure 6.11 was used to simulate the implementation of speed limits and line closures. Transitions $T_{74}^T \rightarrow T_{86}^T$ all have a delay time of zero, so for example as soon as P_{17}^T is marked T_{74}^T will fire (provided there is not already a speed restriction in place ($P_{81}^T \rightarrow P_{83}^T$ marked)). The marking of P_{81}^T will enable T_{79}^T, this will remove the marking in place P_{80}^T. The other restrictions work in the same way.

[8] It is assumed that alignment will not cause a block the line scenario to occur, the speed will just keep being reduced. Other track indicators such as cyclic top can cause a block the line situation.

Following maintenance a reset transition is used to return the system to the initial marking, where only P_{80}^{T} is marked (as in Figure 6.11). If following a repair there is still an asset in a condition that requires a restriction then the appropriate restriction place will be marked again immediately. If the condition worsens before maintenance is scheduled then it may be necessary to increase the level of restriction imposed.

Transition T_{82}^{T} is used to reduce the marking of P_{81}^{T} back to one if both T_{74}^{T} and T_{75}^{T} fire at the same time. This can occur if both the rail and ballast are discovered to be in a state that would require a speed restriction at the same time. Transition T_{86}^{T} performs the same task for the Level 2 speed restriction.

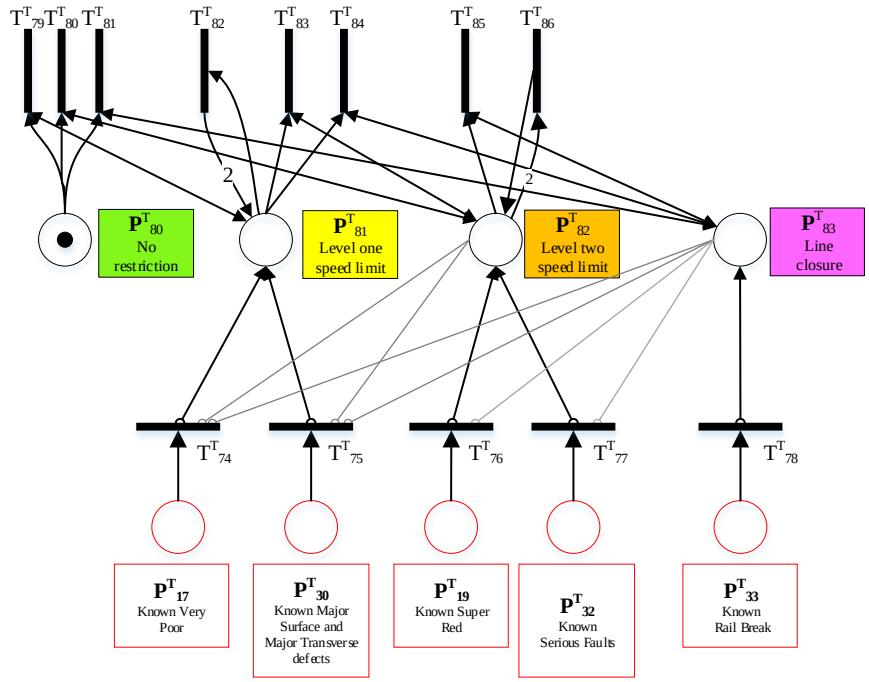


FIGURE 6.11: PETRI NET FOR SPEED RESTRICTIONS AND LINE CLOSURES

When making asset management decisions it is important to consider risk. Asset managers have limited resources so will need to make assessments on the risks of performing certain tasks while not completing others. It is assumed that the highest risk occurs when the deterioration of assets is unrevealed. For this reason asset managers want to ensure the number of days the ballast is unrevealed in the '*Very poor*' or '*Super red*' condition is small.

The final part of the ballast lifecycle that needs considering is ballast cleaning and complete track section renewal. Ballast cleaning and track section renewals are scheduled based on the number of interventions (tamps and stoneblows) that have taken place. Furthermore, it is assumed that the ballast can only be cleaned once in its lifetime. The amount of time between a section being identified as requiring a clean or renewal and the clean or renewal taking place can be significant; months or even years. Therefore even if the section is scheduled to be cleaned or renewed, further tamps and stoneblows must be able to take place. For this reason the Petri net had to be created in such a way as to ensure that once a clean or renewal had been scheduled it did not prevent tamping or stoneblowing.

The Petri net used to simulate cleaning and renewals is shown in Figure 6.12. Test arcs with increasing weights are used to simulate ballast cleans and renewals based on the number of previous interventions. It is assumed that after six interventions (tamps and stoneblows) have occurred a low priority clean would be scheduled. If after eight interventions the clean still has not been performed then a high priority clean is scheduled. The mean firing time of transition T_{32}^{T} was less than that of T_{33}^{T}. After ten interventions a low priority renewal is scheduled, after twelve tamps a medium priority renewal is scheduled and after fourteen tamps a high priority renewal is scheduled. The mean of the distributions used within transitions T_{29}^{T}, T_{30}^{T} and T_{31}^{T} are such that:

$$\mu_{T29} < \mu_{T30} < \mu_{T31} \tag{6.16}$$

and the mean firing times of transitions T_{32}^{T} and T_{33}^{T} are such that:

$$\mu_{T32} < \mu_{T33} \tag{6.17}$$

The firing of T_{32}^{T} or T_{33}^{T} will mark P_{54}^{T}, this will enable RT_{5}^{T} which has a firing time of several days. Following the firing of RT_{5}^{T} place P_{51}^{T} will be marked recording the number of cleans and preventing a second clean taking place, the marking of P_{51}^{T} is only set to zero following a complete renewal. Following a clean the marking of P_{99}^{T} will be set to two and following a complete renewal the marking is set to zero. This is done to model the fact that a clean is not as effective as a complete track section renewal. A full track section renewal can also be scheduled based on the rail condition, this is discussed in the next section.

One other maintenance action was considered in the ballast model; manual interventions. They were modelled as taking place when the ballast is in the *'Very poor'* or *'Super red'* condition and a TSR is in place. As soon as the ballast is known to be in the *'Very poor'* or *'Super red'* condition (Place P_{17}^{T} or P_{19}^{T} marked), then a manual intervention is scheduled supplementary to a tamp or stoneblow. The manual intervention would typically take place that evening, this was assumed to return the ballast condition to '*Poor'* and remove any restrictions, until a tamp or stoneblow took place. A maximum of two manual interventions were permitted in a single lifetime (between track section renewals).

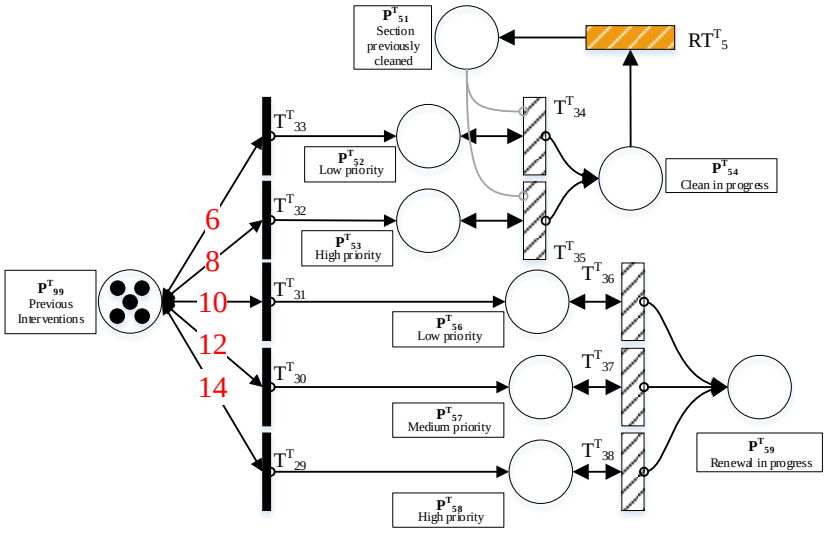


FIGURE 6.12: RENEWAL AND CLEANING SCHEDULER PETRI NET

6.3.1.2 Rail Model

The second part of the track section model simulates the deterioration, inspection and renewal of the rail. There are three factors that limit the service life of rails [29]:

(i) Wear

This occurs primarily on the gauge face of the high rails in the sharper curves, due to the high wheel flanging forces. Some wear also occurs on the running surfaces of all rails due to wheel/rail interaction and also due to rail maintenance (grinding).

(ii) Plastic Flow

This can occur in both high and low rails, primarily in curves subjected to high axle load operations (greater than 20 tonnes). Plastic flow is caused by the applied wheel/rail contact stresses exceeding the strength of the rail.

(iii) Defects

Defects are generally thought of as cracks, these can develop in all rails (and welds) for a wide range of reasons. Defects are of major concern since, if not detected in time, they can grow and possibly cause rail failures, or at least necessitate expensive rail maintenance.

Several assumptions were made about how the rail degrades to enable it to be modelled. Firstly the wear and plastic flow were grouped into a single defect type, and are referred to as *transverse defects*. The remaining defects will be referred to as *surface defects*. In addition it is assumed the rail can experience a *sudden failure* such as a rail break or bolt hole failure. It was assumed the rail could have surface defects, transverse defects or both and furthermore, from any state, except the new state, there was a chance of a sudden failure where the probability increased significantly as the number of defects increased.

These assumptions lead to a nine state Petri net model which can be grouped into four parts, transverse defects, surface defects, surface and transverse defects and sudden failures as shown in Figure 6.13. Starting from place P_5^T (new condition) the marking can evolve to P_6^T or P_8^T, via conditional transitions CT_{11}^T and CT_{13}^T. Note CT_{11}^T and CT_{13}^T have a transition conflict, in the event of a conflict CT_{11}^T fires first as it has a lower ID. From place P_6^T '*Minor surface defects'* the system can evolve in one of three ways ($CT_1^T, CT_{12}^T, CT_{15}^T$). It is considered that the most likely option is that the rail will transition to P_{10}^T '*Surface defects and transverse defects'*, rather than *'Major surface defects*' as major defects, in general, take longer to develop. The likelihood of transitioning to '*Rail break*' from '*Minor surface defects*' is thought to be very low. Hence the mean firing times of transitions CT_1^T, CT_{12}^T and CT_{15}^T are such that:

$$\mu_{CT15} < \mu_{CT12} < \mu_{CT1}. \tag{6.18}$$

Similarly from place P_8^T '*Minor transverse defects'* the system can evolve in one of three ways ($CT_0^T, CT_{14}^T, CT_{17}^T$). It is considered that the most likely option is that the rail will transition to *'Surface defects and transverse defects'*, rather than *'Major transverse defects'* because as before, in general, it takes a long time for major defects to develop, again the

likelihood of reaching '*Rail break*' was thought to be very low. Hence the mean firing times of transitions CT_0^T, CT_{14}^T $and CT_{17}^T$ are such that:

$$\mu_{CT17} < \mu_{CT14} < \mu_{CT0}. \quad (6.19)$$

From places P_7^T, P_9^T and P_{10}^T the rail condition can evolve to place P_{11}^T or P_{13}^T. The likelihood of a rail break is still thought to be low hence:

$$\mu_{CT16} < \mu_{CT4}, \quad (6.20)$$
$$\mu_{CT18} < \mu_{CT3}, \quad (6.21)$$
$$\mu_{CT19} < \mu_{CT2}. \quad (6.22)$$

From P_{11}^T the system can evolve to P_{12}^T. From $P_{11}^T$and P_{12}^T there is the potential for a rail break to occur.

The firing times of the conditional transitions $CT_{11}^T \rightarrow CT_{17}^T$ were sampled from the Weibull distribution based on the analysis in Chapter 5 (shown in Table 5.4 and Appendix B-1). The scale parameter was conditional on the number of passed interventions, the rail age, the rail type and the amount of rail lubrication[9]. The firing times for conditional transitions $CT_0^T \rightarrow CT_6^T$ are sampled from an Exponential distribution, the values are conditional on the rail type and the rail age. The values for these transitions are shown in Appendix B-3.

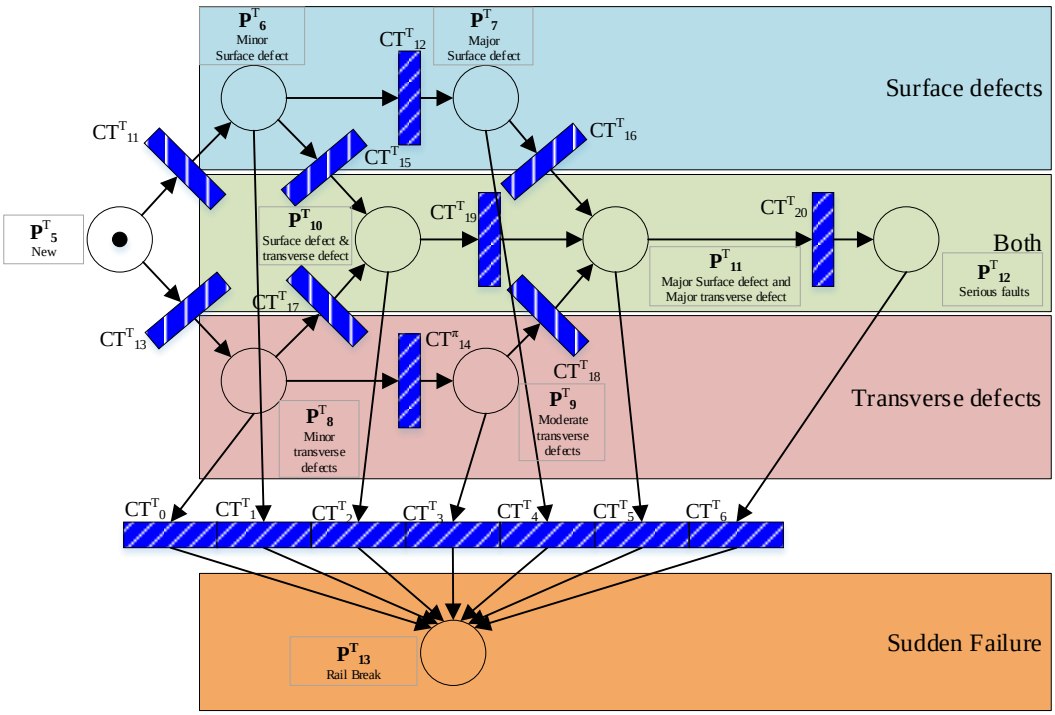


FIGURE 6.13: RAIL CONDITION MODEL

Rail inspection was modelled in a similar way to the ballast inspection loop shown in Figure 6.7. Rail inspection is performed by ultrasonic inspection, with the exception of rail breaks which are detected by a visual inspection. The four types of rail intervention identified (listed in section 2.3.2.3) were modelled in the Petri net. Unlike the ballast model, in the rail model the type of maintenance chosen was mainly selected according to the defect type rather than

[9] A list of rail types is given in Appendix B-2

the history. As discussed in section 2.3.2.3, surface defects (less than 5mm in depth) are generally treated by grinding, however defects deeper than 5mm or not in the rail running surface must be removed using a weld repair or in serious cases the rail must be removed and replaced.

Table 6.5 summarises the maintenance action(s) considered from each of the nine condition states in the model. From places $P_6^T \rightarrow P_9^T$ there is a set maintenance response, note in the individual rail model opportunistic work is not considered (maintenance is not considered from P_7^T *or* P_9^T). From place P_{10}^T where both types of defect are present a conditional probabilistic transition (CPT_7^T) is used to decide whether to perform a grind or weld depending on the number of previous interventions. If the condition of the rail reaches place P_{11}^T or P_{12}^T then there are numerous and severe defects, as such the rail will need replacing. Conditional probabilistic transitions (CPT_8^T, CPT_9^T) decide whether to renew the rails or whether to renew the whole track section, this decision is taken based on the number of passed interventions on both the rails and ballast. As the time to schedule a rail renewal or full track section renewal is significant, if the rail condition reaches place P_{11}^T, or P_{12}^T a partial repair is also scheduled this restores the condition until a full renewal can take place.

If the rail condition reaches P_{11}^T or P_{12}^T then there is an increased safety risk and under a good management strategy this condition will hopefully never be reached, therefore it is undesirable to wait for the rail to reach P_{11}^T or P_{12}^T before scheduling a rail renewal. To address this the number of interventions (welds and grinds) that have taken place on the section are recorded (P_{60}^T, P_{61}^T) and a rail replacement can also be scheduled based on this. Once there have been ten interventions then a low priority rail replacement is requested, if after fourteen interventions, a rail replacement still has not taken place a high priority rail replacement is requested. The Petri net used to model this is shown in Figure 6.14. P_{64}^T records the number of interventions that have taken place, the test arcs linking P_{64}^T to T_{68}^T and T_{69}^T are used to schedule maintenance based on the number of previous welds and grinds.

The amount of lubrication on the rails is also modelled in the Petri net, and is used to influence the distributions for the time for the rails to degrade. The lubrication is modelled using the Petri net shown in Figure 6.15, at the start of the simulation there were ten tokens in place P_{91}^T. Ten tokens in P_{91}^T indicates there is the maximum amount of lubrication and it is having the best possible effect. Gradually the number of tokens in P_{91}^T reduces as T_{94}^T fires. The amount of lubrication is increased by the firing of P_{93}^T. The inhibitor arc ensures that the amount of tokens in P_{91}^T cannot be greater than ten.

There are thought to be dependencies between the condition of the rails and the condition of the ballast. For example poor ballast alignment could lead to faster deterioration of the rails. However numerically quantifying these condition dependencies is very difficult, as a range of external factors such as those discussed in the LI also influence deterioration. Additionally it can be difficult to distinguish between causation and correlation. For this reason dependencies between the ballast and rail condition are not included at this stage.

Maintenance dependencies are considered however; the renewal of the ballast and rail is grouped and Chapter 7 will explain how opportunistic maintenance is considered between multiple different assets.

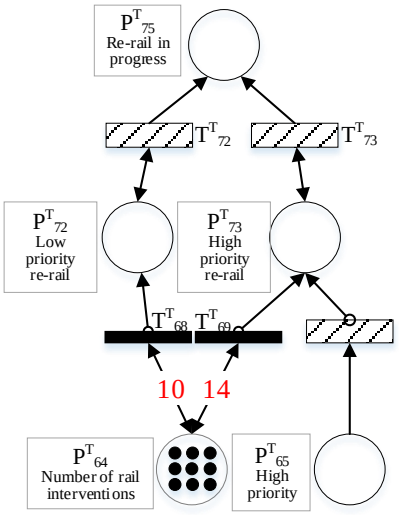


FIGURE 6.14: RAIL RENEWAL SCHEDULE PETRI NET

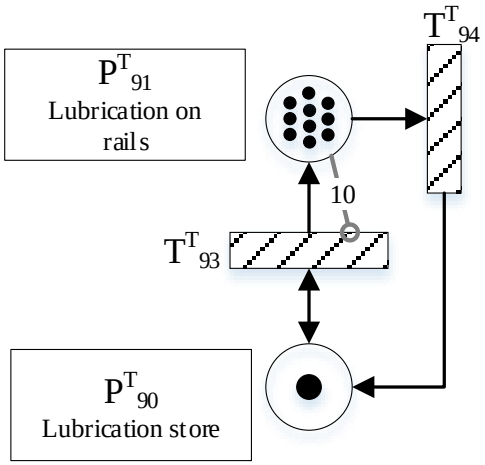


FIGURE 6.15: RAIL LUBRICATION MODEL

Type of Defect	Petri Net Place	Depth of Defect	Length of Defect	Intervention Type
No defects	P_5^T *New*	N/A	N/A	None
Surface defects	P_6^T *Minor surface defects*	D<5	0<L<15	Opportunistic grind[10]
	P_7^T *Major surface defects*	D<5	L>15	Grind
Transverse defects	P_8^T *Minor transverse defects*	5<D<10	0<L<50	Opportunistic weld repair[10]
	P_9^T *Major transverse defects*	D>10	50<L<95	Weld repair
Both	P_{10}^T *Surface defects and transverse defects*	D<5	0<L<20	Grind or weld repair[11]
		5<D<10	0<L<50	
	P_{11}^T *Major surface defects and transverse defects*	D>5	L>20	**Immediate action**: Partial re-rail **Long term**: rail or track section renewal[12]
		D>10	50<L<95	
	P_{12}^T *Critical number of defect*	Surface defects D>5 Transverse defects D>15	Surface defects L>30 Transverse defects L>95	**Immediate action**: Partial re-rail **Long term**: rail or track section renewal[12]
Sudden failure	P_{13}^T *Rail Break*	There is a full break in the rail		Weld repair

TABLE 6.5: SUMMARY OF RAIL MAINTENANCE IN THE RAIL SUBNET

[10] This is only considered in the rail module in the whole system model in Chapter 7.
[11] A conditional probabilistic transition decides whether to schedule a grind or weld based on maintenance history.
[12] A conditional probabilistic transition decides whether to replace just the rail or to renew the track section based on the maintenance history of the ballast and the rail.

Summary of Key Assumptions of the Track Section Model

(i) The ballast can be in one of five condition states.
(ii) The rail can be in one of nine condition states. The rail condition states are grouped into three types: transverse defects, surface defects and sudden failures.
(iii) The deterioration of ballast is conditional on location parameters and maintenance history.
(iv) The deterioration of the rail is conditional on rail lubrication, rail type and maintenance history.
(v) Three types of ballast maintenance are modelled: tamping stoneblowing and manual interventions.
(vi) Four types of rail maintenance are modelled: grinding, welding, partial rail replacement, full rail replacement.
(vii) A ballast clean is requested once six ballast interventions have taken place, it is requested with more urgency following eight interventions.
(viii) Dependencies between the condition of the rails and the ballast are not considered, however maintenance dependencies and maintenance grouping is modelled.
(ix) A full track section renewal is requested once ten ballast interventions have taken place; it is requested with more urgency following 12 and then 14 ballast interventions. A full renewal can also be requested if the rail reaches one of the two worst condition states.
(x) The ballast can only be cleaned once in its lifetime. Following a ballast clean the number of previous interventions is set to two as a clean is not as effective as a full renewal.
(xi) A track section renewal returns the ballast and rails to the new condition and resets the maintenance history of the ballast and rails to zero.
(xii) Tamping, stoneblowing, manual interventions, grinding and welding can take place even if a ballast clean, rail replacement or full renewal has been scheduled.
(xiii) If the condition of the ballast is known to be in one of the two poorest states then a TSR is imposed.
(xiv) If the condition of the rails is known to be in one of the two poorest states then a TSR is imposed.
(xv) If a rail break occurs then the line is closed.
(xvi) High risk occurs if the ballast is unrevealed in the '*Very poor*' or '*Super red'* condition.
(xvii) All of the parameter values are dependent on the track category.

6.3.1.3 Single Track Section Model Results

The single track section model was solved using Monte-Carlo simulations [151]. Bespoke C++ code [152], [153], was used to simulate the Petri net. The code was written and compiled in the Visual Studio intergraded development environment (IDE) [154]. The solution routine is discussed more in Chapter 8.

The single track section model Petri net was simulated 50,000 times for a 50 year period, for categories 1A→5. In the individual model the rail and ballast are assumed to start in the new condition, however in the system model the ballast condition at the start of simulation was calibrated to the geometry recorded at the last inspection. Figure 6.16 shows the ballast deterioration profile (when **no** maintenance is performed) for the various track categories. The difference between the track categories can clearly be seen. For Category 1A track after 50 years there is a 90% chance of the ballast having reached the '*Super red'* condition, if no maintenance is performed, whereas for Category 5 track the probability is only around 15%. There are two main reasons for the difference in deterioration profiles:

(i) Category 1A lines have more trains which are travelling at higher speeds.
(ii) The geometry quality bands are defined differently for each track category.

Figure 6.17 shows the deterioration profile for the rails (when **no** maintenance is performed), again the difference between Category 1A and Category 5 is significant, with Category 1A line having a 95% chance of being in the worst two states after 50 years, however for Category 5 there is only around a 20% chance of being in the worst two states.

Figure 6.18 shows the number of maintenance interventions performed per 10.5 week (fifth year) period for Category 1A, 1, 2 and 3 and per 13 weeks for categories 4 and 5, based on an average of 50,000 simulations when maintenance **is** considered. The spikey nature of the plots for Category 1A, 1, 2 and 3 is due to the 10.5 week periods not aligning with the inspection interval. In a 10.5 week period immediately post inspection work volumes will be higher, than in a 10.5 week period immediately prior to an inspection. Due to there being no common factors between the ultrasonic and NMT inspection frequency (other than seven) it was impossible to choose a period to record the data to keep in line with the inspection cycles. The spikey nature is less pronounced for Category 1A and 1 due to short inspection cycles, meaning work was performed more uniformly. For categories 4 and 5 the NMT and ultrasonic inspection frequencies are the same therefore it was possible to choose an observation period that matched them, hence the spikey nature is removed. Table 6.6 summarises the total number of interventions. There are a number of key observations that can be made:

(i) The difference between the volume of stoneblowing for Category 1A and Category 1; this is due to stoneblowing being used less often for Category 1A lines as it cannot deliver the required alignment.
(ii) As the inspection interval increases, the volume of work performed becomes less uniform.
(iii) As the ballast and rail start in new condition, it is at least ten years before there is any significant probability of a ballast clean or renewal being performed.

(iv) There is a large range in the number of interventions (difference between the minimum and maximum number of interventions shown in Table 6.6). This demonstrates the models ability to capture the stochastic nature of track deterioration. However as discussed in Chapter 5 truncating some of the distributions used within the model to limit extreme values could be considered in the future.

The convergence of the model was assessed based on the overall cost. The overall cost was calculated based on 16 values as shown in Table 6.7. At the request of Network Rail, Network Rail cost figures were not used. The values were based on Spon's [49] and engineering judgement. The cost values used in the track section model are shown in Table 6.7.

Equation (6.23), shows how the overall cost is determined:

$$Cost_c^T = \sum_{j=1}^{16} I_j C_{j,\alpha} \quad \alpha = 0, 1, \dots, 6 , \tag{6.23}$$

where I_j is the number of times the j^{th} cost contributor occurs which is extracted directly from the Petri net, C_j is the cost associated with the j^{th} cost contributor and α represents the track category.

Figure 6.19 shows the convergence of the total cost, for each of the track categories, alongside 95% confidence intervals. As expected Category 1A track is the most expensive and Category 5 is the cheapest. It can also be seen that for all track categories a high level of convergence is achieved by 10,000 simulations.

Figure 6.20 shows how the overall cost, shown in Figure 6.19 is broken down. The cost was broken down into five aspects:

(i) Maintenance
(ii) TSR and line closure penalty costs
(iii) Renewals
(iv) Safety risk
(v) Inspection

It can be seen for the high track Category (1A, 1 and 2) renewals make up the majority of the cost, over ¾ of the total cost. It can be seen that the inspection and maintenance make up the same proportion for Category 1A, 1 and 2 (8% and 5 % respectively). The cost for TSR, varies between 7% and 9%. The safety risk makes up the smallest proportion in all three cases.

For the lower category lines the proportion of the cost associated with renewal gets smaller, the reason for this is as the category decreases the likelihood of renewal occurring in 50 years decreases. The proportion of the cost attributed to speed restrictions and safety risk increases. This is due to the increased inspection interval meaning:

(i) Degradation remains undetected for longer

(ii) The likelihood of reaching the poorest states increases

The less frequent inspections also mean the volume of work performed decreases (work always increases following an inspection when updated condition is revealed).

Finally, Figure 6.21 shows a direct comparison of the overall cost (converged values from Figure 6.19) for the six track categories modelled. As discussed one of the main reasons for categories 4 and 5 having a significantly lower overall cost is due to the reduction in the likelihood of a renewal in 50 years. The cost is also decreased by slower deterioration rates and longer inspection intervals leading to fewer inspections being required.

Category	Intervention	Data	Mean	SD	Max	Min
1A	Tamp	13.02	15.90	5.21	39	1
	Stoneblow	2.48	1.55	2.08	13	0
	Grind	1.74	2.58	1.62	11	0
	Weld	4.95	4.72	2.39	17	0
	Re-rail	n/a	0.83	0.63	4	0
	Clean	n/a	1.17	0.48	4	0
	Renewal	n/a	0.68	0.56	3	0
1	Tamp	9.34	12.38	4.23	33	1
	Stoneblow	4.60	4.78	3.69	24	0
	Grind	1.68	2.47	1.55	11	0
	Weld	6.47	4.52	2.34	17	0
	Re-rail	n/a	0.73	0.61	3	0
	Clean	n/a	1.17	0.45	4	0
	Renewal	n/a	0.71	0.60	3	0
2	Tamp	8.03	11.14	4.08	31	1
	Stoneblow	4.26	4.21	3.49	24	0
	Grind	2.69	2.16	1.46	11	0
	Weld	5.22	3.93	2.07	16	0
	Re-rail	n/a	0.58	0.56	3	0
	Clean	n/a	1.08	0.44	3	0
	Renewal	n/a	0.61	0.59	3	0
3	Tamp	6.43	8.30	3.53	27	0
	Stoneblow	2.44	3.45	3.23	25	0
	Grind	1.91	1.65	1.27	9	0
	Weld	8.99	3.01	1.81	13	0
	Re-rail	n/a	0.34	0.48	2	0
	Clean	n/a	0.78	0.47	3	0
	Renewal	n/a	0.46	0.52	2	0
4	Tamp	5.80	6.18	3.19	23	0
	Stoneblow	1.75	2.79	3.44	22	0
	Grind	3.04	1.24	1.11	8	0
	Weld	7.29	2.28	1.65	14	0
	Re-rail	n/a	0.23	0.42	2	0
	Clean	n/a	0.38	0.49	2	0
	Renewal	n/a	0.23	0.42	2	0
5	Tamp	4.69	4.64	2.95	29	0
	Stoneblow	1.23	1.66	3.16	19	0
	Grind	1.86	0.91	0.97	7	0
	Weld	5.31	1.67	1.43	11	0
	Re-rail	n/a	0.08	0.28	1	0
	Clean	n/a	0.16	0.37	2	0
	Renewal	n/a	0.08	0.27	1	0

TABLE 6.6: SUMMARY OF MAINTENANCE INTERVENTIONS BY TRACK CATEGORY

	Task	Unit	Data Source	Cost Units (By Track Category)					
				1A	1	2	3	4	5
1	Tamp	Each	Estimated	505	455	442	379	379	316
2	Stoneblow	Each	Estimated	750	675	656	563	563	469
3	Weld	Each	Estimated	105	105	105	105	105	105
4	Grind	Each	Estimated	400	400	400	400	400	400
5	Clean	Each	Estimated	53,000	47,700	46,375	39,750	39,750	33,125
6	Renewal	Each	Spon's	105,000	94,500	91,875	78,750	78,750	65,625
7	Full Re-rail	Each	Estimated	30,000	30,000	30,000	26,250	26,250	22,500
8	Partial rail replacement	Each	Estimated	12,000	12,000	12,000	10,500	10,500	9,000
9	Level one Speed Restriction	Per day	Estimated	5,000	4,500	4,500	3,750	2,500	2,500
10	Level two Speed Restriction	Per day	Estimated	25,000	22,500	22,500	18,750	12,500	12,500
11	Line closure	Per day	Estimated	40,000	36,000	36,000	30,000	20,000	20,000
12	Risk due to alignment being undetected in 'Very poor'	Per day	Estimated	1,000	1,000	1,000	1,000	1,000	1,000
13	Risk due to alignment being undetected in 'Super red'	Per day	Estimated	5,000	5,000	5,000	5,000	5,000	5,000
14	Visual inspection	Each	Estimated	8	8	8	8	8	8
15	Geometry inspection (NMT)	Each	Estimated	8	8	8	8	8	8
16	Ultrasonic inspection	Each	Estimated	8	8	8	8	8	8

TABLE 6.7: TRACK SECTION COSTS

.

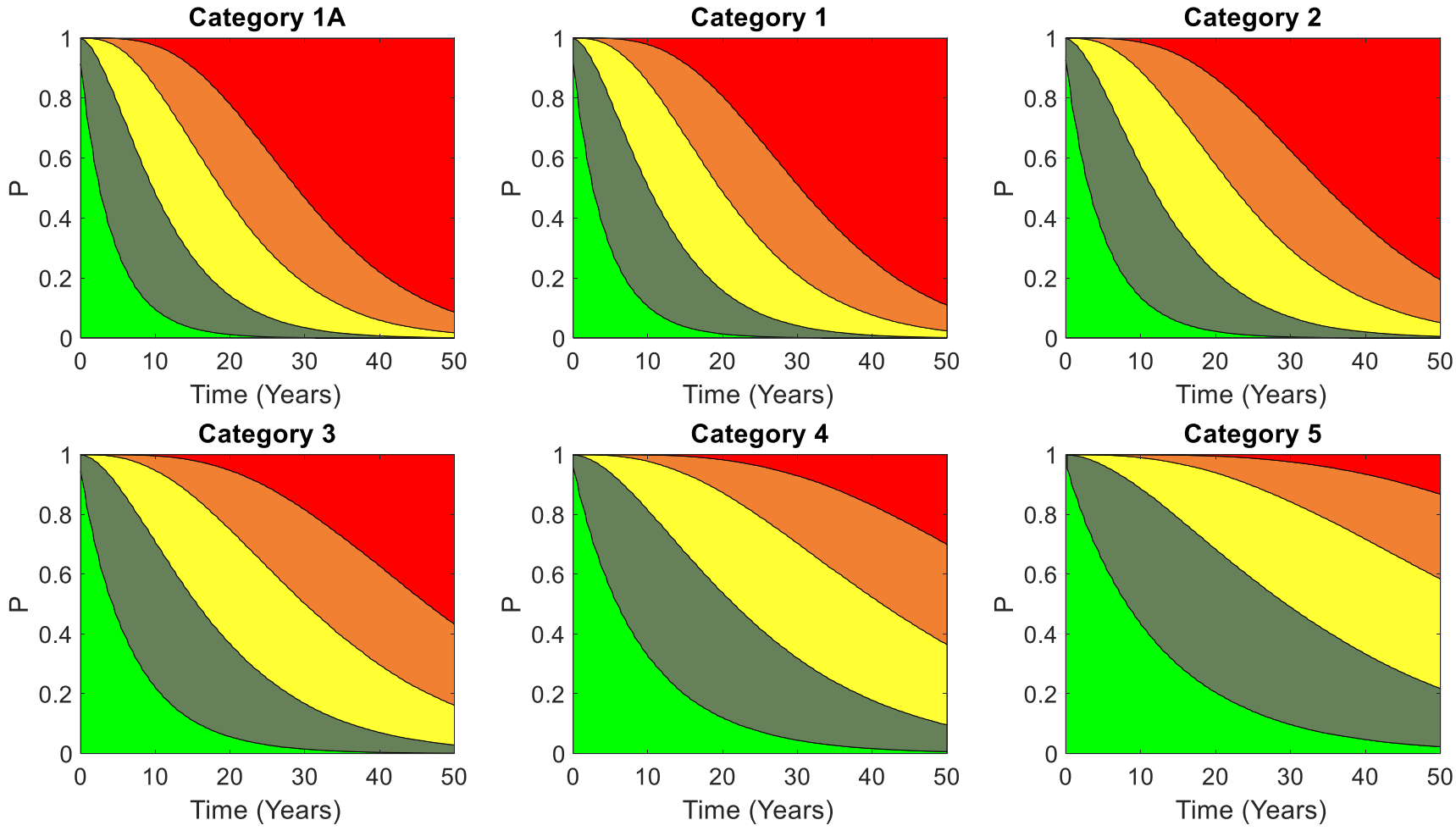


FIGURE 6.16: BALLAST DETERIORATION PROFILES (MAINTENANCE NOT CONSIDERED)
KEY: ●NEW ●SATISFACTORY ●POOR ●VERY POOR ●SUPER RED

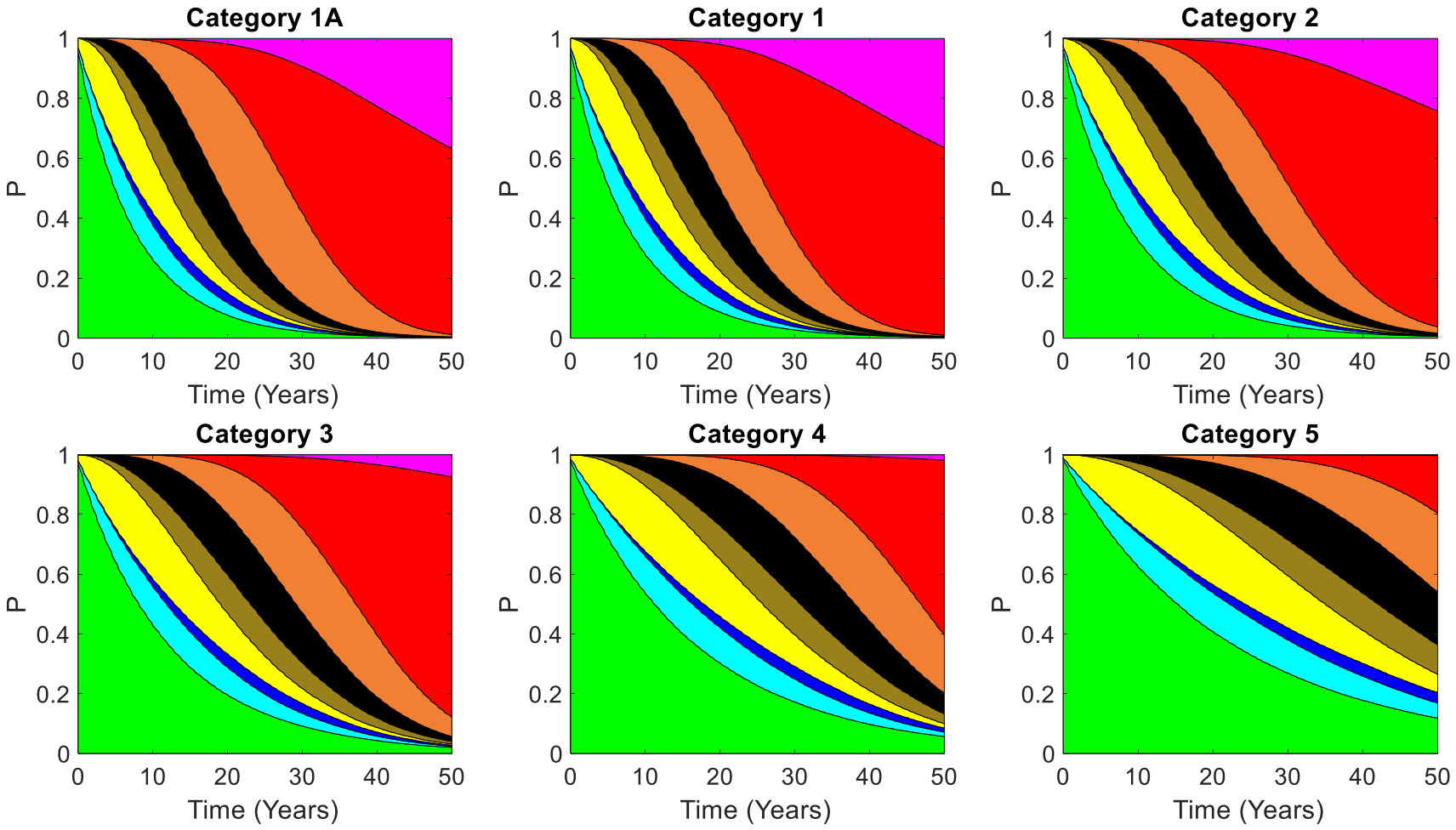


FIGURE 6.17: RAIL DETERIORATION PROFILES (MAINTENANCE NOT CONSIDERED)

KEY: ●NEW ●MINOR SURFACE DEFECTS ●MINOR SURFACE DEFECTS ●MINOR TRANSVERSE DEFECTS ●MAJOR TRANSVERSE DEFECTS ● SURFACE DEFECTS AND TRANSVERSE DEFECTS ●MAJOR SURFACE DEFECTS AND TRANSVERSE DEFECTS ●SERIOUS DEFECTS ●BROKEN RAIL

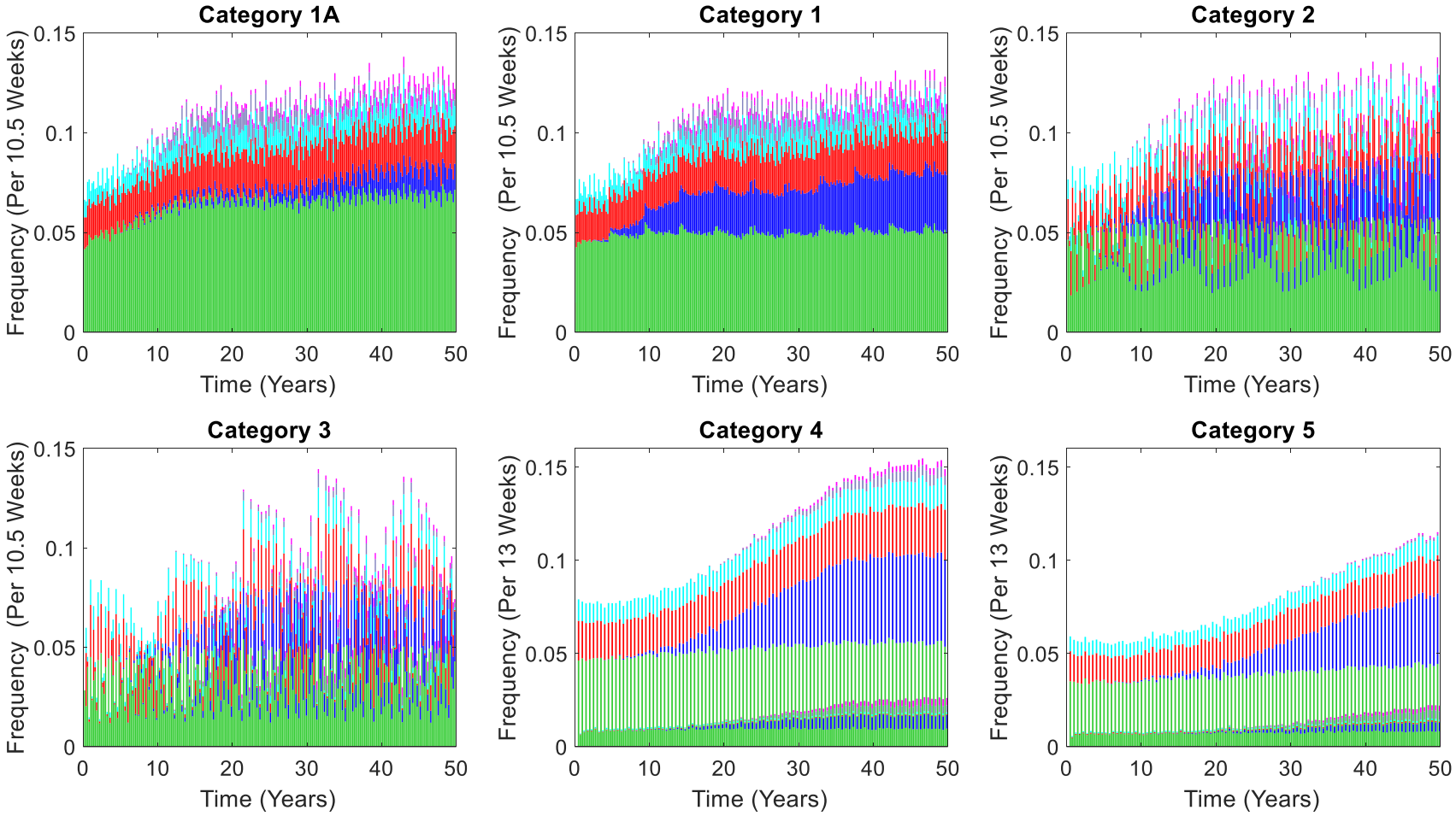


FIGURE 6.18: PROBABILITY OF AN INTERVENTIONS PER 10.5 WEEK PERIOD (CATEGORIES 1A, 1, 2 AND 3) OR 13 WEEK PERIOD (CATEGORIES 4 AND 5)
KEY: ● TAMPING ● STONEBLOWING ● WELDING ● GRINDING ● CLEANING ● RENEWAL

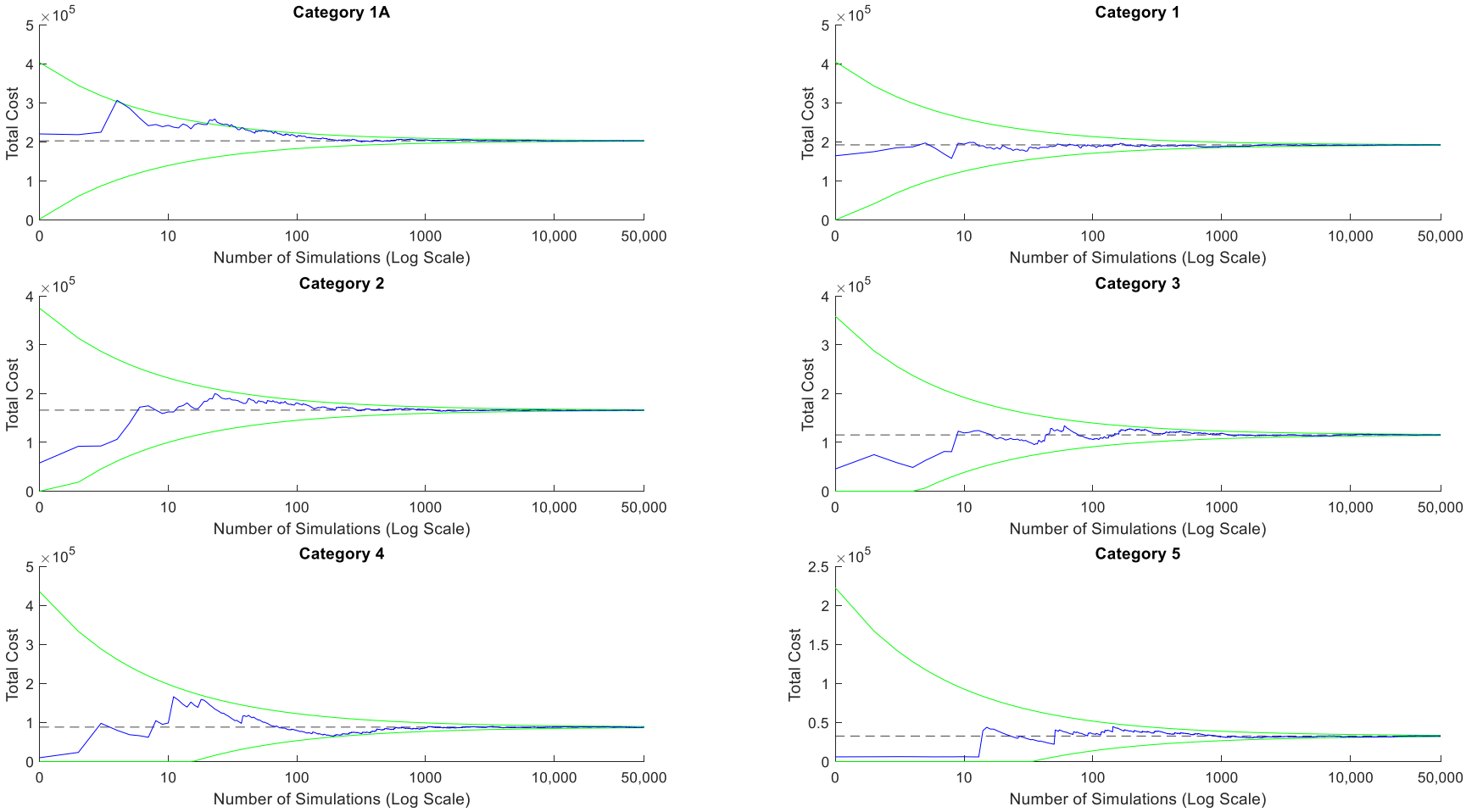


FIGURE 6.19: CONVERGENCE OF TOTAL COST (LOG SCALE)
KEY: ●95% CONVERGENCE BOUNDS ●RUNNING AVERAGE ●CONVERGED VALUE

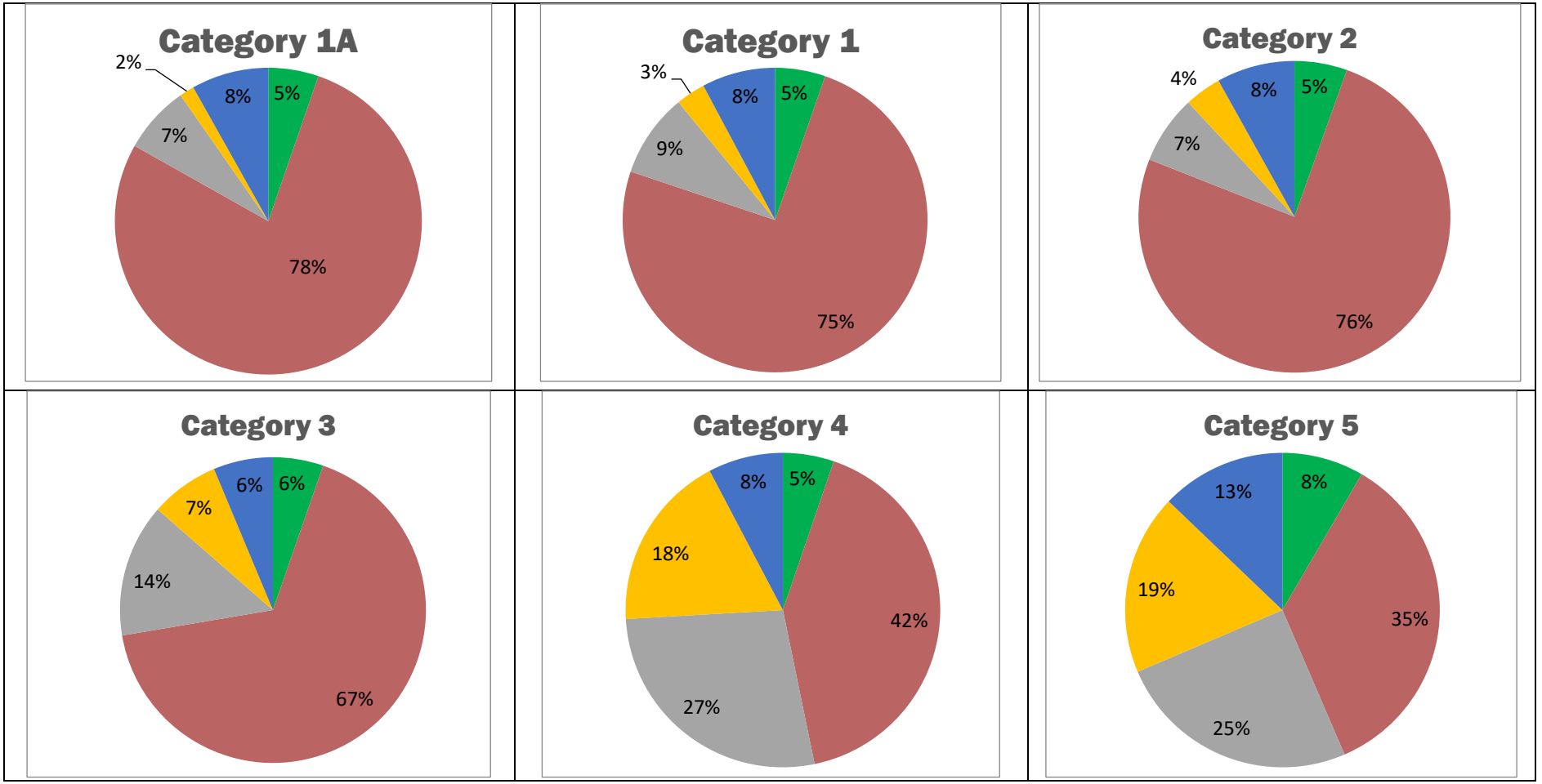


FIGURE 6.20: COST BREAKDOWN

KEY: ●MAINTENANCE ●TSR ●RENEWAL ●SAFETY RISK ●INSPECTION

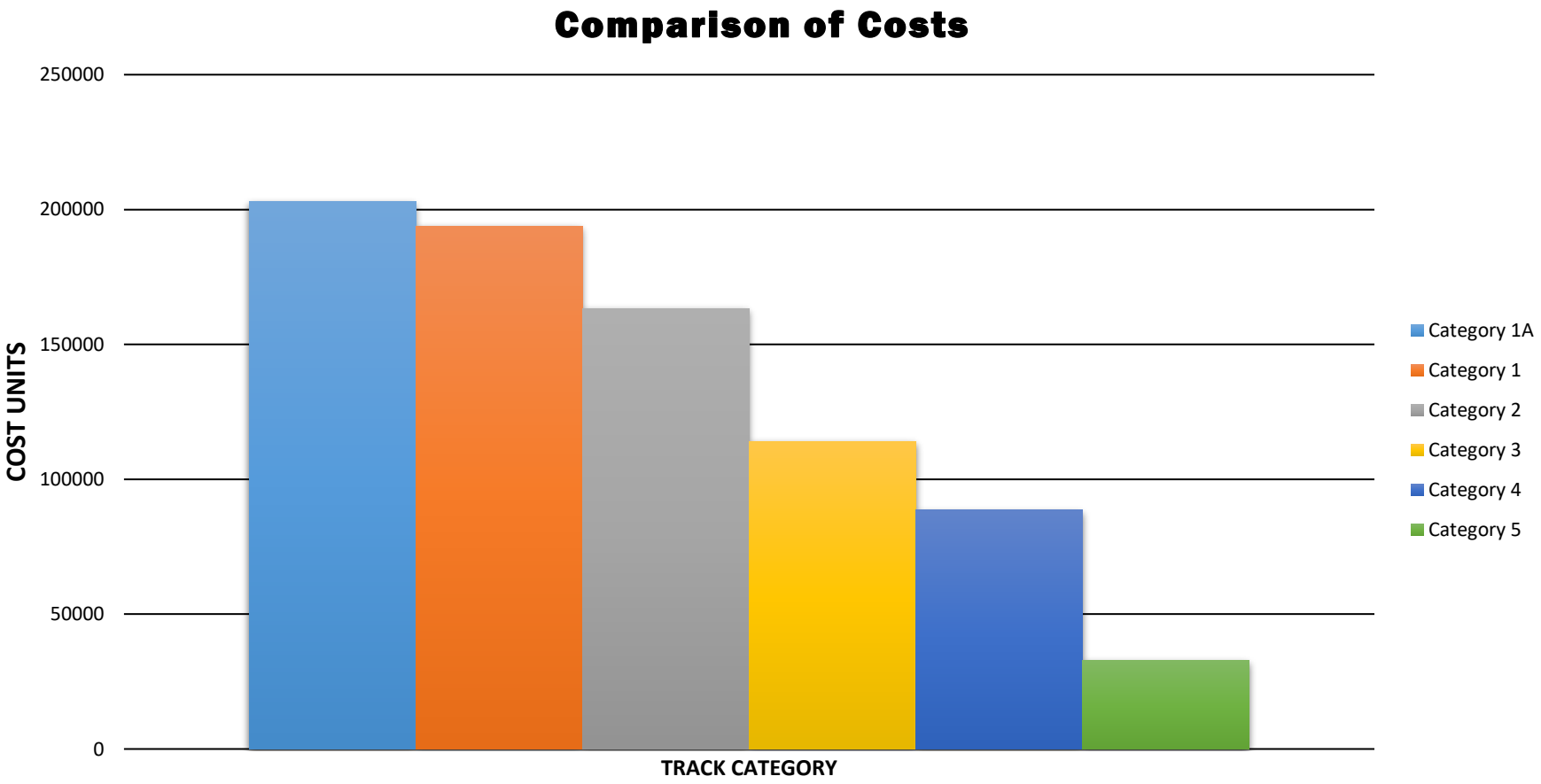


FIGURE 6.21: COST BY TRACK CATEGORY

6.3.1.4 Sensitivity Analysis of Track Section Petri Net Model

A sensitivity analysis was performed for each track category to investigate the factors that influence the overall cost. Nine Parameters were investigated in the sensitivity analysis, the transitions listed are the transitions that were affected. The value sampled from the distribution was adjusted by the percentage shown in Figure 6.22.

(i) Time to schedule ballast maintenance
$T_{19}^{T}, T_{22}^{T}, T_{25}^{T}, T_{27}^{T}$

(ii) Time to schedule rail maintenance
$T_{56}^{T}, T_{59}^{T}, T_{62}^{T}, T_{65}^{T}$

(iii) Time to complete ballast maintenance (tamp and stoneblows)
$RT_{0}^{T}, RT_{1}^{T}, RT_{2}^{T}, RT_{3}^{T}, RT_{4}^{T}$

(iv) Time to complete rail maintenance (grind and weld)
$RT_{7}^{T}, RT_{8}^{T}, RT_{9}^{T}, RT_{10}^{T}, RT_{11}^{T}$

(v) Baseline ballast deterioration rate
$CT_{7}^{T}, CT_{8}^{T}, CT_{9}^{T}, CT_{10}^{T}$

(vi) Baseline rail detonation rate
$CT_{0}^{T} \rightarrow CT_{6}^{T} \& CT_{11}^{T} \rightarrow CT_{20}^{T}$

(vii) Visual inspection frequency
CT_{89}^{T}

(viii) Geometry inspection frequency
$T_{0}^{T} \rightarrow T_{3}^{T}$

(ix) Ultrasonic inspection frequency
$T_{4}^{T} \rightarrow T_{10}^{T}$

The results of the analysis are shown in Figure 6.22. It can be observed that the ballast deterioration rate has the largest effect on the overall cost, this is to be expected as increasing the ballast deterioration rate will increase the number of interventions, which will in turn increase the number of cleans and renewals. There will also be an increased likelihood of reaching the '*Very poor*' and '*Super red'* conditions. The greatest increase in cost can be observed for Categories 4 and 5. The analysis showed that this was due to categories 4 and 5 track generally lasting beyond 50 years, meaning in the baseline case there were very few renewals. However, by accelerating the degradation, the lifetime dropped below 50 years and so the likelihood of renewal increased significantly, dramatically increasing the overall cost. The second biggest effect was rail deterioration; increasing the rail deterioration rates will lead to more rail interventions and a higher number of rail replacements. The deterioration rate of rails does not have such an effect as the ballast as it is not such a big driver of complete renewals.

The remaining seven parameters have a much smaller effect on the overall cost, less than 5% variation in the total cost. Of the remaining factors, the geometry inspection (frequency of NMT) has the next largest effect. It can be seen that reducing the inspection frequency reduces the overall cost, the number of inspections can be reduced without increasing the risk of being undetected in the '*Very poor*' or '*Super red*' state. However in practice the inspection intervals are set in standards and are not negotiable by the rail operators.

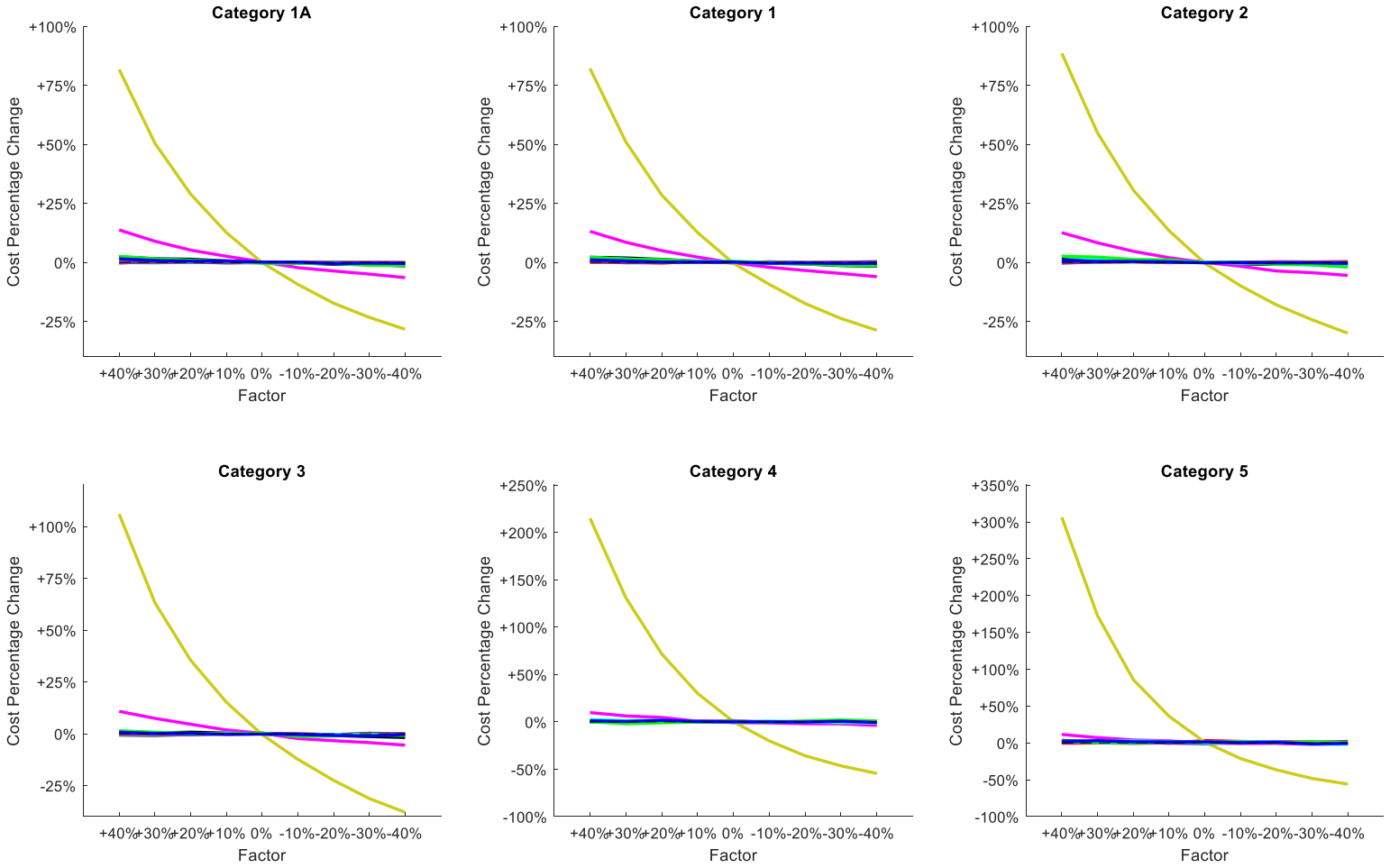


FIGURE 6.22: SENSITIVITY ANALYSIS ON THE TOTAL COST

KEY: ● BALLAST DETERIORATION ● RAIL DETONATION RATE ● BALLAST SCHEDULE TIME ● BALLAST COMPLETION TIME ● RAIL SCHEDULE TIME ● RAIL COMPLETION TIME ● VISUAL INSPECTION FREQUENCY ● GEOMETRY INSPECTION FREQUENCY ● ULTRASONIC INSPECTION FREQUENCY

6.3.2 Sleepers, Fastenings and Pads Petri Net Model

The following sections will introduce the sleeper Petri net asset models and show the results of simulating the models. There are three different materials used for railway sleeper construction: timber/wood, concrete and steel. The degradation mechanics of each are very different and for this reason, a separate Petri net was created for each of the sleeper types. The sleeper models, where appropriate, contained submodules for sleepers, pads and clips/fastenings. The next three sections will detail the Petri net model for each of the three sleeper types.

6.3.2.1 Concrete Sleepers

Concrete sleepers are the most commonly used on the UK railway. The concrete sleeper Petri net model is shown in Figure 6.23, it contains three distinct parts for sleepers, pads and clips as well as an inspection loop (P_{34}^{CS} and P_{35}^{CS}).

It is assumed that sleepers are spaced every half yard (0.46m) hence there are 440 sleepers per track section (eighth mile). The sleeper spacing varies across the network and this spacing was initially chosen so that the number of sleepers divides exactly by the track section length to avoid rounding complications. Nonetheless the Petri net is flexible enough that the number of sleepers can be varied (by varying the initial marking of P_0^{CS}).

Concrete sleeper degradation is influenced by a number of factors (as discussed in Chapter 2). Seven degradation modes are considered:

(i) Deterioration of the rail seat area due to worn pads

This was modelled by transition T_0^{CS}, the firing time of which was sampled from an Exponential distribution, the test arc between T_0^{CS} and place P_{14}^{CS} ensures that this transition can only fire when the pads are in the partly worn condition state.

(ii) Deterioration of rail seat area due to non-functioning pads

This was modelled by transition T_1^{CS}, the firing time of which was also sampled from an Exponential distribution, the test arc between T_1^{CS} and place P_{15}^{CS} ensures that this transition can only fire when the pads are in the heavily worn condition state.

(iii) Damage to the fastening area

This was modelled by transition T_2^{CS}, the firing time of which was sampled from an Exponential distribution. The test arc, with a weight of 20, between T_2^{CS} and place P_{10}^{CS} ensures that this transition can only fire, once at least 20 clips have failed.

(iv) Tamping damage

This was modelled by transition T_3^{CS}, the firing time of which was sampled from an Exponential distribution, this transition was not connected to any other places so can fire at all times. In the system model this transition was connected to '*socket*' places in the ballast model so failures could only occur if a tamp was on going, this is discussed more in Chapter 7 when the system model is introduced.

(v) Poor support due to ballast in '*Very poor*' condition

This was modelled by transition T_4^{CS}, the firing time of which was sampled from an Exponential distribution, this transition was not connected to any other places so can fire at all times. In the system model this transition was connected to a '*socket*' place in the ballast model so that this sort of failure can only occur if the ballast condition is '*Very poor*'.

(vi) Very poor support due to ballast in '*Super red*' condition

This was modelled by transition T_5^{CS}, the firing time of which was sampled from an Exponential distribution, this transition was not connected to any other places so can fire at all times. In the system model this transition was connected to a '*socket*' place in the ballast model so that failures could only occur if the ballast condition is '*Super red*'.

(vii) Concrete type (F27 and F40, more likely to develop defects)

The concrete manufacturing process is constantly improving. Older sleeper designs (F27 and F40) are more likely to develop defects, due to manufacturing errors. This was modelled by transition T_6^{CS}, the firing time of which was sampled from an Exponential distribution. The test arc between transition T_6^{CS} and place P_3^{CS} ensures that this transition can only fire if the sleeper is type F27 or F40. This information was gleaned from the Network Rail track summary database. The sleeper types used in Bletchley Delivery Unit are listed in Appendix J-1.1.

(viii) Baseline failures

In addition to the six failure modes above, which are all attributed to specific events the model also contained a baseline failure mode modelled by transition T_7^{CS}. The baseline failures encapsulate the general deterioration of sleepers due to age, loading and environmental factors. Chapter 5 investigated the relationship between concrete sleeper replacement rates and route tonnage, however no clear link could be established. T_7^{CS} is modelled using a Weibull distribution with shape factor greater than one as failures are thought to increase over time, as the number of loadings the sleeper has experienced increases and the sleeper ages. The scale factor was selected based on the sleeper service life estimations.

The distributions used to model transitions $T_0^{CS} \rightarrow T_7^{CS}$ for each of the six categories considered are shown in Appendix C-1.1.1→ Appendix C-1.1.6.

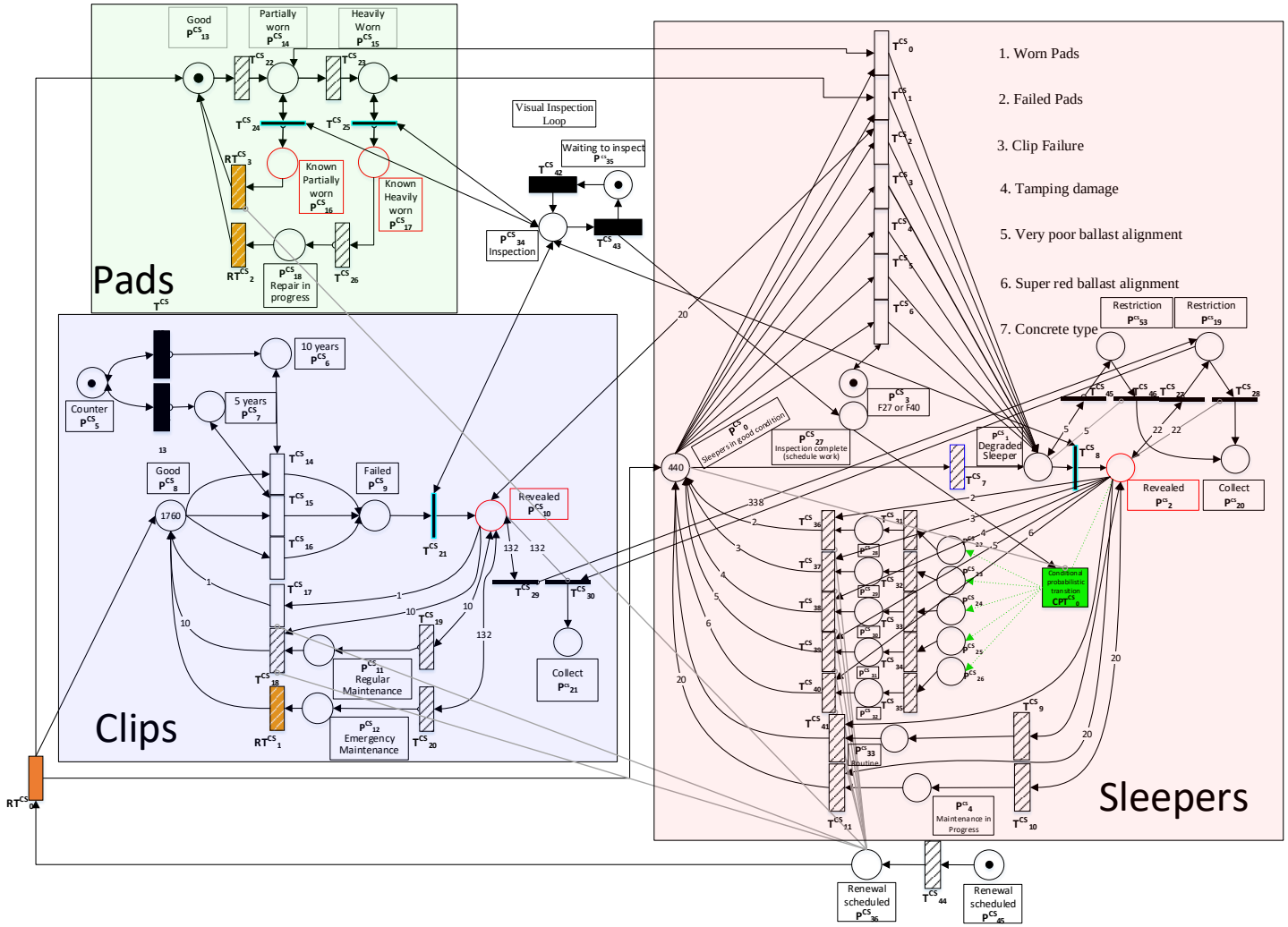


FIGURE 6.23 CONCRETE SLEEPER PETRI NET MODEL

Initially it was proposed to model each sleeper with an individual Petri net consisting of a working and failed place. However this would have required a very high number of transitions and places, and most of the transitions would fire very infrequently. It was therefore, decided to model all 440 sleepers with just one working and one failed place. This was achieved by setting the initial marking of place P_0^{CS} to 440, one token for each sleeper. The Petri net was constructed to ensure that the marking was conserved such that:

$$Marking\ of;\ P_0^{CS} + P_1^{CS} + P_2^{CS} = 440, \qquad \forall\, t \tag{6.24}$$

The distributions used in transitions $T_0^{CS} \rightarrow T_7^{CS}$ had to be altered to reflect that the transitions were now modelling the deterioration of 440 sleepers as opposed to one. For $T_0^{CS} \rightarrow T_6^{CS}$ this is straight forward. Since if $E_1(t)$ and $E_2(t)$ are two independent Exponential processes with rates λ_1 and λ_2 respectively. Then the process $E(t) = E1(t) + E2(t)$ is an Exponential process with rate $\lambda=\lambda_1+\lambda_2$. This is shown in Figure 6.24.

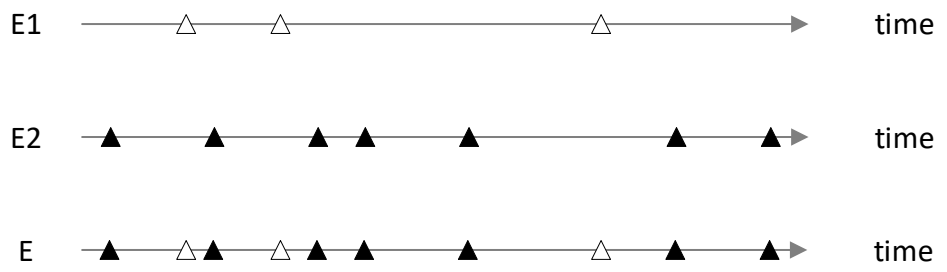


FIGURE 6.24: COMBINING EXPONENTIAL DISTRIBUTIONS

For the Weibull distribution used in T_7^{CS} combining them is more difficult, papers have appeared in literature to provide means to combine Weibull processes [155]. However it is only desired to find failure times. Transition T_7^{CS} was modified so that instead of sampling from a specified Weibull distribution the firing times were sampled from a predetermined vector, $\widehat{\boldsymbol{\Psi}}$. The values of $\widehat{\boldsymbol{\Psi}}$ were determined according to algorithm 6.1. Transitions where the firing time is predetermined using the above algorithm are shown with a blue border in the Petri net diagrams.

Algorithm 6.1

(i) Generate a value ω_1 by sampling from a Weibull distribution, W(β,η) for single sleeper,

If(ω_1<simulation length)

ω_1 added to $\boldsymbol{\Psi_1}$

end

Generate a value ω_2 by sampling from W(β,η)

If($\omega_2 + \omega_1 + MTTR$<simulation length)

$\omega_2 + \omega_1 + MTTR$ added to $\boldsymbol{\Psi_2}$

end

Repeat until $\omega_n + \cdots + \omega_2 + \omega_1 + (n-1)MTTR \geq$simulation length

(ii) Repeat step (i) 440 times to generate failure times for all sleepers.

(iii) Combine vectors $\boldsymbol{\Psi_1}, \ldots, \boldsymbol{\Psi_{440}}$ into a single vector $\widehat{\boldsymbol{\Psi}}$ and then sort $\widehat{\boldsymbol{\Psi}}$ from smallest to largest.

(iv) The final vector $\widehat{\widehat{\boldsymbol{\Psi}}}$ **(**which will be sampled from) is calculated as the difference between the elements of the vector $\widehat{\boldsymbol{\Psi}}$.

Deteriorated sleepers will only be discovered following an inspection, it is assumed that sleeper deterioration will be discovered during a visual inspection. T_8^{CS} is only enabled when the inspection is on going (P_{34}^{CS} marked), the inspection frequency is set in standards and varies by track category as discussed in Chapter 5. Following an inspection maintenance can be scheduled. However, unlike for ballast and rails, concrete sleepers cannot be repaired, and when they are defective they are replaced. Chapter 5 provided an analysis of the concrete sleeper maintenance records. Based on the breakdown of the units complete it was decided to model seven types of sleeper replacement:

(i) Single sleeper replaced
(ii) Two sleepers replaced
(iii) Three sleepers replaced
(iv) Four sleepers replaced
(v) Five sleepers replaced
(vi) Six sleepers replaced
(vii) High number of sleepers replaced, as number of defective sleepers is close to the safety limit

Single sleeper repairs would be scheduled as soon as there was at least one defective sleeper, and a high number of replacements would be scheduled if the number of ineffective sleepers was close to the safety limit. In the remainder of cases the conditional probabilistic transition CPT_0^{CS} would decide whether two, three, four, five or six sleepers would be replaced based on the number that were defective. The probability values are chosen based on the proportion of the total each action represented found in Chapter 5, Figure 5.30. The probabilities used

are shown in Appendix C-4.1. CPT_0^{CS} would re-evaluate after each inspection. The distributions for the schedule ($T_9^{CS}, T_{10}^{CS}, T_{31}^{CS} \rightarrow T_{35}^{CS}$) and repair times ($T_{11}^{CS}, T_{36}^{CS} \rightarrow T_{41}^{CS}$) were those determined in Chapter 5, and are shown in AppendixC-2.1 and C-3.1 respectively.

It is assumed that there are four clips per sleeper (two for each rail) hence in total there are 1760 clips per section. Similar to sleepers, instead of creating a Petri net for each clip, the clips were modelled by setting the initial marking of P_8^{CS} to 1760 and ensuring the marking of the clips subnet was conserved such that:

$$Marking\ of;\ P_8^{CS} + P_9^{CS} + P_{10}^{CS} = 1760 \quad \forall\, t. \tag{6.25}$$

Table 6.8 taken from Network Rail standards [50], details the number of ineffective clips permitted per 60 feet.

	Rail Type	Maintenance Tolerance	Intervention Limit
Number of missing or ineffective fastenings in any 60 feet of track	Bullhead	4	8
	Flat-bottom	6	12

TABLE 6.8: NUMBER OF MISSING OR INEFFECTIVE FASTENINGS PERMITTED PER 60 FEET OF TRACK

Based on these values and observing that an eighth mile section is 660 feet long, three types of clip repair are considered:

(i) Single clip repair (T_{17}^{CS}); this type of intervention is only considered in the system model, it is considered opportunistically (when some other asset in the area is being maintained anyway).

(ii) Multiple clip repair (T_{18}^{CS}); this is the most common type of repair, and is scheduled once the maintenance tolerance is reached (44 Bullhead/88 Flat-bottom).

(iii) Clip renewal (RT_1^{CS}); if the intervention limit (66 Bullhead/132 Flat-bottom) is exceeded then all the clips are assumed to be replaced.

There are two sleeper pads per sleeper (one under each rail). However the pads are not modelled individually as it is difficult to judge the condition of the pads during a visual inspection and it is unlikely that an individual pad would be changed. For this reason only the overall condition of the pads is assessed. The pads can be in one of three condition states:

(i) Good (P_{13}^{CS})
(ii) Partly degraded (P_{14}^{CS})
(iii) Fully degraded (P_{15}^{CS})

As discussed the condition of the pads affects the sleeper deterioration.

The final aspect of the concrete sleeper model that needs to be considered is renewal. The sleepers tend to have a significantly longer service life than the ballast or rails and to replace the sleepers the rails have to be removed and ballast heavily disturbed. Therefore in general the sleepers are renewed when the ballast and rails need renewing also. In the individual

model the time between renewals is governed by transition T_{44}^{CS}, the firing time of T_{44}^{CS} is sampled from a Normal distribution, with mean, μ, equal to the service life of the sleepers. In the whole system model the complete renewal of the track section will also replace the sleepers however track section renewal is seldom determined based on the sleeper condition, so in the track section model, renewal is driven by the ballast and rail condition only. If a section was scheduled for renewal then all but essential (major work to remove speed restrictions) would be prevented, as it is not cost effective to replace individual sleepers if the whole section will be renewed in the near future.

Network Rail safety standards [50] specify that only a certain number of sleepers can be defective in 60 feet of track, this is summarised in Table 6.9.

Speed Limit	Maximum Number of Defective Sleepers Permitted
5-60 mph	66 (15%)
65-100 mph	33 (7.5%)
105-125 mph	22 (5%)

TABLE 6.9: MAXIMUM NUMBER OF DEFECTIVE SLEEPERS PERMITTED PER 60 FEET OF TRACK FOR VARIOUS LINE SPEEDS.

Similar to the track section model, a TSR would be enforced if the asset degradation became too great (more than a given number of sleepers defective). The risk due to a high level of unrevealed defective sleepers was also considered. These phenomena are discussed below.

If more than the permitted number of sleepers become defective, then a speed restriction must be put in place to ensure that it is still safe to run trains. Transitions T_{27}^{CS} and T_{28}^{CS} are used to simulate this, if the marking of place P_2^{CS} exceeds 22 (or 33 or 66) transition T_{27}^{CS} will fire, marking place P_{19}^{CS} and indicating that a speed restriction is in place. Once the number of tokens in place P_2^{CS}drops below 22 again transition T_{28}^{CS} will be uninhibited and will fire immediately, removing the marking of place P_2^{CS}. Similarly, if too many clips are defective then a speed restriction will also be imposed, this is simulated using transitions T_{29}^{CS} and T_{30}^{CS}. In addition to the costs associated with the implementation of speed restrictions, it is also worth considering the impact of undetected sleeper failures; i.e. the number of tokens in place P_1^{CS}. If the marking of P_1^{CS} is greater than Q then there is considered to be too high a risk, and transition T_{45}^{CS} fires, marking place P_{53}^{CS}. A penalty cost is assigned to the number of days that place P_{53}^{CS} is marked as the marking of P_{53}^{CS} indicates there is a high risk of derailment. The value of Q is dependent on the track category. For categories 1A and 1 Q=5, for categories 2 and 3 Q=10 and for categories 4 and 5 Q=15.

The concrete sleeper Petri net was simulated using bespoke C++ code written during the project. The concrete sleeper module was simulated 50,000 times for 165, 16 week (112 days) periods (≈50 years). The costs used in the model are shown in Table 6.10, the cost values were obtained from Spon's [49] (green working values), where no value was given in Spon's the values were estimated. The cost factors were scaled based on the track category. Category 1A lines were assumed to be built using larger (more expensive) sleepers, and have

a higher cost per day for speed restrictions and line closures, the scaling values for the sleeper replacement were determined based on the various costing values for different grades of sleepers listed in Spon's, the scaling factors for risk and restrictions were estimated. It should be noted that the renewal cost was estimated based on the cost of complete renewal (ballast, rail and sleepers).

The results of the concrete sleeper model are shown in Figure 6.25→Figure 6.27 and Table 6.11 → Table 6.12. Table 6.11, summarises the number of failures. Table 6.12 summarises the number of repairs. Figure 6.25 shows the convergence of the total cost (with 95 % confidence bounds), and Figure 6.26 shows how the cost was split between maintenance inspection, TSR, risk and renewal. It can be seen that Category 1A costs more than 10 times that of Category 5. There are a number of reasons why the total cost of Category 5 is significantly less:

(i) Due to the long expected service life, the sleepers do not need renewing in the 50 year simulation period (see Figure 6.26; the only cost is due to maintenance and inspection).
(ii) Due to much lower tolerances required, neither the risk threshold nor restriction threshold are ever reached.
(iii) Inspection costs are lower as inspections were less frequent.
(iv) Replacement costs are lower as a lower quality sleeper was used.

Figure 6.27 shows the frequency of maintenance in each 16 week period of the simulation. Unlike for the track section model it is possible to make sure the 16 week observation period aligns with the inspection interval. For Category 1A to 3 the frequency of maintenance steadily increases from year zero until renewal. Due to the restriction of all but major work, once a renewal has been scheduled it can be seen that leading up to a renewal the volume of work drops.

	Task	Unit	Data Sources	Cost Units (By Track Category)					
				1A	1	2	3	4	5
1	Sleeper	Each	Spon's	50	50	44	44	38	38
2	Sleeper x2	Per intervention	Spon's	100	100	88	88	76	76
3	Sleeper x3	Per intervention	Spon's	150	150	132	132	113	113
4	Sleeper x4	Per intervention	Spon's	200	200	176	176	152	152
5	Sleeper x5	Per intervention	Spon's	250	250	219	219	188	188
6	Sleeper x6	Per intervention	Spon's	300	300	264	264	225	225
7	Major	Per intervention	Spon's	2,500	2,500	4,500	4,500	7,500	7,500
8	Clip replacement	Each	Spon's	8	8	2	2	2	2
9	Pad replacement	Each	Estimated	100	100	100	60	60	60
10	Renewal	Per 220 yards	Estimated	105,000	94,500	91,875	78,750	78,750	65,625
11	Visual inspection	Per intervention	Estimated	8	8	8	8	8	8
12	Restriction	Per day	Estimated	5,000	4,500	3,750	3,750	2,500	2,500
13	Risk	Per day	Estimated	1,000	1,000	1,000	1,000	1,000	1,000

TABLE 6.10: COST BREAKDOWN FOR CONCRETE SLEEPERS BY TRACK CATEGORY

Category	Failure Mode	Per 50 years				Per Year	%[13]
		Mean	SD	Min	Max		
1A	Rail seat area worn due to worn pads	$1.3x10^{-2}$	0.11	0	2	0.000	0.000
	Rail seat area worn due to failed pads	$2.6x10^{-2}$	0.22	0	8	0.001	0.000
	Fastening damage	0.32	0.76	0	8	0.006	0.001
	Cracking due to tamping damaging	14.61	3.83	2	32	0.292	0.066
	Cracking due to poor ballast support (Very poor)	18.24	4.27	3	38	0.365	0.083
	Cracking due to poor ballast support (Super red)	10.96	3.29	1	28	0.219	0.050
	Cracking due to concrete construction (F27 or F40)	22.68	4.72	7	46	0.454	0.103
	General	331.51	18.66	260	430	6.630	1.507
	Total	398.36	n/a	n/a	n/a	7.97	1.81
1	Rail seat area worn due to worn pads	$1.0x10^{-2}$	0.10	0	2	0.000	0.000
	Rail seat area worn due to failed pads	$1.9x10^{-3}$	0.17	0	7	0.000	0.000
	Fastening damage	0.14	0.50	0	7	0.003	0.001
	Cracking due to tamping damage	11.67	3.44	1	28	0.233	0.053
	Cracking due to poor ballast support (Very poor)	14.61	3.79	3	35	0.292	0.066
	Cracking due to poor ballast support (Super red)	8.77	2.96	1	25	0.175	0.040
	Cracking due to concrete construction (F27 or F40)	21.10	4.58	6	41	0.422	0.096
	General	298.49	17.74	225	375	5.970	1.357
	Total	354.79	n/a	n/a	n/a	7.10	1.61
2	Rail seat area worn due to worn pads	$5.9x10^{-3}$	0.08	0	1	0.000	0.00%
	Rail seat area worn due to failed pads	$8.7x10^{-3}$	0.11	0	3	0.000	0.00%
	Fastening damage	$7.9x10^{-2}$	0.37	0	7	0.000	0.00%
	Cracking due to tamping damage	8.19	2.86	0	25	0.164	0.04%
	Cracking due to poor ballast support (Very poor)	10.22	3.19	1	26	0.204	0.05%
	Cracking due to poor ballast support (Super red)	6.14	2.47	0	21	0.123	0.03%
	Cracking due to concrete construction (F27 or F40)	17.25	4.16	4	36	0.345	0.08%
	General	278.69	17.12	211	347	5.574	1.27%
	Total	320.51	n/a	n/a	n/a	6.41	1.46%
3	Rail seat area worn due to worn pads	$4.2x10^{-3}$	0.07	0	1	0.000	0.00%
	Rail seat area worn due to failed pads	$5.9x10^{-3}$	0.09	0	3	0.000	0.00%
	Fastening damage	$4.9x10^{-3}$	0.09	0	4	0.000	0.00%
	Cracking due to tamping damage	6.57	2.55	0	20	0.131	0.03%
	Cracking due to poor ballast support (Very poor)	8.20	2.85	1	22	0.164	0.04%
	Cracking due to poor ballast support (Super red)	4.914	2.22	0	19	0.098	0.02%
	Cracking due to concrete construction (F27 or F40)	16.07	4.00	1	36	0.321	0.07%
	General	266.17	16.71	205	338	5.323	1.21%
	Total	301.94	n/a	n/a	n/a	6.039	1.37%
4	Rail seat area worn due to worn pads	$1.9x10^{-3}$	$4.4x10^{-2}$	0	1	0.000	0.00%
	Rail seat area worn due to failed pads	$2.0x10^{-3}$	$4.5x10^{-2}$	0	3	0.000	0.00%
	Fastening damage	$1.0x10^{-3}$	$3.9x10^{-2}$	0	3	0.000	0.00%
	Cracking due to tamping damage	4.91	2.22	0	17	0.098	0.02%
	Cracking due to poor ballast support (Very poor)	6.15	2.47	0	20	0.123	0.03%
	Cracking due to poor ballast support (Super red)	3.68	1.93	0	14	0.074	0.02%
	Cracking due to concrete construction (F27 or F40)	12.29	3.49	2	31	0.246	0.06%
	General	189.90	14.33	129	260	3.798	0.86%
	Total	216.93	n/a	n/a	n/a	4.339	0.99%
5	Rail seat area worn due to worn pads	$2.2x10^{-3}$	$4.7x10^{-2}$	0	2	0.000	0.00%
	Rail seat area worn due to failed pads	$2.4x10^{-3}$	$5.4x10^{-2}$	0	3	0.000	0.00%
	Fastening damage	$8.0x10^{-5}$	$1.1x10^{-2}$	0	2	0.000	0.00%
	Cracking due to tamping damage	3.44	1.85	0	14	0.069	0.02%
	Cracking due to poor ballast support (Very poor)	4.31	2.08	0	15	0.086	0.02%
	Cracking due to poor ballast support (Super red)	2.58	1.61	0	11	0.052	0.01%
	Cracking due to concrete construction (F27 or F40)	8.61	2.92	0	24	0.172	0.04%
	General	123.07	11.52	75	173	2.461	0.56%
	Total	142.02	n/a	n/a	n/a	2.840	0.65%

TABLE 6.11: MEAN, SD MINIMUM AND MAXIMUM NUMBER OF EACH CAUSE OF CONCRETE SLEEPER FAILURE

[13] For comparison to Figure 5.29

Category	Maintenance Type	Mean	SD	Min	Max
1A	Single sleeper repair	39.28	6.76	14	71
	Sleeper x2	13.80	4.06	2	32
	Sleeper x3	5.72	2.78	0	22
	Sleeper x4	5.22	2.80	0	21
	Sleeper x5	2.30	1.65	0	12
	Sleeper x6	3.10	2.07	0	16
	Major sleeper intervention >20	12.49	1.87	4	20
1	Single sleeper repair	36.87	6.42	15	67
	Sleeper x2	13.38	4.10	1	34
	Sleeper x3	5.33	2.73	0	19
	Sleeper x4	4.79	2.73	0	20
	Sleeper x5	2.12	1.61	0	12
	Sleeper x6	2.84	2.00	0	13
	Major sleeper intervention >20	10.42	1.80	3	17
2	Single sleeper repair	36.17	6.16	14	63
	Sleeper x2	9.66	3.73	0	30
	Sleeper x3	5.06	3.04	0	20
	Sleeper x4	6.84	3.82	0	26
	Sleeper x5	4.16	2.70	0	18
	Sleeper x6	4.92	3.19	0	22
	Major sleeper intervention >40	3.61	1.27	0	8
3	Single sleeper repair	34.92	6.07	12	61
	Sleeper x2	9.85	3.96	0	29
	Sleeper x3	5.93	3.13	0	23
	Sleeper x4	7.11	3.85	0	28
	Sleeper x5	4.26	2.68	0	17
	Sleeper x6	5.09	3.18	0	21
	Major sleeper intervention >40	3.18	1.26	0	7
4	Single sleeper repair	34.67	5.77	13	62
	Sleeper x2	10.35	4.19	1	32
	Sleeper x3	5.38	2.87	0	22
	Sleeper x4	6.52	3.54	0	25
	Sleeper x5	4.01	2.55	0	17
	Sleeper x6	4.78	2.91	0	20
	Major sleeper intervention >60	0.71	0.68	0	3
5	Single sleeper repair	32.12	5.04	15	55
	Sleeper x2	11.48	4.24	0	32
	Sleeper x3	4.01	2.25	0	16
	Sleeper x4	4.10	2.40	0	18
	Sleeper x5	2.30	1.69	0	13
	Sleeper x6	2.87	1.87	0	12
	Major sleeper intervention >60	0.13	0.34	0	2

Table 6.12: MEAN, SD, MINIMUM AND MAXIMUM NUMBER FOR CONCRETE SLEEPER MAINTENANCE INTERVENTIONS

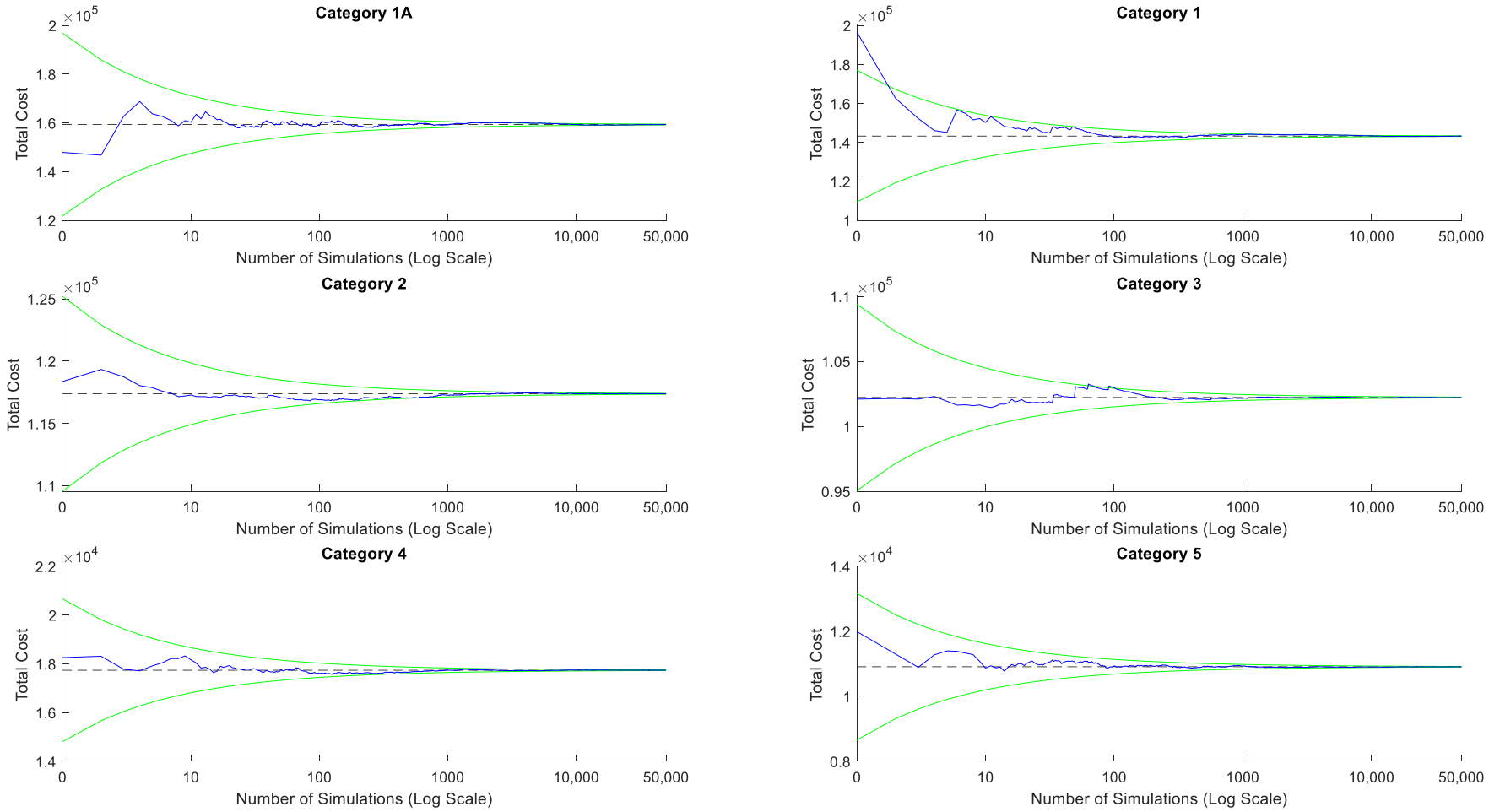


FIGURE 6.25: CONCRETE SLEEPER TOTAL COST CONVERGENCE
KEY: ●95% CONVERGENCE BOUNDS ●RUNNING AVERAGE ●CONVERGED VALUE

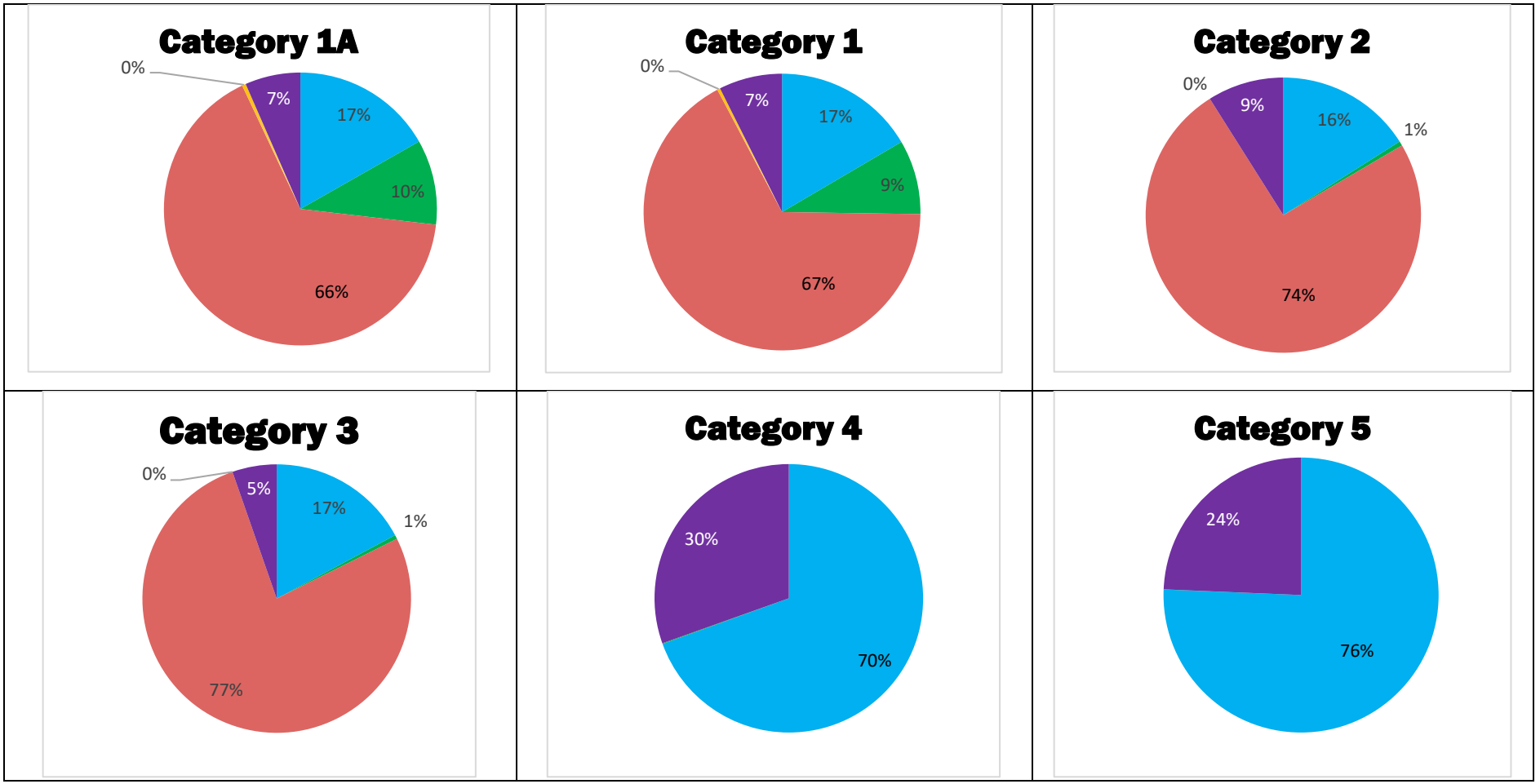


FIGURE 6.26: CONCRETE SLEEPER COST BREAKDOWN
KEY: ●MAINTENANCE ●TSR ●RENEWAL ●SAFETY RISK ●INSPECTION

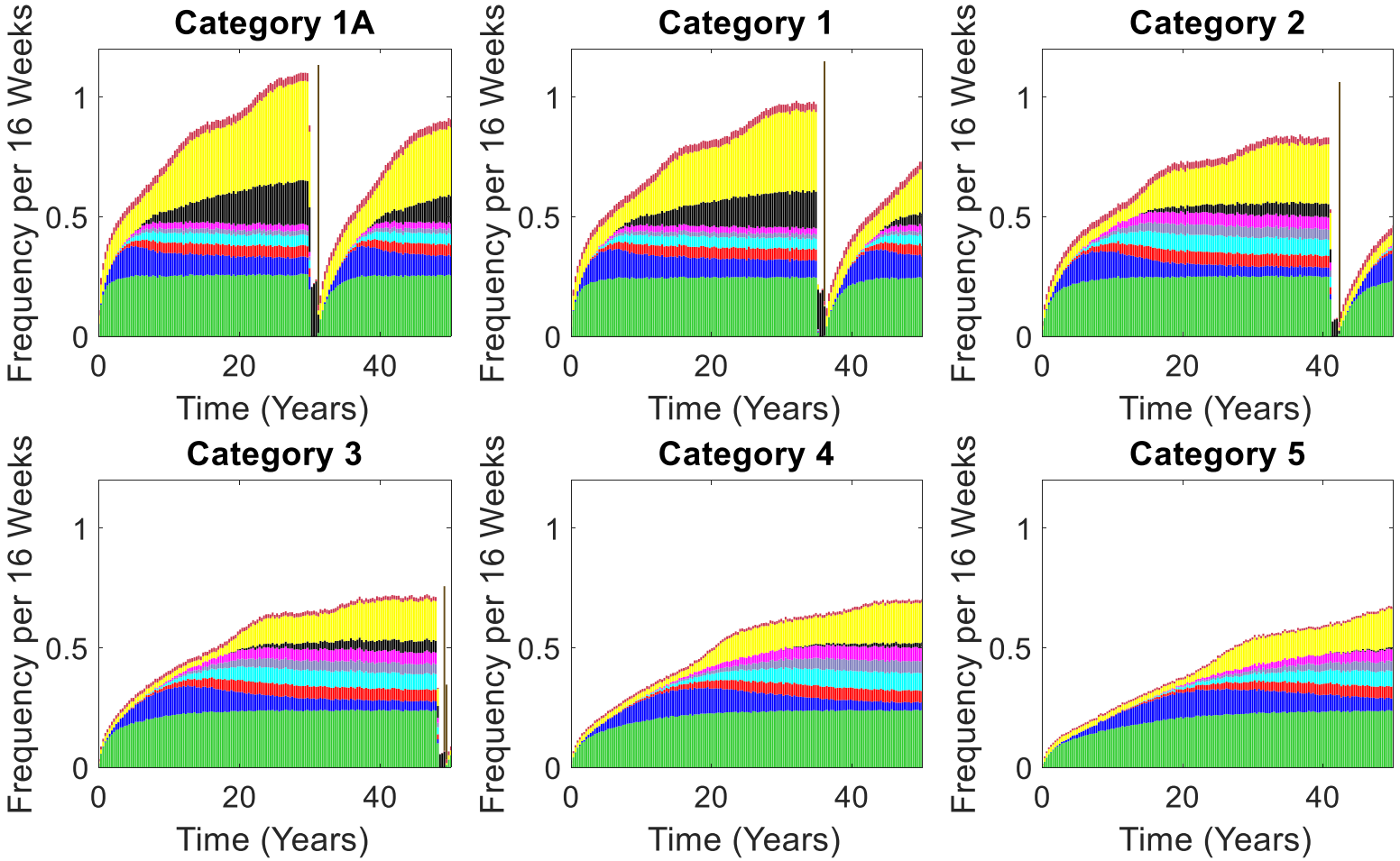


FIGURE 6.27: CONCRETE SLEEPER MAINTENANCE FREQUENCY PER 16 WEEKS

KEY: ●PADS ●CLIPS ●MAJOR SLEEPER REPLACEMENT ● 6X ● 5X ● 4X● 3X ● 2X ● SINGLE SLEEPER REPLACEMENT ●RENEWAL

6.3.2.2 Wooden Sleepers

The second type of sleeper considered is wooden/timber. There are two main types of timber sleeper; softwoods (such as Pine or Beach) and hardwoods (such as Oak or Mahogany). Hardwoods have a much longer service life than softwoods, however they cost significantly more and there are issues around sustainably sourcing hardwoods. The service life of hardwoods is comparable to concrete. However softwood sleepers have a significantly shorter service life. One of the main advantages of timber sleepers is they are considerably lighter than concrete and steel, and hence can be installed much more easily and quickly.

Until recently wooden sleepers were the most common type of sleeper used in the UK, however they have decreased in popularity in favour of concrete sleepers. Wooden sleepers are made of organic materials meaning their degradation is mainly driven by age, and their maximum service life is always limited to around 50 years. Weather conditions in the UK (damp and wet) further reduce the service life of wooden sleepers. Nonetheless wooden sleepers are still regularly used in S&C due to their nonstandard design and in tunnels due to the difficulties in lifting concrete/steel sleepers.

This section will introduce the wooden sleeper Petri net. There are several key differences between the concrete sleeper model and the wooden sleeper model:

(i) The degradation of wooden sleepers is governed by age.
(ii) Wooden sleepers do not have sleeper pads (although they do sometimes have baseplates this will not be considered).

The wooden sleeper model is shown in Figure 6.28. Four failure modes are considered in the wooden sleeper Petri net model:

(i) Damage to the fastening area

This was modelled by transition T_0^{WS}, the firing time of which was sampled from an Exponential distribution. The test arc, with a weight of 20, between T_0^{WS} and place P_{10}^{WS} ensures that this transition can only fire once at least 20 clips have failed.

(ii) Accelerated failure rate due to old sleepers

This was modelled by transition T_1^{WS}, the firing time of which was sampled from an Exponential distribution. The test arc between T_1^{WS} and place P_3^{WS} ensures that this transition can only fire if place P_3^{WS} is marked which only occurs following the firing of T_{46}^{WS} which represents the sleeper being old. The distribution used for T_{46}^{WS} is dependent on the track category and is shown in Appendix C-6.1.

(iii) Very poor support due to ballast in '*Super red*' condition

This was modelled by transition T_2^{WS}, the firing time of which was sampled from an Exponential distribution, this transition was not connected to any other places so can fire at all times. In the system model this transition was connected to a '*socket*' place in the ballast model so that this type of failure can only occur if the ballast condition is '*Super red*', this is discussed in section 7.3.3.

(iv) Baseline deterioration

In addition to the three failure modes above, which are all attributed to specific events the model also considered general failures modelled by transition T_3^{WS}. This transition is included to encapsulate the general deterioration of timber sleepers due to age and loading. T_3^{WS} is modelled using a Weibull distribution with shape factor greater than one as failures are thought to increase as the number of loadings the sleeper has experienced increases and the sleeper ages. The scale factor was estimated based on the sleeper service life estimations discussed in Chapter 2.

The distribution parameters used for transitions $T_0^{WS} \rightarrow T_3^{WS}$ are shown in Appendix C-1.2.1→ Appendix C-1.2.6.

As with the concrete sleeper model, the timber sleeper model was used to model the deterioration of all 440 sleepers in the section. The distributions used for transitions $T_0^{WS} \rightarrow T_3^{WS}$ were altered in the same way as in the concrete sleeper model to allow the transitions to model multiple sleepers simultaneously.

Defective sleepers will only be discovered following an inspection. T_{26}^{WS} is only enabled when the inspection is ongoing (P_{36}^{WS} marked), the inspection frequency is set in standards and varies by track category as discussed in Chapter 5. Based on the variation in the number of sleepers maintained during sleeper work found in Chapter 5 (Figure 5.30) it was decided to model 11 types of timber sleeper replacement:

(i) Single sleeper replaced
(ii) Two sleepers replaced
(iii) Three sleepers replaced
(iv) Four sleepers replaced
(v) Five sleepers replaced
(vi) Six sleepers replaced
(vii) Seven sleepers replaced
(viii) Eight sleepers replaced
(ix) Nine sleepers replaced
(x) Ten sleepers replaced
(xi) High number of sleepers replaced, as number of defective sleepers is close to the safety limit.

Single sleeper repairs would be scheduled as soon as there was at least one defective sleeper, a high number of replacements would be scheduled if the number of ineffective sleepers was close to the safety limit. In the remainder of cases the conditional probabilistic transition CPT_0^{WS} would decide whether two, three, four, five, six, seven, eight, nine or ten sleepers would be replaced based on the total number that were defective. The probability values are chosen based on the proportion of the total each action represented (see Figure 5.30) and are shown in Appendix C-4.2. CPT_0^{WS} would be re-evaluated after each inspection.

The distributions for the schedule times ($T_5^{WS}, T_7^{WS}, T_9^{WS}, T_{11}^{WS}, T_{13}^{WS}, T_{15}^{WS}, T_{17}^{WS}, T_{19}^{WS}, T_{21}^{WS}, T_{23}^{WS}, T_{25}^{WS}$) and repair times ($T_4^{WS}, T_6^{WS}, T_8^{WS}, T_{10}^{WS}, T_{12}^{WS}, T_{14}^{WS}, T_{16}^{WS}, T_{18}^{WS}, T_{20}^{WS}, T_{22}^{WS}, T_{24}^{WS}$) were those determined in Chapter 5, and are shown in Appendix C-2.2 and Appendix C-2.3.

If too many sleepers or clips become defective then it may no longer be safe to run trains at line speed, and a TSR will be put in place. The threshold for a TSR being put in place is the same as in the concrete sleeper model, for both the number of defective sleepers and number of defective clips. The risk threshold was also the same as in the concrete sleeper model.

The cost values used in the wooden sleeper model are shown in Table 6.13, again they are based on Spon's [49] values or estimated when Spon's data did not exist.

As in the case of the concrete sleeper model, the timber sleeper model was simulated 50,000 times for 165, 16 week (112 days) periods (≈50 years) using bespoke C++ software. Table 6.14 shows the average total number of occurrences of each of the four degradation modes discussed above. It can be seen that, as expected, the general failure mode contributed the largest amount to the overall number of failures. For all categories no clip failures occurred, this is due to the number of failed clips never exceeding 20. Categories 2 and 3 do not have any failures due to old sleepers as a renewal occurs before T_{46}^{WS} fires.

Table 6.15 summarises the number of sleeper repairs. For all categories it can be seen that single sleeper repairs contribute the largest proportion of repairs. However it does not form as large of a proportion as compared to the concrete sleeper model.

Figure 6.29 shows the convergence of the total cost for each of the track categories. It can be seen that the cost decreases for categories 1A→3. However it increases again for Category 4; this is due to Category 4 track being assumed to have softwood sleepers (as opposed to hardwood sleepers (categories 1A→3)). Although the cost of renewing softwood sleepers is assumed to be significantly less than that of hardwood, it is assumed that the service life is less than 25 years therefore Category 4 track is renewed twice in the 50 year period. Category 5 has the cheapest overall cost as it is assumed that despite being of softwood construction it will last over 25 years so there is only one renewal in the 50 year period.

Figure 6.30 shows how the overall cost is broken down between inspection, maintenance, renewal, risk and TSRs. It can be seen that a cost due to speed restrictions and high risk only occurs for categories 1A and 1 and the risk never accounts for more than one percent of the total cost. The low value for risk and TSRs is due to the high repair rate for wooden sleepers, as they are cheap and easy to maintain.

Figure 6.31 shows the average frequency of maintenance in each 16 week period based on the 50,000 simulations. It can be seen that initially the overall volume of sleeper repairs increases, the overall work volume then becomes constant, however there is a transition to interventions where the number of sleepers repaired is higher. The double renewal discussed above can clearly be seen in the Category 4 plot.

.	Task	Unit	Data Sources	Cost Units (By Track Category)					
				1A	1	2	3	4[14]	5
1	Sleeper	Each	Spon's	65	65	57	57	41	33
2	Sleeper x2	Per intervention	Spon's	130	130	114	114	81	65
3	Sleeper x3	Per intervention	Spon's	195	195	171	171	122	98
4	Sleeper x4	Per intervention	Spon's	260	260	228	228	163	130
5	Sleeper x5	Per intervention	Spon's	325	325	284	284	203	163
6	Sleeper x6	Per intervention	Spon's	390	390	341	341	244	195
7	Sleeper x7	Per intervention	Spon's	455	455	398	398	284	228
8	Sleeper x8	Per intervention	Spon's	520	520	455	455	325	260
9	Sleeper x9	Per intervention	Spon's	585	585	512	512	366	293
10	Sleeper x10	Per intervention	Spon's	650	650	570	570	410	330
7	Major	Per intervention	Spon's	1430	1430	2500	2500	2700	2150
8	Clip replacement	Each	Spon's	10	10	10	10	10	10
10	Renewal	Per 220 yards	Estimated	390	390	78	0	78	78
11	Visual inspection	Per intervention	Estimated	8	8	8	8	8	8
12	Restriction	Per day	Estimated	5000	4500	3750	3750	2500	2500
13	Risk	Per day	Estimated	195	195	171	171	122	98

TABLE 6.13: TIMBER SLEEPER COSTS

[14] Categories 4 and 5 are assumed to use softwood rather than hardwood so have a much smaller cost.

Category	Failure Mode	Over 50 Years				Per Year	%[15]
		Mean	SD	Min	Max		
1A	Fastening damage	0	0	0	0	0	0%
	Damage due to poor support	18.28	4.26	3	37	0.37	0.08%
	Accelerated failure due to age	38.84	6.60	16	69	0.78	0.18%
	General	401.76	20.58	319	498	8.04	1.83%
	Total	458.88	n/a	n/a	n/a	9.19	2.08%
1	Fastening damage	0	0	0	0	0	0%
	Damage due to poor support	18.26	4.25	5	37	0.37	0.083%
	Accelerated failure due to age	26.58	5.36	9	55	0.53	0.121%
	General	301.19	17.77	227	379	6.024	1.37%
	Total	346.00	n/a	n/a	n/a	6.924	1.57%
2	Fastening damage	0	0	0	0	0	0%
	Damage due to poor support	18.25	4.26	4	40	0.365	0.083%
	Accelerated failure due to age	0	0	0	0	0	0%
	General	255.87	16.50	187	326	5.120	1.16%
	Total	274.12	n/a	n/a	n/a	5.485	1.243%
3	Fastening damage	0	0	0	0	0	0%
	Damage due to poor support	18.27	4.27	5	37	0.365	0.083%
	Accelerated failure due to age	0	0	0	0	0	0%
	General	243.56	16.11	181	312	4.870	1.107%
	Total	261.38	-	-	-	5.235	1.190%
4	Fastening damage	0	0	0	0	0	0%
	Damage due to poor support	18.47	4.29	4	40	0.369	0.084%
	Accelerated failure due to age	8.29	3.25	0	26	0.166	0.038%
	General	593.58	24.81	485	707	11.870	2.70%
	Total	677.76	n/a	n/a	n/a	12.410	2.822%
5	Fastening damage	0	0	0	0	0	0%
	Damage due to poor support	9.25	3.03	0	26	0.185	0.040%
	Accelerated failure due to age	1.46	1.76	0	14	0.029	0.006%
	General	816.11	27.27	695	920	16.320	3.71%
	Total	826.82	- n/a	n/a	n/a	16.534	3.756%

TABLE 6.14: MEAN, SD, MINIMUM AND MAXIMUM NUMBER OF DEFECTIVE SLEEPERS BASED ON THE FOUR DETERIORATION MODES

[15] For comparison to Figure 5.29

Category	Maintenance Type	Mean	SD	Min	Max
1A	Single sleeper repair	12.45	4.92	0	36
	Sleeper x2	10.20	3.77	0	29
	Sleeper x3	4.34	2.11	0	17
	Sleeper x4	8.87	3.48	0	28
	Sleeper x5	2.59	1.96	0	13
	Sleeper x6	2.32	1.66	0	13
	Sleeper x7	2.21	1.46	0	12
	Sleeper x8	2.10	1.30	0	12
	Sleeper x9	1.23	1.11	0	11
	Sleeper x10	2.25	2.37	0	17
	Major sleeper intervention >20	14.00	1.38	2	25
1	Single sleeper repair	13.14	4.92	0	37
	Sleeper x2	9.92	3.91	0	30
	Sleeper x3	4.05	2.23	0	15
	Sleeper x4	8.35	3.61	0	26
	Sleeper x5	2.19	1.55	0	10
	Sleeper x6	1.91	1.51	0	11
	Sleeper x7	1.80	1.49	0	12
	Sleeper x8	1.67	1.41	0	10
	Sleeper x9	0.93	1.11	0	11
	Sleeper x10	1.66	1.61	0	14
	Major sleeper intervention >20	9.32	2.64	0	18
2	Single sleeper repair	13.12	4.95	0	36
	Sleeper x2	8.91	3.78	0	29
	Sleeper x3	3.52	2.11	0	16
	Sleeper x4	7.80	3.45	0	24
	Sleeper x5	3.01	1.96	0	14
	Sleeper x6	2.18	1.64	0	12
	Sleeper x7	1.75	1.47	0	10
	Sleeper x8	1.38	1.29	0	9
	Sleeper x9	0.97	1.12	0	9
	Sleeper x10	3.11	2.36	0	15
	Major sleeper intervention >40	5.46	1.38	0	7
3	Single sleeper repair	12.50	4.80	0	36
	Sleeper x2	9.12	3.91	0	33
	Sleeper x3	3.53	2.13	0	15
	Sleeper x4	7.45	3.39	0	24
	Sleeper x5	2.93	1.93	0	15
	Sleeper x6	2.10	1.62	0	12
	Sleeper x7	1.70	1.45	0	10
	Sleeper x8	1.35	1.29	0	11
	Sleeper x9	0.96	1.11	0	8
	Sleeper x10	3.08	2.34	0	16
	Major sleeper intervention >40	2.15	1.37	0	7
4	Single sleeper repair	24.01	6.87	2	55
	Sleeper x2	8.39	3.61	0	27
	Sleeper x3	3.38	2.08	0	15
	Sleeper x4	8.38	3.62	0	28
	Sleeper x5	6.04	3.25	0	23
	Sleeper x6	3.95	2.42	0	19
	Sleeper x7	2.76	1.92	0	13
	Sleeper x8	1.86	1.57	0	12
	Sleeper x9	1.68	1.52	0	11
	Sleeper x10	7.97	4.49	0	30
	Major sleeper intervention >60	5.20	1.62	0	10
5	Single sleeper repair	25.12	7.25	1	58
	Sleeper x2	8.19	3.79	0	27
	Sleeper x3	3.35	2.11	0	16
	Sleeper x4	8.44	3.71	0	31
	Sleeper x5	7.92	3.92	0	33
	Sleeper x6	5.12	2.84	0	21
	Sleeper x7	3.47	2.20	0	16
	Sleeper x8	2.27	1.77	0	14
	Sleeper x9	2.16	1.75	0	13
	Sleeper x10	11.06	5.64	0	42
	Major sleeper intervention >60	7.88	1.98	0	15

TABLE 6.15: MEAN, SD, MINIMUM AND MAXIMUM NUMBER OF ALL SLEEPER REPLACEMENTS CONSIDERED

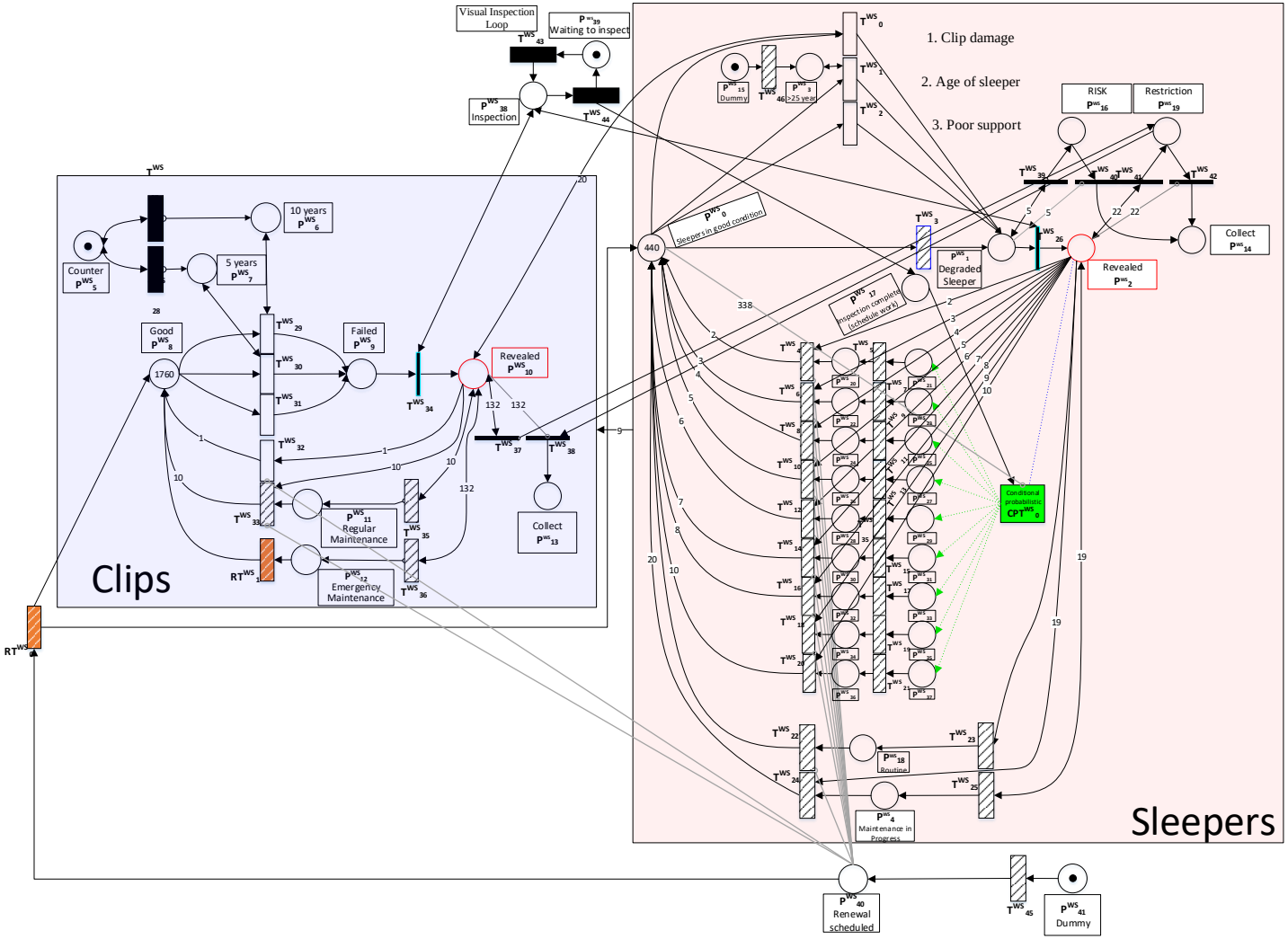


FIGURE 6.28: TIMBER SLEEPER PETRI NET MODEL

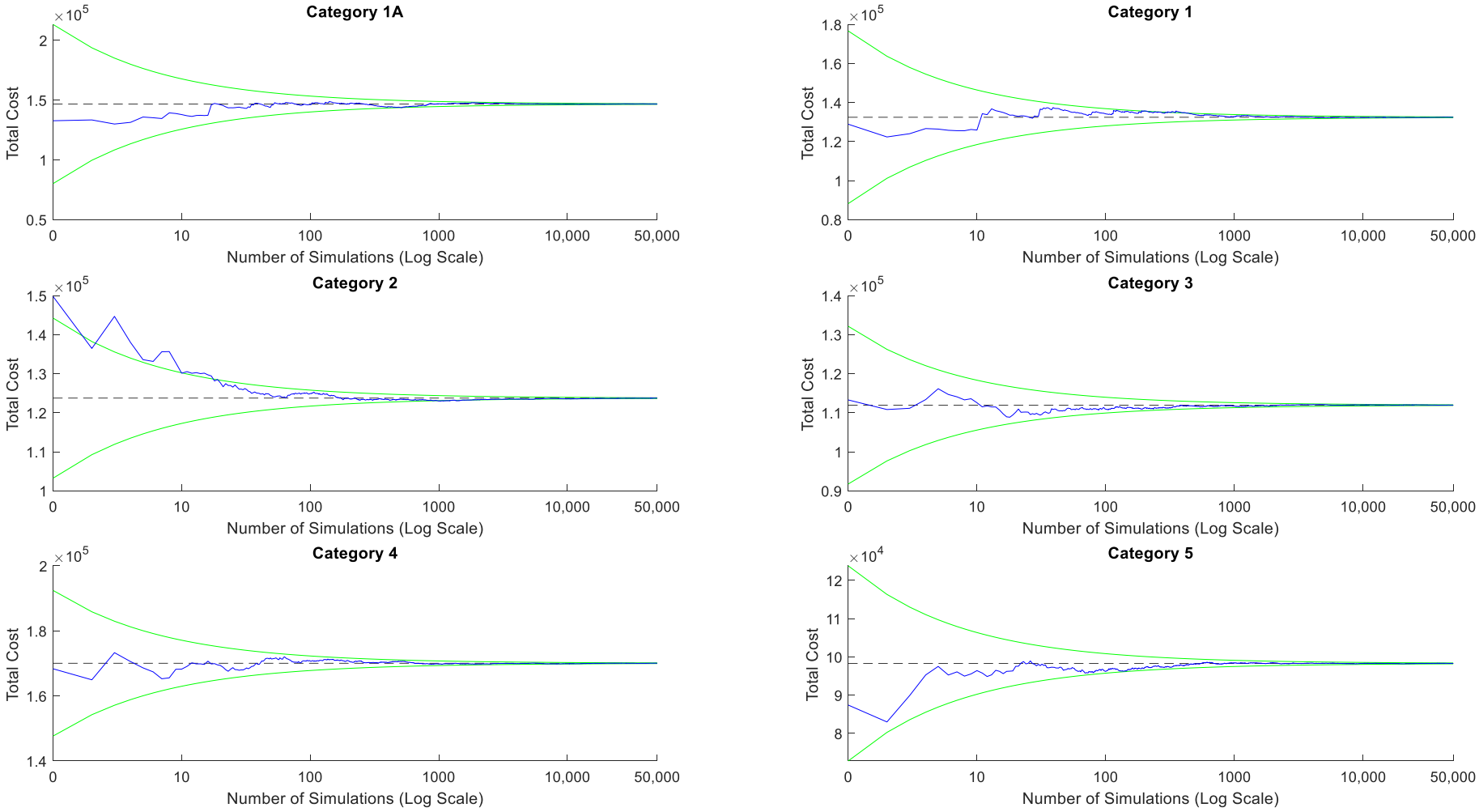


FIGURE 6.29: TIMBER SLEEPER COST CONVERGENCE
KEY: ●95% CONVERGENCE BOUNDS ●RUNNING AVERAGE ●CONVERGED VALUE

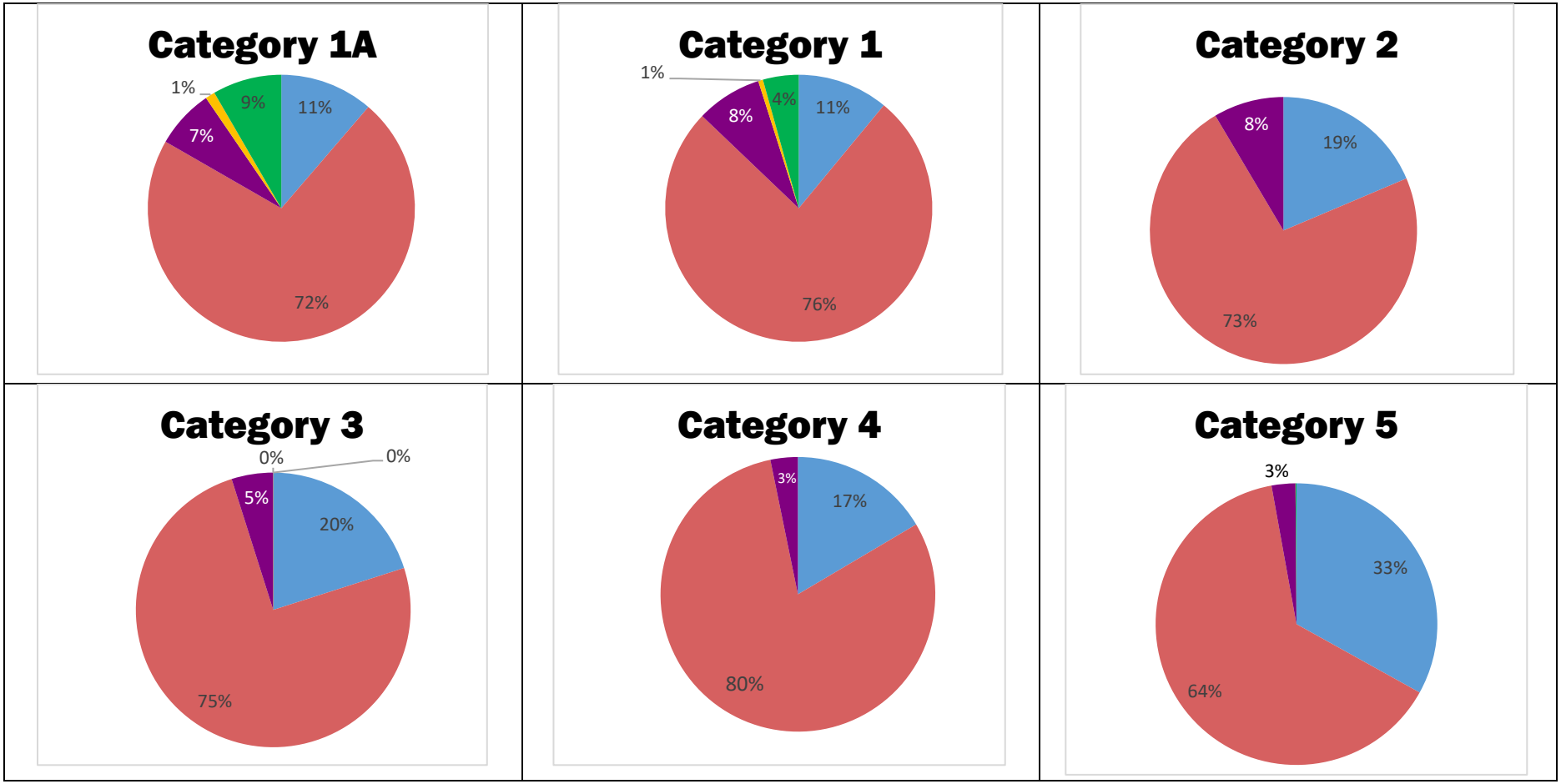


FIGURE 6.30: TIMBER SLEEPER COST BREAKDOWN
KEY: ●MAINTENANCE ●TSR ●RENEWAL ●SAFETY RISK ●INSPECTION

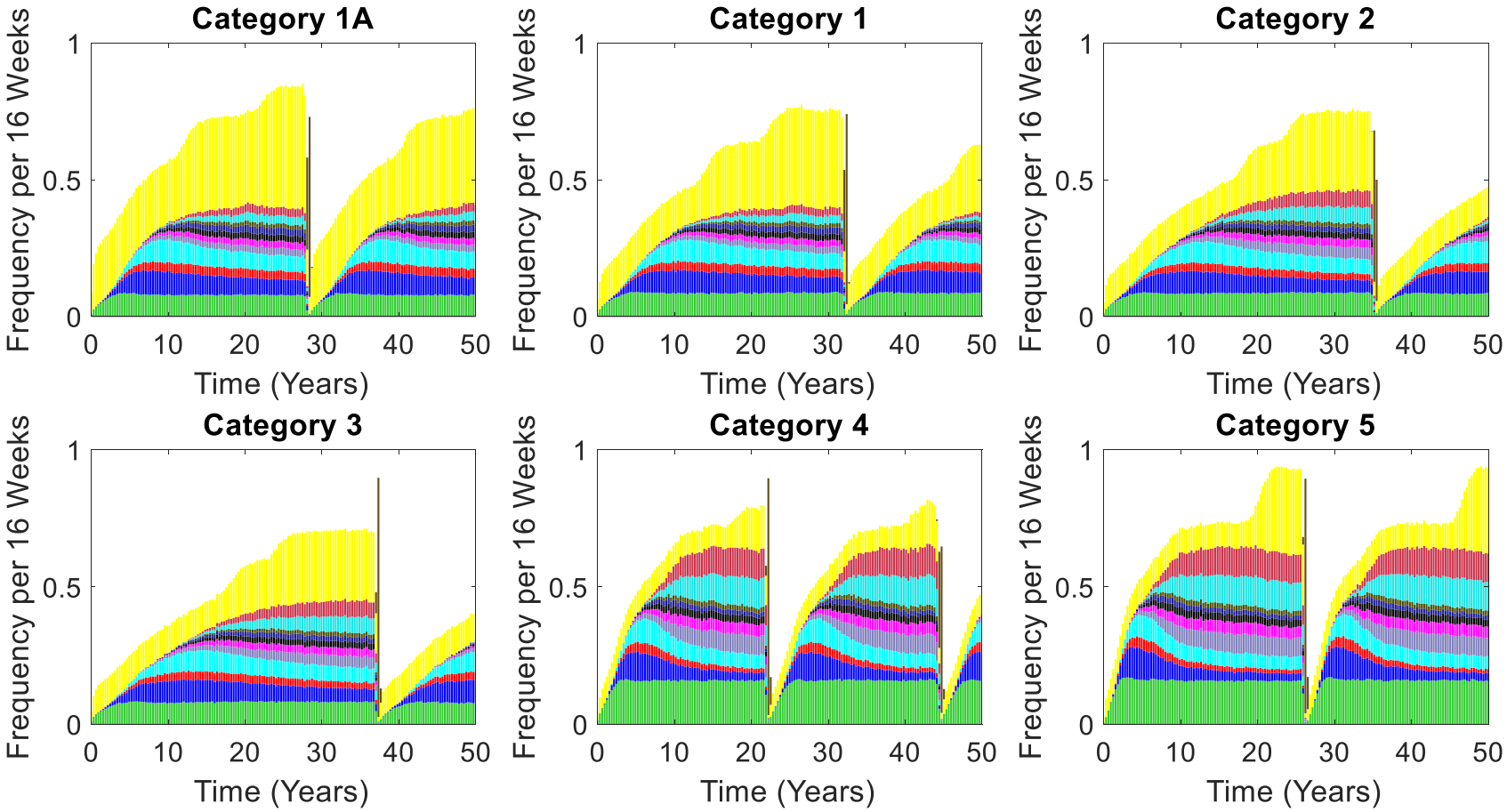


FIGURE 6.31: TIMBER SLEEPER MAINTENANCE FREQUENCY PER 16 WEEKS

KEY: CLIPS MAJOR 10X X9 X8 X7 X6 X5 X4 X3 X2 SINGLE SLEEPER REPLACEMENT RENEWAL

6.3.2.3 Steel Sleepers

The final sleeper type considered is steel sleepers. Steel sleepers are the least common type of sleeper used on the UK railway and the population is very young; as such there were only 169 maintenance records for steel sleeper replacements in CP4. Nonetheless they are used extensively on the Category 5 line between Bedford and Bletchley in the Bletchley Delivery Unit.

Steel sleeper degradation is driven mainly by tonnage; however, unlike concrete sleepers, in the absence of loading the service life of steel sleepers is still limited, as over time, steel sleepers will corrode/rust. This is amplified in damp and wet conditions such as in tunnels. Like concrete sleepers, steel sleepers are also fitted with pads, however in addition to reducing the load on the sleepers they also need to insulate the rails from the sleepers, to ensure there is no interference with the track circuits.

The steel sleeper Petri net is outlined in Figure 6.32 and has subnets for sleepers, clips and pads. Steel sleepers are modelled as having four deterioration modes:

(i) Failure of the isolation between the rail and sleepers
This was modelled by transition T_0^{SS}, the firing time for this transition was sampled from an Exponential distribution, the test arc between T_0^{SS} and place P_{30}^{SS} ensures that this transition can only fire when the pads are in the failed state.

(ii) Fastening failure
This was modelled by transition, T_1^{SS}, the firing time of which was sampled from an Exponential distribution. The test arc, with a weight of 20, between T_1^{SS} and place P_{25}^{SS} ensures that this transition can only fire, once at least 20 clips have failed.

(iii) Failure due to corrosion/age, modelled by transition T_2^{SS}.

(iv) Failure due to usage, modelled by transition T_3^{SS}.

The firing of transition T_2^{SS} was estimated based on the sleeper service life and the firing time of T_3^{SS} was estimated based on the track category and route tonnage. These transitions are modelled with a Weibull distribution, the parameter values are shown in Appendix C-1.3.1→. Appendix C-1.3.6.

The data analysis in Chapter 5 (see Figure 5.24) showed that unlike the other sleeper types for steel sleepers, single sleeper repairs were common with over 40% of the maintenance actions replacing just one sleeper. Based on the breakdown of the units complete it was decided to model seven types of sleeper replacement:

(i) Single sleeper replaced
(ii) Two sleepers replaced
(iii) Three sleepers replaced
(iv) Four sleepers replaced
(v) Five sleepers replaced
(vi) Six sleepers replaced

(vii) High number of sleepers replaced, as the number of defective sleepers is close to the safety limit

Single sleeper repairs would be scheduled as soon as there was at least one defective sleeper and a high number of replacements would be scheduled if the number of ineffective sleepers was close to the safety limit. In the remainder of cases the conditional probabilistic transition CPT_0^{SS} would decide whether two, three, four, five or six sleepers would be replaced based on the number that were degraded. The probability values used in transition CPT_0^{SS} are shown in Appendix C-4.3. The distributions for the schedule time and active repair were sampled from distributions based on the number of sleepers that were defective, the values are shown in Appendix C-2.3 and C-3.3.

The clips were modelled as in the timber and concrete sleeper models, however the distributions of the times to degrade were sampled from were different, the clip repair rate was assumed constant across all three sleeper types. The pads were modelled as in the concrete sleeper model.

As with the previous sleeper models the steel sleeper net was simulated 50,000 times for 165, 16 week periods. The costs used for each of the six track categories are shown in Table 6.16. Table 6.17 shows the statistics on the repair modes and Table 6.18 shows the statistics on the different failure modes.

Figure 6.36 concludes this section by providing a summary of the LCC for the three sleeper types. It can be seen for the higher track categories there is little difference in the overall cost, however for the lower track categories timber is more expensive as timber requires a renewal in the 50 year lifecycle whereas steel and concrete do not.

	Task	Unit	Source	Cost Units (By Track Category)					
				1A	1	2	3	4	5
1	Sleeper	Each	Spon's	56	56	49	49	49	49
2	Sleeper x2	Per intervention	Spon's	112	112	98	98	98	98
3	Sleeper x3	Per intervention	Spon's	168	168	147	147	147	147
4	Sleeper x4	Per intervention	Spon's	224	244	214	214	214	214
5	Sleeper x5	Per intervention	Spon's	280	280	245	245	245	245
6	Sleeper x6	Per intervention	Spon's	336	336	294	294	294	294
7	Major	Per intervention	Spon's	1500	1500	2700	2700	4500	4500
8	Clip replacement	Each	Spon's	8	8	2	2	2	2
9	Pad replacement	Each	Estimate	100	100	100	60	60	60
10	Renewal	Per 220 yards	Estimated	105,000	99,750	89250	84,000	68,250	63,000
11	Visual inspection	Per intervention	Estimated	8	8	8	8	8	8
12	Restriction	Per day	Estimated	5000	4500	3750	3750	2500	2500
13	Risk	Per day	Estimated	1000	1000	1000	1000	1000	1000

TABLE 6.16: STEEL SLEEPER COST BREAKDOWN

Category	Maintenance Type	Mean	SD	Min	Max
1A	Single sleeper repair	159.19	26.53	52	273
	Sleeper x2	54.74	11.50	0	110
	Sleeper x3	12.90	4.43	0	34
	Sleeper x4	1.82	1.44	0	11
	Sleeper x5	0.61	0.80	0	7
	Sleeper x6	0.53	0.84	0	8
	Major sleeper intervention >20	0.87	1.14	0	11
1A	Single sleeper repair	164.57	26.13	58	286
	Sleeper x2	53.74	10.83	2	94
	Sleeper x3	12.58	4.24	0	33
	Sleeper x4	1.64	1.36	0	11
	Sleeper x5	0.54	0.76	0	6
	Sleeper x6	0.41	0.74	0	7
	Major sleeper intervention >20	0.61	0.93	0	8
2	Single sleeper repair	146.01	23.38	46	277
	Sleeper x2	41.68	9.58	1	88
	Sleeper x3	9.64	3.72	0	29
	Sleeper x4	1.15	1.14	0	12
	Sleeper x5	0.45	0.75	0	8
	Sleeper x6	0.47	1.06	0	12
	Major sleeper intervention >40	0.06	0.26	0	3
3	Single sleeper repair	127.62	20.85	40	251
	Sleeper x2	39.76	8.83	1	80
	Sleeper x3	8.14	3.32	0	25
	Sleeper x4	0.72	0.90	0	8
	Sleeper x5	0.24	0.55	0	6
	Sleeper x6	0.24	0.74	0	11
	Major sleeper intervention >40	0.02	0.15	0	3
4	Single sleeper repair	94.51	14.79	32	153
	Sleeper x2	20.41	5.79	1	53
	Sleeper x3	3.97	2.21	0	18
	Sleeper x4	0.22	0.49	0	5
	Sleeper x5	0.05	0.24	0	3
	Sleeper x6	0.03	0.21	0	8
	Major sleeper intervention >60	$2.2x10^{-5}$	$4.4x10^{-3}$	0	1
5	Single sleeper repair	64.33	20	106	10.34
	Sleeper x2	10.98	0	33	4.28
	Sleeper x3	1.67	0	11	1.40
	Sleeper x4	0.04	0	3	0.21
	Sleeper x5	$6.1x10^{-3}$	0	3	0.08
	Sleeper x6	$2.3x10^{-3}$	0	4	0.06
	Major sleeper intervention >60	0	0	0	0

TABLE 6.17: MEAN, SD, MINIMUM AND MAXIMUM NUMBER OF SLEEPERS REPAIRED

Category	Failure	Over 50 Years				Per Year	
		Mean	SD	Min	Max	Mean	%[16]
1A	Fastening damage	0.01	0.11	0	3	$2.0x10^{-4}$	$4.5\ x10^{-5}$
	Damage due to poor support	0.03	0.32	0	11	$6.0x10^{-4}$	$1.4\ x10^{-5}$
	Accelerated failure due to age	173.4	13.86	121	233	3.5	0.8
	General	170.0	13.74	111	234	3.4	0.7
	Total	343.4	n/a	n/a	n/a	6.9	1.6
1	Fastening damage	$3.2x10^{-3}$	0	2	0.06	$6.4x10^{-5}$	$1.5\ x10^{-5}$
	Damage due to poor support	0.01	0	11	0.22	$2.0x10^{-4}$	$4.5\ x10^{-5}$
	Accelerated failure due to age	156.5	100	221	13.14	3.1	0.7
	General	180.1	128	240	14.06	3.6	0.8
	Total	336.6	n/a	n/a	n/a	6.732	1.5
2	Fastening damage	$1.1x10^{-3}$	0.04	0	2	$2.2x10^{-5}$	$5.0\ x10^{-6}$
	Damage due to poor support	0	0	0	0	0	0
	Accelerated failure due to age	127.90	11.74	81	175	2.6	0.6
	General	146.73	12.55	100	203	2.9	0.7
	Total	274.6	n/a	n/a	n/a	5.5	1.3
3	Fastening damage	$9.4x10^{-4}$	0.03	0	2	$1.9x10^{-5}$	$4.3\ x10^{-6}$
	Damage due to poor support	0	0.00	0	0	0	0
	Accelerated failure due to age	112.93	10.95	67	158	2.3	0.5
	General	128.21	11.63	82	182	2.6	0.6
	Total	241.14	n/a	n/a	n/a	4.8	1.1
4	Fastening damage	$4.8x10^{-4}$	0.02	0	2	$9.6x10^{-6}$	$2.2\ x10^{-6}$
	Damage due to poor support	0	0	0	0	0	0
	Accelerated failure due to age	71.24	8.76	38	107	1.4	0.3
	General	78.63	9.36	44	120	1.6	0.4
	Total	149.9	n/a	n/a	n/a	3.0	0.7
5	Fastening damage	$3.8x10^{-4}$	0	2	0.02	$7.6x10^{-6}$	$1.7x10^{-6}$
	Damage due to poor support	0	0	0	0	0	0
	Accelerated failure due to age	44.69	19	76	6.88	0.9	0.2
	General	47.84	21	79	7.29	1	0.2
	Total	92.5	n/a	n/a	n/a	1.85	0.42

TABLE 6.18: MEAN, SD, MINIMUM AND MAXIMUM FOR STEEL SLEEPER FAILURE MODES BY TRACK CATEGORY

[16] For Comparison to Figure 5.29

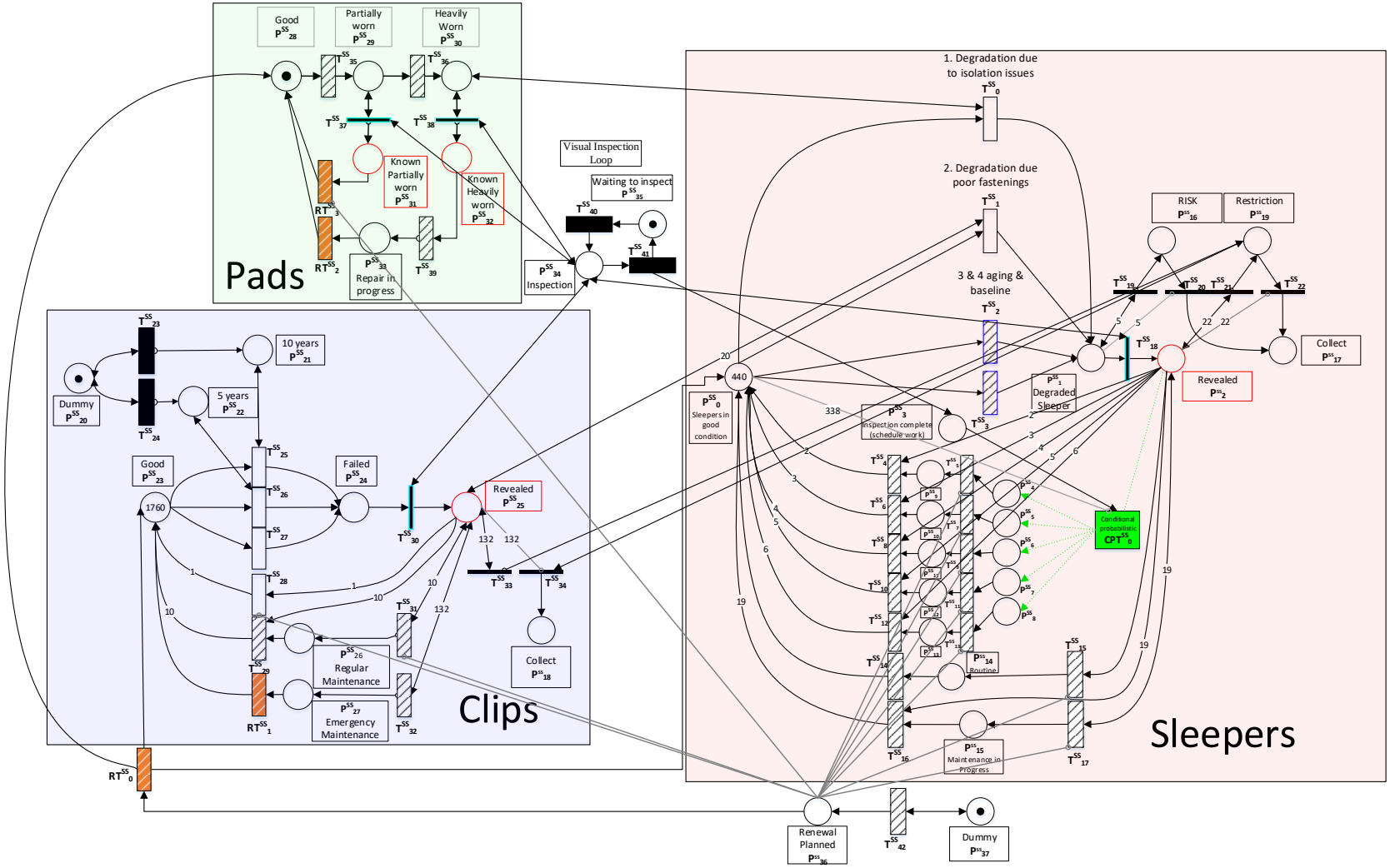


FIGURE 6.32: STEEL SLEEPER PETRI NET

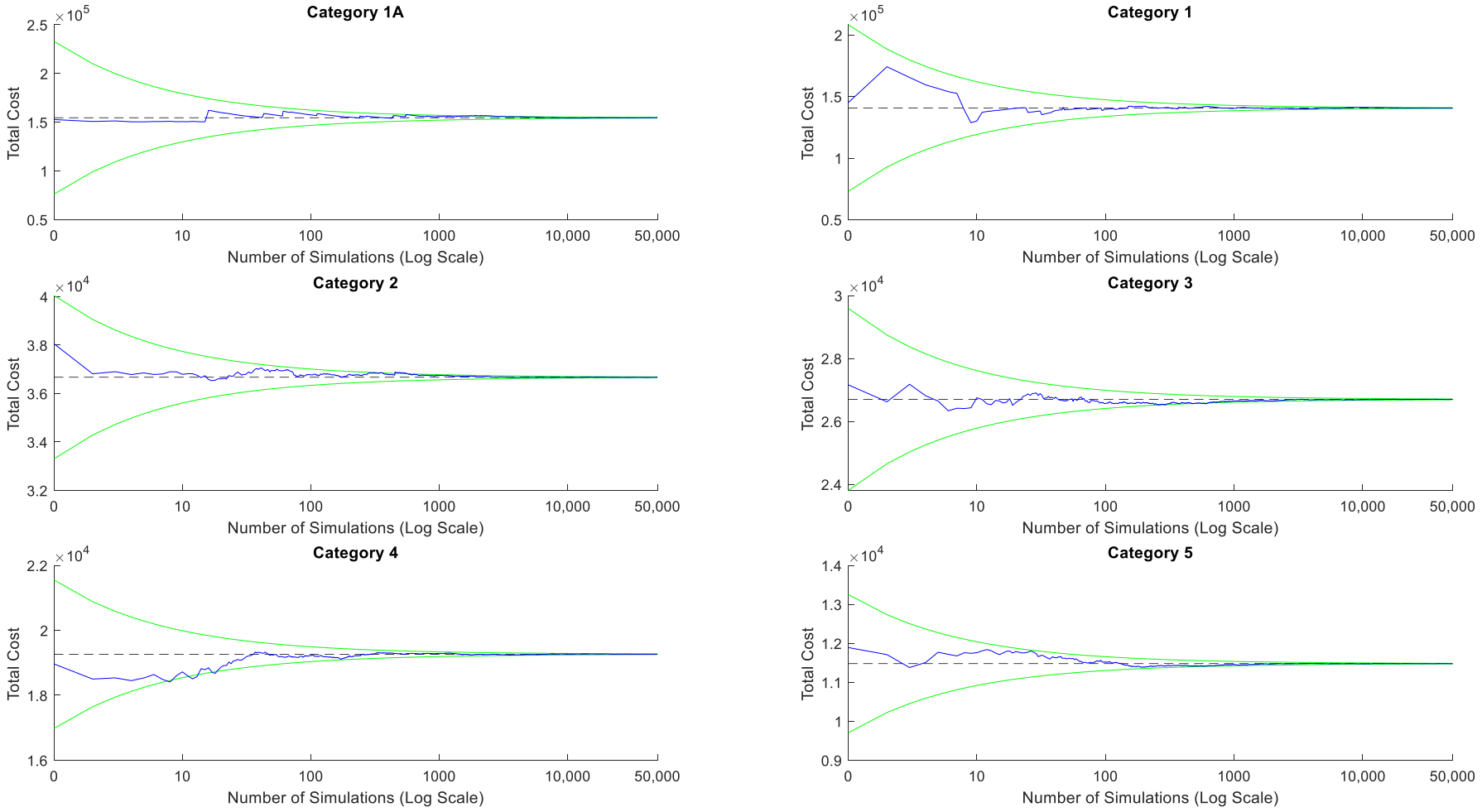


FIGURE 6.33: STEEL SLEEPER TOTAL COST CONVERGENCE
KEY: ●95% CONVERGENCE BOUNDS ●RUNNING AVERAGE ●CONVERGED VALUE

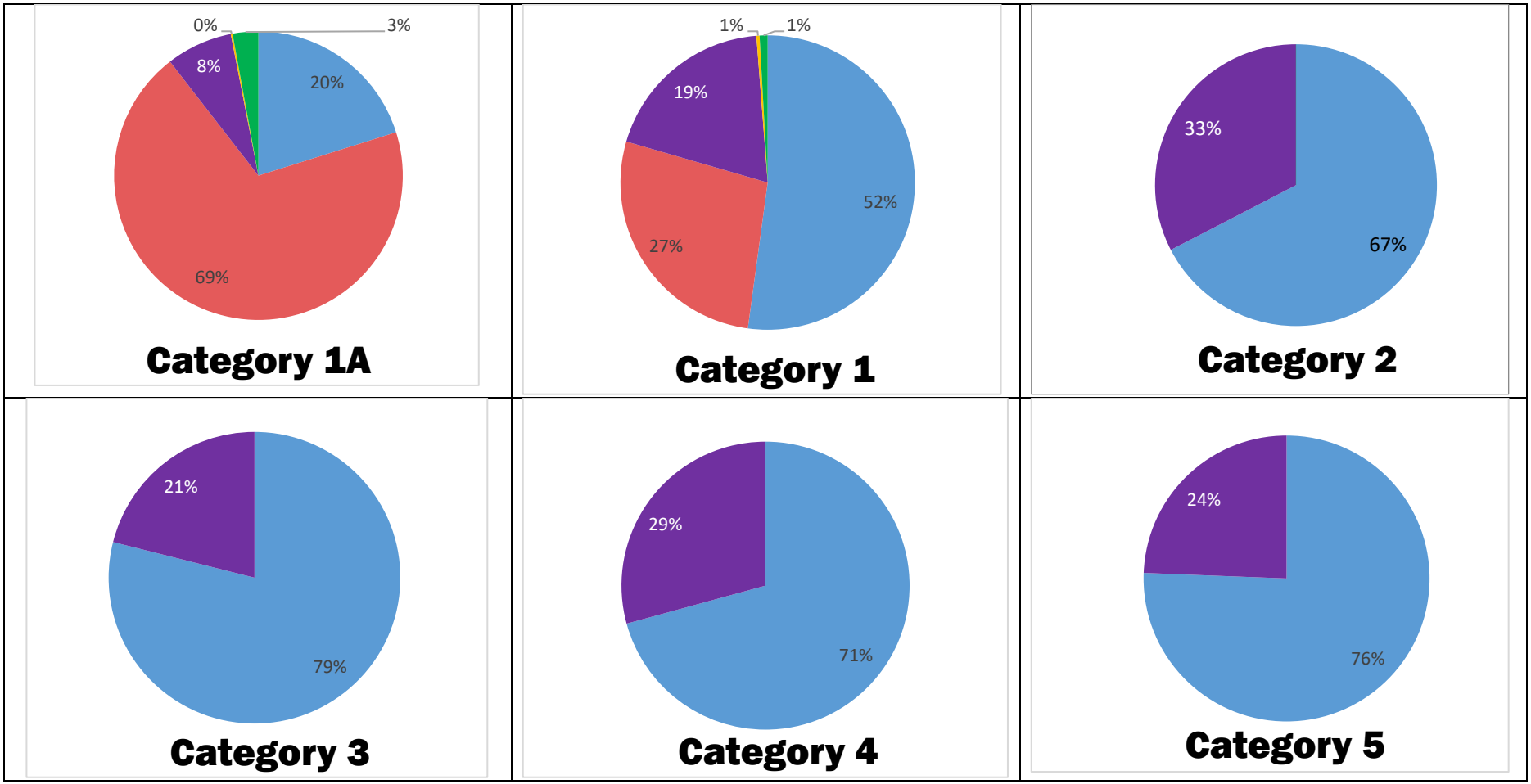


FIGURE 6.34: STEEL SLEEPER COST BREAKDOWN

KEY: ●MAINTENANCE ●TSR ●RENEWAL ●SAFETY RISK ●INSPECTION

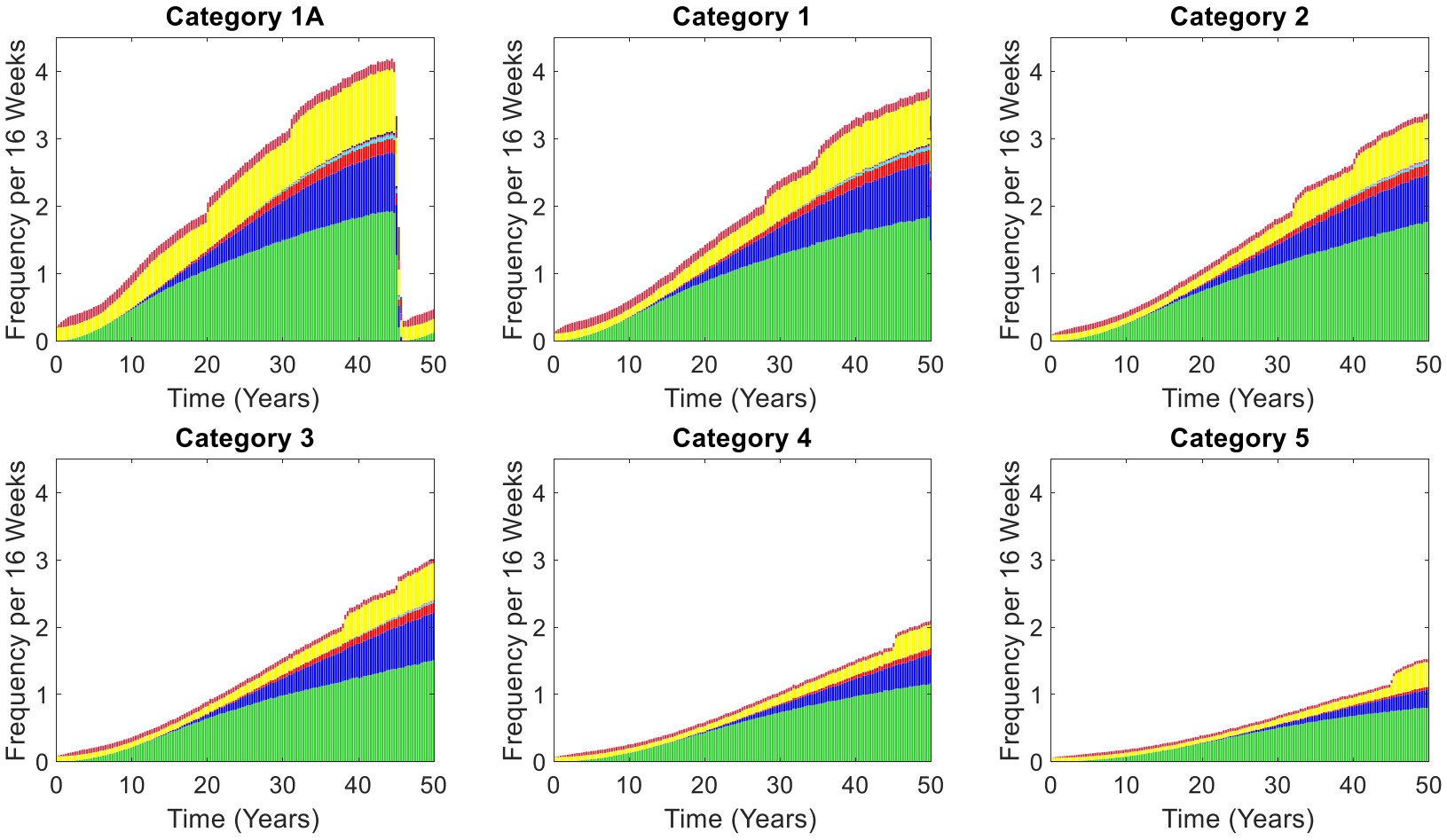


FIGURE 6.35: STEEL SLEEPER MAINTENANCE PER 16 WEEKS

PADS ● CLIPS ● MAJOR SLEEPER REPLACEMENT ● 6X ● 5X ● 4X ● 3X ● 2X ● SINGLE SLEEPER REPLACEMENT ● RENEWAL

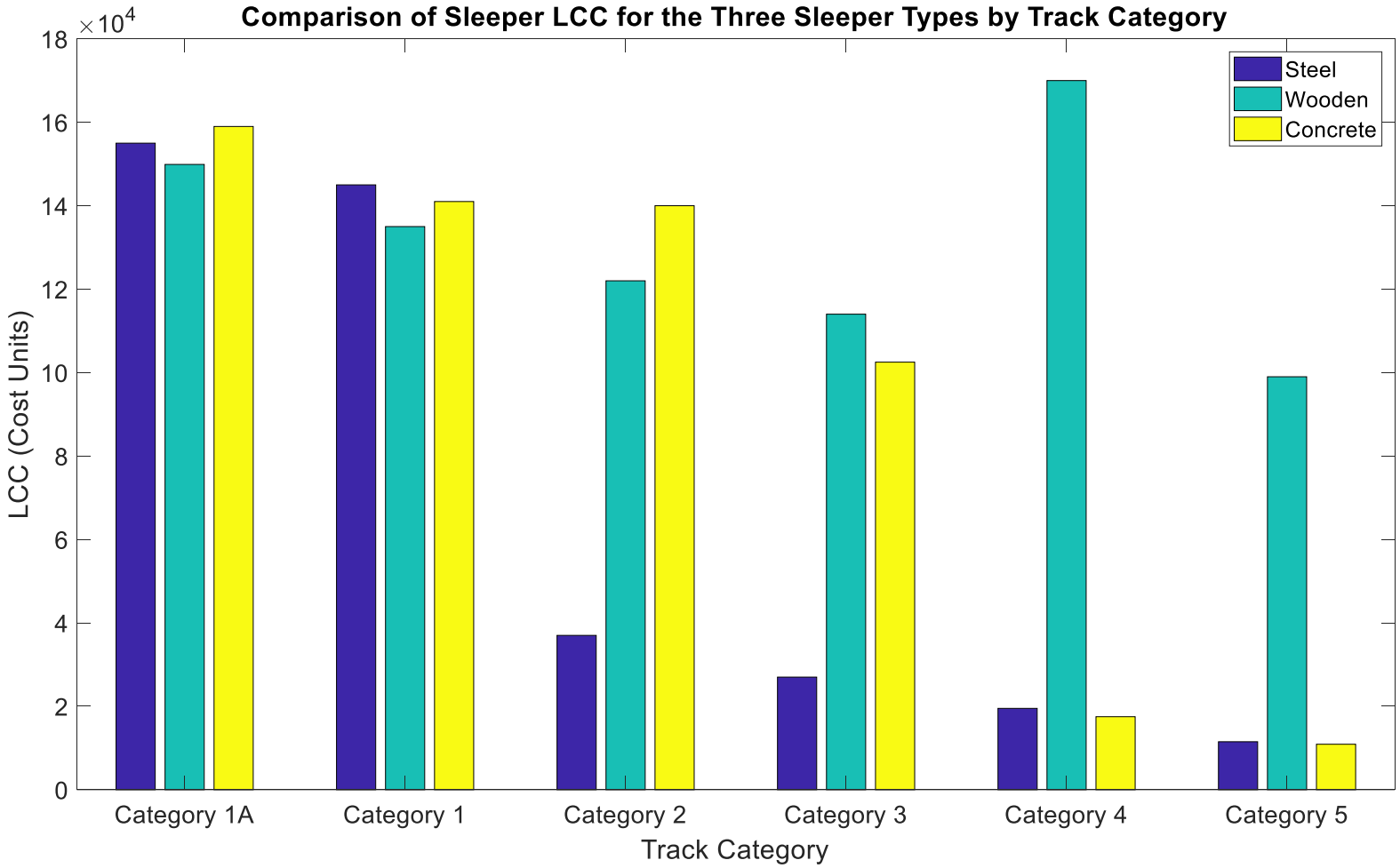


FIGURE 6.36: COMPARISON OF THE LCC COST FOR THE THREE DIFFERENT SLEEPER TYPES (50 YEARS)

6.3.3 Tunnel Petri Net Model

The tunnel model's main purpose is to allow the effect of a tunnel on the assets within the tunnel to be considered. The tunnel model does also contain a simple model to account for the cost associated with the upkeep of the tunnel, however producing a detailed Petri net for tunnel deterioration and maintenance is beyond the scope of this study. It is important to note that the deterioration of tunnels is slow, they require maintenance far less regularly than the other assets discussed.

There are three main differences between track sections in a tunnel and track sections not in a tunnel:

(i) Assets in tunnels deteriorate more quickly due to the damp conditions and because maintenance tasks may not have been performed effectively (see point (ii)).
(ii) Maintenance tasks take longer and cannot be completed to such a high standard due to the damp, dark and cramped conditions within the tunnel. Additionally when working in tunnels lighting and air flow have to be closely monitored.
(iii) There is some additional cost associated with the up keep of the tunnel.

The tunnel Petri net model is shown in Figure 6.37. Two types of maintenance are considered '*Minor*' and '*Major*'. The difference between '*Major*' and '*Minor*' work is that '*Major*' work will return the condition to new (P_0^{TN}) as opposed to repaired (P_1^{TN}) and in the system model for tunnels that are longer than a single section '*Major*' work will return all sections of the tunnel to new (P_0^{TN}). Opportunistic work is also considered in the tunnel model; this allows work to be performed earlier if other work in the section is being performed (modelled by transitions T_5^{TN} and T_7^{TN}). These transitions are not used in the single model but are used in the system model.

As discussed tunnels are inspected visually and by detailed examination. At this stage only visual inspections are considered. Inspection of tunnels happens far less frequently than the track and sleepers, according to standards a visual inspection of structures should be carried out every 12 months [156]. The time interval between the inspections of tunnels is not assumed to be fixed; the time between inspections (T_{17}^{TN}) is sampled from a Normal distribution with μ=365 and σ=10.

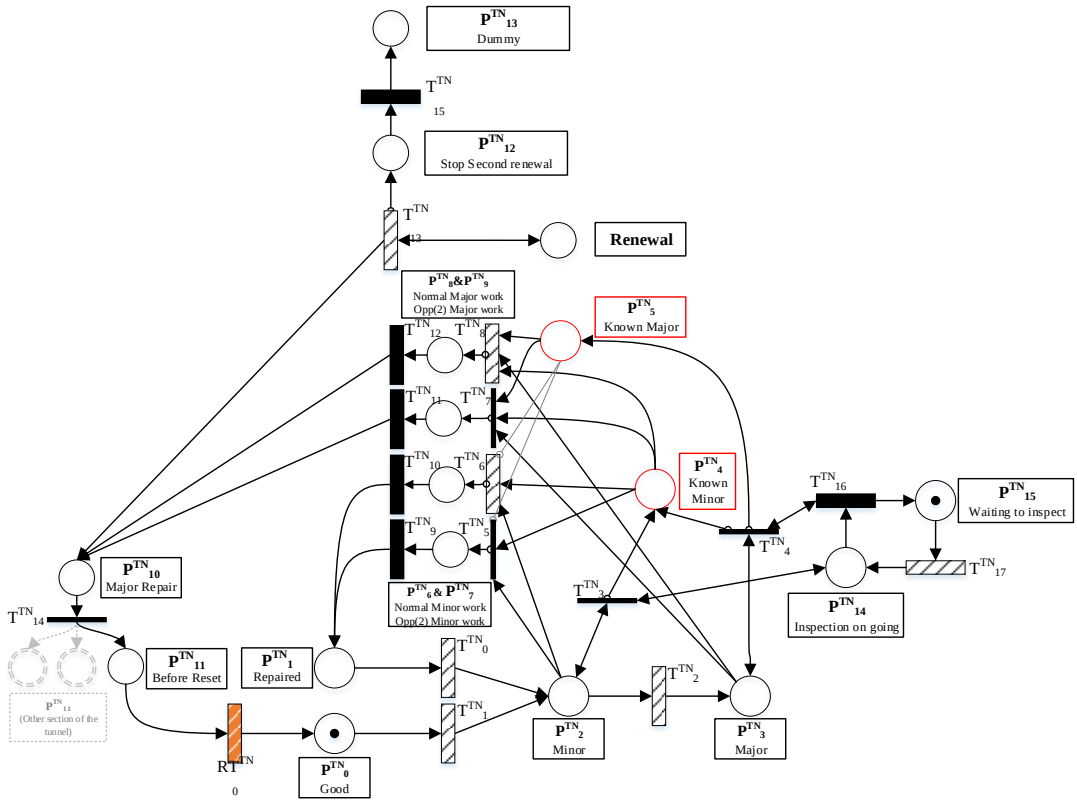


FIGURE 6.37: TUNNEL PETRI NET MODEL

6.3.4 Switches and Crossings Petri Net Model

S&C units are one of the most critical parts of the railway network. This section will present a Petri net to simulate a single S&C unit. The Petri net model for a Size D switch is shown in Figure 6.38. It is made up of eight submodules for the eight switch and crossing components that will be considered:

(i) Stock rail
(ii) Switch rail
(iii) Sleeper/bearer
(iv) Slide chair
(v) Crossing
(vi) Check and wing rail
(vii) Stretcher bar
(viii) Ballast

The components were modelled based on the data analysis in Chapter 5. There were found to be three methodologies required to model S&C components effectively:

(i) Poisson Process (based on the Exponential distribution).
(ii) NHPP (based on the Power Law Process).
(iii) Weibull analysis (based on the Weibull distribution).

The distributions used for the transitions in the Size D S&C model in Figure 6.38 are those determined in Chapter 5 (see Table 5.23), the values were adjusted for the different sized

switches. Conditional transitions were used to model the NHPP, these transitions are shown with a chequered white fill in the Petri net diagrams.

The S&C Petri net model contains inspection loops for visual inspection, NMT inspection and ultrasonic inspection, as the different components within the S&C unit are inspected in different ways. It is assumed the ballast is inspected by the NMT, the rails are inspected ultrasonically and the sleepers and slide chairs are inspected visually. It is assumed that extreme deterioration of the stock rail, switch rail, crossing and check rail can lead to a service affecting failure (P_9^{SC} being marked) and a TSR being imposed.

As with all the other models the S&C Petri net model was simulated 50,000 times for a 50 year period. Table 6.19 summarises the number of faults over the 50 year period. It can be seen that the crossing has the highest density of failures, with an average of 0.2 failures per year, whereas the check and wing rail have the least. This can be explained by the crossing being subject to large forces as the train wheels pass over the crossing whereas the check and wing rails just guide the wheels and do not take the full load of the train.

Table 6.20 summarises the total number of repairs to each of the components. It can be seen that the slide chair has the highest number of repairs. This is due to the high density of slide chairs within an S&C unit. It is assumed that there are two slide chairs per bearer, the number of bearers and slide chairs is dependent on the switch size (see Appendix D-1), for size D there are assumed to be 45 bearers and 90 slide chairs.

Table 6.21 summarises the costs that are used in this research. Spon's [49] provided costings for S&C unit renewals. The costs for maintenance were estimated based on the plain line costs. The larger switch designs (G&H) were assumed to cost more than the smaller designs (A&B) due to them being physically larger, meaning there is more to repair.

Figure 6.39 shows the convergence of the LCC based on 50,000 simulations for S&C sizes A→G and a fixed diamond crossing. It can be seen that sizes A→E have similar cost, size G costs more due to requiring three renewals in the 50 year period rather than two as for all the other types. The fixed diamond crossing costs more than sizes A→E due to having four crossings. Figure 6.40 shows how the overall cost is broken down for a size D turnout. It can be seen, as with the other asset classes, the highest cost is due to renewal (44%). TSRs also form a large part of the cost at 36%. Overall maintenance makes up about 11% with inspections making up the remaining 9%.

Lastly Figure 6.40 shows the number of maintenance interventions performed every 16 weeks for the eight different switch types. The switch is assumed to start in new condition. For the turnouts there is initially a high number of stock and switch rail faults. This represents the early life phase found in the data, caused by poor maintenance and component burn in. Within two years these early life failures die away and the frequency of switch and stock rail repairs becomes small. There is a constant increase in the amount of maintenance up until the renewal. As the fixed diamond crossing does not contain any slide chairs or

switch rails there is no slide chair maintenance or switch rail maintenance, additionally there are four crossing so there is considerably more crossing maintenance.

Component	Per 50 Years				Per Year
	Mean	SD	Min	Max	Mean
Stock Rail	5.51	2.23	0	18	0.11
Switch Rail	4.65	2.12	0	15	0.093
Crossing	9.84	3.12	1	24	0.20
Check & Wing Rail	$2.2_{x10^{-3}}$	0.05	0	1	$4.4_{x10^{-5}}$

TABLE 6.19: S&C FAILURES

Component	Per 50 Years				Per Year
	Mean	SD	Min	Max	Mean
Stock Rail	5.01	2.07	0	15	0.10
Switch Rail	2.98	1.64	0	11	0.06
Sleeper	3.34	1.83	0	13	0.07
Slide Chair	53.89	7.64	13	90	1.18
Crossing	2.83	1.68	0	11	0.06
Check & Wing Rail	0.44	0.66	0	5	$8.8_{x10^{-3}}$
Stretcher Bar	5.40	2.34	0	18	0.11
Ballast	4.91	2.00	0	16	0.01

TABLE 6.20: S&C REPAIRS

	Task	Unit	Data Source	Switch Size							
				A	B	C	D	E	F	G	[17]F-D
1	Stock rail repair	Per intervention	Estimated	200	200	200	250	250	300	300	200
2	Switch rail repair	Per intervention	Estimated	200	200	200	250	250	300	300	200
3	Bearer/sleeper (timber)	Per intervention	Estimated	150	150	150	180	180	210	210	180
4	Slide chair	Per intervention	Estimated	50	50	50	50	50	50	50	50
5	Crossing repair	Per intervention	Estimated	300	300	400	500	500	600	600	400
6	Check and wing rail repairs	Per intervention	Estimated	100	100	100	200	200	300	300	200
7	Stretcher bar renewal	Per bar	Estimated	2000	2000	2000	2000	2000	2000	2000	2000
8	Ballast	Per intervention	Estimated	800	825	850	875	900	925	950	875
9	Complete renewal	Per unit	Spon's	30,000	40,000	50,000	60,000	70,000	80,000	90,000	50,000
10	Visual inspection	Each	Estimated	8	8	8	8	8	8	8	8
11	Geometry inspection (NMT)	Each	Estimated	8	8	8	8	8	8	8	8
12	Ultrasonic inspection	Each	Estimated	8	8	8	8	8	8	8	8
13	Restriction[18]	Per day	Estimated	1000	1000	1000	1000	1000	1000	1000	1000

TABLE 6.21: S&C COST BREAKDOWN FOR VARIOUS SWITCH SIZES

[17] Fixed diamond crossing.
[18] The cost due to restriction would likely be dependent on the track category as opposed to the switch size.

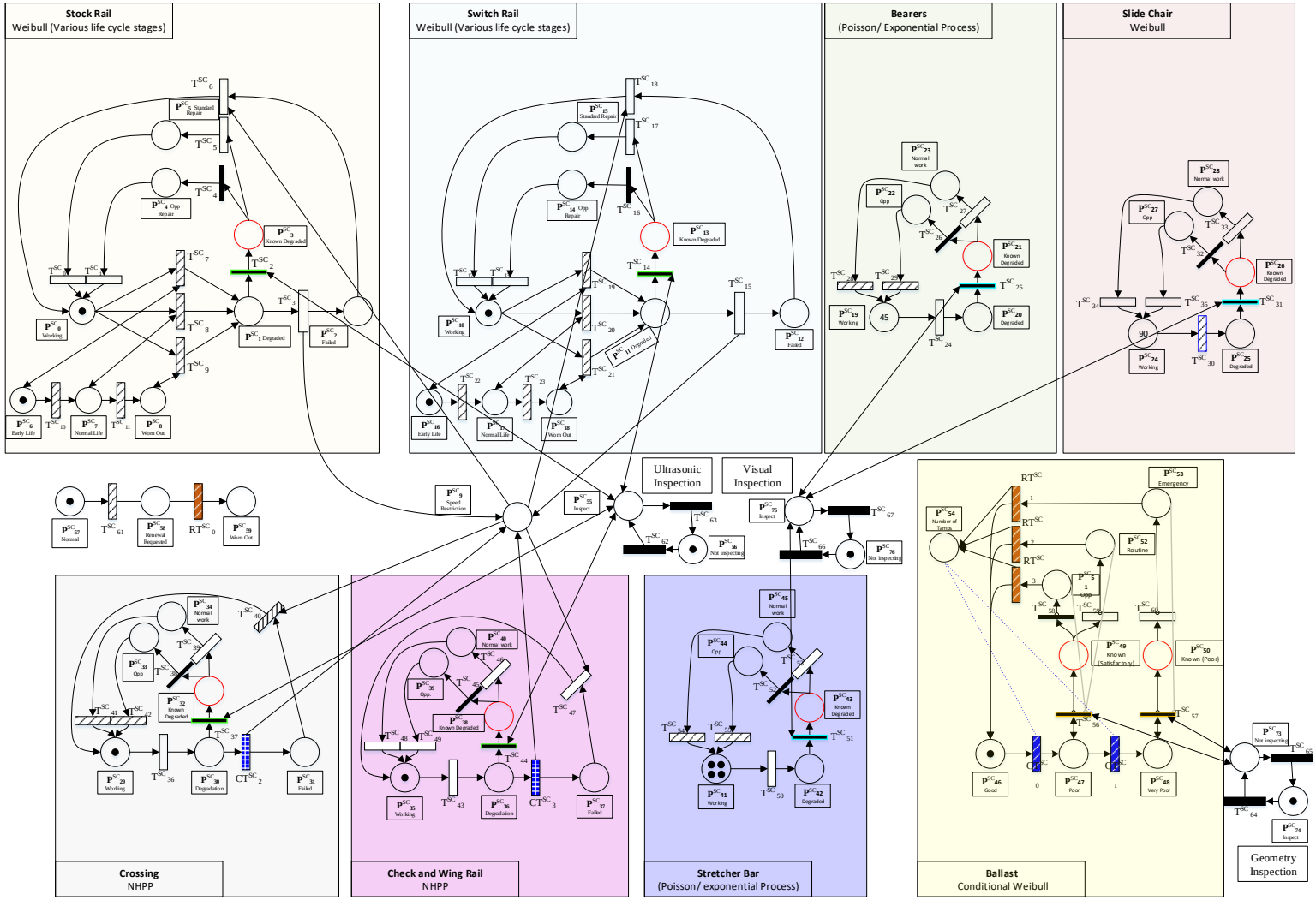


FIGURE 6.38: S&C PETRI NET MODEL (SIZE D)

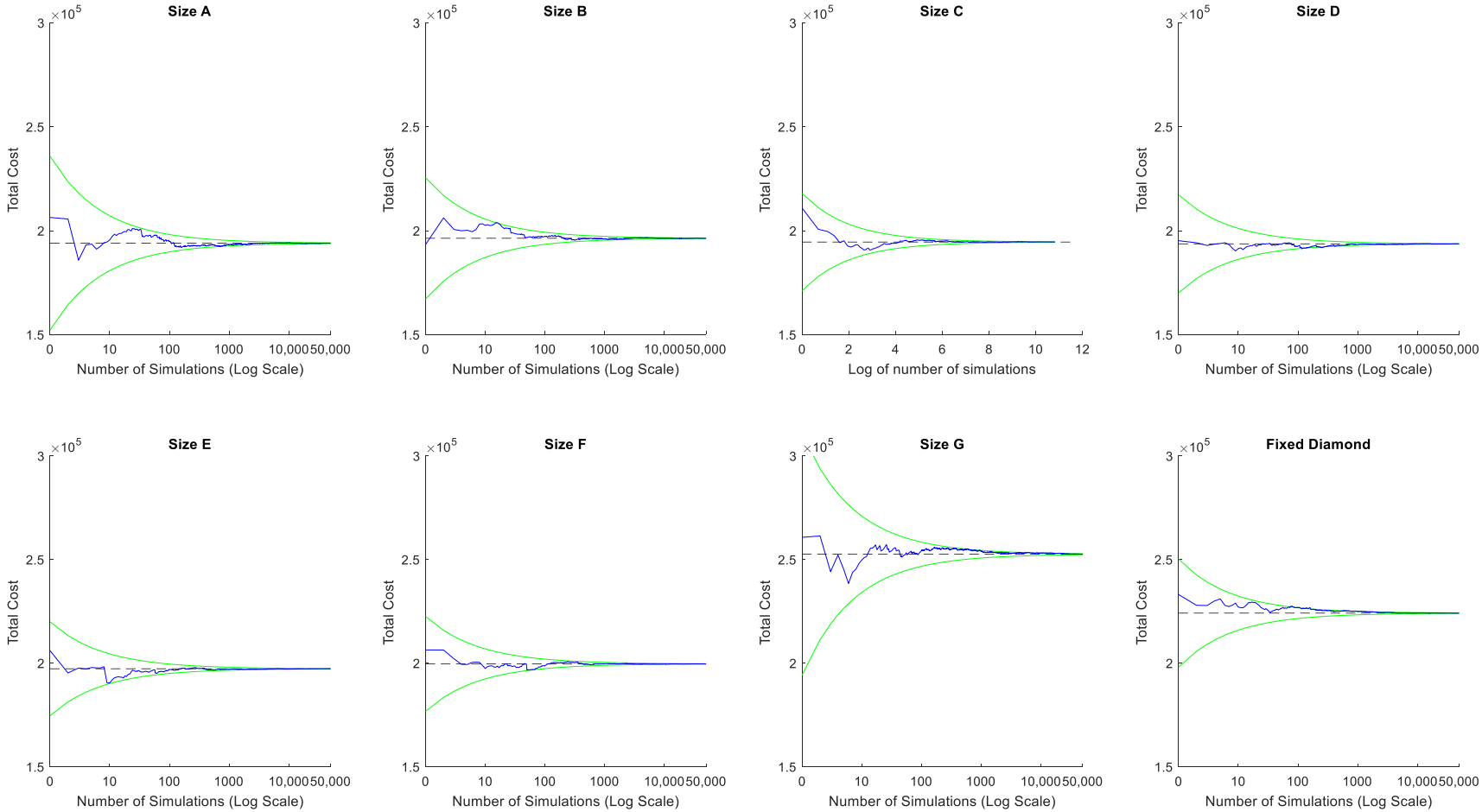


FIGURE 6.39: S&C CONVERGENCE (LOG SCALE)
KEY: ●95% CONVERGENCE BOUNDS ●RUNNING AVERAGE ●CONVERGED VALUE

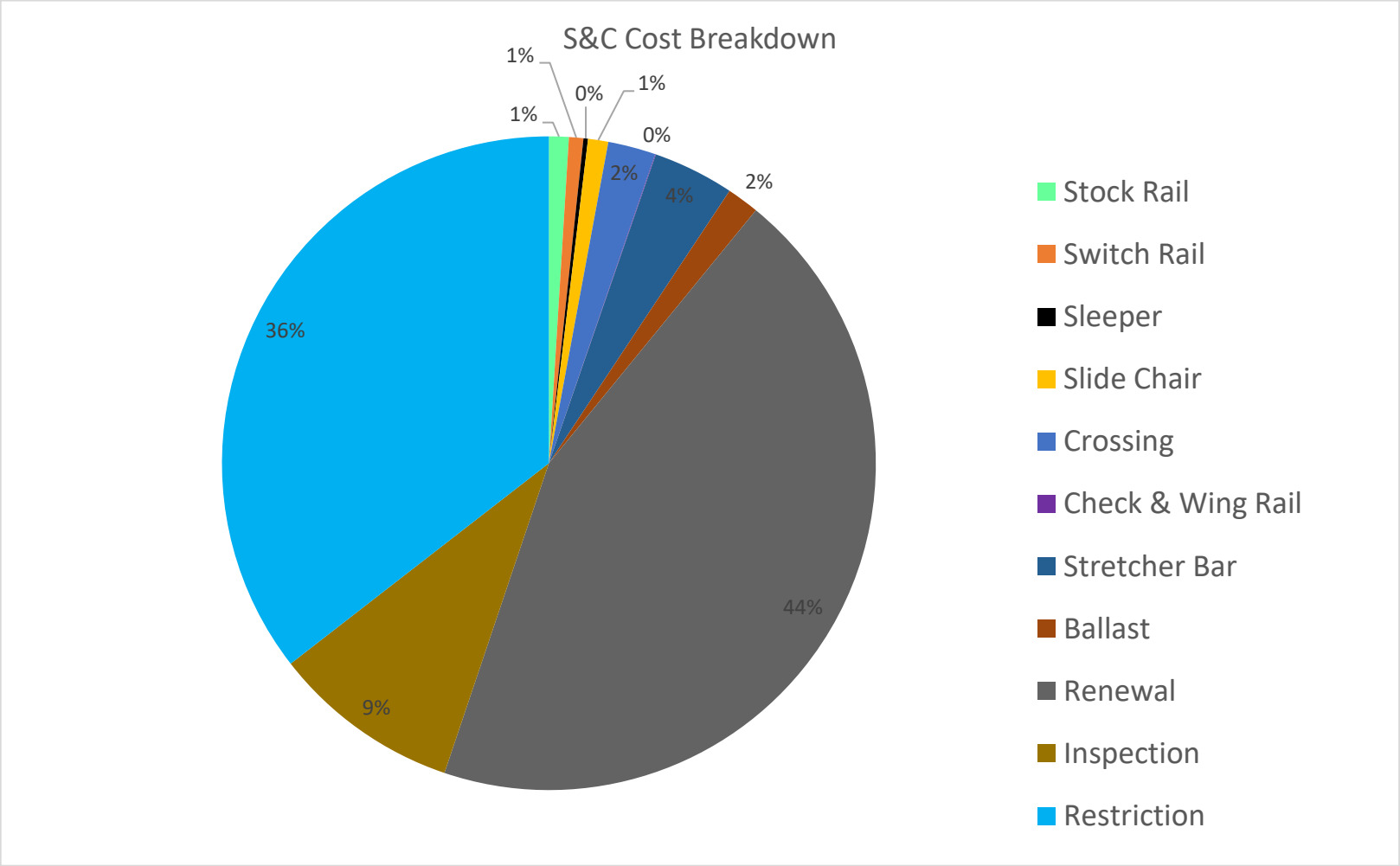


FIGURE 6.40: S&C COST BREAKDOWN (50 YEARS, SIZE D)

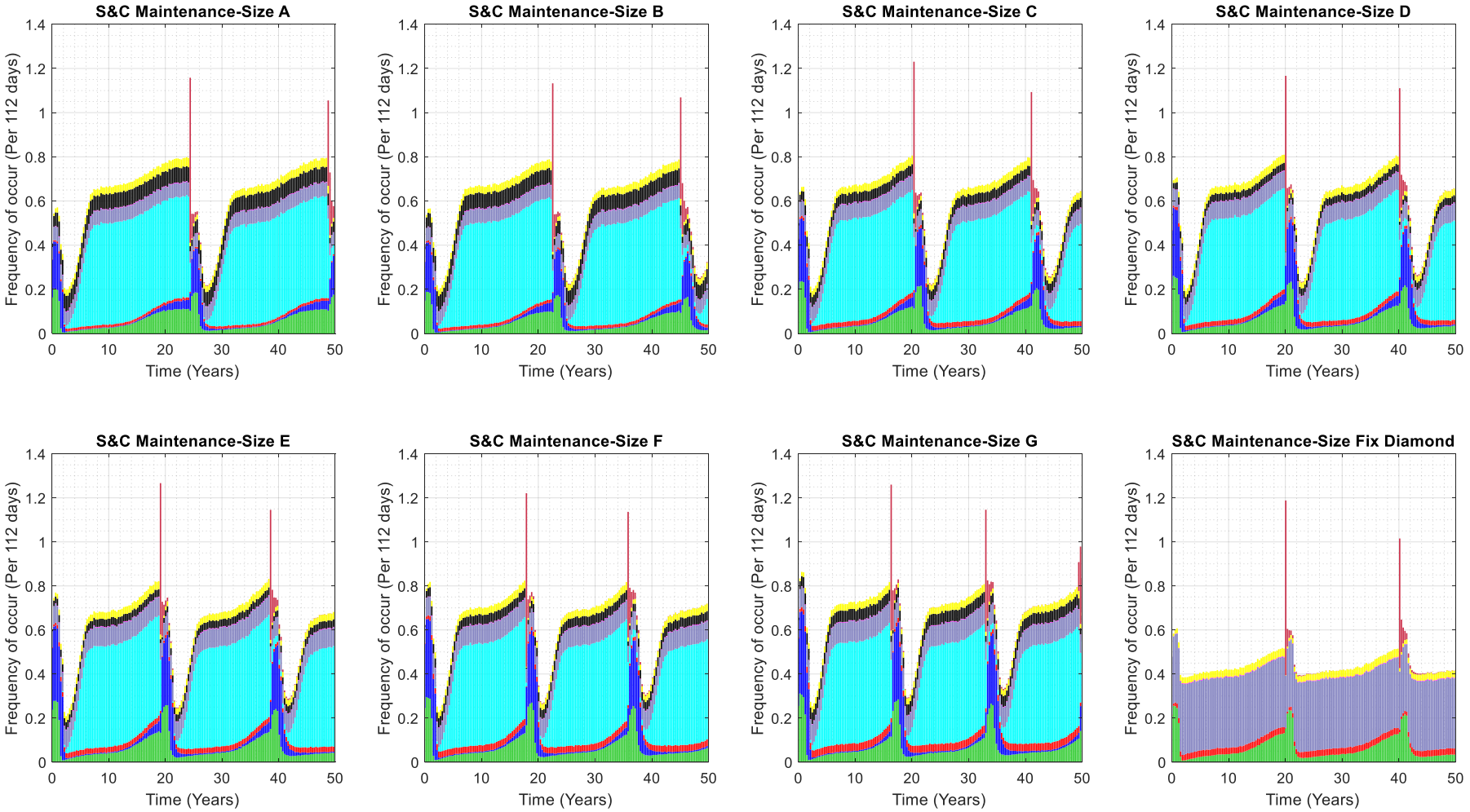


FIGURE 6.41: S&C MAINTENANCE PER 16 WEEK PERIOD (FOR 50 YEARS) BY S&C SIZE

KEY: ●STOCK RAIL ●SWITCH RAIL ●BEARER ●SLIDE CHAIR ●CROSSING ●CHECK & WING RAIL ●STRETCHER BAR ●BALLAST ●RENEWAL

6.3.5 Signalling System Petri Net Model

The final asset considered is the signalling system. This asset is included as it is somewhat different to the previous assets described. The whole signalling system is modelled using just one model consisting of five subsystems:

(i) Axle counter
(ii) AWS
(iii) Track circuits
(iv) Cable
(v) Signal head/lamp

These are some of the main subsystems within the signalling system. The main purpose of the signalling model is to demonstrate the capability of the whole system model to consider a wide range of assets. In the future, when more data is available a more sophisticated signalling model should be used.

The signal model shown in Figure 6.42 is designed to model the signalling system for Bletchley Delivery Unit. The model only simulates the number of failures, the distributions used for the times to failure were those found in Chapter 5 (Table 5.24). As maintenance interventions happen so frequently (see Figure 5.37), they would be occurring at a rate of multiple interventions a day. It was impractical to model this and provided little benefit in terms of considering opportunistic work. For this reason, at this stage the number of repairs (marking of places $P_2^{SG}, P_6^{SG}, P_{10}^{SG}, P_{14}^{SG}$ and P_{18}^{SG}) were just sampled from Normal distributions (see Table 6.22).

Table 6.23 shows the unit costs that were used for the signalling system. It is assumed that the signalling system was inspected every seven days (the inspection costs were calculated directly and not simulated in the Petri net). The disruption caused by a signalling fault is assumed to cause more delays than other assets, as a signalling fault is likely to disrupt the entire route.

As with the other asset modules, the signalling Petri net was simulated 50,000 times for a 50 year period. Table 6.24 summarises the number of faults for the five components considered, as expected the axle counter has the highest number of failures. The number of maintenance interventions is summarised in Table 6.25, these values were sampled directly as explained and not simulated within the Petri net.

Figure 6.43 shows the convergence of the overall cost. It can be seen that the cost converges to around 180 million, this value is several orders of magnitude higher than the other asset models proposed in this chapter. However, this model is for the entire Delivery Unit (100 miles) whereas the other models are just for a small section of track or a single asset. Figure 6.44 shows how the overall cost was broken down, it can be seen that axle counters form the majority of the cost. This is due to the high replacement cost of axle counters. It can be seen that the inspection cost is very small in comparison to the overall cost of the signalling system for Bletchley Delivery Unit.

Component	Distribution for Number of Maintenance Interventions
Axle Counter	Normal(3600, 100)
AWS	Normal(2400, 100)
Track Circuit	Normal(4800, 110)
Cable	Normal(100, 20)
Signal head/lamp	Normal(400, 50)

TABLE 6.22: DISTRIBUTION USED TO DETERMINE THE MARKING OF PLACES P_2^{SG}, P_6^{SG}, P_{10}^{SG}, P_{14}^{SG} AND P_{18}^{SG} (TOTAL NUMBER OF SIGNALLING MAINTENANCE INTERVENTIONS IN BLETCHLEY DELIVERY UNIT IN 50 YEARS)

	Task	Unit	Source	Unit Cost (C)
1	Axle counter	Unit	Spon's	24,000
2	AWS (permanent)	Unit	Spon's	1414
3	Track circuit	Unit	Estimated	1610
4	Cable	metre	Spon's	43
5	Lamp	Unit	Spon's	1950
6	Inspection	Per day	Estimated	8
7	Restriction	Each	Estimated	5000

TABLE 6.23: SIGNALLING SYSTEM COSTS

Component	Per 50 Years				Per Year[19]
	Mean	SD	Min	Max	Mean
Axle Counter	2888.59	53.71	2669	3113	57.77
AWS	55.53	7.42	25	94	1.11
Track Circuit	702.89	26.56	592	837	14.06
Cable	55.50	7.38	27	89	1.11
Signal Head	592.07	24.26	492	702	11.84

TABLE 6.24: SIGNAL MODULE FAILURE RESULTS

Component	Per 50 Years				Per Year[20]
	Mean	SD	Min	Max	Mean
Axle Counter	182,332	5041	166,674	197,862	3646.6
AWS	121,545	5057	105,918	137,106	2430.9
Track Circuit	243,027	5548	225,861	260,188	4860.5
Cable	20,239	2516	12,455	28,049	404.8
Signal Head	5064	1004	1923	8202	101.3

TABLE 6.25: SIGNAL MODULE REPAIR RESULTS

[19] For comparison to Figure 5.28
[20] For comparison to Figure 5.27

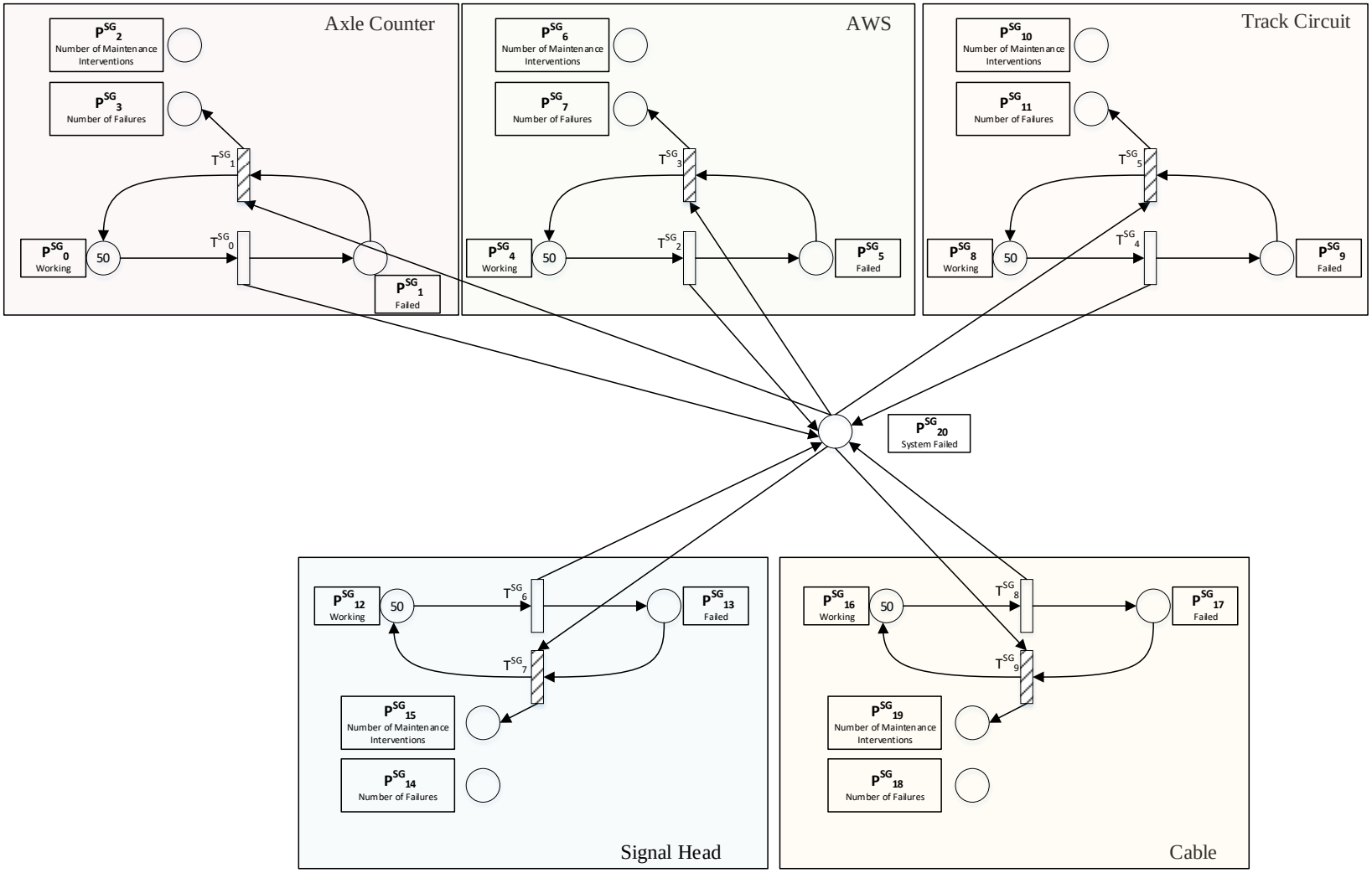


FIGURE 6.42: PETRI NET MODEL FOR THE SIGNALLING SYSTEM

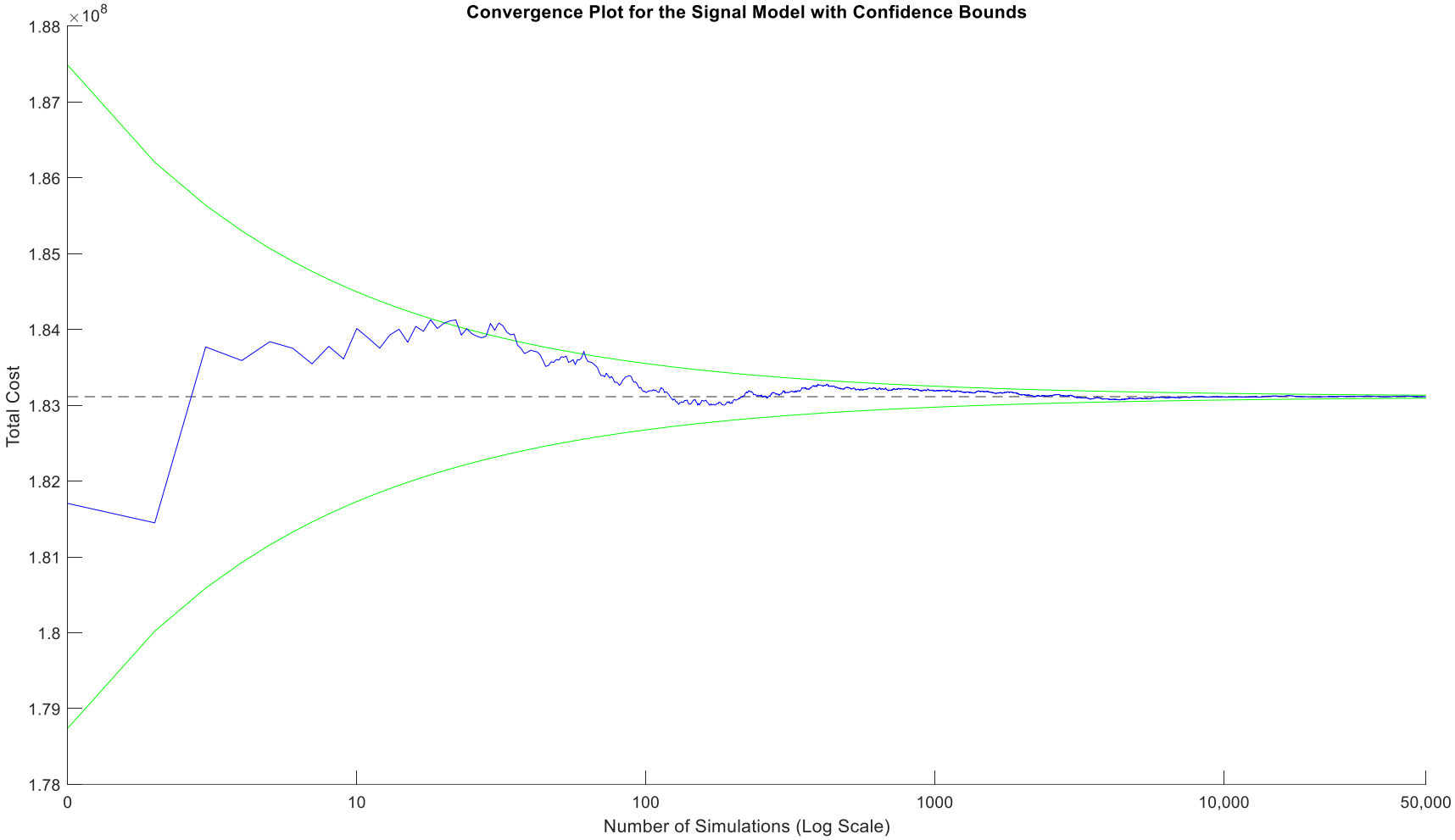


FIGURE 6.43: CONVERGENCE OF THE OVERALL COST OF THE SIGNALLING MODEL
KEY: ●95% CONVERGENCE BOUNDS ●RUNNING AVERAGE ●CONVERGED VALUE

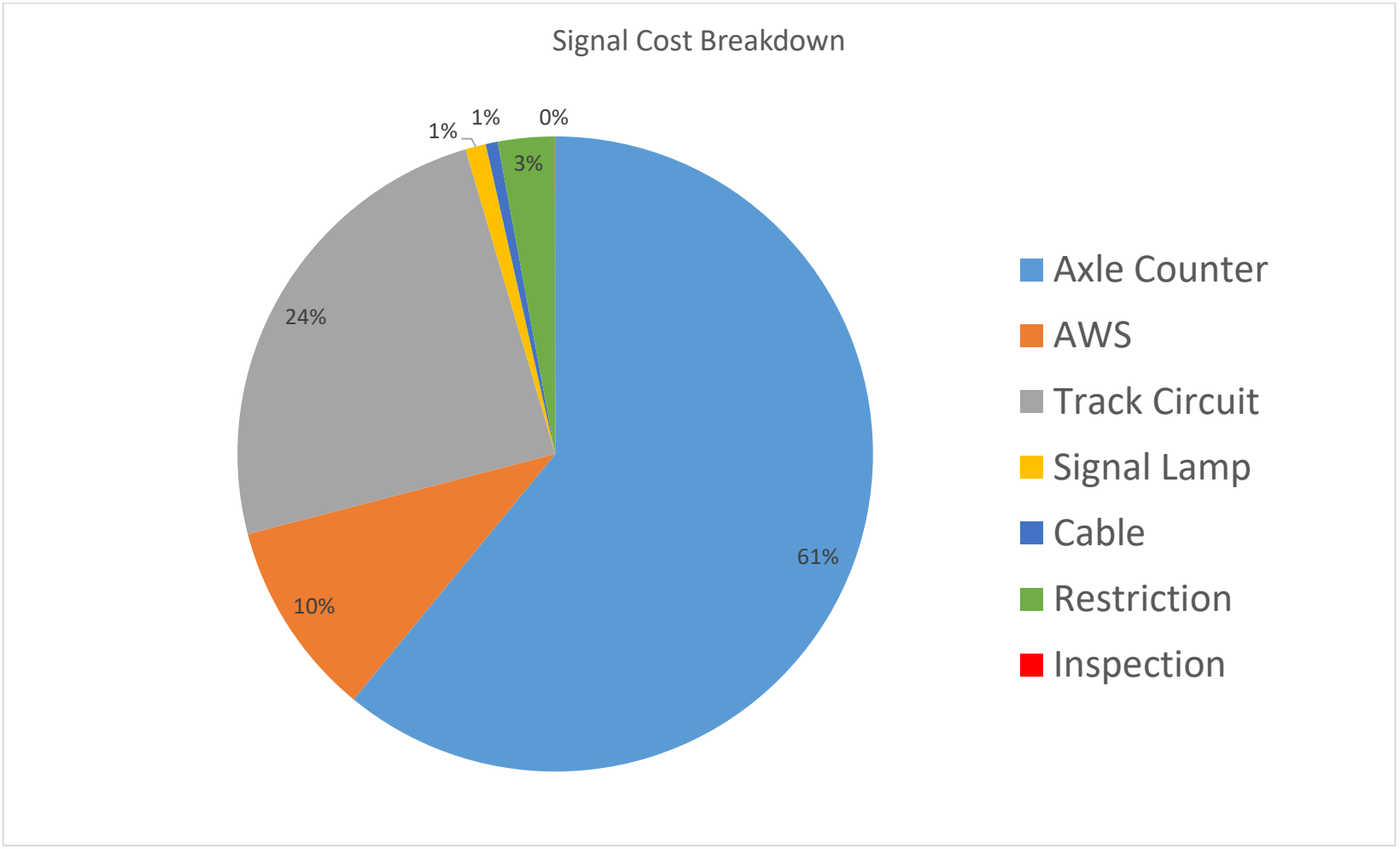


FIGURE 6.44: SIGNALLING SYSTEM COST BREAKDOWN

6.4 Summary and Conclusions

This chapter used the distributions and conclusions found in Chapter 5 to create asset Petri net models for five asset types:

(i) Track (ballast and rails)
(ii) Sleepers (concrete, steel and timber/wooden)
(iii) Tunnels
(iv) S&C (Size A→G and fixed diamond crossing)
(v) Signalling

For track, sleepers and tunnels, Petri net models were proposed for an eighth mile length of track. The Petri nets were then simulated using bespoke C++ software to determine key statistics for these assets. Petri nets were also created to model a range of S&C units. The S&C unit Petri nets contained subnets for the switch rail, stock rail, bearers, slide chairs, crossing, check and wing rails, stretcher bars and ballast. The final Petri net model proposed was for the signalling system. The signalling asset model was slightly different in that it modelled the signalling system for the whole railway corridor in one model, and not at eighth mile section level.

For each asset the number of failures, repairs, renewals, inspections and days when a speed restriction was imposed is predicted, the following conclusions were drawn from the results of the asset models:

Track section

- Category 1A is the most expensive, costing around four times as much as Category 5.
- For the highest track categories (1A, 1 and 2) the LCC over 50 years was dominated by renewal.
- For all categories the inspection cost was higher than the maintenance cost.

Sleepers

- For Categories 1A and 1 lines the analysis suggested that hardwood timber sleepers could be the cheapest, however the cost for all three types was similar for these categories.
- For lower track categories the models suggested that timber sleepers had a significantly higher LCC than concrete or steel.

S&C

- After renewal, the highest proportion of cost during the S&C lifecycle was due to speed restrictions.
- The models predicted that the stretcher bars have the highest LCC of all the components within a S&C unit.

Signalling system

- Axle counters form the highest proportion of the overall cost of the signalling system.

- Due to the very high number of repairs, the number of repairs was sampled from a distribution rather than being simulated using a Petri net.

Chapter 7 will explore how the asset models can be converted into *modules* and be linked together to form a whole system model for a railway corridor.

7 System Framework

7.1 Introduction

The aim of this thesis is to create a whole system framework, which makes better predictions about the future behaviour of railway assets, which can be used by railway asset managers to help make more informed asset management decisions. Chapter 6 introduced Petri net models for the individual assets. This will be extended to a system framework which combines the asset Petri net models to form a system model.

Initially a hierarchical structure is developed that will be used to link the asset models together. A three level hierarchy is proposed, where the asset models which feed into the system hierarchy to make up the system model, are referred to as *modules.* The individual asset Petri net models proposed in Chapter 6 are converted into Petri net modules for use within the whole system framework. The whole system framework is applied to the Bletchley Delivery Unit, a busy railway corridor in England, UK. A discussion on how maintenance such as tamping can be modelled more effectively by using a range of scheduling algorithms is given. The chapter concludes by comparing the cost outputs of the model for Bletchley Delivery Unit to the CP5 expenditure and also compares a ballast profile suggested by the model to an actual ballast profile recorded by the NMT.

7.2 System Hierarchy

To be able to create a whole system model, a framework capable of combining all of the asset models developed is required. The framework would need to be as flexible as possible, so that a range of different asset *modules* could be considered. The framework would also need to be flexible enough to allow additional asset *modules* to be considered in the future.

To create the system model the HPN extension was employed. Jensen and Kristensen [82] proposed the HPN, as a means of showing a large and complete Petri net at the level of abstraction required for human understanding. As discussed in Chapter 4, HPNs have been employed extensively to allow larger Petri nets to be drawn in an understandable way. The hierarchy proposed to create the whole system framework is shown in Figure 7.1. The HPN used is of the format described in section 3.3.3.1, with the levels arranged in a '*master*'/'*slave*' relationship, with a '*port*'/'*socket*' interface used to pass information between *modules*.

The master module, introduced in section 7.3.1, forms the top level of the hierarchy and is master to all other modules. The signal module is considered on the same level as the master module as it affects the whole railway corridor. Nonetheless the signal module is still slave to the master module. The second level of the hierarchy is formed of track section (220 yards) modules. The framework is flexible enough to allow any number of track sections between 10 and 849 to be included. The framework was only limited to 849 track sections as input data was only collected for 849 track sections (Appendix J-1.1). The track section modules are slave to the master module. Each track section module is also linked to the

track section modules adjacent to it, to allow the condition of neighbouring sections to be considered when scheduling maintenance. The number of sections considered when scheduling maintenance depends on the strategy employed. The final level of the hierarchy considers the remaining assets, which are located within the track section:

(i) Sleepers (Concrete, steel or wooden)
(ii) S&C units (Size A→G and fixed diamond crossing)
(iii) Tunnels

Each track section is master to one sleeper module. The framework is adaptable and allows the track section to be modelled with concrete, steel or wooden sleepers. If the section is in a tunnel, a tunnel module is added to the framework. The tunnel module is slave to **one** track section module. If the tunnel is longer than one section then each section requires its own tunnel module, however the tunnel modules are linked together, allowing maintenance to affect the entire tunnel. A track section can also contain S&C units. Each S&C unit is modelled by its own module (allowing the different switch sizes to be considered). A single track section can contain multiple S&C units, in this study the maximum considered is two. The asset modules are all slave to the track section module they are contained within. The asset modules are also linked to the master module to enable budget and resource availability to be considered when scheduling maintenance.

7.2.1 System Dependencies

One of the main benefits of having a system model is that it allows the dependencies between asset models to be considered. Although the dependencies are all interlinked they can be grouped into two main types:

(i) Maintenance/inspection dependencies
When maintenance is planned it is likely the condition of multiple assets will be considered and a collection of assets will be repaired at the same time. Similarly when inspections take place a group of assets are likely to be inspected together.
(ii) Condition profile/deterioration dependencies
The condition of an asset can potentially affect the deterioration of the assets around it. For example poor ballast is likely to lead to poor sleeper support and faster deterioration of the sleeper.

Of the two, modelling the dependencies between asset condition is the more difficult. Modelling how the condition of one asset may affect the deterioration of others is very challenging and there is still debate among engineers about this. Many of the relationships can be two way, and it can be difficult to distinguish between causation and correlation. To demonstrate the capability of the model a few basic dependencies between asset conditions are considered, these are listed in Table 7.1, the implementation in the Petri net models is explained in the following sections. As discussed the signal module is largely a standalone module, the only dependency to other modules is through budget.

Modelling maintenance dependencies is somewhat easier, as maintenance planning is based directly on the condition of assets. Maintenance policy is also well documented in standards

and hence the model can replicate this. In the model maintenance dependencies are considered in detail, with both opportunistic and group work considered between all asset classes, this is discussed in detail in section 7.3.2.2.

Effect on	**Asset Group**				
	Track	Sleepers	S&C	Tunnels	Signalling
Track		Track section renewal possible early if high number of sleepers degraded.	No condition interaction modelled.	Accelerated deterioration of ballast in tunnels. Increased repair times.	-
Sleepers	When the track is tamped there is a probability of the sleepers being damaged. If ballast condition 'Very poor' or 'Super red' the sleeper deterioration rate is accelerated.		No condition interaction modelled.	Increased repair times.	-
S&C	When the track is renewed S&C unit also renewed.	No condition interaction modelled.		Increased repair times.	-
Tunnels	When track renewed tunnel condition improved.	No condition interaction modelled.	No condition interaction modelled.		-
Signalling	-	-	-	-	

TABLE 7.1: CONDITION DEPENDENCIES BETWEEN ASSETS CONSIDERED IN THE SYSTEM PETRI NET MODEL

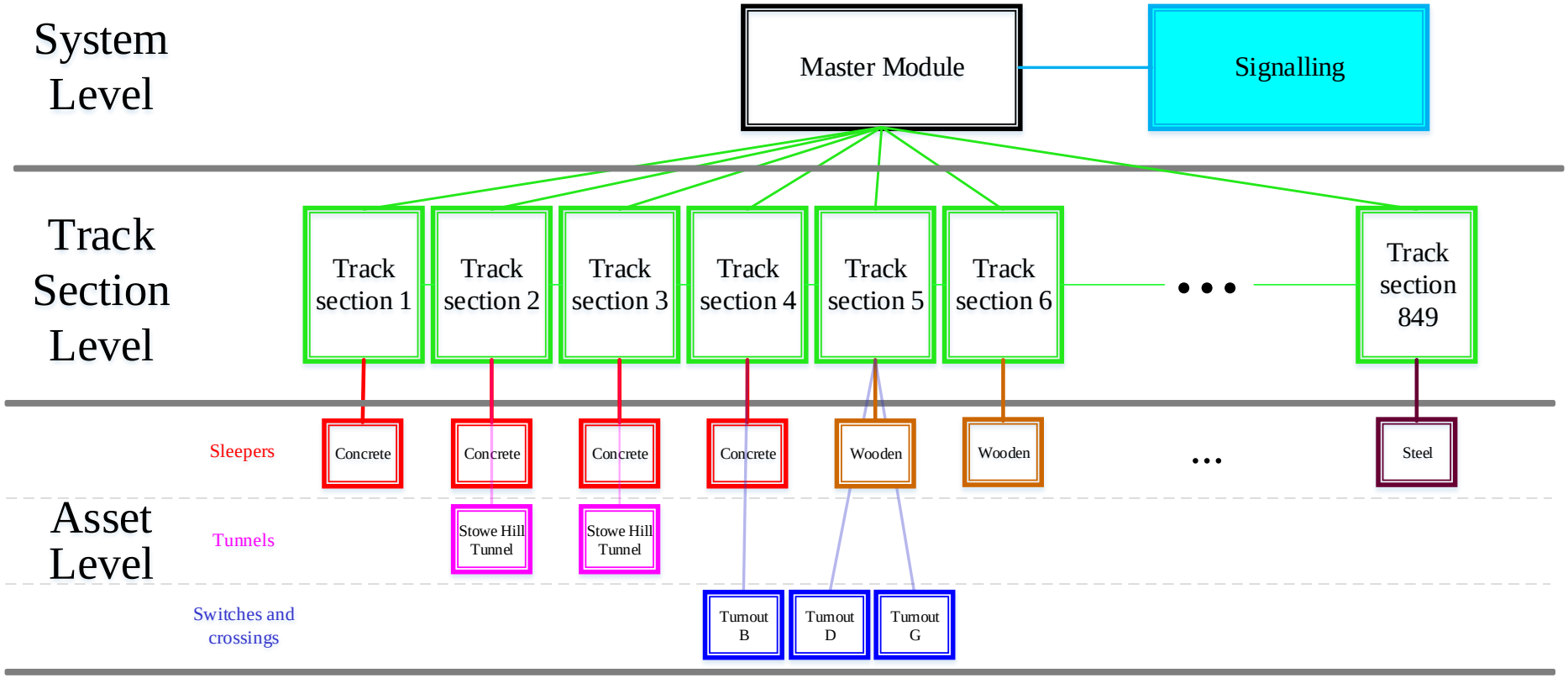


FIGURE 7.1: SYSTEM HIERARCHY

7.3 Whole System Petri Net Modules

To allow modules to be used in the hierarchy shown in Figure 7.1, the asset models presented in Chapter 6 had to be adapted to contain '*port'* and *'socket'* places to allow them to interface with other modules. '*Port*' and '*socket*' places are drawn with a double border to distinguish them from standard places. This section introduces the master module which is used to model resources and other global phenomena.

7.3.1 Master Module

The master module was introduced to enable system phenomena to be modelled and for this reason is linked to all other modules in the system. The master module is shown in Figure 7.2 and is made up of three distinct parts:

1. Resource management (Blue) (see section 7.3.1.1)
2. Condition assessment (Pink) (see section 7.3.1.2)
3. Budget management (Red) (see section 7.3.1.3)

7.3.1.1 Resource Management

Chapter 2 describes the range of maintenance tasks that are performed on the railway. Maintenance tasks require resources (equipment and engineers) which are common to the whole railway corridor. The management of maintenance machines and engineers is simulated by the section of the master module shown in blue in Figure 7.2. Maintenance activities are grouped into two types:

(i) Maintenance tasks that can be performed by hand ('*Manual Work'*)
(ii) Maintenance tasks that require machinery to be performed ('*Machine Work'*)

As *'Manual Work'* is performed using hand tools it is not dependent on machine availability, therefore these tasks are modelled as being independent of machine availability, and can be performed at any time, as long as an engineer is available.

On the other hand *'Machine Work*' requires some specialist machinery. However only a finite number of these machines will be available. '*Machine Work*' tasks can only be performed when there is a free machine in addition to an engineer, and the machine has to be transported to the worksite.

Machine availability was modelled in the following way. Each *'Machine Work*' task has a machine available place in the master module associated with that intervention type ($P_0^M \rightarrow P_5^M \& P_{22}^M$). When a '*Machine Work*' intervention is scheduled (in one of the asset modules) a token is removed from the appropriate place in the master module ($P_0^M \rightarrow P_5^M \; or \; P_{22}^M$). The token is only replaced once the work is complete. If there are no tokens remaining in the place when a *'Machine Work*' task is required, the maintenance is not performed until another module returns a token, indicating a machine is available.

In addition to *'Machine Work*' being restricted due to the machine being unavailable as already performing work in another module, two other phenomena that restrict *'Machine Work*' are considered:

(i) The machine not being available as required outside the railway corridor or being serviced (planned unavailability). This is modelled using two fixed time transitions, which cycle the machine between being available and unavailable on a 365 day cycle, the values for these transitions are shown in Table 7.2.

(ii) The machine not being available due to extreme weather/extreme events (unplanned unavailability). This is modelled using two stochastic transitions which cycle the machine between available and unavailable.

Extreme weather events can restrict and prevent maintenance being carried out on the railway. Events that can disrupt maintenance include prolonged cold and snowy weather such as those experienced in the UK in December 2010 and extremely hot conditions such as those experienced in the 2003 European heatwave. During cold weather it is very difficult for maintenance teams to work on the railway. During extreme heat it is unwise to perform maintenance tasks that stress the rails, as the rails are likely to buckle.

In the master module places $P_{23}^{M} \rightarrow P_{26}^{M}$ are used to model maintenance being restricted due to extreme weather. For example if place P_{23}^{M} was marked then rail maintenance would be restricted on the entire railway corridor. The occurrence of these type of events is modelled using the stochastic transitions $T_{33}^{M} \rightarrow T_{40}^{M}$. The values used for the transitions are shown in Table 7.3 at this stage in the research these values are estimated.

At this stage in the research the logistics of transporting maintenance machines and workers around the network is not considered, merely the availability.

Transition	Description	Time (Days)
T_0^M	Time between HOM planned unavailable	100
T_1^M	Duration of event	265
T_2^M	Time between ballast cleaner planned unavailable	265
T_3^M	Duration of event	100
T_{43}^M	Time between Stoneblower planned unavailable	350
T_{44}^M	Duration of event	15
T_{45}^M	Time between tamp planned unavailable	350
T_{46}^M	Duration of event	15
T_{47}^M	Time between S&C tamper planned unavailable	300
T_{48}^M	Duration of event	65
T_{49}^M	Time between rail replacement planned unavailable	200
T_{50}^M	Duration of event	165
T_{51}^M	Time between rail grinder planned unavailable	340
T_{52}^M	Duration of event	25

TABLE 7.2: TRANSITION USED TO MODEL THE **PLANNED** UNAVAILABILITY OF MAINTENANCE MACHINES

Transition	Description	Time Unit	Distribution
T_{33}^M	Time between extreme events. (Events that prevent tamping).	Days	Weibull(1.1, 2000)
T_{34}^M	Duration of event.	Days	Lognormal(1, 1)
T_{35}^M	Time between extreme events. (Events that prevent stoneblowing).	Days	Weibull(1.1, 2000)
T_{36}^M	Duration of event.	Days	Lognormal(1,1)
T_{37}^M	Time between extreme events. (Events that prevent grinding).	Days	Weibull(1.1, 2500)
T_{38}^M	Duration of event.	Days	Lognormal(1, 1)
T_{39}^M	Time between extreme events. (Events that prevent welding).	Days	Weibull(1.1, 3000)
T_{40}^M	Duration of event.	Days	Lognormal (1, 1)

TABLE 7.3: TRANSITION USED TO MODEL THE **UNPLANNED** UNAVAILABILITY OF MAINTENANCE MACHINES

7.3.1.2 Condition Assessment

The second part of the master module was used to assess the overall condition of the railway corridor. Railway corridors contain a wide range of assets and displaying information on all of these assets simultaneously would be very confusing and it would be difficult to comprehend. It was therefore decided that a means of assessing the overall condition of the railway corridor was required.

As assets degrade it may become unsafe to run trains at line speed, and hence it becomes necessary to implement a TSR. The number of TSRs and line closures will be used as one means of assessing the overall condition of the railway corridor.

The system level Petri net assesses the total number of TSRs and line closures and uses this to give an overview of the whole network. The overall condition of the network can be in one of five states; No Delays (P_{12}^M), Minor Delays (P_{13}^M), Delays (P_{14}^M), Major Delays (P_{15}^M), and Serious Delays (P_{16}^M). The 'calculator' substitution transition marks the appropriate condition place based on the number of TSRs and line closures in the railway corridor.

Table 7.4 shows how the number of level 1 TSRs, level 2 TSRs and line closures are translated into an overall condition state. Table 7.4 is used to assign a condition to all three measures and then the overall condition corresponds to the worst of the three measures. So for example if there were three level 1 TSRs, one level 2 TSR and zero line closures then the condition due to the level 1 TSRs would be 'minor delays', the condition due to the level 2 TSRs would also be 'minor delays' and the condition due to line closures would be 'No delays'. The overall condition is assessed as the worst of these three, so the overall condition would be 'minor delays'.

TSR/Line closures	**Number of track sections with restrictions for overall condition states**				
	No Delay	Minor Delays	Delays	Major Delays	Serious Delays
Level 1	0-1	2-19	20-34	> 34	Any
Level 2	0	1-9	10-14	> 15	Any
Line Closure	0	0	0	0	> 0

TABLE 7.4: NUMBER OF RESTRICTIONS PERMITTED IN EACH OF THE CONDITION STATES

7.3.1.3 Budget

Railway networks are vast systems and as such require significant investment each year. The final part of the master module Petri net (shown in red in Figure 7.2) is used to model the budget. The budget is split into two types track and signalling, and these are divided into maintenance and renewals, creating four *budget places* in total. The number of tokens in each place corresponds to the amount of money left in that budget. All of the track maintenance actions are connected to place P_{18}^M '*Track maintenance budget remaining'* and all the track renewal tasks (Full track section renewal, full re-rail, ballast cleaning, S&C renewal and sleeper renewal) are connected to place P_{20}^M '*Track renewal budget remaining'*. Signal maintenance and renewal tasks are connected to place P_{40}^M or P_{42}^M respectively.

When a maintenance task is performed it removes the appropriate number of tokens from the appropriate budget place. For example a tamp of a Category 1A line costs 505 units. Therefore when a Category 1A line is tamped 505 tokens are removed from P_{18}^M. If there are fewer than 505 tokens in place P_{18}^M then the tamp will not take place until the number of tokens in place P_{18}^M is increased following the next budget allocation. Transitions T_{31}^M, T_{32}^M, T_{49}^M and T_{50}^M are used to add money to the budget remaining places

($P_{18}^{M}, P_{20}^{M}, P_{40}^{M}$ and P_{42}^{M}) at fixed intervals. In this study transitions T_{31}^{M}, T_{32}^{M}, T_{49}^{M} and T_{50}^{M} have a fixed firing time, of five years. These values were chosen to align with Network Rail five year CPs, however any value or distribution could be used.

Table 7.5 details an estimate for the maintenance and renewal budget for Bletchley Delivery Unit for CP5 (5 years), based on Network Rail and ORR funding assessments [157][21]. At this stage only track and signalling are considered. These values were used to initially populate places P_{18}^{M}, P_{20}^{M}, P_{40}^{M} and P_{42}^{M}, the cost outputs of the model are also compared against these expenditure values (see section 7.5). As other assets are included in the system model places can be included to model these asset classes.

Asset Class	**Total (Millions)**			
	Maintenance budget (five years)	Budget place	Renewal budget (five years)	Budget place
Track	30	P_{18}^{M}	44	P_{20}^{M}
Signalling	11	P_{40}^{M}	44	P_{42}^{M}
Civils	6	-	33	-
E&P	6	-	13	-
Telecoms	2	-	5	-
Other[22]	16	-	23	-

TABLE 7.5: ESTIMATE OF BLETCHLEY DELIVERY UNIT MAINTENANCE AND RENEWAL EXPENDITURE (MILLIONS).

[21] Appendix F-1 details maintenance and renewal expenditure for the LNW route, subdivided by asset class. The estimates in Table 7.5 are based on the fact Bletchley Delivery Unit makes up about 6% of the LNW route.

[22] Building and wheel plant

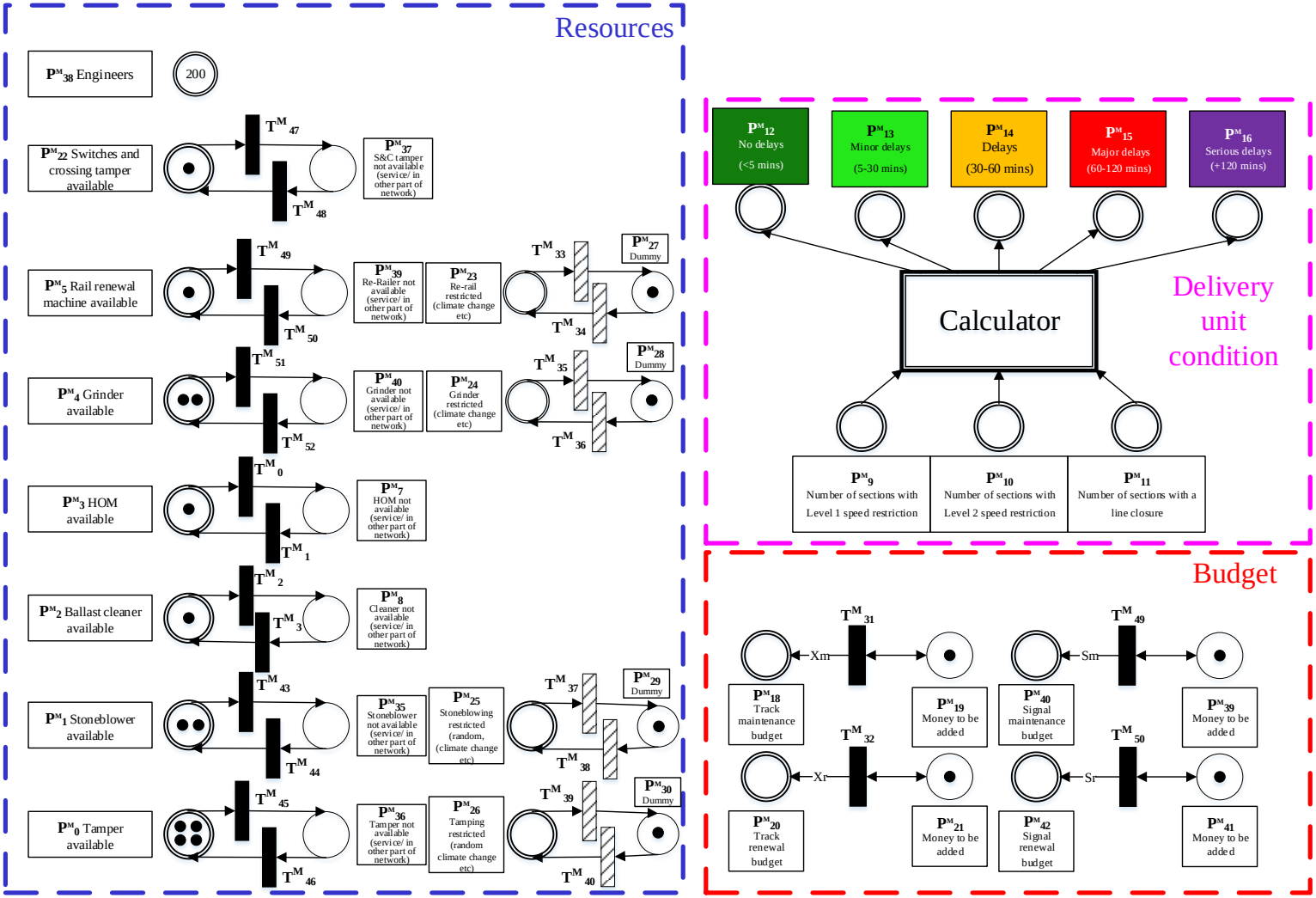


FIGURE 7.2: MASTER MODULE PETRI NET

7.3.2 Additions to the Track Section Model for use in the Whole System Framework

For use in the whole system model, the track section model was converted into a module which included '*port'* and '*socket'* places to allow the track section to interface with the master module and neighbouring track section modules. Three areas of the track section model were altered to allow it to interface with the other modules:

(i) Resource and budget management when scheduling maintenance (section 7.3.2.1)
(ii) Opportunistic maintenance (section 7.3.2.2)
(iii) Renewals (section 7.3.2.3)
(iv) Implementation of TSRs and line closures (section 7.3.2.4)

To allow these additional features to be modelled four '*socket'* places were included in the track section module:

(i) P_{76}^{T} *'Maintenance in this section'*

This place is marked any time work is ongoing in the section. It is a '*socket'* place so that the assets in the bottom level of the hierarchy (sleepers, etc.) can be plugged in to it. This allows the asset modules to know when maintenance is taking place and allows opportunistic work to be scheduled.

(ii) P_{77}^{T} *'Possession units remaining'*

This place is used to limit the number of maintenance tasks that can be performed each day. The default marking is eight. When maintenance tasks are undertaken tokens are removed from P_{77}^{T} and returned when the work is complete. P_{77}^{T} is a '*socket*' place so the asset module can be plugged in, allowing the possession time remaining to be considered for work in the asset modules.

(iii) P_{78}^{T} *'Opportunistic work allowed'*

This place is used to control which type of opportunistic work is permitted.

(iv) P_{79}^{T} *'Stop multiple work'*

This place is used as housekeeping, to ensure only one maintenance machine can be in a section at once, this is important otherwise maintenance machines can become 'lost' in the section.

The following sections will explain how these places were used to convert the track section model in Chapter 6 to a module suitable for use in the system hierarchy.

7.3.2.1 Budget and Resources when Scheduling Maintenance

When scheduling maintenance in the track section module, resources and budget are also considered. The track section module contained '*port*' places which plug into the master module allowing resources and budget to be considered when scheduling maintenance.

In the track section module three additional requirements are considered when scheduling maintenance:

(i) Budget remaining $(P_{18}^{M} \& P_{20}^{M})$
(ii) Machine availability $(P_{0}^{M} \rightarrow P_{5}^{M})$
(iii) Engineer availability (P_{38}^{M})

The transitions used to schedule maintenance were adapted to contain inputs from the above places to ensure that each of these criteria were also met when scheduling maintenance. In the track section module for maintenance to take place there must be:

(i) Budget available
(ii) A maintenance machine available
(iii) An engineer available
(iv) Possession time remaining
(v) No other maintenance being performed in the section

Figure 7.3 shows how the scheduling Petri net in Chapter 6 (Figure 6.9) was adapted to simulate the five additional phenomenon, for routine work. The following section will discuss the further changes that were required in order to consider opportunistic work.

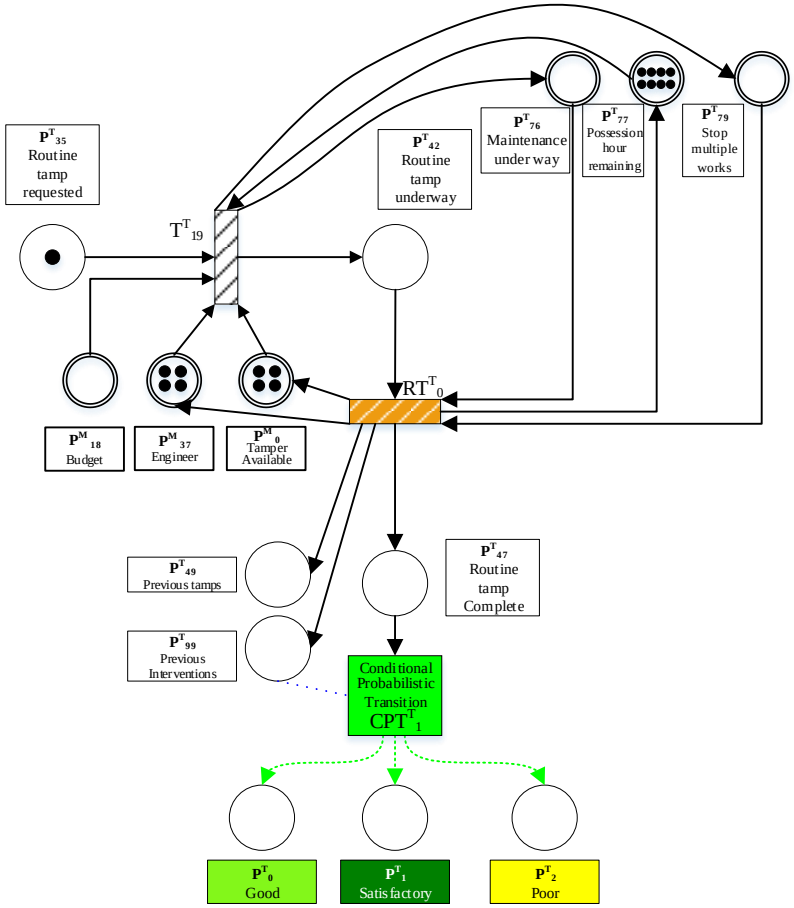


FIGURE 7.3: TAMPING SCHEDULING PETRI NET WITH ADDITIONAL PORT AND SOCKET PLACES

7.3.2.2 Opportunistic Work

In the system model, as multiple track sections are considered it allows opportunistic maintenance to be included. To allow opportunistic maintenance to be considered additional changes had to be made to the Petri net model in Chapter 6. This section will outline how opportunistic work was considered and the additional changes that were required.

Opportunistic work is based on the following assumption:
If an asset is in a state where it has been scheduled for maintenance but work has not yet started, work will be performed immediately (opportunistically) if a 'neighbouring' section or asset is being repaired.

There are four types of opportunistic work that can be considered:

(i) Opportunistic maintenance of a **different** component in the **same** section.
When maintenance is being performed on one asset in the track section work on another asset can be performed if enough resources remain (Figure 7.4).

(ii) Opportunistic maintenance of a **similar** component in a **neighbouring** section.
When maintenance is being performed in one section, the neighbouring section may be maintained in the same way (Figure 7.5).

(iii) Opportunistic maintenance of a **similar** component in the **same** section.
Opportunistic maintenance of the same component in the section is not considered as in the models proposed there is generally only one type of each asset in each section.

(iv) Opportunistic maintenance of a **different** component in a **neighbouring** section.
This is not currently considered as the time required to move to another section and get different equipment organised makes it unlikely this type of work can be performed in the time available.

Places $P_{76}^{T} \rightarrow P_{78}^{T}$ are critical to modelling opportunistic work:

(i) Place P_{76}^{T} is marked whenever any maintenance task is being carried out, and becomes unmarked when the maintenance is complete. If multiple maintenance tasks are performed at the same time the marking will be greater than one. This allows opportunistic work of a different component within the same section to be modelled. As soon as a component within the section is being worked on, any assets within the section that have maintenance scheduled will be repaired immediately (opportunistically) provided there are enough resources remaining.

(ii) P_{77}^{T} was introduced to enable possession time to be considered when scheduling opportunistic work. The modelling of possession time is required in order to limit the amount of opportunistic maintenance that can be performed each day. Without a limit all degraded assets, could in theory, be opportunistically maintained at the same time. Place P_{77}^{T} records the amount of possession time available, each maintenance task requires a given number of possession time units; for track maintenance these are listed in Table 7.6. These values were estimated based on the mean of the distributions for the ART determined in Chapter 5. When a maintenance task is initiated it removes tokens equal to the number of possession units required for that task and returns them upon completion. If there are not enough tokens remaining, then the task does not take place. The default value for $T_{77}^{T}$was eight tokens.

(iii) P_{78}^{T} is used to easily determine the level of opportunistic work that can be carried out:

a) Marking of P_{78}^{T}=0

No opportunistic work

b) Marking of P_{78}^{T}=1
   Opportunistic maintenance of a **similar** component in a **neighbouring** section

c) Marking of P_{78}^{T}=2
   Opportunistic maintenance of a **similar** component in a **neighbouring** section
   And
   Opportunistic maintenance of a **different** component in the **same** section

d) Marking of P_{78}^{T}=3
   Opportunistic maintenance of a **similar** component in a **neighbouring** section
   And
   Opportunistic maintenance of a **different** component in the **same** section
   And
   Grouped/opportunistic renewal see section 7.3.2.2

Opportunistic maintenance of a different component in the same section

It is assumed that tamping, stoneblowing, welding and grinding can all be performed opportunistically, when a different component in the section is being maintained (provided there are resources and time available). Figure 7.4 shows the Petri net used to model opportunistic tamping when another section is being maintained. The ballast condition is known to be '*Poor*' and a '*normal priority'* tamp has been scheduled, place P_{35}^{T} is marked. If maintenance takes place on another asset within the track section place P_{76}^{T} will be marked. The marking of P_{76}^{T} enables transition T_{20}^{T} (provided budget and possession time are available) which has zero delay time so will fire immediately.

Opportunistic maintenance of a similar component in a neighbouring section

Tamping, welding and grinding can also be performed early if a neighbouring section is being maintained in the same way. However, it is assumed that stoneblowing cannot be performed opportunistically when a neighbouring section is being stoneblown, as once a stoneblow has been performed tamping cannot be performed; it is therefore undesirable to stoneblow a section near the beginning of its lifetime.

Figure 7.5 shows the Petri net used to model opportunistic tamping when a neighbouring section is being tamped. The ballast condition is known to be '*Poor*' and a '*normal priority'* tamp has been scheduled, place P_{35}^{T} is marked. If a neighbouring section is being tamped (P_{34}^{T} marked in a neighbouring section) then transition T_{21}^{T} will be enabled (provided budget and possession time are also available), it has a delay time of zero so will fire immediately. Note that T_{21}^{T} does not require work to already be on going in the section ($P_{76}^{T}$is not an input to T_{21}^{T}).

The code was flexible enough that any number of sections can be viewed as neighbouring, however in the examples shown the value chosen is always two either side of the section being maintained. The matrix shown in equation (7.1) summarises the sections that will be

considered for neighbouring opportunistic work, each row represents one track section. *m* indicates the section being maintained, *1* indicates sections considered for opportunistic work when that section is being maintained, *0* indicates the section is not considered for opportunistic work. Notice the first and last sections consider four sections on one side rather than two on either side.

$$\begin{pmatrix} m & 1 & 1 & 1 & 1 & 0 & 0 & 0 & 0 & 0 & \cdots \\ 1 & m & 1 & 1 & 1 & 0 & 0 & 0 & 0 & 0 & \cdots \\ 1 & 1 & m & 1 & 1 & 0 & 0 & 0 & 0 & 0 & \cdots \\ 0 & 1 & 1 & m & 1 & 1 & 0 & 0 & 0 & 0 & \ldots \\ 0 & 0 & 1 & 1 & m & 1 & 1 & 0 & 0 & 0 & \cdots \\ \vdots & \ddots & \ddots & \ddots & \ddots & \ddots & \ddots & \ddots & \ddots & \ddots & \vdots \\ \cdots & 0 & 0 & 0 & 1 & 1 & m & 1 & 1 & 0 & 0 \\ \cdots & 0 & 0 & 0 & 0 & 1 & 1 & m & 1 & 1 & 0 \\ \ldots & 0 & 0 & 0 & 0 & 0 & 1 & 1 & m & 1 & 1 \\ \cdots & 0 & 0 & 0 & 0 & 0 & 1 & 1 & 1 & m & 1 \\ \cdots & 0 & 0 & 0 & 0 & 0 & 1 & 1 & 1 & 1 & m \end{pmatrix} \quad (7.1)$$

Renewals, cleans and rail replacements are not considered opportunistically as firstly they are likely to take considerably longer than regular maintenance tasks. Secondly it is assumed that opportunistic work will not take place during a ballast clean, rail renewal or track section renewal. For this reason renewals, cleans and rails replacement were not linked to the possession remaining place.

Maintenance Task			**Time Units Required**
Tamping	Routine	Regular	3
		Group[23]	4
		Neighbouring[24]	4
	Emergency	Regular	3
		Group	4
		Neighbouring	4
Stoneblowing	Routine	Regular	5
		Group	6
	Emergency	Regular	5
		Group	6
Welding	Routine	Regular	1
		Group	2
		Neighbouring	2
	Emergency	Regular	1
		Group	2
		Neighbouring	2
Grinding	Routine	Regular	3
		Group	4
		Neighbouring	4
	Emergency	Regular	3
		Group	4
		Neighbouring	4

TABLE 7.6: POSSESSION TIME UNITS REQUIRED FOR TRACK MAINTENANCE ACTIONS

[23] Group refers to opportunistic maintenance of a different component in the same section
[24] Neighbouring refers opportunistic maintenance of a similar component in a neighbouring section

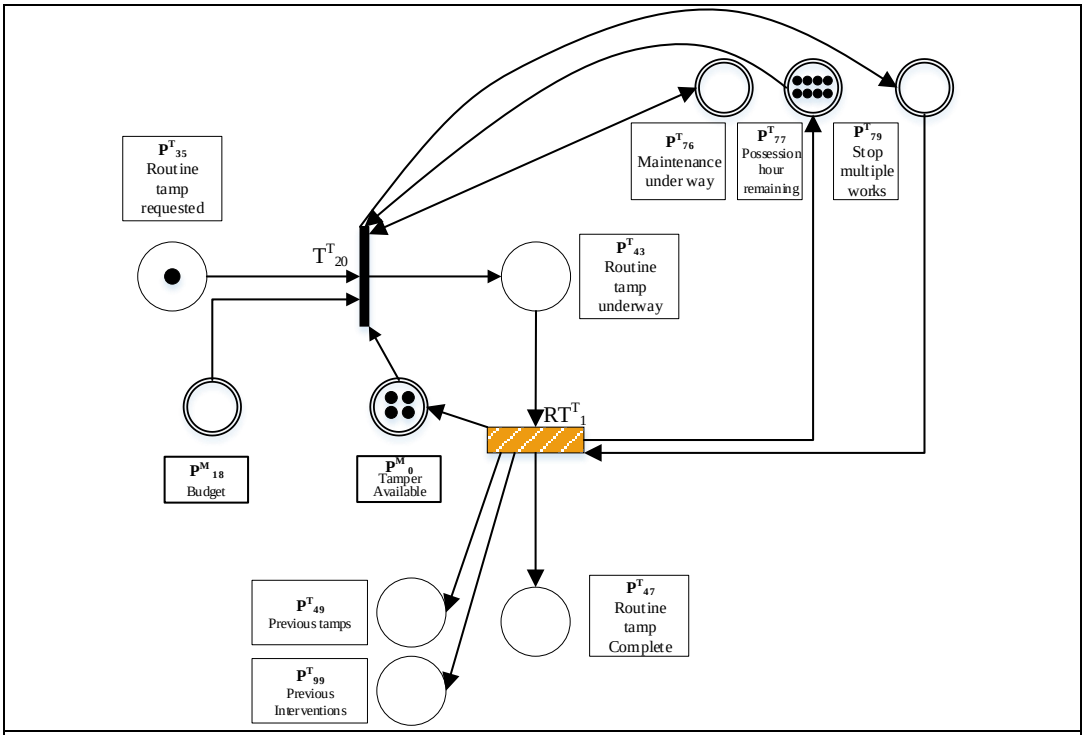


FIGURE 7.4: TAMPING SCHEDULING PETRI NET FOR OPPORTUNISTIC MAINTENANCE OF A DIFFERENT COMPONENT IN THE SAME SECTION WITH ADDITIONAL PORT AND SOCKET PLACES

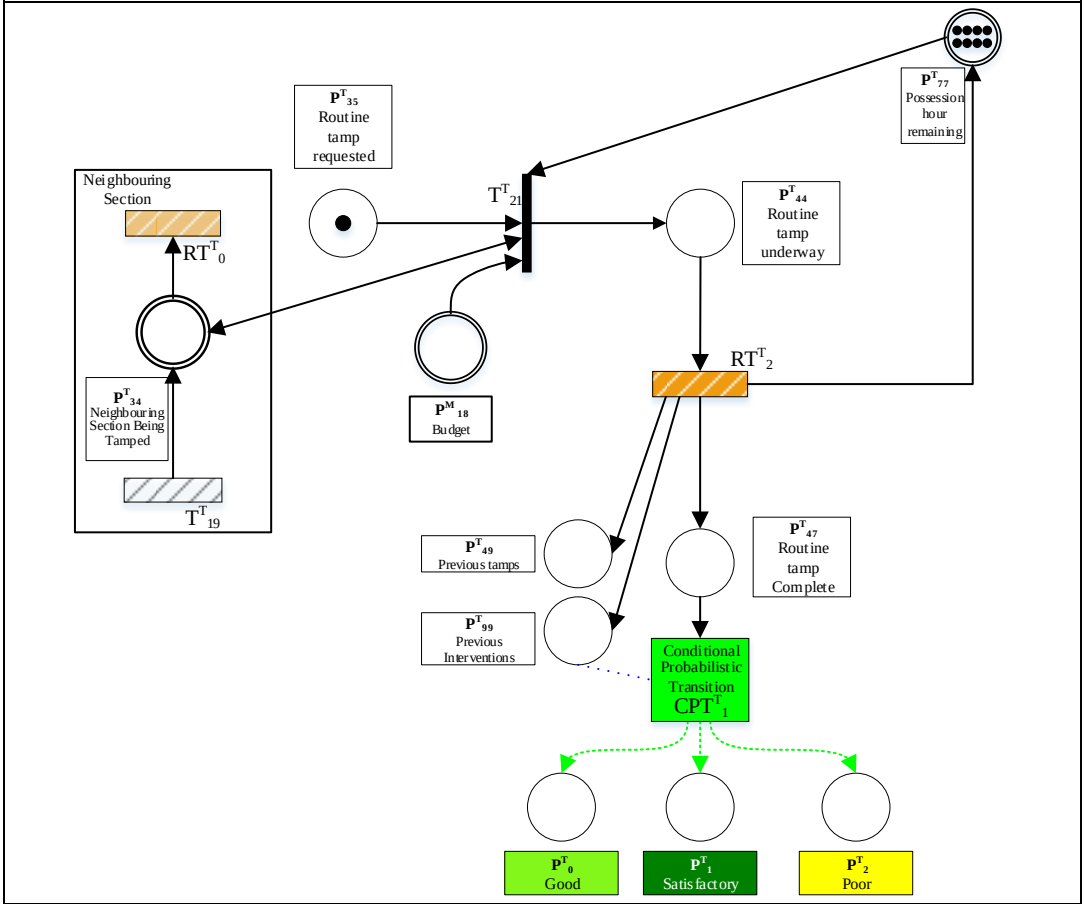


FIGURE 7.5: TAMPING SCHEDULING PETRI NET FOR OPPORTUNISTIC MAINTENANCE OF A SIMILAR COMPONENT IN A NEIGHBOURING SECTION WITH ADDITIONAL PORT AND SOCKET PLACES

7.3.2.3 Grouped Renewals

Section 6.3.1 explained how full renewal of the ballast and rails was implemented in the track section model based on the number of previous interventions. The scheduling of renewals in the system model is slightly different:

(i) In the system model a renewal could be performed early if the condition of the rails, ballast **and** sleepers were all degraded but had not individually reached the threshold for a renewal to take place. Table 7.7 summarises the conditions required for the three types of standard renewal (low, medium and high priority) introduced in the track section model in Chapter 6 as well as the conditions for grouped renewal. Note in the case of grouped renewal the conditions are 'and' meaning that all three must occur, if all three conditions are met simultaneously then a grouped renewal will be scheduled. Due to the long service life of sleepers compared to ballast and rails it is assumed that the sleeper condition alone is not enough to trigger a full renewal.

(ii) When a track section is renewed in the system model all assets within the track section (sleepers, S&C) are renewed.

	Low Priority Renewal	**Medium Priority Renewal**	**High Priority Renewal**	**Grouped Renewal**
Ballast	Ten maintenance interventions (tamps or stoneblows) have been carried out.	12 maintenance interventions (tamps or stoneblows) have been carried out.	14 maintenance interventions (tamps or stoneblows) have been carried out **Or** the Ballast reaches the Super red condition.	Eight maintenance interventions (tamps or stoneblows) have been carried out.
				AND
Sleepers				The number of defective sleepers exceeds a critical amount.
		OR	**OR**	**AND**
Rail		Reaches a condition state such that the rail is known to have 'Major T.D and major S.D' (P_{30}^{T} is marked).	Reaches a condition state such that the rail is known to have 'Serious defects' (P_{32}^{T} is marked).	12 grinds or welds have been carried out on the rail already.

TABLE 7.7: CONDITIONS FOR DIFFERENT TYPES OF RENEWAL

7.3.2.4 Speed Restrictions

The final change to the track section model in Chapter 6 allows information on TSRs and line closures to be transmitted to the master module. The master module kept track of the total number of TSRs (P_9^M and P_{10}^M) and line closures (P_{11}^M) in the railway corridor, and used this to provide an overall condition assessment of the railway corridor. Figure 7.6 shows how information on speed restrictions within the track section is transmitted to the master module so the overall delay can be recorded. The marking is initially as shown in Figure 7.6, there is no speed restriction in place. Eventually place P_{81}^T will be marked indicating that

there is a level 1 speed restriction in the track section. When this happens T_{79}^{T} will fire removing the marking of P_{80}^{T}. Additionally transition T_{88}^{T} will fire, this will absorb the marking of P_{84}^{T} and mark place P_{85}^{T} It also increases the marking of P_{9}^{M} by one. This indicates the total number of level 1 TSRs has increased by one. The marking of P_{85}^{T} inhibits T_{88}^{T} ensuring the TSR is only recorded once.

A level 1 TSR can be removed in one of two ways:

(i) Maintenance is performed in a timely manner and the TSR is removed, this will cause the marking of P_{81}^{T} to be removed and place P_{80}^{T} to be marked. As P_{85}^{T} is also marked and P_{84}^{T} is not marked T_{87}^{T} will fire as soon as P_{80}^{T} is marked. The firing of T_{87}^{T} will remove one from the marking of P_{9}^{M} indicating a decrease of one in the total number of level 1 TSRs. This will also cause the marking of places P_{84}^{T} and P_{85}^{T} to swap, so the marking returns to that shown in Figure 7.6.

(ii) Alternatively if the maintenance is not performed in a timely manner the asset may degrade to the point that a level 2 TSR is required (or another asset in the track section may be found to be defective and require a level 2 TSR). In this case P_{82}^{T} will become marked. The marking of P_{82}^{T} will cause T_{83}^{T} to fire; this will absorb the marking of P_{81}^{T} as well as P_{85}^{T}. It will also remove one from the marking of P_{9}^{M}, and at the same time T_{90}^{T} will fire, increasing the marking of P_{10}^{M} by one. This models a level 1 TSR being removed and a level 2 TSR being imposed. The firing of transition T_{90}^{T} also swaps the marking of P_{86}^{T} and P_{87}^{T}. This stops T_{90}^{T} firing a second time and means that when the restriction is removed transition T_{89}^{T} can fire, removing one from the marking of P_{10}^{M}.

The implementation of line closures (marking of P_{83}^{T}) works in the same way.

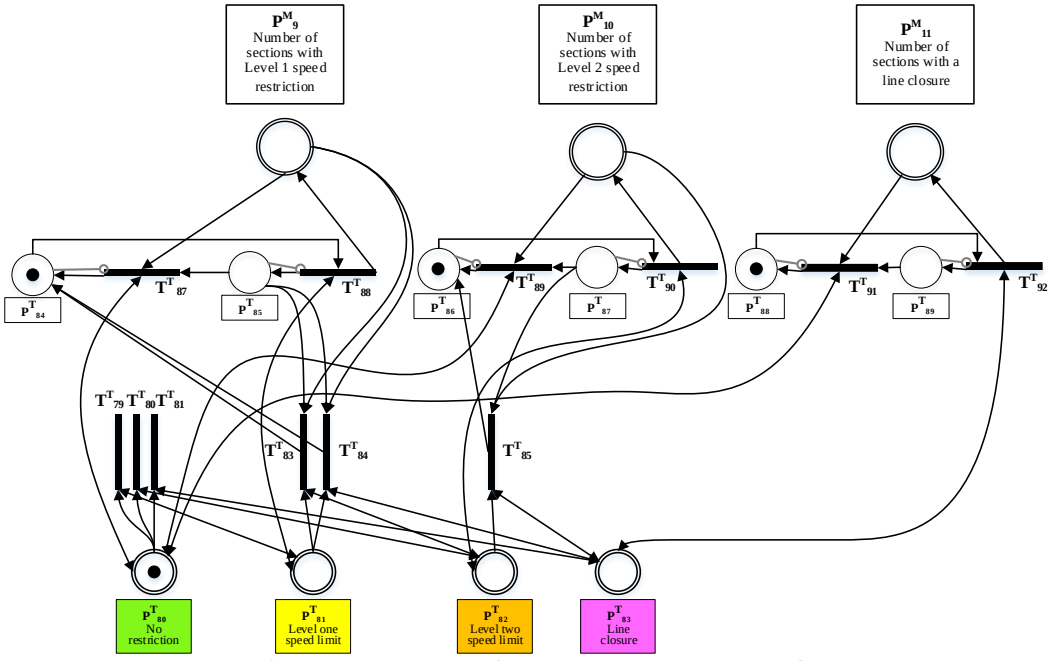


FIGURE 7.6: IMPLEMENTATION OF SPEED RESTRICTIONS AND LINE CLOSURES

7.3.3 Additions to the Sleeper Models for use in the Whole System Framework

Five changes were made to the sleeper models to turn them into modules to allow them to interface with the other modules in the system framework:

(i) Connection to the master module

a. Resource management

It is assumed that spot re-sleepers can be performed by hand so the sleeper maintenance tasks are not linked to a machine available place in the master module, but they are linked to the engineer available place P_{38}^{M}.

b. Budget management

All the sleeper maintenance tasks were linked to P_{18}^{M} in the master module which was used to ensure there was enough budget available to perform the maintenance.

(ii) Connection to the track section module

a. Failure modes based directly on ballast

As the sleeper module was plugged into the track section module, it allowed the failure modes due to tamping damage (T_3^{CS}) and poor ballast condition (T_4^{CS} and T_5^{CS}) to be linked directly to the ballast model; these failure modes were only considered if tamping was in progress (P_{42}^{T}) or the ballast was in '*Very poor*'(P_3^T) or '*Super red*'(P_4^T) condition.

b. Renewal governed by the ballast and rails

As discussed the renewal of sleepers is generally governed by the condition of rails and ballast; in the complete system model the sleepers were renewed when the track section was renewed (based on ballast and rail condition), rather than after a fixed period of time as in the individual sleeper models.

c. Consideration of opportunistic work and the time taken to complete work

In the sleeper modules opportunistic maintenance in the neighbouring section is not considered, however opportunistic work of the sleepers when maintenance takes place on another asset, in the track section, is considered. The sleeper module '*port'* places are plugged into $P_{76}^{T} \rightarrow P_{78}^{T}$ in the relevant track section module. Scheduled work in the sleeper module would be performed early if some other maintenance (place P_{76}^{T} marked) was taking place in the track section module and vice versa if maintenance was performed on the sleeper module, scheduled work in the track section would be performed immediately (opportunistically).

Table 7.8 summarises the time required to perform the various different sleeper maintenance tasks.

d. Speed restrictions

The module was adapted so that speed restrictions would be recorded directly in the track section module ($P_{80}^{T} \rightarrow P_{83}^{T}$). The number of defective sleepers before a speed limit was imposed is as discussed in section 6.3.2.

(iii) Estimation of Weibull distribution for baseline failures

Section 6.3.2.1 explained how the Weibull distribution was combined to allow 440 sleepers to be modelled in one transition, by generating a predetermined list of firing times. However this method is very memory intensive, it requires recording a vector of approximately 1000 integers for each of the sleeper modules. Therefore in the system model a distribution was fitted to the 'predetermined' firing times prior to simulation. The firing times were then sampled from this distribution removing the need for a predetermined list to be stored in memory during the simulation, but still allowing the deterioration of all 440 sleepers to be modelled with one transition. Appendix C-5.1 provides a comparison between the Weibull distribution used in the timber sleeper module and the predetermined values used in the individual timber model.

Diagrams of the system sleeper Petri net modules are shown in Appendix G-1.1 → Appendix G-1.3.

Number of Sleepers Repaired	Time Units		
	Concrete	Timber	Steel
Opp.	1	1	1
1	1	1	1
2	2	1	1
3	3	1	2
4	4	2	2
5	5	2	3
6	6	2	3
7	n/a	3	n/a
8	n/a	3	n/a
9	n/a	4	n/a
10	n/a	4	n/a
Major	7	7	7

TABLE 7.8: REPAIR TIME UNITS FOR VARIOUS SLEEPER MAINTENANCE TASKS

7.3.4 Additions to the S&C Model for use in the Whole System Framework

The following changes were made to the S&C model in section 6.3.4 to convert it into a module suitable for use in the system model; they are similar to the changes made for the sleeper modules:

(i) Connection to the master module

a. Resource management

It is assumed all S&C maintenance is manual except S&C tamping. The S&C tamper availability is modelled using place P_{22}^{M} in the master module, there is assumed to be one S&C tamper in the railway corridor. All S&C maintenance tasks are linked to the engineer available place P_{38}^{M}.

b. Budget management

All the S&C maintenance tasks are linked to P_{18}^{M} in the master module, and S&C renewal is linked to place P_{20}^{M}.

(ii) Connection to the track section module

a. Renewal criteria

In the system model the renewal criteria for S&C were adjusted. In the system S&C module renewals were scheduled in one of two ways; when the track section underwent a full renewal or if the switch had more than three service affecting failures in a year. Following a renewal a second renewal cannot happen for at least ten years.

b. Consideration of opportunistic work

As there is unlikely to be a neighbouring S&C unit, only opportunistic work when maintenance takes place in the track section or sleeper module, associated with the S&C unit is considered. The S&C '*port*' places were plugged into places $P_{76}^{T} \rightarrow P_{78}^{T}$ in the track section model. Scheduled work in the S&C module would be performed early if some other maintenance (place P_{76}^{T} marked) was taking place in the track section module or sleeper module, and vice versa, if maintenance was performed in the S&C module, scheduled work in the track section and sleeper module would be performed immediately (opportunistically) providing there was time allocation remaining (sufficient tokens in place P_{77}^{T}). Table 7.9 shows the hours of maintenance required for the various S&C maintenance tasks considered.

c. Speed restrictions

The S&C model in section 6.3.4 was adapted so that speed restrictions could be recorded directly in the track section module ($P_{80}^{T} \rightarrow P_{83}^{T}$). The criterion for TSRs are the same as in the individual S&C model (section 6.3.4).

(iii) Estimation of Weibull distribution for baseline failure rates

As in the sleeper modules the method which allowed multiple slide chairs to be modelled in one transition was changed to a distribution, to remove the need for a precompiled list to be kept in scope (memory).

The S&C module used in the whole system framework is shown in Appendix G-1.4.

Activity	Type	Time Units
Stock Rail Repair	Routine	2
	Opportunistic	2
Switch Rail Repair	Routine	2
	Opportunistic	2
Sleeper	Routine	8
	Opportunistic	8
Slide Chair	Routine	5
	Opportunistic	5
Crossing	Routine	7
	Opportunistic	7
Check and Wing Rail	Routine	8
	Opportunistic	8
Stretcher Bar	Routine	7
	Opportunistic	7
Ballast	Routine	4
	Opportunistic	4

TABLE 7.9: TIME UNITS REQUIRED FOR S&C MAINTENANCE TASKS

7.3.5 Additions to the Tunnel Model for use in the Whole System Framework

The following changes were made to the tunnel model in section 7.3.5 to allow it to interface with the master module, track section modules, other asset modules and other tunnel modules for use in the whole system framework:

(i) Maintenance affecting all sections of the tunnel

As discussed, if a tunnel was longer than one section it was modelled with multiple tunnel modules. However maintenance is likely to affect the whole tunnel. In the system model major tunnel work would restore all sections of the tunnel to the good condition.

(ii) Connection to the master module

a. Resource management

The tunnel module was linked to P_{38}^{M} to ensure that engineers were available to perform work.

b. Budget management

All the tunnel maintenance tasks were linked to place P_{18}^{M} in the master module, to ensure there was budget available to perform the task.

(iii) Connection to the track section module

a. Renewal

Due to the long service life of tunnels, tunnel renewal is not considered. However when the track section is renewed it is assumed that major maintenance will take place in the tunnel.

b. Consideration of opportunistic work

Each of the tunnel modules was linked to one track section module. The tunnel module '*port'* places were plugged into $P_{76}^{T} \rightarrow P_{78}^{T}$ in the track section model. It was assumed that minor tunnel maintenance could be performed if some other form of maintenance was taking place in the track section or on the assets within the track section and vice versa. However during major tunnel maintenance opportunistic work was not considered as it is thought it would require more time than would ever be available.

c. Accelerated deterioration of assets in the tunnel

The deterioration of the ballast and rails in a tunnel was also increased (although this was done through the LI score rather than directly through the Petri net).

The tunnel Petri net module used in the system framework is shown in appendix G-1.5.

7.3.6 Additions to the Signalling System Model for use in the Whole System Framework

As the signal model is considered at the top level of the hierarchy very few changes were made, the only difference between the signal module used in the system module and the individual one proposed in section 6.3.5 is that the maintenance tasks are connected to the signal maintenance budget place, P_{40}^{M}, this ensures that work will not be complete if financial

resources are not available. The signal module used in the system module is shown in Appendix G-1.6.

It can be seen that, with the exception of the signal module, there is a common theme to the changes that have been made to the individual modules to allow them to be incorporated in the system model. This demonstrates that when it is desired to include additional assets in the framework, a few minor changes will allow them to be easily linked into the whole system framework.

7.4 A Test Case: Bletchley Delivery Unit

The railway corridor that has been considered as a case study is Bletchley Delivery Unit. Bletchley Delivery Unit is a railway corridor in England, North of London see Figure 7.7. It was chosen as it contains a mixture of track categories and a range of assets. An outline of the route is shown in Figure 7.8. The map highlights, stations, tunnels and other major features of the route. The route comprises: a section of the WCML, Northampton Loop and a branch line between Bletchley and Bedford. It is formed of five engineer's line references (ELRs) LEC1, LEC2, BBM, HNR, and RBS1 and contains about one hundred miles of track. No consideration has been taken for multiple running lines; only the up fast (or equivalent) has been considered. A detailed description of the track sections is given in Appendix J-1.1. The system framework for Bletchley Delivery Unit contained 1783 modules, the track summary database was used to determine the nature of the Delivery Unit and the modules that would be required. A breakdown of the modules used is shown in Table 7.10.

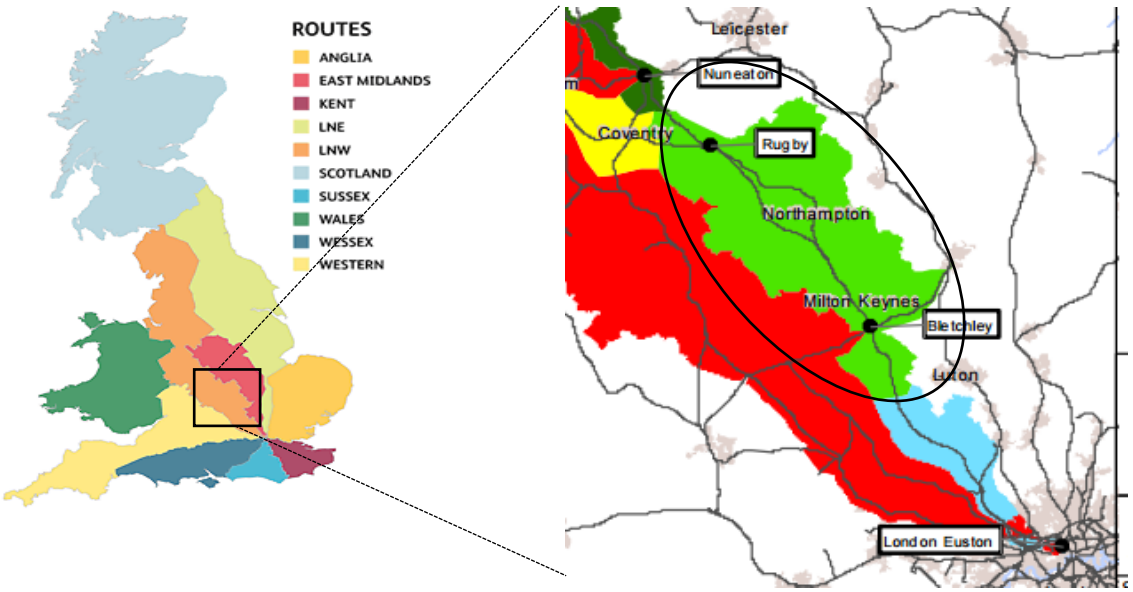


FIGURE 7.7: BLETCHLEY DELIVERY UNIT

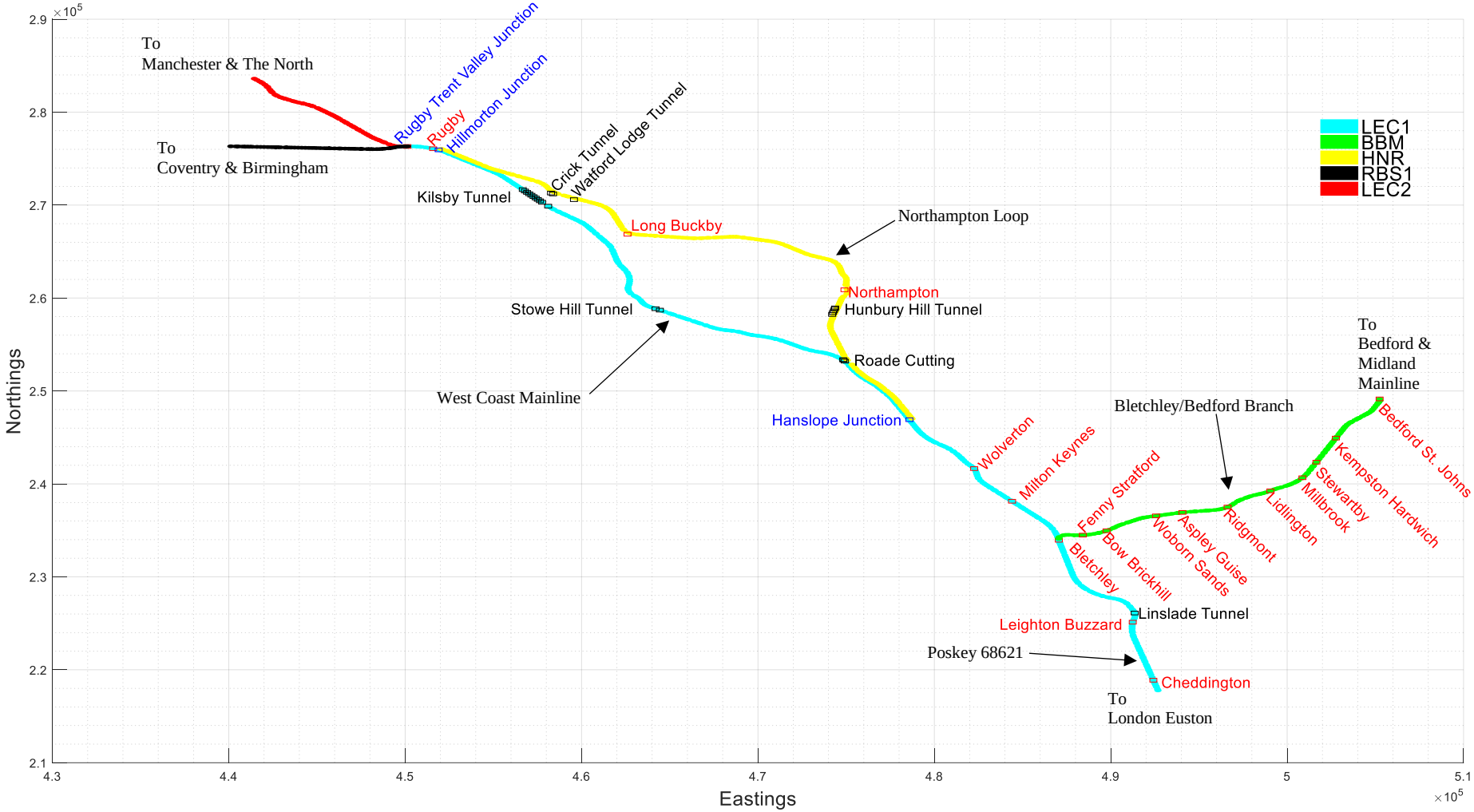


FIGURE 7.8: BLETCHLEY DELIVERY UNIT MAP, INCLUDING STATIONS AND KEY ASSETS

Module Type		Number
Master Module		1
Signal Module		1
Track Section Module	Category 1A	484
	Category 1	60
	Category 2	170
	Category 3	6
	Category 4	0
	Category 5	129
Sleeper Module[25]	Concrete	705
	Timber	51
	Steel	93
Tunnel	Crick Tunnel	2
	Hunbury Hill Tunnel	5
	Kilsby Tunnel	11
	Linslade Tunnel	1
	Stowe Hill Tunnel	2
	Watford Lodge Tunnel	1
Switches and Crossing[26]	Fixed Diamond Crossing	1
	Turnout A	0
	Turnout B	2
	Turnout C	9
	Turnout D	14
	Turnout E	0
	Turnout F	18
	Turnout G	17
	Turnout H	0
	Total	**1783**

TABLE 7.10: SUMMARY OF MODULES IN THE BLETCHLEY DELIVERY UNIT SYSTEM MODEL

7.4.1 Results of Bletchley Delivery Unit Case Study

To attempt to make the system model more realistic, it was decided to start the simulations from a partly degraded condition rather than a new condition. Instead of the ballast always being in good condition at the start of the simulation (P_0^T), the ballast alignment was set equal to the geometry measurement recorded at the last inspection. As the maintenance history is also thought to affect deterioration rates, rather than starting all sections with zero history (no previous interventions), it was decided to sample the number of tokens in the places that record the number of previous interventions for tamps (P_{49}^T), stoneblows (P_{50}^T), cleans (P_{54}^T), grinds(P_{60}^T) and welds (P_{61}^T) from a Normal distribution at the start of each simulation, the distribution parameters for these are shown in Appendix I.1→I.5.

Typical results that can be produced by the whole system model, when simulated for a 35 year period are shown in Figure 7.9 →Figure 7.14.

Figure 7.9 shows a normalised heat map of the cost for the entire Bletchley Delivery Unit predicted by the model. The most expensive section is given a score of one and shown in

[25] Only the up fast was considered.
[26] Only the S&C units on the up fast route were considered in this study. Part of Bletchley to Bedford route is single track (reversible) this is also considered.

red, the least expensive is given a score of zero and coloured dark blue, see the colourmap on the right-hand side. It can be seen that the route between Bletchley and Bedford (BBM), which is mainly Category 5, is a very deep shade of blue, indicating a very low cost, the route between Cheddington and Rugby (LEC1) is a Category 1A route and is coloured green/yellow, indicating it has a much higher overall cost. At Rugby the WCML splits with one route going to Birmingham (RBS1) and the other towards Stafford and Manchester (LEC2), both of these routes are also category 1A but the tonnage that is on the route between Rugby and Cheddington is split between them hence they have a lower cost and are shown in light blue/green. The Northampton Loop (HNR) is formed of categories 2 and 3 and hence also has a relatively low cost, so is a dark blue. The highest costs (orange and red) only occur at a few distinct places on the railway corridor, most notably Hanslope Junction and the Kilsby Tunnel, there is a much higher cost in these areas associated with the additional cost due to TSRs (because of service affecting failures caused by S&C failures) and the increased maintenance volumes in tunnels due to the accelerated deterioration rates.

Figure 7.10 shows a breakdown of the track section costs for the first 400 track sections. Sections 1→367 make up the route between Cheddington and Rugby, all Category 1A. Sections 368 onwards make up the start of the route between Bedford and Bletchley, all Category 5. Hanslope Junction, a major junction on the WCML, containing 16 S&C units, all size G, is highlighted in the figure as well as the Kilsby Tunnel; the track sections containing these have a significantly higher cost. It can be seen that for Category 1A line the majority of the cost is spent on renewals, with ballast cleans, level 1 speed restrictions and sleeper maintenance also making up significant proportions of the overall cost. Additional costs for S&C maintenance can be seen for Ledburn Junction and S&C units in the Milton Keynes area. These switches have a lower failure rate than those at Hanslope Junction, as they are smaller in size. For the Category 5 track section it can be observed that the majority of the cost is due to sleeper maintenance.

Figure 7.11 shows a breakdown of the yearly cost for the 35 year simulation period. It can be seen that there is a gradual increase in cost between year one and eight, and beyond this the cost remains relatively constant. The initial variation is caused by the initial conditions, there is a disproportionately high number of assets in the good condition at the start of the simulation. The other interesting observation is that the penalty costs due to line closures gradually increase during the simulation period, this is due to ageing of the rails.

Figure 7.12 shows how the overall cost is split between TSRs, maintenance, inspections and renewals for Bletchley Delivery Unit. As with all of the asset models the biggest proportion of the total cost is renewals, however the difference between the proportion spent on maintenance and the proportion spent on renewals is much smaller than for the majority of the individual models. It can be seen in the system model that the inspection cost accounts for a far smaller proportion of the total cost than in the individual models. A breakdown of the inspections and inspection costs for all the assets in the system model is shown in Appendix E-1.1.

Figure 7.13 shows a plot of the Delivery Unit Condition based on the five condition states introduced in section 7.3.1.2. It can be seen that at the start of the simulation the initial conditions inflate the overall condition. There is an exponential decline in the overall condition of the Delivery Unit; the amount of time there is no speed restriction in place, gradually falls to zero. Also over time the probability that there is 'No Service' increases as the chance of there being a rail break somewhere in the route increases. This is caused by an ageing of the rail. The spikey nature of the figure was due to the same reason as in the asset model maintenance plots; the condition assessment did not align exactly with the inspection period, in periods after an inspection the condition was likely to be better as many repairs would have been performed, immediately prior to an inspection the condition is likely to be worse.

The final plot, Figure 7.14, shows the convergence of the overall cost. The system framework was simulated 1800 times, using a graphics processing unit (GPU) accelerated approach (this is discussed more in Chapter 8). It can be seen that after approximately 1500 simulations reasonable convergence is achieved. The system model was found to converge much faster than the individual track section model, a discussion of convergence is given in section 8.4, the system model was thought to converge faster as rare events such as rail breaks have a much smaller effect in the system model (due to the vast number of track sections modelled).

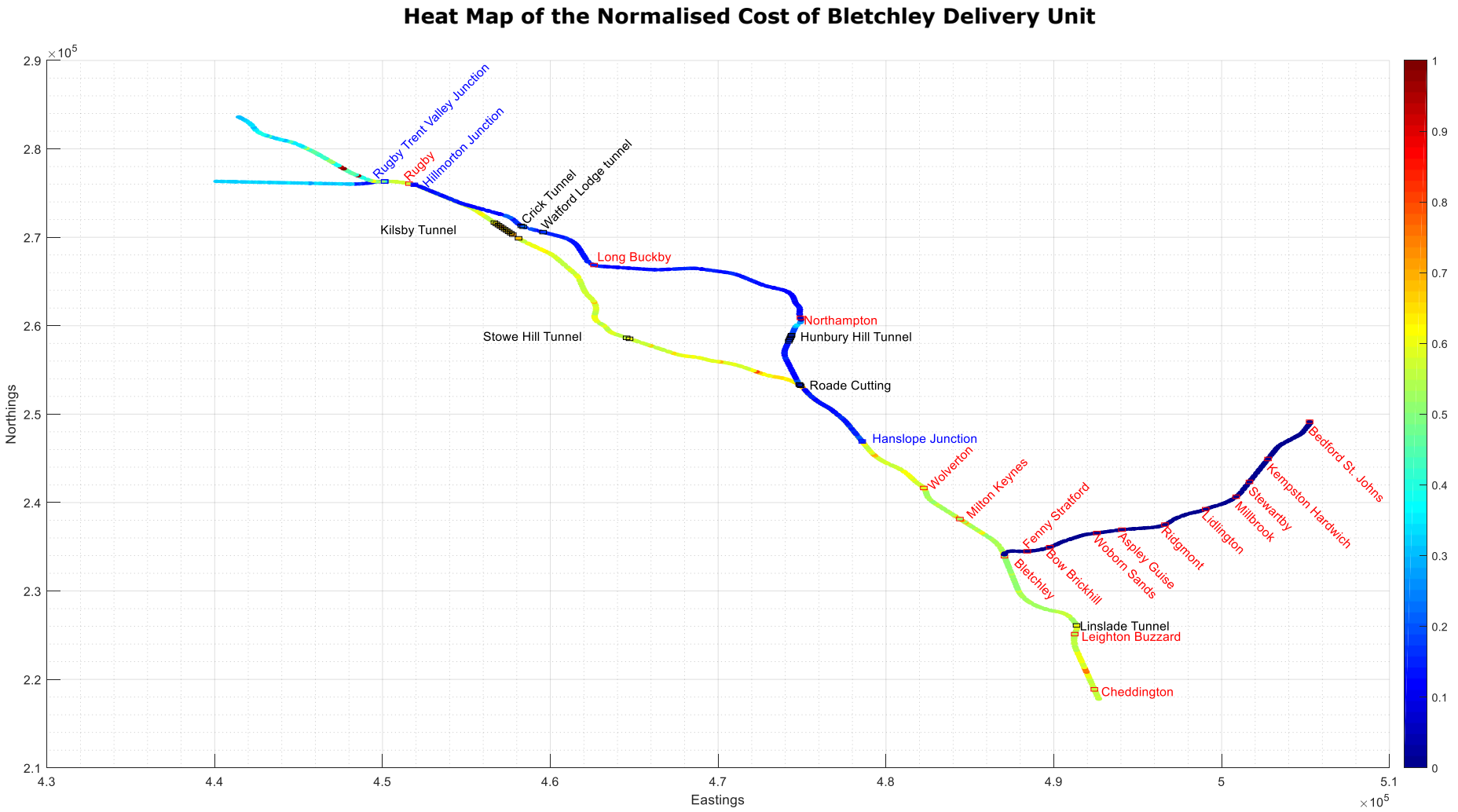


FIGURE 7.9: BLETCHLEY DELIVERY UNIT HEAT MAP OF COST, NORMALISED

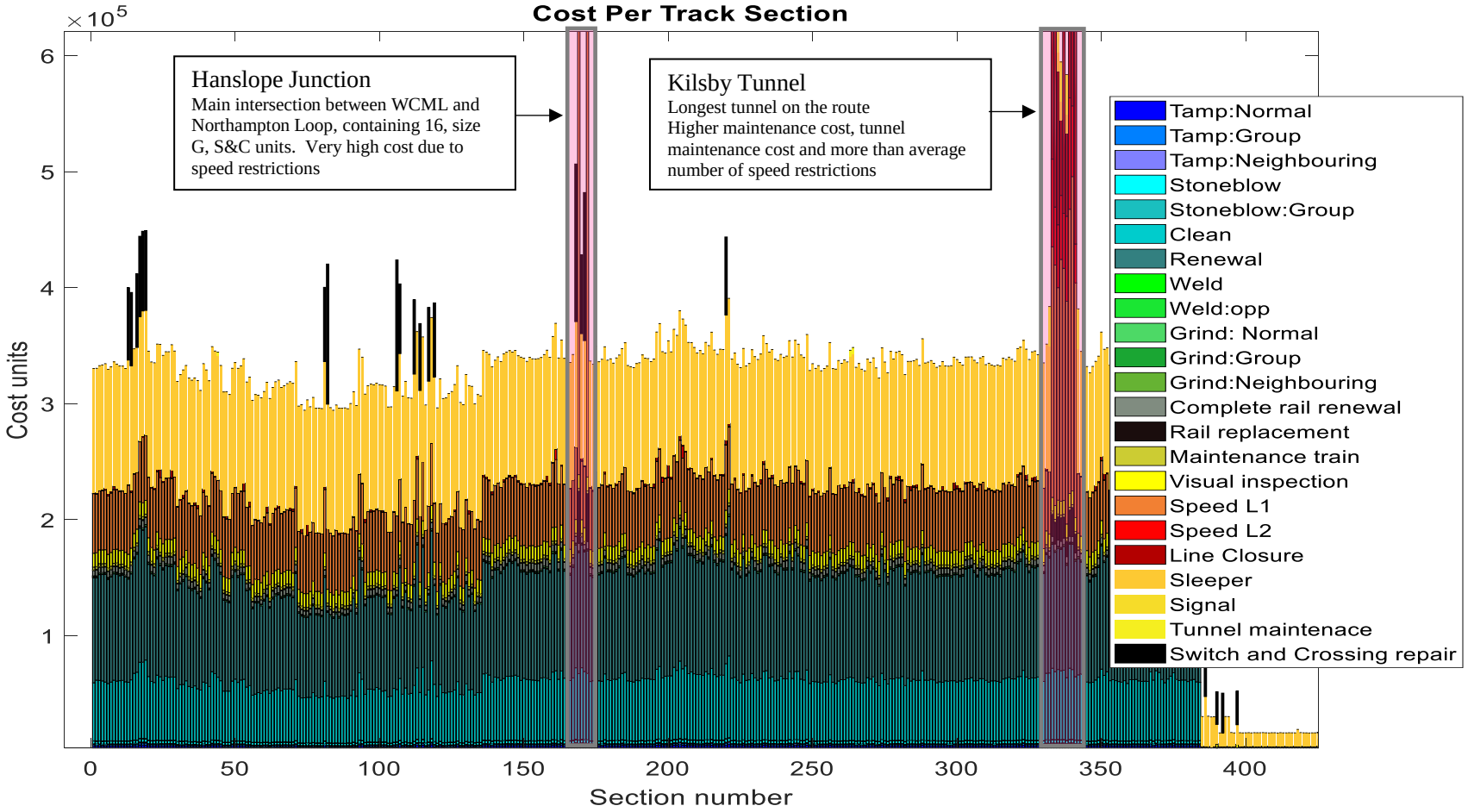


FIGURE 7.10: BLETCHLEY DELIVERY UNIT COST BREAKDOWN SECTIONS 1-400

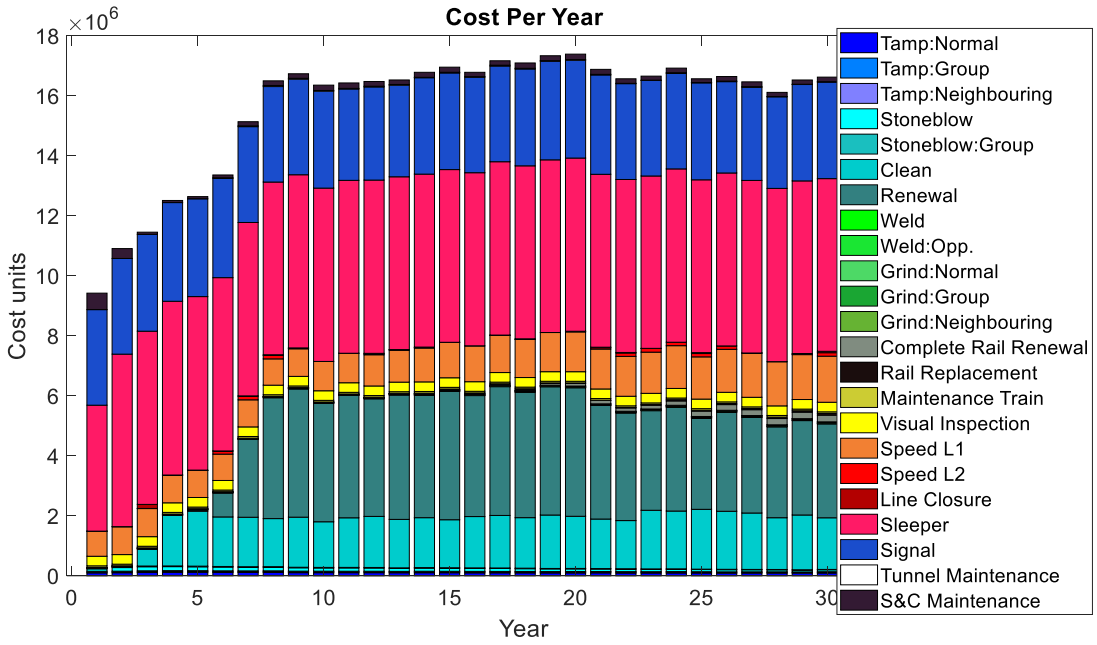


FIGURE 7.11: BLETCHLEY DELIVERY UNIT COST BREAKDOWN BY YEAR

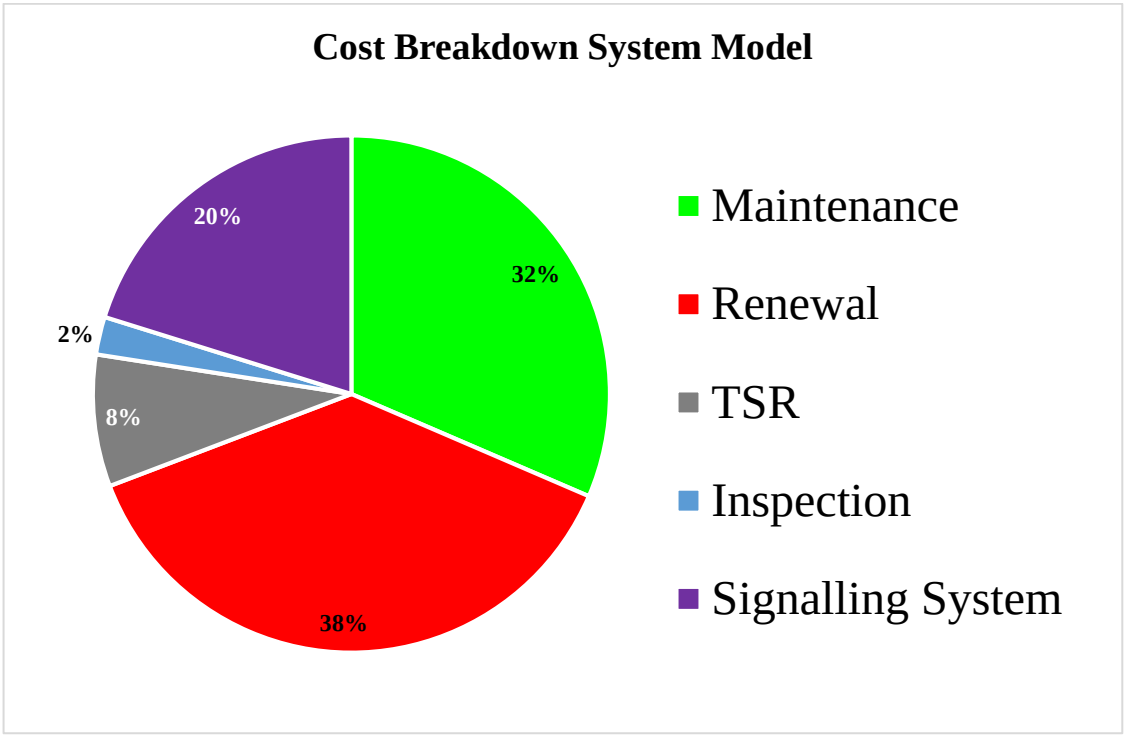


FIGURE 7.12: BLETCHLEY DELIVERY UNIT TOTAL COST BREAKDOWN

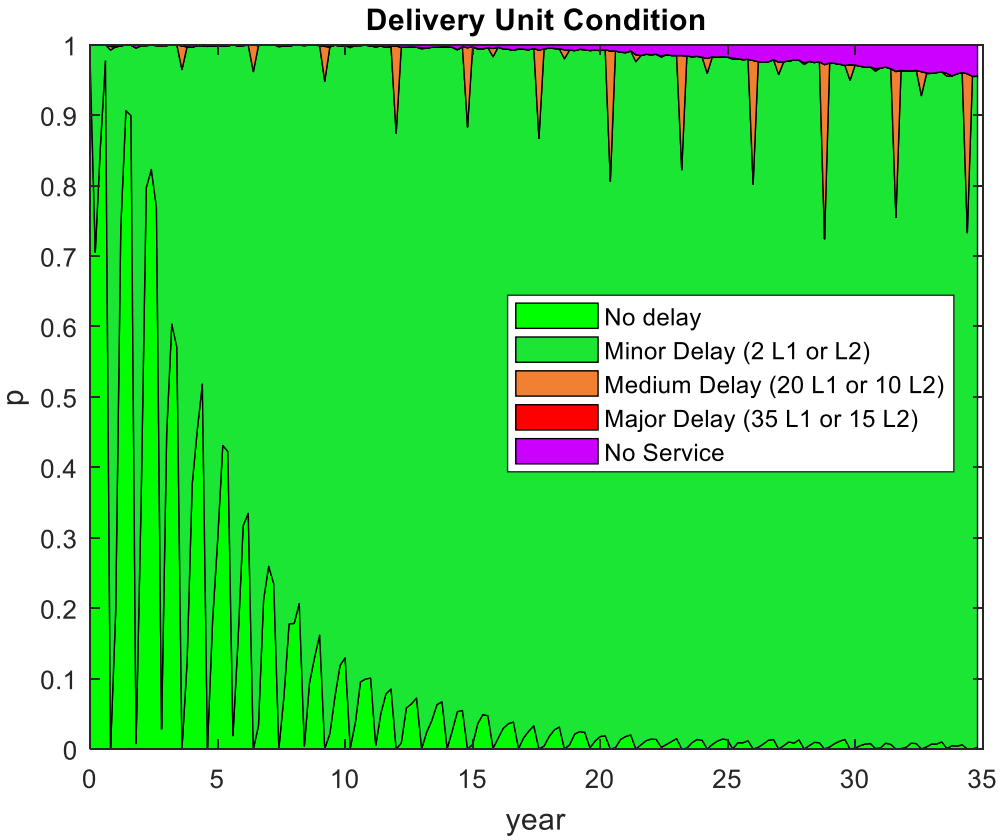


FIGURE 7.13: DELIVERY UNIT CONDITION

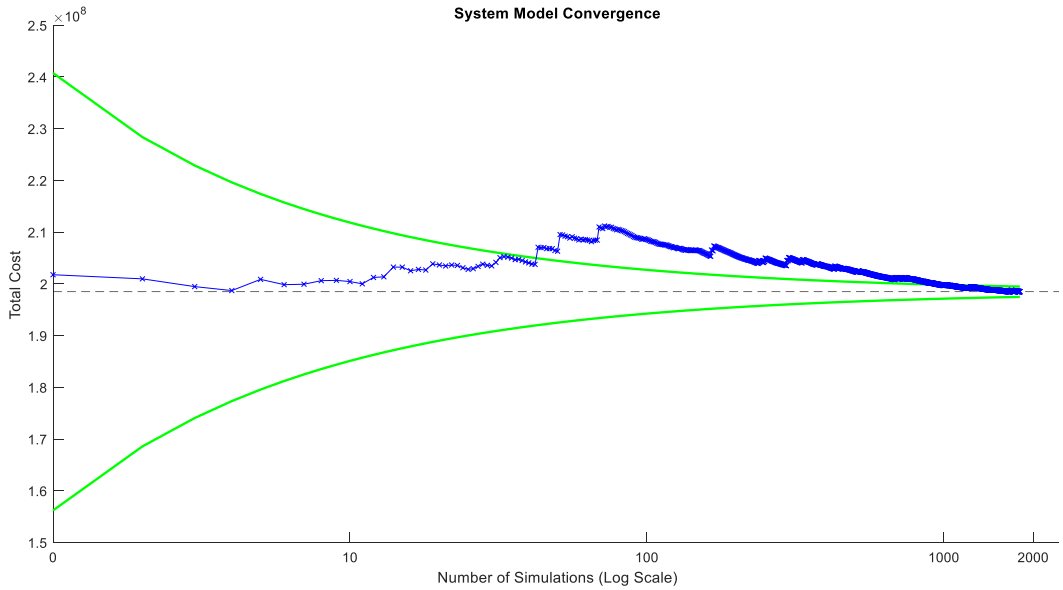


FIGURE 7.14: BLETCHLEY DELIVERY UNIT CONVERGENCE PLOT
KEY: ●95% CONVERGENCE BOUNDS ●RUNNING AVERAGE ●CONVERGED VALUE

7.5 Model Validation

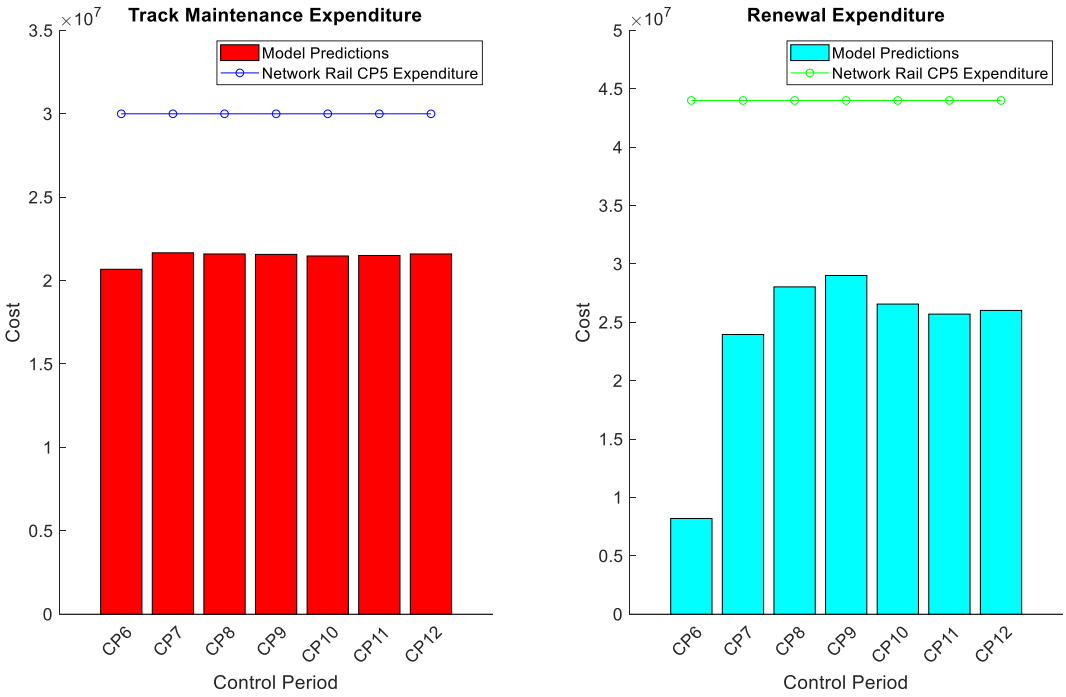
This section will provide some validation of the model results by comparing the outputs of the model to current practice. Two areas are considered. Firstly, the overall expenditure of the model is compared to Network Rail's CP5 expenditure. Secondly, a condition profile of the ballast predicted by the model is compared to an actual condition profile measured by the NMT.

7.5.1 Cost Outputs

Table 7.5 summarised Network Rail's assessment of CP5 expenditure. The expected expenditure on track was £30 million and the expected expenditure on renewals was £44 million. The yearly cost outputs from the Bletchley Delivery Unit system model (Figure 7.11) were compared against these values, the comparison is shown in Figure 7.15. To calculate the control period (five year) expenditure, the yearly cost outputs from the model were summed together in five year blocks. It can be seen that the track maintenance expenditure suggested by the model is between 21 and 23 million per control period, which is slightly less than the CP5 expenditure of 30 million, see Figure 7.15 (a). The reason for this is thought to be uncertainty in the cost assigned to the maintenance actions and due to some track maintenance such as drainage work not being considered. It can also be noted that the track expenditure does not vary significantly from control period to control period as the network usage is modelled as being constant and no consideration is given to inflation. The lower cost in CP6 is due to the initial conditions of the model artificially improving the condition of the assets, the asset condition quickly reaches equilibrium.

Figure 7.15 (b) shows a comparison between Network Rail's CP5 renewal expenditure and the model's predicted renewal expenditure. Assigning initial maintenance history was difficult and the initial conditions artificially reduced the maintenance history, leading to significantly lower renewal volumes in CP6. This also led to an increased number of track sections requiring renewal in CP9 as many were in the same initial state and hence needed renewing at similar times. The difference between the model's predicted outputs and Network Rail CP5 expenditure was thought to be due to three reasons:

(i) The model assigns a fixed cost to renewal, yet in reality there is significant uncertainty and variation in renewal costs.
(ii) The model did not consider enhancements.
(iii) The model did not consider drainage or earthworks renewals which may have contributed to Network Rail's CP5 track renewal expenditure.



(a) (b)

FIGURE 7.15: COMPARISON BETWEEN MODEL OUTPUTS FOR CP6→CP12 (35 YEARS) AND NETWORK RAIL'S CP5 EXPENDITURE ON RENEWALS AND TRACK MAINTENANCE

7.5.2 Ballast Condition Profile Condition

Comparing the condition outputs of the model to actual data is somewhat tricky as the data only provides a deterministic view of the asset's past, whereas, due to the variation in asset lifetime, the model produces a stochastic prediction of the future. To attempt to validate the results for the condition profile of the ballast, the condition profile prediction from a single simulation for a specific poskey was compared to historical records of that poskey's condition.

Network Rail provided geometry measurements from 2006 to 2016 for use in this study. Figure 7.16 (a) shows the vertical top geometry measurement (with 35 m filter applied) for poskey number 68621 which is located between Cheddington and Leighton Buzzard (see Figure 7.8). In the figure the horizontal lines represent the maximum threshold for the condition bound, so if the condition goes above the *'Good'* line then it enters satisfactory condition. From the figure two maintenance interventions can be identified, one in 2009 and one at the end of 2012. However it was difficult to match these interventions (condition improvements) to maintenance records in the Ellipse maintenance database. It was somewhat unclear why interventions were performed at these points; the condition was very stable leading up to the intervention in 2009 and following this intervention the condition quickly returned to the pre maintained condition. The intervention in 2012 had a much larger effect, and improved the condition for longer, however the alignment was still '*Good*' at the point of intervention. A possible reason for the early intervention is to keep the track alignment *'Good'*.

Figure 7.16 (b) shows the model output for the ballast condition for poskey 68621. The Petri net model contains discrete states and hence the geometry recorded is discrete. It can be observed in the model output the condition is initially in the '*Good*' state and maintenance is not considered until the condition reaches '*Satisfactory*', and in fact the section briefly enters '*Poor*' before being maintained. A second intervention is requested in 2029 when the condition again reaches satisfactory.

As mentioned comparing stochastic model outputs to deterministic historical records is difficult. Nonetheless some comparison between the historical condition records and the model outputs can be made. It can be seen that in a ten year period both have two interventions, it can also be seen that both heavily favour *'Good'* condition; the historical records showed the section to be in *'Good'* condition 100% of the time compared to 92.3% in the model. Based on these comparisons it was concluded that the model results were reasonable, and were certainly good enough to demonstrate the capability of the system model. The main difference between the model and the historical records is that the model does not consider maintenance from '*Good*' condition, whereas in reality maintenance clearly is performed even when the alignment is '*Good*'. Section 9.7.1 discusses how an alternative scheduling strategy could be considered in the model which allows maintenance from *'Good'* condition.



(a) (b)

FIGURE 7.16: COMPARISON BETWEEN THE BALLAST GEOMETRY RECORDED BY THE NMT AND A BALLAST PROFILE GENERATED IN ONE SIMULATION OF THE PETRI NET

In the future, further model validation can be performed by considering how historical data for each poskey can be matched to the model outputs for each track section, this could also help with refining location parameters as it would highlight sections that have traditionally performed differently. A means of comparing the average condition across all simulations against the historical records should also be considered, to ensure that the average predicted condition also matches historical records. A final consideration is that the maintenance records only covered a ten year period and the maintenance history prior to 2006 was unknown, if more data becomes available then model validation should be considered with a larger data set.

7.6 Discussion and Conclusions

The aim of this chapter was to combine the asset models presented in Chapter 6 to form a system framework. A three-level hierarchical framework is proposed to link the asset models together. The top level considers the master module and the signal model. The second level contains the track section models and the final level contains additional assets that are located within the track section, such as an S&C unit.

The chapter explored how each of the asset models presented in Chapter 6 could be converted into modules for use in the system hierarchy. Although the changes varied from asset to asset, there was a common theme to the changes that were needed, highlighting the ease with which additional asset models could be added in the future.

The chapter presented an application of the whole system framework to Bletchley Delivery Unit, a range of results were presented including a heat map and yearly cost breakdown plot. The outputs of the model can be used by asset managers to help understand which areas are costing the most, and allows them to see how the condition of their assets will change over the next 35 years. It also allows them to determine the budgets and maintenance interventions required to deliver a given condition profile.

The chapter concluded by comparing the outputs of the model to Network Rail's CP5 expenditure and comparing the predicted ballast condition profile to historical records of the ballast condition.

8 Simulating Large Petri Nets and Code Validation

8.1 Introduction

The thesis has presented asset Petri net models for a range of railway assets and explored how these models can be converted into modules for use in a whole system framework. This demonstrates that the Petri net framework has the capability to deliver a whole system framework and can model the functions required. Consideration is now given to the computational requirements that are needed to solve such large scale Petri nets, and the areas that might limit the size and complexity of the system model that can be solved.

The first part of this will scrutinise how the Petri net algorithm was implemented and explain three ways in which the code was validated, to ensure it was solving the model correctly. Then it will go on to explore the computation and areas that currently limit the size and complexity of whole system model that can be created. The chapter will conclude by investigating means to maximise and improve the computational performance through parallel programming, GPU acceleration and algorithm improvements.

8.2 Code Validation

Section 7.5 explained how the results were validated however, as the code was entirely developed during the project, it was important to validate the code to make sure it was simulating the Petri net correctly, before obtaining results. As it is not possible to calculate the exact solution, the Petri net code cannot be validated by comparison to a known result. Therefore a range of other means were used to validate the code. Three approaches were used:

(i) Calculate the solution to the system model in special cases.
(ii) Compare the results to proven software.
(iii) Compare general-purpose computation on graphics processing unit (GPGPU) results with central processing unit (CPU) results.

8.2.1 Calculating Solution in Special Cases

Generally it is not possible to know how the Petri net will evolve, however in certain '*special cases*' it is possible to predict the behaviour of the model, and know the results the Petri net should give. Three special cases were considered:

(i) Very large time between inspections (greater than the simulation length)
In the S&C module it is assumed that failures will be discovered immediately; therefore these events still occur, and have a cost; both to repair the component and due to speed restrictions while the component is in the failed state. Costs were also incurred from sections that are assumed to start in the degraded condition, as they are assumed to be known to be degraded. The results when the system Petri net

was simulated in this way are shown in Appendix H-1.1. Note in the system model, the risk of being in a degraded state is not considered.

(ii) Very slow degradation rate (significantly longer than the simulation length)
As the deterioration rate is slow, all assets will remain in good condition for the duration of the simulation, the only cost will be due to inspections. Furthermore, as the inspection interval is fixed and the cost of an inspection is known, it is possible to calculate the exact cost.

(iii) No maintenance machines
If no maintenance machines are available then certain types of maintenance for example tamping, cannot take place. The result when the system Petri net was simulated with no tampers is shown in Appendix H-1-2. It can be seen that no cost is incurred from tamping, but the cost due to TSRs increases as the condition of the ballast is poorer, as tamper requests are never met and so sections are never tamped, the lack of tamping also means that renewals are not requested.

In all three cases the results found, matched the expected outcomes and it was concluded that the code was not simulating the model in an obviously incorrect way.

8.2.2 Comparison to Other Codes and Software

The second method of validation was to compare the results of the code, for a simple Petri net, to a known result. A small Petri net was created (see Figure 8.1) and simulated using the code developed in this research. The Petri net was simulated 20,000 times and the number of tokens in the *expenditure* place was recorded after 100,000 time units. The results are summarised in Table 8.1. A mean value of 63,450 was also achieved from a number of other pieces of Petri net software, including the Macchiato software.

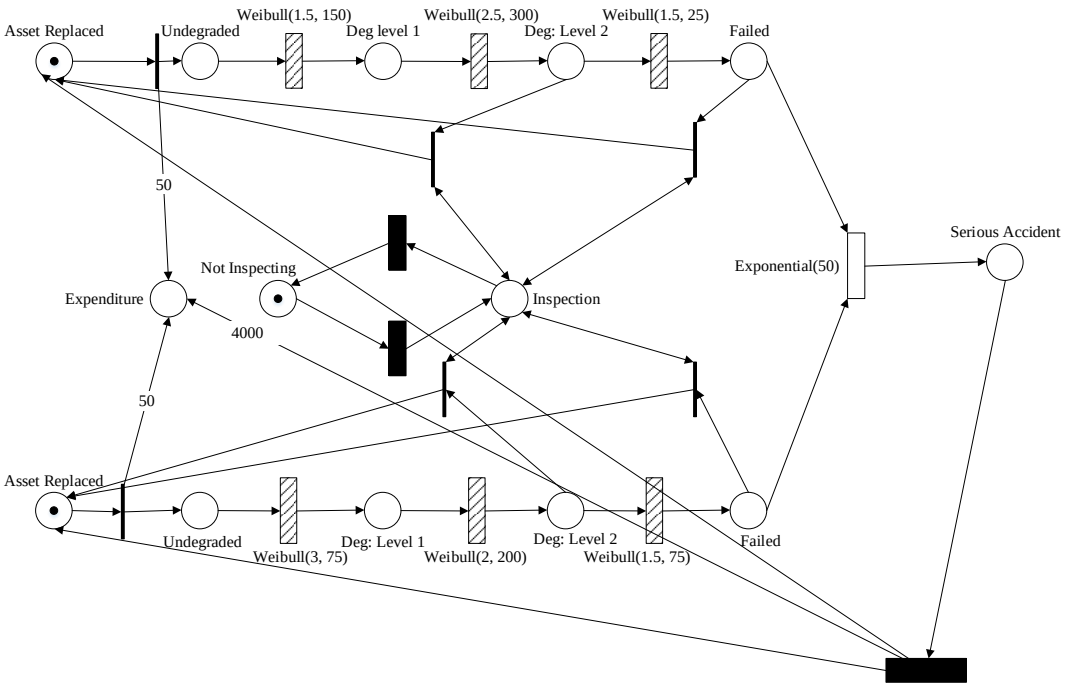


FIGURE 8.1: SAMPLE PETRI NET MODEL

	Mean	Minimum	Maximum
Expenditure Place	63,450	60,350	78,700

TABLE 8.1: MARKING OF THE EXPENDITURE PLACE AFTER 100,000 TIME UNITS BASED ON 20,000 SIMULATIONS

8.2.3 CPU V GPGPU Results

The final means used to validate the code was comparing the results of GPGPU (code performed on the graphics processing unit (GPU)) and code performed on the CPU. GPGPU coding is discussed more in section 8.3.4. The code had to be completely re-written to make it suitable for simulation on a GPU. However when the random number generator was seeded with the same value the GPU and CPU code gave the same results.

8.3 Reducing Computer Resources Required

The Petri net proposed for the whole system model was solved using Monte Carlo simulations. The resources (computation time and memory) required to solve such a large Petri net using Monte Carlo simulations can be prohibitive. This section will explore ways to reduce these issues and explore the factors that limit the overall size of whole system Petri net model that can be simulated.

To improve simulation time two methods were explored:

(i) Improving the Petri net structure and solution algorithm
This involved investigating which Petri net structures and parts of the algorithm were slow and improving them.

(ii) Parallel processing and GPGPU programming
This technique makes use of the fact that, as all Monte Carlo Simulations are independent, it is possible to perform multiple simulations at the same time (parallel) rather than sequentially (series).

8.3.1 The Petri Net Solution Routine

The first method used to increase the performance was to identify which Petri net structures and which parts of the solution routine were computationally expensive and investigate ways to improve these parts of the solution algorithm. To investigate the computation time a method of timing the code was required; the methodology implemented was the *Chrono Library*. The *Chrono Library* is a precision neutral library, the library contains three clocks; *system clock, steady clock* and *high resolution clock*. The *system clock* is not steady as the computer operator has the power to change this clock, furthermore the clock may automatically update for example moving from Greenwich Mean Time to British Summer Time, hence timing the program with the *system clock* is not recommended. Therefore the *steady clock* function was used to time the code.

8.3.1.1 Petri Net Structure

This section explores how the Petri net structure, the way the places and transitions are arranged affects the overall simulation time. There were found to be three factors that influenced the computation time needed to solve a Petri net model:

(i) The number of transitions in the model. To quantify the effect the number of transitions had on the simulation time a series Petri net loop (transitions and places connected one after another, where the n^{th} transition links the n^{th} place back to the first place) was created. The size of loop was increased from 100 transitions and 100 places to 1000 transitions and 1000 places. Increasing the size of the series loop did not affect the number of transitions that fired during the simulation period (number of steps). There was found to be a linear relationship between the number of transitions and simulation time as shown in Figure 8.3. The number of places was found to have a slight effect on the memory required but had very little impact on the overall computation time.

(ii) The number of transitions that fire in the simulation period (number of steps). To investigate this a Petri net loop of 100 transitions was used and the delay time of the transitions was reduced. This was also found to have an effect on the simulation time, see Figure 8.4. The relationship was not as obviously linear as with the number of transitions, however there was undoubtedly correlation between the two.

(iii) The complexity of the net. To quantify the effect of the complexity of the net, a Petri net was created with a collection of transitions in series, followed by a collection in parallel see Figure 8.2. Initially there were 900 transitions in parallel and 100 in series, the number of transitions in parallel was increased from 100 to 1000 (while the number in series was decreased from 900 to zero). In the original algorithm the Petri net structure was found to have little effect on the computation time, except when transitions were in an entirely parallel arrangement, see Figure 8.5. Arranging all 1000 transitions in parallel caused a tenfold increase in the computation time. This was due to there being a 1000 way transition conflict (see section 6.2.7) at every time step, whereas until this point there was a conflict, at most, every 100 time steps. When the *advanced algorithm* (see section 8.3.2) was employed it was found to be significantly faster when there were few transitions in parallel, however as the number of transitions in parallel was increased the speed up factor was reduced and indeed when all the transitions were arranged in parallel the *advanced algorithm* was found to be slower.

Finally, Figure 8.6 shows the effect of increasing the number of transitions **and** the number of transitions that fire (number of steps). This is a more realistic expectation of what would happen in an actual Petri net model; in the whole system model proposed, as the number of assets is increased the number of transitions and the number of transitions that fire **both** increase. It can be seen in this case the increase in computation time is initially exponential, until it reaches a *saturation point*, as initially both the number of transitions and the number of transitions that fire (number of time steps) is increasing. At the *saturation point* a transition is firing at every time step, and therefore it is not possible to further increase the number of time steps in the simulation period. As a result beyond the *saturation point* the computation time increase is linearly, as only the number of transitions in the net is increasing.

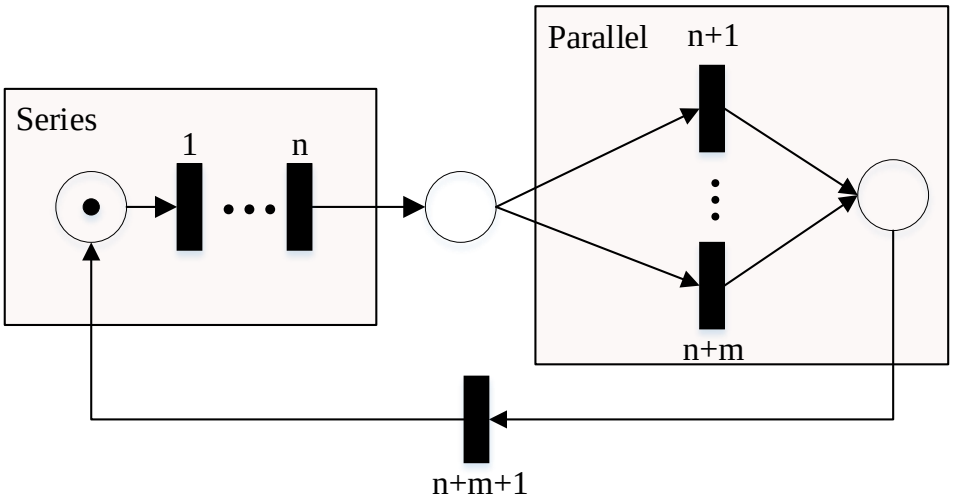


FIGURE 8.2: PARALLEL AND SERIES PETRI NET STRUCTURE

Effect of a range of Petri net charteristics on the simulation time

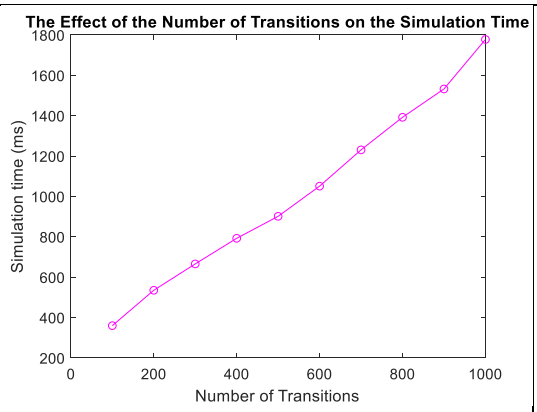


FIGURE 8.3: EFFECT OF THE NUMBER OF TRANSITIONS (CONSTANT NUMBER OF TIME STEPS) ON THE SIMULATION TIME

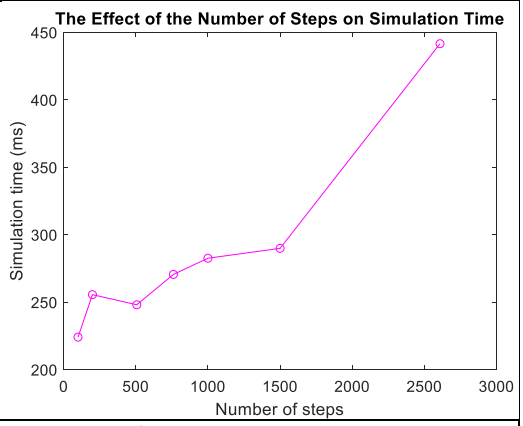


FIGURE 8.4: EFFECT OF THE NUMBER OF TRANSITIONS THAT FIRE (NUMBER OF TIME STEPS) ON THE SIMULATIONS TIME (CONSTANT NUMBER OF TRANSITIONS)

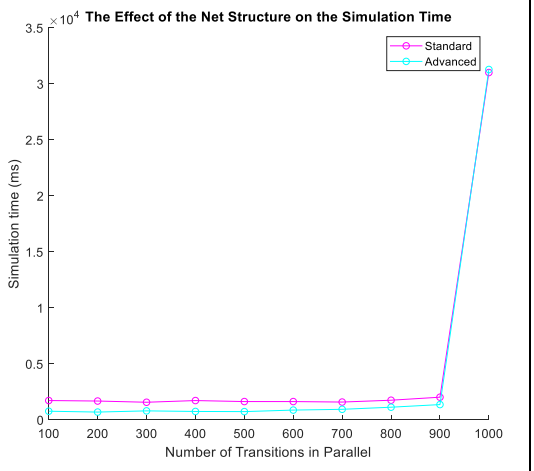


FIGURE 8.5: THE EFFECT OF A PARALLEL VS SERIES NET STRUCTURE (SEE FIGURE 8.2) ON SIMULATION TIME (CONSTANT NUMBER OF TRANSITIONS AND CONSTANT NUMBER OF STEPS)

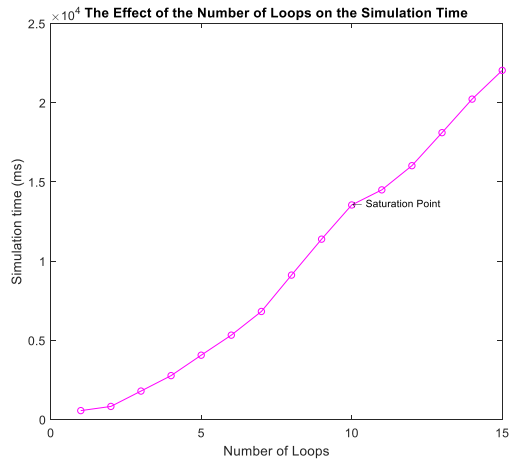


FIGURE 8.6: THE EFFECT OF INCREASING THE NUMBER OF TRANSITIONS AND THE NUMBER OF TRANSITIONS THAT FIRE (TIME STEPS) ON THE SIMULATION TIME

8.3.1.2 Petri Net Solution Algorithm

As well as the net structure the solution algorithm used was also investigated to determine which parts of the algorithm were slow and if they could be improved. A flowchart of the Petri net solution algorithm is shown in Figure 8.7. There are two main features that influence how long each function takes to run; the number of operations that are performed within the function and the type of operation.

Table 8.2 shows the computation time for a number of operations in C++ in the Microsoft Visual Studio IDE. Three operations in particular were identified as requiring significant computation time: generation of random numbers, dynamic vector operations (resizing) and vector sorting operations.

Within the Petri net algorithm Function 1 and Function 2 were found to require the largest amount of computation time. Function 1 had a long simulation time as it had to cycle through every single transition and perform checks to see if it was enabled, this led to a very high number of operations. Function 2 was found to take a long time due to the number of calls to the random number generator and due to calls to the sort function.

Operation	Time (ns)
Addition of two integers	293
Write one value to a vector	880
Write one value to an array	293
Generate one random number using the Mersenne Twister Engine	586
Find the minimum element of a vector size 100 (Generated using the Mersenne Twister Engine)	10,557
‘Push Back’ one element to a vector size 100	10,557
Sort a vector size 100 (Generated using the Mersenne Twister Engine)	120,525

TABLE 8.2: TIME TO PERFORM VARIOUS OPERATIONS IN C++ (USING VISUAL STUDIO, X64 BIT, DEBUG MODE)

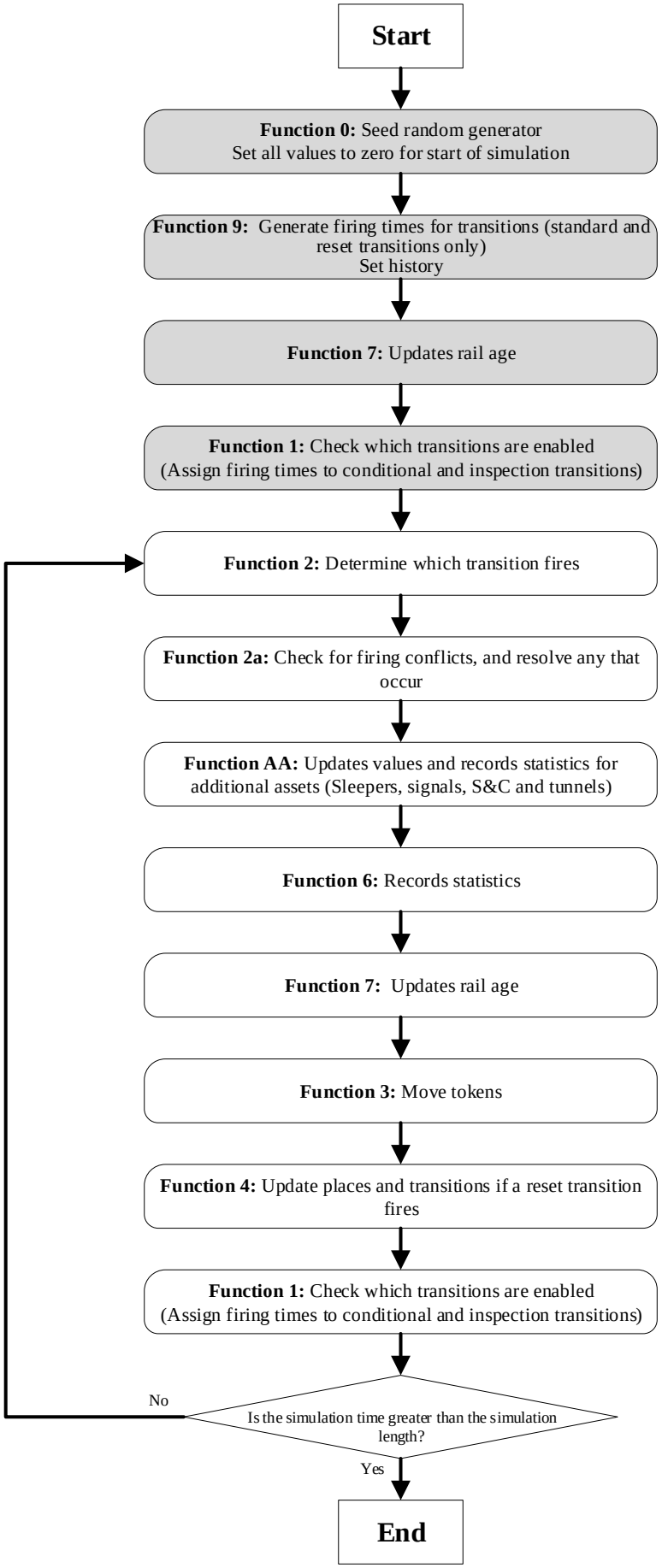


FIGURE 8.7: FLOWCHART OF THE PETRI NET SOLUTION ALGORITHM

8.3.2 Petri Net Solution Routine Improvements Implemented

The previous section highlighted how the structure of the Petri net as well as the Petri net solution algorithm can affect the computation time. To address some of these issues the following changes were made:

(i) Include inspection transitions. The inspection loop was found to be very inefficient as the network would be inspected regularly (weekly), however the condition of assets would often degrade slowly (years or even decades). So almost all the inspections would not reveal any defects, yet the inspection loop transitions would be firing at a very high frequency. This is a common problem when modelling inspections with Petri nets, hence a solution has been found: the Periodical Transition [158]. Periodical Transitions have two input parameters: the time from the start of the simulation until the instant the transition becomes able to fire, T, and the length of time between two periodic events such as inspections, p. The firing time is then equal to the remainder when T is divided by p. By replacing the inspection loop with a periodical transition the number of time steps was reduced and hence the overall simulation time was reduced.

(ii) Only checking a select number of transitions when deciding which transitions are enabled. Function 1 (the part of the algorithm which checks which transitions are enabled after a transition has fired) was found to be the slowest part of the solution algorithm, as it had to cycle through every transition and perform a range of checks on each transition to see if it was enabled. This process was often very inefficient as it checks all transitions even though very few will have changed. Therefore a means of checking only the transitions that could be affected was developed; the *'advanced algorithm'*. In the *'advanced algorithm'* each transition contained a list of all the transitions that could become enabled or become disabled if that transition were to fire. Only these transitions would be checked rather than the full net. It can be seen in Figure 8.5 that for nets with a limited number of transitions in parallel there was significant computational savings using the *'advanced algorithm'*. However the computation savings were much less for complex nets where the firing of one transition affected a high number of other transitions. There is a further drawback, for large complex nets each transition has many transitions that need to be checked and storing this list for every transition is memory intense.

(iii) The Petri nets were designed with the aim of limiting the number of transitions in parallel, however when modelling dependencies this becomes very difficult.

(iv) Function 2 was adapted to use a minimum element function rather than a sort function to determine which transition would fire first.

8.3.3 Parallel Programming

In the early days of computing performance, increases were achieved by increasing the speed at which the CPU could perform calculations, going from KIPS (Kilo instructions per cycle) to MIPS (Mega instructions per cycle) and then GIPS (Giga instructions per cycle). Figure 8.8 shows the increase in processor speed from 1980 to 2000. By 2019 the most advanced Intel processors such as the X-series processors run at up to 4GHz [159] and perform over 300 GIPS.

However there is a limit to the speed that the CPU can perform calculations; the speed of light argument can be used to argue a theoretical maximum speed. However currently the major limiting factor is heat transfer; '*Further improvements in microprocessor technology are currently limited by our ability to cool these tiny devices'* [160]. As such a new method of increasing performance has been developed; parallel processing through the use of multiple CPUs and multiple CPU cores. A multi-core processor is essentially multiple independent processing units in one. Multi-core processors allow independent tasks to be performed in parallel, which can dramatically reduce computation time. Figure 8.9 shows the difference between tasks computed in series (sequentially) and tasks computed in parallel. Computer programmers have long known about the benefits of parallel programming. Most computers, laptops and even smart phones now have multi-core processors allowing parallel processing and improving performance. Many CPUs have four or eight cores with the most advanced and up-to-date having 16-18 cores.

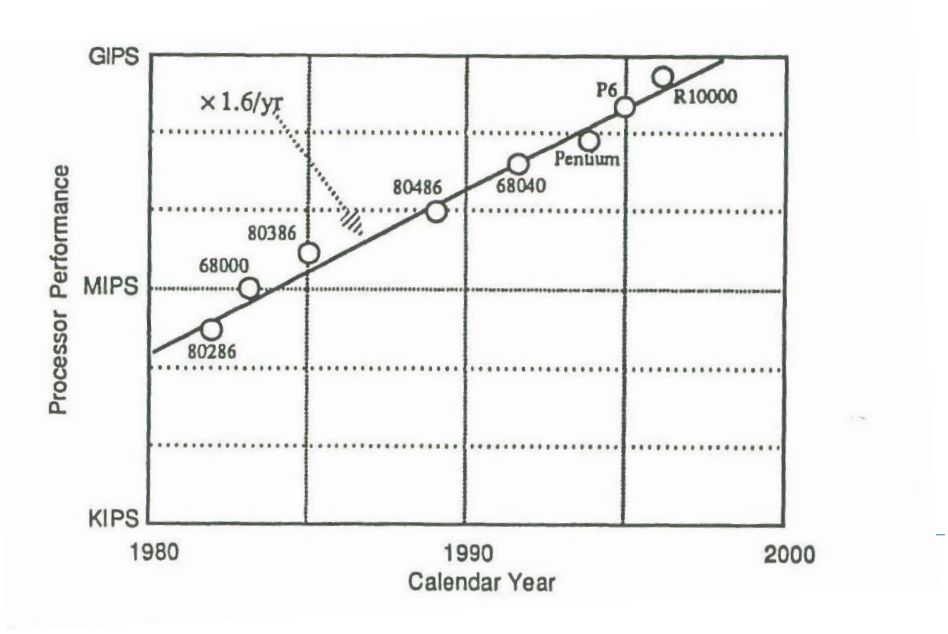


FIGURE 8.8: INCREASE IN PROCESSOR SPEED 1980→2000 [161]

The speedup factor achieved by adding more cores to execute computer tasks is however sublinear. The speedup factor is considered to follow Amdahl's Law [162]:

$$Speedup = \frac{1}{(1-f) + {}^{f}/_{s}}, \tag{8.1}$$

where

s is the speedup of the part of the task that benefits from improved system resources.

f is the proportion of execution time that the part benefiting from improved resources originally occupied.

Amdahl's Law implies that parallel processing is most effective when the number of parallel cores is small. Amdahl's Law and the heat transfer issues limit the number of cores that can be contained within a CPU. The increase in the number of cores has slowed down recently, hence computer programmers have looked for alternative ways to improve performance. One such method is GPGPU programming.

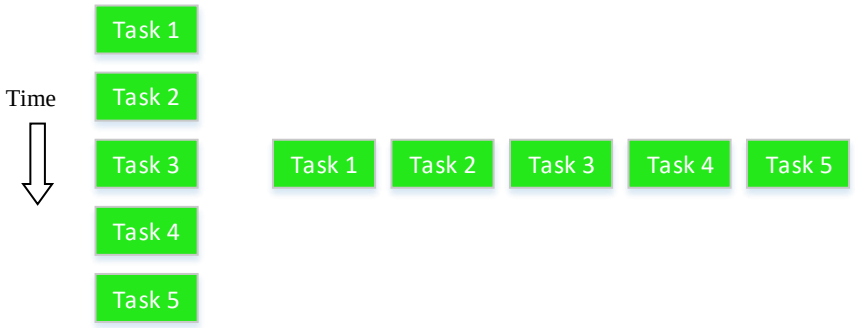


FIGURE 8.9: TASKS IN SERIES (LEFT) AND TASKS IN PARALLEL (RIGHT)

8.3.4 GPGPU Programming

In recent years there have been significant developments in the field of GPUs. As the computing power of GPUs has increased they have begun to be used to perform general purpose tasks, rather than the specific tasks they were designed for; this is known as GPGPU. As discussed, the number of cores within the CPU is limited to around 16-18 [159], however GPUs can have thousands of cores [163]. When referring to GPU and CPU programing, the CPU and random-access memory (RAM) is generally referred to as *host*, whereas the GPU and memory on the GPU is referred to as *device.*

GPUs were traditionally developed to rapidly create images and display them on screen. Originally GPU cores were far less powerful than CPU cores and so were only able to perform very simple tasks such as render a pixel. However in recent years the processing power of GPUs has rapidly increased and it is now possible to perform general computing tasks on a GPU. The capability of GPUs and CPUs is often measured according to two values:

(i) Memory bandwidth
This is the ratio at which memory can be read and stored. Normally measured in Gigabytes per second (GB/s)

(ii) The maximum computing power

This is the maximum number of floating point operations that can be performed each second (FLOPS) or trillion floating point operations per second (TFLOPS). Figure 8.10 shows how since 2008 GPUs have started to outstrip CPUs in both of these areas. This essentially means it should be possible to perform general purpose tasks on the GPU faster than on the CPU. Table 8.3 compares the two values for the CPU (Intel i3 3220) and GPU (Tesla K40) used in this research.

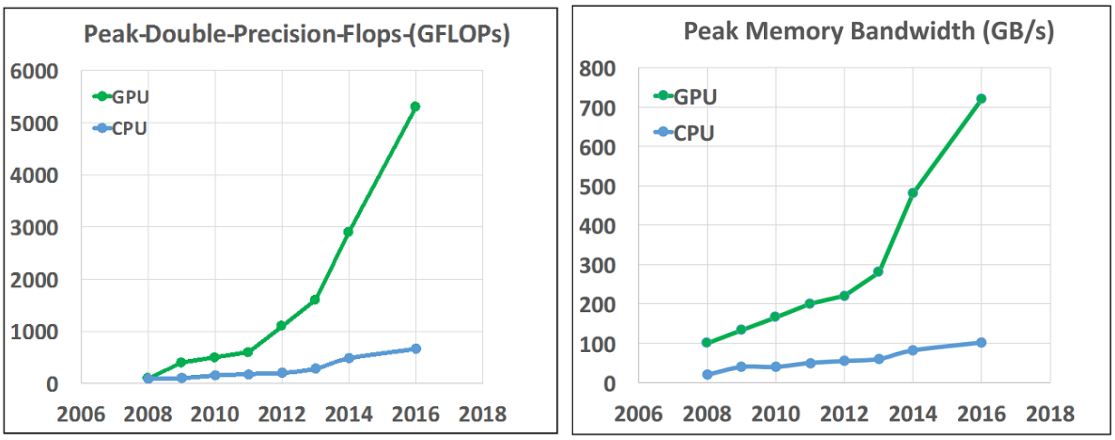


FIGURE 8.10: GPU V CPU GFLOPS FROM 2008 TO 2016 (LEFT) AND GPU V CPU MEMORY BANDWIDTH 2008 TO 2016 (RIGHT) [164]

	CPU Intel i3 -3220	GPU Tesla K40
Memory bandwidth (GB/s)	25.6	288
Maximum computing power (TFLOPS)	0.95	429

TABLE 8.3: CPU AND GPU USED IN THIS RESEARCH

Nonetheless GPUs are not designed to replace CPUs, they are designed to complement them. GPUs are good at dealing with data parallel computation intensive tasks whereas CPUs are good at control-intensive tasks [165]. The best results are achieved when the CPU and GPU work together, this is known as heterogeneous computing.

To be able to perform general computing tasks on the GPU an interface between standard C/C++ and the GPU is required. This is done using CUDA. CUDA is a computing language developed by NVIDIA to provide a programming interface to execute a wide range of tasks on the GPU. GPUs have many cores, however parallelising tasks on the GPU is not as simple as just running one task on each core. On a GPU the cores are located within streaming multiprocessors (SMs) and on each SM numerous threads are executed. The SM framework is grouped into grids, blocks, threads and warps as described below:

Grid

Collection of blocks.

Block

This is a collection of threads. They can be launched in one, two or three dimensions.

Thread

A thread on the GPU is a basic element of the data to be processed. By multi-threading we can process lots of data at the same time.

Warp

Is a collection of 32 threads. All threads in a warp execute the same code**.**

Figure 8.11 shows a possible grid, block and thread layout. The grid contains 27 blocks arranged in a three dimensional (3*3*3) cube. Each block contains 96 threads arranged into three warps. Hence there are 2592 threads in total.

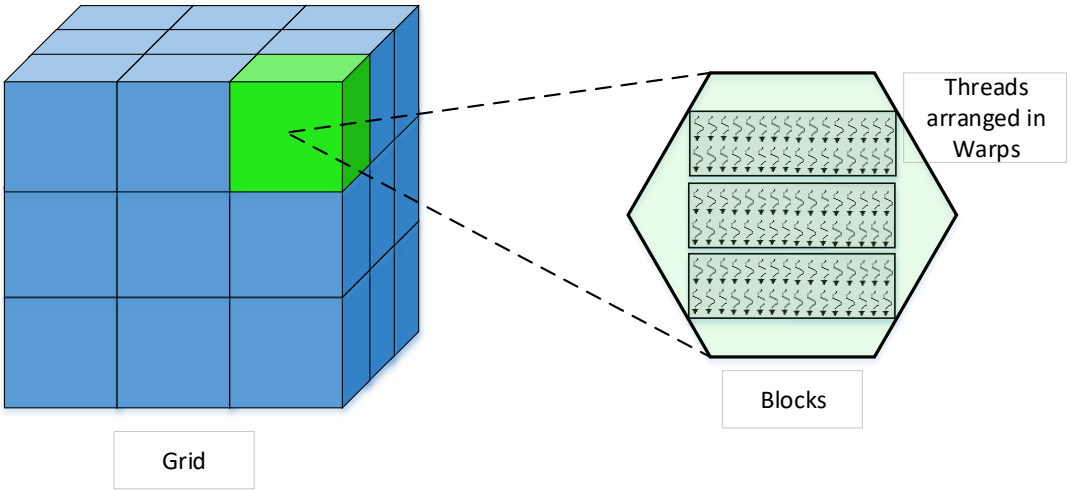


FIGURE 8.11: BLOCK, GRID, THREAD AND WARP CONFIGURATION

There are two types of GPU architecture: Fermi and Kepler. The more recent Kepler architecture will be focused on as the Tesla K40 uses the Kepler architecture. The Kepler architecture comprises 15 SMs. Figure 8.12 shows an SM schematic. Each SM contains:

(i) 192 Single precision CUDA cores (CUDA core)
Each CUDA core can execute one single precision floating point calculation per clock cycle.

(ii) 64 Double precision units (DP Units)
Each DP unit can execute one double precision floating point calculation per clock cycle.

(iii) 32 Special function units
These perform essential functions such as sine, cosine and square root.

(iv) 32 Load/store units
These calculate the source and destination of each half warp (16 threads).

(v) 4 Warp schedulers

(vi) 8 Dispatch units
When a *block* of threads is assigned to the SM the warp scheduler and dispatch unit split the threads into warps across the SM.

(vii) Instruction cache

(viii) Register file

Variables such as integers which are declared on the device are stored in the register file. Registers are the fastest memory on the GPU but there is very limited space available in the register file.

(ix) Shared memory/L1 cache

All cores in the SM have access to this memory.

(x) Read only constant memory/Data cache

The values stored in constant memory cannot be changed during the simulation.

(xi) Read only texture memory (TEX)

TEX is similar to constant memory however it is designed specifically for memory access patterns that have high spatial locality [166]. In simple terms this means a thread is likely to access memory 'near' to the memory the thread before used.

Each SM can schedule 64 warps (2048 threads) per time step.

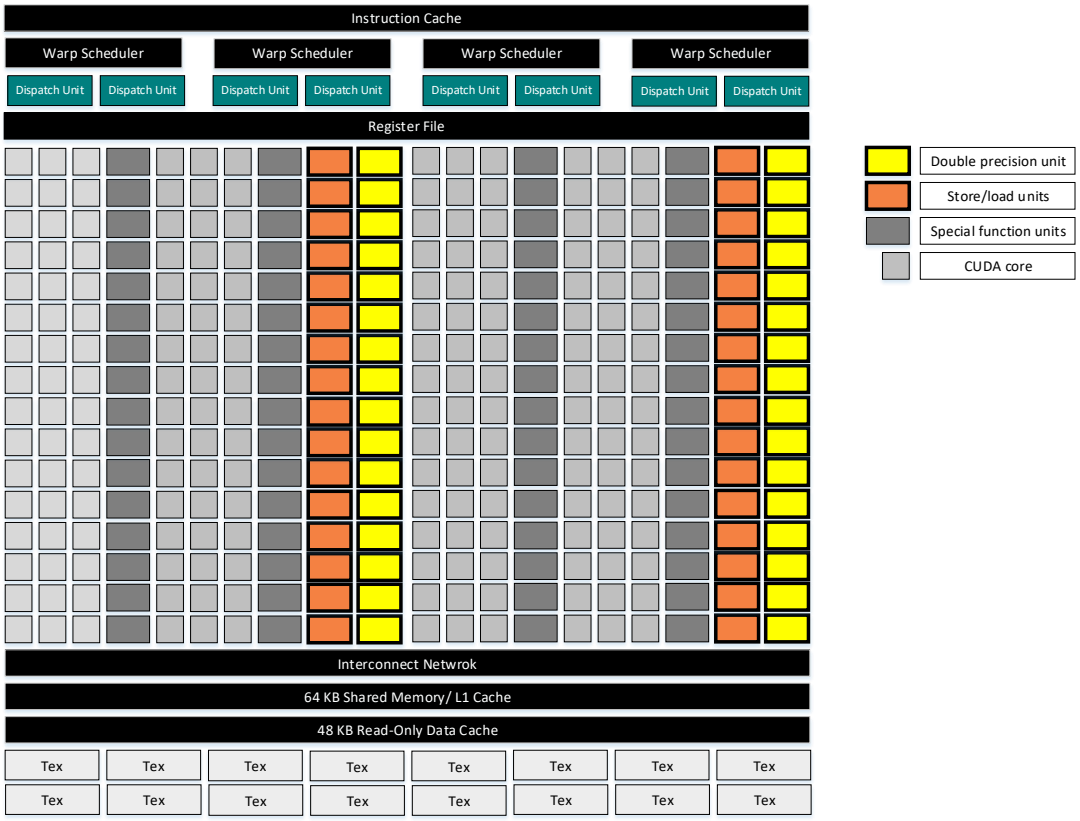


FIGURE 8.12: KEPLER STREAMING MULTIPROCESSOR

The Tesla K40 has 15 SMs which are arranged as shown in Figure 8.13. The L2 cache is memory shared by all 15 SMs hence all threads have access to values stored in here. The GPU and CPU interact through the peripheral component interconnect (PCI) express interface on the motherboard.

The complex arrangement of the GPU makes writing efficient GPU code difficult and it is often not straightforward to determine which code structure will be most efficient. To achieve the most efficient code the best kernel (grid, block and thread) structure is needed as

well as the correct memory allocations. There are two main factors that are needed to achieve good performance on the GPU:

(i) Reduce the number of read/writes between the host and device
(ii) Maximise the occupation of the kernel

As the GPU can perform a very high number of FLOPS often it is not possible to copy the variables to and from cache fast enough and therefore the maximum computing power of the GPU is not reached. This is known as memory bottleneck. TEX and constant memory can be used to reduce this.

For best performance all the cores should be calculating all of the time. However if care is not taken when creating GPU code then many of the cores may become idle during the simulation, this is called latency. Latency is the number of clock cycles between an instruction being issued and it being completed. During this time the core is not doing any work, the warp has stalled. However if there are multiple warps in the SM, then when one warp stalls calculations can be performed on another warp. This is only possible if there are sufficient warps on the SM. This is known as latency hiding; it is very important to have high levels of latency hiding to obtain high levels of efficiency. Little's Law shown in equation (8.2) gives an approximation of the number of threads required to hide latency, where throughput is the number of calculations per second measured in TFLOPS.

$$\text{Number of required warps} = \text{Latency} * \text{Throughput} \tag{8.2}$$

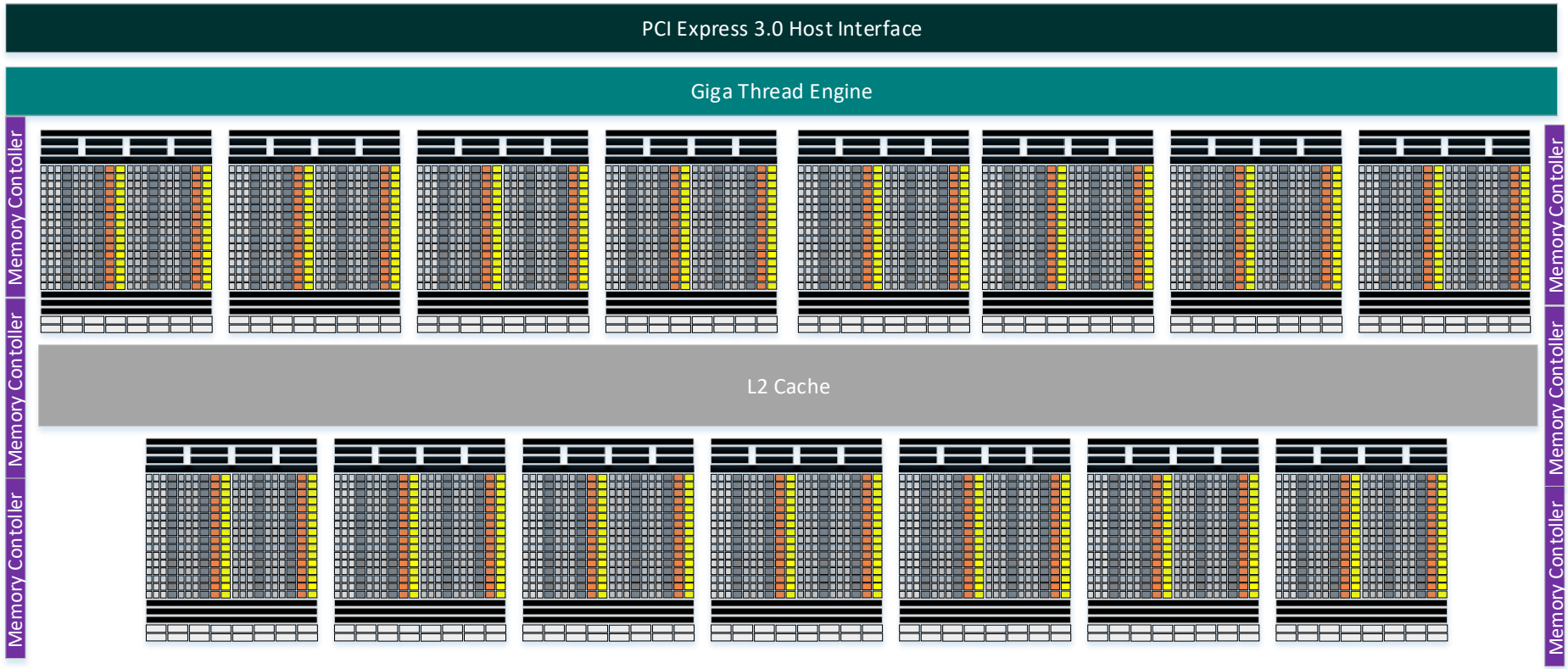


FIGURE 8.13: TESLA K40 SCHEMATIC, COMPRISING 15 MSS

8.3.4.1 GPU Applications

Due to their potential computation time reduction there has been considerable interest in GPUs in areas where computation time limits performance. Barash et al. [167] used a GPU to apply the population annealing algorithm to calculate internal energy, specific heat, magnetisation moments, entropy and free energy of the 2D Ising model on a square lattice. The population annealing method is a hybrid method combining Markov Chain updates with population control. The complete algorithm is given in [167]. There are three computationally heavy parts of the algorithm that are of interest in terms of GPGPU:

(i) Resampling of the population
(ii) Updating the configuration using Markov Chain Monte Carlo
(iii) Recording results

Barash et al. implemented the algorithm on an Intel Xeon E5-2683 CPU and Tesla K80 graphics card (both high-end products). The results are summarised in Table 8.4 for the single spin code (SSC) and multi spin code (MSC). The results show that the GPU implementation of the MSC achieves a peak speedup of about 2400, as compared to the scalar program.

Lattice Size	CPU	GPU			
	t (ns)	SSC		MSC	
		Time per spin flip (ns)	Speed-up	Time per spin flip (ns)	Speed-up
16	23.1	0.092	251	0.0096	2406
32	22.9	0.094	243	0.0095	2410
64	22.6	0.095	238	0.0098	2306
128	22.6	0.098	230	0.0098	2306
256	22.5	0.099	227	0.0098	2295

TABLE 8.4: GPU V CPU [167]

GPUs have also been used to speed up Petri net algorithms. Yianni [168] proposed a detailed Petri net for modelling bridge asset management. He used GPU programming to speed up the simulation of his bridge asset management model. The results are summarised in Table 8.5.

Device	CPU (1 core)	CPU (4 cores)	GPU (Tesla K40)
Simulation time (s)	16.51	4.358	0.886

TABLE 8.5: GPU V CPU FOR SOLVING BRIDGE ASSET MANAGEMENT PETRI NET [168]

The speed up on the GPU was significantly less than that achieved in the population annealing algorithm however there was still an 18.6 times increase compared to the single core code. Yianni noted a number of reasons why using a GPU to implement a Petri net algorithm might be inefficient:

(i) Large amounts of data were needed to simulate such a large Petri net, leading to latency.
(ii) There were imbalanced workloads (work was not well balanced between the GPU and CPU to get maximum performance from both).

Chalkidis et al. [169] proposed a hybrid Petri net to simulate biological pathways. A hybrid Petri net is a combined, discrete and continuous Petri net; in a continuous Petri net the place markings are not restricted to being integer tokens. Chalkidis et al. investigated several randomly-generated biological models consisting of a varying number of processes. Figure 8.14 shows how the computation time was impacted by the number of processes simulated, for both a GPU and CPU model.

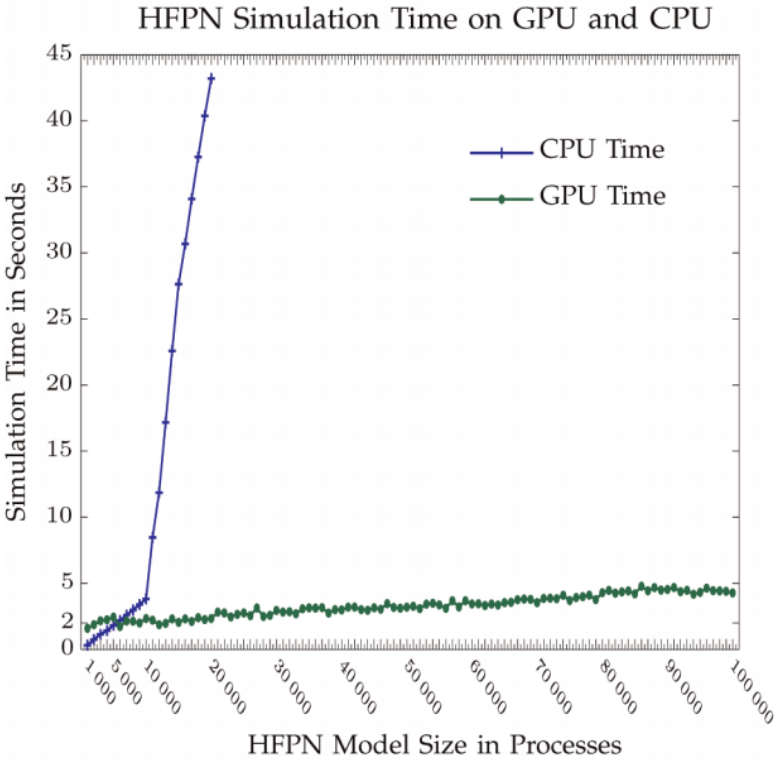


FIGURE 8.14: CPU V GPU SIMULATION TIME FOR RANDOMLY GENERATE BIOLOGICAL MODELS WITH VARYING NUMBERS OF PROCESSES [169]

Their results produced a number of key findings. Firstly, as expected as, the number of processes increased, the simulation time for the CPU model increased linearly. The change in gradient at 10,000 processes is due to a change in the optimisation level of the GNU gcc-compiler used. Furthermore beyond 20,000 the GNU gcc-compiler was unable to compile on the CPU due to the size. By contrast the GPU performance remains near constant as the number of processes is increased, as it can run them in parallel. For a small number of processes the CPU performs better, however after approximately 5,000 processes the GPU performance becomes superior. Like Yianni, the speedup factor was found to be about 18 times (at 20,000 processes).

8.3.5 Parallel Processing in this Research

The Petri net model proposed is solved using Monte Carlo Simulations. Based on the suggested benefits seen in the literature it was decided to explore solving the Petri Net in parallel, both on the CPU and GPU. An Intel i3-3220 and Tesla K40 GPU were used to solve the Petri net model. To investigate the benefits of parallel processing four methods of simulating the Petri net were considered:

(i) All simulations run in series on CPU.
(ii) All simulations run in parallel on the CPU.
(iii) All simulations run on the GPU.
(iv) Simulations run on the CPU and GPU heterogeneously.

The results of the four methods are shown in Figure 8.15, the analysis was performed on a reduced version of the system model and a simulation period of just one year. The simulation time of the full model is detailed in the next section.

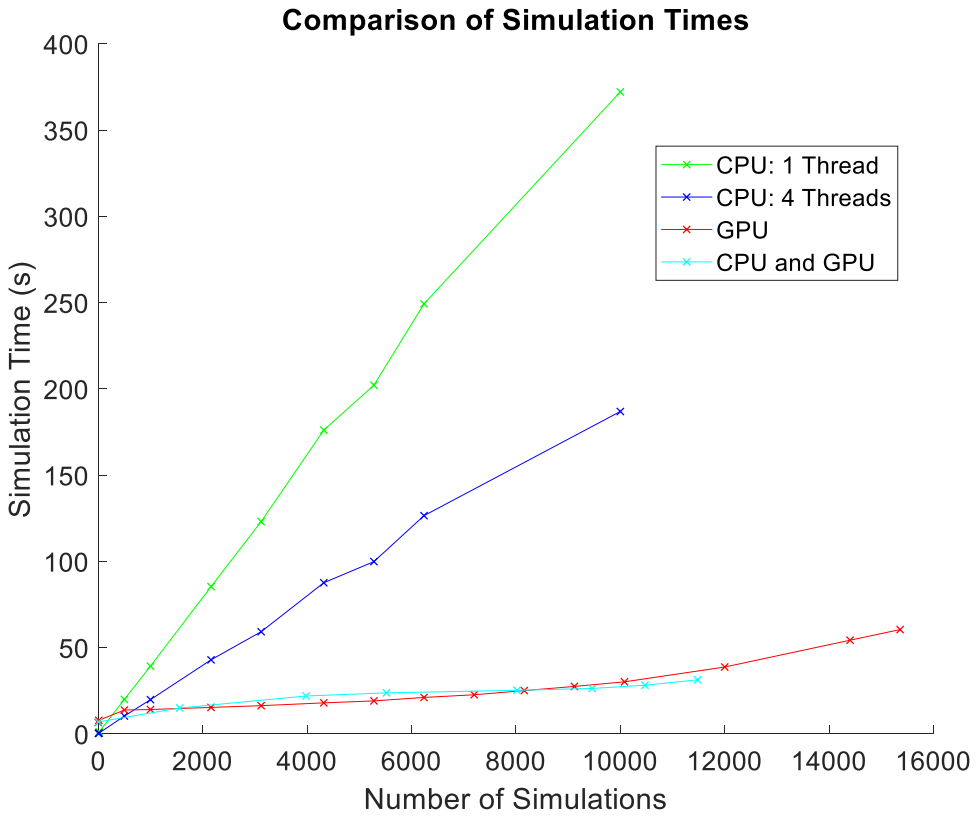


FIGURE 8.15: SIMULATION TIME FOR VARIOUS CPU AND GPU SETUPS

The following key conclusions were drawn from the analysis:

(i) For simulations performed on the CPU there is a linear relationship between the number of simulations and the simulation time.
(ii) The speed up factor achieved using four CPU threads compared to a single CPU thread was about 2.8 times. This was less than the expected four times increase due to overheads in managing the threads.
(iii) For the GPU the simulation time was largely constant as the number of simulations was increased. This was because more and more threads could be launched.
(iv) For a low number of simulations the CPU performed better than the GPU.

The analysis also revealed that there were a number of issues with solving the system model using GPGPU:

(i) Maximum benefit from the GPU was achieved with a very high number of simulations, however to perform a high number of simulations, a large amount of

memory is required; all of the information on all of the nodes for all of the simulations is required to be in memory simultaneously. The memory required to simulate on the GPU meant that for the system model the number of parallel threads that could be launched was limited, only about 1200 threads could be launched in parallel on the GPU to solve the system model.

(ii) GPU code does not allow dynamic resizing of vectors (all vectors must be defined at compile time). This had two limitations, firstly many of the algorithm improvements discussed could not be implemented or at least not implemented as effectively as in the CPU code. It also meant that all vectors had to be created to accommodate the largest value possible and this meant memory was not allocated effectively adding to the memory issue (discussed in (i)).

(iii) The whole system framework led to a very complex Petri net structure with the firing of many of the transitions affecting a large number of others. This was especially noticeable in the master module, where the firing of transitions in the master module could affect 1000's of other transitions. This means the advantages of the *'advanced algorithm'* were limited in the system model. There were also memory issues around the *'advanced algorithm'* in the system model due to the high amount of memory required to contain the vast amount of information needed for the *'advanced algorithm'*. As such the *'advanced algorithm'* was not used in the GPU code.

(iv) The Petri net algorithm for the system model did not appear to be well suited to GPGPU; there appeared to be a high level of latency as the speedup factor was considerably less than that achieved in the literature.

The above highlights that one of the main issues when using GPGPU is the memory required. To reduce the amount of memory required, it was decided to combine several pieces of information in the same integer, as opposed to using an array or vector, for example:

```
int C[9] = { 1,1,1,0,0,0,1,1,1 };          (8.3)
int D =  111000111;                         (8.4)
```

It would be possible to use equation (8.3) or (8.4) to record the same piece of information however the first method requires (9*4) =36 bytes, but the second requires four bytes. An integer can store values up to nine digits. This method only works, however, when values of the array are strictly between zero and nine, for example:

```
int C1[4] = {6,34,321,20};                  (8.5)
int D1 =  63432120;                         (8.6)
```

There is no easy way of splitting the integer D1 back into the four values expressed in array C1.

Algorithm 8.1 shows how the *enabled* vector was processed when the information for nine transitions was combined into a single integer. This method is used for the *enabled* and *fire* vectors as their elements are binary, it is not used for the *delay time* vector as the delay time is not restricted to a Boolean. Although using this method reduced the memory requirement it came with a time cost, as for each transition Algorithm 8.1 would have to be implemented to test if it was enabled and implemented again when the transition fired.

Algorithm 8.1

element = Floor((*n* + *i*) / 9);
ad = *n* + *i* - (9 * element);
x = pow10(*ad* + 1);
y = ENABLE[Floor((*n* + *i*) / 9)] % x;
y = y / pow10(*ad*);

where *%* finds the remainder and the function *pow10*, raises 10 to the power of the input argument

8.4 Convergence Rates

All the solution methods so far have performed a fixed number of simulations and the previous sections have discussed reducing the simulation time by increasing the number of simulations performed in a fixed amount of time. An alternative way to reduce simulation time and indeed the memory required is to stop simulating once a sufficient level of convergence is reached. If this approach is taken then means to reduce the simulation time by increasing the convergence rate of the model can be explored.

The convergence of Monte Carlo simulations can be assessed in a number of ways. In this research the convergence was be assessed based on the variance of the sample, $\bar{s}$, (with respect to the sample mean) divided by the square root of the number of simulations *N* based on equation (3.21). The convergence criterion, ζ, was determined by considering this value as a proportion of the sample mean, $\bar{x}$, as shown in equation (8.7).

$$\zeta = \frac{\bar{x}\sqrt{N}}{\bar{s}} \tag{8.7}$$

All the models presented were executed for a specific number of simulations and the convergence criterion, ζ, was assessed afterwards. However, it could be possible to set the level of convergence required, ζ_{crit}, before simulation and stop simulating once the value of ζ was smaller than ζ_{crit} hence reducing the number of simulations required. However this would be difficult to implement with a highly parallelised code as it would not be possible to calculate the convergence criterion after each simulation, only at the end after all simulations had finished. For this reason a convergence criterion was not used to determine the number of simulations complete, a fixed number of simulations was chosen prior to simulating.

The convergence criterion, ζ, after 2000 simulations for each of the individual models and the system model is given in Table 8.6 for comparison. As discussed it can be seen that the track section model is the slowest to converge whereas the system model is one of the fastest. The track section model is slow to converge due to rare events (rail breaks) leading to a very small number of simulations having a significantly high cost. In the system model, as the track section model is repeated many times, the same effect would only occur if a rail break happened in all track sections in the same simulation, which never occurs.

8.5 Simulation Times

The complete system model was solved heterogeneously on the CPU and GPU, with the algorithm improvements and Petri net structure improvements discussed in section 8.3.2 applied. The memory reduction method in the previous section was also applied to the GPU code. It took about nine days to simulate the complete whole system model 1800 times (1200 GPU simulations and 600 CPU simulations) for a 35 year period and used up to 12GB of device memory and up to 15GB of host memory. Table 8.6 shows the simulation time and convergence criteria, for each of the asset models, alongside the simulation time for the system model both with and without GPU acceleration.

The speed up factor achieved by the GPU in solving the complete system model compared to the single threaded approach was 8.20 and the speedup factor compared to the multi-threaded code (four threads) was 2.73. The low speed up factor was down to three reasons:

(i) The '*advanced algorithm'* could not be used in the GPU code.
(ii) The memory saving method used to allow GPU simulations, reduce the GPU performance.
(iii) Poor latency hiding.

	Module	Number of Places	Number of Transitions	Number of Conditional Transitions	Number of Reset Transitions	Number of Probabilistic Transitions	Number of Conditional Probabilistic Transitions	Number of Simulations	Simulation Period (Years)	Complete Simulation Time (Minutes)	Time for One Simulation (Milliseconds)	Convergence Criteria[27]	
												$\frac{\bar{s}}{\sqrt{N}}$	ζ
1	Master	31	43	0	0	0	0	n/a	n/a	n/a	n/a	n/a	n/a
2	Track Section (Category 1A)	99	93	21	14	3	7	50,000	50	0.550	0.660	2347	1.141
3	Concrete Sleeper (Category 1A)	31	33	1	5	0	1	50,000	50	4.634	5.561	432	0.270
4	Wooden Sleeper (Category 1A)	24	26	1	3	0	1	50,000	50	3.459	4.151	747	0.506
5	Steel Sleeper (Category 1A)	32	31	2	5	0	1	50,000	50	4.397	5.277	1079	0.689
6	Tunnel	14	16	0	1	0	0	n/a	n/a	n/a	n/a	n/a	n/a
7	S&C (Size D)	78	68	4	4	0	0	50,000	50	6.115	7.338	11	0.005
8	Signalling	21	10	0	0	0	0	50,000	50	4.469	5.363	49,248	0.027
9	System Model	133,596	134,279	18,073	16,295	1698	7641	**1000**	35	17,554	1,053,240	n/a[28]	n/a
10	System Model with GPU Acceleration	133,596	134,279	18,073	16,295	1698	7641	**2000**	35	12,841	385,224	498,598	0.251

TABLE 8.6: SUMMARY OF MODELS AND SIMULATION TIMES

[27] After 2000 simulations

[28] Only 1000 simulations run, so not possible to calculate the value after 2000 simulations, however the value would be the same as the GPU accelerated approach.

8.6 Summary and Conclusions

The aim of this chapter was to explore the solving of the whole system Petri net framework proposed, and to explore the factors that might limit the size and complexity of model that could be created. The first part of the chapter showed how a range of validation methods were used in order to validate the code and conclude that the algorithm proposed was implementing the Petri net correctly. A range of techniques to reduce the computation time including parallel processing, GPU acceleration and algorithm improvements were explored. A methodology to reduce the memory requirements by storing multiple *bits* of information in a single integer rather than an array or vector was also shown.

It was concluded that there were two main areas that limited performance: memory resources and computation time. Currently the system model for Bletchley Delivery Unit requires eight to ten days to simulate and a maximum of 12 GB of device memory and 15 GB of host memory. If the size of the model were increased the memory requirements would likely become an issue before the computation time.

The overall conclusion of this chapter is that the system model proposed in Chapter 7 can comfortably be solved with a mid-range computer. If the system model was increased in size it is likely to be memory requirement that would limit performance. However a high performance computer would be more than capable of solving the model even if it was increased in size considerably.

9 Conclusions

9.1 Introduction

This chapter provides a summary of the work completed, the conclusions of the individual asset models are then discussed, followed by the conclusions drawn from the system model. Lastly conclusions relating to the computational requirements are discussed. These conclusions are used to justify the completion of the aims and the contribution to the research field. The chapter concludes by discussing the limitations of the work and how these could be addressed in future developments.

9.2 Summary of Work Completed

Railway networks are complex systems. Asset managers only have finite resources and budget with which to maintain the railway. The aim of this thesis was to create a whole system framework for railway asset management, to allow asset managers to make more informed asset management decisions based on the whole system condition and whole life cost.

An extensive literature review of asset management and current modelling techniques used within asset management was completed. Based on the literature it was concluded that Petri nets would provide the best framework as they were flexible enough to model the wide range of processes that take place in a railway system. Additionally, the literature revealed that HPNs allow a complex system model to be expressed at a satisfactory level of abstraction and furthermore, provide an appropriate means to add and remove modules with ease from the framework.

Based on the literature, analysis of Network Rail data and expert judgement, models were created for five asset classes:

(i) Track (including rails and ballast)
(ii) Sleepers (steel, concrete and timber construction)
(iii) S&C (Size A→G and fixed diamond crossing)
(iv) Tunnels
(v) Signalling system

The asset models were created using timed Petri nets with four additional transition types: reset transition, conditional transition, probabilistic transition and conditional probabilistic transition. Conditional probabilistic transitions were created to allow the Petri net to make choices based on the condition of the system.

Each of the asset models was simulated individually using bespoke C++ software developed during the project. Each of the asset models was simulated for a 50 year period, for 50,000 simulations. The conclusions drawn from the asset models are discussed in section 9.3.

The models created were transformed into *modules* which could be combined to form a system framework. A master *module* was also introduced to simulate system phenomena. An HPN was used to create a system model by combining the asset modules and the master module. The HPN composed a three level hierarchy, with the '*port*'/ '*socket*' interface between the levels. The top level of the hierarchy comprised the master module. The signal module was also considered at the top level of the hierarchy as the signal module spans the whole railway corridor. The second level of the hierarchy contained the track section modules (ballast and rails). The third and final level of the hierarchy contained models for the remaining assets: sleepers, S&C and tunnels.

The system model was implemented on Bletchley Delivery Unit, a railway corridor in England, north of London, as a case study. The Bletchley Delivery Unit model was made up of 1783 modules: one master module, one signal module, 849 track section modules, 705 concrete sleeper modules, 51 timber sleeper modules, 93 steel sleeper modules, 61 S&C modules (of various sizes) and 22 tunnel modules. The system model considered two types of opportunistic work:

(i) Opportunistic maintenance of a different component in the same section.
(ii) Opportunistic maintenance of a similar component in a neighbouring section.

The output costs of the case study were compared to Network Rail's CP5 expenditure and a ballast profile produced by the model was compared to a ballast profile measured by the NMT. The conclusions drawn from the system model are summarised in section 9.3.2.

The final part of the thesis investigated the computational requirements for solving large Petri net models. Two areas were identified as possibly limiting performance: the memory required and the computation time. Two methods were investigated to reduce the simulation time:

(i) Parallel processing and GPU acceleration
(ii) Improving the Petri net algorithm and Petri net structure

A means of reducing the memory required on the GPU by storing multiple bits of information in a single integer rather than using an array or vector was also explored.

9.3 Conclusions

The following section will outline the main conclusions of the work, the conclusions are grouped into three subsections: conclusions drawn from the asset models, conclusions from the system model and conclusions drawn on the computation requirements.

9.3.1 Conclusions Drawn from the Asset Models

The following conclusions were drawn from the asset models:

Track section

(i) Tamping and stoneblowing interventions tended to span more than one section, and so there would be significant benefit to modelling this in a system model.

(ii) On the other hand welding and grinding tended to be performed on a section by section basis.
(iii) Category 1A was the most expensive, costing around four times as much as Category 5.
(iv) For the highest track categories (1A, 1 and 2) the LCC over 50 years was dominated by renewals; lower category lines generally lasted beyond 50 years (particularly with a clean) and so were often not renewed in the 50 year simulation period, leading to a significantly lower LCC.
(v) For all categories the inspection cost was higher than the maintenance cost.

Sleepers

(i) There was significant variation in the number of sleepers replaced during an intervention. Therefore to create the most accurate model, a means of varying the number of sleepers that were replaced during an intervention was needed; a conditional probabilistic transition was proposed to achieve this.
(ii) For Category 1A and 1 timber sleepers were found to be the cheapest, however all three construction types have a similar cost for Category 1A and 1. For lower track categories timber has the highest cost, due to the service life being limited by time, meaning it still requires a renewal within 50 years. By contrast concrete and steel would last beyond the 50 year simulation period.

S&C

(i) As with all other components, the renewal formed the largest proportion of the budget. However, the second highest proportion was due to speed restrictions; there were more speed restrictions in the S&C model compared to the sleeper and track section models.
(ii) Due to the high number of components within the S&C model, it took the longest to simulate.

Signalling system

(i) The signalling system was modelled as a single model for the whole railway corridor rather than as 220 yard sections.
(ii) Axle counters formed the highest proportion of the overall cost, this was largely due to the high replacement cost of axle counters.
(iii) Due to the high number of repairs, the number of repairs was sampled from a distribution rather than being simulated using a Petri net, as the rate of occurrence of events made it impractical to simulate.

9.3.2 Conclusions Drawn from the System Framework

The following conclusions were drawn from the system model:

(i) As the number of track sections increased the number of speed restrictions increased, this is thought to be due to faster deterioration rates due to the consideration of local factors modelled using an LI in the system model and due to the consideration of resources, engineers and budget which restricted when maintenance could be performed.

(ii) Rare events (rail breaks) led to significant spikes in the overall cost, leading to certain sections costing considerably more than the baseline.
(iii) The convergence of the system model was faster than individual asset models due to the repetitive nature of the system model.
(iv) As expected, the overall cost was dominated by Category 1A line. The highest cost was incurred in sections containing an S&C unit and sections in tunnels
(v) Although renewals still made up the biggest proportion of the overall cost, the share was smaller than for many of the other assets.
(vi) The model's predicted expenditure for the Bletchley Delivery Unit was less than Network Rail's CP5 expenditure, this was concluded to be due to earthworks and drainage not being modelled but being considered in Network Rail's CP5 expenditure, another explanation was enhancement projects not being considered in the model.

9.3.3 Conclusions Drawn on the Computational Requirements

There were a number of conclusions drawn from Chapter 8 about the computational requirements:

(i) The model proposed in Chapter 7 could be solved relatively efficiently on a mid-range computer.
(ii) As the model size was increased it was likely to be memory resources that became restrictive before time.
(iii) Solving the model using GPGPU reduced the computation time by around eight times compared to single threaded code, this was less than for other applications seen in the literature. This was largely due to speed performance being sacrificed in order to decrease memory usage and a lack of memory limiting the number of simulations that could be performed in parallel.
(iv) If the model was increased in size it may have to be solved using a high performance computer yet it could be expanded considerably before it was beyond the capabilities of a high performance computer.

9.4 Overall Conclusions

The following overall conclusions were drawn:

(i) Petri nets were found to be a very powerful technique as they allowed decisions to be made based on the condition of the whole system; they were capable of simulating any distribution and they were flexible enough to model any process that was needed in this research. They are particularly good for building individual asset models, computation time and memory requirements are not an issue for these models.
(ii) When creating system models, the Petri net technique was still found to be beneficial; the '*port*' and '*socket*' interface made it easy to add additional assets to the core framework. The Petri net framework was again found to be flexible enough to model a wide range of factors, including variations in deterioration based on location parameters and interactions between modules. The level of uncertainty in the system model was found to be a barrier to implementation, the uncertainty would

need quantifying, and likely reducing before a system model could be used in practice.

(iii) The computation time required to solve the Petri net was found to be between eight and ten days; however, the limiting factor in the size of system model that could be created was found to be the memory.

The main conclusion of this research is that it is currently possible to create a system model for railway asset management. The system model has the ability to consider a wide range of assets and make decisions based on whole system condition and LCC. Furthermore, computational requirements do not prohibit the solving of the model at its current size. The model has the potential to deliver significant benefits to the rail sector by allowing better predictions of asset service life and maintenance planning and scheduling. However the data to support such a model is lacking, particularly for non-track assets. Therefore railway operators would be best placed to invest in better data collection and development of their understanding of deterioration processes and the factors that influence them, if they wish to fully exploit the benefits of whole system asset management. Until these areas are addressed the benefit of any system model will be significantly limited due to the high level of uncertainty within the model.

9.5 Completion of Aims and Contributions to Research

The fundamental aim of this research, to develop a whole system model for a railway network with capabilities to model a range of railway assets, has been achieved. The research demonstrates how a Petri net framework can be developed to model a railway corridor. The model's effectiveness in assisting asset managers is currently limited, however, by a lack of understanding of the interaction between assets, leading to a high level of uncertainty in the results. However, in time, if these dependencies and interactions become well understood the research has demonstrated that whole system models can be beneficial. Table 9.1 summarises how the objectives listed in Chapter 1 were completed, to complement the realisation of the aim.

Two main contributions to the field of railway asset management have been made. Firstly, the demonstration of the effectiveness of Petri nets in whole system asset management. The thesis has shown the capability of the Petri net modelling technique to form a whole system model. The Petri net model proposed is one of the largest created in the field of railway asset management and considers a wider range of assets simultaneously than previous studies. An incomplete understanding of the interactions and dependencies between assets was identified as limiting the adoption of whole system models in railway asset management.

The second area of novelty in this research is the solving of the Petri net using heterogeneous programming, allowing simulations to be performed on both the GPU and CPU simultaneously. This led to an eight times reduction in the simulation time compared to a single-threaded approach. Memory restrictions limited the benefit that could be achieved from heterogeneous programming.

	Objectives	Completion Notes
1	Gain an understanding of railway systems and current asset management strategies.	Chapter 2 & Chapter 3: a range of asset management techniques were reviewed.
2	Review asset management models for assets which influence the whole system service performance of a railway.	Chapter 4: a range of literature was reviewed, track was found to have the most data available and have been studied the most.
3	Identify the best modelling approach which will support maintenance decision making, taking a whole system, whole life prospective.	Chapter 4: Petri nets were found to be the most suitable.
4	Analyse Network Rail data to determine deterioration and repair times.	Chapter 5: a range of Network Rail data was reviewed.
5	Develop asset state models for each asset group considered.	Chapter 6: presents asset models for five asset classes.
6	Establish dependencies and links between asset types to include in the whole system model.	Chapter 7: current understanding on this is limited and limits the overall effectiveness of a whole system model.
7	Link track section models together to create a whole system model for a large railway corridor.	Chapter 7: the Petri net framework was trialled on an example railway corridor; Bletchley Delivery Unit.
8	Investigate the simulation times for such large-scale models.	Chapter 8: it was concluded that the simulation time could be prohibitive, however memory limitations were much more likely to restrict model size. Memory restrictions also limited the benefits that could be achieved from parallel processing.
9	Develop ways to speed up the run time of the model, to allow a complete system model to be simulated in a reasonable time duration.	Chapter 8: algorithm improvements and parallel processing were explored. It was found that memory limitations were likely to become prohibitive before computation time.

TABLE 9.1: COMPLETION OF OBJECTIVES LISTED IN CHAPTER 1

9.6 Limitations

As discussed, the major factor currently limiting the progression of whole system models in railway asset management is the lack of understanding of the interactions and dependencies between assets.

In terms of the proposed framework a number of limitations in this were also identified:

(i) The proposed track section model did not consider multiple running lines, which may impact the effectiveness of maintenance scheduling.

(ii) The signalling model was a large simplification of reality, which again may impact decisions made using the framework.

(iii) There are a number of asset classes such as electrification & power and structures that are not included in the framework.

(iv) The framework does not consider the logistics of transporting staff or machines, merely their availability.

9.7 Future Work

Due to the scale of the project there is still considerable work that can be undertaken in the field and which the author is keen to pursue. As future work further model validation should be prioritised, such that the model outputs can be compared to Network Rail's own forecasts. The following steps are considered critical:

(i) Explore more ways to validate the model outputs, with respect to both the costs and work volumes performed, as this is critical to model adoption in industry. The cost was only validated against a single control period overall route expenditure. In the future costs could be compared against a more detailed breakdown of the spending, however this information is commercially sensitive. Additionally more work should be undertaken to validate the condition of the ballast in all poskeys modelled against historical NMT condition records, as well as considering means to validate the condition profile of the other assets modelled.

(ii) Alongside additional validation better quantification of the uncertainty within the model is also required for wider industry adoption.

Following industry adoption/ validation the following additions could also be considered:

(i) Consider alternative methods for scheduling maintenance across multiple track sections (see section 9.7.1).

(ii) Alongside this it could be possible to explore how the Petri net could be interfaced with other modelling/scheduling techniques both in terms of maintenance scheduling and indeed if other assets are introduced to the framework. The use of a continuous Petri net could be beneficial in modelling the ballast condition.

(iii) Better modelling/understanding of the effect local factors have on deterioration, and how these factors may change. The LI score proposed was mainly used to demonstrate the model's capability, in the future a Cox Proportional Hazard model could be developed as a mathematically sound means of quantifying the effect of location factors on deterioration. Additionally the location parameters were

modelled as remaining constant throughout the simulation period, it could be possible to predict how factors such as tonnage and sleeper design may change and the effect this would have on deterioration.

(iv) Better modelling/understanding of the dependencies between asset condition and how the condition of one asset can affect the deterioration profile of other assets. In the model only a few basic cross asset condition dependencies were considered, in the future this area could be explored and conditional probability could be used to model cross asset condition dependencies.

(v) Alternative distribution fitting methods could be considered, such as bootstrapping or using an empirical distribution function to capture multimodal phenomena and remove unrealistically long deterioration times.

(vi) Consideration of additional assets such as structures in the system framework.

Following validation, the research in the future that, the author feels, would be most beneficial to the development of a system model would be further analysis of the interactions and dependencies between the deterioration of assets. In terms of asset models, it would appear that the development of the signalling asset model would be the most useful. Signalling and track are similar in both the budget allocated and number of failures (and considerably more than any other asset class (see Figure 9.1)) yet signalling has been studied considerably less than track.

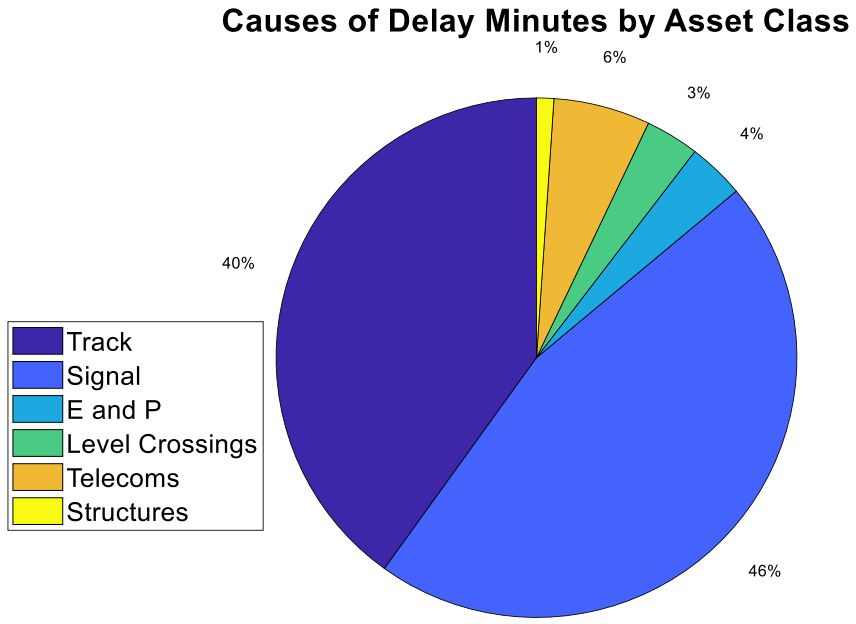


FIGURE 9.1: CAUSES OF DELAY MINUTES BY ASSET CLASS (TRANSPENNINE ROUTE 2014-2019)

9.7.1 Future Developments of Tamping and Stoneblowing Scheduling

Based on the observation that tamping and stoneblowing interventions tended to span several sections, two possible alternative means of scheduling tamping and stoneblowing were considered, where tamping and stoneblowing maintenance would be carried out on a number of sections at the same time. The two methodologies considered were:

Method A

The first method is based on the observation that during a tamp or stoneblow on average approximately 1000 yards (five sections) were maintained. To capture this an alternative method, to '*Normal priority*' maintenance (from '*Satisfactory*' or '*Poor*' condition), was proposed. Under method A, as in the standard model when the ballast reaches '*Satisfactory*' or '*Poor*' condition following an inspection the known condition state is marked and following this a conditional probabilistic transition is used to decide whether a tamp or stoneblow is performed. However, under method A work will only be scheduled once a block of five adjacent sections have a routine tamp scheduled or five adjacent sections have a routine stoneblow scheduled, rather than as soon as one section has a tamp or stoneblow scheduled.

Figure 9.2 shows the Petri net used to implement method A. The central section in the block of five is linked to the machine available place (P_0^M or P_1^M), the budget remaining place (P_{18}^M), engineer available place (P_{38}^M), the possession remaining place (P_{77}^T) and the maintenance ongoing in this section place, (P_{78}^T). The other sections are not linked to these places as the resources are only required once.

Emergency maintenance (From '*Very poor*' or '*Super red*' condition) should still be performed on an individual bases.

Method B

Method B aims to take account of two features, in addition to the observation that the average length of a tamp or stoneblow during an intervention was five sections, these are:

(i) Although the average length maintained is five sections there is significant variation in the length maintained.

(ii) A high number of sections were tamped despite being in '*Good*' condition, (this was observed in the data and verified by Network Rail engineers). The previous methodologies did not allow work to be performed from the good condition.

Method B involves giving each of the track sections a score, based on a number of attributes of the section. An example means of calculating the score is:

$$s = k.\frac{10.\alpha.\gamma}{9+\beta}, \qquad (9.1)$$

where k is the time since the condition was improved, α is a scaling factor based on the quality band ('*Good*', '*Satisfactory*' etc.) (Table 9.2), β is a scaling factor based on the track category (1A, 1, etc.) (Table 9.3) and lastly γ is a scaling factor based on the proportion of the budget that has been spent so far (Table 9.4).

The track section score was updated after each inspection. The proportion of budget spent was calculated by assuming the budget should be spent evenly between each inspection in the CP. For example if there are 500 inspections in the CP and the budget is 500m then 1m should be spent between each inspection. If at the second inspection the budget remaining is less than 499m (meaning more than the 1m allocation has been spent) then the scores following the inspection would be weighted heavily, to reduce the amount of work performed in the next period. If the value was greater than 499m the score would be weighted lightly, to increase the likelihood of work in the next period.

The scores s are then used to form work banks. Initially groups of ten adjacent sections are reviewed, the scores of all of the ten sections are added together to determine an overall score, S. S is then compared against a threshold value, δ_i, the values of δ_i are shown in Table 9.5. If,

$$S > \delta_{i,} \tag{9.2}$$

then all ten sections in the batch are placed in the work bank. The process is then repeated with blocks of decreasing length, from nine to one section. A record is kept of which sections have been added to the work bank and the total number of sections placed in the work bank. A maximum value is placed on the number of sections that can be placed in the work bank to limit the number of sections that are placed in the work bank between each inspection.

The implementation of method B is not possible with standard Petri nets. It is modelled using a *calculation transition*. The calculation transition reviews all the relevant input places and marks the output places based on the rules outlined above. A possible implementation of this is shown in Figure 9.3.

Condition	α
'Good'	1
'Satisfactory'	2
'Poor'	3
'Very poor'	4
'Super red'	5

TABLE 9.2: CONDITION SCALING FACTOR, α

Category	β
1A	1
1	2
2	3
3	4
4	5
5	6

TABLE 9.3: CONDITION SCALING FACTOR, β

Percentage Budget	γ
<30%	0.2
30%	0.4
20%	0.6
10%	0.8
0%	1
-10%	2
-20%	3
-30%	4
>-30%	5

TABLE 9.4: CONDITION SCALING FACTOR, γ

δ_i	Value
δ_1	1,500
δ_2	2,500
δ_3	3,500
δ_4	4,500
δ_5	5,500
δ_6	6,500
δ_7	7,500
δ_8	8,500
δ_9	9,500
δ_{10}	10,500

TABLE 9.5: THRESHOLD VALUES FOR WORK BANK PLACEMENT, METHOD B

As well as the parameters introduced in equation (9.1) there are a number of other factors that can be used to determine when the track section should be tamped, such as subgrade and the proximity of tampers. In addition to this a number of experts said the time since last intervention would have little to no consideration on when the next time would be scheduled so could be removed from equation (9.1).

As a future study these methodologies could be worked into the system model to better predict tamping and stoneblowing maintenance.

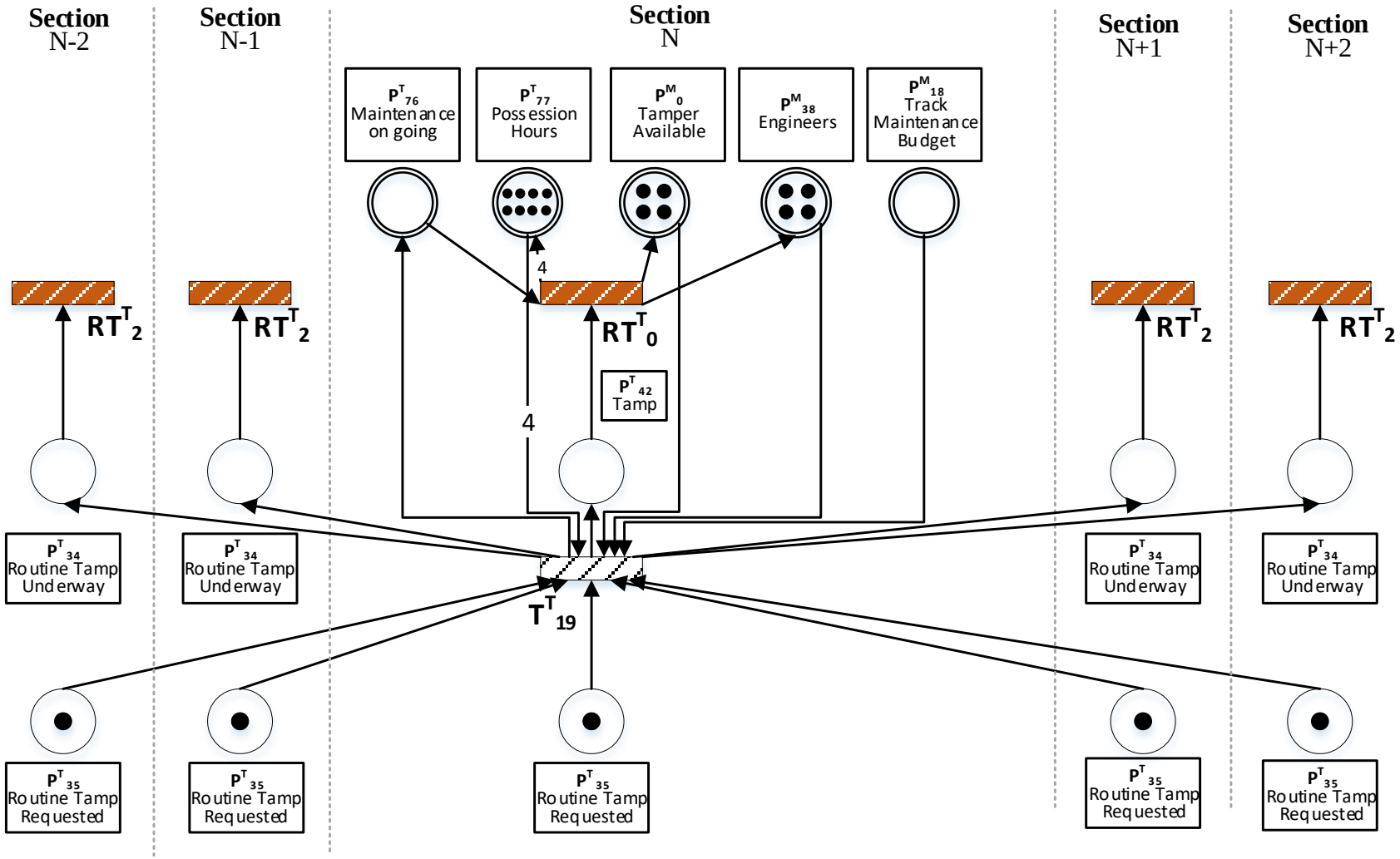


FIGURE 9.2: TAMPING SCHEDULING METHOD A

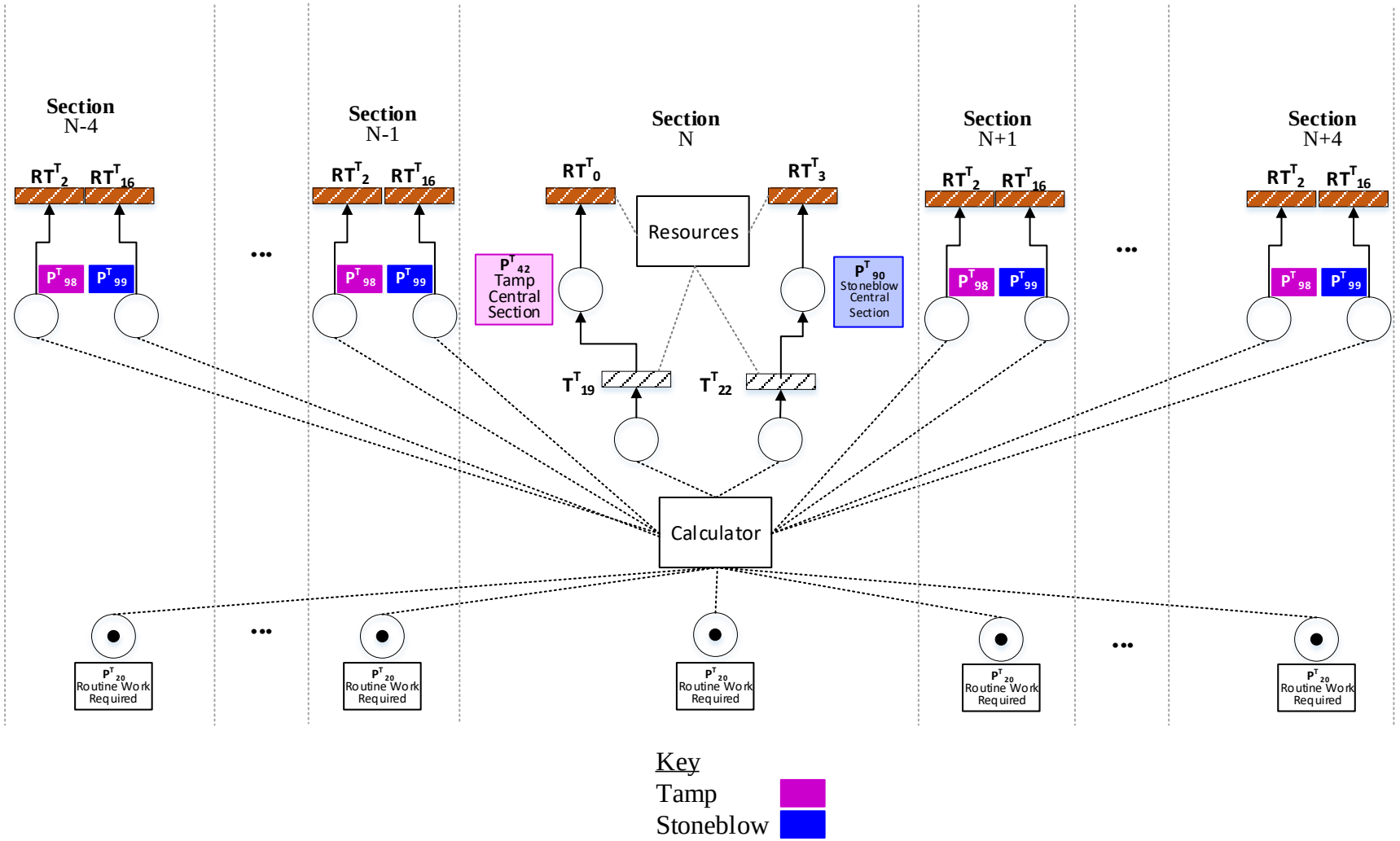


FIGURE 9.3: TAMPING AND STONEBLOWING SCHEDULING METHOD B

References

[1] Virgin Trains, “Back to the Future as History made with East Coast Rail Icons,” 2017. [Online]. Available: http://www.mynewsdesk.com/uk/virgintrains/pressreleases/back-to-the-future-as-history-made-with-east-coast-rail-icons-1929402. [Accessed: 25-May-2019].

[2] SNCF Reseau, “The Railway Network,” 2017. [Online]. Available: https://www.sncf-reseau.fr/en/the-railway-network. [Accessed: 19-Apr-2018].

[3] G. Ollivier, R. Bullock, Y. Jin, and N. Zhou, “High-Speed Railways in China : A Look at Traffic,” *China Transp. Top.*, vol. 11, 2014.

[4] Office of Road and Rail, “Passenger Rail Usage 2015-16 Q4 Statistical Release,” London: Office of Road and Rail, 2016.

[5] British Railway Board, “The Reshaping of British Railways,” London: British Railway Board, 1963.

[6] Office of Road and Rail, “Rail Infrastructure, Assets and Environmental 2016-17 Annual Statistical Release,” London: Office of Road and Rail, 2017.

[7] Department for Transport, “Length of National Railway Route at Year End, and Passenger Travel by National Railway and London Underground,” Table TSGB0601 (RAI0101) London: Department for Transport, 2016.

[8] Technical Strategy Leadership Group (TSLG), “Rail Technical Strategy,” Technical Report, Rail Research UK Association, London, 2012.

[9] Technical Leadership Group, “Rail Technical Strategy- Capability Delivery Plan,” Technical Report, Rail Delivery Group, London, 2017.

[10] Office of Road and Rail, “Passenger Rail Usage 2017-18 Q4 Statistical Release,” London: Office of Road and Rail, 2018.

[11] Office or Rail and Road, “Schedules 4 and 8 possessions and performance regimes,” 2012. [Online]. Available: http://orr.gov.uk/rail/consultations/policy-consultations-by-topic/pr13-consultations/schedules-4-and-8-possessions-and-performance-regimes. [Accessed: 03-May-2018].

[12] Office or Rail and Road, “Who Are We?,” 2019. [Online]. Available: https://orr.gov.uk/about-orr/who-we-are. [Accessed: 02-Sep-2019].

[13] C. Esveld, *Modern Railway Track*, 2nd ed. Zaltbommel: MRT-Productions, 2001.

[14] E. Selig and J. Waters, *Track Geotechnology and Substructure Management*. London: Thomas Telford, 1994.

[15] W. Salim, D. Christie, H. Khabbaz, and B. Indraratna, “Geotechnical Properties of Ballast and the Role of Geosynthetics in Rail Track Stabilisation,” *Proc. ICE - Gr. Improv.*, vol. 10, no. 3, pp. 91–101, 2006.

[16] N. Tennakoon, B. Indraratna, C. Rujikiatkamjorn, S. Nimbalkar, and T. Neville, “The Role of Ballast Fouling Characteristics on the Drainage Capacity of Rail Substructure,” *Geotech. Test. J.*, vol. 35, no. 4, pp. 1–12, 2012.

[17] A. Hudson, G. Watson, L. Le Pen, and W. Powrie, “Remediation of Mud Pumping on a Ballasted Railway Track,” *Procedia Eng.*, vol. 143, pp. 1043–1050, 2016.

[18] Rail Accident Investigation Branch (RAIB), “Passenger train derailment, London Paddington,” London, Department for Transport, 2017.

[19] AMEC Rail *et al.*, “Management of Cyclic Top,” CEC/DG/002, Civil Engineering Conference, Birmingham, 2002.

[20] Rail Accident Investigation Branch (RAIB), “Freight Train Derailment Near Gloucester,” London: Department for Transport, 2014.

[21] J. D. Andrews, “A modelling approach to railway track asset management,” *Proc. Inst. Mech. Eng. Part F J. Rail Rapid Transit*, vol. 227, no. 1, pp. 56–73, 2013.

[22] Network Rail, “Wet Bed Repair,” 2014. [Online]. Available: https://www.youtube.com/watch?v=oB0mSUh4DUc. [Accessed: 06-Feb-2018].

[23] Network Rail, “Network Rail Standards; Track Inspection, NR/L2/TRK/001/mod02,” 2013.

[24] Network Rail, “Network Rail Standards; Track Geometry - Inspections and Minimum Actions NR/L2/TRK/001/mod11,” 2012.

[25] Network Rail, “Network Rail: Track Treatment Fleet,” 2019. [Online]. Available: https://www.networkrail.co.uk/running-the-railway/looking-after-the-railway/fleet-machines-vehicles/track-treatment/. [Accessed: 29-Apr-2019].

[26] Office of Rail Regulation, “Regional Usage Profiles,” London: Office of Rail Regulation, 2012.

[27] Network Rail, “High Output,” 2019. [Online]. Available: https://www.networkrail.co.uk/running-the-railway/looking-after-the-railway/fleet-machines-vehicles/high-output/. [Accessed: 22-May-2019].

[28] British Steel, “Interactive Product Guide; Unlocking the Potential with Steel,” London: British Steel, 2017.

[29] A. Wilson and M. Kerr, *Rail Defects Handbook: TMC 226*. Sydney: RailCorp, 2012.

[30] S. Kumar, “A Study of the Rail Degradation Process to Predict Rail Breaks,” Doctorial Dissertation, Luleå Tekniska Universitet, 2006.

[31] D. Hoffman, K. Dahle, and F. David, *Welding*. New York: Persons, 2012.

[32] Network Rail, “Network Rail Standards; Visual Inspection and Ultrasonic Testing of Rails NR/L2/TRK/001/mod06,” 2012.

[33] C. Esveld, “Recent Developments in Slab Track,” *Eur. Railw. Rev.*, vol. 9, pp. 81–85, 2003.

[34] P. Gautier, “Slab track : Review of existing systems and optimization potentials including very high speed,” *Constr. Build. Mater.*, vol. 92, pp. 9–15, 2015.

[35] British Standards Institution, “BS EN 13230-1:2016 Railway Applications - Track - Concrete Sleepers and Bearers Part 1 : General Requirements,” London: BSI, 2016.

[36] W. Ferdous and A. Manalo, “Sleepers: Failures of mainline railway sleepers and suggested remedies - Review of current practice,” *Eng. Fail. Anal.*, vol. 44, pp. 17–35, 2014.

[37] A. Manalo, T. Aravinthan, W. Karunasena, and A. Ticoalu, “A review of alternative materials for replacing existing timber sleepers,” *Compos. Struct.*, vol. 92, no. 3, pp. 603–611, 2010.

[38] P. Qiao, J. F. Davalos, and M. G. Zipfelh, “Modeling and optimal design of composite-reinforced crosstie,” *Compos. Struct.*, vol. 41, no. 1, pp. 87–96, 1998.

[39] R. C. Hibbeler, *Statics and Mechanics of Materials*. New Jersey: Pearson Prentice Hall, 2004.

[40] K. S. Elliott, *Precast Concrete Structures*, 2nd ed. Boca Raton: Taylor & Francis Group, 2016.

[41] R. H. Lutch, D. K. Harris, and T. M. Ahlborn, “Prestressed Concrete Ties in North

America," in *Proceeding of AREMA Annual Conference*, 2009, pp. 1–39.

[42] R. H. Lutch, D. K. Harris, and T. M. Ahlborn, "Causes and Preventative Methods for Rail Seat Abrasion in North America 's Railroads," *Cold Reg. Eng. 2009 Cold Reg. Impacts Res. Des. Constr.*, no. May, pp. 455–466, 2009.

[43] R. You, K. Goto, C. Ngamkhanong, and S. Kaewunruen, "Nonlinear finite element analysis for structural capacity of railway prestressed concrete sleepers with rail seat abrasion," *Eng. Fail. Anal.*, vol. 95, pp. 47–65, 2019.

[44] S. Mohammadzadeh and E. Vahabi, "Time-dependent reliability analysis of B70 pre-stressed concrete sleeper subject to deterioration," *Eng. Fail. Anal.*, vol. 18, no. 1, pp. 421–432, 2011.

[45] R. Reiff, R. Walker, P. Schreiber, N. Wilson, and T. H, "Assessment of Rail Seat Abrasion Patterns and Environment," Washington DC, 2012.

[46] S. Townsend, E. McCombe, M. Kerr, and M. French, "Cost Efficient Track by the use of Steel Sleepers," *CORE 2002 Cost Effic. Railw. through Eng.*, no. 349, 2002.

[47] British Steel, "Steel sleeper: Lower lifetime cost and more efficient logistics," Scunthorpe, 2017.

[48] New Civil Engineer, "Steel Sleepers," 2001. [Online]. Available: https://www.newcivilengineer.com/steel-sleepers/814302.article. [Accessed: 20-Mar-2019].

[49] Franklin + Andrews Ltd, *Spon's Railways Construction Price Book*, 2nd ed. New York: Spon Press, 2003.

[50] Network Rail, "Network Rail Standards; Plain Line Track NR/L2/TRK/001/mod03," 2012.

[51] Aveng Infraset, "Railway Products:Fastening System," 2015. [Online]. Available: http://www.infraset.co.za. [Accessed: 22-Apr-2018].

[52] P. Wang, *Design of high-speed railway turnouts: theory and applications*. London: Academic Press, 2015.

[53] D. Rama and J. D. Andrews, "A reliability analysis of railway switches," *Proc. Inst. Mech. Eng. Part F J. Rail Rapid Transit*, vol. 227, no. 4, pp. 344–363, 2013.

[54] HSE Investigation Board, "Train Derailment at Potters Bar 10 May 2002," Bootle, 2003.

[55] F. B. Zhou, M. D. Duta, M. P. Henry, S. Baker, and C. Burton, "Remote Condition Monitoring for Railway Point Machine," in *ASME/IEEE 2002 Joint Rail Conference*, 2002, pp. 103–108.

[56] M. Vileiniskis, R. Remenyte-Prescott, and D. Rama, "A fault detection method for railway point systems," *Proc. Inst. Mech. Eng. Part F J. Rail Rapid Transit*, vol. 230, no. 3, pp. 852–865, 2016.

[57] Network Rail, "The Challenges of Working in Tunnels," 2019. [Online]. Available: https://www.networkrail.co.uk/the-challenges-of-working-in-tunnels/. [Accessed: 22-May-2019].

[58] Theeg G. & Vlasenko S., *Railway Signalling & Interlocking*. Hamburg: DVV Media Group, 2009.

[59] W. D. Cullen, "The Ladbroke Grove Rail Inquiry: Part 1," London: Health & Safety Commission, 2001.

[60] International Union of Railways (UIC), "Guidelines for the Application of Asset Management in Railway Infrastructure Organisations," Paris, 2010.

[61] International Standards Organisation, "Asset Management - Overview, Principles

and Terminology," 2014.

[62] The Institute of Asset Management, "The Institute of Asset Management; the Professional Body for Whole Life Management of Physical Assets," 2019. [Online]. Available: https://theiam.org/. [Accessed: 09-Apr-2019].

[63] British Standards Institution, "BS EN 50126-1:2017 Railway Applications - The Specification and Demonstration of Reliability, Availability, Maintainability and Safety(RAMS)," London: BSI, 2017.

[64] The Institute of Asset Management, "Asset Management - An Anatomy Volume 3," Bristol, UK, 2015.

[65] International Electrotechnical Commission, "IEC 60050-192:2015. International Electrotechnical Vocabulary - Part 192: Dependability: International Electrotechnical Commission," Geneva, Switzerland, 2015.

[66] International Standards Organisation, "EB ISO 16194:2017 Pneumatic Fluid Power — Assessment of Component Reliability by Accelerated Life Testing — General Guidelines and Procedures," Geneva, Switzerland, 2017.

[67] J. D. Andrews and T. R. Moss, *Reliability and Risk Assessment*, 2nd ed. Bury St Edmunds: Professional Engineering Publishing, 2002.

[68] Q. Mahboob and E. ZIO, *Handbook of RAMS in Railway Systems; Theory and Practice*. Boca Raton: Taylor & Francis Group, 2018.

[69] INNOTRACK, "Deliverable D6.5.4; Guideline for LCC and RAMS Analysis," Thematic Priority 6: Sustainable Development, Global Change and Ecosystems. Project No. TIP5-CT-2006-031415, 2006.

[70] Office of Road and Rail, "Rail Safety Statistics: 2016-17 Annual Statistical Release," London: Office of Road and Rail, 2017.

[71] Department for Transport, "Reported Road Casualties In Great Britain: Quarterly Provisional Estimates Year Ending June 2017," London: Department for Transport, 2017.

[72] W. J. Fabrycky and S. B. Blanchard, *Life-Cycle Cost and Economic Analysis*. New Jersey: Prentice Hall International, 1991.

[73] G. Rubino and B. Sericola, *Markov Chains and Dependability Theory*. Cambridge: Cambridge University Press, 2014.

[74] P. Do Van, A. Barros, and C. Bérenguer, "Reliability importance analysis of Markovian systems at steady state using perturbation analysis," *Reliab. Eng. Syst. Saf.*, vol. 93, no. 11, pp. 1605–1615, 2008.

[75] D. R. Westhead and M. . Vijayabaskar, *Hidden Markov Models; Methods and Protocols*. New York: Springer Science+Business Media, 2017.

[76] J. Jannssen and N. Limnios, *Semi-Markov Models and Applications*. Dordrecht, Netherlands: Kluwer Academic Publishers, 1999.

[77] J. Van der Hoek and R. J. Elliott, *Introduction to Hidden Semi-Markov Models*, Vol. 445. Cambridge: Cambridge University Press, 2018.

[78] C. A. Petri, "Kommunikation mit automaten.," PhD Thesis, University of Bonn, 1962.

[79] T. Murata, "Petri nets: Properties, Analysis and Applications," *Proc. IEEE*, vol. 77, no. 4, pp. 541–580, 1989.

[80] S. K. D'souza, "Asset Management of Offshore Oil and Gas Installations," PhD Thesis: University of Nottingham, 2017.

[81] British Standards, "BS EN 62551:2012, Analysis techniques for dependability- Petri

net techniques," London: BSI, 2012.

[82] K. Jensen and L. Kristensen, *Coloured Petri Nets*. Heidelberg, Berlin: Springer-Verlag, 2009.

[83] Jensen Kurt, *Coloured Petri Nets; Basic Concepts, Analysis Methods and Practical Use Volume 1*. Heidelberg, Berlin: Springe-Verlag, 1997.

[84] L. Liu, X. Liu, and G. Liu, "The Risk Management of Perishable Supply Chain Based on Coloured Petri Net Modeling," *Inf. Process. Agric.*, vol. 5, no. 1, pp. 47–59, 2017.

[85] M. D. Lloyd, J. D. Andrews, R. Remenyte-Prescott, J. T. Pearson, and P. Hubbard, "A Petri Net Approach to Fault Verification in Phased Mission Systems using the Standard Deviation Technique," *Qual. Reliab. Eng. Int.*, vol. 30, no. 1, pp. 83–95, 2014.

[86] P. Kilsby, R. Remenyte-Prescott, and J. Andrews, "A modelling approach for railway overhead line equipment asset management," *Reliab. Eng. Syst. Saf.*, vol. 168, pp. 326–337, 2017.

[87] R. David and H. Alla, *Discrete, Continuous and Hybrid Petri Net*. Berlin: Springer, 2010.

[88] L. Recalde, S. Haddad, and M. Silva, "Continuous Petri Nets: Expressive Power and Decidability Issues," *Int. J. Found. Comput. Sci.*, vol. 21, pp. 235–256, 2010.

[89] R. David, "Modelling Hybrid Systems Using Continuous and Hybrid Petri Nets," in *Proceedings of the Seventh International Workshop on Petri Nets and Performance Models*, 1997, pp. 47–58.

[90] D. P. Kroese, T. Taimre, and Z. I. Botev, *Handbook of Monte Carlo Method*. Hoboken, New Jersey: Wiley, 2011.

[91] W. L. Dunn and J. K. Shultis, "Exploring Monte Carlo Methods." Elsevier, Amsterdam, The Netherlands, 2011.

[92] M. J. Wootton, J. Andrews, A. L. Lloyd, R. Smith, and A. J. Arul, "Petri Nets and Pseudo-Bond Graphs for a Nuclear Reactor Primary Coolant System," in *29th European Safety and Reliability Conference*, 2019, pp. 978–981.

[93] J. E. Alva-Hurtado and E. T. Selig, "Permanent Strain Behavior of Railroad Ballast," in *The 10th International Conference on Soil Mechanics and Foundation Engineering*, 1981.

[94] Shenton M.J., "Ballast Deformation and Track Deterioration," in *In Proceedings of a Conference on Track Technology*, 1985, pp. 253–265.

[95] B. Lichtberger, "Das system Gleis und seine Instandhaltung," *Der Eisenbahningenieur*, vol. 58, no. 1, 2007.

[96] L. M. Quiroga and E. Schnieder, "Monte Carlo simulation of railway track geometry deterioration and restoration," *J. Risk Reliab.*, vol. 226, no. 3, pp. 274–282, 2012.

[97] A. Gross and A. Bing, "Development of Railroad Track Degradation Models," *Transp. Res. Rec.*, vol. 939, pp. 27–31, 1983.

[98] S. Chrismer and E. Selig, "Computer model for ballast maintenance planning.," in *IHHA Board (ed.) Proceedings of fifth international heavy haul railway conference*, 1993, pp. 223–227.

[99] A. Hamid and A. Gross, "Track-Quality Indices and Track-Degradation Models for Maintenance-of-Way Planning," *Transp Res Rec*, vol. 802:, pp. 2–8, 1981.

[100] Y. Sato, "Optimum track structure considering deterioration in ballasted track," in

IHHA Board (ed.) Proceedings of sixth international heavy haul conference, 1997, p. 576.

[101] J. Sadeghi and H. Askarinejad, "Development of improved railway track degradation models," *Struct. Infrastruct. Eng.*, vol. 6, no. 6, pp. 675–688, 2010.

[102] A. R. Andrade and P. F. Teixeira, "Statistical modelling of railway track geometry degradation using Hierarchical Bayesian models," *Reliab. Eng. Syst. Saf.*, vol. 142, pp. 169–183, 2015.

[103] Q. Mahboob, "A Bayesian Network Methodology for Railway Risk, Safety and Decision Support," PhD Thesis, Technische Universität Dresdon, Dersden, 2014.

[104] Y. Shafahi and R. Hakhamaneshi, "Application of a Maintenance Management Model for Iranian Railways Based on the Markov Chain and Probabilistic Dynamic Programming," *Sci. Iran.*, vol. 16, no. 1, pp. 87–97, 2009.

[105] D. Prescott and J. D. Andrews, "Modelling maintenance in railway infrastructure management," *2013 Proc. Annu. Reliab. Maintainab. Symp.*, pp. 1–6, 2013.

[106] N. Lyngby, P. Hokstad, and J. Vatn, "RAMS Management of Railway Tracks," in *Handbook of Performability Engineering*, Springer, 2008, pp. 1123–1145.

[107] L. Bai, R. Liu, Q. Sun, F. Wang, and P. Xu, "Markov-based model for the prediction of railway track irregularities," *Proc IMechE, Part F J Rail Rapid Transit*, vol. 229, no. 2, pp. 150–159, 2013.

[108] B. Le, "Modelling Railway Bridge Asset Management," PhD Thesis: University of Nottingham, 2014.

[109] M. Audley, "Rail Track Geometry Degradation and Maintenance Decision Making," PhD Thesis: University of Nottingham, 2014.

[110] D. Prescott and J. Andrews, "A track ballast maintenance and inspection model for a rail network," *Proc. Inst. Mech. Eng. Part O J. Risk Reliab.*, vol. 227, no. 3, pp. 251–266, 2013.

[111] J. Andrews, D. Prescott, and F. De Rozières, "A stochastic model for railway track asset management," *Reliab. Eng. Syst. Saf.*, vol. 130, pp. 76–84, 2014.

[112] S. Mercier, C. Meier-hirmer, and M. Roussignol, "Bivariate Gamma wear processes for track geometry modelling , with application to intervention scheduling," *Struct. Infrastruct. Eng.*, vol. 8, no. 4, pp. 357–366, 2012.

[113] R. You, D. Li, C. Ngamkhanong, R. Janeliukstis, and S. Kaewunruen, "Fatigue life assessment method for prestressed concrete sleepers," *Front. Built Environ.*, vol. 3, pp. 1–13, 2017.

[114] S. Laryea, M. S. Baghsorkhi, J. Ferellec, G. R. Mcdowell, and C. Chen, "Comparison of performance of concrete and steel sleepers using experimental and discrete element methods," *Transp. Geotech.*, vol. 1, no. 4, pp. 225–240, 2014.

[115] UIC Track and Structures Sector Repair Panel of Structural Experts, "Repair Works in Tunnels; Comparison of International Practices & Overview of Innovative Projects," Paris, 2018.

[116] D. Chapman, N. Metje, and A. Stärk, *Introduction to Tunnel Construction*, 2nd ed. Boca Raton: Talyor & Francis Group, 2018.

[117] Getlink, "Maintenance for a Smart Tunnel," 2019. [Online]. Available: https://www.getlinkgroup.com/uk/the-channel-tunnel/maintenance/. [Accessed: 22-Mar-2019].

[118] T. Cronvall, "Maintenance of railway tunnels in Finland," NRC Group Finland Oy (VR Track), Helsinki, 2014.

[119] S. J. Cox and A. Wang, “Effect of track stiffness on vibration levels in railway tunnels,” *J. Sound Vib.*, vol. 267, pp. 565–573, 2003.

[120] L. Guang-cheng, X. I. E. You-jun, D. De-hua, and L. I. Xiao-kun, “Deterioration of concrete in railway tunnel suffering from sulfate attack,” *J. Cent. South Univ. Technol.*, vol. 18, no. 3, pp. 881–888, 2011.

[121] J. A. Silmon and C. Roberts, “Improving railway switch system reliability with innovative condition monitoring algorithms,” *Proc. Inst. Mech. Eng. Part F J. Rail Rapid Transit*, vol. 224, no. 4, pp. 293–302, 2010.

[122] B. A. Pålsson and J. C. O. Nielsen, “Wheel – rail interaction and damage in switches and crossings,” vol. 50, no. 1, pp. 42–58, 2012.

[123] J. Pombo *et al.*, “Development of a wear prediction tool for steel railway wheels using three alternative wear functions,” *Wear*, vol. 271, no. 1–2, pp. 238–245, 2011.

[124] D. Prescott and J. D. Andrews, “A railway track ballast maintenance and inspection model for multiple track sections,” in *11th International Probabilistic Safety Assessment and Management Conference and the Annual European Safety and Reliability Conference 2012, PSAM11 ESREL 2012*, 2012, vol. 1, pp. 41–50.

[125] H. Shang, “Maintenance modelling, simulation and performance assessment for railway asset management,” PhD Thesis, University of Technology of Troyes, 2015.

[126] N. Lethanh, B. T. Adey, and M. Sigrist, “A Mixed-Integer Linear Model for Determining Optimal Work Zones on a Road Network,” in *International Conference on Engineering and Applied Sciences Optimization*, 2014.

[127] R. Hajdin and B. T. Adey, “Optimal worksites on highway networks subject to constraints,” in *IFED International Forum on Engineering Decision Making*, 2006, vol. 26–29.

[128] C. Kielhauser, B. T. Adey, and N. Lethanh, “Investigation of a static and a dynamic neighbourhood methodology to develop work programs for multiple close municipal infrastructure networks,” *Struct. Infrastruct. Eng. Maint. , Manag.*, vol. 13, no. 3, pp. 361–389, 2017.

[129] ReliaSoft Corporation, “Weibull++5 Software, Version 5.0.” 2000.

[130] D. Kececioglu, *Reliability and life testing handbook*, Volume I. New Jersey: Prentice Hall, Inc, 1993.

[131] R. Mooney, C. F., Mooney, C. L., Mooney, C. Z., Duval, R. D., & Duvall, *Bootstrapping: A nonparametric approach to statistical inference*. Newbury Park, California: SAGE, 1993.

[132] M. Audley and J. D. Andrews, “The effects of tamping on railway track geometry degradation,” *Proc. Inst. Mech. Eng. Part F J. Rail Rapid Transit*, vol. 227, no. 4, pp. 376–391, 2013.

[133] S. Clarke and D. Prescott, “Identifying the factors influencing track degradation on the UK rail network,” in *Stephenson Conference : Research for Railways*, 2017.

[134] R. Vandoorne and P. J. Gra, “Stochastic rail life cycle cost maintenance modelling using Monte Carlo simulation,” vol. 232, no. 4, pp. 1240–1251, 2018.

[135] S. Kumar, U. Espling, and U. Kumar, “Holistic procedure for rail maintenance in Sweden,” vol. 222, pp. 331–344, 2008.

[136] J. M. Chambers, W. S. Cleveland, B. Kleiner, and P. A. Tukey, *Graphical Methods for Data Analysis*. New Jersey: Wadsworth, 1983.

[137] D. R. COX, “Regression Models and Life-Tables,” *J. R. Stat. Soc. Ser. B*, vol. 34, no. 2, pp. 187–220, 1972.

[138] M. Nikulin and H.-D. I. Wu, *The Cox model and its applications*. Berlin Heidelberg: Springer, 2016.

[139] R. An, Q. Sun, F. Wang, W. Bai, X. Zhu, and R. Liu, "Improved Railway Track Geometry Degradation Modeling for Tamping Cycle Prediction," *J. Transp. Eng. Part A Syst.*, vol. 144, no. 7, p. 04018025, 2018.

[140] K. Terzaghi, *Theoretical soil mechanics*. New York: John Wiley & Sons, 1943.

[141] British Geological Survey, "Geology of Britain Viewer," 2019. [Online]. Available: http://mapapps.bgs.ac.uk/geologyofbritain/home.html. [Accessed: 01-May-2019].

[142] M. Antoni, "Degradation laws of railway ballasted track," in *Estimation of the need of maintenance, proceedings of 3rd international conference on accelerated life testing*, 2010.

[143] L. Blanco Casteneda, V. Arunachalam, and S. Dharmaraja, *Introduction to Probability and Stochastic Processes with Applications*. 2012.

[144] V. V Krivtsov, "Practical extensions to NHPP application in repairable system reliability analysis," *Reliab. Eng. Syst. Saf.*, vol. 92, no. 5, pp. 560–562, 2007.

[145] L. H. Crow, "Reliability Analysis for Complex, Repairable Systems," (No. AMSAA-TR-138). Army Materiel Systems Analysis Activity Aberdeen Proving Ground Md., 1975.

[146] V. J. Rayward-Smith, I. H. . Osman, C. R. Reeves, and G. D. Smith, *Modern Heuristic Search Methods*. New York: John Wiley, 1996.

[147] Amey, "S & C EDS Degradation and Risk Modelling; Summary Report Version 1," Oxford, UK, 2014.

[148] J. Litherland and J. D. Andrews, "A Petri Net Methodology for Modelling the Maintenance of Railway Route Sections," in *Proceedings of the 29th European Safety and Reliability Conference (ESREL 2019)*, 2019, pp. 452–459.

[149] S. Winitzki, "A handy approximation for the error function and its inverse," A lecture note obtained through private communication, 2008.

[150] Network Rail, "Track Asset Policy," 2015.

[151] N. Thomopoulos, *Essentials of Monte Carlo Simulation; Statistical Methods for Building Simulation Models*. New York, USA: Springer Science & Business Media, 2013.

[152] J. P. Mueller and J. Cogswell, *C++ All-In-One For Dummies*, 3rd ed. Hoboken, New Jersey: John Wiley & Sons, 2014.

[153] B. Stroustrup, *The C++ Programming Language*, 4th ed. Michigan: Addison Wesley, 2013.

[154] B. Johnson, *Professional Visual Studio 2017*. Indianapolis, Indiana: Wrox, 2017.

[155] A. M. Razali and A. A. Salih, "Combining Two Weibull Distributions Using a Mixing Parameter," *Eur. J. Sci. Res.*, vol. 31, no. 2, pp. 296–305, 2009.

[156] Network Rail, "Network Rail Standards; Handbook for the Examination of Structures – Part 1C: Determining the Examination Regime NR/L3/CIV/006/1C," 2014.

[157] Office or Rail and Road, "Periodic Review 2013: Final determination of Network Rail's outputs and funding for 2014-19," London: Office of Road and Rail, 2013.

[158] D. Rama and J. D. Andrews, "A holistic modelling framework for railway infrastructure asset management," *Int. J. Performability Eng.*, vol. 11, no. 2, pp. 107–120, 2015.

[159] Intel, “Product Brief: New Intel Core X-series Processor Family,” 2017.

[160] D. P. Bergman, T. L., Incropera, F. P., Lavine, A. S., & DeWitt, *Introduction to Heat transfer*, 6th ed. Jefferson City: John Wiley & Sons, 2011.

[161] B. Parhami, *Introduction to Parallel Processing*. New York: Plenum Press, 1999.

[162] G. M. Amdahl, “Validity of the single processor approach to achieving large scale computing capabilities,” in *April 18-20, 1967 Spring joint computer conference*, 1967, pp. 438–485.

[163] Nvidia, “Compare 10 Series GPUs,” 2017. [Online]. Available: https://www.nvidia.com/en-us/geforce/products/10series/compare/. [Accessed: 22-Mar-2018].

[164] V. Natoli, “Architecting Performance Efficiency and Choice in HPC,” 2016. [Online]. Available: https://www.hpcwire.com/2016/08/23/2016-important-year-hpc-two-decades/. [Accessed: 18-Jun-2019].

[165] J. Cheng, M. Grossman, and T. McKercher, *Professional CUDA C Programming*. Indianapolis, Indiana: Wrox. A Wiley Brand, 2014.

[166] J. Sanders and E. Kandrot, *CUDA by Example; An Introduction to General-Purpose GPU Programming*. Ann Arbor, Michigan, USA: Addison Wesley, 2010.

[167] L. Y. Barash, M. Weigel, M. Borovský, W. Janke, and L. N. Shchur, “GPU Accelerated Population Annealing algorithm,” *Comput. Phys. Commun.*, vol. 220, pp. 341–350, 2017.

[168] P. Yianni, “A Modelling Approach to Railway Bridge Asset Management,” PhD Thesis: University of Nottingham, 2017.

[169] G. Chalkidis, M. Nagasaki, and S. Miyano, “High performance hybrid functional petri net simulations of biological pathway models on CUDA,” *IEEE/ACM Trans. Comput. Biol. Bioinforma.*, vol. 8, no. 6, pp. 1545–1556, 2011.

Appendix A: Ballast Parameters

A-1: Ballast Model Conditional Probabilistic Transitions

A-1.1: Conditional probabilistic transition (CPT_1^T), after tamping.

Number of Interventions	Condition after tamping (p)		
	Good	Satisfactory	Poor
1	0.990	0.010	0
2	0.900	0.090	0.010
3	0.800	0.150	0.050
4	0.700	0.200	0.100
5	0.600	0.300	0.100
6	0.550	0.350	0.100
7	0.510	0.375	0.115
8	0.450	0.500	0.050
9	0.410	0.400	0.190
10	0.380	0.400	0.220
11	0.300	0.500	0.200
12	0.250	0.500	0.250
13	0.220	0.400	0.380
>13	0.200	0.300	0.500

A-1.2: Conditional probabilistic transition (CPT_2^T), after stoneblowing.

Number of Interventions	Condition after stoneblowing (p)		
	Good	Satisfactory	Poor
1	0.99	0.01	0
2	0.95	0.05	0
3	0.90	0.09	0.01
4	0.80	0.18	0.02
5	0.75	0.20	0.05
6	0.70	0.24	0.06
7	0.60	0.34	0.06
8	0.50	0.42	0.08
9	0.43	0.40	0.17
10	0.38	0.40	0.22
11	0.30	0.50	0.20
12	0.25	0.50	0.25
13	0.22	0.40	0.38
>13	0.20	0.30	0.50

Appendix B: Rail Parameters

B-1: Rail Deterioration Distributions Categories 1→5[29]

B-1.1: Rail deterioration rates Category 1

Category	State	Transition	Time Unit	Distribution
1	New→ Minor Surface Defects	CT_{11}^{T-1}	Days	Weibull(1.7, 525)
	Minor Surface Defects→ Major Surface Defects	CT_{12}^{T-1}	Days	Weibull(1.7, 260)
	New→ Minor Transverse Defects	CT_{13}^{T-1}	Days	Weibull(1.7, 495)
	Minor Transverse Defects → Major Transverse Defects	CT_{14}^{T-1}	Days	Weibull(1.7, 250)
	Minor Surface Defects→ Surface Defects and Transverse Defects	CT_{15}^{T-1}	Days	Weibull(1.7,255)
	Major Surface Defects→ Major Surface Defects and Transverse Defects	CT_{16}^{T-1}	Days	Weibull(1.7, 345)
	Minor Transverse Defects → Surface Defects and Transverse Defects	CT_{17}^{T-1}	Days	Weibull(1.7, 255)
	Major Transverse Defects → Major Surface Defects and Transverse Defects	CT_{18}^{T-1}	Days	Weibull(1.7, 345)
	Surface Defects and transverse → Major Surface Defects and Transverse Defects	CT_{19}^{T-1}	Days	Weibull(1.7, 320)
	Major Surface Defects and Transverse Defects→Serious Faults	CT_{20}^{T-1}	Days	Weibull(1.7, 160)

B-1.2: Rail deterioration rates Category 2

Category	State	Transition	Time Unit	Distribution
2	New→ Minor Surface Defects	CT_{11}^{T-2}	Days	Weibull(1.7, 580)
	Minor Surface Defects→ Major Surface Defects	CT_{12}^{T-2}	Days	Weibull(1.7, 280)
	New→ Minor Transverse Defects	CT_{13}^{T-2}	Days	Weibull(1.7,550)
	Minor Transverse Defects → Major Transverse Defects	CT_{14}^{T-2}	Days	Weibull(1.7, 265)
	Minor Surface Defects→ Surface Defects and Transverse Defects	CT_{15}^{T-2}	Days	Weibull(1.7, 300)
	Major Surface Defects→ Major Surface Defects and Transverse Defects	CT_{16}^{T-2}	Days	Weibull(1.7, 385)
	Minor Transverse Defects → Surface Defects and Transverse Defects	CT_{17}^{T-2}	Days	Weibull(1.7, 300)
	Major Transverse Defects → Major Surface Defects and Transverse Defects	CT_{18}^{T-2}	Days	Weibull(1.7, 385)
	Surface Defects and transverse → Major Surface Defects and Transverse Defects	CT_{19}^{T-2}	Days	Weibull(1.7, 340)
	Major Surface Defects and Transverse Defects→Serious Faults	CT_{20}^{T-2}	Days	Weibull(1.7, 180)

[29] Category 1A values shown in Table 5.4

B-1.3: Rail deterioration rates Category 3

Category	State	Transition	Time Unit	Distribution
3	New→ Minor Surface Defects	CT_{11}^{T-3}	Days	Weibull(1.7, 710)
	Minor Surface Defects→ Major Surface Defects	CT_{12}^{T-3}	Days	Weibull(1.7, 365)
	New→ Minor Transverse Defects	CT_{13}^{T-3}	Days	Weibull(1.7, 680)
	Minor Transverse Defects → Major Transverse Defects	CT_{14}^{T-3}	Days	Weibull(1.7, 355)
	Minor Surface Defects→ Surface Defects and Transverse Defects	CT_{15}^{T-3}	Days	Weibull(1.7, 320)
	Major Surface Defects→ Major Surface Defects and Transverse Defects	CT_{16}^{T-3}	Days	Weibull(1.7, 400)
	Minor Transverse Defects → Surface Defects and Transverse Defects	CT_{17}^{T-3}	Days	Weibull(1.7, 320)
	Major Transverse Defects → Major Surface Defects and Transverse Defects	CT_{18}^{T-3}	Days	Weibull(1.7, 400)
	Surface Defects and transverse → Major Surface Defects and Transverse Defects	CT_{19}^{T-3}	Days	Weibull(1.7, 350)
	Major Surface Defects and Transverse Defects→Serious Faults	CT_{20}^{T-3}	Days	Weibull(1.7, 190)

B-1.4: Rail deterioration rates Category 4

Category	State	Transition	Time Unit	Distribution
4	New→ Minor Surface Defects	CT_{11}^{T-4}	Days	Weibull(1.7, 825)
	Minor Surface Defects→ Major Surface Defects	CT_{12}^{T-4}	Days	Weibull(1.7, 430)
	New→ Minor Transverse Defects	CT_{13}^{T-4}	Days	Weibull(1.7, 805)
	Minor Transverse Defects → Major Transverse Defects	CT_{14}^{T-4}	Days	Weibull(1.7, 420)
	Minor Surface Defects→ Surface Defects and Transverse Defects	CT_{15}^{T-4}	Days	Weibull(1.7, 340)
	Major Surface Defects→ Major Surface Defects and Transverse Defects	CT_{16}^{T-4}	Days	Weibull(1.7, 420)
	Minor Transverse Defects → Surface Defects and Transverse Defects	CT_{17}^{T-4}	Days	Weibull(1.7, 340)
	Major Transverse Defects → Major Surface Defects and Transverse Defects	CT_{18}^{T-4}	Days	Weibull(1.7, 420)
	Surface Defects and transverse → Major Surface Defects and Transverse Defects	CT_{19}^{T-4}	Days	Weibull(1.7, 380)
	Major Surface Defects and Transverse Defects→ Serious Faults	CT_{20}^{T-4}	Days	Weibull(1.7, 210)

B-1.5: Rail deterioration rates Category 5

Category	State	Transition	Time Unit	Distribution
5	New→ Minor Surface Defects	CT_{11}^{T-5}	Days	Weibull(1.7, 1205)
	Minor Surface Defects→ Major Surface Defects	CT_{12}^{T-5}	Days	Weibull(1.7, 600)
	New→ Minor Transverse Defects	CT_{13}^{T-5}	Days	Weibull(1.7, 1105)
	Minor Transverse Defects → Major Transverse Defects	CT_{14}^{T-5}	Days	Weibull(1.7, 520)
	Minor Surface Defects→ Surface Defects and Transverse Defects	CT_{15}^{T-5}	Days	Weibull(1.7, 380)
	Major Surface Defects→ Major Surface Defects and Transverse Defects	CT_{16}^{T-5}	Days	Weibull(1.7, 440)
	Minor Transverse Defects → Surface Defects and Transverse Defects	CT_{17}^{T-5}	Days	Weibull(1.7, 380)
	Major Transverse Defects → Major Surface Defects and Transverse Defects	CT_{18}^{T-5}	Days	Weibull(1.7, 440)
	Surface Defects and transverse → Major Surface Defects and Transverse Defects	CT_{19}^{T-5}	Days	Weibull(1.7, 400)
	Major Surface Defects and Transverse Defects→ Serious Faults	CT_{20}^{T-5}	Days	Weibull(1.7, 225)

B-2: Rail Types

	Rail Types
1	UIC 60 Flat-bottom Rail (CEN-60-E-1)
2	BS113A Flat-bottom Rail
3	113lb Flat-bottom Rail
4	BS110A Flat-bottom Rail
5	109lb Flat-bottom Rail
6	97.5lb Bullhead Rail
7	95lb Bullhead Rail
8	85lb Bullhead Rail
9	Transition Rail

B-3: Rail Break Distributions

Category	**Exponential Lambda Values, time unit days**															
	Age (Years)	**1→5**			**5→10**			**10→15**			**15→20**			**>20**		
	Rail type	Bullhead	Flat-bottom (Low grades)	Flat-bottom (High grade)	Bullhead	Flat-bottom (Low grades)	Flat-bottom (High grade)	Bullhead	Flat-bottom (Low grades)	Flat-bottom (High grade)	Bullhead	Flat-bottom (Low grades)	Flat-bottom (High grade)	Bullhead	Flat-bottom (Low grades)	Flat-bottom (High grade)
1A&1	CT_0^{T-1A}, CT_0^{T-1}	3.00x10^{-6}	4.00 x10^{-6}	5.00 x10^{-6}	3.50 x10^{-6}	4.50 x10^{-6}	5.50 x10^{-6}	4.00 x10^{-6}	5.00 x10^{-6}	6.00 x10^{-6}	4.50 x10^{-6}	5.50 x10^{-6}	6.50 x10^{-6}	5.00 x10^{-6}	6.00 x10^{-6}	7.00 x10^{-6}
	CT_1^{T-1A}, CT_1^{T-1}	3.00 x10^{-6}	4.00 x10^{-6}	5.00 x10^{-6}	3.50 x10^{-6}	4.50 x10^{-6}	5.50 x10^{-6}	4.00 x10^{-6}	5.00 x10^{-6}	6.00 x10^{-6}	4.50 x10^{-6}	5.50 x10^{-6}	6.50 x10^{-6}	5.00 x10^{-6}	6.00 x10^{-6}	7.00 x10^{-6}
	CT_2^{T-1A}, CT_2^{T-1}	4.00 x10^{-6}	5.00 x10^{-6}	6.00 x10^{-6}	4.50 x10^{-6}	5.50 x10^{-6}	6.50 x10^{-6}	5.00 x10^{-6}	6.00 x10^{-6}	7.00 x10^{-6}	5.50 x10^{-6}	6.50 x10^{-6}	7.50 x10^{-6}	6.00 x10^{-6}	7.00 x10^{-6}	8.00 x10^{-6}
	CT_3^{T-1A}, CT_3^{T-1}	4.00 x10^{-6}	5.00 x10^{-6}	6.00 x10^{-6}	4.50 x10^{-6}	5.50 x10^{-6}	6.50 x10^{-6}	5.00 x10^{-6}	6.00 x10^{-6}	7.00 x10^{-6}	5.50 x10^{-6}	6.50 x10^{-6}	7.50 x10^{-6}	6.00 x10^{-6}	7.00 x10^{-6}	8.00 x10^{-6}
	CT_4^{T-1A}, CT_4^{T-1}	8.00 x10^{-6}	9.00 x10^{-6}	1.00 x10^{-5}	8.50 x10^{-6}	9.50 x10^{-6}	1.05 x10^{-5}	9.00 x10^{-6}	1.00 x10^{-5}	1.10 x10^{-5}	9.50 x10^{-6}	1.05 x10^{-5}	1.15 x10^{-5}	1.00 x10^{-5}	1.10 x10^{-5}	1.20 x10^{-5}
	CT_5^{T-1A}, CT_5^{T-1}	8.00 x10^{-6}	9.00 x10^{-6}	1.00 x10^{-5}	8.50 x10^{-6}	9.50 x10^{-6}	1.05 x10^{-5}	9.00 x10^{-6}	1.00 x10^{-5}	1.10 x10^{-5}	9.50 x10^{-6}	1.05 x10^{-5}	1.15 x10^{-5}	1.00 x10^{-5}	1.10 x10^{-5}	1.20 x10^{-5}
	CT_6^{T-1A}, CT_6^{T-1}	4.80 x10^{-5}	4.90 x10^{-5}	5.00 x10^{-5}	4.85 x10^{-5}	4.95 x10^{-5}	5.05 x10^{-5}	4.90 x10^{-5}	5.00 x10^{-5}	5.10 x10^{-5}	4.95 x10^{-5}	5.05 x10^{-5}	5.15 x10^{-5}	5.00 x10^{-5}	5.10 x10^{-5}	5.20 x10^{-5}
2&3	CT_0^{T-2}, CT_0^{T-3}	7.78 x10^{-7}	1.78 x10^{-6}	2.78 x10^{-6}	1.28 x10^{-6}	2.28 x10^{-6}	3.28 x10^{-6}	1.78 x10^{-6}	2.78 x10^{-6}	3.78 x10^{-6}	2.28x106	3.28 x10^{-6}	4.28 x10^{-6}	2.78 x10^{-6}	3.78 x10^{-6}	4.78 x10^{-6}
	CT_1^{T-2}, CT_1^{T-3}	7.78 x10^{-7}	1.78 x10^{-6}	2.78 x10^{-6}	1.28 x10^{-6}	2.28 x10^{-6}	3.28 x10^{-6}	1.78X106	2.78 x10^{-6}	3.78 x10^{-6}	2.28X106	3.28 x10^{-6}	4.28 x10^{-6}	2.78 x10^{-6}	3.78 x10^{-6}	4.78 x10^{-6}
	CT_2^{T-2}, CT_2^{T-3}	1.00 x10^{-6}	2.00X106	3.00 x10^{-6}	1.50 x10^{-6}	2.50 x10^{-6}	3.50 x10^{-6}	2.00 x10^{-6}	3.00 x10^{-6}	4.00 x10^{-6}	2.50 x10^{-6}	3.50 x10^{-6}	4.50 x10^{-6}	3.00 x10^{-6}	4.00 x10^{-6}	5.00 x10^{-6}
	CT_3^{T-2}, CT_3^{T-3}	1.00 x10^{-6}	2.00 x10^{-6}	3.00 x10^{-6}	1.50 x10^{-6}	2.50 x10^{-6}	3.50 x10^{-6}	2.00 x10^{-6}	3.00 x10^{-6}	4.00 x10^{-6}	2.50 x10^{-6}	3.50 x10^{-6}	4.50 x10^{-6}	3.00 x10^{-6}	4.00 x10^{-6}	5.00 x10^{-6}
	CT_4^{T-2}, CT_4^{T-3}	8.00 x10^{-6}	9.00 x10^{-6}	1.00 x10^{-5}	8.50 x10^{-6}	9.50 x10^{-6}	1.05 x10^{-5}	9.00 x10^{-6}	1.00 x10^{-5}	1.10 x10^{-5}	9.50 x10^{-6}	1.05 x10^{-5}	1.15 x10^{-5}	1.00 x10^{-5}	1.10 x10^{-5}	1.20 x10^{-5}
	CT_5^{T-2}, CT_5^{T-3}	8.00 x10^{-6}	9.00 x10^{-6}	1.00 x10^{-5}	8.50 x10^{-6}	9.50 x10^{-6}	1.05 x10^{-5}	9.00 x10^{-6}	1.00 x10^{-5}	1.10 x10^{-5}	9.50 x10^{-6}	1.05 x10^{-5}	1.15 x10^{-5}	1.00 x10^{-5}	1.10 x10^{-5}	1.20 x10^{-5}
	CT_6^{T-2}, CT_6^{T-3}	1.80 x10^{-5}	1.90 x10^{-5}	2.00 x10^{-5}	1.85 x10^{-5}	1.95 x10^{-5}	2.05 x10^{-5}	1.90 x10^{-5}	2.00 x10^{-5}	2.10 x10^{-5}	1.95 x10^{-5}	2.05 x10^{-5}	2.15 x10^{-5}	2.00 x10^{-5}	2.10 x10^{-5}	2.20 x10^{-5}
4&5	CT_0^{T-4}, CT_0^{T-5}	4.67 x10^{-7}	5.67 x10^{-7}	6.67 x10^{-7}	5.17 x10^{-7}	6.17 x10^{-7}	7.17 x10^{-7}	5.67 x10^{-7}	6.67 x10^{-7}	7.67 x10^{-7}	6.17 x10^{-7}	7.17 x10^{-7}	8.17 x10^{-7}	6.67 x10^{-7}	7.67 x10^{-7}	8.67 x10^{-7}
	CT_1^{T-4}, CT_1^{T-5}	4.67 x10^{-7}	5.67 x10^{-7}	6.67 x10^{-7}	5.17 x10^{-7}	6.17 x10^{-7}	7.17 x10^{-7}	5.67 x10^{-7}	6.67 x10^{-7}	7.67 x10^{-7}	6.17 x10^{-7}	7.17 x10^{-7}	8.17 x10^{-7}	6.67 x10^{-7}	7.67 x10^{-7}	8.67 x10^{-7}
	CT_2^{T-4}, CT_2^{T-5}	7.00 x10^{-7}	8.00 x10^{-7}	9.00 x10^{-7}	7.50 x10^{-7}	8.50 x10^{-7}	9.50 x10^{-7}	8.00 x10^{-7}	9.00 x10^{-7}	1.00 x10^{-6}	8.50 x10^{-7}	9.50 x10^{-7}	1.05 x10^{-6}	9.00 x10^{-7}	1.00 x10^{-6}	1.10 x10^{-6}
	CT_3^{T-4}, CT_3^{T-5}	7.00 x10^{-7}	8.00 x10^{-7}	9.00 x10^{-7}	7.50 x10^{-7}	8.50 x10^{-7}	9.50 x10^{-7}	8.00 x10^{-7}	9.00 x10^{-7}	1.00 x10^{-6}	8.50 x10^{-7}	9.50 x10^{-7}	1.05 x10^{-6}	9.00 x10^{-7}	1.00 x10^{-6}	1.10 x10^{-6}
	CT_4^{T-4}, CT_4^{T-5}	8.00 x10^{-7}	9.00 x10^{-7}	1.00 x10^{-6}	8.50 x10^{-7}	9.50 x10^{-7}	1.05 x10^{-6}	9.00 x10^{-7}	1.00 x10^{-6}	1.10 x10^{-6}	9.50 x10^{-7}	1.05 x10^{-6}	1.15 x10^{-6}	1.00 x10^{-6}	1.10 x10^{-6}	1.20 x10^{-6}
	CT_5^{T-4}, CT_5^{T-5}	8.00 x10^{-7}	9.00 x10^{-7}	1.00 x10^{-6}	8.50 x10^{-7}	9.50 x10^{-7}	1.05 x10^{-6}	9.00 x10^{-7}	1.00 x10^{-6}	1.10 x10^{-6}	9.50 x10^{-7}	1.05 x10^{-6}	1.15 x10^{-6}	1.00 x10^{-6}	1.10 x10^{-6}	1.20 x10^{-6}
	CT_6^{T-4}, CT_6^{T-5}	9.80 x10^{-6}	9.90 x10^{-6}	100. x10^{-5}	9.85 x10^{-6}	9.95 x10^{-6}	1.01 x10^{-5}	9.90 x10^{-6}	1.00 x10^{-5}	1.01 x10^{-5}	9.95 x10^{-6}	1.01 x10^{-5}	1.02 x10^{-5}	1.00 x10^{-5}	1.01 x10^{-5}	1.02 x10^{-5}

Appendix C: Sleeper Parameters

C-1: Deterioration Rates

C-1.1.1: Concrete sleeper Category 1A deterioration distributions

Category		Degradation	Transition	Time Unit	Distribution
1A	1	Deterioration of the rail seat area due to worn pads	T_0^{CS-1A}	Days	Exponential(0.0002)
	2	Deterioration of rail seat are due to no functioning pads	T_1^{CS-1A}	Days	Exponential(0.004)
	3	Damage to the fastening area	T_2^{CS-1A}	Days	Exponential(0.0008)
	4	Tamping damage	T_3^{CS-1A}	Days	Exponential(0.0008)
	5	Poor support due to ballast in Very poor condition	T_4^{CS-1A}	Days	Exponential(0.001)
	6	Very poor support due to ballast in Super red condition	T_5^{CS-1A}	Days	Exponential(0.0006)
	7	Concrete type (F27 and F40)	T_6^{CS-1A}	Days	Exponential(0.002)
	8	Baseline failure rate	T_7^{CS-1A}	Days	Weibull(2.3, 15330)

C-1.1.2: Concrete sleeper Category 1 deterioration distributions

Category		Degradation	Transition	Time Unit	Distribution
1	1	Deterioration of the rail seat area due to worn pads	T_0^{CS-1}	Days	Exponential(0.00016)
	2	Deterioration of rail seat are due to no functioning pads	T_1^{CS-1}	Days	Exponential(0.0032)
	3	Damage to the fastening area	T_2^{CS-1}	Days	Exponential(0.00064)
	4	Tamping damage	T_3^{CS-1}	Days	Exponential(0.00064)
	5	Poor support due to ballast in Very poor condition	T_4^{CS-1}	Days	Exponential(0.0008)
	6	Very poor support due to ballast in Super red condition	T_5^{CS-1}	Days	Exponential(0.00048)
	7	Concrete type (F27 and F40)	T_6^{CS-1}	Days	Exponential(0.0016)
	8	Baseline failure rate	T_7^{CS-1}	Days	Weibull(2.2, 17520)

C-1.1.3: Concrete sleeper Category 2 deterioration distributions

Category		Degradation	Transition	Time Unit	Distribution
2	1	Deterioration of the rail seat area due to worn pads	T_0^{CS-2}	Days	Exponential(0.000112)
	2	Deterioration of rail seat are due to no functioning pads	T_1^{CS-2}	Days	Exponential(0.00224)
	3	Damage to the fastening area	T_2^{CS-2}	Days	Exponential(0.000448)
	4	Tamping damage	T_3^{CS-2}	Days	Exponential(0.000448)
	5	Poor support due to ballast in Very poor condition	T_4^{CS-2}	Days	Exponential(0.00056)
	6	Very poor support due to ballast in Super red condition	T_5^{CS-2}	Days	Exponential(0.000336)
	7	Concrete type (F27 and F40)	T_6^{CS-2}	Days	Exponential(0.0012)
	8	Baseline failure rate	T_7^{CS-2}	Days	Weibull(2.2, 20075)

C-1.1.4: Concrete sleeper Category 3 deterioration distributions

Category		Degradation	Transition	Time Unit	Distribution
3	1	Deterioration of the rail seat area due to worn pads	T_0^{CS-3}	Days	Exponential(0.0000896)
	2	Deterioration of rail seat are due to no functioning pads	T_1^{CS-3}	Days	Exponential(0.001792)
	3	Damage to the fastening area	T_2^{CS-3}	Days	Exponential(0.000358)
	4	Tamping damage	T_3^{CS-3}	Days	Exponential(0.000358)
	5	Poor support due to ballast in Very poor condition	T_4^{CS-3}	Days	Exponential(0.000448)
	6	Very poor support due to ballast in Super red condition	T_5^{CS-3}	Days	Exponential(0.000269)
	7	Concrete type (F27 and F40)	T_6^{CS-3}	Days	Exponential(0.000896)
	8	Baseline failure rate	T_7^{CS-3}	Days	Weibull(2.4, 22995)

C-1.1.5: Concrete sleeper Category 4 deterioration distributions

Category		Degradation	Transition	Time Unit	Distribution
4	1	Deterioration of the rail seat area due to worn pads	T_0^{CS-4}	Days	Exponential(0.0000672)
	2	Deterioration of rail seat are due to no functioning pads	T_1^{CS-4}	Days	Exponential(0.001344)
	3	Damage to the fastening area	T_2^{CS-4}	Days	Exponential(0.000269)
	4	Tamping damage	T_3^{CS-4}	Days	Exponential(0.000269)
	5	Poor support due to ballast in Very poor condition	T_4^{CS-4}	Days	Exponential(0.000336)
	6	Very poor support due to ballast in Super red condition	T_5^{CS-4}	Days	Exponential(0.000202)
	7	Concrete type (F27 and F40)	T_6^{CS-4}	Days	Exponential(0.000672)
	8	Baseline failure rate	T_7^{CS-4}	Days	Weibull(2.45, 27375)

C-1.1.6 Concrete sleeper Category 5 deterioration distributions

Category		Degradation	Transition	Time Unit	Distribution
5	1	Deterioration of the rail seat area due to worn pads	T_0^{CS-5}	Days	Exponential(0.000047)
	2	Deterioration of rail seat are due to no functioning pads	T_1^{CS-5}	Days	Exponential(0.000941)
	3	Damage to the fastening area	T_2^{CS-5}	Days	Exponential(0.000188)
	4	Tamping damage	T_3^{CS-5}	Days	Exponential(0.000188)
	5	Poor support due to ballast in Very poor condition	T_4^{CS-5}	Days	Exponential(0.000235)
	6	Very poor support due to ballast in Super red condition	T_5^{CS-5}	Days	Exponential(0.000141)
	7	Concrete type (F27 and F40)	T_6^{CS-5}	Days	Exponential(0.00047)
	8	Baseline failure rate	T_7^{CS-5}	Days	Weibull(2.45, 32850)

C-1.2.1: Timber sleeper Category 1A deterioration distributions

Category		Degradation	Transition	Time Unit	Distribution
1A	1	Clip damage	T_0^{WS-1A}	Days	Exponential(0.1)
	2	Age of sleeper	T_1^{WS-1A}	Days	Exponential(0.01)
	3	Poor support	T_2^{WS-1A}	Days	Exponential(0.001)
	4	Baseline	T_3^{WS-1A}	Days	Weibull(2.8, 13000)

C-1.2.2: Timber sleeper Category 1 deterioration distributions

Category		Degradation	Transition	Time Unit	Distribution
1	1	Clip damage	T_0^{WS-1}	Days	Exponential(0.1)
	2	Age of sleeper	T_1^{WS-1}	Days	Exponential(0.01)
	3	Poor support	T_2^{WS-1}	Days	Exponential(0.001)
	4	Baseline	T_3^{WS-1}	Days	Weibull(2.75, 1512)

C-1.2.3: Timber sleeper Category 2 deterioration distributions

Category		Degradation	Transition	Time Unit	Distribution
2	1	Clip damage	T_0^{WS-2}	Days	Exponential(0.1)
	2	Age of sleeper	T_1^{WS-2}	Days	Exponential(0.01)
	3	Poor support	T_2^{WS-2}	Days	Exponential(0.001)
	4	Baseline	T_3^{WS-2}	Days	Weibull(2.65, 1712)

C-1.2.4: Timber sleeper Category 3 deterioration distributions

Category		Degradation	Transition	Time Unit	Distribution
3	1	Clip damage	T_0^{WS-3}	Days	Exponential(0.1)
	2	Age of sleeper	T_1^{WS-3}	Days	Exponential(0.01)
	3	Poor support	T_2^{WS-3}	Days	Exponential(0.001)
	4	Baseline	T_3^{WS-3}	Days	Weibull(2.65, 1812)

C-1.2.5 Timber sleeper Category 4 deterioration distributions

Category		Degradation	Transition	Time Unit	Distribution
4	1	Clip damage	T_0^{WS-4}	Days	Exponential(0.1)
	2	Age of sleeper	T_1^{WS-4}	Days	Exponential(0.01)
	3	Poor support	T_2^{WS-4}	Days	Exponential(0.001)
	4	Baseline	T_3^{WS-4}	Days	Weibull(2.65, 9856)

C-1.2.6 Timber sleeper Category 5 deterioration distributions

Category		Degradation	Transition	Time Unit	Distribution
5	1	Clip damage	T_0^{WS-5}	Days	Exponential(0.1)
	2	Age of sleeper	T_1^{WS-5}	Days	Exponential(0.01)
	3	Poor support	T_2^{WS-5}	Days	Exponential(0.0005)
	4	Baseline	T_3^{WS-5}	Days	Weibull(2.4, 10000)

C-1.3.1: Steel sleeper Category 1A deterioration distributions

Category		Degradation	Transition	Time Unit	Distribution
1A	1	Pad/isolation issues	T_0^{SS-1A}	Days	Exponential(0.002)
	2	Fastening issues	T_1^{SS-1A}	Days	Exponential(0.002)
	3	Ageing	T_2^{SS-1A}	Days	Weibull (2.75, 24000)
	4	Loading	T_3^{SS-1A}	Days	Weibull(2.8, 24000)

C-1.3.2: Steel sleeper Category 1 deterioration distributions

Category		Degradation	Transition	Time Unit	Distribution
1	1	Pad/isolation issues	T_0^{SS-1}	Days	Exponential(0.002)
	2	Fastening issues	T_1^{SS-1}	Days	Exponential(0.002)
	3	Ageing	T_2^{SS-1}	Days	Weibull (2.75, 27500)
	4	Loading	T_3^{SS-1}	Days	Weibull(2.85, 26000)

C-1.3.3: Steel sleeper Category 2 deterioration distributions

Category		Degradation	Transition	Time Unit	Distribution
2	1	Pad/isolation issues	T_0^{SS-2}	Days	Exponential(0.002)
	2	Fastening issues	T_1^{SS-2}	Days	Exponential(0.0016)
	3	Ageing	T_2^{SS-2}	Days	Weibull (2.85, 29500)
	4	Loading	T_3^{SS-2}	Days	Weibull(2.9, 28000)

C-1.3.4: Steel sleeper Category 3 deterioration distributions

Category		Degradation	Transition	Time Unit	Distribution
3	1	Pad/isolation issues	T_0^{SS-3}	Days	Exponential(0.002)
	2	Fastening issues	T_1^{SS-3}	Days	Exponential(0.0016)
	3	Ageing	T_2^{SS-3}	Days	Weibull (2.85, 31500)
	4	Loading	T_3^{SS-3}	Days	Weibull(2.9, 30000)

C-1.3.5: Steel sleeper Category 4 deterioration distributions

Category		Degradation	Transition	Time Unit	Distribution
4	1	Pad/isolation issues	T_0^{SS-4}	Days	Exponential(0.002)
	2	Fastening issues	T_1^{SS-4}	Days	Exponential(0.0016)
	3	Ageing	T_2^{SS-4}	Days	Weibull (2.85, 36500)
	4	Loading	T_3^{SS-4}	Days	Weibull(2.9, 35000)

C-1.3.6: Steel sleeper Category 5 deterioration distributions

Category		Degradation	Transition	Time Unit	Distribution
5	1	Pad/isolation issues	T_0^{SS-5}	Days	Exponential(0.002)
	2	Fastening issues	T_1^{SS-5}	Days	Exponential(0.0011)
	3	Ageing	T_2^{SS-5}	Days	Weibull (2.85, 42500)
	4	Loading	T_3^{SS-5}	Days	Weibull(2.9, 41000)

C-2: Sleeper Schedule Time

C-2.1: Concrete Sleeper Schedule Time

	Degradation	Transition	Time Unit	Distribution
1	Single Sleeper	T_9^{CS}	Days	Weibull(0.9,400)
2	Two Sleepers	T_{31}^{CS}	Days	Exponential(0.0014)
3	Three Sleepers	T_{32}^{CS}	Days	Weibull(0.5067,348.86)
4	Four Sleepers	T_{33}^{CS}	Days	Lognormal(3.834,2.344)
5	Five Sleepers	T_{34}^{CS}	Days	Lognormal(3.932,2.259)
6	Six Sleepers	T_{35}^{CS}	Days	Lognormal(3.640,2.139)
8	Major	T_{10}^{CS}	Days	Lognormal(3.004,1.933)

C-2.2: Timber/Wooden Sleeper Schedule Time

	Degradation	Transition	Time Unit	Distribution
1	Single Sleeper	T_{23}^{WS}	Days	Weibull(0.666, 520.48)
2	Two Sleepers	T_5^{WS}	Days	Weibull (0.595, 333.61)
3	Three Sleepers	T_7^{WS}	Days	Weibull(0.569, 324.96)
4	Four Sleepers	T_9^{WS}	Days	Weibull (0.517, 208.99)
5	Five Sleepers	T_{11}^{WS}	Days	Lognormal(4.198, 2.223)
6	Six Sleepers	T_{13}^{WS}	Days	Lognormal(4.055, 2.195)
7	Seven Sleepers	T_{15}^{WS}	Days	Lognormal(4.179, 2.153)
8	Eight Sleepers	T_{17}^{WS}	Days	Lognormal(4.122, 2.197)
9	Nine Sleepers	T_{19}^{WS}	Days	Lognormal(4.473, 2.112)
10	Ten Sleepers	T_{21}^{WS}	Days	Lognormal(3.922, 1.908)
11	Major	T_{25}^{WS}	Days	Lognormal(1,1)

C-2.3: Steel Sleeper Schedule Time

	Degradation	Transition	Time Unit	Distribution
1	Single Sleeper	T_{15}^{SS}	Days	Lognormal (2.172, 1.763)
2	Two Sleepers	T_5^{SS}	Days	Lognormal l(2.869, 1.697)
3	Three Sleepers	T_7^{SS}	Days	2[30]
4	Four Sleepers	T_9^{SS}	Days	Lognormal(1.726, 0.774)
5	Five Sleepers	T_{11}^{SS}	Days	Lognormal(3.492, 2.076)
6	Six Sleepers	T_{13}^{SS}	Days	Normal(400, 332.268)
8	Major	T_{17}^{SS}	Days	Lognormal(1,1)

[30] Due to the lack of data point was not possible to fit a distribution

C-3: Sleeper ART

C-3.1: Concrete Sleeper ART

	Degradation	Transition	Time Unit	Distribution
1	Single Sleeper	T_{41}^{CS}	Hours	Weibull(1.285, 7.358)
2	Two Sleepers	T_{36}^{CS}	Hours	Weibull (1.307, 11.878)
3	Three Sleepers	T_{37}^{CS}	Hours	Weibull(1.479, 16.682)
4	Four Sleepers	T_{38}^{CS}	Hours	Weibull (1.472, 17.501)
5	Five Sleepers	T_{39}^{CS}	Hours	Weibull (1.506 ,24.512)
6	Six Sleepers	T_{40}^{CS}	Hours	Weibull (1.693, 24.448)
7	Major	T_{11}^{CS}	Hours	Weibull(1.062,13.114)

C-3.2: Timber Sleeper ART

	Degradation	Transition	Time Unit	Distribution
1	Single Sleeper	T_{22}^{WS}	Hours	Lognormal (1.087, 0.882)
2	Two Sleepers	T_{4}^{WS}	Hours	Lognormal (1.671, 0.776)
3	Three Sleepers	T_{6}^{WS}	Hours	Weibull(1.440, 10.048)
4	Four Sleepers	T_{8}^{WS}	Hours	Weibull (1.458, 12.945)
5	Five Sleepers	T_{10}^{WS}	Hours	Weibull (1.612, 16.344)
6	Six Sleepers	T_{12}^{WS}	Hours	Weibull (1.584, 19.319)
7	Seven Sleepers	T_{14}^{WS}	Hours	Weibull (1.632, 21.894)
8	Eight Sleepers	T_{16}^{WS}	Hours	Weibull (1.312, 21.929)
9	Nine Sleepers	T_{18}^{WS}	Hours	Normal(21.030, 11.937)
10	Ten Sleepers	T_{20}^{WS}	Hours	Weibull (1.806, 29.907)
11	Major	T_{24}^{WS}	Hours	Lognormal(1,1)

C-3.3: Steel Sleeper ART

	Degradation	Transition	Time Unit	Distribution
1	Single Sleeper	T_{14}^{SS}	Hours	Lognormal(1.521, 0.919)
2	Two Sleepers	T_{4}^{SS}	Hours	Weibull(1.1092, 10.986)
3	Three Sleepers	T_{6}^{SS}	Hours	Lognormal(1.263, 0.750)
4	Four Sleepers	T_{8}^{SS}	Hours	Lognormal(2.426, 1.046)
5	Five Sleepers	T_{10}^{SS}	Hours	Lognormal(2.571, 0.210)
6	Six Sleepers	T_{12}^{SS}	Hours	Normal(31.6, 17.636)
7	Major	T_{16}^{SS}	Hours	Lognormal(1, 1)

C-4: Conditional Probabilistic Values

C-4.1: Concrete sleeper, probability of repairing: two, three, four, five or six sleepers based on the number that are degraded (CPT_0^{CS})

		Number of sleepers repaired (p)				
		2	3	4	5	6
Number of degraded sleepers	2	1.000	0.000	0.000	0.000	0.000
	3	0.999	0.001	0.000	0.000	0.000
	4	0.998	0.001	0.001	0.000	0.000
	4	0.900	0.090	0.010	0.000	0.000
	5	0.750	0.180	0.020	0.050	0.000
	6	0.700	0.190	0.070	0.030	0.010
	7	0.600	0.100	0.090	0.030	0.180
	8	0.500	0.170	0.120	0.040	0.170
	9	0.450	0.200	0.150	0.050	0.150
	10	0.300	0.230	0.200	0.150	0.120
	11	0.250	0.250	0.200	0.100	0.200
	12	0.200	0.270	0.270	0.110	0.150
	13	0.100	0.290	0.280	0.120	0.210
	14	0.090	0.350	0.280	0.100	0.180
	15	0.080	0.330	0.310	0.110	0.170
	16	0.070	0.370	0.350	0.100	0.110
	17	0.060	0.350	0.400	0.110	0.080
	18	0.050	0.250	0.410	0.200	0.090
	19	0.010	0.250	0.420	0.210	0.110
	20	0.010	0.250	0.350	0.220	0.170
	21	0.010	0.250	0.350	0.230	0.160
	22	0.010	0.150	0.300	0.240	0.300
	>22	1.000	0.000	0.000	0.000	0.000

C-4.2: Timber sleeper probability of repairing: two, three, four, five, six, seven, eight, nine or ten sleepers based on the number that are degraded (CPT_0^{WS})

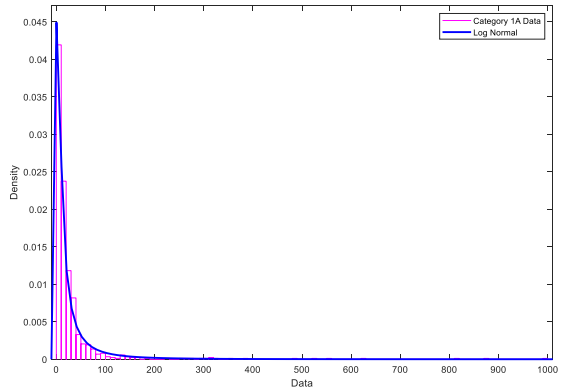
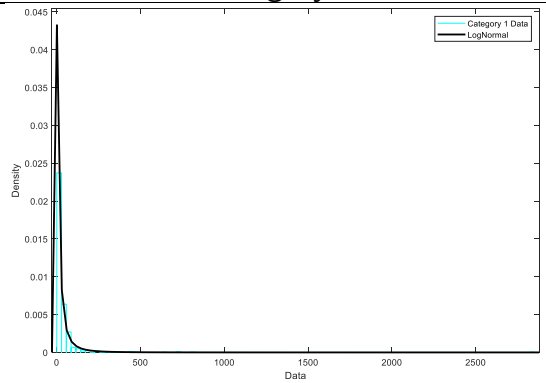
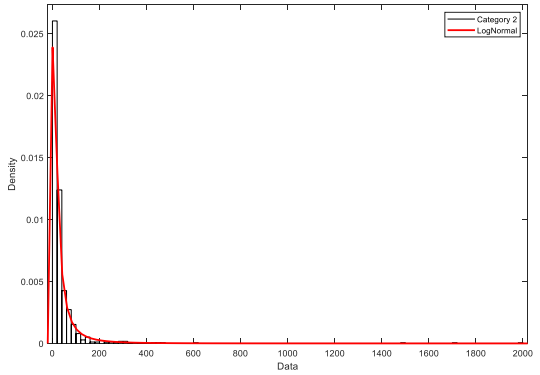
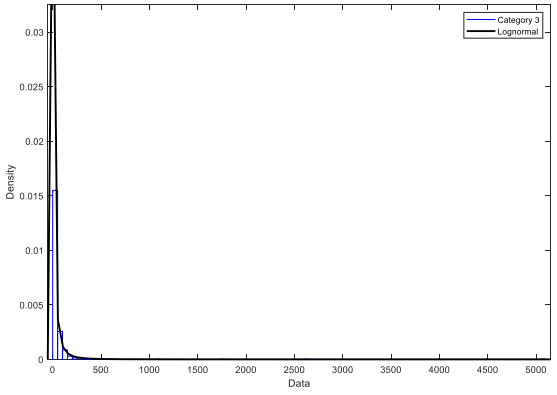
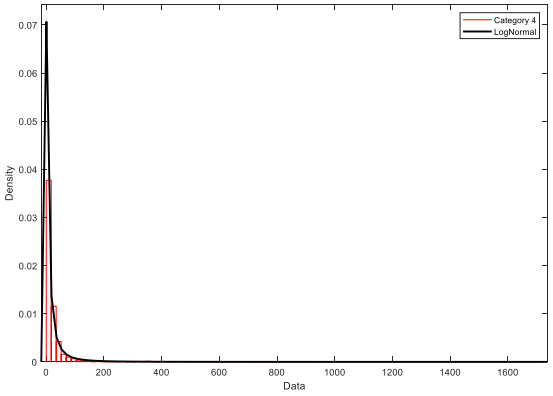
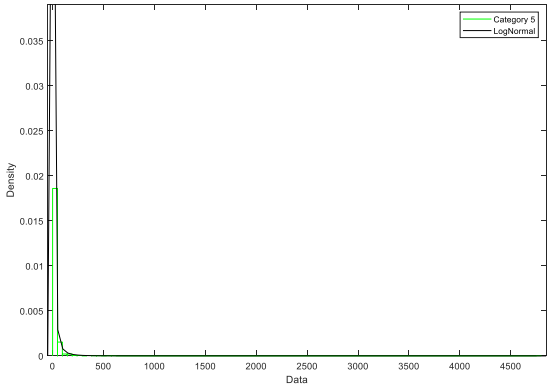
		Number of sleepers repaired (p)								
		2	3	4	5	6	7	8	9	10
Number of degraded sleepers	2	1.000	0.000	0.000	0.000	0.000	0.000	0.000	0.000	0.000
	3	0.750	0.250	0.000	0.000	0.000	0.000	0.000	0.000	0.000
	4	0.500	0.100	0.400	0.000	0.000	0.000	0.000	0.000	0.000
	5	0.450	0.200	0.300	0.050	0.000	0.000	0.000	0.000	0.000
	6	0.400	0.150	0.200	0.100	0.150	0.000	0.000	0.000	0.000
	7	0.100	0.190	0.200	0.180	0.010	0.320	0.000	0.000	0.000
	8	0.100	0.100	0.240	0.080	0.200	0.030	0.250	0.000	0.000
	9	0.090	0.170	0.120	0.090	0.150	0.200	0.039	0.141	0.000
	10	0.080	0.150	0.270	0.050	0.050	0.100	0.070	0.009	0.221
	11	0.070	0.090	0.160	0.150	0.050	0.040	0.050	0.200	0.190
	12	0.065	0.080	0.150	0.100	0.100	0.060	0.200	0.090	0.155
	13	0.065	0.070	0.155	0.110	0.125	0.060	0.190	0.090	0.135
	14	0.060	0.065	0.160	0.120	0.125	0.100	0.180	0.090	0.100
	15	0.050	0.050	0.100	0.100	0.125	0.110	0.170	0.080	0.215
	16	0.009	0.040	0.170	0.110	0.125	0.120	0.160	0.070	0.196
	17	0.008	0.009	0.100	0.100	0.125	0.130	0.150	0.032	0.346
	18	0.007	0.008	0.100	0.110	0.125	0.135	0.130	0.034	0.351
	19	0.006	0.007	0.100	0.200	0.125	0.140	0.135	0.130	0.157
	20	0.001	0.003	0.150	0.170	0.180	0.100	0.140	0.135	0.121
	21	0.001	0.001	0.100	0.220	0.125	0.060	0.100	0.140	0.253
	22	0.001	0.001	0.100	0.230	0.125	0.060	0.002	0.100	0.381
	>22	0.001	0.001	0.100	0.240	0.125	0.060	0.002	0.035	0.436

C-4.3: Steel sleeper, probability of repairing: two, three, four, five or six sleepers based on the number that are degraded (CPT_0^{SS})

		Number of sleepers repaired				
		2	3	4	5	6
Number of degraded sleepers	2	1.000	0.000	0.000	0.000	0.000
	3	0.999	0.001	0.000	0.000	0.000
	4	0.998	0.001	0.001	0.000	0.000
	4	0.900	0.090	0.010	0.000	0.000
	5	0.750	0.180	0.020	0.050	0.000
	6	0.700	0.190	0.070	0.030	0.010
	7	0.600	0.100	0.090	0.030	0.180
	8	0.500	0.170	0.120	0.040	0.170
	9	0.450	0.200	0.150	0.050	0.150
	10	0.300	0.230	0.200	0.150	0.120
	11	0.250	0.250	0.200	0.100	0.200
	12	0.200	0.270	0.270	0.110	0.150
	13	0.100	0.290	0.280	0.120	0.210
	14	0.090	0.350	0.280	0.100	0.180
	15	0.080	0.330	0.310	0.110	0.170
	16	0.070	0.370	0.350	0.100	0.110
	17	0.060	0.350	0.400	0.110	0.080
	18	0.050	0.250	0.410	0.200	0.090
	19	0.010	0.250	0.420	0.210	0.110
	20	0.010	0.250	0.350	0.220	0.170
	21	0.010	0.250	0.350	0.230	0.160
	22	0.010	0.150	0.300	0.240	0.300
	>22	1.000	0.000	0.000	0.000	0.000

C-5: Goodness of Fit for Transition T_3^{WS}

C-5.1: Comparison between the distribution used for T_3^{WS} in the system model and the predetermined value used in the individual model for Categories 1A→5

<table>
<tr><th>Category 1A</th><th>Category 1</th><th>Category 2</th></tr>
<tr><td>
</td><td>
</td><td>
</td></tr>
<tr><th>Category 3</th><th>Category 4</th><th>Category 5</th></tr>
<tr><td>
</td><td>
</td><td>
</td></tr>
</table>

C-6: Distributions for Transition T_{46}^{WS}

C-6.1: Distributions for Transition T_{46}^{WS}, time to 'old'

Category	Wood type	Transition	Time Unit	Distribution
1A	Hardwood	T_{46}^{WS-1A}	Days	Normal(7300, 160)
1	Hardwood	T_{46}^{WS-1}	Days	Normal(9125, 150)
2	Hardwood	T_{46}^{WS-2}	Days	Normal(10220, 150)
3	Hardwood	T_{46}^{WS-3}	Days	Normal(10950, 150)
4	Softwood	T_{46}^{WS-4}	Days	Normal(7300, 150)
5	Softwood	T_{46}^{WS-5}	Days	Normal(8760, 150)

Appendix D: Switches and Crossings Summary

C-1 S&C Size Summary

D-1.1 UK S&C by switch size including number of stretcher bars, bearers and slide chairs; note each S&C is unique, the numbers listed are just a guide

	S&C type	Turnout length (m)	Switch radius (m)	Max speed (mph)	Number of units	Number of stretcher bars	Number of bearers	Number of slide chairs	Number of crossings
1	Turnout A	7.3	141.1	10	280	2	25	50	1
2	Turnout B	8.7	184.0	20	1700	2	30	60	1
3	Turnout C	11.9	245.8	30	8000	3	35	70	1
4	Turnout D	12.4	332.7	40	2850	4	45	90	1
5	Turnout E	17.3	645.1	50	2290	4	50	100	1
6	Turnout F	20.8	980.9	60	760	5	60	120	1
7	Turnout G	24.4	1264	70	390	6	70	140	1
8	Turnout H	>24.4	>1264	90	14	>6	>70	>140	1
9	Catch points	N/A	N/A	N/A	890	variable	variable	variable	1
10	Other (including fixed diamond crossing and scissors)	N/A	N/A	Variable	1125	Variable (Zero for fixed diamond crossing)	Variable (60 for fixed diamond crossing)	Variable (Zero for fixed diamond crossing)	Variable (Four for fixed diamond crossing)

D-2: S&C Stretcher Bar Summary

D-2.1 CP4 stretcher bar maintenance tasks

	Job Code	Maintenance Description	Number of Occurrences
1	1151	S&C Replace/Adjust A Pts Stretcher Bar	4528
2	1152	S&C Pt Mach - Install Stretcher Bar	163
3	1153	S&C Pt Mach - Refit Stretcher Bar	713
4	6969	S&C Renew Stretcher Bar Assemble Hardlock Bolts	502
5	6974	S&C Replace Lock Stretcher Bolts	130
6	7415	S&C Maintain Tubular Stretcher Bar	1
7	8040	S&C Sin110 Replace Adjustable Stretcher Bar	1441
8	8043	S&C Sin110 Refurbish Adjustable Stretcher Bar	730
9	9218	S&C - Renew Stretcher Bar	1025
		Total:	9233

Appendix E: Inspection Costs

E-2: Summary of Inspections in the System Model

E-2.1 Inspection Cost Breakdown for the System Model

Asset class		Inspection type	Inspection frequency	Inspections per year	Inspections in 35 years	Number of assets to inspect	Inspection cost	Total cost
Track section	Category 1A	Visual	14	26.07	912.5	484	8	3,533,200
		Ultra Sonic	56	6.52	228.1	484	8	883,300
		Maintenance Train	42	8.69	304.2	484	8	1,177,733
	Category 1	Visual	14	26.07	912.5	60	8	438,000
		Ultra Sonic	56	6.52	228.1	60	8	109,500
		Maintenance Train	70	5.21	182.5	60	8	87,600
	Category 2	Visual	14	26.07	912.5	170	8	1,241,000
		Ultra Sonic	112	3.26	114.1	170	8	155,125
		Maintenance Train	98	3.72	130.4	170	8	177,286
	Category 3	Visual	28	13.04	456.3	6	8	21,900
		Ultra Sonic	182	2.01	70.2	6	8	3,369
		Maintenance Train	126	2.90	101.4	6	8	4,867
	Category 5	Visual	56	6.52	228.1	129	8	235,425
		Ultra Sonic	182	2.01	70.2	129	8	72,438
		Maintenance Train	182	2.01	70.2	129	8	72,438
Tunnel		Visual	365	1	35	6	200	42,000
S&C		Visual	7	52.14	1825.0	61	8	890,600
		Ultra Sonic	56	6.52	228.1	61	8	111,325
		Maintenance Train	112	3.26	114.1	61	8	55,663
							Total	**9,312,769**

Appendix F: Budget Parameters

F-1: Assessment of Funding

F-1.1: ORR and Network Rail Assessment of LNW Route Maintenance Expenditure for CP5 (Millions) [157].

Total(£m)	2014-15	2015-16	2016-17	2017-18	2018-19	CP5 Total
Network Rail	280	269	267	259	250	1326
ORR	277	266	259	250	244	1296
Average Value	279	268	263	255	247	1311

F-1.2: ORR Assessment of LNW Route Maintenance Expenditure Breakdown for CP5 [157].

Asset Breakdown (%)	2014-15	2015-16	2016-17	2017-18	2018-19	CP5 Total
Track	38%	38%	38%	37%	37%	38%
Signalling	14%	14%	14%	14%	14%	14%
Civils and buildings	7%	8%	8%	8%	8%	8%
Electrification and fixed plant	8%	8%	8%	9%	9%	8%
Telecoms	2%	2%	2%	2%	2%	2%
Other maintenance	20%	20%	20%	20%	19%	20%
Reactive maintenance	11%	11%	11%	11%	10%	11%
Total	100%	100%	100%	100%	100%	100%

F-1.3: Network Rail Assessment of LNW Route Renewal Expenditure for CP5 (Millions) [157].

Total(£m)	2014-15	2015-16	2016-17	2017-18	2018-19	CP5 Total
Network Rail	536	557	571	571	534	2722

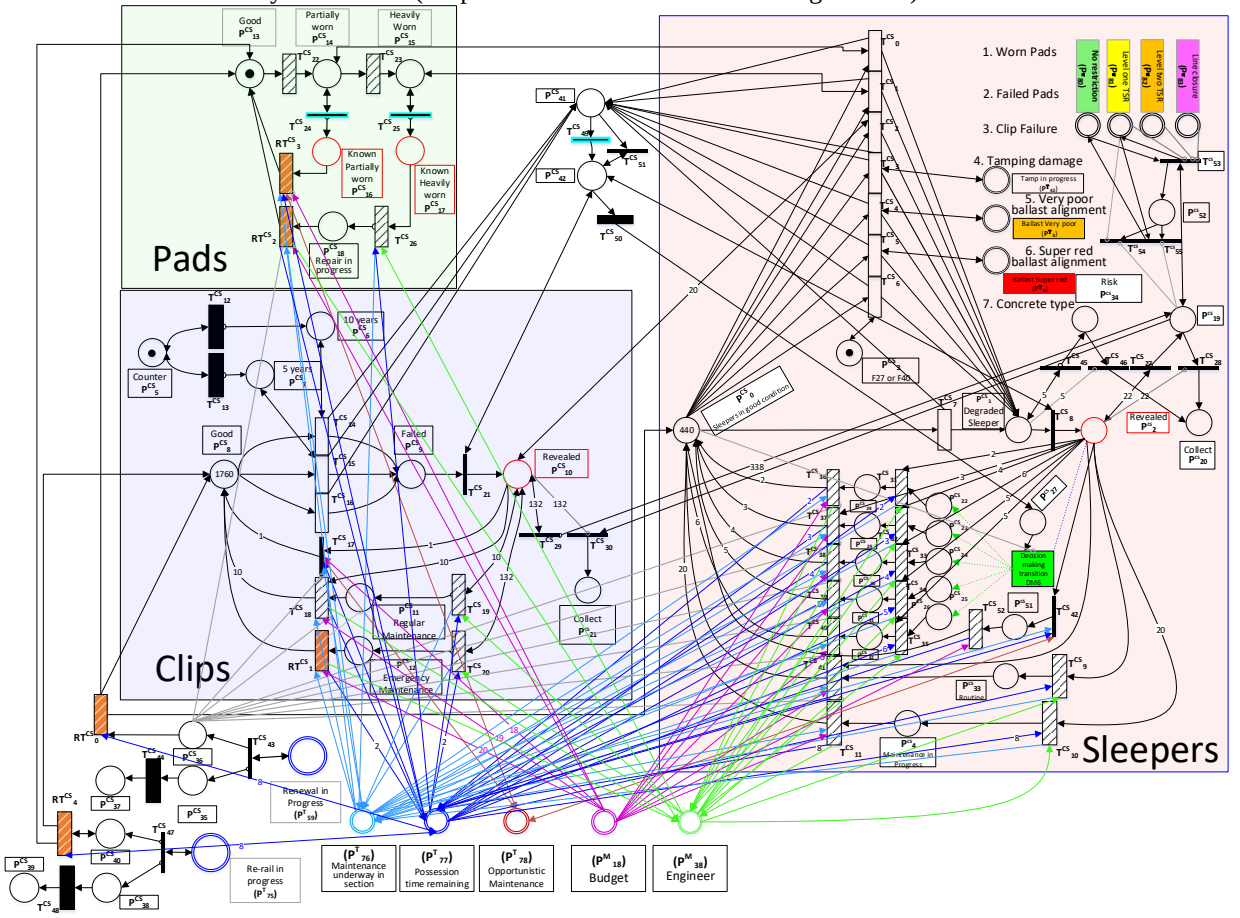
F-1.4: Network Rail Assessment of LNW Route Renewal Expenditure by Asset Type CP5 [157].

Asset Class	CP5 Total
Track	27.35%
Signalling	27.16%
Civils and buildings	20.08%
Electrification and fixed plant	9.64%
Telecoms	8.15%
Other maintenance	3.22%
Reactive maintenance	4.40%
Total	100%

Appendix G: System Level Asset Module Petri Nets

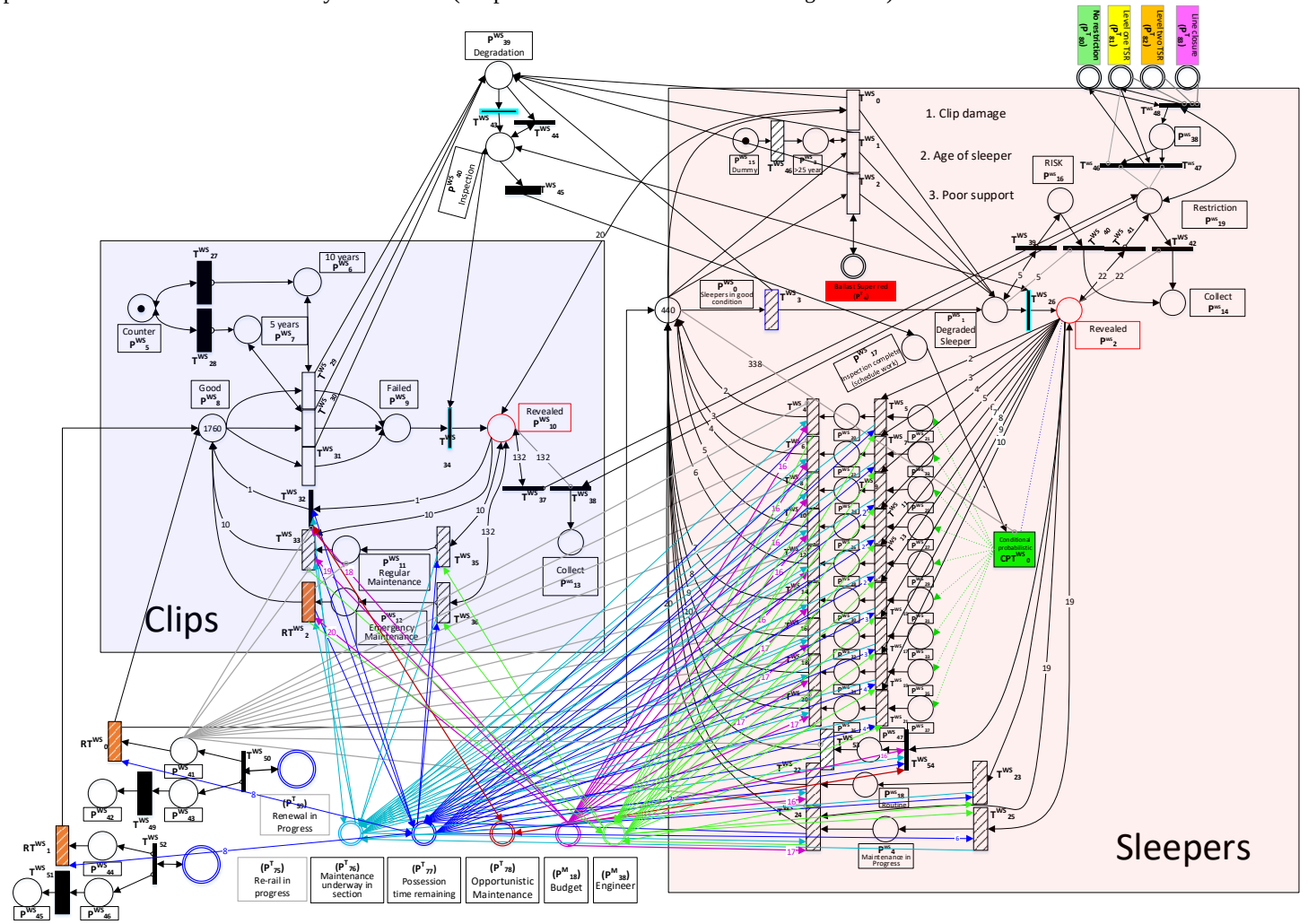
G-1: System Petri Net Module Diagrams

G-1.1: Concrete sleeper Petri net module used in the system model (adapted from individual model in Figure 6.23)



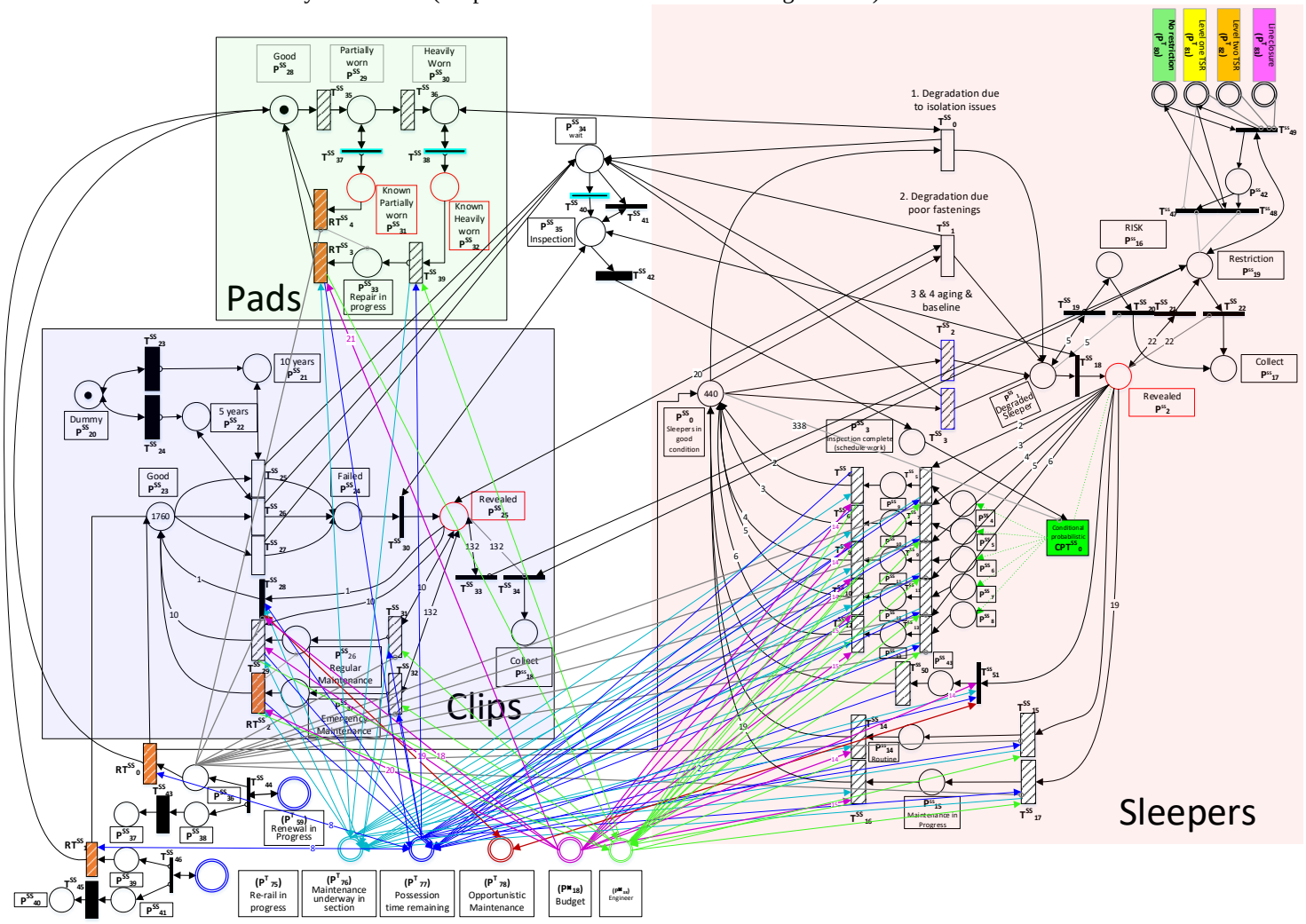
Coloured arcs used for clarity in diagrams

G-1.2: Timber sleeper Petri net module used in the system model (adapted from individual model in Figure 6.28)



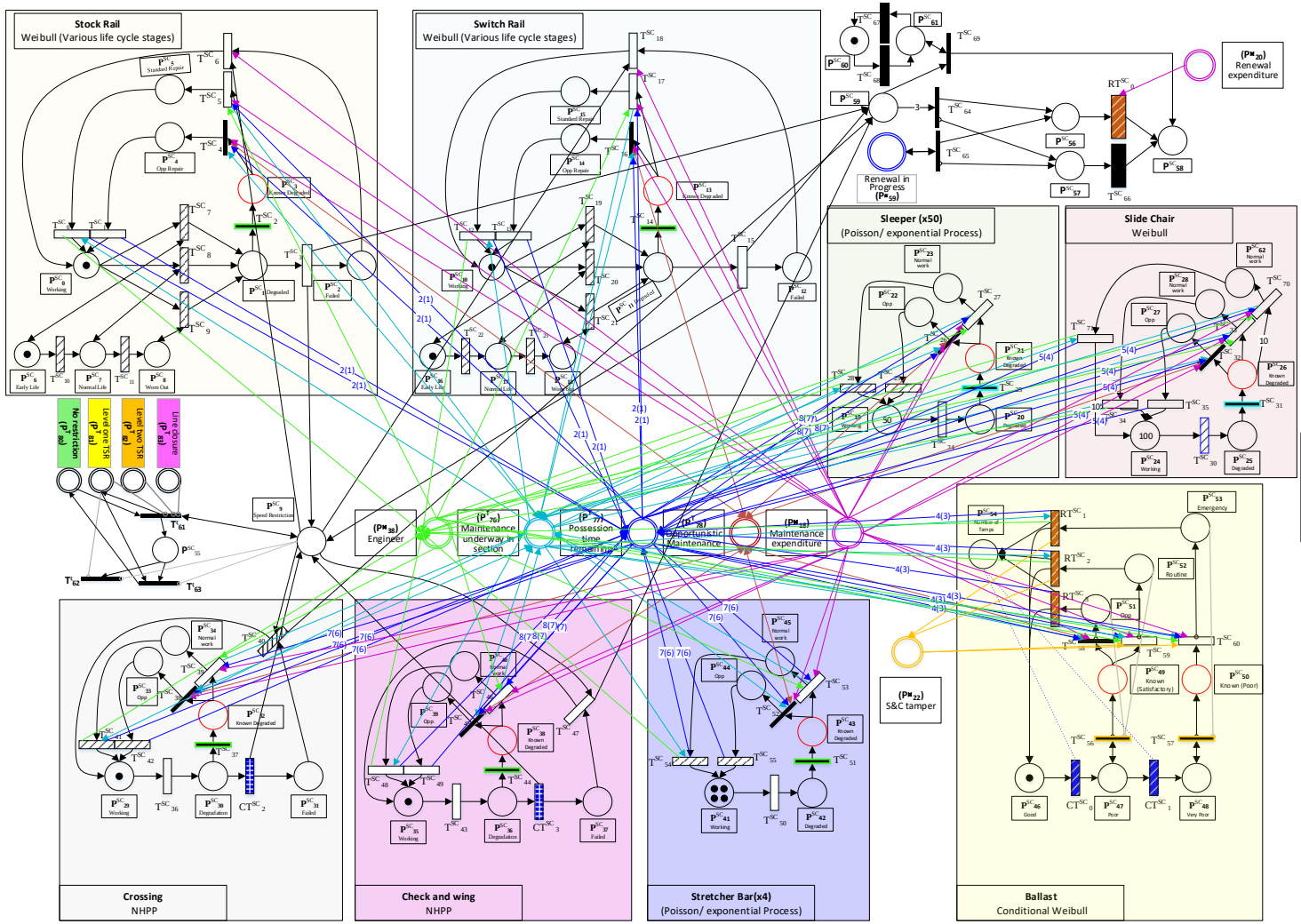
Coloured arcs used for clarity in diagrams

G-1.3: Steel sleeper Petri net module used in the system model (adapted from individual model in Figure 6.32)



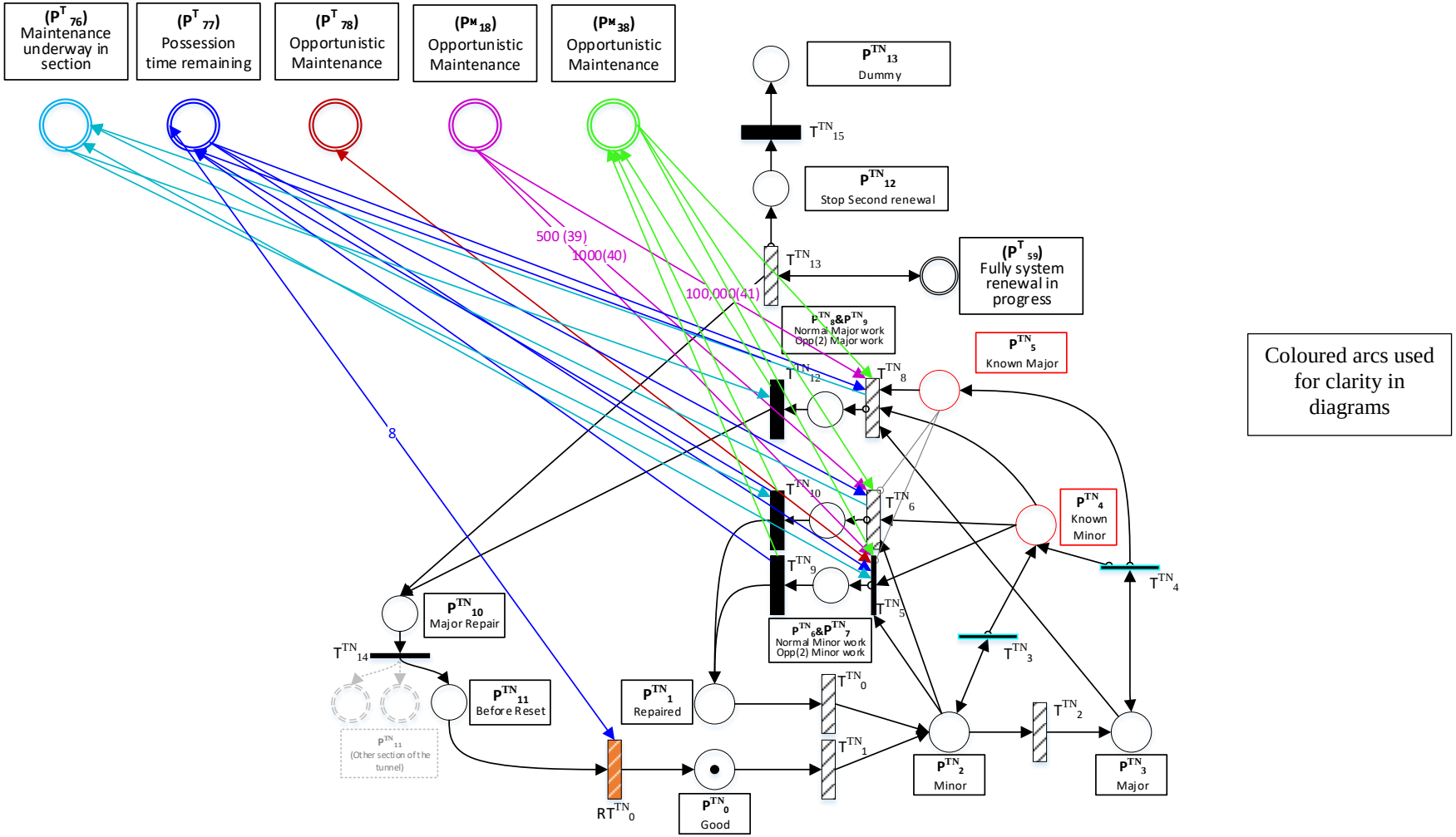
Coloured arcs used for clarity in diagrams

G-1.4: S&C Petri net module used in the system model (adapted from individual model in Figure 6.38)

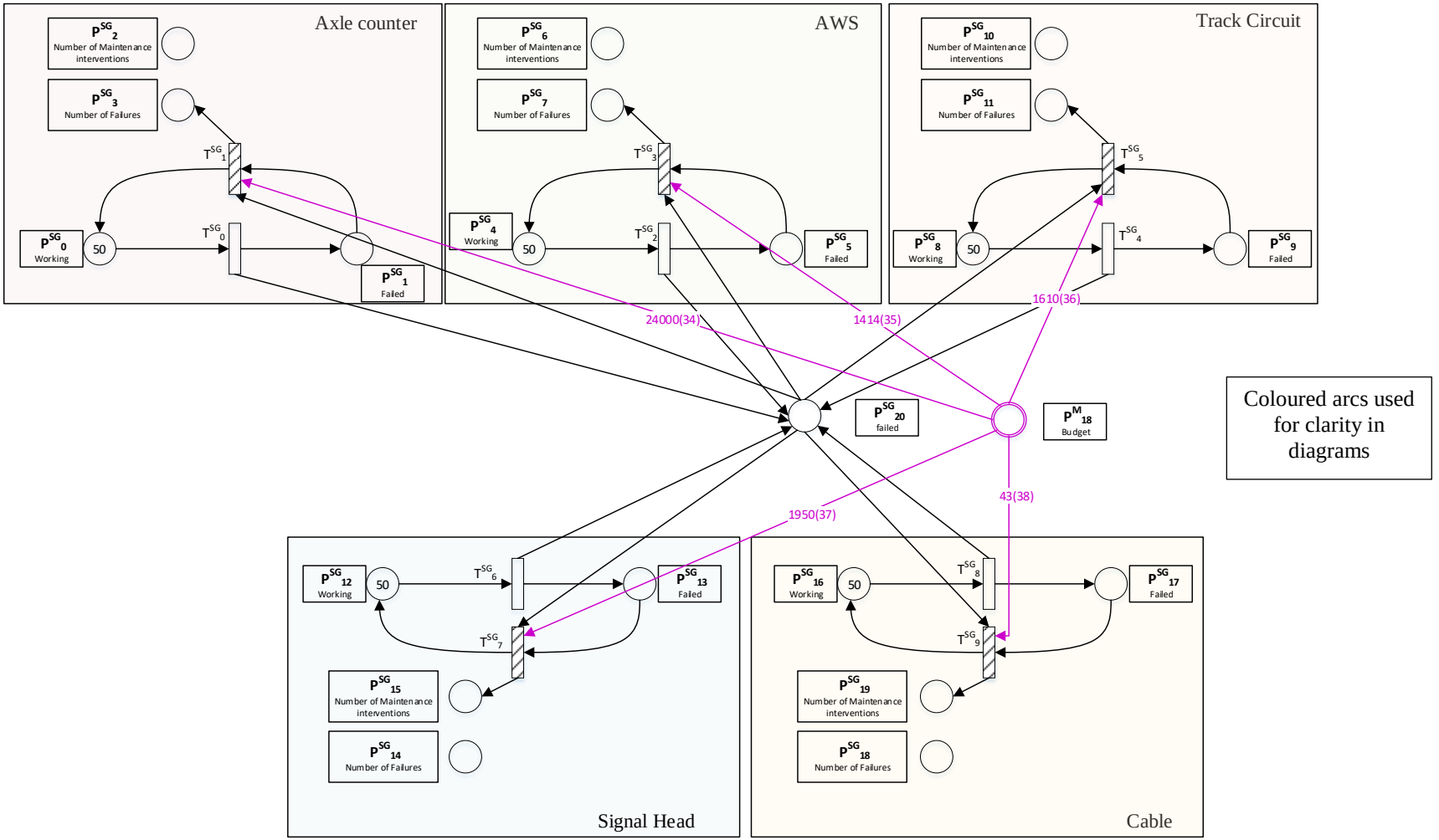


Coloured arcs used for clarity in diagrams

G-1.5: Tunnel Petri net module used in the system model (adapted from individual model in Figure 6.37)



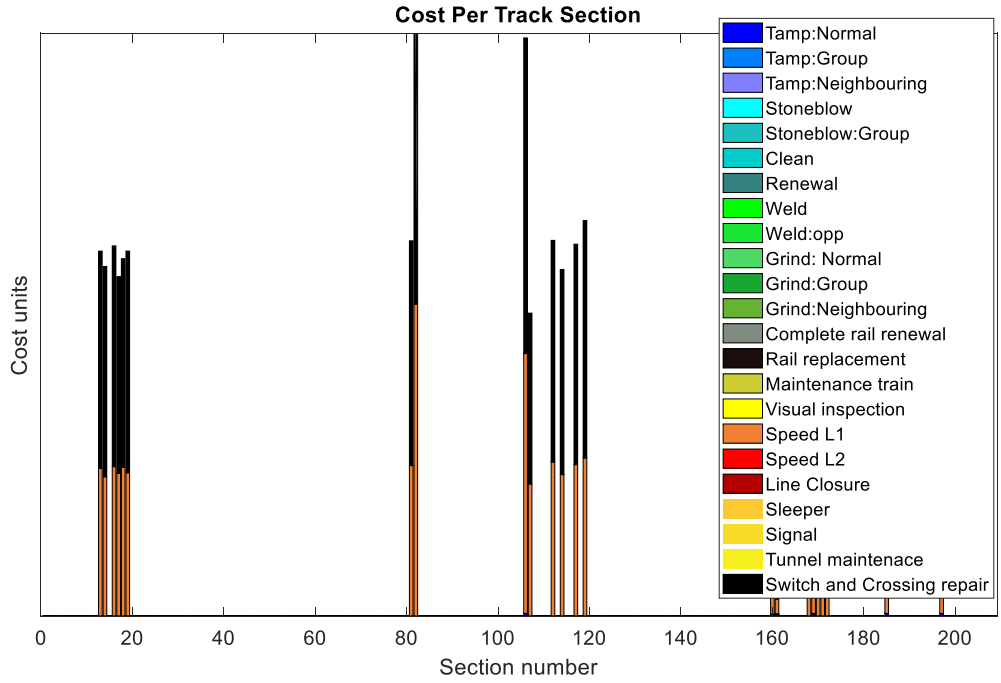
G-1.6: Signal Petri net module used in the system model (adapted from individual model in Figure 6.42)



Appendix H: Special Case Solutions to the System Model

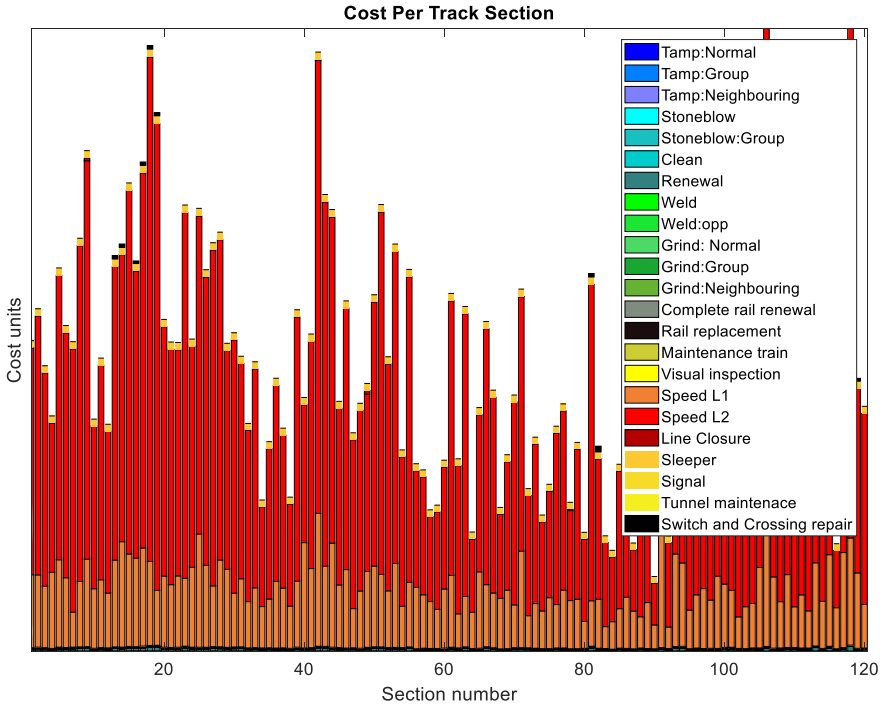
H-1: Special Case Solution for Validation

H-1.1: Case 1: Very large time between inspections



Major cost incurred is S&C failures and the speed restrictions associated with them, tamping/stoneblowing occurs in sections that start in a *known* degraded condition

H-1.2: Case 3: No tampers



No tamping costs and very high cost due to TSR as tamping requests are never met.

Appendix I: System Model Initial Marking Distributions

I-1: Tamping Previous Intervention Distributions

I-1.1: Distribution for the number of previous tamps

Category	Distribution
Category 1A	Lognormal(0.6, 1)
Category 1	Lognormal(0.8, 0.8)
Category 2	Lognormal(0.7, 0.65)
Category 3	Lognormal(0.6, 0.6)
Category 4	Lognormal(0.3, 0.4)
Category 5	Lognormal(0.1, 0.1)

I-2: Stoneblowing Previous Intervention Distributions

I-2.1: Distribution for the number of previous stoneblows

Category	Distribution
Category 1A	Lognormal(0.1, 0.1)
Category 1	Lognormal(0.8, 0.8)
Category 2	Lognormal(0.7, 0.65)
Category 3	Lognormal(0.6, 0.6)
Category 4	Lognormal(0.3, 0.4)
Category 5	Lognormal(0.1, 0.1)

I-3: Cleaning Previous Intervention Distributions

I-3.1: Distribution for the number of previous cleans

Category	Distribution
Category 1A	Lognormal(0.1, 0.5)
Category 1	Lognormal(0.8, 0.8)
Category 2	Lognormal(0.7, 0.65)
Category 3	Lognormal(0.6, 0.6)
Category 4	Lognormal(0.3, 0.4)
Category 5	Lognormal(0.1, 0.1)

I-4: Grinding Previous Intervention Distributions

I-4.1: Distribution for the number of previous grinds

Category	Distribution
Category 1A	Lognormal(1.5, 0.2)
Category 1	Lognormal(0.8, 0.8)
Category 2	Lognormal(0.7, 0.65)
Category 3	Lognormal(0.6, 0.6)
Category 4	Lognormal(0.3, 0.4)
Category 5	Lognormal(0.1, 0.1)

I-5: Welding Previous Intervention Distributions

I-5.1: Distribution for the number of previous welds

Category	Distribution
Category 1A	Lognormal(1.6, 0.3)
Category 1	Lognormal(0.8, 0.8)
Category 2	Lognormal(0.7, 0.65)
Category 3	Lognormal(0.6, 0.6)
Category 4	Lognormal(0.3, 0.4)
Category 5	Lognormal(0.1, 0.1)

Appendix J: Location Parameters

J-1: List of Location Parameters and Associated LI Score for Bletchley Delivery Unit Track Sections

J-1.1: LI scores

Section Number	Tonnage (EMGTPA)		Speed (mph)		Jointed		Sleeper design		Bed Rock		Electrification		Curvature (m^{-1})		Tunnel		Overall Score
	Value/ LI Score		Value/ LI Score		Value/ LI Score		Value/ LI Score		Value/ LI Score		Value/ LI Score		Value/ LI Score		Value/ LI		
1	54.48	190.7	125	280.0	C	0	G44 Concrete Sleeper With Fastclip	0	Gault Formation And Upper Greensand Formation	30	Overhead Line	0	0.00000	0.0	0	0	500.7
2	54.48	190.7	125	280.0	C	0	G44 Concrete Sleeper With Fastclip	0	Gault Formation And Upper Greensand Formation	30	Overhead Line	0	0.00000	0.0	0	0	500.7
3	54.48	190.7	125	280.0	C	0	G44 Concrete Sleeper With Fastclip	0	Gault Formation And Upper Greensand Formation	30	Overhead Line	0	0.00000	0.0	0	0	500.7
4	54.48	190.7	125	280.0	C	0	G44 Concrete Sleeper With Fastclip	0	Gault Formation And Upper Greensand Formation	30	Overhead Line	0	0.00000	0.0	0	0	500.7
5	54.48	190.7	125	280.0	C	0	G44 Concrete Sleeper With Fastclip	0	Gault Formation And Upper Greensand Formation	30	Overhead Line	0	0.00000	0.0	0	0	500.7
6	54.48	190.7	125	280.0	C	0	G44 Concrete Sleeper With Fastclip	0	Gault Formation And Upper Greensand Formation	30	Overhead Line	0	0.00000	0.0	0	0	500.7
7	54.49	190.7	125	280.0	C	0	G44 Concrete Sleeper With Fastclip	0	Gault Formation And Upper Greensand Formation	30	Overhead Line	0	0.00000	0.0	0	0	500.7
8	54.49	190.7	125	280.0	C	0	G44 Concrete Sleeper With Fastclip	0	Gault Formation And Upper Greensand Formation	30	Overhead Line	0	0.00000	0.0	0	0	500.7
9	54.49	190.7	125	280.0	C	0	G44 Concrete Sleeper With Fastclip	0	Gault Formation And Upper Greensand Formation	30	Overhead Line	0	0.00000	0.0	0	0	500.7
10	54.49	190.7	125	280.0	C	0	G44 Concrete Sleeper With Fastclip	0	Gault Formation And Upper Greensand Formation	30	Overhead Line	0	0.00000	0.0	0	0	500.7
11	54.49	190.7	125	280.0	C	0	G44 Concrete Sleeper With Fastclip	0	Gault Formation And Upper Greensand Formation	30	Overhead Line	0	0.00000	0.0	0	0	500.7
12	54.49	190.7	125	280.0	C	0	G44 Concrete Sleeper With Fastclip	0	Gault Formation And Upper Greensand Formation	30	Overhead Line	0	0.00000	0.0	0	0	500.7
13	54.49	190.7	125	280.0	C	0	G44 Concrete Sleeper With Fastclip	0	Gault Formation And Upper Greensand Formation	30	Overhead Line	0	0.00000	0.0	0	0	500.7
14	54.49	190.7	125	280.0	C	0	G44 Concrete Sleeper With Fastclip	0	Gault Formation And Upper Greensand Formation	30	Overhead Line	0	0.00000	0.0	0	0	500.7
15	54.49	190.7	125	280.0	C	0	G44 Concrete Sleeper With Fastclip	0	Gault Formation And Upper Greensand Formation	30	Overhead Line	0	0.00000	0.0	0	0	500.7
16	54.49	190.7	125	280.0	C	0	G44 Concrete Sleeper With Fastclip	0	Gault Formation And Upper Greensand Formation	30	Overhead Line	0	0.00000	0.0	0	0	500.7
17	54.49	190.7	125	280.0	C	0	Concrete Bearer R (Shallow Depth)	80	Gault Formation And Upper Greensand Formation	30	Overhead Line	0	0.00000	0.0	0	0	650.7
18	54.49	190.7	125	280.0	C	0	Concrete Bearer R (Shallow Depth)	80	Gault Formation And Upper Greensand Formation	30	Overhead Line	0	0.00000	0.0	0	0	650.7
19	54.49	190.7	125	280.0	C	0	Concrete Bearer R (Shallow Depth)	80	Gault Formation And Upper Greensand Formation	30	Overhead Line	0	0.00000	0.0	0	0	650.7
20	54.49	190.7	125	280.0	C	0	F27 Concrete Sleeper	40	Gault Formation And Upper Greensand Formation	30	Overhead Line	0	0.00000	0.0	0	0	540.7
21	54.49	190.7	125	280.0	C	0	G44 Concrete Sleeper With Fastclip	0	Gault Formation And Upper Greensand Formation	30	Overhead Line	0	0.00000	0.0	0	0	500.7
22	54.49	190.7	125	280.0	C	0	G44 Concrete Sleeper With Fastclip	0	Gault Formation And Upper Greensand Formation	30	Overhead Line	0	0.00000	0.0	0	0	500.7
23	54.49	190.7	125	280.0	C	0	F27 Concrete Sleeper	40	Gault Formation And Upper Greensand Formation	30	Overhead Line	0	0.00000	0.0	0	0	540.7
24	50.19	175.7	125	280.0	C	0	F27 Concrete Sleeper	40	Gault Formation And Upper Greensand Formation	30	Overhead Line	0	0.00000	0.0	0	0	525.7
25	50.19	175.7	125	280.0	C	0	F27 Concrete Sleeper	40	Gault Formation And Upper Greensand Formation	30	Overhead Line	0	0.00000	0.0	0	0	525.7
26	50.19	175.7	125	280.0	C	0	F27 Concrete Sleeper	40	Gault Formation And Upper Greensand Formation	30	Overhead Line	0	0.00000	0.0	0	0	525.7
27	50.19	175.7	125	280.0	C	0	F27 Concrete Sleeper	40	Gault Formation And Upper Greensand Formation	30	Overhead Line	0	0.00000	0.0	0	0	525.7
28	50.19	175.7	125	280.0	C	0	F27 Concrete Sleeper	40	Gault Formation And Upper Greensand Formation	30	Overhead Line	0	0.00000	0.0	0	0	525.7
29	50.19	175.7	125	280.0	C	0	F27 Concrete Sleeper	40	Gault Formation And Upper Greensand Formation	30	Overhead Line	0	0.00000	0.0	0	0	525.7
30	50.19	175.7	125	280.0	C	0	G44 Concrete Sleeper With Fastclip	0	Gault Formation And Upper Greensand Formation	30	Overhead Line	0	0.00000	0.0	0	0	485.7
31	50.19	175.7	125	280.0	C	0	G44 Concrete Sleeper With Fastclip	0	Gault Formation And Upper Greensand Formation	30	Overhead Line	0	0.00016	6.4	0	0	492.1
32	50.19	175.7	125	280.0	C	0	G44 Concrete Sleeper With Fastclip	0	Gault Formation And Upper Greensand Formation	30	Overhead Line	0	0.00016	6.4	0	0	492.1
33	50.19	175.7	125	280.0	C	0	G44 Concrete Sleeper With Fastclip	0	Gault Formation And Upper Greensand Formation	30	Overhead Line	0	0.00016	6.4	0	0	492.1
34	50.19	175.7	125	280.0	C	0	G44 Concrete Sleeper With Fastclip	0	Lower Greensand Group	15	Overhead Line	0	0.00016	6.4	0	0	477.1
35	50.19	175.7	125	280.0	C	0	G44 Concrete Sleeper With Fastclip	0	Lower Greensand Group	15	Overhead Line	0	0.00016	6.4	0	0	477.1
36	50.19	175.7	125	280.0	C	0	G44 Concrete Sleeper With Fastclip	0	Lower Greensand Group	15	Overhead Line	0	0.00016	6.4	0	0	477.1
37	50.19	175.7	125	280.0	C	0	G44 Concrete Sleeper With Fastclip	0	Lower Greensand Group	15	Overhead Line	0	0.00008	3.1	0	0	473.8
38	50.19	175.7	125	280.0	C	0	G44 Concrete Sleeper With Fastclip	0	Lower Greensand Group	15	Overhead Line	0	0.00022	8.7	0	0	479.4
39	50.19	175.7	125	280.0	C	0	F40 Concrete Sleeper	10	Lower Greensand Group	15	Overhead Line	0	0.00039	15.7	0	0	486.4
40	50.10	175.4	125	280.0	C	0	F40 Concrete Sleeper	10	Lower Greensand Group	15	Overhead Line	0	0.00024	9.6	0	0	479.9
41	50.10	175.4	125	280.0	C	0	G44 Concrete Sleeper With Fastclip	0	Lower Greensand Group	15	Overhead Line	0	0.00029	11.4	0	0	481.8
42	50.10	175.4	125	280.0	C	0	G44 Concrete Sleeper With Fastclip	0	Lower Greensand Group	15	Overhead Line	0	0.00080	31.9	0	0	502.2

43	50.10	175.4	125	280.0	C	0	G44 Concrete Sleeper With Fastclip	0	Lower Greensand Group	15	Overhead Line	0	0.00080	31.9	0	0	502.2
44	50.10	175.4	125	280.0	C	0	EG47 Concrete Sleeper With FASTCLIP	0	Lower Greensand Group	15	Overhead Line	0	0.00080	31.9	1	50	542.2
45	50.10	175.4	125	280.0	C	0	EG47 Concrete Sleeper With FASTCLIP	0	Lower Greensand Group	15	Overhead Line	0	0.00080	31.9	0	0	502.2
46	50.10	175.4	125	280.0	C	0	G44 Concrete Sleeper With Fastclip	0	Lower Greensand Group	15	Overhead Line	0	0.00000	0.0	0	0	470.4
47	50.10	175.4	125	280.0	C	0	G44 Concrete Sleeper With Fastclip	0	Lower Greensand Group	15	Overhead Line	0	0.00000	0.0	0	0	470.4
48	50.10	175.4	125	280.0	C	0	G44 Concrete Sleeper With Fastclip	0	Lower Greensand Group	15	Overhead Line	0	0.00000	0.0	0	0	470.4
49	50.10	175.4	125	280.0	C	0	G44 Concrete Sleeper With Fastclip	0	Lower Greensand Group	15	Overhead Line	0	0.00079	31.7	0	0	502.0
50	50.10	175.4	125	280.0	C	0	G44 Concrete Sleeper With Fastclip	0	Lower Greensand Group	15	Overhead Line	0	0.00079	31.7	0	0	502.0
51	50.10	175.4	125	280.0	C	0	G44 Concrete Sleeper With Fastclip	0	Lower Greensand Group	15	Overhead Line	0	0.00077	30.8	0	0	501.2
52	50.10	175.4	125	280.0	C	0	G44 Concrete Sleeper With Fastclip	0	Lower Greensand Group	15	Overhead Line	0	0.00077	30.8	0	0	501.2
53	50.10	175.4	125	280.0	C	0	G44 Concrete Sleeper With Fastclip	0	Lower Greensand Group	15	Overhead Line	0	0.00077	30.8	0	0	501.2
54	50.10	175.4	125	280.0	C	0	G44 Concrete Sleeper With Fastclip	0	Lower Greensand Group	15	Overhead Line	0	0.00034	13.7	0	0	484.0
55	50.10	175.4	125	280.0	C	0	G44 Concrete Sleeper With Fastclip	0	Lower Greensand Group	15	Overhead Line	0	0.00032	12.8	0	0	483.1
56	50.10	175.4	125	280.0	C	0	G44 Concrete Sleeper With Fastclip	0	Kellaways Formation And Oxford Clay Formation	0	Overhead Line	0	0.00025	9.9	0	0	465.3
57	50.10	175.4	125	280.0	C	0	G44 Concrete Sleeper With Fastclip	0	Kellaways Formation And Oxford Clay Formation	0	Overhead Line	0	0.00025	9.9	0	0	465.3
58	50.10	175.4	125	280.0	C	0	G44 Concrete Sleeper With Fastclip	0	Kellaways Formation And Oxford Clay Formation	0	Overhead Line	0	0.00025	9.9	0	0	465.3
59	50.10	175.4	125	280.0	C	0	G44 Concrete Sleeper With Fastclip	0	Kellaways Formation And Oxford Clay Formation	0	Overhead Line	0	0.00025	9.9	0	0	465.3
60	50.10	175.4	125	280.0	C	0	G44 Concrete Sleeper With Fastclip	0	Kellaways Formation And Oxford Clay Formation	0	Overhead Line	0	0.00025	9.9	0	0	465.3
61	50.10	175.4	125	280.0	C	0	G44 Concrete Sleeper With Fastclip	0	Kellaways Formation And Oxford Clay Formation	0	Overhead Line	0	0.00025	9.9	0	0	465.3
62	50.10	175.4	125	280.0	C	0	G44 Concrete Sleeper With Fastclip	0	Kellaways Formation And Oxford Clay Formation	0	Overhead Line	0	0.00025	9.9	0	0	465.3
63	50.10	175.4	125	280.0	C	0	F40 Concrete Sleeper	10	Kellaways Formation And Oxford Clay Formation	0	Overhead Line	0	0.00025	9.9	0	0	465.3
64	50.10	175.4	125	280.0	C	0	F40 Concrete Sleeper	10	Kellaways Formation And Oxford Clay Formation	0	Overhead Line	0	0.00025	9.9	0	0	465.3
65	50.10	175.4	125	280.0	C	0	F40 Concrete Sleeper	10	Kellaways Formation And Oxford Clay Formation	0	Overhead Line	0	0.00036	14.4	0	0	469.7
66	50.10	175.4	125	280.0	C	0	F40 Concrete Sleeper	10	Kellaways Formation And Oxford Clay Formation	0	Overhead Line	0	0.00022	8.8	0	0	464.2
67	50.10	175.4	125	280.0	C	0	F40 Concrete Sleeper	10	Kellaways Formation And Oxford Clay Formation	0	Overhead Line	0	0.00031	12.3	0	0	467.7
68	50.10	175.4	125	280.0	C	0	F40 Concrete Sleeper	10	Kellaways Formation And Oxford Clay Formation	0	Overhead Line	0	0.00031	12.3	0	0	467.7
69	50.10	175.4	125	280.0	C	0	F40 Concrete Sleeper	10	Kellaways Formation And Oxford Clay Formation	0	Overhead Line	0	0.00031	12.3	0	0	467.7
70	50.10	175.4	125	280.0	C	0	F40 Concrete Sleeper	10	Kellaways Formation And Oxford Clay Formation	0	Overhead Line	0	0.00031	12.3	0	0	467.7
71	50.10	175.4	125	280.0	C	0	F19 Concrete Sleeper	60	Kellaways Formation And Oxford Clay Formation	0	Overhead Line	0	0.00031	12.3	0	0	507.7
72	50.10	175.4	125	280.0	C	0	G44 Concrete Sleeper With Fastclip	0	Kellaways Formation And Oxford Clay Formation	0	Overhead Line	0	0.00013	5.3	0	0	460.7
73	50.10	175.4	125	280.0	C	0	G44 Concrete Sleeper With Fastclip	0	Kellaways Formation And Oxford Clay Formation	0	Overhead Line	0	0.00000	0.0	0	0	455.4
74	50.10	175.4	125	280.0	C	0	G44 Concrete Sleeper With Fastclip	0	Kellaways Formation And Oxford Clay Formation	0	Overhead Line	0	0.00000	0.0	0	0	455.4
75	50.10	175.4	125	280.0	C	0	G44 Concrete Sleeper With Fastclip	0	Kellaways Formation And Oxford Clay Formation	0	Overhead Line	0	0.00000	0.0	0	0	455.4
76	50.10	175.4	125	280.0	C	0	G44 Concrete Sleeper With Fastclip	0	Kellaways Formation And Oxford Clay Formation	0	Overhead Line	0	0.00000	0.0	0	0	455.4
77	50.10	175.4	125	280.0	C	0	F40 Concrete Sleeper	10	Kellaways Formation And Oxford Clay Formation	0	Overhead Line	0	0.00000	0.0	0	0	455.4
78	50.10	175.4	125	280.0	C	0	G44 Concrete Sleeper With Fastclip	0	Kellaways Formation And Oxford Clay Formation	0	Overhead Line	0	0.00000	0.0	0	0	455.4
79	50.10	175.4	125	280.0	C	0	G44 Concrete Sleeper With Fastclip	0	Kellaways Formation And Oxford Clay Formation	0	Overhead Line	0	0.00000	0.0	0	0	455.4
80	50.10	175.4	125	280.0	C	0	G44 Concrete Sleeper With Fastclip	0	Kellaways Formation And Oxford Clay Formation	0	Overhead Line	0	0.00000	0.0	0	0	455.4
81	50.10	175.4	125	280.0	C	0	F27 Concrete Sleeper	40	Kellaways Formation And Oxford Clay Formation	0	Overhead Line	0	0.00000	0.0	0	0	495.4
82	50.10	175.4	125	280.0	C	0	G44 Concrete Sleeper With Fastclip	0	Kellaways Formation And Oxford Clay Formation	0	Overhead Line	0	0.00000	0.0	0	0	455.4
83	50.10	175.4	125	280.0	C	0	G44 Concrete Sleeper With Fastclip	0	Kellaways Formation And Oxford Clay Formation	0	Overhead Line	0	0.00000	0.0	0	0	455.4
84	50.10	175.4	125	280.0	C	0	G44 Concrete Sleeper With Fastclip	0	Kellaways Formation And Oxford Clay Formation	0	Overhead Line	0	0.00000	0.0	0	0	455.4
85	50.10	175.4	125	280.0	C	0	G44 Concrete Sleeper With Fastclip	0	Kellaways Formation And Oxford Clay Formation	0	Overhead Line	0	0.00000	0.0	0	0	455.4
86	50.10	175.4	125	280.0	C	0	G44 Concrete Sleeper With Fastclip	0	Kellaways Formation And Oxford Clay Formation	0	Overhead Line	0	0.00000	0.0	0	0	455.4
87	50.10	175.4	125	280.0	C	0	G44 Concrete Sleeper With Fastclip	0	Kellaways Formation And Oxford Clay Formation	0	Overhead Line	0	0.00000	0.0	0	0	455.4
88	50.10	175.4	125	280.0	C	0	G44 Concrete Sleeper With Fastclip	0	Kellaways Formation And Oxford Clay Formation	0	Overhead Line	0	0.00000	0.0	0	0	455.4
89	50.10	175.4	125	280.0	C	0	G44 Concrete Sleeper With Fastclip	0	Kellaways Formation And Oxford Clay Formation	0	Overhead Line	0	0.00000	0.0	0	0	455.4
90	50.10	175.4	125	280.0	C	0	G44 Concrete Sleeper With Fastclip	0	Kellaways Formation And Oxford Clay Formation	0	Overhead Line	0	0.00000	0.0	0	0	455.4
91	50.10	175.4	125	280.0	C	0	G44 Concrete Sleeper With Fastclip	0	Kellaways Formation And Oxford Clay Formation	0	Overhead Line	0	0.00000	0.0	0	0	455.4
92	50.80	177.8	125	280.0	C	0	G44 Concrete Sleeper With Fastclip	0	Kellaways Formation And Oxford Clay Formation	0	Overhead Line	0	0.00000	0.0	0	0	457.8
93	50.80	177.8	125	280.0	C	0	F23 Concrete Sleeper	60	Kellaways Formation And Oxford Clay Formation	0	Overhead Line	0	0.00000	0.0	0	0	497.8
94	50.80	177.8	125	280.0	C	0	F27 Concrete Sleeper	40	Kellaways Formation And Oxford Clay Formation	0	Overhead Line	0	0.00030	11.9	0	0	509.7
95	50.80	177.8	125	280.0	C	0	G44 Concrete Sleeper With Fastclip	0	Kellaways Formation And Oxford Clay Formation	0	Overhead Line	0	0.00030	11.9	0	0	469.7
96	50.80	177.8	125	280.0	C	0	F40 Concrete Sleeper	10	Kellaways Formation And Oxford Clay Formation	0	Overhead Line	0	0.00030	11.9	0	0	469.7

97	50.80	177.8	125	280.0	C	0	F40 Concrete Sleeper	10	Kellaways Formation And Oxford Clay Formation	0	Overhead Line	0	0.00030	11.9	0	0	469.7
98	50.80	177.8	125	280.0	C	0	F40 Concrete Sleeper	10	Kellaways Formation And Oxford Clay Formation	0	Overhead Line	0	0.00030	11.9	0	0	469.7
99	50.80	177.8	125	280.0	C	0	F40 Concrete Sleeper	10	Kellaways Formation And Oxford Clay Formation	0	Overhead Line	0	0.00030	11.9	0	0	469.7
100	50.80	177.8	125	280.0	C	0	F40 Concrete Sleeper	10	Kellaways Formation And Oxford Clay Formation	0	Overhead Line	0	0.00030	11.9	0	0	469.7
101	50.80	177.8	125	280.0	C	0	F40 Concrete Sleeper	10	Kellaways Formation And Oxford Clay Formation	0	Overhead Line	0	0.00030	11.9	0	0	469.7
102	50.80	177.8	125	280.0	C	0	F40 Concrete Sleeper	10	Kellaways Formation And Oxford Clay Formation	0	Overhead Line	0	0.00030	11.9	0	0	469.7
103	50.80	177.8	125	280.0	C	0	G44 Concrete Sleeper With Fastclip	0	Kellaways Formation And Oxford Clay Formation	0	Overhead Line	0	0.00000	0.2	0	0	458.0
104	50.80	177.8	125	280.0	C	0	G44 Concrete Sleeper With Fastclip	0	Kellaways Formation And Oxford Clay Formation	0	Overhead Line	0	0.00000	0.0	0	0	457.8
105	50.80	177.8	125	280.0	C	0	G44 Concrete Sleeper With Fastclip	0	Kellaways Formation And Oxford Clay Formation	0	Overhead Line	0	0.00000	0.0	0	0	457.8
106	50.80	177.8	125	280.0	C	0	G44 Concrete Sleeper With Fastclip	0	Kellaways Formation And Oxford Clay Formation	0	Overhead Line	0	0.00000	0.0	0	0	457.8
107	50.90	178.2	125	280.0	C	0	Hardwood Sleeper / Bearer	60	Kellaways Formation And Oxford Clay Formation	0	Overhead Line	0	0.00000	0.0	0	0	518.2
108	50.90	178.2	125	280.0	C	0	F40 Concrete Sleeper	10	Kellaways Formation And Oxford Clay Formation	0	Overhead Line	0	0.00000	0.0	0	0	458.2
109	50.90	178.2	125	280.0	C	0	F40 Concrete Sleeper	10	Kellaways Formation And Oxford Clay Formation	0	Overhead Line	0	0.00000	0.0	0	0	458.2
110	50.90	178.2	125	280.0	C	0	F40 Concrete Sleeper	10	Kellaways Formation And Oxford Clay Formation	0	Overhead Line	0	0.00000	0.0	0	0	458.2
111	50.90	178.2	125	280.0	C	0	F40 Concrete Sleeper	10	Kellaways Formation And Oxford Clay Formation	0	Overhead Line	0	0.00000	0.0	0	0	458.2
112	50.90	178.2	125	280.0	C	0	F40 Concrete Sleeper	10	Kellaways Formation And Oxford Clay Formation	0	Overhead Line	0	0.00000	0.0	0	0	458.2
113	50.90	178.2	125	280.0	C	0	Concrete Bearer R (Shallow Depth)	80	Kellaways Formation And Oxford Clay Formation	0	Overhead Line	0	0.00000	0.0	0	0	608.2
114	50.90	178.2	125	280.0	C	0	F40 Concrete Sleeper	10	Kellaways Formation And Oxford Clay Formation	0	Overhead Line	0	0.00000	0.0	0	0	458.2
115	50.90	178.2	125	280.0	C	0	Concrete Bearer R (Shallow Depth)	80	Kellaways Formation And Oxford Clay Formation	0	Overhead Line	0	0.00000	0.0	0	0	608.2
116	50.90	178.2	125	280.0	C	0	G44 Concrete Sleeper With Fastclip	0	Kellaways Formation And Oxford Clay Formation	0	Overhead Line	0	0.00000	0.0	0	0	458.2
117	50.22	175.8	125	280.0	C	0	G44 Concrete Sleeper With Fastclip	0	Kellaways Formation And Oxford Clay Formation	0	Overhead Line	0	0.00000	0.0	0	0	455.8
118	50.22	175.8	125	280.0	C	0	Concrete Bearer R (Shallow Depth)	80	Kellaways Formation And Oxford Clay Formation	0	Overhead Line	0	0.00000	0.0	0	0	605.8
119	50.22	175.8	125	280.0	C	0	F40 Concrete Sleeper	10	Kellaways Formation And Oxford Clay Formation	0	Overhead Line	0	0.00000	0.0	0	0	455.8
120	50.22	175.8	125	280.0	C	0	G44 Concrete Sleeper With Fastclip	0	Kellaways Formation And Oxford Clay Formation	0	Overhead Line	0	0.00000	0.0	0	0	455.8
121	50.22	175.8	125	280.0	C	0	G44 Concrete Sleeper With Fastclip	0	Lower Greensand Group	15	Overhead Line	0	0.00000	0.0	0	0	470.8
122	50.22	175.8	125	280.0	C	0	G44 Concrete Sleeper With Fastclip	0	Lower Greensand Group	15	Overhead Line	0	0.00000	0.0	0	0	470.8
123	50.22	175.8	125	280.0	C	0	G44 Concrete Sleeper With Fastclip	0	Lower Greensand Group	15	Overhead Line	0	0.00000	0.0	0	0	470.8
124	50.22	175.8	125	280.0	C	0	G44 Concrete Sleeper With Fastclip	0	Lower Greensand Group	15	Overhead Line	0	0.00000	0.0	0	0	470.8
125	50.22	175.8	125	280.0	C	0	G44 Concrete Sleeper With Fastclip	0	Lower Greensand Group	15	Overhead Line	0	0.00000	0.0	0	0	470.8
126	50.22	175.8	125	280.0	C	0	G44 Concrete Sleeper With Fastclip	0	Lower Greensand Group	15	Overhead Line	0	0.00000	0.0	0	0	470.8
127	50.22	175.8	125	280.0	C	0	F27 Concrete Sleeper	40	Kellaways Formation And Oxford Clay Formation	0	Overhead Line	0	0.00009	3.4	0	0	499.2
128	50.22	175.8	125	280.0	C	0	G44 Concrete Sleeper With Fastclip	0	Kellaways Formation And Oxford Clay Formation	0	Overhead Line	0	0.00020	8.1	0	0	463.9
129	50.22	175.8	125	280.0	C	0	G44 Concrete Sleeper With Fastclip	0	Kellaways Formation And Oxford Clay Formation	0	Overhead Line	0	0.00014	5.7	0	0	461.5
130	50.22	175.8	125	280.0	C	0	G44 Concrete Sleeper With Fastclip	0	Kellaways Formation And Oxford Clay Formation	0	Overhead Line	0	0.00057	22.8	0	0	478.5
131	50.22	175.8	125	280.0	C	0	G44 Concrete Sleeper With Fastclip	0	Kellaways Formation And Oxford Clay Formation	0	Overhead Line	0	0.00057	22.8	0	0	478.5
132	50.22	175.8	125	280.0	C	0	G44 Concrete Sleeper With Fastclip	0	Kellaways Formation And Oxford Clay Formation	0	Overhead Line	0	0.00057	22.8	0	0	478.5
133	50.22	175.8	125	280.0	C	0	G44 Concrete Sleeper With Fastclip	0	Kellaways Formation And Oxford Clay Formation	0	Overhead Line	0	0.00014	5.8	0	0	461.5
134	50.22	175.8	125	280.0	C	0	G44 Concrete Sleeper With Fastclip	0	Lower Greensand Group	15	Overhead Line	0	0.00008	3.2	0	0	474.0
135	50.22	175.8	125	280.0	C	0	G44 Concrete Sleeper With Fastclip	0	Lower Greensand Group	15	Overhead Line	0	0.00000	0.0	0	0	470.8
136	50.22	175.8	125	280.0	C	0	G44 Concrete Sleeper With Fastclip	0	Lower Greensand Group	15	Overhead Line	0	0.00073	29.2	0	0	499.9
137	50.22	175.8	125	280.0	C	0	G44 Concrete Sleeper With Fastclip	0	Lower Greensand Group	15	Overhead Line	0	0.00073	29.2	0	0	499.9
138	50.20	175.7	125	280.0	C	0	G44 Concrete Sleeper With Fastclip	0	Lower Greensand Group	15	Overhead Line	0	0.00073	29.2	0	0	499.9
139	50.20	175.7	125	280.0	C	0	G44 Concrete Sleeper With Fastclip	0	Lias Group	40	Overhead Line	0	0.00040	15.8	0	0	511.5
140	50.20	175.7	125	280.0	C	0	G44 Concrete Sleeper With Fastclip	0	Lias Group	40	Overhead Line	0	0.00046	18.2	0	0	514.0
141	50.20	175.7	125	280.0	C	0	F40 Concrete Sleeper	10	Lias Group	40	Overhead Line	0	0.00032	12.8	0	0	508.6
142	50.20	175.7	125	280.0	C	0	F40 Concrete Sleeper	10	Lias Group	40	Overhead Line	0	0.00000	0.0	0	0	495.7
143	50.20	175.7	125	280.0	C	0	F40 Concrete Sleeper	10	Lias Group	40	Overhead Line	0	0.00000	0.0	0	0	495.7
144	50.20	175.7	125	280.0	C	0	F40 Concrete Sleeper	10	Great Oolite Group	85	Overhead Line	0	0.00000	0.0	0	0	535.7
145	50.20	175.7	125	280.0	C	0	G44 Concrete Sleeper With Fastclip	0	Great Oolite Group	85	Overhead Line	0	0.00024	9.6	0	0	545.4
146	50.20	175.7	125	280.0	C	0	G44 Concrete Sleeper With Fastclip	0	Great Oolite Group	85	Overhead Line	0	0.00030	11.8	0	0	547.6
147	50.20	175.7	125	280.0	C	0	G44 Concrete Sleeper With Fastclip	0	Great Oolite Group	85	Overhead Line	0	0.00030	11.8	0	0	547.6
148	50.20	175.7	125	280.0	C	0	G44 Concrete Sleeper With Fastclip	0	Great Oolite Group	85	Overhead Line	0	0.00030	11.8	0	0	547.6
149	50.20	175.7	125	280.0	C	0	F40 Concrete Sleeper	10	Lias Group	40	Overhead Line	0	0.00030	11.8	0	0	507.6
150	50.20	175.7	125	280.0	C	0	5f40 Concrete Sleeper	0	Lias Group	40	Overhead Line	0	0.00030	11.8	0	0	507.6
151	50.20	175.7	125	280.0	C	0	F40 Concrete Sleeper	10	Lias Group	40	Overhead Line	0	0.00030	11.8	0	0	507.6
152	50.20	175.7	125	280.0	C	0	F40 Concrete Sleeper	10	Lias Group	40	Overhead Line	0	0.00030	11.8	0	0	507.6

153	50.20	175.7	125	280.0	C	0	F40 Concrete Sleeper	10	Lias Group	40	Overhead Line	0	0.00002	0.9	0	0	496.6
154	50.20	175.7	125	280.0	C	0	F40 Concrete Sleeper	10	Lias Group	40	Overhead Line	0	0.00022	8.9	0	0	504.6
155	50.20	175.7	125	280.0	C	0	F40 Concrete Sleeper	10	Lias Group	40	Overhead Line	0	0.00022	8.9	0	0	504.6
156	50.20	175.7	125	280.0	C	0	F40 Concrete Sleeper	10	Lias Group	40	Overhead Line	0	0.00022	8.9	0	0	504.6
157	50.20	175.7	125	280.0	C	0	F40 Concrete Sleeper	10	Lias Group	40	Overhead Line	0	0.00022	8.9	0	0	504.6
158	50.20	175.7	125	280.0	C	0	F40 Concrete Sleeper	10	Lias Group	40	Overhead Line	0	0.00022	8.9	0	0	504.6
159	50.20	175.7	125	280.0	C	0	F40 Concrete Sleeper	10	Lias Group	40	Overhead Line	0	0.00022	8.9	0	0	504.6
160	50.20	175.7	125	280.0	C	0	F40 Concrete Sleeper	10	Lias Group	40	Overhead Line	0	0.00022	8.9	0	0	504.6
161	50.20	175.7	125	280.0	C	0	F40 Concrete Sleeper	10	Lias Group	40	Overhead Line	0	0.00022	8.9	0	0	504.6
162	50.20	175.7	125	280.0	C	0	F40 Concrete Sleeper	10	Lias Group	40	Overhead Line	0	0.00022	8.9	0	0	504.6
163	50.20	175.7	125	280.0	C	0	G44 Concrete Sleeper With Fastclip	0	Lias Group	40	Overhead Line	0	0.00022	8.9	0	0	504.6
164	50.20	175.7	125	280.0	C	0	F40 Concrete Sleeper	10	Lias Group	40	Overhead Line	0	0.00022	8.9	0	0	504.6
165	50.20	175.7	125	280.0	C	0	F40 Concrete Sleeper	10	Lias Group	40	Overhead Line	0	0.00000	0.0	0	0	495.7
166	50.20	175.7	125	280.0	C	0	F40 Concrete Sleeper	10	Lias Group	40	Overhead Line	0	0.00000	0.0	0	0	495.7
167	50.20	175.7	125	280.0	C	0	F27 Concrete Sleeper	40	Lias Group	40	Overhead Line	0	0.00000	0.0	0	0	535.7
168	50.20	175.7	125	280.0	C	0	F27 Concrete Sleeper	40	Lias Group	40	Overhead Line	0	0.00000	0.0	0	0	535.7
169	50.20	175.7	125	280.0	C	0	Hardwood Sleeper / Bearer	60	Lias Group	40	Overhead Line	0	0.00000	0.0	0	0	555.7
170	50.20	175.7	125	280.0	C	0	Ef33 Concrete Sleeper	40	Lias Group	40	Overhead Line	0	0.00000	0.0	0	0	535.7
171	50.20	175.7	125	280.0	C	0	G44 Concrete Sleeper With Fastclip	0	Lias Group	40	Overhead Line	0	0.00000	0.0	0	0	495.7
172	51.05	178.7	125	280.0	C	0	Hardwood Sleeper / Bearer	60	Lias Group	40	Overhead Line	0	0.00000	0.0	0	0	558.7
173	51.05	178.7	125	280.0	C	0	F40 Concrete Sleeper	10	Lias Group	40	Overhead Line	0	0.00000	0.0	0	0	498.7
174	51.05	178.7	125	280.0	C	0	F40 Concrete Sleeper	10	Lias Group	40	Overhead Line	0	0.00000	0.0	0	0	498.7
175	51.05	178.7	125	280.0	C	0	F40 Concrete Sleeper	10	Lias Group	40	Overhead Line	0	0.00000	0.0	0	0	498.7
176	51.05	178.7	125	280.0	C	0	F40 Concrete Sleeper	10	Lias Group	40	Overhead Line	0	0.00000	0.0	0	0	498.7
177	51.05	178.7	125	280.0	C	0	F40bs Concrete Sleeper	0	Lias Group	40	Overhead Line	0	0.00000	0.0	0	0	498.7
178	51.05	178.7	125	280.0	C	0	F40bs Concrete Sleeper	0	Lias Group	40	Overhead Line	0	0.00000	0.0	0	0	498.7
179	51.05	178.7	125	280.0	C	0	F40bs Concrete Sleeper	0	Lias Group	40	Overhead Line	0	0.00000	0.0	0	0	498.7
180	51.05	178.7	125	280.0	C	0	F40 Concrete Sleeper	10	Lias Group	40	Overhead Line	0	0.00009	3.5	0	0	502.2
181	51.05	178.7	125	280.0	C	0	G44 Concrete Sleeper With Fastclip	0	Lias Group	40	Overhead Line	0	0.00023	9.3	0	0	508.0
182	51.05	178.7	125	280.0	C	0	F40 Concrete Sleeper	10	Lias Group	40	Overhead Line	0	0.00023	9.3	0	0	508.0
183	51.05	178.7	125	280.0	C	0	F40 Concrete Sleeper	10	Lias Group	40	Overhead Line	0	0.00023	9.3	0	0	508.0
184	51.05	178.7	125	280.0	C	0	G44 Concrete Sleeper With Fastclip	0	Lias Group	40	Overhead Line	0	0.00011	4.3	0	0	503.0
185	51.05	178.7	125	280.0	C	0	G44 Concrete Sleeper With Fastclip	0	Lias Group	40	Overhead Line	0	0.00000	0.0	0	0	498.7
186	51.05	178.7	125	280.0	C	0	G44 Concrete Sleeper With Fastclip	0	Lias Group	40	Overhead Line	0	0.00000	0.0	0	0	498.7
187	51.05	178.7	125	280.0	C	0	G44 Concrete Sleeper With Fastclip	0	Lias Group	40	Overhead Line	0	0.00000	0.0	0	0	498.7
188	51.05	178.7	125	280.0	C	0	G44 Concrete Sleeper With Fastclip	0	Lias Group	40	Overhead Line	0	0.00000	0.0	0	0	498.7
189	51.05	178.7	125	280.0	C	0	G44 Concrete Sleeper With Fastclip	0	Lias Group	40	Overhead Line	0	0.00039	15.4	0	0	514.1
190	51.05	178.7	125	280.0	C	0	G44 Concrete Sleeper With Fastclip	0	Lias Group	40	Overhead Line	0	0.00040	15.8	0	0	514.5
191	51.05	178.7	125	280.0	C	0	F40 Concrete Sleeper	10	Lias Group	40	Overhead Line	0	0.00040	15.8	0	0	514.5
192	51.05	178.7	125	280.0	C	0	F40 Concrete Sleeper	10	Lias Group	40	Overhead Line	0	0.00011	4.6	0	0	503.3
193	51.05	178.7	125	280.0	C	0	F40 Concrete Sleeper	10	Lias Group	40	Overhead Line	0	0.00014	5.5	0	0	504.2
194	51.05	178.7	125	280.0	C	0	F40 Concrete Sleeper	10	Lias Group	40	Overhead Line	0	0.00014	5.5	0	0	504.2
195	51.05	178.7	125	280.0	C	0	F40as Concrete Sleeper	0	Lias Group	40	Overhead Line	0	0.00014	5.5	0	0	504.2
196	51.05	178.7	125	280.0	C	0	F27 Concrete Sleeper	40	Great Oolite Group	85	Overhead Line	0	0.00014	5.5	0	0	584.2
197	51.05	178.7	125	280.0	C	0	G44 Concrete Sleeper With Fastclip	0	Great Oolite Group	85	Overhead Line	0	0.00014	5.5	0	0	544.2
198	51.05	178.7	125	280.0	C	0	G44 Concrete Sleeper With Fastclip	0	Great Oolite Group	85	Overhead Line	0	0.00014	5.5	0	0	544.2
199	51.05	178.7	125	280.0	C	0	G44 Concrete Sleeper With Fastclip	0	Great Oolite Group	85	Overhead Line	0	0.00014	5.5	0	0	544.2
200	51.05	178.7	125	280.0	C	0	G44 Concrete Sleeper With Fastclip	0	Great Oolite Group	85	Overhead Line	0	0.00014	5.5	0	0	544.2
201	51.05	178.7	125	280.0	C	0	G44 Concrete Sleeper With Fastclip	0	Great Oolite Group	85	Overhead Line	0	0.00014	5.5	0	0	544.2
202	51.05	178.7	125	280.0	C	0	F27 Concrete Sleeper	40	Great Oolite Group	85	Overhead Line	0	0.00014	5.5	0	0	584.2
203	51.05	178.7	125	280.0	C	0	F27 Concrete Sleeper	40	Great Oolite Group	85	Overhead Line	0	0.00028	11.0	0	0	589.7
204	51.05	178.7	125	280.0	C	0	F27 Concrete Sleeper	40	Great Oolite Group	85	Overhead Line	0	0.00043	17.1	0	0	595.8
205	51.05	178.7	125	280.0	C	0	F27 Concrete Sleeper	40	Great Oolite Group	85	Overhead Line	0	0.00043	17.1	0	0	595.8
206	51.05	178.7	125	280.0	C	0	F40 Concrete Sleeper	10	Great Oolite Group	85	Overhead Line	0	0.00043	17.1	0	0	555.8
207	51.05	178.7	125	280.0	C	0	F40 Concrete Sleeper	10	Great Oolite Group	85	Overhead Line	0	0.00043	17.1	0	0	555.8
208	51.05	178.7	125	280.0	C	0	F40 Concrete Sleeper	10	Great Oolite Group	85	Overhead Line	0	0.00043	17.1	0	0	555.8

209	51.05	178.7	125	280.0	C	0	G44 Concrete Sleeper With Fastclip	0	Great Oolite Group	85	Overhead Line	0	0.00043	17.1	0	0	555.8
210	51.05	178.7	125	280.0	C	0	G44 Concrete Sleeper With Fastclip	0	Great Oolite Group	85	Overhead Line	0	0.00043	17.1	0	0	555.8
211	51.05	178.7	125	280.0	C	0	G44 Concrete Sleeper With Fastclip	0	Great Oolite Group	85	Overhead Line	0	0.00043	17.1	0	0	555.8
212	51.05	178.7	125	280.0	C	0	G44 Concrete Sleeper With Fastclip	0	Great Oolite Group	85	Overhead Line	0	0.00043	17.1	0	0	555.8
213	51.05	178.7	125	280.0	C	0	G44 Concrete Sleeper With Fastclip	0	Great Oolite Group	85	Overhead Line	0	0.00043	17.1	0	0	555.8
214	51.05	178.7	125	280.0	C	0	F40 Concrete Sleeper	10	Great Oolite Group	85	Overhead Line	0	0.00043	17.1	0	0	555.8
215	51.05	178.7	125	280.0	C	0	F40 Concrete Sleeper	10	Great Oolite Group	85	Overhead Line	0	0.00030	11.8	0	0	550.5
216	51.05	178.7	125	280.0	C	0	G44 Concrete Sleeper With Fastclip	0	Great Oolite Group	85	Overhead Line	0	0.00030	11.8	0	0	550.5
217	51.05	178.7	125	280.0	C	0	G44 Concrete Sleeper With Fastclip	0	Great Oolite Group	85	Overhead Line	0	0.00030	11.8	0	0	550.5
218	51.05	178.7	125	280.0	C	0	G44 Concrete Sleeper With Fastclip	0	Great Oolite Group	85	Overhead Line	0	0.00030	11.8	0	0	550.5
219	51.05	178.7	125	280.0	C	0	G44 Concrete Sleeper With Fastclip	0	Great Oolite Group	85	Overhead Line	0	0.00026	10.3	0	0	549.0
220	51.05	178.7	125	280.0	C	0	F27 Concrete Sleeper	40	Great Oolite Group	85	Overhead Line	0	0.00006	2.3	0	0	581.0
221	51.05	178.7	125	280.0	C	0	Concrete Bearer R (Shallow Depth)	80	Great Oolite Group	85	Overhead Line	0	0.00000	0.0	0	0	688.7
222	51.05	178.7	125	280.0	C	0	G44 Concrete Sleeper With Fastclip	0	Great Oolite Group	85	Overhead Line	0	0.00000	0.0	0	0	538.7
223	51.05	178.7	125	280.0	C	0	G44 Concrete Sleeper With Fastclip	0	Great Oolite Group	85	Overhead Line	0	0.00000	0.0	0	0	538.7
224	51.05	178.7	125	280.0	C	0	G44 Concrete Sleeper With Fastclip	0	Lias Group	40	Overhead Line	0	0.00000	0.0	0	0	498.7
225	51.05	178.7	125	280.0	C	0	G44 Concrete Sleeper With Fastclip	0	Lias Group	40	Overhead Line	0	0.00017	6.6	0	0	505.3
226	51.05	178.7	125	280.0	C	0	G44 Concrete Sleeper With Fastclip	0	Lias Group	40	Overhead Line	0	0.00025	10.1	0	0	508.8
227	51.05	178.7	125	280.0	C	0	G44 Concrete Sleeper With Fastclip	0	Lias Group	40	Overhead Line	0	0.00025	10.1	0	0	508.8
228	51.05	178.7	125	280.0	C	0	G44 Concrete Sleeper With Fastclip	0	Lias Group	40	Overhead Line	0	0.00025	10.1	0	0	508.8
229	51.05	178.7	125	280.0	C	0	G44 Concrete Sleeper With Fastclip	0	Lias Group	40	Overhead Line	0	0.00025	10.1	0	0	508.8
230	51.05	178.7	125	280.0	C	0	F40 Concrete Sleeper	10	Lias Group	40	Overhead Line	0	0.00025	10.1	0	0	508.8
231	51.05	178.7	125	280.0	C	0	F40 Concrete Sleeper	10	Lias Group	40	Overhead Line	0	0.00025	10.1	0	0	508.8
232	51.05	178.7	125	280.0	C	0	F40 Concrete Sleeper	10	Lias Group	40	Overhead Line	0	0.00025	10.1	0	0	508.8
233	51.05	178.7	125	280.0	C	0	F40 Concrete Sleeper	10	Lias Group	40	Overhead Line	0	0.00025	10.1	0	0	508.8
234	51.05	178.7	125	280.0	C	0	F40 Concrete Sleeper	10	Lias Group	40	Overhead Line	0	0.00013	5.1	0	0	503.8
235	51.05	178.7	125	280.0	C	0	F40 Concrete Sleeper	10	Lias Group	40	Overhead Line	0	0.00043	17.0	0	0	515.7
236	51.05	178.7	125	280.0	C	0	F40 Concrete Sleeper	10	Lias Group	40	Overhead Line	0	0.00043	17.0	0	0	515.7
237	51.05	178.7	125	280.0	C	0	F40 Concrete Sleeper	10	Lias Group	40	Overhead Line	0	0.00050	20.1	0	0	518.8
238	51.05	178.7	125	280.0	C	0	F40 Concrete Sleeper	10	Lias Group	40	Overhead Line	0	0.00031	12.2	0	0	510.9
239	51.05	178.7	125	280.0	C	0	F40 Concrete Sleeper	10	Lias Group	40	Overhead Line	0	0.00045	18.1	0	0	516.8
240	51.05	178.7	125	280.0	C	0	F40 Concrete Sleeper	10	Lias Group	40	Overhead Line	0	0.00045	18.1	0	0	516.8
241	51.05	178.7	125	280.0	C	0	F40 Concrete Sleeper	10	Lias Group	40	Overhead Line	0	0.00039	15.6	0	0	514.3
242	51.05	178.7	125	280.0	C	0	F40 Concrete Sleeper	10	Lias Group	40	Overhead Line	0	0.00039	15.6	0	0	514.3
243	51.05	178.7	125	280.0	C	0	F40 Concrete Sleeper	10	Lias Group	40	Overhead Line	0	0.00027	10.8	0	0	509.5
244	51.05	178.7	125	280.0	C	0	F40 Concrete Sleeper	10	Lias Group	40	Overhead Line	0	0.00038	15.3	0	0	514.0
245	51.05	178.7	125	280.0	C	0	F40 Concrete Sleeper	10	Lias Group	40	Overhead Line	0	0.00028	11.3	0	0	510.0
246	51.05	178.7	125	280.0	C	0	F40 Concrete Sleeper	10	Lias Group	40	Overhead Line	0	0.00027	10.7	0	0	509.4
247	51.05	178.7	125	280.0	C	0	F40 Concrete Sleeper	10	Lias Group	40	Overhead Line	0	0.00045	17.8	0	0	516.5
248	51.05	178.7	125	280.0	C	0	F27 Concrete Sleeper	40	Lias Group	40	Overhead Line	0	0.00006	2.2	0	0	540.9
249	51.05	178.7	125	280.0	C	0	G44 Concrete Sleeper With Fastclip	0	Lias Group	40	Overhead Line	0	0.00000	0.0	0	0	498.7
250	51.05	178.7	125	280.0	C	0	G44 Concrete Sleeper With Fastclip	0	Lias Group	40	Overhead Line	0	0.00000	0.0	0	0	498.7
251	51.05	178.7	125	280.0	C	0	G44 Concrete Sleeper With Fastclip	0	Lias Group	40	Overhead Line	0	0.00000	0.0	0	0	498.7
252	51.05	178.7	125	280.0	C	0	G44 Concrete Sleeper With Fastclip	0	Lias Group	40	Overhead Line	0	0.00000	0.0	0	0	498.7
253	51.05	178.7	125	280.0	C	0	G44 Concrete Sleeper With Fastclip	0	Lias Group	40	Overhead Line	0	0.00000	0.0	0	0	498.7
254	51.05	178.7	125	280.0	C	0	G44 Concrete Sleeper With Fastclip	0	Lias Group	40	Overhead Line	0	0.00000	0.0	0	0	498.7
255	51.05	178.7	125	280.0	C	0	G44 Concrete Sleeper With Fastclip	0	Lias Group	40	Overhead Line	0	0.00000	0.0	0	0	498.7
256	51.05	178.7	125	280.0	C	0	G44 Concrete Sleeper With Fastclip	0	Lias Group	40	Overhead Line	0	0.00000	0.0	0	0	498.7
257	51.05	178.7	125	280.0	C	0	G44 Concrete Sleeper With Fastclip	0	Lias Group	40	Overhead Line	0	0.00000	0.0	0	0	498.7
258	51.05	178.7	125	280.0	C	0	G44 Concrete Sleeper With Fastclip	0	Lias Group	40	Overhead Line	0	0.00000	0.0	0	0	498.7
259	51.05	178.7	125	280.0	C	0	G44 Concrete Sleeper With Fastclip	0	Lias Group	40	Overhead Line	0	0.00000	0.0	0	0	498.7
260	51.05	178.7	125	280.0	C	0	G44 Concrete Sleeper With Fastclip	0	Lias Group	40	Overhead Line	0	0.00000	0.0	0	0	498.7
261	51.05	178.7	125	280.0	C	0	G44 Concrete Sleeper With Fastclip	0	Lias Group	40	Overhead Line	0	0.00000	0.0	0	0	498.7
262	51.05	178.7	125	280.0	C	0	G44 Concrete Sleeper With Fastclip	0	Lias Group	40	Overhead Line	0	0.00000	0.0	0	0	498.7
263	51.05	178.7	125	280.0	C	0	EG47 Concrete Sleeper With FASTCLIP	0	Lias Group	40	Overhead Line	0	0.00000	0.0	1	50	538.7

264	51.05	178.7	125	280.0	C	0	EG47 Concrete Sleeper With FASTCLIP	0	Lias Group	40	Overhead Line	0	0.00000	0.0	1	50	538.7
265	51.05	178.7	125	280.0	C	0	EG47 Concrete Sleeper With FASTCLIP	0	Lias Group	40	Overhead Line	0	0.00000	0.0	0	0	498.7
266	51.05	178.7	125	280.0	C	0	G44 Concrete Sleeper With Fastclip	0	Lias Group	40	Overhead Line	0	0.00000	0.0	0	0	498.7
267	51.05	178.7	125	280.0	C	0	G44 Concrete Sleeper With Fastclip	0	Lias Group	40	Overhead Line	0	0.00000	0.0	0	0	498.7
268	51.05	178.7	125	280.0	C	0	G44 Concrete Sleeper With Fastclip	0	Lias Group	40	Overhead Line	0	0.00000	0.0	0	0	498.7
269	51.05	178.7	120	268.8	C	0	G44 Concrete Sleeper With Fastclip	0	Lias Group	40	Overhead Line	0	0.00091	36.5	0	0	524.0
270	51.05	178.7	120	268.8	C	0	G44 Concrete Sleeper With Fastclip	0	Lias Group	40	Overhead Line	0	0.00091	36.5	0	0	524.0
271	51.05	178.7	120	268.8	C	0	G44 Concrete Sleeper With Fastclip	0	Lias Group	40	Overhead Line	0	0.00091	36.5	0	0	524.0
272	51.05	178.7	120	268.8	C	0	G44 Concrete Sleeper With Fastclip	0	Lias Group	40	Overhead Line	0	0.00015	5.9	0	0	493.4
273	51.05	178.7	120	268.8	C	0	G44 Concrete Sleeper With Fastclip	0	Lias Group	40	Overhead Line	0	0.00000	0.0	0	0	487.5
274	51.05	178.7	120	268.8	C	0	G44 Concrete Sleeper With Fastclip	0	Lias Group	40	Overhead Line	0	0.00084	33.5	0	0	521.0
275	51.05	178.7	120	268.8	C	0	G44 Concrete Sleeper With Fastclip	0	Lias Group	40	Overhead Line	0	0.00036	14.3	0	0	501.8
276	51.14	179.0	120	268.8	C	0	G44 Concrete Sleeper With Fastclip	0	Lias Group	40	Overhead Line	0	0.00000	0.0	0	0	487.8
277	51.14	179.0	120	268.8	C	0	G44 Concrete Sleeper With Fastclip	0	Lias Group	40	Overhead Line	0	0.00090	36.2	0	0	524.0
278	51.14	179.0	120	268.8	C	0	G44 Concrete Sleeper With Fastclip	0	Lias Group	40	Overhead Line	0	0.00090	36.2	0	0	524.0
279	51.14	179.0	120	268.8	C	0	G44 Concrete Sleeper With Fastclip	0	Lias Group	40	Overhead Line	0	0.00090	36.2	0	0	524.0
280	51.14	179.0	120	268.8	C	0	G44 Concrete Sleeper With Fastclip	0	Lias Group	40	Overhead Line	0	0.00090	36.2	0	0	524.0
281	51.14	179.0	120	268.8	C	0	G44 Concrete Sleeper With Fastclip	0	Lias Group	40	Overhead Line	0	0.00090	36.2	0	0	524.0
282	51.14	179.0	120	268.8	C	0	G44 Concrete Sleeper With Fastclip	0	Lias Group	40	Overhead Line	0	0.00000	0.0	0	0	487.8
283	51.14	179.0	120	268.8	C	0	G44 Concrete Sleeper With Fastclip	0	Lias Group	40	Overhead Line	0	0.00042	16.8	0	0	504.6
284	51.14	179.0	125	280.0	C	0	G44 Concrete Sleeper With Fastclip	0	Lias Group	40	Overhead Line	0	0.00042	16.8	0	0	515.8
285	51.14	179.0	125	280.0	C	0	G44 Concrete Sleeper With Fastclip	0	Lias Group	40	Overhead Line	0	0.00042	16.8	0	0	515.8
286	51.14	179.0	125	280.0	C	0	G44 Concrete Sleeper With Fastclip	0	Lias Group	40	Overhead Line	0	0.00042	16.8	0	0	515.8
287	51.14	179.0	125	280.0	C	0	G44 Concrete Sleeper With Fastclip	0	Lias Group	40	Overhead Line	0	0.00042	16.8	0	0	515.8
288	51.14	179.0	125	280.0	C	0	G44 Concrete Sleeper With Fastclip	0	Lias Group	40	Overhead Line	0	0.00042	16.8	0	0	515.8
289	51.14	179.0	125	280.0	C	0	G44 Concrete Sleeper With Fastclip	0	Lias Group	40	Overhead Line	0	0.00042	16.8	0	0	515.8
290	51.14	179.0	125	280.0	C	0	G44 Concrete Sleeper With Fastclip	0	Lias Group	40	Overhead Line	0	0.00042	16.8	0	0	515.8
291	51.14	179.0	125	280.0	C	0	G44 Concrete Sleeper With Fastclip	0	Lias Group	40	Overhead Line	0	0.00042	16.8	0	0	515.8
292	51.14	179.0	125	280.0	C	0	G44 Concrete Sleeper With Fastclip	0	Lias Group	40	Overhead Line	0	0.00021	8.2	0	0	507.2
293	51.14	179.0	125	280.0	C	0	G44 Concrete Sleeper With Fastclip	0	Lias Group	40	Overhead Line	0	0.00032	12.8	0	0	511.8
294	51.14	179.0	125	280.0	C	0	G44 Concrete Sleeper With Fastclip	0	Lias Group	40	Overhead Line	0	0.00032	12.8	0	0	511.8
295	51.14	179.0	125	280.0	C	0	G44 Concrete Sleeper With Fastclip	0	Lias Group	40	Overhead Line	0	0.00032	12.8	0	0	511.8
296	51.14	179.0	125	280.0	C	0	G44 Concrete Sleeper With Fastclip	0	Lias Group	40	Overhead Line	0	0.00032	12.8	0	0	511.8
297	51.14	179.0	125	280.0	C	0	G44 Concrete Sleeper With Fastclip	0	Lias Group	40	Overhead Line	0	0.00000	0.0	0	0	499.0
298	51.14	179.0	125	280.0	C	0	F40 Concrete Sleeper	10	Lias Group	40	Overhead Line	0	0.00000	0.0	0	0	499.0
299	51.14	179.0	125	280.0	C	0	F40 Concrete Sleeper	10	Lias Group	40	Overhead Line	0	0.00000	0.0	0	0	499.0
300	51.14	179.0	125	280.0	C	0	F40 Concrete Sleeper	10	Lias Group	40	Overhead Line	0	0.00000	0.0	0	0	499.0
301	51.14	179.0	125	280.0	C	0	F40 Concrete Sleeper	10	Lias Group	40	Overhead Line	0	0.00000	0.0	0	0	499.0
302	51.14	179.0	125	280.0	C	0	F40 Concrete Sleeper	10	Lias Group	40	Overhead Line	0	0.00000	0.0	0	0	499.0
303	51.14	179.0	125	280.0	C	0	G44 Concrete Sleeper With Fastclip	0	Lias Group	40	Overhead Line	0	0.00065	25.9	0	0	524.9
304	51.14	179.0	125	280.0	C	0	G44 Concrete Sleeper With Fastclip	0	Lias Group	40	Overhead Line	0	0.00065	25.9	0	0	524.9
305	51.14	179.0	125	280.0	C	0	G44 Concrete Sleeper With Fastclip	0	Lias Group	40	Overhead Line	0	0.00042	16.6	0	0	515.6
306	51.14	179.0	125	280.0	C	0	G44 Concrete Sleeper With Fastclip	0	Lias Group	40	Overhead Line	0	0.00000	0.0	0	0	499.0
307	51.14	179.0	125	280.0	C	0	G44 Concrete Sleeper With Fastclip	0	Lias Group	40	Overhead Line	0	0.00000	0.0	0	0	499.0
308	51.14	179.0	125	280.0	C	0	F40 Concrete Sleeper	10	Lias Group	40	Overhead Line	0	0.00000	0.0	0	0	499.0
309	51.14	179.0	125	280.0	C	0	F27 Concrete Sleeper	40	Lias Group	40	Overhead Line	0	0.00000	0.0	0	0	539.0
310	51.14	179.0	125	280.0	C	0	G44 Concrete Sleeper With Fastclip	0	Lias Group	40	Overhead Line	0	0.00000	0.0	0	0	499.0
311	51.14	179.0	125	280.0	C	0	G44 Concrete Sleeper With Fastclip	0	Lias Group	40	Overhead Line	0	0.00000	0.0	0	0	499.0
312	51.14	179.0	125	280.0	C	0	G44 Concrete Sleeper With Fastclip	0	Lias Group	40	Overhead Line	0	0.00000	0.0	0	0	499.0
313	51.14	179.0	125	280.0	C	0	G44 Concrete Sleeper With Fastclip	0	Lias Group	40	Overhead Line	0	0.00000	0.0	0	0	499.0
314	51.14	179.0	125	280.0	C	0	G44 Concrete Sleeper With Fastclip	0	Lias Group	40	Overhead Line	0	0.00000	0.0	0	0	499.0
315	51.14	179.0	125	280.0	C	0	G44 Concrete Sleeper With Fastclip	0	Lias Group	40	Overhead Line	0	0.00000	0.0	0	0	499.0
316	51.14	179.0	125	280.0	C	0	G44 Concrete Sleeper With Fastclip	0	Lias Group	40	Overhead Line	0	0.00030	11.9	0	0	510.9
317	51.14	179.0	125	280.0	C	0	G44 Concrete Sleeper With Fastclip	0	Lias Group	40	Overhead Line	0	0.00039	15.4	0	0	514.4

318	51.14	179.0	125	280.0	C	0	G44 Concrete Sleeper With Fastclip	0	Lias Group	40	Overhead Line	0	0.00039	15.4	0	0	514.4
319	51.14	179.0	125	280.0	C	0	G44 Concrete Sleeper With Fastclip	0	Lias Group	40	Overhead Line	0	0.00039	15.4	0	0	514.4
320	51.14	179.0	125	280.0	C	0	G44 Concrete Sleeper With Fastclip	0	Lias Group	40	Overhead Line	0	0.00039	15.4	0	0	514.4
321	51.14	179.0	125	280.0	C	0	F27 Concrete Sleeper	40	Lias Group	40	Overhead Line	0	0.00000	0.0	0	0	539.0
322	51.14	179.0	125	280.0	C	0	F27 Concrete Sleeper	40	Lias Group	40	Overhead Line	0	0.00000	0.0	0	0	539.0
323	51.14	179.0	125	280.0	C	0	F27 Concrete Sleeper	40	Lias Group	40	Overhead Line	0	0.00000	0.0	0	0	539.0
324	51.14	179.0	125	280.0	C	0	F27 Concrete Sleeper	40	Lias Group	40	Overhead Line	0	0.00000	0.0	0	0	539.0
325	51.14	179.0	125	280.0	C	0	F27 Concrete Sleeper	40	Lias Group	40	Overhead Line	0	0.00000	0.0	0	0	539.0
326	51.14	179.0	125	280.0	C	0	F27 Concrete Sleeper	40	Lias Group	40	Overhead Line	0	0.00000	0.0	0	0	539.0
327	51.14	179.0	125	280.0	C	0	F27 Concrete Sleeper	40	Lias Group	40	Overhead Line	0	0.00000	0.0	0	0	539.0
328	51.14	179.0	125	280.0	C	0	F27 Concrete Sleeper	40	Lias Group	40	Overhead Line	0	0.00002	0.6	0	0	539.6
329	51.14	179.0	125	280.0	C	0	G44 Concrete Sleeper With Fastclip	0	Lias Group	40	Overhead Line	0	0.00018	7.4	0	0	506.4
330	51.14	179.0	125	280.0	C	0	G44 Concrete Sleeper With Fastclip	0	Lias Group	40	Overhead Line	0	0.00018	7.4	0	0	506.4
331	51.14	179.0	125	280.0	C	0	G44 Concrete Sleeper With Fastclip	0	Lias Group	40	Overhead Line	0	0.00018	7.4	0	0	506.4
332	51.00	178.5	110	246.4	C	0	G44 Concrete Sleeper With Fastclip	0	Lias Group	40	Overhead Line	0	0.00015	6.0	1	50	510.9
333	51.00	178.5	110	246.4	C	0	Hardwood Sleeper / Bearer	60	Lias Group	40	Overhead Line	0	0.00000	0.0	1	50	564.9
334	51.00	178.5	110	246.4	C	0	Hardwood Sleeper / Bearer	60	Lias Group	40	Overhead Line	0	0.00000	0.0	1	50	564.9
335	51.00	178.5	110	246.4	C	0	Hardwood Sleeper / Bearer	60	Lias Group	40	Overhead Line	0	0.00000	0.0	1	50	564.9
336	51.00	178.5	110	246.4	C	0	Hardwood Sleeper / Bearer	60	Lias Group	40	Overhead Line	0	0.00000	0.0	1	50	564.9
337	51.00	178.5	110	246.4	C	0	Hardwood Sleeper / Bearer	60	Lias Group	40	Overhead Line	0	0.00000	0.0	1	50	564.9
338	51.00	178.5	110	246.4	C	0	Hardwood Sleeper / Bearer	60	Lias Group	40	Overhead Line	0	0.00000	0.0	1	50	564.9
339	51.00	178.5	110	246.4	C	0	Hardwood Sleeper / Bearer	60	Lias Group	40	Overhead Line	0	0.00000	0.0	1	50	564.9
340	51.00	178.5	110	246.4	C	0	Hardwood Sleeper / Bearer	60	Lias Group	40	Overhead Line	0	0.00000	0.0	1	50	564.9
341	51.00	178.5	110	246.4	C	0	Hardwood Sleeper / Bearer	60	Lias Group	40	Overhead Line	0	0.00000	0.0	1	50	564.9
342	51.00	178.5	110	246.4	C	0	Hardwood Sleeper / Bearer	60	Lias Group	40	Overhead Line	0	0.00000	0.0	1	50	564.9
343	51.14	179.0	125	280.0	C	0	Hardwood Sleeper / Bearer	60	Lias Group	40	Overhead Line	0	0.00000	0.0	0	0	559.0
344	51.14	179.0	125	280.0	C	0	G44 Concrete Sleeper With Fastclip	0	Lias Group	40	Overhead Line	0	0.00000	0.0	0	0	499.0
345	51.14	179.0	125	280.0	C	0	G44 Concrete Sleeper With Fastclip	0	Lias Group	40	Overhead Line	0	0.00000	0.0	0	0	499.0
346	51.14	179.0	125	280.0	C	0	G44 Concrete Sleeper With Fastclip	0	Lias Group	40	Overhead Line	0	0.00000	0.0	0	0	499.0
347	51.14	179.0	125	280.0	C	0	G44 Concrete Sleeper With Fastclip	0	Lias Group	40	Overhead Line	0	0.00000	0.0	0	0	499.0
348	51.14	179.0	125	280.0	C	0	F27p Concrete Sleeper	10	Lias Group	40	Overhead Line	0	0.00000	0.0	0	0	499.0
349	51.14	179.0	125	280.0	C	0	F19 Concrete Sleeper	60	Lias Group	40	Overhead Line	0	0.00000	0.0	0	0	539.0
350	51.14	179.0	125	280.0	C	0	F19 Concrete Sleeper	60	Lias Group	40	Overhead Line	0	0.00000	0.0	0	0	539.0
351	51.14	179.0	125	280.0	C	0	G44 Concrete Sleeper With Fastclip	0	Lias Group	40	Overhead Line	0	0.00000	0.0	0	0	499.0
352	51.14	179.0	125	280.0	C	0	G44 Concrete Sleeper With Fastclip	0	Lias Group	40	Overhead Line	0	0.00023	9.4	0	0	508.4
353	51.14	179.0	125	280.0	C	0	G44 Concrete Sleeper With Fastclip	0	Lias Group	40	Overhead Line	0	0.00023	9.4	0	0	508.4
354	51.14	179.0	125	280.0	C	0	G44 Concrete Sleeper With Fastclip	0	Lias Group	40	Overhead Line	0	0.00032	12.8	0	0	511.8
355	51.14	179.0	125	280.0	C	0	G44 Concrete Sleeper With Fastclip	0	Lias Group	40	Overhead Line	0	0.00032	12.8	0	0	511.8
356	51.14	179.0	125	280.0	C	0	G44 Concrete Sleeper With Fastclip	0	Lias Group	40	Overhead Line	0	0.00008	3.2	0	0	502.2
357	51.14	179.0	125	280.0	C	0	G44 Concrete Sleeper With Fastclip	0	Lias Group	40	Overhead Line	0	0.00000	0.0	0	0	499.0
358	51.14	179.0	125	280.0	C	0	G44 Concrete Sleeper With Fastclip	0	Lias Group	40	Overhead Line	0	0.00000	0.0	0	0	499.0
359	51.14	179.0	125	280.0	C	0	G44 Concrete Sleeper With Fastclip	0	Lias Group	40	Overhead Line	0	0.00000	0.0	0	0	499.0
360	51.14	179.0	125	280.0	C	0	F40 Concrete Sleeper	10	Lias Group	40	Overhead Line	0	0.00000	0.0	0	0	499.0
361	51.14	179.0	125	280.0	C	0	F40 Concrete Sleeper	10	Lias Group	40	Overhead Line	0	0.00000	0.0	0	0	499.0
362	51.14	179.0	125	280.0	C	0	F40 Concrete Sleeper	10	Lias Group	40	Overhead Line	0	0.00000	0.0	0	0	499.0
363	51.14	179.0	125	280.0	C	0	F40 Concrete Sleeper	10	Lias Group	40	Overhead Line	0	0.00000	0.0	0	0	499.0
364	51.14	179.0	125	280.0	C	0	G44 Concrete Sleeper With Fastclip	0	Lias Group	40	Overhead Line	0	0.00000	0.0	0	0	499.0
365	51.14	179.0	125	280.0	C	0	G44 Concrete Sleeper With Fastclip	0	Lias Group	40	Overhead Line	0	0.00000	0.0	0	0	499.0
366	51.14	179.0	125	280.0	C	0	G44 Concrete Sleeper With Fastclip	0	Lias Group	40	Overhead Line	0	0.00000	0.0	0	0	499.0
367	51.14	179.0	125	280.0	C	0	G44 Concrete Sleeper With Fastclip	0	Lias Group	40	Overhead Line	0	0.00000	0.0	0	0	499.0
368	51.14	179.0	125	280.0	C	0	G44 Concrete Sleeper With Fastclip	0	Lias Group	40	Overhead Line	0	0.00000	0.0	0	0	499.0
369	51.14	179.0	125	280.0	C	0	G44 Concrete Sleeper With Fastclip	0	Lias Group	40	Overhead Line	0	0.00000	0.0	0	0	499.0
370	51.14	179.0	125	280.0	C	0	G44 Concrete Sleeper With Fastclip	0	Lias Group	40	Overhead Line	0	0.00000	0.0	0	0	499.0
371	51.14	179.0	125	280.0	C	0	G44 Concrete Sleeper With Fastclip	0	Lias Group	40	Overhead Line	0	0.00000	0.0	0	0	499.0
372	51.14	179.0	125	280.0	C	0	G44 Concrete Sleeper With Fastclip	0	Lias Group	40	Overhead Line	0	0.00000	0.0	0	0	499.0
373	51.14	179.0	125	280.0	C	0	G44 Concrete Sleeper With Fastclip	0	Lias Group	40	Overhead Line	0	0.00055	22.0	0	0	521.0

374	51.14	179.0	125	280.0	C	0	G44 Concrete Sleeper With Fastclip	0	Lias Group	40	Overhead Line	0	0.00102	50.0	0	0	539.0
375	51.14	179.0	125	280.0	C	0	G44 Concrete Sleeper With Fastclip	0	Lias Group	40	Overhead Line	0	0.00028	11.3	0	0	510.3
376	51.14	179.0	125	280.0	C	0	G44 Concrete Sleeper With Fastclip	0	Lias Group	40	Overhead Line	0	0.00028	11.3	0	0	510.3
377	51.14	179.0	125	280.0	C	0	G44 Concrete Sleeper With Fastclip	0	Lias Group	40	Overhead Line	0	0.00028	11.3	0	0	510.3
378	51.14	179.0	125	280.0	C	0	G44 Concrete Sleeper With Fastclip	0	Lias Group	40	Overhead Line	0	0.00025	9.9	0	0	508.9
379	51.14	179.0	125	280.0	C	0	G44 Concrete Sleeper With Fastclip	0	Lias Group	40	Overhead Line	0	0.00032	12.8	0	0	511.8
380	51.14	179.0	125	280.0	C	0	G44 Concrete Sleeper With Fastclip	0	Lias Group	40	Overhead Line	0	0.00028	11.2	0	0	510.2
381	51.14	179.0	125	280.0	C	0	G44 Concrete Sleeper With Fastclip	0	Lias Group	40	Overhead Line	0	0.00028	11.2	0	0	510.2
382	51.14	179.0	125	280.0	C	0	G44 Concrete Sleeper With Fastclip	0	Lias Group	40	Overhead Line	0	0.00028	11.2	0	0	510.2
383	51.14	179.0	125	280.0	C	0	G44 Concrete Sleeper With Fastclip	0	Lias Group	40	Overhead Line	0	0.00000	0.0	0	0	499.0
384	51.14	179.0	125	280.0	C	0	G44 Concrete Sleeper With Fastclip	0	Lias Group	40	Overhead Line	0	0.00000	0.0	0	0	499.0
385	0.70	2.5	25	56.0	C	0	Concrete Bearer (Unknown)	80	Kellaways Formation And Oxford Clay Formation	0	Not Electrified	50	0.00000	0.0	0	0	248.5
386	0.70	2.5	25	56.0	C	0	Concrete Bearer (Unknown)	80	Kellaways Formation And Oxford Clay Formation	0	Not Electrified	50	0.00000	0.0	0	0	248.5
387	0.80	2.8	25	56.0	C	0	Concrete Bearer (Unknown)	80	Kellaways Formation And Oxford Clay Formation	0	Not Electrified	50	0.00000	0.0	0	0	248.8
388	0.80	2.8	25	56.0	C	0	F27 Concrete Sleeper	40	Kellaways Formation And Oxford Clay Formation	0	Not Electrified	50	0.00000	0.0	0	0	138.8
389	0.80	2.8	25	56.0	C	0	F27 Concrete Sleeper	40	Kellaways Formation And Oxford Clay Formation	0	Not Electrified	50	0.00000	0.0	0	0	138.8
390	1.03	3.6	55	123.2	J	120	Hardwood Sleeper / Bearer	60	Kellaways Formation And Oxford Clay Formation	0	Not Electrified	50	0.00000	0.0	0	0	416.8
391	1.03	3.6	55	123.2	C	0	W560h Steel Sleepers	60	Kellaways Formation And Oxford Clay Formation	0	Not Electrified	50	0.00000	0.0	0	0	226.8
392	1.03	3.6	55	123.2	C	0	W560h Steel Sleepers	60	Kellaways Formation And Oxford Clay Formation	0	Not Electrified	50	0.00000	0.0	0	0	226.8
393	1.08	3.8	60	134.4	C	0	F27 Concrete Sleeper	40	Kellaways Formation And Oxford Clay Formation	0	Not Electrified	50	0.00017	6.6	0	0	224.8
394	1.08	3.8	60	134.4	C	0	F27 Concrete Sleeper	40	Kellaways Formation And Oxford Clay Formation	0	Not Electrified	50	0.00038	15.1	0	0	233.3
395	1.08	3.8	60	134.4	C	0	W560h Steel Sleepers	60	Kellaways Formation And Oxford Clay Formation	0	Not Electrified	50	0.00030	11.9	0	0	250.1
396	1.08	3.8	60	134.4	C	0	W560h Steel Sleepers	60	Kellaways Formation And Oxford Clay Formation	0	Not Electrified	50	0.00019	7.6	0	0	245.8
397	0.47	1.7	60	134.4	TC	120	Hardwood Sleeper / Bearer	60	Kellaways Formation And Oxford Clay Formation	0	Not Electrified	50	0.00000	0.0	0	0	426.1
398	0.47	1.7	60	134.4	C	0	W560 Steel Sleeper	80	Kellaways Formation And Oxford Clay Formation	0	Not Electrified	50	0.00034	13.6	0	0	249.7
399	0.47	1.7	60	134.4	C	0	W560 Steel Sleeper	80	Kellaways Formation And Oxford Clay Formation	0	Not Electrified	50	0.00034	13.6	0	0	249.7
400	0.47	1.7	60	134.4	C	0	W560 Steel Sleeper	80	Kellaways Formation And Oxford Clay Formation	0	Not Electrified	50	0.00034	13.6	0	0	249.7
401	0.47	1.7	60	134.4	C	0	W560 Steel Sleeper	80	Kellaways Formation And Oxford Clay Formation	0	Not Electrified	50	0.00034	13.4	0	0	249.5
402	0.47	1.7	60	134.4	C	0	W560 Steel Sleeper	80	Kellaways Formation And Oxford Clay Formation	0	Not Electrified	50	0.00033	13.2	0	0	249.3
403	0.47	1.7	60	134.4	C	0	W560 Steel Sleeper	80	Kellaways Formation And Oxford Clay Formation	0	Not Electrified	50	0.00033	13.2	0	0	249.3
404	0.47	1.7	60	134.4	C	0	W560 Steel Sleeper	80	Kellaways Formation And Oxford Clay Formation	0	Not Electrified	50	0.00033	13.2	0	0	249.3
405	0.47	1.7	60	134.4	C	0	W560h Steel Sleepers	60	Kellaways Formation And Oxford Clay Formation	0	Not Electrified	50	0.00074	29.7	0	0	265.7
406	0.47	1.7	60	134.4	C	0	W560h Steel Sleepers	60	Kellaways Formation And Oxford Clay Formation	0	Not Electrified	50	0.00059	23.6	0	0	259.7
407	0.47	1.7	60	134.4	C	0	W560h Steel Sleepers	60	Kellaways Formation And Oxford Clay Formation	0	Not Electrified	50	0.00000	0.0	0	0	236.1
408	0.47	1.7	60	134.4	C	0	W560h Steel Sleepers	60	Kellaways Formation And Oxford Clay Formation	0	Not Electrified	50	0.00000	0.0	0	0	236.1
409	0.47	1.7	60	134.4	C	0	W560h Steel Sleepers	60	Kellaways Formation And Oxford Clay Formation	0	Not Electrified	50	0.00000	0.0	0	0	236.1
410	0.47	1.7	60	134.4	C	0	W560h Steel Sleepers	60	Kellaways Formation And Oxford Clay Formation	0	Not Electrified	50	0.00000	0.0	0	0	236.1
411	0.47	1.7	60	134.4	C	0	W560h Steel Sleepers	60	Kellaways Formation And Oxford Clay Formation	0	Not Electrified	50	0.00000	0.0	0	0	236.1
412	0.47	1.7	60	134.4	C	0	W560h Steel Sleepers	60	Kellaways Formation And Oxford Clay Formation	0	Not Electrified	50	0.00034	13.6	0	0	249.7
413	0.47	1.7	60	134.4	C	0	W560h Steel Sleepers	60	Kellaways Formation And Oxford Clay Formation	0	Not Electrified	50	0.00061	24.4	0	0	260.4
414	0.47	1.7	60	134.4	C	0	W560h Steel Sleepers	60	Kellaways Formation And Oxford Clay Formation	0	Not Electrified	50	0.00061	24.4	0	0	260.4
415	0.47	1.7	60	134.4	C	0	W560h Steel Sleepers	60	Kellaways Formation And Oxford Clay Formation	0	Not Electrified	50	0.00000	0.0	0	0	236.1
416	0.47	1.7	60	134.4	C	0	W560h Steel Sleepers	60	Kellaways Formation And Oxford Clay Formation	0	Not Electrified	50	0.00000	0.0	0	0	236.1
417	0.47	1.7	60	134.4	C	0	W560h Steel Sleepers	60	Kellaways Formation And Oxford Clay Formation	0	Not Electrified	50	0.00000	0.0	0	0	236.1
418	0.47	1.7	60	134.4	C	0	Hardwood Sleeper / Bearer	60	Kellaways Formation And Oxford Clay Formation	0	Not Electrified	50	0.00000	0.0	0	0	236.1
419	0.47	1.7	60	134.4	C	0	W560h Steel Sleepers	60	Kellaways Formation And Oxford Clay Formation	0	Not Electrified	50	0.00000	0.0	0	0	236.1
420	0.47	1.7	60	134.4	C	0	W560h Steel Sleepers	60	Kellaways Formation And Oxford Clay Formation	0	Not Electrified	50	0.00000	0.0	0	0	236.1
421	0.47	1.7	60	134.4	C	0	W560h Steel Sleepers	60	Kellaways Formation And Oxford Clay Formation	0	Not Electrified	50	0.00000	0.0	0	0	236.1
422	0.47	1.7	60	134.4	C	0	W560h Steel Sleepers	60	Kellaways Formation And Oxford Clay Formation	0	Not Electrified	50	0.00000	0.0	0	0	236.1
423	0.47	1.7	60	134.4	C	0	W560h Steel Sleepers	60	Kellaways Formation And Oxford Clay Formation	0	Not Electrified	50	0.00000	0.0	0	0	236.1
424	0.47	1.7	60	134.4	C	0	W560h Steel Sleepers	60	Kellaways Formation And Oxford Clay Formation	0	Not Electrified	50	0.00000	0.0	0	0	236.1
425	0.47	1.7	60	134.4	C	0	W560h Steel Sleepers	60	Kellaways Formation And Oxford Clay Formation	0	Not Electrified	50	0.00077	30.7	0	0	266.7
426	0.47	1.7	60	134.4	C	0	W560h Steel Sleepers	60	Kellaways Formation And Oxford Clay Formation	0	Not Electrified	50	0.00001	0.4	0	0	236.5
427	0.47	1.7	60	134.4	C	0	560D Steel Sleeper CEN60 / 113A	80	Kellaways Formation And Oxford Clay Formation	0	Not Electrified	50	0.00000	0.0	0	0	326.1
428	0.47	1.7	60	134.4	C	0	560D Steel Sleeper CEN60 / 113A	80	Kellaways Formation And Oxford Clay Formation	0	Not Electrified	50	0.00000	0.0	0	0	326.1
429	0.47	1.7	60	134.4	C	0	560D Steel Sleeper CEN60 / 113A	80	Kellaways Formation And Oxford Clay Formation	0	Not Electrified	50	0.00000	0.0	0	0	326.1

430	0.47	1.7	60	134.4	C	0	560D Steel Sleeper CEN60 / 113A	80	Kellaways Formation And Oxford Clay Formation	0	Not Electrified	50	0.00000	0.0	0	0	326.1
431	0.47	1.7	60	134.4	C	0	560D Steel Sleeper CEN60 / 113A	80	Kellaways Formation And Oxford Clay Formation	0	Not Electrified	50	0.00000	0.0	0	0	326.1
432	0.47	1.7	60	134.4	C	0	560D Steel Sleeper CEN60 / 113A	80	Kellaways Formation And Oxford Clay Formation	0	Not Electrified	50	0.00000	0.0	0	0	326.1
433	0.47	1.7	60	134.4	C	0	Hardwood Sleeper / Bearer	60	Kellaways Formation And Oxford Clay Formation	0	Not Electrified	50	0.00000	0.0	0	0	236.1
434	0.47	1.7	60	134.4	C	0	W560h Steel Sleepers	60	Kellaways Formation And Oxford Clay Formation	0	Not Electrified	50	0.00052	20.7	0	0	256.7
435	0.47	1.7	60	134.4	C	0	W560h Steel Sleepers	60	Kellaways Formation And Oxford Clay Formation	0	Not Electrified	50	0.00058	23.3	0	0	259.3
436	0.47	1.7	60	134.4	C	0	W560h Steel Sleepers	60	Kellaways Formation And Oxford Clay Formation	0	Not Electrified	50	0.00066	26.3	0	0	262.3
437	0.47	1.7	60	134.4	C	0	W560h Steel Sleepers	60	Kellaways Formation And Oxford Clay Formation	0	Not Electrified	50	0.00058	23.0	0	0	259.1
438	0.47	1.7	60	134.4	C	0	W560h Steel Sleepers	60	Kellaways Formation And Oxford Clay Formation	0	Not Electrified	50	0.00063	25.1	0	0	261.1
439	0.47	1.7	60	134.4	A	120	Hardwood Sleeper / Bearer	60	Kellaways Formation And Oxford Clay Formation	0	Not Electrified	50	0.00063	25.1	0	0	451.1
440	0.47	1.7	60	134.4	C	0	F27 Concrete Sleeper	40	Kellaways Formation And Oxford Clay Formation	0	Not Electrified	50	0.00063	25.1	0	0	241.1
441	0.47	1.7	60	134.4	C	0	F27 Concrete Sleeper	40	Kellaways Formation And Oxford Clay Formation	0	Not Electrified	50	0.00000	0.0	0	0	216.1
442	0.47	1.7	60	134.4	C	0	F27 Concrete Sleeper	40	Kellaways Formation And Oxford Clay Formation	0	Not Electrified	50	0.00060	24.1	0	0	240.2
443	0.47	1.7	60	134.4	C	0	F27 Concrete Sleeper	40	Kellaways Formation And Oxford Clay Formation	0	Not Electrified	50	0.00060	24.1	0	0	240.2
444	0.47	1.7	60	134.4	C	0	F27 Concrete Sleeper	40	Kellaways Formation And Oxford Clay Formation	0	Not Electrified	50	0.00008	3.1	0	0	219.1
445	0.47	1.7	60	134.4	C	0	Softwood Sleeper / Bearer	120	Kellaways Formation And Oxford Clay Formation	0	Not Electrified	50	0.00000	0.0	0	0	276.1
446	0.47	1.7	60	134.4	C	0	Softwood Sleeper / Bearer	120	Kellaways Formation And Oxford Clay Formation	0	Not Electrified	50	0.00000	0.0	0	0	276.1
447	0.47	1.7	60	134.4	C	0	F27 Concrete Sleeper	40	Kellaways Formation And Oxford Clay Formation	0	Not Electrified	50	0.00056	22.3	0	0	238.3
448	0.47	1.7	60	134.4	C	0	F27 Concrete Sleeper	40	Kellaways Formation And Oxford Clay Formation	0	Not Electrified	50	0.00051	20.3	0	0	236.4
449	0.47	1.7	60	134.4	C	0	F27 Concrete Sleeper	40	Kellaways Formation And Oxford Clay Formation	0	Not Electrified	50	0.00000	0.0	0	0	216.1
450	0.47	1.7	60	134.4	C	0	F27 Concrete Sleeper	40	Kellaways Formation And Oxford Clay Formation	0	Not Electrified	50	0.00000	0.0	0	0	216.1
451	0.47	1.7	60	134.4	C	0	Hardwood Sleeper / Bearer	60	Kellaways Formation And Oxford Clay Formation	0	Not Electrified	50	0.00061	24.5	0	0	260.6
452	0.47	1.7	60	134.4	C	0	W560h Steel Sleepers	60	Kellaways Formation And Oxford Clay Formation	0	Not Electrified	50	0.00060	24.0	0	0	260.1
453	0.47	1.7	60	134.4	C	0	W560h Steel Sleepers	60	Kellaways Formation And Oxford Clay Formation	0	Not Electrified	50	0.00000	0.0	0	0	236.1
454	0.47	1.7	60	134.4	C	0	Softwood Sleeper / Bearer	120	Kellaways Formation And Oxford Clay Formation	0	Not Electrified	50	0.00000	0.0	0	0	276.1
455	0.47	1.7	60	134.4	C	0	W560h Steel Sleepers	60	Kellaways Formation And Oxford Clay Formation	0	Not Electrified	50	0.00012	4.6	0	0	240.7
456	0.47	1.7	60	134.4	C	0	W560h Steel Sleepers	60	Kellaways Formation And Oxford Clay Formation	0	Not Electrified	50	0.00061	24.3	0	0	260.3
457	0.47	1.7	60	134.4	C	0	Softwood Sleeper / Bearer	120	Kellaways Formation And Oxford Clay Formation	0	Not Electrified	50	0.00031	12.6	0	0	288.6
458	0.47	1.7	60	134.4	C	0	W560h Steel Sleepers	60	Kellaways Formation And Oxford Clay Formation	0	Not Electrified	50	0.00031	12.6	0	0	248.6
459	0.47	1.7	60	134.4	C	0	W560h Steel Sleepers	60	Kellaways Formation And Oxford Clay Formation	0	Not Electrified	50	0.00031	12.6	0	0	248.6
460	0.47	1.7	60	134.4	C	0	W560h Steel Sleepers	60	Kellaways Formation And Oxford Clay Formation	0	Not Electrified	50	0.00031	12.6	0	0	248.6
461	0.47	1.7	60	134.4	C	0	W560h Steel Sleepers	60	Kellaways Formation And Oxford Clay Formation	0	Not Electrified	50	0.00031	12.6	0	0	248.6
462	0.47	1.7	60	134.4	C	0	W560h Steel Sleepers	60	Kellaways Formation And Oxford Clay Formation	0	Not Electrified	50	0.00031	12.6	0	0	248.6
463	0.47	1.7	60	134.4	C	0	W560h Steel Sleepers	60	Kellaways Formation And Oxford Clay Formation	0	Not Electrified	50	0.00031	12.6	0	0	248.6
464	0.47	1.7	60	134.4	C	0	W560h Steel Sleepers	60	Kellaways Formation And Oxford Clay Formation	0	Not Electrified	50	0.00031	12.6	0	0	248.6
465	0.47	1.7	60	134.4	A	120	Hardwood Sleeper / Bearer	60	Kellaways Formation And Oxford Clay Formation	0	Not Electrified	50	0.00031	12.6	0	0	438.6
466	0.47	1.7	60	134.4	J	120	Softwood Sleeper / Bearer	120	Kellaways Formation And Oxford Clay Formation	0	Not Electrified	50	0.00031	12.6	0	0	478.6
467	0.47	1.7	60	134.4	J	120	Softwood Sleeper / Bearer	120	Kellaways Formation And Oxford Clay Formation	0	Not Electrified	50	0.00032	12.9	0	0	479.0
468	0.47	1.7	60	134.4	J	120	Softwood Sleeper / Bearer	120	Kellaways Formation And Oxford Clay Formation	0	Not Electrified	50	0.00030	11.9	0	0	477.9
469	0.47	1.7	60	134.4	J	120	Softwood Sleeper / Bearer	120	Kellaways Formation And Oxford Clay Formation	0	Not Electrified	50	0.00000	0.0	0	0	466.1
470	0.47	1.7	60	134.4	J	120	Softwood Sleeper / Bearer	120	Kellaways Formation And Oxford Clay Formation	0	Not Electrified	50	0.00000	0.0	0	0	466.1
471	0.47	1.7	60	134.4	J	120	Softwood Sleeper / Bearer	120	Kellaways Formation And Oxford Clay Formation	0	Not Electrified	50	0.00000	0.0	0	0	466.1
472	0.47	1.7	60	134.4	J	120	Softwood Sleeper / Bearer	120	Kellaways Formation And Oxford Clay Formation	0	Not Electrified	50	0.00000	0.0	0	0	466.1
473	0.47	1.7	60	134.4	J	120	Softwood Sleeper / Bearer	120	Kellaways Formation And Oxford Clay Formation	0	Not Electrified	50	0.00000	0.0	0	0	466.1
474	0.47	1.7	60	134.4	J	120	Softwood Sleeper / Bearer	120	Kellaways Formation And Oxford Clay Formation	0	Not Electrified	50	0.00000	0.0	0	0	466.1
475	0.47	1.7	60	134.4	J	120	W560 Steel Sleeper	80	Kellaways Formation And Oxford Clay Formation	0	Not Electrified	50	0.00000	0.0	0	0	426.1
476	0.47	1.7	60	134.4	C	0	W560 Steel Sleeper	80	Kellaways Formation And Oxford Clay Formation	0	Not Electrified	50	0.00000	0.0	0	0	236.1
477	0.47	1.7	60	134.4	C	0	W560 Steel Sleeper	80	Kellaways Formation And Oxford Clay Formation	0	Not Electrified	50	0.00000	0.0	0	0	236.1
478	0.47	1.7	60	134.4	C	0	W560 Steel Sleeper	80	Kellaways Formation And Oxford Clay Formation	0	Not Electrified	50	0.00000	0.0	0	0	236.1
479	0.47	1.7	60	134.4	C	0	W560 Steel Sleeper	80	Kellaways Formation And Oxford Clay Formation	0	Not Electrified	50	0.00000	0.0	0	0	236.1
480	0.47	1.7	60	134.4	C	0	W560 Steel Sleeper	80	Kellaways Formation And Oxford Clay Formation	0	Not Electrified	50	0.00000	0.0	0	0	236.1
481	0.47	1.7	60	134.4	C	0	W560 Steel Sleeper	80	Kellaways Formation And Oxford Clay Formation	0	Not Electrified	50	0.00000	0.0	0	0	236.1
482	0.48	1.7	60	134.4	C	0	W560 Steel Sleeper	80	Kellaways Formation And Oxford Clay Formation	0	Not Electrified	50	0.00000	0.0	0	0	236.1
483	0.48	1.7	60	134.4	C	0	W560 Steel Sleeper	80	Kellaways Formation And Oxford Clay Formation	0	Not Electrified	50	0.00000	0.0	0	0	236.1
484	0.48	1.7	60	134.4	C	0	W560 Steel Sleeper	80	Kellaways Formation And Oxford Clay Formation	0	Not Electrified	50	0.00000	0.0	0	0	236.1
485	0.48	1.7	60	134.4	C	0	W560 Steel Sleeper	80	Kellaways Formation And Oxford Clay Formation	0	Not Electrified	50	0.00000	0.0	0	0	236.1

486	0.48	1.7	60	134.4	C	0	W560 Steel Sleeper	80	Kellaways Formation And Oxford Clay Formation	0	Not Electrified	50	0.00000	0.0	0	0	236.1
487	0.48	1.7	60	134.4	C	0	W560 Steel Sleeper	80	Kellaways Formation And Oxford Clay Formation	0	Not Electrified	50	0.00000	0.0	0	0	236.1
488	0.48	1.7	60	134.4	C	0	W560 Steel Sleeper	80	Kellaways Formation And Oxford Clay Formation	0	Not Electrified	50	0.00000	0.0	0	0	236.1
489	0.48	1.7	60	134.4	C	0	W560 Steel Sleeper	80	Kellaways Formation And Oxford Clay Formation	0	Not Electrified	50	0.00000	0.0	0	0	236.1
490	0.48	1.7	60	134.4	C	0	W560 Steel Sleeper	80	Kellaways Formation And Oxford Clay Formation	0	Not Electrified	50	0.00000	0.0	0	0	236.1
491	0.48	1.7	60	134.4	C	0	W560 Steel Sleeper	80	Kellaways Formation And Oxford Clay Formation	0	Not Electrified	50	0.00000	0.0	0	0	236.1
492	0.48	1.7	60	134.4	C	0	W560 Steel Sleeper	80	Kellaways Formation And Oxford Clay Formation	0	Not Electrified	50	0.00000	0.0	0	0	236.1
493	0.48	1.7	60	134.4	C	0	W560 Steel Sleeper	80	Kellaways Formation And Oxford Clay Formation	0	Not Electrified	50	0.00000	0.0	0	0	236.1
494	0.48	1.7	60	134.4	C	0	W560 Steel Sleeper	80	Kellaways Formation And Oxford Clay Formation	0	Not Electrified	50	0.00000	0.0	0	0	236.1
495	0.48	1.7	60	134.4	C	0	W560 Steel Sleeper	80	Kellaways Formation And Oxford Clay Formation	0	Not Electrified	50	0.00048	19.3	0	0	255.3
496	0.48	1.7	60	134.4	C	0	W560 Steel Sleeper	80	Kellaways Formation And Oxford Clay Formation	0	Not Electrified	50	0.00060	23.9	0	0	259.9
497	0.48	1.7	60	134.4	C	0	W560 Steel Sleeper	80	Kellaways Formation And Oxford Clay Formation	0	Not Electrified	50	0.00060	23.9	0	0	259.9
498	0.48	1.7	60	134.4	C	0	W560 Steel Sleeper	80	Kellaways Formation And Oxford Clay Formation	0	Not Electrified	50	0.00014	5.6	0	0	241.6
499	0.48	1.7	60	134.4	C	0	W560 Steel Sleeper	80	Kellaways Formation And Oxford Clay Formation	0	Not Electrified	50	0.00000	0.0	0	0	236.1
500	0.48	1.7	60	134.4	C	0	W560 Steel Sleeper	80	Kellaways Formation And Oxford Clay Formation	0	Not Electrified	50	0.00000	0.0	0	0	236.1
501	0.48	1.7	60	134.4	C	0	W560 Steel Sleeper	80	Kellaways Formation And Oxford Clay Formation	0	Not Electrified	50	0.00000	0.0	0	0	236.1
502	0.48	1.7	60	134.4	C	0	W560 Steel Sleeper	80	Kellaways Formation And Oxford Clay Formation	0	Not Electrified	50	0.00000	0.0	0	0	236.1
503	0.48	1.7	60	134.4	C	0	W560h Steel Sleepers	60	Kellaways Formation And Oxford Clay Formation	0	Not Electrified	50	0.00000	0.0	0	0	236.1
504	0.48	1.7	60	134.4	C	0	W560h Steel Sleepers	60	Kellaways Formation And Oxford Clay Formation	0	Not Electrified	50	0.00000	0.0	0	0	236.1
505	0.48	1.7	60	134.4	C	0	W560h Steel Sleepers	60	Kellaways Formation And Oxford Clay Formation	0	Not Electrified	50	0.00085	33.9	0	0	269.9
506	0.48	1.7	60	134.4	C	0	W560h Steel Sleepers	60	Kellaways Formation And Oxford Clay Formation	0	Not Electrified	50	0.00092	36.6	0	0	272.7
507	0.48	1.7	60	134.4	C	0	W560h Steel Sleepers	60	Great Oolite Group	85	Not Electrified	50	0.00017	6.7	0	0	322.7
508	0.48	1.7	60	134.4	C	0	W560h Steel Sleepers	60	Great Oolite Group	85	Not Electrified	50	0.00000	0.0	0	0	316.1
509	0.48	1.7	60	134.4	C	0	W560h Steel Sleepers	60	Great Oolite Group	85	Not Electrified	50	0.00000	0.0	0	0	316.1
510	0.48	1.7	60	134.4	C	0	W560h Steel Sleepers	60	Great Oolite Group	85	Not Electrified	50	0.00000	0.0	0	0	316.1
511	0.48	1.7	60	134.4	C	0	W560h Steel Sleepers	60	Great Oolite Group	85	Not Electrified	50	0.00000	0.0	0	0	316.1
512	0.86	3.0	15	33.6	J	120	Hardwood Sleeper / Bearer	60	Great Oolite Group	85	Not Electrified	50	0.00000	0.0	0	0	406.6
513	0.86	3.0	15	33.6	J	120	Hardwood Sleeper / Bearer	60	Great Oolite Group	85	Not Electrified	50	0.00000	0.0	0	0	406.6
514	24.67	86.4	100	224.0	C	0	G44 Concrete Sleeper With Fastclip	0	Great Oolite Group	85	Overhead Line	0	0.00000	0.0	0	0	390.4
515	24.67	86.4	100	224.0	C	0	F40 Concrete Sleeper	10	Great Oolite Group	85	Overhead Line	0	0.00000	0.0	0	0	390.4
516	24.67	86.4	100	224.0	C	0	F40 Concrete Sleeper	10	Great Oolite Group	85	Overhead Line	0	0.00000	0.0	0	0	390.4
517	24.67	86.4	100	224.0	C	0	F23 Concrete Sleeper	60	Great Oolite Group	85	Overhead Line	0	0.00000	0.0	0	0	430.4
518	24.67	86.4	100	224.0	C	0	G44 Concrete Sleeper With Fastclip	0	Great Oolite Group	85	Overhead Line	0	0.00000	0.0	0	0	390.4
519	24.67	86.4	100	224.0	C	0	G44 Concrete Sleeper With Fastclip	0	Great Oolite Group	85	Overhead Line	0	0.00000	0.0	0	0	390.4
520	24.67	86.4	100	224.0	C	0	G44 Concrete Sleeper With Fastclip	0	Great Oolite Group	85	Overhead Line	0	0.00000	0.0	0	0	390.4
521	24.67	86.4	100	224.0	C	0	G44 Concrete Sleeper With Fastclip	0	Great Oolite Group	85	Overhead Line	0	0.00000	0.0	0	0	390.4
522	24.67	86.4	100	224.0	C	0	G44 Concrete Sleeper With Fastclip	0	Lias Group	40	Overhead Line	0	0.00000	0.0	0	0	350.4
523	24.67	86.4	100	224.0	C	0	F27 Concrete Sleeper	40	Lias Group	40	Overhead Line	0	0.00000	0.0	0	0	390.4
524	24.67	86.4	100	224.0	C	0	F27 Concrete Sleeper	40	Lias Group	40	Overhead Line	0	0.00000	0.0	0	0	390.4
525	24.67	86.4	100	224.0	C	0	G44 Concrete Sleeper With Fastclip	0	Lias Group	40	Overhead Line	0	0.00019	7.5	0	0	357.9
526	24.67	86.4	100	224.0	C	0	G44 Concrete Sleeper With Fastclip	0	Lias Group	40	Overhead Line	0	0.00020	7.9	0	0	358.3
527	24.67	86.4	100	224.0	C	0	G44 Concrete Sleeper With Fastclip	0	Lias Group	40	Overhead Line	0	0.00020	7.9	0	0	358.3
528	24.67	86.4	100	224.0	C	0	G44 Concrete Sleeper With Fastclip	0	Lias Group	40	Overhead Line	0	0.00020	7.9	0	0	358.3
529	24.67	86.4	100	224.0	C	0	F27 Concrete Sleeper	40	Lias Group	40	Overhead Line	0	0.00000	0.0	0	0	390.4
530	24.67	86.4	100	224.0	C	0	F27 Concrete Sleeper	40	Lias Group	40	Overhead Line	0	0.00000	0.0	0	0	390.4
531	24.67	86.4	100	224.0	C	0	G44 Concrete Sleeper With Fastclip	0	Lias Group	40	Overhead Line	0	0.00000	0.0	0	0	350.4
532	24.67	86.4	100	224.0	C	0	G44 Concrete Sleeper With Fastclip	0	Lias Group	40	Overhead Line	0	0.00000	0.0	0	0	350.4
533	24.67	86.4	100	224.0	C	0	G44 Concrete Sleeper With Fastclip	0	Lias Group	40	Overhead Line	0	0.00007	2.9	0	0	353.2
534	24.51	85.8	90	201.6	C	0	G44 Concrete Sleeper With Fastclip	0	Lias Group	40	Overhead Line	0	0.00041	16.6	0	0	343.9
535	24.51	85.8	90	201.6	C	0	F40as Concrete Sleeper	0	Lias Group	40	Overhead Line	0	0.00042	16.6	0	0	344.0
536	24.51	85.8	90	201.6	C	0	F40as Concrete Sleeper	0	Lias Group	40	Overhead Line	0	0.00027	11.0	0	0	338.3
537	24.51	85.8	90	201.6	C	0	F40as Concrete Sleeper	0	Lias Group	40	Overhead Line	0	0.00035	14.1	0	0	341.5
538	24.51	85.8	90	201.6	C	0	F40as Concrete Sleeper	0	Lias Group	40	Overhead Line	0	0.00035	13.9	0	0	341.3
539	24.51	85.8	90	201.6	C	0	F40as Concrete Sleeper	0	Lias Group	40	Overhead Line	0	0.00043	17.2	0	0	344.6
540	24.51	85.8	90	201.6	C	0	F40 Concrete Sleeper	10	Lias Group	40	Overhead Line	0	0.00018	7.2	0	0	334.5
541	24.51	85.8	90	201.6	C	0	F40 Concrete Sleeper	10	Lias Group	40	Overhead Line	0	0.00045	18.0	0	0	345.4

542	24.51	85.8	90	201.6	C	0	F40 Concrete Sleeper	10	Lias Group	40	Overhead Line	0	0.00000	0.0	0	0	327.4
543	24.51	85.8	90	201.6	C	0	F40 Concrete Sleeper	10	Lias Group	40	Overhead Line	0	0.00039	15.4	0	0	342.8
544	24.51	85.8	90	201.6	C	0	F27 Concrete Sleeper	40	Lias Group	40	Overhead Line	0	0.00024	9.4	0	0	376.8
545	24.51	85.8	90	201.6	C	0	F27 Concrete Sleeper	40	Lias Group	40	Overhead Line	0	0.00021	8.4	0	0	375.7
546	24.51	85.8	90	201.6	C	0	F27 Concrete Sleeper	40	Lias Group	40	Overhead Line	0	0.00002	0.7	0	0	368.1
547	24.51	85.8	90	201.6	C	0	G44 Concrete Sleeper With Fastclip	0	Lias Group	40	Overhead Line	0	0.00018	7.0	0	0	334.4
548	24.51	85.8	90	201.6	C	0	G44 Concrete Sleeper With Fastclip	0	Lias Group	40	Overhead Line	0	0.00026	10.4	0	0	337.8
549	24.51	85.8	90	201.6	C	0	Hardwood Sleeper / Bearer	60	Lias Group	40	Overhead Line	0	0.00038	15.4	0	0	402.7
550	24.51	85.8	90	201.6	C	0	Hardwood Sleeper / Bearer	60	Lias Group	40	Overhead Line	0	0.00038	15.4	0	0	402.7
551	24.51	85.8	90	201.6	C	0	Hardwood Sleeper / Bearer	60	Lias Group	40	Overhead Line	0	0.00082	32.7	0	0	420.1
552	24.51	85.8	90	201.6	C	0	F40 Concrete Sleeper	10	Lias Group	40	Overhead Line	0	0.00082	32.7	0	0	360.1
553	24.51	85.8	90	201.6	C	0	Softwood Sleeper / Bearer	120	Lias Group	40	Overhead Line	0	0.00000	0.0	0	0	427.4
554	24.51	85.8	90	201.6	C	0	Softwood Sleeper / Bearer	120	Lias Group	40	Overhead Line	0	0.00000	0.0	0	0	427.4
555	24.51	85.8	90	201.6	C	0	F40 Concrete Sleeper	10	Lias Group	40	Overhead Line	0	0.00000	0.0	0	0	327.4
556	24.51	85.8	90	201.6	C	0	F40 Concrete Sleeper	10	Lias Group	40	Overhead Line	0	0.00000	0.0	0	0	327.4
557	24.51	85.8	90	201.6	C	0	F40 Concrete Sleeper	10	Lias Group	40	Overhead Line	0	0.00000	0.0	0	0	327.4
558	24.51	85.8	90	201.6	C	0	F40 Concrete Sleeper	10	Lias Group	40	Overhead Line	0	0.00000	0.0	0	0	327.4
559	24.51	85.8	90	201.6	C	0	F40 Concrete Sleeper	10	Lias Group	40	Overhead Line	0	0.00000	0.0	0	0	327.4
560	24.51	85.8	90	201.6	C	0	F40 Concrete Sleeper	10	Lias Group	40	Overhead Line	0	0.00000	0.0	0	0	327.4
561	24.51	85.8	90	201.6	C	0	F40 Concrete Sleeper	10	Lias Group	40	Overhead Line	0	0.00000	0.0	0	0	327.4
562	24.51	85.8	90	201.6	C	0	G44 Concrete Sleeper With Fastclip	0	Lias Group	40	Overhead Line	0	0.00000	0.0	0	0	327.4
563	24.51	85.8	90	201.6	C	0	G44 Concrete Sleeper With Fastclip	0	Lias Group	40	Overhead Line	0	0.00000	0.0	0	0	327.4
564	24.51	85.8	90	201.6	C	0	G44 Concrete Sleeper With Fastclip	0	Lias Group	40	Overhead Line	0	0.00000	0.0	0	0	327.4
565	24.51	85.8	90	201.6	C	0	G44 Concrete Sleeper With Fastclip	0	Lias Group	40	Overhead Line	0	0.00000	0.0	0	0	327.4
566	24.51	85.8	90	201.6	C	0	G44 Concrete Sleeper With Fastclip	0	Lias Group	40	Overhead Line	0	0.00000	0.0	0	0	327.4
567	24.51	85.8	90	201.6	C	0	F27 Concrete Sleeper	40	Lias Group	40	Overhead Line	0	0.00042	16.8	0	0	384.1
568	23.41	81.9	75	168.0	C	0	F27 Concrete Sleeper	40	Lias Group	40	Overhead Line	0	0.00042	16.8	0	0	346.7
569	23.41	81.9	75	168.0	C	0	G44 Concrete Sleeper With Fastclip	0	Lias Group	40	Overhead Line	0	0.00042	16.8	0	0	306.7
570	23.41	81.9	75	168.0	C	0	G44 Concrete Sleeper With Fastclip	0	Lias Group	40	Overhead Line	0	0.00042	16.8	0	0	306.7
571	23.41	81.9	75	168.0	C	0	G44 Concrete Sleeper With Fastclip	0	Lias Group	40	Overhead Line	0	0.00042	16.8	0	0	306.7
572	23.41	81.9	75	168.0	C	0	G44 Concrete Sleeper With Fastclip	0	Lias Group	40	Overhead Line	0	0.00042	16.8	0	0	306.7
573	23.41	81.9	75	168.0	C	0	G44 Concrete Sleeper With Fastclip	0	Lias Group	40	Overhead Line	0	0.00000	0.0	0	0	289.9
574	23.41	81.9	75	168.0	C	0	G44 Concrete Sleeper With Fastclip	0	Lias Group	40	Overhead Line	0	0.00000	0.0	0	0	289.9
575	23.41	81.9	75	168.0	C	0	G44 Concrete Sleeper With Fastclip	0	Lias Group	40	Overhead Line	0	0.00000	0.0	0	0	289.9
576	23.41	81.9	75	168.0	C	0	G44 Concrete Sleeper With Fastclip	0	Lias Group	40	Overhead Line	0	0.00000	0.0	1	50	329.9
577	23.41	81.9	75	168.0	C	0	G44 Concrete Sleeper With Fastclip	0	Lias Group	40	Overhead Line	0	0.00000	0.0	1	50	329.9
578	23.41	81.9	75	168.0	C	0	G44 Concrete Sleeper With Fastclip	0	Lias Group	40	Overhead Line	0	0.00000	0.0	1	50	329.9
579	23.41	81.9	75	168.0	C	0	G44 Concrete Sleeper With Fastclip	0	Lias Group	40	Overhead Line	0	0.00000	0.0	1	50	329.9
580	23.41	81.9	75	168.0	C	0	G44 Concrete Sleeper With Fastclip	0	Lias Group	40	Overhead Line	0	0.00000	0.0	1	50	329.9
581	23.41	81.9	75	168.0	C	0	F27 Concrete Sleeper	40	Inferior Oolite Group	60	Overhead Line	0	0.00000	0.0	0	0	349.9
582	23.41	81.9	75	168.0	C	0	F27 Concrete Sleeper	40	Inferior Oolite Group	60	Overhead Line	0	0.00000	0.0	0	0	349.9
583	23.41	81.9	75	168.0	C	0	F27 Concrete Sleeper	40	Inferior Oolite Group	60	Overhead Line	0	0.00000	0.0	0	0	349.9
584	23.41	81.9	75	168.0	C	0	F27 Concrete Sleeper	40	Inferior Oolite Group	60	Overhead Line	0	0.00000	0.0	0	0	349.9
585	23.41	81.9	75	168.0	C	0	Softwood Sleeper / Bearer	120	Inferior Oolite Group	60	Overhead Line	0	0.00166	50.0	0	0	449.9
586	23.41	81.9	75	168.0	J	120	Softwood Sleeper / Bearer	120	Lias Group	40	Overhead Line	0	0.00000	0.0	0	0	579.9
587	16.70	58.5	35	78.4	J	120	Softwood Sleeper / Bearer	120	Lias Group	40	Overhead Line	0	0.00000	0.0	0	0	466.9
588	16.70	58.5	35	78.4	J	120	Concrete Bearer R (Shallow Depth)	80	Lias Group	40	Overhead Line	0	0.00202	50.0	0	0	556.9
589	16.70	58.5	20	44.8	C	0	Hardwood Sleeper / Bearer	60	Lias Group	40	Overhead Line	0	0.00000	0.0	0	0	203.3
590	15.62	54.7	30	67.2	C	0	F40 Concrete Sleeper	10	Lias Group	40	Overhead Line	0	0.00000	0.0	0	0	161.9
591	15.62	54.7	30	67.2	C	0	Concrete Bearer D Or R (Unknown)	80	Inferior Oolite Group	60	Overhead Line	0	0.00000	0.0	0	0	331.9
592	15.62	54.7	30	67.2	C	0	Hardwood Sleeper / Bearer	60	Inferior Oolite Group	60	Overhead Line	0	0.00000	0.0	0	0	241.9
593	14.66	51.3	60	134.4	C	0	Hardwood Sleeper / Bearer	60	Inferior Oolite Group	60	Overhead Line	0	0.00015	6.0	0	0	311.7
594	14.66	51.3	60	134.4	C	0	G44 Concrete Sleeper With Fastclip	0	Inferior Oolite Group	60	Overhead Line	0	0.00025	10.1	0	0	255.8
595	14.66	51.3	60	134.4	C	0	G44 Concrete Sleeper With Fastclip	0	Inferior Oolite Group	60	Overhead Line	0	0.00100	50.0	0	0	285.7
596	14.66	51.3	60	134.4	C	0	F40 Concrete Sleeper	10	Inferior Oolite Group	60	Overhead Line	0	0.00100	50.0	0	0	285.7
597	14.70	51.5	60	134.4	C	0	F40 Concrete Sleeper	10	Inferior Oolite Group	60	Overhead Line	0	0.00100	50.0	0	0	285.9

598	14.70	51.5	60	134.4	C	0	F40 Concrete Sleeper	10	Lias Group	40	Overhead Line	0	0.00100	50.0	0	0	265.9
599	14.70	51.5	60	134.4	C	0	G44 Concrete Sleeper With Fastclip	0	Lias Group	40	Overhead Line	0	0.00096	38.6	0	0	264.4
600	14.70	51.5	60	134.4	C	0	G44 Concrete Sleeper With Fastclip	0	Lias Group	40	Overhead Line	0	0.00000	0.0	0	0	225.9
601	14.70	51.5	60	134.4	C	0	Hardwood Sleeper / Bearer	60	Lias Group	40	Overhead Line	0	0.00018	7.0	0	0	292.9
602	14.70	51.5	60	134.4	C	0	F27 Concrete Sleeper	40	Lias Group	40	Overhead Line	0	0.00000	0.0	0	0	265.9
603	18.35	64.2	60	134.4	C	0	F40 Concrete Sleeper	10	Lias Group	40	Overhead Line	0	0.00075	29.9	0	0	268.6
604	18.35	64.2	60	134.4	C	0	G44 Concrete Sleeper With Fastclip	0	Lias Group	40	Overhead Line	0	0.00094	37.8	0	0	276.4
605	18.35	64.2	60	134.4	C	0	G44 Concrete Sleeper With Fastclip	0	Lias Group	40	Overhead Line	0	0.00076	30.4	0	0	269.0
606	18.35	64.2	60	134.4	C	0	G44 Concrete Sleeper With Fastclip	0	Lias Group	40	Overhead Line	0	0.00076	30.4	0	0	269.0
607	18.35	64.2	60	134.4	C	0	G44 Concrete Sleeper With Fastclip	0	Lias Group	40	Overhead Line	0	0.00076	30.4	0	0	269.0
608	18.35	64.2	60	134.4	C	0	F40 Concrete Sleeper	10	Lias Group	40	Overhead Line	0	0.00035	14.0	0	0	252.7
609	20.31	71.1	75	168.0	C	0	F40 Concrete Sleeper	10	Lias Group	40	Overhead Line	0	0.00000	0.0	0	0	279.1
610	20.31	71.1	75	168.0	C	0	G44 Concrete Sleeper With Fastclip	0	Lias Group	40	Overhead Line	0	0.00000	0.0	0	0	279.1
611	20.31	71.1	75	168.0	C	0	G44 Concrete Sleeper With Fastclip	0	Lias Group	40	Overhead Line	0	0.00000	0.0	0	0	279.1
612	20.31	71.1	75	168.0	C	0	F40 Concrete Sleeper	10	Lias Group	40	Overhead Line	0	0.00000	0.0	0	0	279.1
613	20.31	71.1	75	168.0	C	0	F40 Concrete Sleeper	10	Lias Group	40	Overhead Line	0	0.00057	23.0	0	0	302.1
614	20.31	71.1	75	168.0	C	0	F40 Concrete Sleeper	10	Lias Group	40	Overhead Line	0	0.00040	16.1	0	0	295.2
615	20.31	71.1	75	168.0	C	0	F40 Concrete Sleeper	10	Lias Group	40	Overhead Line	0	0.00040	16.1	0	0	295.2
616	20.31	71.1	75	168.0	C	0	F40 Concrete Sleeper	10	Lias Group	40	Overhead Line	0	0.00000	0.0	0	0	279.1
617	20.31	71.1	75	168.0	C	0	F40 Concrete Sleeper	10	Lias Group	40	Overhead Line	0	0.00000	0.0	0	0	279.1
618	20.31	71.1	75	168.0	C	0	Ef29 Concrete Sleeper	40	Lias Group	40	Overhead Line	0	0.00000	0.0	0	0	319.1
619	20.31	71.1	75	168.0	C	0	F40 Concrete Sleeper	10	Lias Group	40	Overhead Line	0	0.00000	0.0	0	0	279.1
620	20.31	71.1	75	168.0	C	0	F27 Concrete Sleeper	40	Lias Group	40	Overhead Line	0	0.00000	0.0	0	0	319.1
621	20.31	71.1	75	168.0	C	0	F27 Concrete Sleeper	40	Lias Group	40	Overhead Line	0	0.00000	0.0	0	0	319.1
622	20.31	71.1	75	168.0	C	0	G44 Concrete Sleeper With Fastclip	0	Lias Group	40	Overhead Line	0	0.00000	0.0	0	0	279.1
623	20.31	71.1	75	168.0	C	0	G44 Concrete Sleeper With Fastclip	0	Lias Group	40	Overhead Line	0	0.00041	16.2	0	0	295.3
624	20.31	71.1	75	168.0	C	0	G44 Concrete Sleeper With Fastclip	0	Lias Group	40	Overhead Line	0	0.00041	16.2	0	0	295.3
625	20.31	71.1	75	168.0	C	0	F27 Concrete Sleeper	40	Lias Group	40	Overhead Line	0	0.00041	16.2	0	0	335.3
626	20.31	71.1	75	168.0	C	0	F27 Concrete Sleeper	40	Lias Group	40	Overhead Line	0	0.00041	16.2	0	0	335.3
627	20.31	71.1	75	168.0	C	0	F40 Concrete Sleeper	10	Lias Group	40	Overhead Line	0	0.00013	5.3	0	0	284.4
628	20.31	71.1	75	168.0	C	0	G44 Concrete Sleeper With Fastclip	0	Lias Group	40	Overhead Line	0	0.00000	0.0	0	0	279.1
629	20.31	71.1	75	168.0	C	0	G44 Concrete Sleeper With Fastclip	0	Lias Group	40	Overhead Line	0	0.00000	0.0	0	0	279.1
630	20.31	71.1	75	168.0	C	0	G44 Concrete Sleeper With Fastclip	0	Lias Group	40	Overhead Line	0	0.00000	0.0	0	0	279.1
631	20.31	71.1	75	168.0	C	0	F27 Concrete Sleeper	40	Lias Group	40	Overhead Line	0	0.00000	0.0	0	0	319.1
632	20.31	71.1	75	168.0	C	0	F27 Concrete Sleeper	40	Lias Group	40	Overhead Line	0	0.00000	0.0	0	0	319.1
633	20.31	71.1	75	168.0	C	0	F27 Concrete Sleeper	40	Lias Group	40	Overhead Line	0	0.00000	0.0	0	0	319.1
634	20.31	71.1	75	168.0	C	0	G44 Concrete Sleeper With Fastclip	0	Lias Group	40	Overhead Line	0	0.00000	0.0	0	0	279.1
635	20.31	71.1	75	168.0	C	0	G44 Concrete Sleeper With Fastclip	0	Lias Group	40	Overhead Line	0	0.00000	0.0	0	0	279.1
636	20.31	71.1	75	168.0	C	0	G44 Concrete Sleeper With Fastclip	0	Lias Group	40	Overhead Line	0	0.00058	23.2	0	0	302.3
637	20.31	71.1	75	168.0	C	0	G44 Concrete Sleeper With Fastclip	0	Lias Group	40	Overhead Line	0	0.00058	23.2	0	0	302.3
638	20.31	71.1	75	168.0	C	0	G44 Concrete Sleeper With Fastclip	0	Lias Group	40	Overhead Line	0	0.00026	10.3	0	0	289.4
639	20.31	71.1	75	168.0	C	0	Hardwood Sleeper / Bearer	60	Lias Group	40	Overhead Line	0	0.00000	0.0	0	0	339.1
640	20.31	71.1	75	168.0	C	0	F27 Concrete Sleeper	40	Lias Group	40	Overhead Line	0	0.00000	0.0	0	0	319.1
641	20.31	71.1	75	168.0	C	0	F27 Concrete Sleeper	40	Lias Group	40	Overhead Line	0	0.00000	0.0	0	0	319.1
642	20.31	71.1	75	168.0	C	0	F27 Concrete Sleeper	40	Lias Group	40	Overhead Line	0	0.00000	0.0	0	0	319.1
643	20.31	71.1	75	168.0	C	0	F27 Concrete Sleeper	40	Lias Group	40	Overhead Line	0	0.00000	0.0	0	0	319.1
644	20.31	71.1	75	168.0	C	0	G44 Concrete Sleeper With Fastclip	0	Lias Group	40	Overhead Line	0	0.00000	0.0	0	0	279.1
645	20.31	71.1	75	168.0	C	0	G44 Concrete Sleeper With Fastclip	0	Lias Group	40	Overhead Line	0	0.00000	0.0	0	0	279.1
646	20.31	71.1	75	168.0	C	0	G44 Concrete Sleeper With Fastclip	0	Lias Group	40	Overhead Line	0	0.00000	0.0	0	0	279.1
647	20.31	71.1	75	168.0	C	0	F40 Concrete Sleeper	10	Lias Group	40	Overhead Line	0	0.00029	11.6	0	0	290.7
648	20.31	71.1	75	168.0	C	0	G44 Concrete Sleeper With Fastclip	0	Lias Group	40	Overhead Line	0	0.00032	12.6	0	0	291.7
649	20.31	71.1	75	168.0	C	0	G44 Concrete Sleeper With Fastclip	0	Lias Group	40	Overhead Line	0	0.00032	12.6	0	0	291.7
650	20.31	71.1	75	168.0	C	0	G44 Concrete Sleeper With Fastclip	0	Lias Group	40	Overhead Line	0	0.00015	6.0	0	0	285.1
651	20.31	71.1	75	168.0	C	0	G44 Concrete Sleeper With Fastclip	0	Lias Group	40	Overhead Line	0	0.00000	0.0	0	0	279.1
652	20.31	71.1	75	168.0	C	0	G44 Concrete Sleeper With Fastclip	0	Lias Group	40	Overhead Line	0	0.00000	0.0	0	0	279.1
653	20.31	71.1	75	168.0	C	0	G44 Concrete Sleeper With Fastclip	0	Lias Group	40	Overhead Line	0	0.00000	0.0	0	0	279.1

654	20.31	71.1	75	168.0	C	0	G44 Concrete Sleeper With Fastclip	0	Lias Group	40	Overhead Line	0	0.00000	0.0	0	0	279.1
655	20.31	71.1	75	168.0	C	0	G44 Concrete Sleeper With Fastclip	0	Lias Group	40	Overhead Line	0	0.00000	0.0	0	0	279.1
656	20.31	71.1	75	168.0	C	0	G44 Concrete Sleeper With Fastclip	0	Lias Group	40	Overhead Line	0	0.00000	0.0	0	0	279.1
657	20.31	71.1	75	168.0	C	0	G44 Concrete Sleeper With Fastclip	0	Lias Group	40	Overhead Line	0	0.00000	0.0	0	0	279.1
658	20.31	71.1	75	168.0	C	0	F40 Concrete Sleeper	10	Lias Group	40	Overhead Line	0	0.00000	0.0	0	0	279.1
659	20.31	71.1	75	168.0	C	0	G44 Concrete Sleeper With Fastclip	0	Lias Group	40	Overhead Line	0	0.00000	0.0	0	0	279.1
660	20.31	71.1	75	168.0	C	0	G44 Concrete Sleeper With Fastclip	0	Lias Group	40	Overhead Line	0	0.00000	0.0	0	0	279.1
661	20.31	71.1	75	168.0	C	0	G44 Concrete Sleeper With Fastclip	0	Lias Group	40	Overhead Line	0	0.00000	0.0	0	0	279.1
662	20.31	71.1	75	168.0	C	0	G44 Concrete Sleeper With Fastclip	0	Lias Group	40	Overhead Line	0	0.00000	0.0	0	0	279.1
663	20.31	71.1	75	168.0	C	0	G44 Concrete Sleeper With Fastclip	0	Lias Group	40	Overhead Line	0	0.00000	0.0	0	0	279.1
664	20.31	71.1	75	168.0	C	0	G44 Concrete Sleeper With Fastclip	0	Lias Group	40	Overhead Line	0	0.00000	0.0	0	0	279.1
665	20.31	71.1	75	168.0	C	0	G44 Concrete Sleeper With Fastclip	0	Lias Group	40	Overhead Line	0	0.00091	36.6	0	0	315.7
666	20.31	71.1	75	168.0	C	0	F40 Concrete Sleeper	10	Lias Group	40	Overhead Line	0	0.00100	50.0	0	0	319.1
667	20.33	71.1	75	168.0	C	0	F40 Concrete Sleeper	10	Lias Group	40	Overhead Line	0	0.00100	50.0	0	0	319.1
668	20.33	71.1	75	168.0	C	0	F40 Concrete Sleeper	10	Lias Group	40	Overhead Line	0	0.00100	50.0	0	0	319.1
669	20.33	71.1	75	168.0	C	0	F40 Concrete Sleeper	10	Lias Group	40	Overhead Line	0	0.00100	50.0	0	0	319.1
670	20.33	71.1	75	168.0	C	0	F40 Concrete Sleeper	10	Lias Group	40	Overhead Line	0	0.00100	50.0	0	0	319.1
671	20.33	71.1	75	168.0	C	0	F40 Concrete Sleeper	10	Lias Group	40	Overhead Line	0	0.00000	0.0	0	0	279.1
672	20.33	71.1	75	168.0	C	0	F40 Concrete Sleeper	10	Lias Group	40	Overhead Line	0	0.00000	0.0	0	0	279.1
673	20.33	71.1	75	168.0	C	0	F40 Concrete Sleeper	10	Lias Group	40	Overhead Line	0	0.00000	0.0	0	0	279.1
674	20.33	71.1	75	168.0	C	0	F40 Concrete Sleeper	10	Lias Group	40	Overhead Line	0	0.00000	0.0	0	0	279.1
675	20.33	71.1	75	168.0	C	0	F40 Concrete Sleeper	10	Lias Group	40	Overhead Line	0	0.00000	0.0	0	0	279.1
676	20.33	71.1	75	168.0	C	0	G44 Concrete Sleeper With Fastclip	0	Lias Group	40	Overhead Line	0	0.00000	0.0	0	0	279.1
677	20.33	71.1	75	168.0	C	0	G44 Concrete Sleeper With Fastclip	0	Lias Group	40	Overhead Line	0	0.00000	0.0	0	0	279.1
678	20.33	71.1	75	168.0	C	0	G44 Concrete Sleeper With Fastclip	0	Lias Group	40	Overhead Line	0	0.00013	5.2	0	0	284.3
679	20.33	71.1	75	168.0	C	0	G44 Concrete Sleeper With Fastclip	0	Lias Group	40	Overhead Line	0	0.00048	19.1	0	0	298.3
680	20.33	71.1	75	168.0	C	0	G44 Concrete Sleeper With Fastclip	0	Lias Group	40	Overhead Line	0	0.00048	19.1	0	0	298.3
681	20.33	71.1	75	168.0	C	0	G44 Concrete Sleeper With Fastclip	0	Lias Group	40	Overhead Line	0	0.00049	19.4	0	0	298.6
682	20.33	71.1	75	168.0	C	0	F40 Concrete Sleeper	10	Lias Group	40	Overhead Line	0	0.00048	19.3	0	0	298.5
683	20.33	71.1	75	168.0	C	0	F40 Concrete Sleeper	10	Lias Group	40	Overhead Line	0	0.00048	19.3	0	0	298.5
684	20.33	71.1	75	168.0	C	0	F27 Concrete Sleeper	40	Lias Group	40	Overhead Line	0	0.00048	19.3	0	0	338.5
685	20.33	71.1	75	168.0	C	0	F27 Concrete Sleeper	40	Lias Group	40	Overhead Line	0	0.00048	19.3	0	0	338.5
686	20.33	71.1	75	168.0	C	0	G44 Concrete Sleeper With Fastclip	0	Lias Group	40	Overhead Line	0	0.00039	15.5	0	0	294.6
687	20.33	71.1	75	168.0	C	0	F27 Concrete Sleeper	40	Lias Group	40	Overhead Line	0	0.00000	0.0	0	0	319.1
688	20.33	71.1	75	168.0	C	0	F27 Concrete Sleeper	40	Lias Group	40	Overhead Line	0	0.00000	0.0	0	0	319.1
689	20.33	71.1	75	168.0	C	0	F27 Concrete Sleeper	40	Lias Group	40	Overhead Line	0	0.00000	0.0	0	0	319.1
690	20.33	71.1	75	168.0	C	0	F27 Concrete Sleeper	40	Lias Group	40	Overhead Line	0	0.00000	0.0	0	0	319.1
691	20.33	71.1	75	168.0	C	0	F23 Concrete Sleeper	60	Lias Group	40	Overhead Line	0	0.00000	0.0	0	0	319.1
692	20.33	71.1	75	168.0	C	0	F27 Concrete Sleeper	40	Lias Group	40	Overhead Line	0	0.00000	0.0	1	50	359.1
693	20.33	71.1	75	168.0	C	0	F27 Concrete Sleeper	40	Lias Group	40	Overhead Line	0	0.00000	0.0	0	0	319.1
694	20.33	71.1	75	168.0	C	0	G44 Concrete Sleeper With Fastclip	0	Lias Group	40	Overhead Line	0	0.00000	0.0	0	0	279.1
695	20.33	71.1	75	168.0	C	0	G44 Concrete Sleeper With Fastclip	0	Lias Group	40	Overhead Line	0	0.00000	0.0	0	0	279.1
696	20.33	71.1	75	168.0	C	0	F27 Concrete Sleeper	40	Lias Group	40	Overhead Line	0	0.00000	0.0	0	0	319.1
697	20.33	71.1	75	168.0	C	0	Hardwood Sleeper / Bearer	60	Lias Group	40	Overhead Line	0	0.00028	11.1	0	0	350.3
698	20.33	71.1	75	168.0	C	0	Hardwood Sleeper / Bearer	60	Lias Group	40	Overhead Line	0	0.00062	25.0	1	50	404.1
699	20.33	71.1	75	168.0	C	0	Hardwood Sleeper / Bearer	60	Lias Group	40	Overhead Line	0	0.00062	25.0	1	50	404.1
700	20.33	71.1	75	168.0	C	0	F27as Concrete Sleeper	40	Lias Group	40	Overhead Line	0	0.00062	25.0	0	0	344.1
701	20.33	71.1	75	168.0	C	0	G44 Concrete Sleeper With Fastclip	0	Lias Group	40	Overhead Line	0	0.00062	25.0	0	0	304.1
702	20.33	71.1	75	168.0	C	0	F27as Concrete Sleeper	40	Lias Group	40	Overhead Line	0	0.00062	25.0	0	0	344.1
703	20.33	71.1	75	168.0	C	0	F27as Concrete Sleeper	40	Lias Group	40	Overhead Line	0	0.00062	24.7	0	0	343.9
704	18.18	63.6	75	168.0	C	0	G44 Concrete Sleeper With Fastclip	0	Lias Group	40	Overhead Line	0	0.00062	24.7	0	0	296.3
705	18.18	63.6	75	168.0	C	0	Softwood Sleeper / Bearer	120	Lias Group	40	Overhead Line	0	0.00062	24.7	0	0	396.3
706	18.18	63.6	75	168.0	C	0	Softwood Sleeper / Bearer	120	Lias Group	40	Overhead Line	0	0.00062	24.7	0	0	396.3
707	18.18	63.6	75	168.0	C	0	Softwood Sleeper / Bearer	120	Lias Group	40	Overhead Line	0	0.00062	24.7	0	0	396.3
708	18.18	63.6	75	168.0	C	0	G44 Concrete Sleeper With Fastclip	0	Lias Group	40	Overhead Line	0	0.00000	0.0	0	0	271.6
709	18.18	63.6	75	168.0	C	0	G44 Concrete Sleeper With Fastclip	0	Lias Group	40	Overhead Line	0	0.00000	0.0	0	0	271.6

710	18.18	63.6	75	168.0	C	0	G44 Concrete Sleeper With Fastclip	0	Lias Group	40	Overhead Line	0	0.00000	0.0	0	0	271.6
711	22.33	78.2	75	168.0	C	0	F40 Concrete Sleeper	10	Lias Group	40	Overhead Line	0	0.00000	0.0	0	0	286.2
712	22.33	78.2	75	168.0	C	0	G44 Concrete Sleeper With Fastclip	0	Lias Group	40	Overhead Line	0	0.00000	0.0	0	0	286.2
713	22.33	78.2	75	168.0	C	0	G44 Concrete Sleeper With Fastclip	0	Lias Group	40	Overhead Line	0	0.00000	0.0	0	0	286.2
714	22.33	78.2	75	168.0	C	0	G44 Concrete Sleeper With Fastclip	0	Lias Group	40	Overhead Line	0	0.00000	0.0	0	0	286.2
715	22.33	78.2	75	168.0	C	0	G44 Concrete Sleeper With Fastclip	0	Lias Group	40	Overhead Line	0	0.00000	0.0	0	0	286.2
716	22.33	78.2	75	168.0	C	0	G44 Concrete Sleeper With Fastclip	0	Lias Group	40	Overhead Line	0	0.00000	0.0	0	0	286.2
717	22.33	78.2	75	168.0	C	0	G44 Concrete Sleeper With Fastclip	0	Lias Group	40	Overhead Line	0	0.00000	0.0	0	0	286.2
718	22.33	78.2	75	168.0	C	0	G44 Concrete Sleeper With Fastclip	0	Lias Group	40	Overhead Line	0	0.00000	0.0	0	0	286.2
719	22.33	78.2	75	168.0	C	0	G44 Concrete Sleeper With Fastclip	0	Lias Group	40	Overhead Line	0	0.00000	0.0	0	0	286.2
720	22.33	78.2	75	168.0	C	0	G44 Concrete Sleeper With Fastclip	0	Lias Group	40	Overhead Line	0	0.00000	0.0	0	0	286.2
721	22.33	78.2	75	168.0	C	0	G44 Concrete Sleeper With Fastclip	0	Lias Group	40	Overhead Line	0	0.00037	15.0	0	0	301.1
722	22.33	78.2	75	168.0	C	0	G44 Concrete Sleeper With Fastclip	0	Lias Group	40	Overhead Line	0	0.00037	15.0	0	0	301.1
723	22.33	78.2	75	168.0	C	0	G44 Concrete Sleeper With Fastclip	0	Lias Group	40	Overhead Line	0	0.00000	0.0	0	0	286.2
724	22.33	78.2	75	168.0	C	0	F27as Concrete Sleeper	40	Lias Group	40	Overhead Line	0	0.00000	0.0	0	0	326.2
725	22.33	78.2	75	168.0	C	0	F27as Concrete Sleeper	40	Lias Group	40	Overhead Line	0	0.00000	0.0	0	0	326.2
726	22.33	78.2	75	168.0	C	0	F27as Concrete Sleeper	40	Lias Group	40	Overhead Line	0	0.00000	0.0	0	0	326.2
727	22.33	78.2	75	168.0	C	0	F40as Concrete Sleeper	0	Lias Group	40	Overhead Line	0	0.00000	0.0	0	0	286.2
728	22.33	78.2	75	168.0	C	0	F40as Concrete Sleeper	0	Lias Group	40	Overhead Line	0	0.00000	0.0	0	0	286.2
729	22.33	78.2	75	168.0	C	0	F40as Concrete Sleeper	0	Lias Group	40	Overhead Line	0	0.00000	0.0	0	0	286.2
730	22.33	78.2	75	168.0	C	0	F27 Concrete Sleeper	40	Lias Group	40	Overhead Line	0	0.00000	0.0	0	0	326.2
731	22.33	78.2	75	168.0	C	0	F27 Concrete Sleeper	40	Lias Group	40	Overhead Line	0	0.00000	0.0	0	0	326.2
732	22.33	78.2	75	168.0	C	0	G44 Concrete Sleeper With Fastclip	0	Lias Group	40	Overhead Line	0	0.00000	0.0	0	0	286.2
733	22.33	78.2	75	168.0	C	0	G44 Concrete Sleeper With Fastclip	0	Lias Group	40	Overhead Line	0	0.00000	0.0	0	0	286.2
734	22.33	78.2	75	168.0	C	0	G44 Concrete Sleeper With Fastclip	0	Lias Group	40	Overhead Line	0	0.00000	0.0	0	0	286.2
735	22.33	78.2	75	168.0	C	0	G44 Concrete Sleeper With Fastclip	0	Lias Group	40	Overhead Line	0	0.00022	8.9	0	0	295.0
736	22.33	78.2	75	168.0	C	0	G44 Concrete Sleeper With Fastclip	0	Lias Group	40	Overhead Line	0	0.00041	16.2	0	0	302.4
737	22.33	78.2	75	168.0	C	0	G44 Concrete Sleeper With Fastclip	0	Lias Group	40	Overhead Line	0	0.00000	0.0	0	0	286.2
738	22.33	78.2	75	168.0	C	0	G44 Concrete Sleeper With Fastclip	0	Lias Group	40	Overhead Line	0	0.00000	0.0	0	0	286.2
739	22.33	78.2	75	168.0	C	0	G44 Concrete Sleeper With Fastclip	0	Lias Group	40	Overhead Line	0	0.00000	0.0	0	0	286.2
740	22.05	77.2	75	168.0	C	0	F27 Concrete Sleeper	40	Triassic Rocks	0	Overhead Line	0	0.00000	0.0	0	0	285.2
741	22.05	77.2	75	168.0	C	0	F27 Concrete Sleeper	40	Triassic Rocks	0	Overhead Line	0	0.00016	6.2	0	0	291.4
742	22.05	77.2	75	168.0	C	0	Hardwood Sleeper / Bearer	60	Triassic Rocks	0	Overhead Line	0	0.00000	0.0	0	0	305.2
743	22.05	77.2	75	168.0	C	0	Hardwood Sleeper / Bearer	60	Triassic Rocks	0	Overhead Line	0	0.00066	26.6	0	0	331.7
744	22.05	77.2	75	168.0	C	0	Hardwood Sleeper / Bearer	60	Triassic Rocks	0	Overhead Line	0	0.00016	6.4	0	0	311.6
745	24.38	85.3	110	246.4	C	0	G44 Concrete Sleeper With Fastclip	0	Triassic Rocks	0	Overhead Line	0	0.00039	15.5	0	0	347.2
746	24.38	85.3	110	246.4	C	0	G44 Concrete Sleeper With Fastclip	0	Triassic Rocks	0	Overhead Line	0	0.00000	0.0	0	0	331.7
747	24.38	85.3	110	246.4	C	0	G44 Concrete Sleeper With Fastclip	0	Triassic Rocks	0	Overhead Line	0	0.00042	16.9	0	0	348.7
748	24.38	85.3	110	246.4	C	0	Hardwood Sleeper / Bearer	60	Triassic Rocks	0	Overhead Line	0	0.00027	10.9	0	0	402.6
749	24.38	85.3	110	246.4	C	0	G44 Concrete Sleeper With Fastclip	0	Lias Group	40	Overhead Line	0	0.00017	6.9	0	0	378.6
750	24.44	85.5	125	280.0	C	0	G44 Concrete Sleeper With Fastclip	0	Lias Group	40	Overhead Line	0	0.00017	6.9	0	0	412.4
751	24.44	85.5	125	280.0	C	0	G44 Concrete Sleeper With Fastclip	0	Lias Group	40	Overhead Line	0	0.00008	3.3	0	0	408.8
752	24.44	85.5	125	280.0	C	0	G44 Concrete Sleeper With Fastclip	0	Lias Group	40	Overhead Line	0	0.00000	0.0	0	0	405.5
753	24.44	85.5	125	280.0	C	0	G44 Concrete Sleeper With Fastclip	0	Lias Group	40	Overhead Line	0	0.00000	0.0	0	0	405.5
754	24.44	85.5	125	280.0	C	0	G44 Concrete Sleeper With Fastclip	0	Lias Group	40	Overhead Line	0	0.00000	0.0	0	0	405.5
755	24.44	85.5	125	280.0	C	0	G44 Concrete Sleeper With Fastclip	0	Lias Group	40	Overhead Line	0	0.00000	0.0	0	0	405.5
756	24.44	85.5	125	280.0	C	0	G44 Concrete Sleeper With Fastclip	0	Lias Group	40	Overhead Line	0	0.00000	0.0	0	0	405.5
757	24.44	85.5	125	280.0	C	0	G44 Concrete Sleeper With Fastclip	0	Lias Group	40	Overhead Line	0	0.00000	0.0	0	0	405.5
758	24.44	85.5	125	280.0	C	0	G44 Concrete Sleeper With Fastclip	0	Lias Group	40	Overhead Line	0	0.00000	0.0	0	0	405.5
759	24.44	85.5	125	280.0	C	0	G44 Concrete Sleeper With Fastclip	0	Lias Group	40	Overhead Line	0	0.00000	0.0	0	0	405.5
760	24.44	85.5	125	280.0	C	0	F40 Concrete Sleeper	10	Lias Group	40	Overhead Line	0	0.00000	0.0	0	0	405.5
761	24.44	85.5	125	280.0	C	0	F40 Concrete Sleeper	10	Lias Group	40	Overhead Line	0	0.00000	0.0	0	0	405.5
762	24.44	85.5	125	280.0	C	0	G44 Concrete Sleeper With Fastclip	0	Triassic Rocks	0	Overhead Line	0	0.00000	0.0	0	0	365.5
763	24.44	85.5	125	280.0	C	0	G44 Concrete Sleeper With Fastclip	0	Triassic Rocks	0	Overhead Line	0	0.00000	0.0	0	0	365.5
764	24.44	85.5	125	280.0	C	0	G44 Concrete Sleeper With Fastclip	0	Lias Group	40	Overhead Line	0	0.00000	0.0	0	0	405.5
765	24.44	85.5	125	280.0	C	0	G44 Concrete Sleeper With Fastclip	0	Lias Group	40	Overhead Line	0	0.00000	0.0	0	0	405.5

766	24.44	85.5	125	280.0	C	0	G44 Concrete Sleeper With Fastclip	0	Lias Group	40	Overhead Line	0	0.00000	0.0	0	0	405.5
767	24.44	85.5	125	280.0	C	0	G44 Concrete Sleeper With Fastclip	0	Lias Group	40	Overhead Line	0	0.00000	0.0	0	0	405.5
768	24.44	85.5	125	280.0	C	0	G44 Concrete Sleeper With Fastclip	0	Lias Group	40	Overhead Line	0	0.00000	0.0	0	0	405.5
769	24.44	85.5	125	280.0	C	0	G44 Concrete Sleeper With Fastclip	0	Lias Group	40	Overhead Line	0	0.00000	0.0	0	0	405.5
770	24.44	85.5	125	280.0	C	0	G44 Concrete Sleeper With Fastclip	0	Lias Group	40	Overhead Line	0	0.00000	0.0	0	0	405.5
771	24.44	85.5	125	280.0	C	0	G44 Concrete Sleeper With Fastclip	0	Lias Group	40	Overhead Line	0	0.00000	0.0	0	0	405.5
772	24.44	85.5	125	280.0	C	0	G44 Concrete Sleeper With Fastclip	0	Lias Group	40	Overhead Line	0	0.00000	0.0	0	0	405.5
773	24.44	85.5	125	280.0	C	0	G44 Concrete Sleeper With Fastclip	0	Lias Group	40	Overhead Line	0	0.00000	0.0	0	0	405.5
774	24.44	85.5	125	280.0	C	0	G44 Concrete Sleeper With Fastclip	0	Lias Group	40	Overhead Line	0	0.00000	0.0	0	0	405.5
775	24.44	85.5	125	280.0	C	0	G44 Concrete Sleeper With Fastclip	0	Lias Group	40	Overhead Line	0	0.00000	0.0	0	0	405.5
776	24.44	85.5	125	280.0	C	0	G44 Concrete Sleeper With Fastclip	0	Lias Group	40	Overhead Line	0	0.00000	0.0	0	0	405.5
777	24.44	85.5	125	280.0	C	0	G44 Concrete Sleeper With Fastclip	0	Lias Group	40	Overhead Line	0	0.00000	0.0	0	0	405.5
778	24.44	85.5	125	280.0	C	0	G44 Concrete Sleeper With Fastclip	0	Lias Group	40	Overhead Line	0	0.00000	0.0	0	0	405.5
779	24.44	85.5	125	280.0	C	0	G44 Concrete Sleeper With Fastclip	0	Lias Group	40	Overhead Line	0	0.00000	0.0	0	0	405.5
780	24.44	85.5	125	280.0	C	0	G44 Concrete Sleeper With Fastclip	0	Lias Group	40	Overhead Line	0	0.00000	0.0	0	0	405.5
781	24.44	85.5	125	280.0	C	0	G44 Concrete Sleeper With Fastclip	0	Lias Group	40	Overhead Line	0	0.00000	0.0	0	0	405.5
782	24.44	85.5	125	280.0	C	0	G44 Concrete Sleeper With Fastclip	0	Lias Group	40	Overhead Line	0	0.00000	0.0	0	0	405.5
783	24.44	85.5	125	280.0	C	0	G44 Concrete Sleeper With Fastclip	0	Lias Group	40	Overhead Line	0	0.00003	1.2	0	0	406.7
784	24.44	85.5	125	280.0	C	0	G44 Concrete Sleeper With Fastclip	0	Lias Group	40	Overhead Line	0	0.00000	0.0	0	0	405.5
785	24.44	85.5	125	280.0	C	0	EG47 Concrete Sleeper With FASTCLIP	0	Lias Group	40	Overhead Line	0	0.00000	0.0	0	0	405.5
786	24.44	85.5	125	280.0	C	0	F40 Concrete Sleeper	10	Lias Group	40	Overhead Line	0	0.00000	0.0	0	0	405.5
787	24.44	85.5	125	280.0	C	0	F40 Concrete Sleeper	10	Lias Group	40	Overhead Line	0	0.00000	0.0	0	0	405.5
788	24.44	85.5	125	280.0	C	0	F40 Concrete Sleeper	10	Lias Group	40	Overhead Line	0	0.00000	0.0	0	0	405.5
789	24.44	85.5	125	280.0	C	0	F40 Concrete Sleeper	10	Lias Group	40	Overhead Line	0	0.00000	0.0	0	0	405.5
790	24.44	85.5	125	280.0	C	0	F40 Concrete Sleeper	10	Lias Group	40	Overhead Line	0	0.00000	0.0	0	0	405.5
791	33.51	117.3	125	280.0	C	0	G44 Concrete Sleeper With Fastclip	0	Lias Group	40	Overhead Line	0	0.00000	0.0	0	0	437.3
792	33.51	117.3	125	280.0	C	0	G44 Concrete Sleeper With Fastclip	0	Lias Group	40	Overhead Line	0	0.00062	24.7	0	0	462.0
793	33.51	117.3	125	280.0	C	0	G44 Concrete Sleeper With Fastclip	0	Lias Group	40	Overhead Line	0	0.00083	33.3	0	0	470.6
794	33.51	117.3	125	280.0	C	0	G44 Concrete Sleeper With Fastclip	0	Lias Group	40	Overhead Line	0	0.00083	33.3	0	0	470.6
795	33.51	117.3	125	280.0	C	0	G44 Concrete Sleeper With Fastclip	0	Lias Group	40	Overhead Line	0	0.00083	33.3	0	0	470.6
796	33.51	117.3	125	280.0	C	0	G44 Concrete Sleeper With Fastclip	0	Lias Group	40	Overhead Line	0	0.00083	33.3	0	0	470.6
797	33.51	117.3	125	280.0	C	0	G44 Concrete Sleeper With Fastclip	0	Lias Group	40	Overhead Line	0	0.00026	10.6	0	0	447.8
798	33.51	117.3	125	280.0	C	0	G44 Concrete Sleeper With Fastclip	0	Lias Group	40	Overhead Line	0	0.00000	0.0	0	0	437.3
799	33.51	117.3	125	280.0	C	0	G44 Concrete Sleeper With Fastclip	0	Lias Group	40	Overhead Line	0	0.00000	0.0	0	0	437.3
800	33.51	117.3	125	280.0	TG	120	Concrete Bearer R (Shallow Depth)	80	Lias Group	40	Overhead Line	0	0.00000	0.0	0	0	777.3
801	33.51	117.3	125	280.0	C	0	5f40 Concrete Sleeper	0	Lias Group	40	Overhead Line	0	0.00000	0.0	0	0	437.3
802	33.51	117.3	125	280.0	C	0	5f40 Concrete Sleeper	0	Lias Group	40	Overhead Line	0	0.00033	13.2	0	0	450.5
803	33.51	117.3	125	280.0	C	0	F40 Concrete Sleeper	10	Lias Group	40	Overhead Line	0	0.00033	13.2	0	0	450.5
804	33.51	117.3	125	280.0	C	0	F40 Concrete Sleeper	10	Lias Group	40	Overhead Line	0	0.00013	5.2	0	0	442.5
805	33.51	117.3	125	280.0	C	0	F40 Concrete Sleeper	10	Lias Group	40	Overhead Line	0	0.00000	0.0	0	0	437.3
806	33.51	117.3	125	280.0	TF	120	Concrete Bearer R (Shallow Depth)	80	Lias Group	40	Overhead Line	0	0.00000	0.0	0	0	777.3
807	33.51	117.3	125	280.0	TF	120	Concrete Bearer R (Shallow Depth)	80	Lias Group	40	Overhead Line	0	0.00000	0.0	0	0	777.3
808	33.51	117.3	125	280.0	C	0	G44 Concrete Sleeper With Fastclip	0	Lias Group	40	Overhead Line	0	0.00000	0.0	0	0	437.3
809	33.51	117.3	125	280.0	C	0	G44 Concrete Sleeper With Fastclip	0	Lias Group	40	Overhead Line	0	0.00000	0.0	0	0	437.3
810	33.51	117.3	125	280.0	C	0	G44 Concrete Sleeper With Fastclip	0	Lias Group	40	Overhead Line	0	0.00000	0.0	0	0	437.3
811	33.51	117.3	125	280.0	C	0	F27 Concrete Sleeper	40	Lias Group	40	Overhead Line	0	0.00000	0.0	0	0	477.3
812	33.51	117.3	125	280.0	C	0	F27 Concrete Sleeper	40	Lias Group	40	Overhead Line	0	0.00000	0.0	0	0	477.3
813	33.51	117.3	125	280.0	C	0	F27 Concrete Sleeper	40	Lias Group	40	Overhead Line	0	0.00000	0.0	0	0	477.3
814	33.51	117.3	125	280.0	C	0	F40 Concrete Sleeper	10	Lias Group	40	Overhead Line	0	0.00000	0.0	0	0	437.3
815	33.51	117.3	125	280.0	C	0	G44 Concrete Sleeper With Fastclip	0	Lias Group	40	Overhead Line	0	0.00000	0.0	0	0	437.3
816	33.51	117.3	125	280.0	C	0	F40 Concrete Sleeper	10	Lias Group	40	Overhead Line	0	0.00000	0.0	0	0	437.3
817	33.51	117.3	125	280.0	C	0	F40 Concrete Sleeper	10	Lias Group	40	Overhead Line	0	0.00000	0.0	0	0	437.3
818	33.51	117.3	125	280.0	C	0	F40 Concrete Sleeper	10	Lias Group	40	Overhead Line	0	0.00018	7.3	0	0	444.6
819	33.51	117.3	125	280.0	C	0	F40 Concrete Sleeper	10	Lias Group	40	Overhead Line	0	0.00027	10.7	0	0	448.0
820	33.51	117.3	125	280.0	C	0	F40 Concrete Sleeper	10	Lias Group	40	Overhead Line	0	0.00000	0.0	0	0	437.3

821	33.51	117.3	125	280.0	C	0	F40 Concrete Sleeper	10	Lias Group	40	Overhead Line	0	0.00000	0.0	0	0	437.3
822	33.51	117.3	125	280.0	C	0	Hardwood Sleeper / Bearer	60	Lias Group	40	Overhead Line	0	0.00000	0.0	0	0	497.3
823	33.51	117.3	125	280.0	C	0	F40 Concrete Sleeper	10	Lias Group	40	Overhead Line	0	0.00000	0.0	0	0	437.3
824	33.51	117.3	125	280.0	C	0	F40 Concrete Sleeper	10	Triassic Rocks	0	Overhead Line	0	0.00000	0.0	0	0	397.3
825	33.51	117.3	125	280.0	C	0	F40 Concrete Sleeper	10	Triassic Rocks	0	Overhead Line	0	0.00032	12.7	0	0	410.0
826	33.51	117.3	125	280.0	C	0	F40 Concrete Sleeper	10	Triassic Rocks	0	Overhead Line	0	0.00032	12.7	0	0	410.0
827	33.51	117.3	125	280.0	C	0	F40 Concrete Sleeper	10	Triassic Rocks	0	Overhead Line	0	0.00032	12.7	0	0	410.0
828	33.51	117.3	125	280.0	C	0	F40 Concrete Sleeper	10	Triassic Rocks	0	Overhead Line	0	0.00032	12.7	0	0	410.0
829	33.51	117.3	125	280.0	C	0	G44 Concrete Sleeper With Fastclip	0	Triassic Rocks	0	Overhead Line	0	0.00032	12.7	0	0	410.0
830	33.51	117.3	125	280.0	C	0	G44 Concrete Sleeper With Fastclip	0	Triassic Rocks	0	Overhead Line	0	0.00018	7.0	0	0	404.3
831	33.51	117.3	125	280.0	C	0	F40 Concrete Sleeper	10	Triassic Rocks	0	Overhead Line	0	0.00029	11.6	0	0	408.9
832	33.51	117.3	125	280.0	C	0	F40 Concrete Sleeper	10	Triassic Rocks	0	Overhead Line	0	0.00030	12.1	0	0	409.4
833	33.51	117.3	125	280.0	C	0	F40 Concrete Sleeper	10	Triassic Rocks	0	Overhead Line	0	0.00000	0.0	0	0	397.3
834	33.51	117.3	125	280.0	C	0	F40 Concrete Sleeper	10	Triassic Rocks	0	Overhead Line	0	0.00000	0.0	0	0	397.3
835	33.51	117.3	125	280.0	C	0	F40 Concrete Sleeper	10	Triassic Rocks	0	Overhead Line	0	0.00000	0.0	0	0	397.3
836	33.51	117.3	125	280.0	C	0	F40 Concrete Sleeper	10	Triassic Rocks	0	Overhead Line	0	0.00000	0.0	0	0	397.3
837	33.51	117.3	125	280.0	C	0	F40 Concrete Sleeper	10	Triassic Rocks	0	Overhead Line	0	0.00065	26.1	0	0	423.4
838	33.51	117.3	125	280.0	C	0	F40 Concrete Sleeper	10	Triassic Rocks	0	Overhead Line	0	0.00065	26.1	0	0	423.4
839	33.51	117.3	125	280.0	C	0	F40 Concrete Sleeper	10	Triassic Rocks	0	Overhead Line	0	0.00065	26.1	0	0	423.4
840	33.51	117.3	125	280.0	C	0	G44 Concrete Sleeper With Fastclip	0	Triassic Rocks	0	Overhead Line	0	0.00065	26.1	0	0	423.4
841	33.51	117.3	125	280.0	C	0	G44 Concrete Sleeper With Fastclip	0	Triassic Rocks	0	Overhead Line	0	0.00065	26.1	0	0	423.4
842	33.51	117.3	125	280.0	C	0	G44 Concrete Sleeper With Fastclip	0	Triassic Rocks	0	Overhead Line	0	0.00000	0.0	0	0	397.3
843	33.51	117.3	125	280.0	C	0	G44 Concrete Sleeper With Fastclip	0	Triassic Rocks	0	Overhead Line	0	0.00043	17.3	0	0	414.6
844	33.51	117.3	125	280.0	C	0	G44 Concrete Sleeper With Fastclip	0	Triassic Rocks	0	Overhead Line	0	0.00043	17.3	0	0	414.6
845	33.51	117.3	125	280.0	C	0	G44 Concrete Sleeper With Fastclip	0	Triassic Rocks	0	Overhead Line	0	0.00039	15.6	0	0	412.8
846	33.51	117.3	125	280.0	C	0	G44 Concrete Sleeper With Fastclip	0	Triassic Rocks	0	Overhead Line	0	0.00047	18.8	0	0	416.1
847	33.51	117.3	125	280.0	C	0	G44 Concrete Sleeper With Fastclip	0	Triassic Rocks	0	Overhead Line	0	0.00019	7.5	0	0	404.8
848	33.51	117.3	125	280.0	C	0	G44 Concrete Sleeper With Fastclip	0	Triassic Rocks	0	Overhead Line	0	0.00000	0.0	0	0	397.3
849	33.51	117.3	125	280.0	C	0	G44 Concrete Sleeper With Fastclip	0	Triassic Rocks	0	Overhead Line	0	0.00000	0.0	0	0	397.3